

REACTING FLUIDS LABORATORY

(NASA-CR-112026) STAGNATION REGION HEATING
OF A PHENOLIC-NYLON ABLATOR DURING RETURN
FROM PLANETARY MISSIONS Final Report D.D.
Esch, et al (Louisiana State Univ.) 1 Sep.
1971 488 p

N72-18951

Unclas
17801

CSCL 20M G3/33

FINAL REPORT

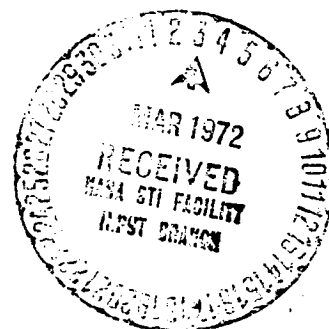
ON

NASA GRANT NGR 19-001-059

STAGNATION REGION HEATING OF A PHENOLIC-NYLON ABLATOR DURING RETURN FROM PLANETARY MISSIONS

by

Donald D. Esch, Research Associate
Ralph W. Pike, Co-principal Investigator
Carl D. Engel, Research Associate
Richard C. Farmer, Co-principal Investigator
John F. Balhoff, Research Associate
Department of Chemical Engineering



September 1, 1971

Reproduced by
NATIONAL TECHNICAL
INFORMATION SERVICE
Springfield, Va. 22151

LOUISIANA STATE UNIVERSITY



STAGNATION REGION HEATING OF A
PHENOLIC-NYLON ABLATOR DURING RETURN
FROM PLANETARY MISSIONS

by

Donald D. Esch
Ralph W. Pike
Carl D. Engel
Richard C. Farmer
John F. Balhoff

Prepared under
Grant NGR 19-001-059

by

Reacting Fluids Laboratory
Department of Chemical Engineering
Louisiana State University
Baton Rouge, Louisiana 70803

for

Langley Research Center
NATIONAL AERONAUTICS AND SPACE ADMINISTRATION

PREFACE

This report gives the results, in detail, for a stagnation-line analysis of the radiative heating of a phenolic-nylon ablator. The analysis includes flowfield coupling with the ablator surface, equilibrium chemistry, multicomponent or binary diffusion and a coupled line and continuum radiation calculation. This report serves as the documentation, i.e. users manual and operating instructions, for the computer programs listed in the report. Copies of the decks have been transferred to Mr. James N. Moss, grant monitor, of the Langley Research Center, and can be obtained from him or from the authors.

Due to the length of this report an abbreviated version giving the key information has been submitted to the Langley Research Center for reviewing and issuing as a NASA contractor's report. This report also served as the dissertation in chemical engineering for Donald D. Esch.

ACKNOWLEDGEMENTS

The authors express their appreciation to Mr. Robert T. Swann of NASA who was responsible for initiating the study and whose interest and consultation was very valuable as the work progressed. Also the efforts of Mr. James N. Moss, the grant monitor, are gratefully acknowledged. Also we are most appreciative of the helpful discussions with Mr. K. H. Wilson of the Lockheed Missles and Space Company and Dr. W. S. Rigdon and Dr. R. B. Dirling of the McDonnell-Douglas Astronautics Company.

The assistance of Mr. Dean Mayers, Mr. James Callender and Mr. Simon Hacker for special contributions to preparation of the report is gratefully acknowledged. The typing chores were very capably performed by Mrs. Elida Aronstein and Mrs. Carol Esch.

TABLE OF CONTENTS

	Page
ACKNOWLEDGMENTS.....	ii
LIST OF TABLES.....	vii
LIST OF FIGURES.....	viii
ABSTRACT.....	xii
CHAPTER	
I. INTRODUCTION AND BACKGROUND.....	1
Introduction.....	1
Aerodynamic Heating.....	2
The Importance of Accurate Radiative Heating Rate Predictions.....	9
Statement of Objectives.....	14
II. A REVIEW OF PREVIOUS ANALYSES IN MULTICOMPONENT REACTING GAS SYSTEMS.....	18
Historical Development of Dilute-Gas Transport Equations.....	18
Diffusion in Dilute Multicomponent Gases....	20
Analytical Studies of Diffusion.....	31
Previous Analyses of Ablating Thermal Protection Systems with Radiation Coupling.....	35

CHAPTER	Page
	Numerical Multicomponent Diffusion Analyses Related to the Study of Ablating Thermal Protection Systems..... 46
	Coupled Analyses of the Effects of Transport and Thermodynamic Properties..... 50
	Summary..... 54
III.	DEVELOPMENT OF EQUATIONS FOR A STAGNATION REGION FLOWFIELD ANALYSIS..... 63
	Introduction..... 63
	Stagnation Line Thin Shock Equations..... 65
	Derivation of Surface Interaction Relations..... 79
	Ablator Response and the Quasi-steady Assumption..... 90
	Shock Boundary Conditions..... 96
	Nondimensionalization and Transformation of the Flowfield Equations..... 99
	Summary.....104
IV.	TRANSPORT, THERMODYNAMIC AND RADIATIVE PROPERTIES.....107
	Theoretical Predictions of High Temperature Gas Properties.....107
	Transport Properties.....107
	Thermodynamic Properties.....126
	Radiation Properties.....132
	Summary.....138

CHAPTER		Page
V.	NUMERICAL IMPLEMENTATION OF THIN SHOCK LAYER EQUATIONS.....	144
	Introduction.....	144
	Coupled Stagnation Line Analysis with Binary Diffusion.....	145
	Overall Analysis.....	164
	Stagnation Region Heating Analysis with Multicomponent Diffusion.....	175
	Summary.....	185
VI.	RESULTS OF STAGNATION REGION HEATING ANALYSIS.....	189
	Coupled Ablator-Flowfield Analyses.....	195
	The Effects of Simplifications in Property Models Upon Radiation Heating Prediction.....	198
	Comparisons of Heating Rate Predictions Using Ablation Product-Air and Pure Air Transport and Thermodynamic Properties.....	208
	The Effectiveness of Phenolic Nylon Ablators in Reducing Radiative Heat Transfer to the Wall.....	216
	Further Observations.....	219
	Summary.....	221
VII.	CONCLUSIONS AND RECOMMENDATIONS.....	223
	Conclusions.....	223
	Recommendation for Design Calculations....	224
	Recommendations for the Improvement of the SLAB Program.....	225

NOMENCLATURE.....	227
APPENDICES	
A	TRANSFORMATION OF SPECIES CONTINUITY EQUATIONS TO ELEMENTAL CONTINUITY EQUATIONS.....232
B	DERIVATION OF TOTAL THERMAL CONDUCTIVITY AND HEAT CAPACITY EXPRESSIONS.....235
C	ESTIMATION OF COLLISION PARAMETERS FOR BINARY DIFFUSION COEFFICIENTS.....239
D	DETERMINATION OF POLYNOMIAL COEFFICIENTS FOR THERMODYNAMIC PROPERTIES.....245
E	DETERMINATION OF EQUILIBRIUM COMPOSITIONS.....252
F	COMPUTER PROGRAM FOR A VISCOUS COUPLED STAGNATION LINE HEATING ANALYSIS.....255
G	COMPUTER PROGRAM FOR MULTICOMPONENT DIFFUSION ANALYSIS.....395
H	GRAPHICAL RESULTS OF CASES RUN.....462
I	<u>POSTERIORI</u> EXAMINATION OF SORET EFFECT.....471
DISTRIBUTION	475

LIST OF TABLES

TABLE		Page
1.1.	Expected Earth Entry Velocities for Several Planetary Missions.....	11
2.1.	A Summary of Related Studies Which Include Multicomponent Diffusion.....	47
3.1.	Dimensionless Groups Used for Nondimensionalization of the Governing Transport Equations.....	100
4.1.	Empirical Constants for Viscosity Correlation.....	115
4.2.	Empirical Constants for Thermal Conductivity Correlation.....	118
4.3.	Collision Parameters Employed in the Current Study.....	127
5.1.	Comparison of Elemental Carbon Distribution for ETA Distributions of 59 and 126 Steps.....	156
6.1.	Comparison of Elemental Composition (Mass Percent) of Phenolic-Nylon and Carbon-Phenolic Ablators.....	194
6.2.	Summary of Major Flowfield Parameters and Corresponding Heating Rate Predictions.	196
6.3.	Comparison of Heating Rate Predictions for Binary and Multicomponent Analyses.....	201
6.4.	Comparison of Heating Rate Predictions Obtained by Assuming Air Properties for Injected Species.....	210

LIST OF FIGURES

Figure	Page
1.1. Total Kinetic Energy of a Body in Motion....	3
1.2. Illustration of Charring-Ablator and Flowfield Interaction.....	6
1.3. Illustration of Heat Transfer Mechanisms in Ablating Thermal Protection Systems.....	8
1.4. Peak Stagnation Point Heating Rates; Blunt Body, $L/D = 0.5$	12
1.5. Weight Sensitivity for Planetary Return (Eight Man Crew).....	13
2.1. Diffusion Velocities as a Function of Mole Fraction Gradient.....	33
2.2. Comparison of Radiation Coupled Stagnation Line Analyses with Mass Injection of Ablation Products.....	39
2.3. Comparison of Dimensionless Radiative Heating Rates ($P_s = 1.0$ atm, $R = 9$ ft.).....	45
2.4. Comparison of Properties of Air and Carbon Phenolic-Air Mixture.....	52
2.5. Effect of Thermodynamic and Transport Properties on the Radiative Flux Toward the Wall.....	53
3.1. Body Oriented Coordinate System and Shock Layer Geometrical Relations.....	68
3.2. Illustration of Overall Surface Material Balance.....	82

Figure	Page
3.3. Illustration of Typical Density and Temperature Profiles in an Ablative Composite.....	91
3.4. Thickness of the Char and Virgin Plastic as a Function of Time.....	93
3.5. Illustration of Flowfield Coupling and Quasi-steady Ablator Response.....	94
3.6. Equilibrium Mass Injection Rates Versus Wall Heating Rates for Various Surface Pressures and Corresponding Temperatures.....	97
4.1. Viscosity of Air Species at 1 atm.....	110
4.2. Viscosity of Ablation Products at 1 atm....	111
4.3. Viscosity of Air at 1 atm.....	113
4.4. Frozen Thermal Conductivity of Air Species at 1 atm.....	116
4.5. Frozen Thermal Conductivity of Ablation Products at 1 atm.....	117
4.6. Comparison of Predictions for Frozen Thermal Conductivity of Air at 1 atm.....	120
4.7. Total Thermal Conductivity of Air at 1 atm.....	122
4.8. Comparison of Several Predictions of the Reacting Thermal Conductivity of Air at 1.0 Atmosphere Pressure.....	123
4.9. Comparison of Mixture Reacting Heat Capacity for Air at 1 atm.....	133
4.10. Spectral Absorption Coefficient of Air-Carbon Phenolic Ablation Products Mixture for $P = 1$ atm and $T = 16,000^{\circ}\text{K}$	135

Figure		Page
4.11.	Typical Variation of k_w Across the Shock Layer with Ablation Productions Injection (Ref. 4.24).....	136
4.12.	Comparison of Dimensionless Radiative Heating Rates (Ref. 4.21)....	139
5.1.	Simplified Flow Diagram for Stagnation Line Heating Analysis with Binary Diffusion (SLAB).....	146
5.2.	Composition Profiles of Elemental Carbon with Various Characteristic Diffusion Parameters.....	151
5.3.	Illustration of One-dimensional Finite-difference Network.....	154
5.4.	Comparison of Stagnation Line Momentum Equation Solutions.....	162
5.5.	Comparison of Dimensionless Radiative Heating Rates ($P_s = 1.0$ atm, $R = 9$ ft).....	166
5.6.	Illustration of the Effect of Temperature Variations Upon Radiative Flux Divergence.....	168
5.7.	Variation in Temperature Profiles From Iteration to Iteration.....	170
5.8.	Variation in Temperature Profiles From Iteration to Iteration.....	171
5.9.	Variation in Temperature Profiles From Iteration to Iteration.....	172
5.10.	Variation in Temperature Profiles From Iteration to Iteration.....	173
5.11.	Converged Temperature Profile.....	174
5.12.	Diffusion Rates of CO_2 As a Function of Y_{CO_2}	180
5.13.	Simplified Flow Diagram of Species Solution with Multicomponent Diffusion.	183

Figure		Page
5.14.	Comparisons of Numerical Results With and Without $d\ln\bar{D}_i/d\eta$	186
6.1.	Typical Trajectories for Earth Entry From Space Origins.....	190
6.2.	Ablator-Coupled Heating Rate Predictions for Phenolic-Nylon Ablator.....	199
6.3.	Comparison of Elemental Profiles Obtained From Binary and Multi- component Diffusion Calculations.....	202
6.4.	Composition Profiles for Air and Major Ablation Species.....	204
6.5.	Composition Profiles for Minor Ablation Species.....	205
6.6.	Composition Profiles for Air and Major Ablation Species.....	206
6.7.	Composition Profiles for Minor Ablation Species.....	207
6.8.	Temperature and Flux Divergence Profiles for Various Property Models...	211
6.9.	Temperature and Flux Divergence Profiles for Various Property Models...	212
6.10.	Comparison Between Phenolic Nylon and Air Mixture Properties to Those of Pure Air.....	214
6.11.	Comparison Between Effectiveness of Phenolic-Nylon and Carbon-Phenolic Ablators.....	218

ABSTRACT

A coupled numerical analysis of the radiative heating of ablative thermal protection systems was developed. The analysis includes flowfield coupling with the ablator surface, multicomponent diffusion, and a coupled line and continuum radiation calculation. With emphasis toward re-entry from planetary flight, the effects of assuming simplified transport and thermodynamic models were examined.

Comparisons were made in wall heating rate calculations assuming both binary and multicomponent diffusion. Further comparisons were made by performing heating rate analysis based upon the proper values of thermal conductivity and viscosity for the injected species and based upon using air properties for the injected species. Heat capacity was examined in a similar manner.

On the basis of this research, it was concluded that the binary diffusion assumption, as opposed to a rigorous multicomponent diffusion analysis, can yield accurate heating rate predictions provided the appropriate binary coefficient is employed. For low mass injection

rates, it was also observed that the choice of the binary coefficient was very critical in determining the correct wall heating rate.

For large blowing rates it was confirmed that the transport mechanisms (i.e., diffusion, conduction, and viscous transport) contribute very little ($\leq 5\%$) to the heat transfer process. Therefore, variations in property models are of little consequence. For low mass injection rates, thermal conductivity was observed to contribute significantly in determining heat transfer to the surface.

Heat capacity was found to be an important factor in determining temperature distributions throughout the flowfield. In the presence of high radiative heating, large differences in the temperature distributions were observed when the simplified (air) property was used instead of the appropriate value.

In comparison with the performance of carbon-phenolic ablators, the 40% nylon-60% phenolic resin ablator was observed to be approximately 5% less effective in blocking radiation to the ablator surface.

CHAPTER I

INTRODUCTION AND BACKGROUND

Introduction

It is the purpose of this research to quantitatively establish the effects of several assumptions used in the prediction of gas-dynamic heating of re-entry vehicles. Particular emphasis will be given to analyses at flight conditions characteristic of re-entry from planetary missions. This chapter will serve as a general introduction to the subject of re-entry heating and will establish the appropriate groundwork for analytical development in subsequent chapters.

The chapter will consist of three parts with the first being a brief overview of aerodynamic heating and thermal protection systems, specifically the charring ablator. This discussion will then be followed by an evaluation of the importance of, and difficulties associated with, accurate heating rate calculations for future manned and unmanned planetary missions. The chapter will be concluded with a specific statement of objectives for the current study.

Aerodynamic Heating

If a body entering a planetary atmosphere utilizes aerodynamic drag to reduce its speed for a soft landing, all of the kinetic energy possessed by the vehicle at entry must be converted to heat. As shown in Figure 1.1, this quantity of energy can be very large (10^3 - 10^5 BTU/lb). This figure also demonstrates the relative advantage of ablative materials over heat sinks as thermal protection systems (Ref. 1.1).

The heating rates suggested by Figure 1.1 are somewhat misleading since, as will be demonstrated, it is not necessary for the energy equivalent to the total kinetic energy to reach the surface of the vehicle. It can be shown that the total heat input for re-entry can be approximated by the following relationship (Ref. 1.1):

$$H = \frac{c_h}{c_d} \left(\frac{1}{2} m U_{\infty}^2 \right) = \frac{c_f}{2c_d} \left(\frac{1}{2} m U_{\infty}^2 \right) \quad (1.1)$$

where

H = total heat input to the vehicle

m = vehicle mass

U_{∞} = entry velocity

c_h = heat-transfer coefficient

c_d = drag coefficient

c_f = friction coefficient

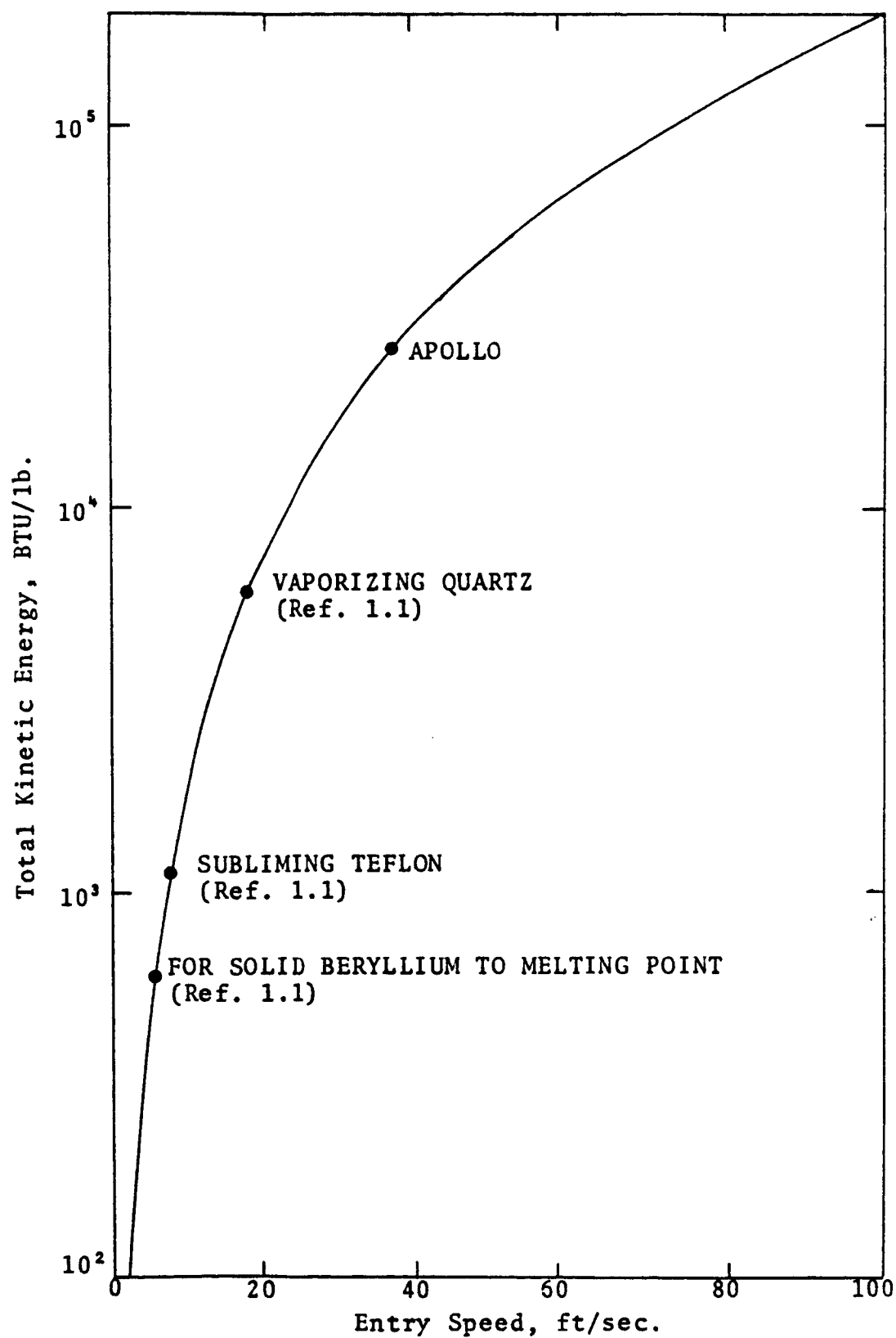


Figure 1.1. Total Kinetic Energy of a Body in Motion.

For blunt bodies (i.e., those having high drag coefficients), the ratio of the heat-transfer coefficient to the drag coefficient is less than for streamline bodies under the same conditions. A typical value for this ratio of coefficients for hypersonic flow over a blunt body is 0.005, assuming laminar boundary layer (Ref. 1.1).

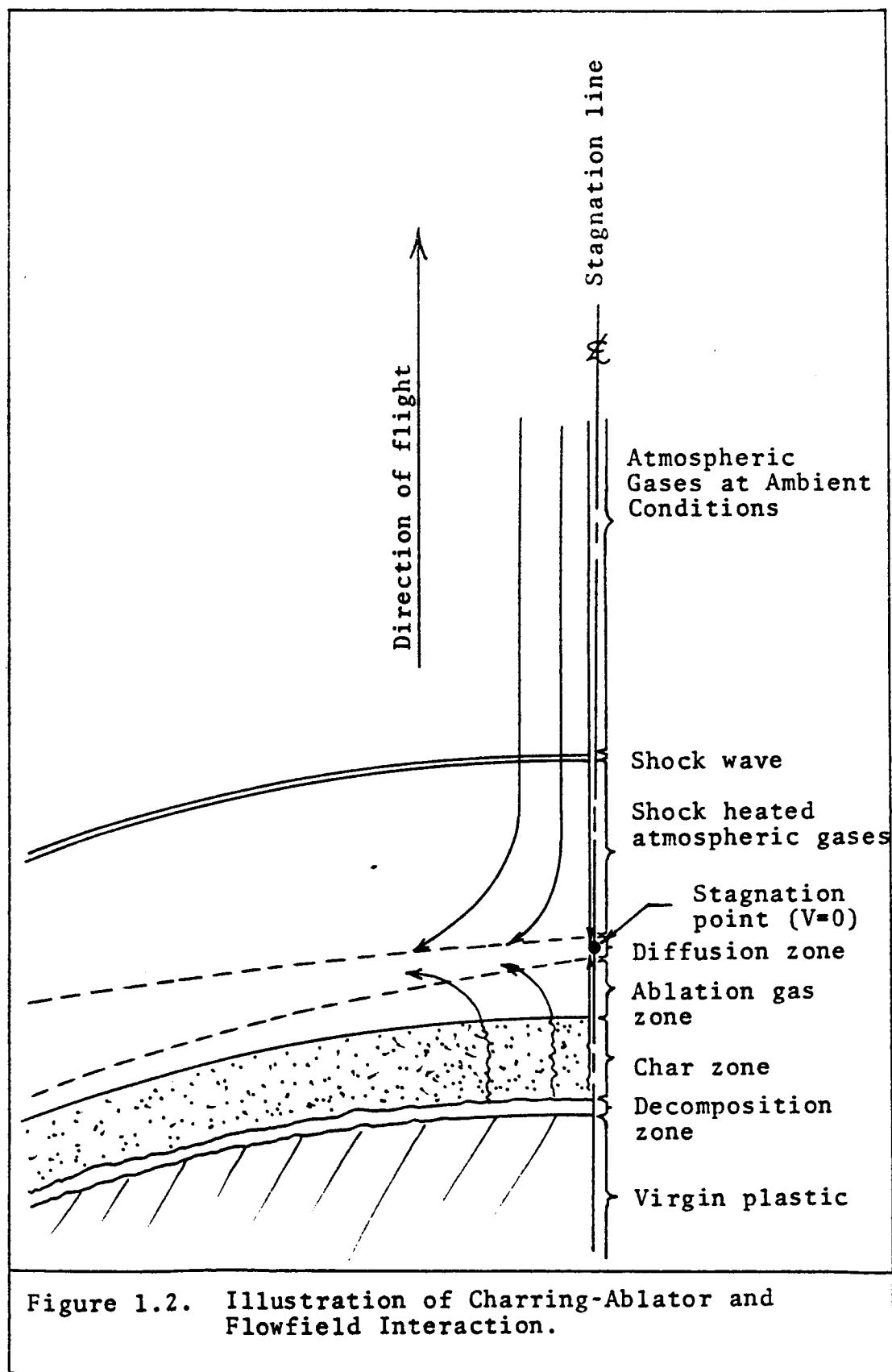
In spite of the reduction in total heating achieved by using blunt bodies for re-entry vehicles, the relative amount of heat absorbed by the vehicle is still sufficient to produce surface temperatures in excess of 3000°K. Thus highly efficient thermal protection systems are required. As previously noted in Figure 1.1 the ablative thermal protection system is more effective than simple heat sinks since large amounts of energy are absorbed by the phase and chemical changes that occur.

Charring Ablators

A wide range of ablative materials have been investigated extensively for use as thermal protection systems for high speed Earth entry and planetary atmospheric flight. A selected list of these investigations is reported in Reference 1.2. As a result of these studies it was found that charring ablators, such as reinforced plastics and castable epoxy resins, provide

a relatively efficient heat protection system with a wide range of versatility (Ref. 1.2). Currently, the technology associated with charring ablators is quite well established as the result of numerous analytical and experimental studies over the last decade; for example, see References 1.3 to 1.10. Considering the advanced technology of charring ablators, this thermal protection system is currently most desirable for the early manned planetary missions.

An illustration of the process of charring ablation is given in Figure 1.2. The ablation process and accompanying flow-field interaction occurs as follows: the virgin plastic, e.g., virgin, phenolic resin-nylon composite, is heated by conduction to its decomposition temperature (approximately 1000°K), where endothermic cracking of the polymer occurs, producing hydrocarbon gases which pass outward through the porous, charred remains of previously decomposed plastic. The pyrolysis products are then expelled into the boundary layer adjacent to the charred surface, carrying with them an additional quantity of carbon gas provided by the subliming char interface. Thus at equilibrium, the surface temperature of the gas-solid interface is approximately equal to the sublimation temperature of the solid ($\sim 3450^{\circ}\text{K}$ for carbon).



At the outer edge of the boundary layer, shock heated atmospheric gases ($\sim 15,000^\circ\text{K}$) move primarily by convection toward the stagnation point, where the diffusive mechanism becomes predominant. The region in the immediate vicinity of the stagnation point is thus indicated in Figure 1.2, as a diffusion zone.

Although simply depicted in Figure 1.2, the overall process is quite complex and presents a significant challenge to an accurate mathematical analysis. The major difficulty arises in determining the net radiative heating incident upon the ablating surface. In Figure 1.3, the primary heat transfer mechanisms associated with this problem are illustrated. The discussion to follow will consist of an elementary description of these mechanisms.

In the shock-heated, atmospheric gas region, while radiative absorption does occur, the predominant radiation effect is emission, which naturally occurs in all directions. Precursor heating arises when the radiative flux through the shock is absorbed by the ambient gases thus increasing the free-stream enthalpy and resulting in even higher temperatures subsequent to the shock heating. The radiative flux in the direction of the body is partially absorbed in the ablation layer, increasing the temperature of the gases in the region; the

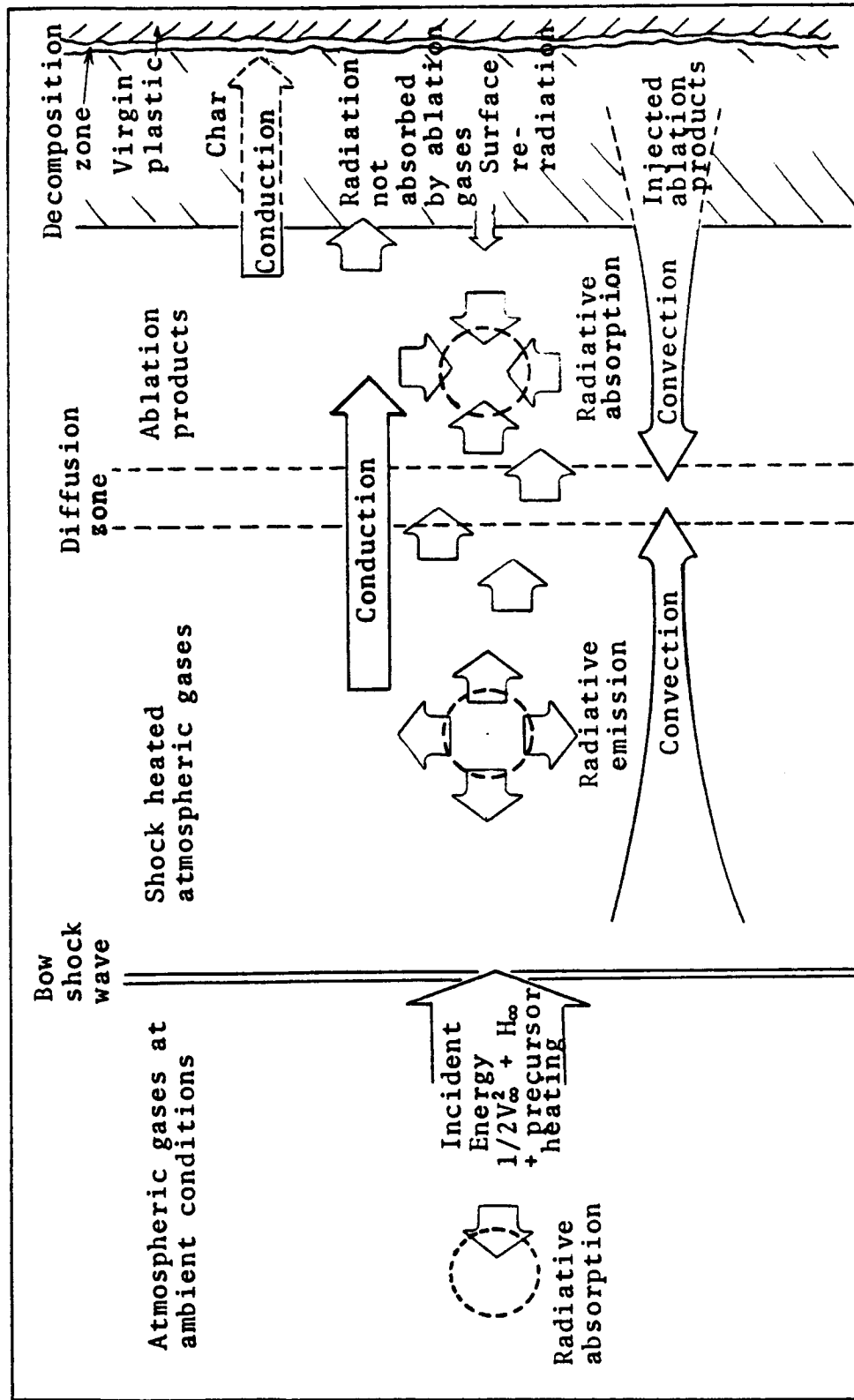


Figure 1.3. Illustration of Heat Transfer Mechanisms in Ablating Thermal Protection Systems.

remaining energy is absorbed by the solid interface to be re-radiated or transported by conduction through the char into the decomposition zone. In the ablator the energy is absorbed by the endothermic reactions of the pyrolysis gases in the char zone and the decomposition of the polymer. The small fraction of energy not assimilated in the char and decomposition zones is finally absorbed by conduction into the virgin plastic.

The preceding description clearly shows the intimate coupling between the response of the thermal protection system and the radiation heat transfer process. Since radiative transport is determined by the temperature and composition of the system, it stands to reason that any approximation used in the evaluation of these dependent variables would be reflected in the radiation calculation and thus the ablator response. Correspondingly, more rigorous calculations could substantially alter the prediction of flowfield characteristics and the surface heating rates.

The Importance of Accurate Radiative Heating Rate Predictions

The current uncertainty in radiative heating rate predictions at entry velocities characteristic of lunar return is minimal compared to other uncertainties

in predicting heat shield performance at this flight condition. Consequently refinements in these calculations would yield relatively small increases in accuracy. However, for those velocities anticipated for planetary entry and return, radiative heating is expected to play a far more important role (See Table 1.1). An estimate of the increase in radiative and convective heating for increasing entry velocity is shown in Figure 1.4. As a result of the dramatic increase in radiation heating, many of the currently acceptable assumptions in heating rate calculations may become intolerable, particularly those assumptions which relate to the prediction of species compositions. One such assumption is that of local chemical equilibrium as opposed to finite-rate chemistry. Another is the assumption of binary diffusion (Fick's Law) versus a multicomponent diffusion analysis. Others include-- simplifications in transport properties, such as using air properties throughout the flowfield and neglecting thermal diffusion; simplified radiation models; and the assumption of a laminar flowfield. In Figure 1.5, the uncertainties in heat shield weight requirements are estimated for the approximate range of entry velocities anticipated in future planetary missions. According to

Table 1.1
Expected Earth Entry Velocities for Several Planetary Missions

VELOCITY (ft/sec)	30,000	40,000	50,000	60,000	70,000	80,000	REFERENCE	
MERCURY							1.12	
VENUS							1.11,1.12, 1.13,1.15	
MARS (SWINGBY)							1.12,1.14	
MARS (DIRECT)							1.12,1.13	
MARS-VENUS							1.14	
CERES							1.12	
JUPITER							1.12	
APOLLO								
VELOCITY (km/sec)	10	12	14	16	18	20	22	24

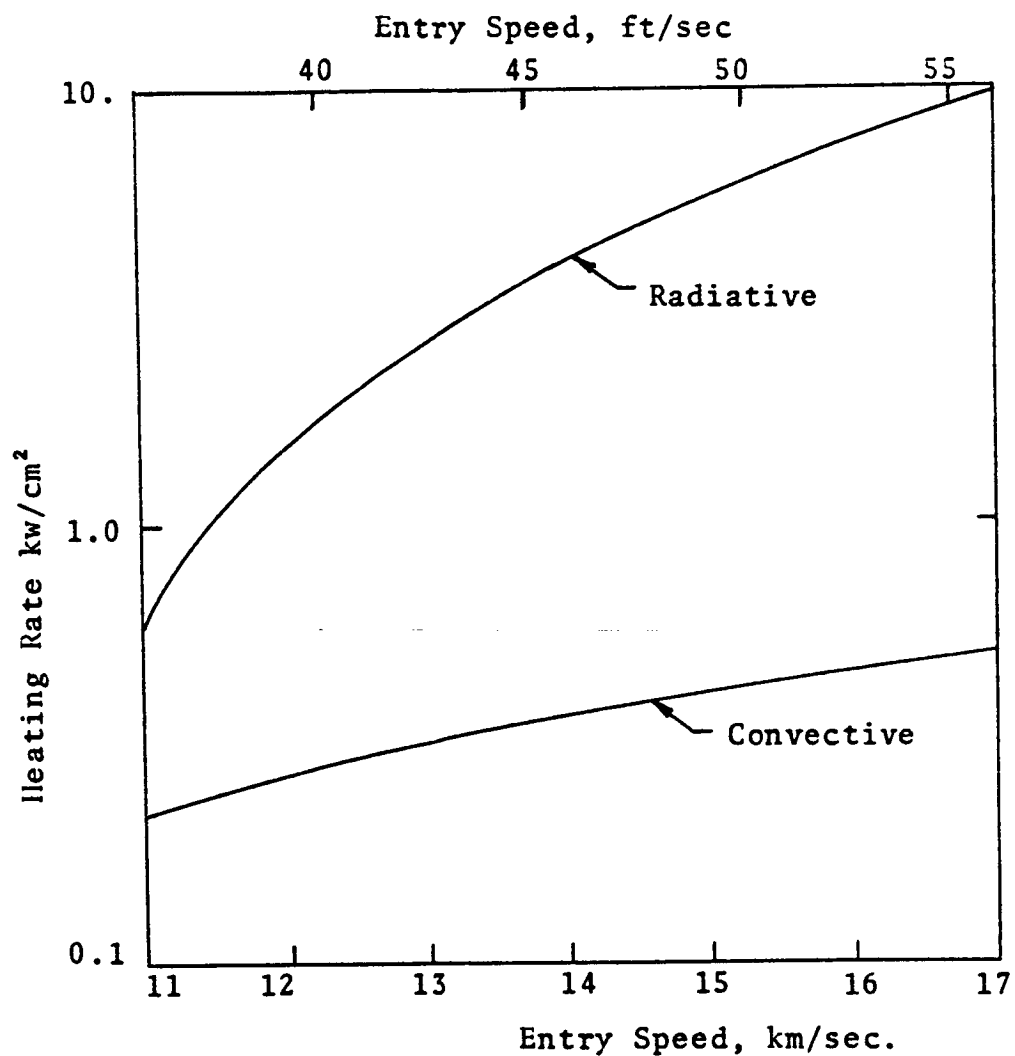


Figure 1.4. Peak Stagnation Point Heating Rates; Blunt Body, $L/D = 0.5$ (Ref. 1.12).

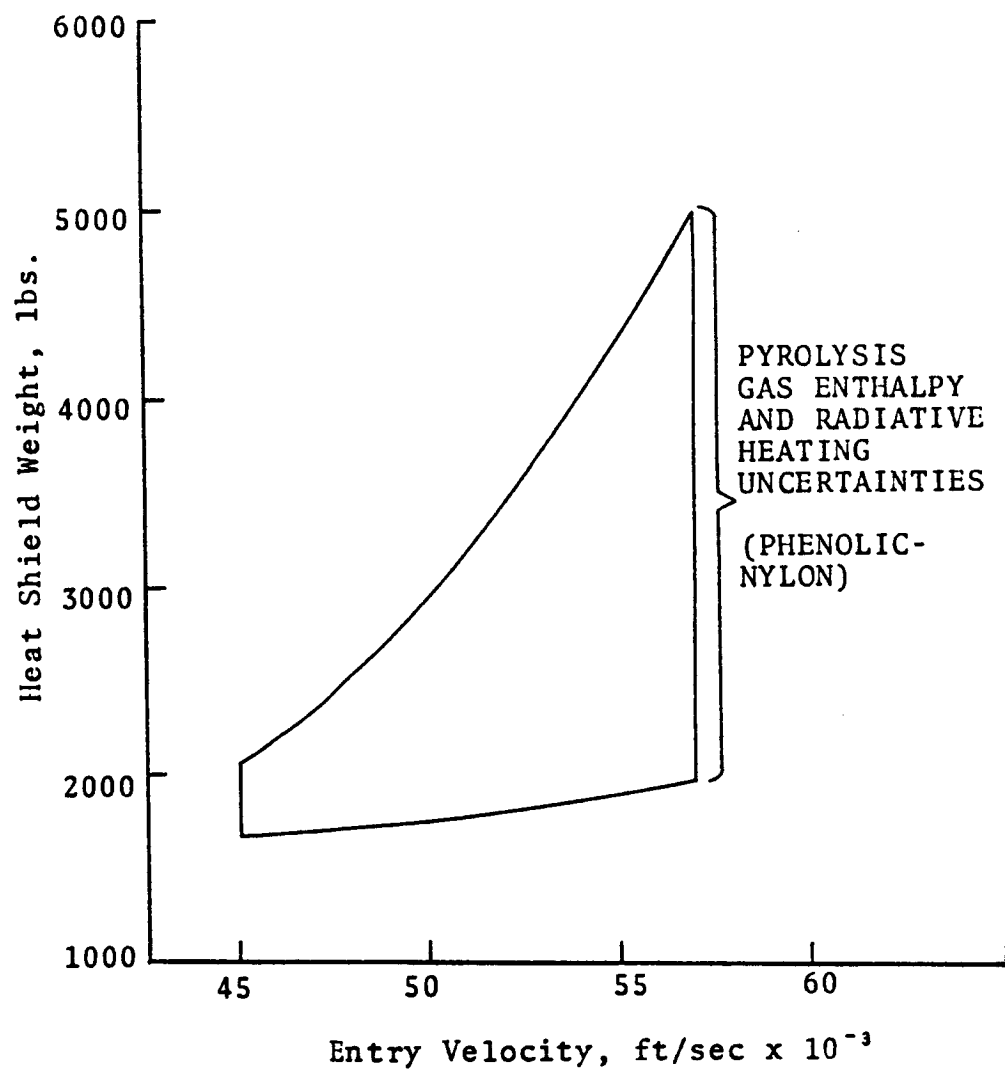


Figure 1.5. Weight Sensitivity for Planetary Return (Eight Man Crew, Ref. 1.11).

one estimate, each pound carried throughout a manned planetary mission can represent between 300 and 1000 pounds on the launch pad (Ref. 1.12). Assume that each pound of heat shield only represents 300 pounds of launch pad weight. Using Figure 1.5 an uncertainty of 180 tons in the weight of the launch vehicle would then exist for an entry velocity of 50,000 feet per second.

Statement of Objectives

In an effort to reduce uncertainties such as those previously illustrated, the current research was undertaken. Specifically, the current study will include the assessment of two important effects:

1. The effect upon radiation heating of the more accurate multicomponent diffusion analysis versus simple Fickian diffusion.
2. An evaluation of the effect upon radiant heating of using appropriate transport and thermodynamic properties, as opposed to the simplification of using air properties throughout the flowfield.

The flight conditions selected for these comparisons will be characteristic of those anticipated for re-entry from planetary missions.

Subsequent studies will be aimed at resolving additional uncertainties in current analyses by including finite-rate chemistry, by performing a thorough assessment

of radiation properties, and including these results in a fully coupled analysis of the ablator-flowfield interaction. The overall goal of all of the studies will be to develop an optimum model for use in thermal protection system design calculations where radiant heating is the dominant heat transfer mechanism.

The following chapter will consist of a detailed review of previous literature on multicomponent diffusion studies and of pertinent investigations in the prediction of high temperature transport and thermodynamic properties. In addition, a review and comparison of previous investigations of radiation coupled heating rate analyses will be presented.

REFERENCES

- 1.1. Allen, Julian H., "Some Problems of Planetary Atmospheric Entry," J. Roy. Aero. Soc. (January 1968).
- 1.2. Diaconis, N. S., W. R. Warren, Jr. and T. E. Shaw, "The Hypervelocity Heat Protection Problem," in Propulsion and Re-entry. Proceedings of the XVIth International Astronautical Congress (Gauthier-Villars, Paris, 1966), pp. 397-434.
- 1.3. April, G. C., Evaluation of the Energy Transfer in the Char Zone During Ablation, Ph.D. Dissertation, Louisiana State University, Baton Rouge, Louisiana (1969).
- 1.4. Beecher, N. and R. E. Roseweeg, "Ablation Mechanisms in Plastics With Inorganic Reinforcement," ARS Journal, Vol. 31, No. 1 (January 1961), pp. 532-538.
- 1.5. Lagedrost, J. F., et al., "Thermophysical and Chemical Characterization of Charring Ablative Materials," NASA CR-73399 (December 1968).
- 1.6. Moss, James N. and W. E. Howell, "A Study of the Performance of Low-Density Phenolic-Nylon Ablators," NASA TN D-5257 (June 1969).
- 1.7. Matting, F. W., "Analysis of Charring Ablation With Description of Associated Computing Program," NASA TN D-6085 (November 1970).
- 1.8. McLain, A. G., K. Sutton, and G. D. Walberg, "Experimental and Theoretical Investigation of the Ablative Performance of Five Phenolic-Nylon-Based Polymers," NASA TN D-4374 (April 1968).
- 1.9. Scala, S. M. and L. M. Gilbert, "Thermal Degradation of a Char-Forming Plastic During Hypersonic Flight," ARS Journal, Vol. 32, No. 6 (June 1962), pp. 917-924.

- 1.10. Witte, William G., "Flight Test of High-Density Phenolic-Nylon on a Spacecraft Launched by the Pacemaker Vehicle System," NASA TM X-1910 (November 1969).
- 1.11. Stewart, J. D. and D. H. Greenshields, "Entry Vehicles for Space Programs," Journal of Spacecraft and Rockets, Vol. 6, No. 10 (October 1969), pp. 1089-1102.
- 1.12. Syvertson, C. A., "Research Problems in Atmospheric Entry and Landing for Manned Planetary Missions," NASA TM D-4977 (January 1969).
- 1.13. Allen, Julian H., "Hypersonic Aerodynamic Problems of the Future," in The High Temperature Aspects of Hypersonic Flow, ed. by W. C. Nelson (Pergamon Press, MacMillan Co., New York, New York), 1964, pp. 1-42.
- 1.14. Willis, E. A., Jr. and J. A. Padruft, "Round-Trip Trajectories with Stopovers at Both Mars and Venus," NASA TN D-5758 (April 1970).
- 1.15. Jaworski, W. and R. G. Nagler, "A Parametric Analysis of Venus Entry Heat Shield Requirements," Jet Propulsion Laboratory Tech. Rept. No. 32-1468, (California Inst. of Tech., Pasadena, Calif. 1970).

CHAPTER II

A REVIEW OF PREVIOUS ANALYSES IN MULTICOMPONENT REACTING GAS SYSTEMS

Historical Development of Dilute-Gas Transport Equations

An excellent historical summary of the early development of the hydrodynamic transport equations is given in Chapman and Cowling (Ref. 2.1). The formulation and development had its origins in a classic paper by J. C. Maxwell, in 1867 (Ref. 2.2). His paper, "On the Dynamical Theory of Gases", contains a derivation of the general equations of transfer describing the total rate of change of any mean property. The solution to these relationships required the specification of a molecular velocity distribution function. To obtain a solution, Maxwell, thus proposed the distribution function which is given his name today. Boltzmann, in 1872 (Ref. 2.3) gave his famous integro-differential equation* which the velocity distribution function must satisfy. From the Boltzmann equation, the equations of change (the equations of conservation of mass, momentum

*See Ref. 2.8, p. 452, Equation 7.1-25.

and energy) could theoretically be derived without having specified the velocity distribution function. Assuming a Maxwellian distribution, Boltzmann confirmed the equations proposed by Maxwell; however, he was never able to obtain a satisfactory solution to his own equation.

He gave a complicated approximate method of solution with the object of calculating viscosity. The investigation, which in all occupies 168 pages of his Collected Works, appeared to yield no simple result, and Boltzmann remarked that one must despair of the general solution of his equation. (Ref. 2.1)

Nearly a half a century later the general solution was finally realized. Independently, solutions were derived by Chapman (Ref. 2.4) in 1916 and Enskog (Ref. 2.5) in 1917. With the exception of minor theoretical revisions, their solution to the Boltzmann equation has remained unchanged during the past four decades. Hence the name, "Chapman-Enskog Theory", has come to mean the rigorous kinetic theory of dilute (low pressure) monatomic gas mixtures. Accordingly, the "Chapman-Enskog" equations are those describing the transport coefficients (viscosity, thermal conductivity, and diffusion coefficients) of dilute gases. With a few modifications to account for the presence of polyatomic molecules, these equations will serve as a basis for the current analyses.

For the most part, the remainder of this chapter will be devoted specifically to a review of one aspect of dilute gas transport phenomena, the diffusion of chemical species in reacting gas mixtures. In the course of surveying this topic, it will be necessary to include a discussion of the various formulations and nomenclature commonly employed in gaseous diffusion calculations, for example: the Stefan-Maxwell equations; multicomponent, binary and effective diffusion coefficients; and frames of reference. Following the survey of multicomponent diffusion studies, the chapter will be concluded with a review of current radiation-coupled analyses of ablating thermal protection systems and a summary of the results of previous studies into the effects of transport property variations upon heating rate predictions.

Diffusion in Dilute Multicomponent Gases

Multicomponent Diffusion Coefficients: Through solutions of the Boltzmann equation, Hellund (Ref. 2.6) and later Curtiss and Hirschfelder (Ref. 2.7) obtained theoretical formulations describing the diffusive behavior of a mixture of several gases. The equation describing the diffusive mass flux vector (\mathbf{J}_i) of the i th species relative to the mass average velocity ($\bar{\mathbf{v}}$) is given in Hirschfelder,

Curtiss, and Bird (Ref. 2.8, p. 516). The flux vector (neglecting pressure diffusion and forced diffusion) is written as,*

$$\mathbf{J}_i = \frac{n^2}{\rho} \sum_{j=1}^v m_i m_j D_{ij} \bar{\nabla} Y_j - D_i^T \bar{\nabla} \ln T$$

$$i=1, 2, \dots, v \quad (2.1)$$

$$\text{where } \mathbf{J}_i = \rho_i \bar{\mathbf{V}}_i = \rho_i (\bar{\mathbf{v}}_i - \bar{\mathbf{v}}) \quad (2.2)$$

The D_{ij} 's appearing in Equation 2.1 are referred to as multicomponent diffusion coefficients. These are not to be confused with the binary diffusion coefficients, \mathcal{D}_{ij} , which are computed directly from molecular properties by the following Chapman-Enskog equation:

$$\mathcal{D}_{ij} = 2.28 \times 10^{-7} T^{3/2} \left(\frac{M_i + M_j}{2 M_i M_j} \right)^{1/2} / p \sigma_{ij} \Omega_{ij}^{(1,1)} \text{ ft}^2/\text{sec}$$

$$(2.3)$$

From the composition and the binary diffusion coefficients, the multicomponent diffusion coefficients can be determined by means of the matrix formulation given in Hirschfelder, Curtiss, and Bird (Ref. 2.8, p. 541). The

*For specific definition of terms, the reader is referred to the nomenclature section.

same reference gives a similar formulation from which the thermal diffusion coefficients, D_1^T , can be computed (p. 543).

For most calculations, the effects of pressure, forced and thermal diffusion can be neglected and, Equation 2.1 can be expressed as follows:

$$J_i = \frac{\rho}{M} \sum_{j=1}^n M_i M_j D_{ij} \nabla Y_j \quad i=1, 2, \dots, v \quad (2.4)$$

Because of the concentration dependence of the multi-component diffusion coefficients, this type of formulation is inconvenient to use (Ref. 2.9). For this reason various modifications of the previous form are frequently more desirable for computational purposes. In Reference 2.7, Curtiss and Hirschfelder demonstrated that for an ideal gas mixture, Equation 2.1 (or Equation 2.4) could be rearranged into a form which is expressed entirely in terms of the binary diffusion coefficients. This form is referred to as the Stefan-Maxwell Equations.*

* Maxwell's contribution to the development of the transport equations has been discussed earlier in this chapter. The inclusion of Stefan's name in the title of the equations is most likely based upon his being the first to specifically examine the diffusion aspect of transport equations (Ref. 2.12).

The Stefan-Maxwell Equations. The most frequently used approach to the solution of multicomponent, gas-diffusion problems involves the use of the Maxwell or Stefan-Maxwell Equations. A derivation of these relations from Equation 2.1 is given in Reference 2.8 (p. 485). In the absence of the thermal diffusion, forced and pressure diffusion, the equations are written as follows (Ref. 2.9, p. 570):

$$\nabla Y_i = \sum_{j=1}^v \frac{Y_i Y_j}{D_{ij}} (\nabla_j - \nabla_i) \quad i=1, 2, \dots, v \quad (2.5)$$

In matrix form these equations can be conveniently represented in the following way for one coordinate direction

$$\bar{A} \nabla_y = \frac{\partial Y}{\partial y} \quad (2.6)$$

where the coefficients a_{ik} are,

$$a_{ik} = \frac{Y_i Y_k}{D_{ik}} \quad (i \neq k) \quad (2.7)$$

$$a_{ii} = - Y_i \sum_{j \neq i} \frac{Y_j}{D_{ij}} \quad (2.8)$$

and ∇_y is the vector of diffusion velocities of the v species in the y direction.

The system given by Equations 2.5 or 2.6 is not linearly independent as discussed in Reference 2.11. In fact, there are only $v-1$ linearly independent equations. The physical meaning of this occurrence arises from the fact that the diffusion velocities, V_i , are relative to the mixture flow velocity as defined in Equation 2.2. It is therefore necessary to establish some frame of reference, which can be applied to obtain an independent set of equations.

Reference Frames in Diffusion. The specification of the required reference frame is equivalent to defining the mixture flow velocity. Definitions of mixture flow velocity which are commonly employed are the local mass average velocity, molar average velocity or the volume average velocity, the choice being based upon the convenience of formulation. Several good discussions concerning the choice of these and other reference frames are available throughout the literature (Refs. 2.9-2.11). In this study, the mixture flow velocity is defined as the local mass average velocity:

$$\bar{v} = \frac{\sum_{i=1}^v \rho_i \bar{v}_i}{\sum_{i=1}^v \rho_i} \quad (2.9)$$

where \bar{v}_i is the velocity of the i th species with respect to stationary coordinate axis. As previously stated, the diffusion velocities, \bar{V}_i appearing in Equation 2.6 are expressed relative to the mixture flow velocity.

$$V_i = (\bar{v}_i - \bar{v}) \quad (2.10)$$

From this relationship and the assumed frame of reference, the local mass average velocity, the sum of the mass fluxes over all species can be determined:

$$\sum_{i=1}^v \rho_i \bar{v}_i = \sum_{i=1}^v \rho_i \bar{v}_i - \bar{v} \sum_{i=1}^v \rho_i \quad (2.11)$$

From Equation 2.9,

$$\sum_{i=1}^v \rho_i \bar{v}_i = \bar{v} \sum_{i=1}^v \rho_i \quad (2.12)$$

therefore

$$\sum \rho_i \bar{V}_i = 0 \quad (2.13)$$

Since this relationship between mass fluxes is based upon the selected frame of reference, it provides the necessary condition for completely defining the diffusion

velocities, \bar{V}_i . By replacing one of Equations 2.5 by Equation 2.13, the diffusion velocities can be determined. Analogous developments can be performed for various other reference frames.*

Common Diffusion Coefficients. For a binary system of components A and B, Equation 2.4 simplifies to Fick's law such that,

$$\bar{J}_A = - \rho / M^2 \quad M_A M_B \mathcal{D}_{AB} \frac{\bar{V}_{YA}}{dy} \quad (2.14)$$

$$\bar{J}_B = - \rho / M^2 \quad M_A M_B \mathcal{D}_{BA} \frac{\bar{V}_{YA}}{dy} \quad (2.15)$$

When expressed in terms of mass fractions rather than mole fractions, these equations become,

$$\bar{J}_A = - \rho \mathcal{D}_{AB} \bar{V}_{CA} \quad (2.16)$$

$$\bar{J}_B = - \rho \mathcal{D}_{BA} \bar{V}_{CB} \quad (2.17)$$

Upon examining the Chapman-Enskog equations from which the binary diffusion coefficients are computed (Equation 2.3) it is seen that the coefficients \mathcal{D}_{AB} and \mathcal{D}_{BA} are equal. Thus the diffusive behavior of binary system can

*A discussion of several other frames of reference is given in Reference 2.11.

be determined from the specification of a single coefficient. In an effort to extend this simplification to multicomponent systems, several authors (Refs. 2.13-2.17) have replaced the exact expression for mass flux in multicomponent mixtures (Equation 2.4) by Fick's Law,

$$J_i = - \rho D \nabla C_i \quad i=1, 2, \dots, v \quad (2.18)$$

The selection of the appropriate diffusion coefficient usually is satisfactory as long as the mixture is composed of similar species. However, for systems containing very dissimilar molecules, no basis exists for estimating a characteristic diffusion coefficient (Ref. 2.27). In the subsequent discussions, the use of the formulation given in Equation 2.18 will be referred as the "binary diffusion approximation."

Effective Diffusion Coefficients. When using the terminology, "effective diffusion coefficients", a distinction must be made between the approximate coefficients obtained from the derivation of Wilke (Ref. 2.18) and those obtained from the exact formulation employed by Tirskaa (Refs. 2.19-2.21). The Wilke equation, given below, is derived from the Stefan-Maxwell equations assuming the diffusion of one

component, A, into a stagnant mixture of gases, B, C, D . . . The equation, which is exact only under the above conditions is,*

$$D_A = \frac{1 - Y_A}{\frac{Y_B}{D_{AB}} + \frac{Y_C}{D_{AC}} + \frac{Y_D}{D_{AD}} + \dots} \quad (2.19)$$

The effective diffusion coefficient referred to by Tirskaa is not limited by the previous assumption and is obtained in the following manner:

Assume a Fickian-like diffusion where

$$J_{i,y} = J_i = - \rho D_i \frac{\partial C_i}{\partial y} \quad (2.20)$$

In terms of mass concentrations, the Stefan-Maxwell equations can be written in one dimensional form as shown below:

$$\frac{\partial C_i}{\partial y} = \frac{M}{\rho} \left[\sum_j \frac{C_i J_j - C_j J_i}{D_{ij} M_j} - C_i \sum_k \sum_j \frac{C_k J_j - C_j J_k}{D_{kj} M_j} \right] \quad (2.21)$$

By combining Equations 2.20 and 2.21 an exact relationship for the effective coefficient, D_i , is thus obtained.

*Excellent agreement was found in the experimental verification of this equation (Refs. 2.18 and 2.22). These results are an encouraging indication of the validity of the Stefan-Maxwell equations.

$$\frac{1}{D_i} = \frac{M}{J_i} \left[C_i \sum_k \sum_j \frac{C_k J_j - C_j J_k}{D_{kj} M_j} - \sum_j \frac{C_i J_j - C_j J_i}{D_{ij} M_j} \right] \quad (2.22)$$

Such a relationship as Equation 2.22 is best suited for an iterative numerical solution such as that proposed in Tirskaa's latter paper (Ref. 2.21) and as that employed in this study.*

The Bifurcation Approximation. In Reference 2.23, Bird demonstrated that a bifurcation (separation) of the effects of the interaction between species permits an explicit solution to the Stefan-Maxwell equations for the mass fluxes. The empirical approximation used for this simplification was

$$D_{ij} \approx \bar{D} / F_i F_j \quad (2.23)$$

where \bar{D} is an arbitrary reference diffusion coefficient and the parameters, F_i and F_j , are diffusion factors for species i and j .**

Using Equation 2.23, the explicit solution can be developed as shown in Reference 2.25 (Appendix B). The result is expressed as:

*Presented in Chapter V.

**A method for computing these parameters is described in Reference 2.25 (Appendix C).

$$J_{i,y} = \frac{\rho \bar{D}}{\psi_1} \left[\frac{\psi_2}{M} \frac{\partial z_i}{\partial y} + \frac{(z_i - C_i)}{M} \frac{\partial \psi_2}{\partial y} + C_i \left(\frac{1}{F_i^2} \frac{dF_i}{dT} - \psi_4 \right) \frac{\partial T}{\partial y} \right] \quad (2.24)$$

where,

$$z_i = M_i Y_i / F_i \psi_2 = M C_i / F_i \psi_2 \quad (2.25)$$

$$\psi_1 = \sum_j Y_j F_j = M \sum_j C_j F_j / M_j \quad (2.26)$$

$$\psi_2 = \sum_j M_j Y_j / F_j = M \sum_j C_j / F_j \quad (2.27)$$

$$\psi_4 = \sum_j (C_j / F_j^2) \frac{\partial F_j}{\partial T} \quad (2.28)$$

It has been found that it is often consistent with the level of approximation to consider F_i independent of temperature (Refs. 2.24 and 2.26) Equation 2.24 is thus simplified to the following form:

$$J_{i,y} = \rho \frac{\bar{D} \psi_2}{\psi_1 M} \left[\frac{\partial z_i}{\partial y} + \left(\frac{z_i - C_i}{\psi_2} \right) \frac{\partial \psi_2}{\partial y} \right] \quad (2.29)$$

The accuracy of the foregoing approximation to multicomponent mass fluxes has been investigated by Bartlett and Grose (Ref. 2.28) and Graves (Ref. 2.29). The former study involved a coupled ablator-flowfield analysis in which the use of the bifurcation approximation gave predictions of mass injection rates which agreed within 5.0% of those predicted using an exact method. The investigation by Graves gave results which were quite favorable of the bifurcation model. It was reported that in general there was little detectable difference between the multicomponent and the bifurcation diffusion models. More discussion of the latter analysis will be included in a later development.

In the following section, the review of multicomponent diffusion analyses will be extended by examining the results of some analytical solutions. From these studies, certain phenomena are found to occur which might not be predicted by some of the previously discussed approximate methods.

Analytical Studies of Diffusion

Cross-effects Unique to Multicomponent Analyses:

Several specific solutions to the Stefan-Maxwell equations have been reported in the literature (for example, Refs. 2.30-2.36). Although these solutions are all limited

to tertiary systems, some anomalies unique to multi-component diffusion are revealed. From the previously discussed multicomponent formulations, Equations 2.1 and 2.5, it is observed that the diffusive behavior of each component is not simply a function of its own gradient as is the case with binary diffusion. Instead, an additional dependency upon the gradients of the other components is seen to exist. As reported in the analytical investigation of Toor (Ref. 2.35), this occurrence gives rise to the following phenomena:

Under certain conditions there exists,

- (1) a "diffusion barrier" such that the rate of diffusion of a component is zero even though its own concentration gradient is finite.
- (2) a condition, "osmotic diffusion," under which diffusion of a component may occur in spite of its own gradient being zero.
- (3) "reverse diffusion," when a component diffuses against its own gradient.

In Figure 2.1, an analytical solution to the Stefan-Maxwell equations for a tertiary system consisting of CO_2 , H_2O , and H_2 , are shown to demonstrate these occurrences. If effective diffusion coefficients were employed, a negative effective coefficient would

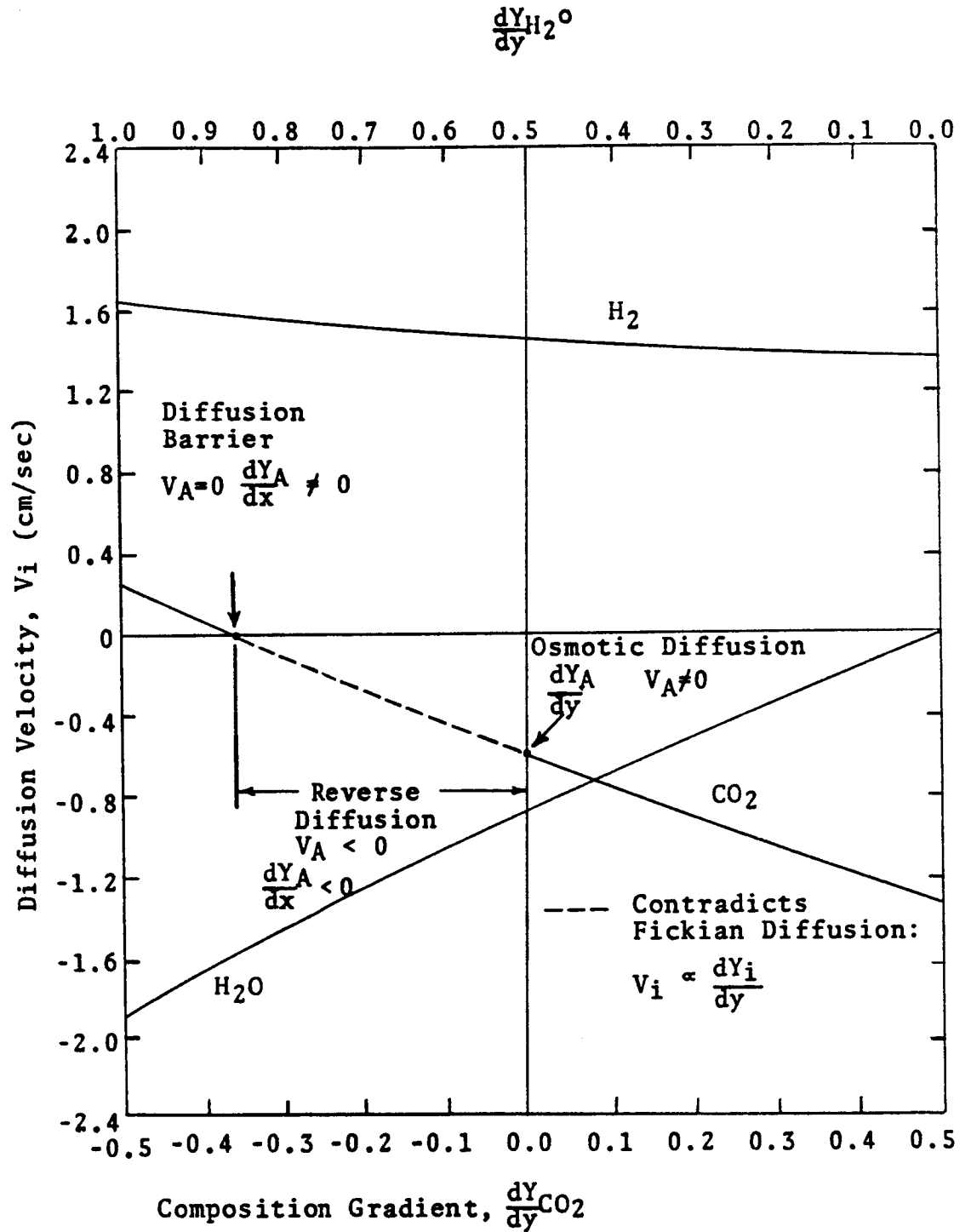


Figure 2.1. Diffusion Velocities as a Function of Mole Fraction Gradient (Ref. 2.35).

appear for CO_2 in the reverse diffusion region while the other coefficients would be positive. Since the binary diffusion approximation requires a common coefficient for all species, it is quite obvious that such an assumption is in contradiction to multicomponent behavior when reverse diffusion occurs.

Linearization of Diffusion Formulation. In recent papers by Toor (Ref. 2.37) and Cullinan (Ref. 2.38) it has been demonstrated that the species equations with mass fluxes expressed in the form of Equation 2.1, can be transformed in such a way that the equations become uncoupled in the diffusion terms. In matrix form, Equation 2.1 can be written:

$$\bar{J}_y = \frac{\rho}{M^2} \bar{D} \frac{\partial Y}{\partial y} \quad (2.30)$$

where

$$D_{ij} = M_i M_j D_{ij}$$

Toor and Cullihan demonstrated that a non-singular matrix, \bar{T} , exists, such that \bar{D} reduces to a diagonal matrix by the following transformation:

$$\bar{T}^{-1} \bar{D} \bar{T} = \begin{bmatrix} \tilde{D}_{11} & \bigcirc \\ \bigcirc & \tilde{D}_{\nu\nu} \end{bmatrix} \quad (2.31)$$

In this way the diffusion terms of the species equations can be decoupled by assuming that \tilde{D}_{i_i} is concentration independent. The latter assumption severely restricts the use of the Toor-Cullinan transformation to systems where concentration differences are relatively small.

Previous Analyses of Ablating Thermal Protection Systems With Radiation Coupling

There are four research groups that have reported stagnation line analyses which include mass injection of ablation products with radiation coupling. These investigators are: Rigdon, Dirling, and Thomas of the McDonnell Douglas Corporation (Refs. 2.15 and 2.48); Hoshizaki, Wilson, and Lasher of Lockheed Missiles and Space Company (Refs. 2.16, 2.49, and 2.50); Smith, Suttles, Sullivan, and Graves at NASA Langley Research Center (Ref. 2.14); and Chin, also at Lockheed (Ref. 2.51).

Rigdon, Dirling, and Thomas derived from the thin shock equations and subsequently solved the following viscous, stagnation-line, equations over the entire flowfield. The equation set solved was:

Continuity and X-Momentum:

$$\frac{d}{dy} \left(\mu \frac{d}{dy} \frac{1}{\rho} \frac{d(\rho v)}{dy} \right) - \rho v \frac{d}{dy} \left(\frac{1}{\rho} \frac{d(\rho v)}{dy} \right) + \frac{\rho}{2} \left(\frac{1}{\rho} \frac{d(\rho v)}{dy} \right)^2 + 2 \left(\frac{d^2 P}{dx^2} \right) = 0 \quad (2.32)$$

Y-Momentum

$$\frac{dP}{dy} = 0$$

Energy:

$$\rho v c_p \frac{dT}{dy} = \frac{d}{dy} \left(k \frac{dT}{dy} \right) - \frac{dq_R}{dy} \quad (2.33)$$

Species Continuity:

$$\rho v \frac{d\tilde{C}_A}{dy} - \frac{d}{dy} \rho \mathcal{D}_{12} \frac{d\tilde{C}_A}{dy} = 0 \quad (2.34)$$

where \tilde{C}_A is the total elemental concentration of ablation products.

In order to avoid the numerical difficulties which occur when initial value (marching) finite difference approximations are used with mass injection,* this group obtained solutions by beginning the integration of the conservation equations at the stagnation point and proceeding in both directions (toward the wall and toward the shock), and iterating until the boundary conditions at both the wall and shock were satisfied.

The binary diffusion coefficient, \mathcal{S}_{12} , used in Equation 2.34 was that of the C-N interaction. This choice was rather intuitive, but was based upon the fact that the ablation products (carbon-phenolic ablator) consists primarily of carbon while air is predominately nitrogen. It was reported that a posteriori analysis revealed that the choice of the binary diffusion was not critical in the prediction of wall heating rates. For this study, thermodynamic and transport properties of air were used for the injected gases.

The most recent study by Wilson (Ref. 2.16) involves an inviscid analysis of the ablation layer

*This difficulty is discussed by Rigdon in Reference 2.48 and has been encountered by several other investigators (Refs. 2.14, 2.16, 2.39, 2.41, and 2.43). The difficulties originate from trying to maintain numerical precision when taking small differences between numbers of the same size.

coupled with a viscous analysis of the air layer. In Figure 2.2 the regions of viscous and inviscid flow are graphically illustrated and compared to the assumptions employed by the other investigators. The equations governing the inviscid region are equivalent to those employed by Rigdon, Dirling, and Thomas (Ref. 2.15), with the coefficients of diffusion, viscosity, and thermal conductivity set equal to zero. The following equations correspond to the transformed equations used by Wilson in the ablation layer:

Continuity and X-Momentum:

$$\rho f \frac{d}{dy} \left(\frac{1}{\rho} \frac{d(\rho v)}{dy} \right) = \frac{\rho}{2} \frac{1}{\rho} \left(\frac{d(\rho v)}{dy} \right)^2 + 2 \frac{d^2 P}{dx^2} \quad (2.35)$$

Y-Momentum:

$$\frac{dP}{dy} = 0 \quad (2.36)$$

Energy:

$$\rho v \frac{dH}{dy} = - \frac{dq_R}{dy} \quad (2.37)$$

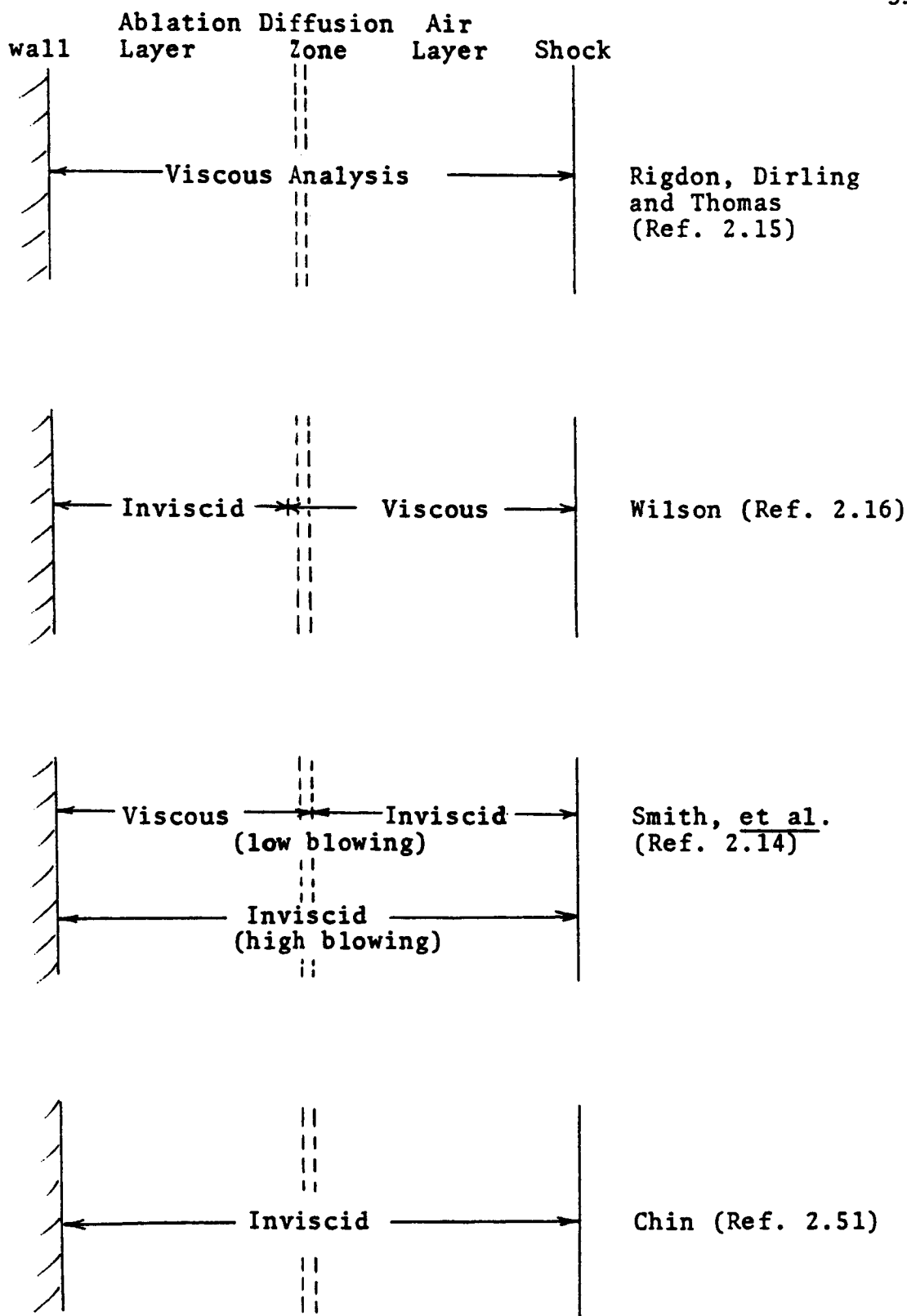


Figure 2.2. Comparison of Radiation Coupled Stagnation Line Analyses with Mass Injection of Ablation Products.

Species Continuity:

$$\frac{d\tilde{C}_A}{dy} = 0 \quad (2.38)$$

In this viscous region, the following equations were transformed and solved:

Continuity and X-Momentum:

$$\begin{aligned} \frac{d}{dy} \left(\mu \frac{d}{dy} \left(\frac{1}{\rho} \frac{d(\rho v)}{dy} \right) \right) - \rho v \frac{d}{dy} \left(\frac{1}{\rho} \frac{d(\rho v)}{dy} \right) \\ + \frac{\rho}{2} \left(\frac{1}{\rho} \frac{d(\rho v)}{dy} \right)^2 + 2 \left(\frac{d^2 P}{dx^2} \right) = 0 \end{aligned} \quad (2.39)$$

Y-Momentum:

$$\frac{dP}{dy} = 0 \quad (2.40)$$

Energy:

$$\rho v \frac{dH}{dy} = \frac{d}{dy} \left(\frac{\mu}{Pr} \frac{dH}{dy} \right) - \frac{dq_R}{dy} \quad (2.41)$$

Species Continuity:

$$\rho v \frac{d\tilde{C}_A}{dy} - \frac{d}{dy} \left(\rho \mathcal{Q}_{12} \frac{d\tilde{C}_A}{dy} \right) = 0 \quad (2.42)$$

In transforming the viscous momentum equation (Eq. 2.39) to the final form required for solution, the assumption was made that the $\rho\mu$ product was constant. Although this assumption resulted in errors as high as 25% (Ref. 2.55) in the velocity profile when compared to a more rigorous solution, no assessment was made of its effects upon a coupled solution. The choice of the binary diffusion coefficient as used in Equation 2.42 was not reported. However, it was stated that the N_2-N interaction was used for the flux term in the prediction of total thermal conductivity (See Appendix A).

Wilson obtained numerical solutions by assuming enthalpy and velocity profiles and performing a forward integration from the wall to the shock, excluding the viscous terms in the ablation layer and including them in the air layer. This procedure was repeated until convergence of the velocity and enthalpy profiles was achieved. The analyses performed included thermodynamic properties of ablation products, but apparently did not include the transport properties of the same species.*

*Wilson's discussion of transport properties is somewhat vague, but includes only references and discussion of air transport data.

The analysis by Smith, et al. (Ref. 2.14) was accomplished by assuming a viscous ablation products region and an inviscid air layer. In this analysis, it was assumed the radiation between the ablation and air layers was uncoupled. For low blowing, the ablation layer was represented by the following equations:*

Continuity:

$$2 \frac{du}{dx} = - \frac{1}{\rho} \frac{d(\rho v)}{dy} \quad (2.43)$$

x-Momentum:

$$\begin{aligned} \rho v \frac{d}{dy} \left(\frac{du}{dx} \right) - \frac{d}{dy} \left(\mu \frac{d}{dy} \left(\frac{du}{dx} \right) \right) \\ + \rho \left(\frac{du}{dx} \right)^2 + \frac{d^2 P}{dx^2} = 0 \end{aligned} \quad (2.44)$$

y-Momentum:

$$\frac{dP}{dy} = 0 \quad (2.45)$$

Energy:

$$\rho v \frac{dH}{dy} = \frac{d}{dy} \left(\frac{\mu}{Pr} \frac{dH}{dy} \right) - \frac{dq_R}{dy} \quad (2.46)$$

*These equations are the untransformed equivalents to the final forms employed in the analysis by Smith, et al., (Ref. 2.14). As with the previous discussion of Wilson's study (Ref. 2.16), the equations are presented in this form for comparative purposes.

Elemental Continuity:

$$\rho v \frac{d\tilde{C}_j}{dy} - \frac{d}{dy} \rho \sum_{12} \frac{d\tilde{C}_j}{dy} \quad j = 1, 2, \dots, \quad (2.47)$$

The characteristics of the inviscid air layer were determined by the same set of equations, neglecting the viscous terms as in Equations 2.35 to 2.38.

For large blowing it was assumed that the ablation layer was a region of constant shear and negligible conduction. The elemental compositions were then computed by assuming a cubic relationship in a narrow region between air and ablation layer. With the exception of allowing for an elemental mixing zone, these assumptions result in a completely inviscid analysis for the case of large blowing.* The numerical technique employed in this analysis was a one strip integral technique developed by Suttles in Reference 2.52.

Chin (Ref. 2.51) assumed the entire flowfield to be inviscid with a discontinuous (step function) composition interface between the ablation layer and air

*The mass injection cases reported in Reference 2.14 were apparently solved in this manner.

layer. The equations employed for this study were equivalent to those used by Wilson (Ref. 2.16) and Smith, et al. (Ref. 2.14) for their inviscid regions of analysis. Unlike the analysis of Smith, et al. (Ref. 2.14) the radiative coupling between the ablation and air layers was included. By obtaining solutions in each layer separately while lagging on the solution for the other layer, a fully coupled radiation analysis was obtained.

In a recent study by Page, et al. (Ref. 2.53) of radiation coupled stagnation flow (without mass injection), a comparison was made between their results and those of several other investigators. The comparison included both inviscid and viscous analyses. As shown in Figure 2.3, the results of these investigations are in reasonable agreement. The cases reported by Smith, et al. (Ref. 2.14) all included mass injection and therefore cannot be compared in Figure 2.3. However, comparisons to the results of Chin (Ref. 2.51) and Rigdon, Dirling, and Thomas (Ref. 2.48) were reported in Reference 2.14. For these cases, considerable disagreement in wall heating rates were found (33% and 20% respectively). This discrepancy is most likely due to the fact that the radiation analysis of Smith, et al. does not include line radiation from C and H, both of which are included

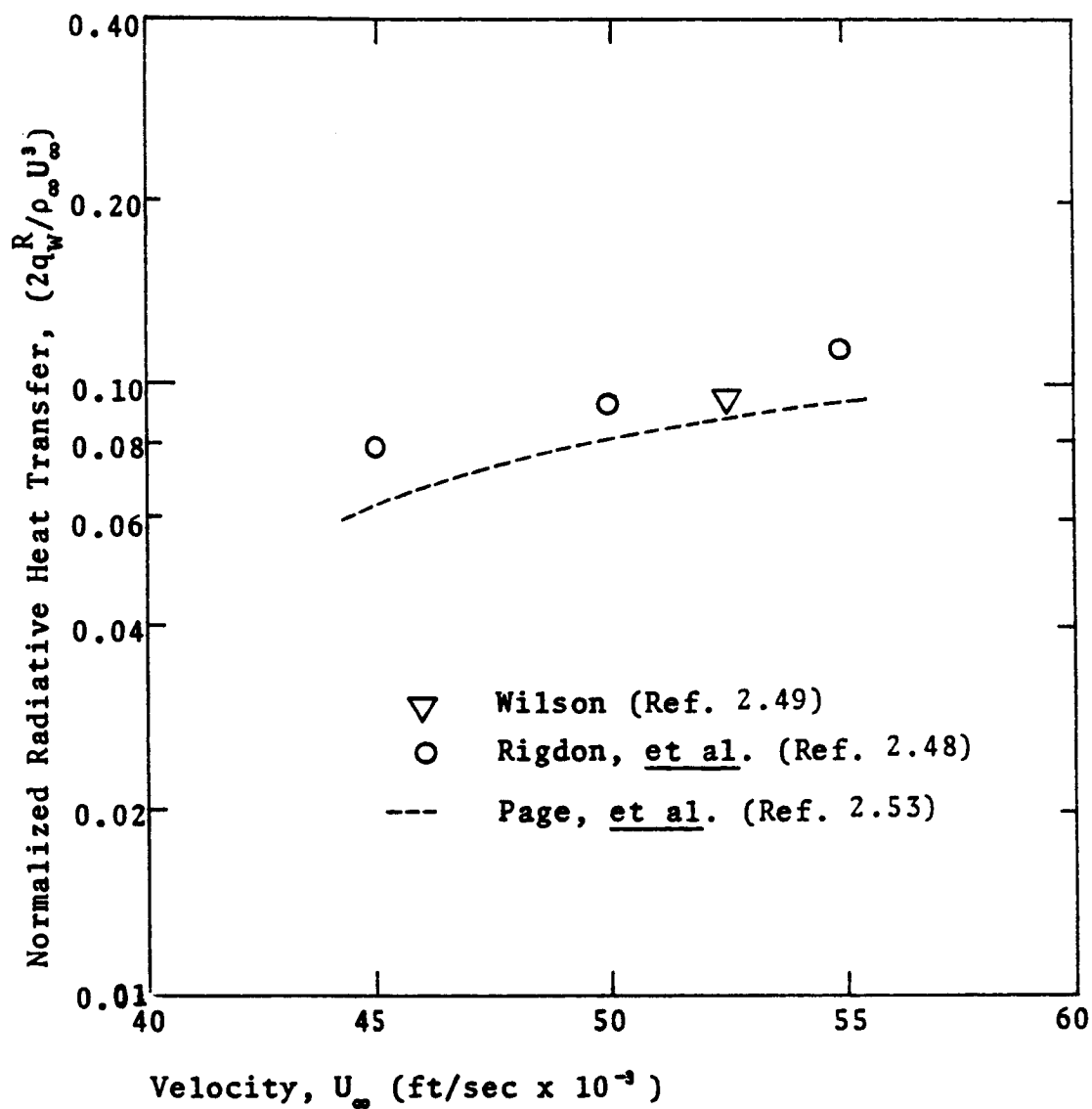


Figure 2.3. Comparison of Dimensionless Radiative Heating Rates ($P_s = 1.0$ atm., $R = 9$ ft.)

2

in the analyses of Rigdon, et al. (Ref. 2.48), Wilson (Ref. 2.16), Chin (Ref. 2.51), as well as the current study.

Numerical Multicomponent Diffusion Analyses
Related to the Study of Ablating Thermal
Protection Systems

Relatively few of the studies pertaining to stagnation region heating shields have included multicomponent diffusion effects. A summary of these investigations is given in Table 2.1. Until recently no comparisons between the binary and the multicomponent analyses have been reported. In the past year, the results of two such investigations have been published (Refs. 2.29, 2.43 and 2.44).

In the analysis of Davy, Craig and Lyle (Ref. 2.43), coupled solutions of the transport equations were obtained using both the binary assumption and the Stefan-Maxwell equations to represent the diffusive mass fluxes. Their results confirmed the previously discussed hypothesis that systems of similar molecules would be well represented by the binary approximation. However, for a system containing H_2 , N_2 , H , and NH_3 , the binary approximation gave species profiles which were substantially in error. A general conclusion of this investigation was that a multicomponent solution is required for analyses

TABLE 2.1
A SUMMARY OF RELATED STUDIES WHICH INCLUDE MULTICOMPONENT DIFFUSION

Investigator(s)	System	Diffusion Analysis	Numerical Method
Libby and Pierucci, 1964 (Ref. 2.39)	O ₂ , H ₂ , H ₂ O and N ₂	Multicomponent Diffusion Coefficients (Eq. 2.4)	Initial Value With Kutta- Runga-Gil Integration Method
Blotner, 1970 (Ref. 2.54)	N, O, N ₂ , O ₂ , NO and NO ⁺	Multicomponent Diffusion Coefficients	Implicit Two. Point Boundary Value Formulation
Nachtsheim, 1967 (Ref. 2.41)	O ₂ , H ₂ , H ₂ O, OH, H, O	Stefan-Maxwell Equations (Eq. 2.5)	Initial Value With Runga- Kutta Startup and Adams- Moulton Continuation
Davy, Craig, and Lyle, 1969 (Ref. 2.43)	(1) NH ₃ , H ₂ , H, and N ₂ (2) Ar, H ₂ , H, and N ₂ (3) H ₂ O, H ₂ , H, OH, N ₂ , NO, O ₂ , and O	Stefan-Maxwell Equations	

TABLE 2.1 (continued)

Investigator(s)	System	Diffusion Analysis	Numerical Method
Graves, 1970* (Ref. 2.29)	O ₂ , H ₂ , H ₂ O, and N ₂	Stefan-Maxwell Equations	Implicit Two Point Boundary Value Formulation
Present Investigation	O ₂ , N ₂ , O, N, O ⁺ , N ⁺ , e ⁻ , H, H ₂ , CO, C ₂ , C ₃ , CN, C ₂ H, C ₂ H ₂ , C ₃ H, C ₄ H, HCN, C ⁺	Exact Effective Diffusion Co- efficients Obtained From Stefan-Maxwell Equations	Implicit Two Point Boundary Value Formulation

*Couette flow, $\rho v = \text{constant}$.

in which accurate species profiles and local temperatures are important.

The studies by Graves (Ref. 2.29 and 2.44) are perhaps the most valuable with respect to the current investigation. In his analysis of Couette flow with four components, Graves compared three diffusion models: the binary assumption, the bifurcation approximation, and the Stefan-Maxwell equations. In conjunction with the binary assumption, a comparison of three methods of estimating a representative diffusion coefficient was also given. The most accurate method for estimating the characteristic binary diffusion coefficient is given as follows:*

$$D_{12} = 26.28 \times 10^{-4} \frac{T^{3/2} v}{P} \frac{Y_i}{\sum_{i=1} \sqrt{M_i \sigma_i^2 \Omega_{ii}^{(1,1)}}} \text{ cm}^2/\text{sec} \quad (2.32)$$

However, the binary model using a diffusion coefficient predicted by this equation gave at best, only a "fair" approximation to the rigorous solution. As mentioned in the previous discussion of the bifurcation approximation, the results of the Graves study indicated that the latter approximation gave essentially the same

*An empirical modification of Equation 2.3.

results as the multicomponent diffusion model. It should be pointed out, however, that for the system studied the diffusion factors, F_i (See Equation 2.33), give excellent agreement with the theoretical values of Δ_{ij} , the maximum error being 2.44%. As shown by Kendall in Reference 2.25, such agreement is certainly not typical since errors as high as 46% were reported.

With the exception of Graves' analysis (Ref. 2.29), all of the previous related studies involving multicomponent diffusion are limited to low mass injection rates, of approximately 1.5% of the free stream mass flux. As previously mentioned, this limitation is characteristic of initial value formulations of problems involving mass injection. The implicit formulation employed in the current study and in the Couette flow study by Graves is not subject to this limitation. Further discussion of these implicit formulations will be included in Chapter V.

Coupled Analyses of the Effects of Transport and Thermodynamic Properties

A survey of the literature revealed only two investigations into the effects of uncertainties in transport and thermodynamic properties upon convective

and radiative heating of ablating heat shields. In a study by Howe and Sheaffer (Ref. 2.45), the effect of uncertainties in the thermal conductivity of air on convective heating was examined. Comparing the thermal conductivity models employed by Hansen (Ref. 2.46) and Yos (Ref. 2.47), Howe and Sheaffer found the differences in convective heating to be negligible. However, the resulting temperature profiles were in disagreement by as much as 20%. Such a difference in temperature could greatly effect radiant heating predictions.

Rigdon, Dirling, and Thomas (Ref. 2.15) performed coupled analyses with mass injection of ablation products (carbon phenolic ablator) to determine the effect of using air properties for the ablation products. A comparison of the ratio of these properties is shown in Figure 2.4. The results of their analysis showing the behavior of the radiative flux toward the wall as a function of assumed thermodynamic and transport properties is shown in Figure 2.5. These results indicate that the change in density and heat capacity substantially modified the radiative energy transport in the ablation layer. This phenomena was attributed to the increased absorption (because of the increase in heat capacity) by the injected gases. The negligible effect of the addition of the more

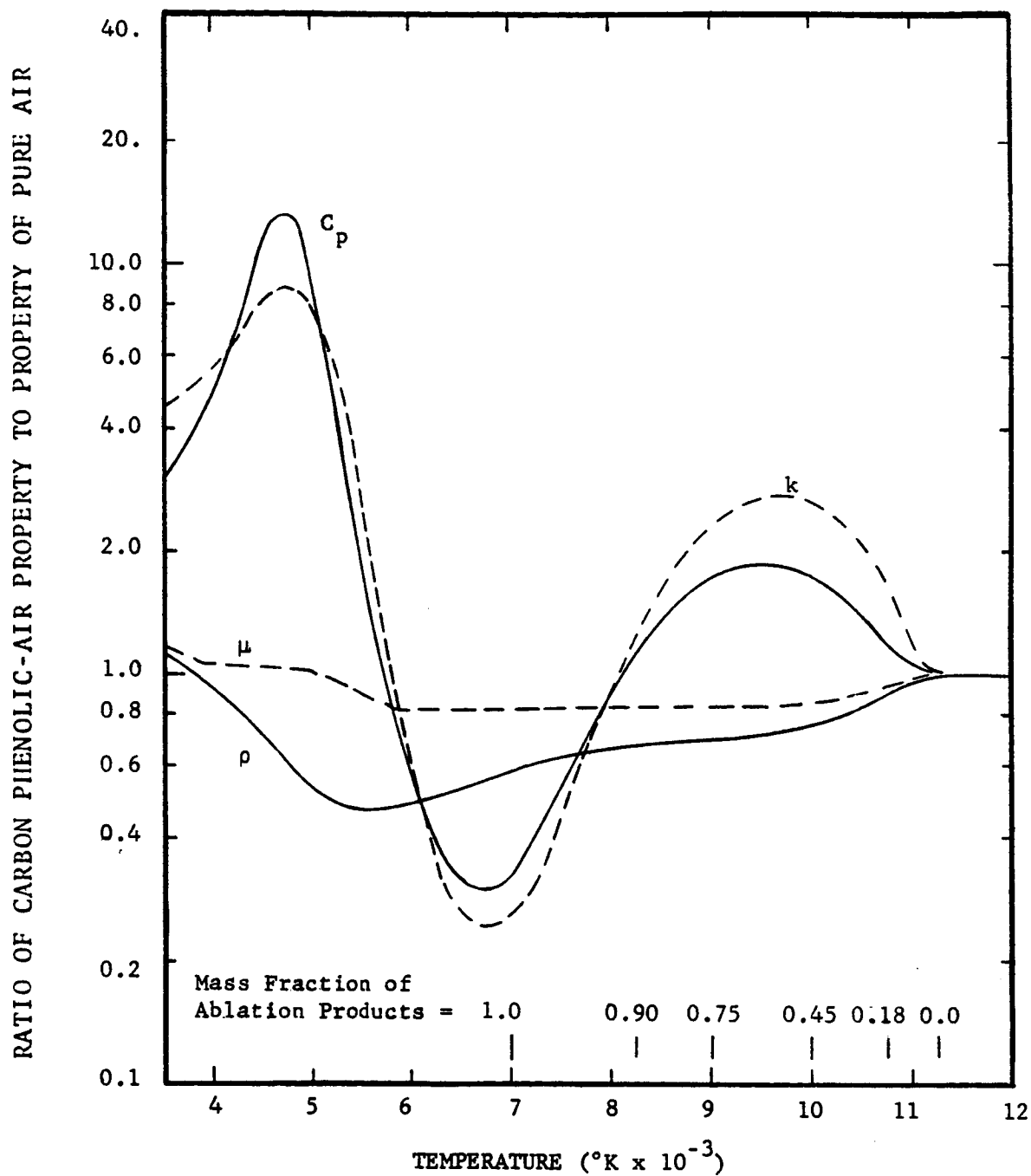


Figure 2.4. Comparison of Properties of Air and Carbon Phenolic-Air Mixture (Ref. 2.15).

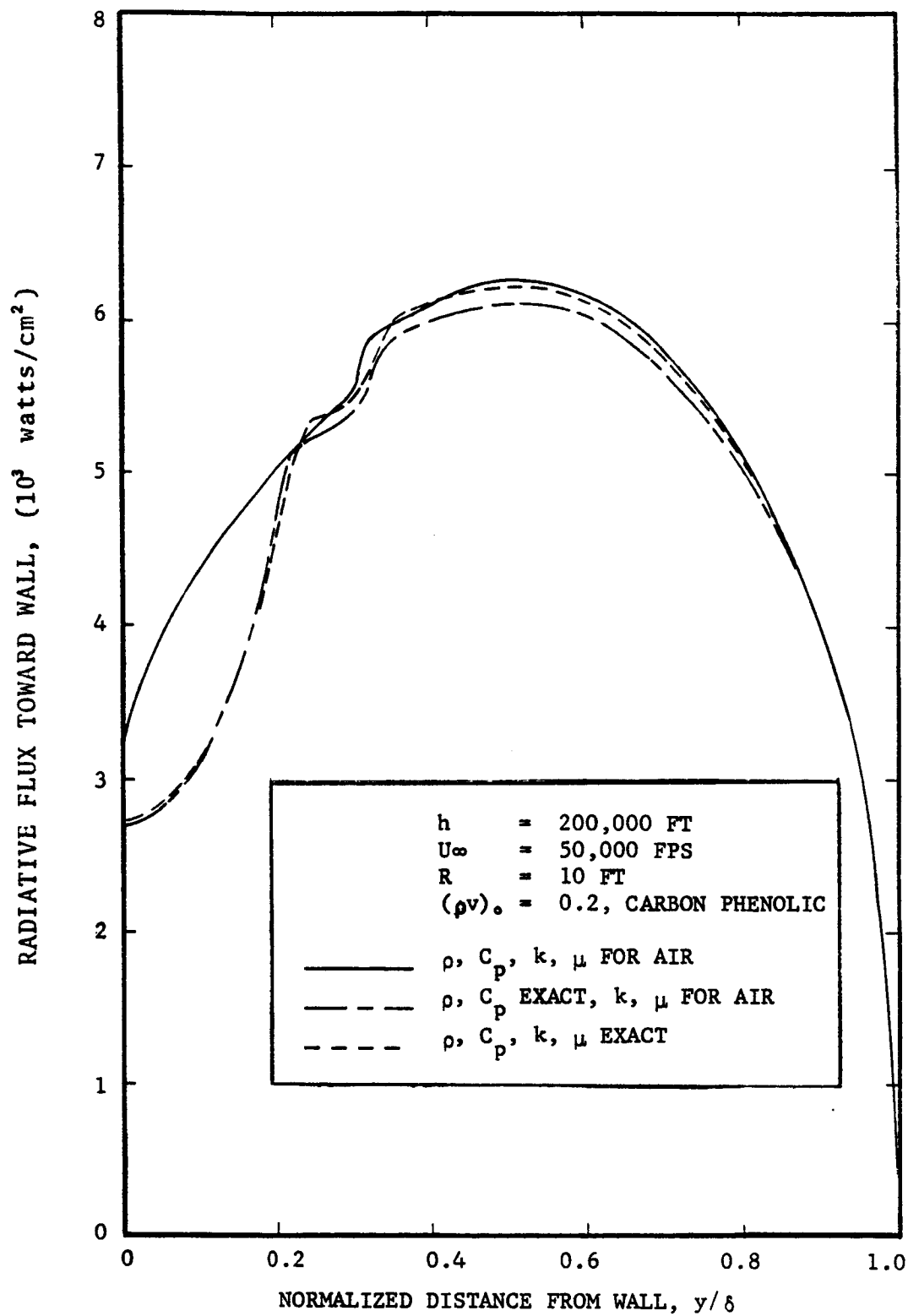


FIGURE 2.5. Effect of Thermodynamic and Transport Properties on the Radiative Flux Toward the Wall.

accurate thermal conductivity was accounted for by the fact that the contribution of this variable is confined to a relatively narrow region around the stagnation point.*

Summary

In this chapter an attempt has been made to perform a detailed survey of the previous work associated with diffusion analyses of multicomponent systems. A survey has been performed of previous investigations into the effects of variations in transport and thermodynamic properties. The primary objective of this review has been that of making an assessment of the relative importance of an exact multicomponent analysis as opposed to approximate methods. Particular emphasis has been given to assessing the reliability of the binary diffusion approximation which has been employed (almost without question) by several major investigators of the blunt-body problem (Refs. 2.13-2.17). From this review it is clear that substantial errors can be introduced in calculations of radiation flowfields through the use of simplified diffusion models. Upon examining the

*This region was referred to as the diffusion zone in Figures 1.2 and 1.3.

currently existing radiation coupled analyses of ablating thermal protection systems, it was found that at best some investigators assume binary diffusion while others neglect diffusion effects entirely.

It was further noted in the review of current radiation heat shield analyses that as a matter of convenience some investigators have assumed the transport properties of air for the ablation layer. Others dispose of the problem entirely by assuming inviscid flow which eliminates all terms containing the transport coefficients. The results of a single study by Rigdon, et al. (Ref. 2.15) suggest that while the proper thermodynamic properties may be important, the differences in transport properties may be of little consequence.

In summary, existing analyses of radiation heating of charring ablators contain several assumptions relating to the transport and thermodynamic properties which have not been thoroughly investigated. As a result, vital questions remain unanswered in the accurate design of ablative thermal protection systems. The major question to be answered by the current study is, "How important are accurate transport and thermodynamic properties in the prediction of radiative heating of

charring ablators?" In conjunction with this question, how accurate is a binary diffusion approximation? When are transport (viscous) effects important?

The objectives of this research are to answer these questions by performing theoretical analyses with and without the effects under question, and to thus obtain quantitative estimates of their importance. In so doing, this work will improve the reliability of the results obtained by currently existing analyses and will yield a more thorough understanding of the problems which must be solved in order to obtain more accuracy in the design of ablative thermal protection systems.

REFERENCES

- 2.1. Chapman, S. and T. G. Cowling, The Mathematical Theory of Non-Uniform Gases, Cambridge, England: Cambridge University Press, 1960.
- 2.2. Maxwell, J. C., "On the Dynamical Theory of Gases," Phil. Trans. Roy. Soc., Vol. 157 (1867), p. 49 f., (Referenced in Chapman and Cowling, op. cit.).
- 2.3. Boltzmann, L., "Further Studies on the Thermal Equilibrium Among Gas-molecules," Wren. Ber., Vol. 66, 1872, p. 275 f., (Referenced in Chapman op. cit.).
- 2.4. Chapman, S., "On the Law of Distribution of Velocities, and on the Theory of Viscosity and Thermal Conduction, in a Non-uniform Simple Monatomic Gas," Phil. Trans. Roy Soc. A., Vol. 216 (1916), p. 279 f., (Referenced in Chapman and Cowling, op. cit.).
- 2.5. Enskog, D., "The Kinetic Theory of Phenomena in Fairly Rare Gases," Dissertation, Upsala, 1917 (Referenced in Chapman and Cowling, op. cit.).
- 2.6. Hellund, F. J., Phys. Rev., Vol. 57 (1940), p. 319 (Referenced in Chapman and Cowling, op. cit.).
- 2.7. Curtiss, C. F. and J. O. Hirschfelder, "Transport Properties of Multicomponent Gas Mixtures," Journal of Chem. Phys., Vol. 17, No. 6 (June, 1949), pp. 550-555.
- 2.8. Hirschfelder, J. O., C. F. Curtiss and R. B. Bird, Molecular Theory of Gases and Liquids, New York: John Wiley and Sons, Inc., 1967.
- 2.9. Bird, R. B., W. E. Stewart, and E. N. Lightfoot Transport Phenomena, New York: John Wiley and Sons, Inc., 1966.

- 2.10. Toor, H. L., "Reference Frames in Diffusion," AICHE Journal, Vol. 8, (1962), p. 561.
- 2.11. Frank-Kamenetskii, D. A., Diffusion and Heat Transfer in Chemical Kinetics, New York: Plenum Press, 1969.
- 2.12. Stefan, J., Sitzber, Akad. Wiss. Wien., 65 (Abt. III), 323 (1872), Referenced in H. L. Toor, "Diffusion in Three-Component Gas Mixtures," AICHE Journal, (June 1957), pp. 198-207.
- 2.13. Lees, L., "Convective Heat Transfer with Mass Addition and Chemical Reactions," presented at Third Combustion and Propulsion Colloquium, AGARD, NATO, Palermo, Italy, March 17-21, 1958.
- 2.14. Smith, G. L., J. T. Suttles, E. M. Sullivan, and R. A. Graves, Jr., "Viscous Radiating Flow Field on An Ablating Blunt Body," AIAA Paper No. 70-218 presented at AIAA 8th Aerospace Sciences Meeting, New York, (January 19-21, 1970).
- 2.15. Rigdon, W. S., R. B. Dirling, and M. Thomas, "Stagnation Point Heat Transfer During Hypervelocity Atmospheric Entry," NASA CR-1462, (February, 1970).
- 2.16. Wilson, K. H., "Stagnation Point Analysis of Coupled Viscous-Radiating Flow with Massive Blowing," NASA CR-1548, (June, 1970).
- 2.17. Davis, R. T., "Hypersonic Flow of a Chemically Reacting Binary Mixture Past a Blunt Body," AIAA Paper No. 70-805 presented at AIAA 3rd Fluid and Plasma Dynamics Conference, Los Angeles, (June 29-July 1, 1970).
- 2.18. Wilke, C. R., "Diffusional Properties of Multicomponent Gases," CEP, Vol. 46, No. 2, (February, 1950).
- 2.19. Tirskii, G. A., "Analysis of the Chemical Composition of the Laminar Multicomponent Boundary Layer on the Surface of Hot Plastics," Trans. from Kosmicheskie Issledovaniya, Vol. 2, No. 4, (July-August, 1964), pp. 570-594.

- 2.20. Tirskii, G. A., "Calculating the Effective Diffusion Coefficients in a Laminar Dissociated Multicomponent Boundary Layer," PPM, Vol. 33, No. 1, (1969), pp. 180-192.
- 2.21. Tirskii, G. A., "Method of Successive Approximations for the Integration of Equations of a Laminar Multicomponent Boundary Layer with Chemical Reactions Including Ionization," NASA TT F-13, 379, N71-11532, (November, 1970).
- 2.22. Fairbanks, D. F., and C. R. Wilke, "Diffusion Coefficients in Multicomponent Gas Mixtures," Ind. Eng. Chem., Vol. 42, (March, 1950), pp. 471-475.
- 2.23. Bird, R. B., "Diffusion in Multicomponent Gas Mixtures," NASA TT-F-10, 925.
- 2.24. Bartlett, E. P., R. M. Kendall, and R. A. Rindal, "An Analysis of the Coupled Chemically Reacting Boundary Layer and Charring Ablator, Part IV," NASA CR-1063, (1968).
- 2.25. Engel, C. D., D. D. Esch, R. C. Farmer, and R. W. Pike, "Formulation, Derivation and Development of the Analysis of the Interaction of Ablating Protection Systems and Stagnation Region Heating," NASA CR-66931 (January 1, 1970).
- 2.26. Gomez, A. V. and A. F. Mills, "Multicomponent, Foreign Species Injection, Heat Transfer, Skin Friction, and Mass Transfer Correlations for the Hypersonic, Laminar Boundary Layer in the Stagnation Region Including Chemical Reactions," TRW Proj. Rept. TASK E-45B, (June, 1969).
- 2.27. Kunth, E. L., "Multicomponent Diffusion and Fick's Law," Phys. Fluids, Vol. 2, no. 3, (May-June, 1959), pp. 339-340.
- 2.28. Bartlett, E. P. and R. D. Grose, "An Evaluation of a Transfer Coefficient Approach for Unequal Diffusion Coefficients," AIAA Journal, Vol. 8, No. 6, (June, 1970), pp. 1146-47.

- 2.29. Graves, R. A., Jr., "Diffusion Model Study in Chemically Reacting Air Couette Flow with Hydrogen Injection," NASA TR R-349, (October, 1970).
- 2.30. Sherwood, T. K., Absorption and Extraction, McGraw-Hill Book Company, Inc., New York, (1949).
- 2.31. Hoopes, J. W., Jr., Ph.D. Thesis, Columbia Univ., New York, (1951), Referenced in Toors, H. L., "Diffusion in Three-component Gas Mixtures," AIChE Journal, Vol. 3, No. 2, (June, 1957), pp. 198-207.
- 2.32. Benedict, Manson, and A. Boas, "Separation of Gas Mixtures by Mass Diffusion," Chem. Engr. Prog., Vol. 47, No. 51 (1951), pp. 111-122.
- 2.33. Cichelli, M. T., U. D. Weatherford, Jr., and J. R. Bowman, "Sweep Diffusion Gas Separation Process," Chem. Engr. Prog., Vol. 47, No. 63 (1951), pp. 123-133.
- 2.34. Keyes, J. J., Jr. and R. L. Pigford, Chem. Engr. Sci., Vol. 6, (1957), p. 215 f., Referenced in Hsu, H. and R. B. Bird, "Multicomponent Diffusion Problems," AIChE Journal, Vol. 6, No. 3, (September, 1960), pp. 516-524.
- 2.35. Toor, H. L., "Diffusion in Three-Component Gas Mixtures," AIChE Journal, Vol. 3, No. 2, (June, 1957), pp. 198-207.
- 2.36. Hsu, H. and R. B. Bird, "Multicomponent Diffusion Problems," AIChE Journal, Vol. 6, No. 3, (September, 1960), pp. 516-524.
- 2.37. Toor, H. L., "Solution of the Linearized Equations of Multicomponent Mass Transfer: II Matrix Methods," AIChE Journal, Vol. 10, No. 4, (July, 1964), pp. 460-465.
- 2.38. Cullinan, H. T., Jr., "Analysis of the Flux Equations of Multicomponent Diffusion," I. & E. C. Fund., Vol. 4, No. 2, (May, 1965), pp. 133-139).

- 2.39. Libby, P. A. and M. Pierucci, "Laminary Boundary Layer with Hydrogen Injection Including Multi-component Diffusion," AIAA Journal, Vol. 2, No. 12, (December, 1964), pp. 2118-2126.
- 2.40. Scala, M. S. and L. M. Gilbert, "Sublimation of Graphite at Hypersonic Speeds," AIAA Journal, Vol. 3, No. 9, (September, 1965), pp. 1635-1643.
- 2.41. Nachtsheim, P. R., "Multicomponent Diffusion in Chemically Reacting Laminar Boundary Layers," Proceedings Heat Transfer and Fluid Mechanics Institute, Stanford Univ. Press (1967).
- 2.42. Blottner, F. G., "Viscous Shock Layer at the Stagnation Point with Nonequilibrium Air Chemistry," AIAA Journal, Vol. 7, No. 12, (December, 1969), pp. 2281-2288.
- 2.43. Davy, W. C., R. A. Craig and G. C. Lyle, "An Evaluation of Approximations Used in the Analysis of Chemically Reacting, Stagnation Point Boundary Layers with Wall Injection," in Proceedings of the 1970 Heat Transfer and Fluid Mechanics Institute, ed. by Turgut Sarpkaya, (Stanford University Press: Stanford, California), 1970, p. 222-237.
- 2.44. Graves, Randolph A., Jr., "Chemically Reacting Couette Flow With Hydrogen Injection for Two Diffusion Models," M.S. Thesis, Virginia Polytech. Inst., 1969.
- 2.45. Howe, J. T. and Y. S. Sheaffer, "The Effects of Uncertainties in the Thermal Conductivity of Air on Convective Heat Transfer for Stagnation Temperatures up to 30,000°K," NASA TN D-2678, (February, 1965).
- 2.46. Hansen, C. F., "Approximations for the Thermodynamic and Transport Properties of High-Temperature Air," NASA TR R-50, (1959).
- 2.47. Yos, J. M., "Transport Properties of Nitrogen, Hydrogen, Oxygen, and Air to 30,000°K," AVCO Corp., RAD-TM-63-7 (March, 1963), AD-435053.

- 2.48. Rigdon, W. S., R. B. Dirling, Jr. and M. Thomas, "Radiative and Convective Heating During Atmospheric Entry," NASA C12-1170 (September, 1968).
- 2.49. Wilson, K. H. and H. Hoshizaki, "Effect of Ablation Product Absorption and Line Transitions on Shock Layer Radiative Transport," NASA CR-1264 (February, 1969).
- 2.50. Hoshizaki, H. and L. E. Lasher, "Convective and Radiative Heat Transfer to an Ablating Body," AIAA, Vol. 6 (1968), p. 1441-1449.
- 2.51. Chin, J. H., "Radiation Transport for Stagnation Flow Including the Effects of Lines and Ablation Layer," AIAA Paper No. 68-644, (June, 1968).
- 2.52. Suttles, John T., "A Method of Integral Relations Solution for Radiating Non-Adiabatic Inviscid Flow Over a Blunt Body," NASA TN D-5480.
- 2.53. Page, W. A., et al., "Radiative Transport in Inviscid Nonadiabatic Stagnation-Region Shock Layers," AIAA Paper No. 68-784, AIAA 3rd Thermophysics Conference, June 1968.
- 2.54. Blottner, F. G., "Finite Difference Methods of Solution of the Boundary-Layer Equations," AIAA Journal, Vol. 8, No. 2 (February, 1970), pp. 193-205.
- 2.55. Engel, C. D. and R. C. Farmer, "Stagnation Line Momentum and Energy Equations," Louisiana State University, NASA-RFL-TR 70-2 (September, 1970).

CHAPTER III

DEVELOPMENT OF EQUATIONS FOR A STAGNATION REGION FLOWFIELD ANALYSIS

Introduction

It is the purpose of this chapter to present and develop the necessary equations describing the multicomponent, reacting and radiating flowfield encountered in the aerodynamic heating of ablating, blunt bodies. A detailed development of the governing flowfield equations is presented in Reference 3.1. The development in this reference is a complete derivation of the thin shock layer equations from general transport equations and includes intermediate formulations of varying degrees of rigor. At each stage of the development, the inherent assumptions are indicated so that a logical selection of the appropriate equations can be made.

The following criteria have been established for use in selecting the proper equations for the purposes of this study.

1. Since the most severe heating occurs at and near the leading edge, or stagnation region, of the vehicle special attention should be given to the representation of the flowfield in this vicinity.

2. The equations selected should yield an accurate representation of the flowfield behavior for the body radius and flight conditions selected.

3. The equations must be coupled properly to the surface boundary conditions and must be valid for both large and small mass injection rates.

4. Enough rigor must be maintained such that the effects of diffusion can be properly assessed.

On the basis of these criteria the first order stagnation line, shock layer equations given in Reference 3.1 were selected and will be presented in the following development.

Following the presentation of the stagnation line shock layer equations, several modifications required for each equation will be separately performed and discussed. Subsequently, an analysis of the required boundary conditions for the flowfield equations will be given. Particular emphasis will be directed to the formulation of the surface boundary conditions through which the ablator and flowfield are coupled. The development of the necessary equations will then be concluded by a Dorodnitsyn transformation of the final system of equations to reduce density effects and to place them in final form for a computer solution.

Stagnation Line Thin Shock Equations

A frequently employed simplification in the formulation of hypersonic flow problems is the thin shock layer assumption (Refs. 3.2, 3.7-3.9, 3.13). This assumption implies that the thickness (δ) of the shock layer (the region between the body and shock wave) is much less than the radius of curvature (R) of the adjacent surface. In specific terms, this condition is expressed as,

$$\frac{\delta}{R} \ll 1 \quad (3.1)$$

For hypersonic flow, it has been shown that the ratio given in Equation 3.1 is of the same order of magnitude as the density ratio across the shock wave, $\bar{\rho}$, (Ref. 3.13). Further, it has been shown that for $Re \geq 100$,* $\bar{\rho}$ will be of order 0.1 or less. For the flight conditions of interest in the current investigation Reynold's numbers of approximately 10^4 are expected; therefore, the thin shock layer assumption is applicable for the present study.

*The Reynolds number employed here is based upon the freestream density and velocity, the body radius, and the viscosity on the body side of the shock wave. For typical entry conditions of $U_\infty \approx 50,000$ fps, $\rho_\infty \approx 10^{-5}$ lb/ft³ and $R = 1.0$ ft., a value of $T_s \approx 15,000$ is obtained therefore $\mu_s \approx 10^{-4}$ lb_m/ft^m-sec, and $Re_s \approx 5 \times 10^3$.

Assuming a thin shock layer, an order analysis of the general conservation equations, neglecting all terms less than the order of $\bar{\rho}$, yields the following equations (Refs. 3.1, 3.2, and 3.13):

Global Continuity:

$$\frac{\partial}{\partial x} (\rho r^A u) + \frac{\partial}{\partial y} (\rho \tilde{\kappa} r^A v) = 0 \quad (3.2)$$

Species Continuity:

$$\frac{\partial}{\partial x} (r^A \rho C_i u) + \frac{\partial}{\partial y} (\tilde{\kappa} r^A \rho C_i v) = - \frac{\partial}{\partial y} (\tilde{\kappa} r^A J_{i,\gamma}) + \tilde{\kappa} r^A \omega_i \quad (3.3)$$

x-Momentum:

$$\rho r^A u \frac{\partial u}{\partial x} + \rho \tilde{\kappa} r^A v \frac{\partial u}{\partial y} = - r^A \frac{\partial P}{\partial x} + \frac{\partial}{\partial y} \left[\tilde{\kappa} r^A \mu \frac{\partial u}{\partial y} \right] \quad (3.4)$$

y-Momentum:

$$\rho \kappa u^2 = \tilde{\kappa} \frac{\partial P}{\partial y} \quad (3.5)$$

Energy:

$$\begin{aligned} r^A \rho u \frac{\partial H}{\partial x} + \tilde{\kappa} r^A \rho v \frac{\partial H}{\partial y} = \frac{\partial}{\partial y} \left(\tilde{\kappa} r^A k_f \frac{\partial T}{\partial y} \right) - \frac{\partial}{\partial y} (\tilde{\kappa} r^A [h_i J_{i,y}]) \\ - \tilde{\kappa} r^A \frac{\partial q_{R,y}^*}{\partial y} + \frac{\partial}{\partial y} \left(\tilde{\kappa} r^A \mu u \frac{\partial u}{\partial y} \right) \end{aligned} \quad (3.6)$$

where: $\tilde{\kappa} = 1 + \kappa y$

The body oriented coordinate system and shock layer geometrical relations pertinent to these equations is given in Figure 3.1.

Along the stagnation line, these equations can be simplified to obtain the following:

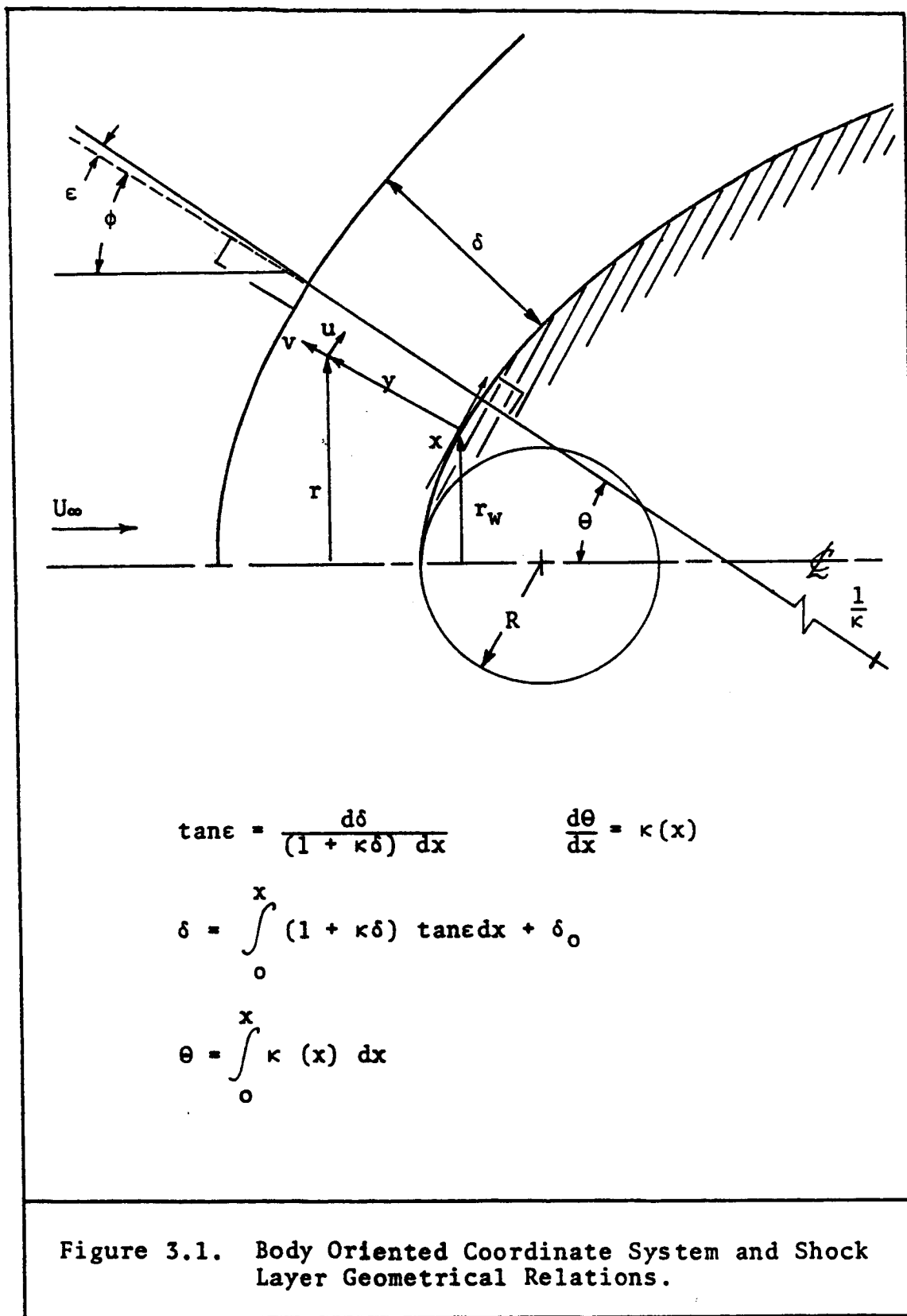
Global Continuity:

$$2 \frac{\partial(\rho u)}{\partial x} + \frac{\partial}{\partial y} (\tilde{\kappa} \rho v) + \kappa \rho v = 0 \quad (3.7)$$

Species Continuity:

$$\tilde{\kappa} \rho v \frac{\partial C_i}{\partial y} = - \frac{\partial}{\partial y} (\tilde{\kappa} J_i) - \kappa J_i + \tilde{\kappa} \omega_i \quad (3.8)$$

*The term $\partial q_{R,y}/\partial y$ is the radiative flux divergence. The details of its computation are given in Chapter IV.



x-Momentum:

$$\begin{aligned}
 & \frac{\partial}{\partial y} \left[\bar{\kappa} \mu \frac{\partial}{\partial y} \left(\frac{\partial u}{\partial x} \right) \right] + [\kappa \mu - \bar{\kappa} \rho v] \frac{\partial}{\partial y} \left(\frac{\partial u}{\partial x} \right) \\
 & - \kappa [\rho v + \mu \frac{\kappa}{\bar{\kappa}} + \frac{1}{2} \frac{\partial \mu}{\partial y}] \left(\frac{\partial u}{\partial x} \right) - \rho \left(\frac{\partial u}{\partial x} \right)^2 \\
 & - \frac{\partial^2 p}{\partial x^2} = 0
 \end{aligned} \tag{3.9}$$

y-Momentum:

$$\frac{\partial p}{\partial y} = 0 \tag{3.10}$$

Energy:

$$\begin{aligned}
 \bar{\kappa} \rho v \frac{\partial H}{\partial y} = & - \left(1 + \frac{\kappa}{\bar{\kappa}} \right) \frac{\partial}{\partial y} \left[- \bar{\kappa} k \frac{\partial T}{\partial y} + \bar{\kappa} \sum h_i J_i \right] \\
 & - \bar{\kappa} \frac{\partial q_R}{\partial y}
 \end{aligned} \tag{3.11}$$

Since the boundary layer thickness is small in comparison to the local body radius (Eq. 1.1), the following additional simplifications exist:

$$\kappa \approx 0 \tag{3.12}$$

$$\bar{\kappa} \approx 1 \tag{3.13}$$

Applying these simplifications to Equations 3.7-3.11, the first order stagnation line, thin shock equations are obtained:

Global Continuity:

$$2 \frac{\partial u}{\partial x} = - \frac{1}{\rho} \frac{\partial}{\partial y} (\rho v) \quad (3.14)$$

Species Continuity:

$$\rho v \frac{\partial C_i}{\partial y} = - \frac{\partial J_i}{\partial y} + \omega_i \quad i=1, 2, \dots, v \quad (3.15)$$

x-Momentum:

$$\frac{\partial}{\partial y} \left[\mu \frac{\partial}{\partial y} \left(\frac{\partial u}{\partial x} \right) \right] - \rho v \frac{\partial}{\partial y} \left(\frac{\partial u}{\partial x} \right) - \rho \left(\frac{\partial u}{\partial x} \right)^2 + \left(\frac{\partial^2 P}{\partial x^2} \right)_{x=0} = 0 \quad (3.16)$$

y-Momentum:

$$\frac{\partial P}{\partial y} = 0 \quad (3.17)$$

Energy:

$$\rho v \frac{\partial H}{\partial y} = - \frac{\partial}{\partial y} \left[- k \frac{\partial T}{\partial y} + \sum h_i J_i \right] - \frac{\partial q_R}{\partial y} \quad (3.18)$$

In the sections to follow the formulation of these equations will be further developed to obtain more convenient forms for numerical solutions.

Species Equations. For studies of reacting flow systems in chemical equilibrium, a useful simplification which eliminates the reaction rate term in the species equation can be realized by transforming the v species equations (Eqs. 3.15) to elemental equations. The transformation, referred to as the Shvab-Zeldovich transformation (Refs. 3.3-3.5), is accomplished by means of the following relationships:

$$\tilde{C}_j = \tilde{M}_j \sum_{i=1}^v \frac{A_{ij}C_i}{M_i} = \text{mass fraction of element } j \quad (3.19)$$

$$\tilde{J}_j = \tilde{M}_j \sum_{i=1}^v \frac{A_{ij}J_i}{M_i} = \text{mass flux of element } j \quad (3.20)$$

where A_{ij} represents the moles of element j per mole of compound i , \tilde{M}_j is the atomic weight of the element j and M_i is the molecular weight of the compound i . The details of the transformation are given in Appendix A. The resulting form of the elemental conservation equations is

$$\rho v \frac{d\tilde{C}_j}{dy} = - \frac{d\tilde{J}_j}{dy} \quad j = 1, 2, \dots, l \quad (3.21)$$

The species mass flux, J_i , appearing in Equation 3.15 is generally computed by assuming binary (Fick's Law) diffusion (Refs. 3.7-3.10):

$$J_i = - \rho \mathcal{D}_{12} \frac{dC_i}{dy} \quad (3.22)$$

where a single diffusion coefficient, \mathcal{D}_{12} , is chosen to represent the diffusive behavior of all species in the system. As shown in Appendix A, the binary flux expression (Eq. 3.22) can be conveniently transformed by the Shvab-Zeldovich transformation to an elemental basis.

$$\tilde{J}_j = - \rho \mathcal{D}_{12} \frac{d\tilde{C}_j}{dy} \quad (3.23)$$

This relationship can be substituted into the elemental continuity equations (Eqs. 3.21) to yield the following second order ordinary differential equations,

$$\rho v \frac{d\tilde{C}_j}{dy} = \rho \mathcal{D}_{12} \frac{d^2 \tilde{C}_j}{dy^2} + \frac{d(\rho \mathcal{D}_{12})}{dy} \frac{d\tilde{C}_j}{dy} \quad j = 1, 2, \dots, \quad (3.24)$$

or

$$\frac{d^2 \tilde{C}_j}{dy^2} + p(y) \frac{d\tilde{C}_j}{dy} = 0 \quad j = 1, 2, \dots, \ell \quad (3.25)$$

where

$$p(y) = \frac{d \ln \mathcal{Q}_{12}}{dy} + \frac{d \ln \rho}{dy} - \frac{v}{\mathcal{Q}_{12}} \quad (3.26)$$

For situations, such as the current study, where more accuracy is required in determining species distribution, the Stefan-Maxwell equations can be utilized to compute the diffusive mass fluxes. The Stefan-Maxwell Equations were presented in the Chapter II (Eq. 2.5) as follows:

$$\frac{dY_i}{dy} = \sum_{j=1}^v \frac{Y_i Y_j}{\mathcal{Q}_{ij}} (V_j - V_i) \quad i = 1, 2, \dots, v-1 \quad (2.5)$$

As discussed in the previous chapter, these equations do not form an independent set. It is therefore necessary to replace one of the Stefan-Maxwell Equations by Equation 2.13:

$$\sum_{i=1}^v \rho_i V_i = \sum_{i=1}^v J_i = 0 \quad (2.13)$$

Unfortunately, the resulting system of v equations which accurately describes the multicomponent diffusion velocities cannot be simplified by means of the Shvab-Zeldovich transformation. However, it is still possible, as will be demonstrated in Chapter V, to use the present forms of Equations 2.5 and 2.13 with the elemental equations (Eqs. 3.21) to obtain accurate species distributions in equilibrium flow.

Momentum Equation. To obtain a more classical form of the momentum equation a velocity function (f') is defined

$$f' = \frac{\partial u}{\partial x} / \left(\frac{\partial u}{\partial x} \right)_s \quad (3.27)$$

where the quantity $\left(\frac{\partial u}{\partial x} \right)_s$ is the tangential velocity gradient at the shock and can be determined from the Rankine-Hugoniot Equations (to be subsequently discussed). Substituting Equation 3.27 into the momentum equation (Eq. 3.16) gives the following:

$$\frac{d}{dy} \left(\mu \frac{df'}{dy} \right) - \rho v \frac{df'}{dy} - \rho \left(\frac{\partial u}{\partial x} \right)_s (f')^2 - \frac{\partial^2 p}{\partial x^2} = 0 \quad (3.28)$$

The tangential pressure gradient term appearing in this equation is a function of the flow downstream and consequently cannot be rigorously determined without an analysis of the downstream effects. It has been shown that for a thin shock layer, this term is constant along the stagnation line (Ref. 3.1) and therefore can be evaluated at any point. From the Rankine-Hugoniot Equations the pressure behind the shock can be expressed as

$$P_s = [(1 - \bar{\rho}) \cos^2 \phi] \rho_\infty U_\infty^2 \quad (3.29)$$

differentiation yields

$$\frac{\partial^2 P_s}{\partial x^2} = -2(1 - \bar{\rho}) \left(\frac{\partial \phi}{\partial x} \right)^2 [\cos^2 \phi - \sin^2 \phi] \rho_\infty U_\infty^2 \quad (3.30)$$

An approximation of a concentric shock is consistent with the thin shock layer analysis. For a concentric shock, $\left(\frac{d\phi}{dx} \right)_{x=0} = 1$ (See Figure 3.1). Furthermore, $\phi = 0$ at $x = 0$. Therefore, Equation 3.30 becomes

$$\left(\frac{\partial^2 P}{\partial x^2} \right)_{x=0} = -2(1 - \bar{\rho}) \rho_\infty U_\infty^2 \quad (3.31)$$

Substituting Equation 3.31 into the momentum equation (Eq. 3.27), the following equation is obtained:

$$\frac{d}{dy} \mu \frac{df'}{dy} - \rho v \frac{df'}{dy} - \rho \left(\frac{\partial u}{\partial x} \right)_s (f')^2 + 2 (1 - \bar{\rho}) \rho_{\infty} U_{\infty}^2 = 0 \quad (3.32)$$

A simultaneous solution of the above equation with the Global Continuity Equation (Eq. 3.14), expressed in terms of f' (Eq. 3.27), thus defines the velocity distribution. The necessary form of the Global Continuity Equation is given as follows:

$$2 f' \left(\frac{\partial u}{\partial x} \right)_s = - \frac{1}{\bar{\rho}} \frac{d}{dy} (\rho v) \quad (3.33)$$

Energy Equation: Since the available thermodynamic and transport properties* are expressed in terms of temperature, it is desirable to reformulate the energy equation in terms of temperature rather than enthalpy as the dependent variable. The required manipulations for this conversion are given in Reference 3.6 and are shown in the development to follow.

Consider the term on the left hand side of Equation 3.18,

$$\rho v \frac{dH}{dy} = \rho v \frac{d}{dy} \left(h + \frac{u^2 + v^2}{2} \right) \quad (3.34)$$

*Presented in Chapter IV.

Noting that

$$h = \sum_{i=1}^v C_i h_i \quad (3.35)$$

$$\frac{dh}{dy} = \sum_{i=1}^v h_i \frac{dC_i}{dy} + \left(\sum_{i=1}^v C_i \frac{dh_i}{dT} \right) \frac{dT}{dy} \quad (3.36)$$

$$\frac{dh}{dy} = \sum_{i=1}^v h_i \frac{dC_i}{dy} + \left(\sum C_i c_{pi} \right) \frac{dT}{dy}$$

$$\frac{dh}{dy} = \sum_{i=1}^v h_i \frac{dC_i}{dy} + c_{pf} \frac{dT}{dy} \quad (3.37)$$

Substitution of Equation 3.37 into Equation 3.33 and noting that $u = 0$ at $x = 0$ gives,

$$\rho v \frac{dH}{dy} = \rho v \left[\sum_{i=1}^v h_i \frac{dC_i}{dy} + c_{pf} \frac{dT}{dy} + \frac{d}{dy} \left(\frac{v^2}{2} \right) \right] \quad (3.38)$$

Combining Equations 3.38 and 3.18 yields

$$\begin{aligned} \rho v c_{pf} \frac{dT}{dy} = \frac{d}{dy} \left(k_f \frac{dT}{dy} \right) - \rho v \sum_{i=1}^v h_i \frac{dC_i}{dy} - \rho v^2 \frac{dv}{dy} \\ - \frac{d}{dy} \left(\sum_{i=1}^v h_i J_i \right) - \frac{dq_R}{dy} \end{aligned} \quad (3.39)$$

In the experimental measurement of the thermal conductivity and heat capacity of gaseous mixtures, certain effects attributed to the reactive behavior of the mixture are observed. As will be illustrated by the following development, these effects are predicted by the energy equation, but are not included in the terms normally associated with ordinary thermal conductivity and heat capacity. Therefore it is convenient to incorporate the additional terms into these coefficients for consistency with experimental observations.

The quantities c_{pf} and k_f appearing in Equation 3.39 are referred to respectively as the "frozen" heat capacity and thermal conductivity. As shown in Appendix B, the summation terms of Equation 3.39 can be rearranged to combine with the above coefficients to yield the following form of the energy equation:

$$\rho v c_p \frac{dT}{dy} = \frac{d}{dy} \left(k \frac{dT}{dy} \right) - \rho v^2 \frac{dv}{dy} - \frac{dq_R}{dy} \quad (3.40)$$

where

$$c_p = c_{pf} + \sum h_i \left(\frac{\partial C_i}{\partial T} \right) \quad (3.41)$$

and

$$k = k_f + \rho \sum D_i h_i \left(\frac{\partial C_i}{\partial T} \right) \quad (3.42)$$

As given in the preceding equation, the total heat capacity, c_p , includes the effects of chemical heats of reaction as an additional mechanism of energy absorption. The total thermal conductivity, k , accounts for the additional transport of energy through the diffusion of high energy molecules into regions of lower energy. This effect is not to be confused with the related phenomena of thermal diffusion which accounts for the flux of mass due to temperature gradients.

For a fully coupled analysis, it is important that the behavior of the ablative material be properly incorporated in the formulation. In the current investigation, the contribution of the ablator appears as a boundary condition to the flowfield equations. A derivation of these relationships is given in the following discussion.

Derivation of Surface Interaction Relations

The boundary conditions for this investigation can be derived in either of two ways. The first, and most frequently used, technique consists of simply formulating a physical balance across the boundaries of

the system. A second technique involves the use of the flowfield equations themselves, which are integrated across the system boundaries and then contracted by taking the limit as the spacial increment approaches zero. Both of these methods should yield identical results. In this development both of these techniques will be employed. The first method has the advantage that the physical significance of each term in the resulting equation is more readily evident. The second, the integration technique, will assure that all of the necessary terms have been considered.

Species Boundary Conditions: At the char surface the following general surface balance is applicable:

$$\begin{aligned}
 & \left[\begin{array}{l} \text{convective flux} \\ \text{of species } i \text{ on} \\ \text{the char side} \\ \text{of the interface} \end{array} \right] + \left[\begin{array}{l} \text{diffusive flux} \\ \text{of species } i \text{ on} \\ \text{the char side} \\ \text{of the interface} \end{array} \right] + \left[\begin{array}{l} \text{all contribu-} \\ \text{tions to the} \\ \text{net flux of} \\ \text{species } i \text{ due} \\ \text{to surface} \\ \text{phenomena} \end{array} \right] \\
 & = \left[\begin{array}{l} \text{convective flux} \\ \text{of species } i \text{ on} \\ \text{flowfield side} \\ \text{of the interface} \end{array} \right] + \left[\begin{array}{l} \text{diffusive} \\ \text{flux of} \\ \text{species } i \\ \text{on flow-} \\ \text{field side} \\ \text{of the} \\ \text{interface} \end{array} \right]
 \end{aligned}
 \tag{3.43}$$

or

$$\rho v C_i^- + J_i^- + S_i = \rho v C_i^+ + J_i^+ \quad (3.44)$$

The surface generation (S_i) can now be quantitatively defined and the remaining terms of the equation verified by examining an integral derivation of this relationship. It can be shown that the following equation describes the heterogeneous system which exists at the char interface:

$$\rho v \frac{dC_i}{dy} = - \frac{dJ_i}{dy} + \omega_{i_{\text{homo}}} + \omega_{i_{\text{hetero}}} + \omega_{i_{\text{subl}}} \quad (3.45)$$

In this relationship, both the solid and gas phases have been included. As shown in Figure 3.2, the following overall material balance exists at the surface:

$$(\rho v)_{\text{wall}} = \rho_g v_g + \rho_c v_r = \text{mass injection rate} \quad (3.46)$$

The generation terms appearing in Equation 3.45 are defined as follows

$$\omega_{i_{\text{homo}}} = \begin{array}{l} \text{net generation of species } i \text{ by} \\ \text{means of homogeneous chemical} \\ \text{reactions} \end{array} \quad (3.47)$$

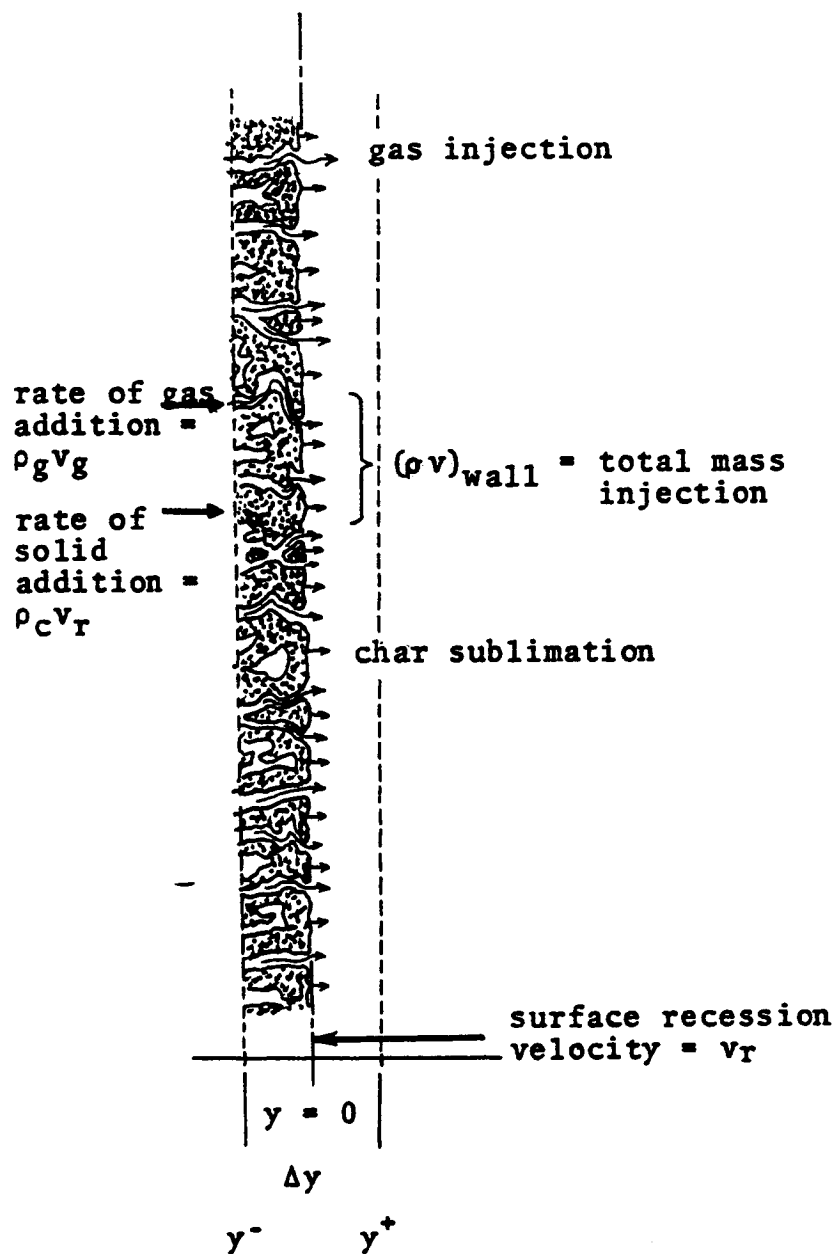


Figure 3.2. Illustration of Overall Surface Material Balance.

$$\omega_{i \text{ hetero}} = \text{net generation of species } i \text{ by means of heterogeneous reactions (excluding sublimation)} \quad (3.48)$$

$$\omega_{i \text{ subl}} = \text{net generation of species } i \text{ by means of sublimation of the solid phase} \quad (3.49)$$

Each of the previous terms represents a generation of mass of species i by reaction per unit time per unit volume. For the ablator this unit volume contains both gas and solid. Thus if r_i is the rate of formation of species i by heterogeneous reaction per unit area of solid surface, A_r , then $\omega_{i \text{ hetero}}$ is given by the following equation:

$$\omega_{i \text{ hetero}} = \frac{r_i A_r}{A \Delta y} \quad (3.50)$$

The ratio of $A_r/A \Delta y$ represents the concentration of surface area, i.e., the area of available surface per unit volume of the reacting system. In the subsequent steps of this analysis Equation 3.45 will be integrated across the char interface a distance of Δy which will define the thickness of a control volume

of cross-sectional area A which contains a total reactive surface area A_r . Equation 3.50 can also be conveniently expressed in terms of char porosity, (volume of voids per unit volume), which for an isotropic material is equal to $(A - A_r)/A$. Thus,

$$\omega_{i_hetero} = r_i (1 - \epsilon_p)/\Delta y \quad (3.51)$$

In a similar manner the sublimation term can be derived as,

$$\omega_{i_subl} = s_i (1 - \epsilon_p)/\Delta y \quad (3.52)$$

where s_i , is the mass rate of sublimation per unit area of solid surface. The homogeneous reaction rate term represents the net rate of formation of species i in the gas phase and requires no rearrangement.

Having now defined, quantitatively, the total generation term in the species continuity equation, the integration technique will be used to define s_i in terms of w_i . Equation 3.45 can be integrated as follows:

$$\int_{y^-}^{y^+} \rho v \frac{dC_i}{dy} dy = - \int_{y^-}^{y^+} \frac{dJ_i}{dy} dy + \int_{y^-}^{y^+} (\omega_{i_homo} + \omega_{i_hetero} + \omega_{i_subl}) dy \quad (3.53)$$

Substituting Equations 3.51 and 3.52, into the above gives:

$$\int_{y^-}^{y^+} \rho v dC_i = - \int_{y^-}^{y^+} dJ_i + \int_{y^-}^{y^+} \omega_{i_{\text{homo}}} dy$$

$$\int_{y^-}^{y^+} (r_i + s_i) (1 - \epsilon_p) dy \quad (3.54)$$

Integrating the above equation noting that ρv is a constant gives

$$\rho v C_i^+ - \rho v C_i^- = J_i^- - J_i^+ + (\omega_{i_{\text{homo mean}}}) \Delta y + (r_i + s_i)(1 - \epsilon_p) \Delta y$$

(3.55)

Taking the limit as $\Delta y \rightarrow 0$, and rearranging gives:

$$\rho v C_i^- + J_i^- + (r_i + s_i) (1 - \epsilon_p) = \rho v C_i^+ + J_i^+ \quad (3.56)$$

Comparing the above equation with Equation 3.44 confirms our previous surface balance and defines, S_i the dimensionless surface generation term as:

$$S_i = (r_i + s_i) (1 - \epsilon_p)$$

Although Equation 3.57 is completely rigorous for all species which may exist either in the flow-field or the char, a more specific interpretation of this equation can be arrived at for various types of species which can be grouped into distinct categories. For example: pyrolysis gases (excluding carbon), carbon gas, all remaining gases, and finally the solid carbon.

Elemental Boundary Conditions. Following the procedure of Appendix A, the species boundary condition equations can be transformed to elemental boundary conditions. Multiplication of Equation 3.56 by the appropriate elemental distributions and summing over the species gives

$$\rho v \sum_{i=1}^V e_{ij} C_i^- + \sum_{i=1}^V e_{ij} J_i^- = \rho v \sum_{i=1}^V e_{ij} C_i^+ + \sum_{i=1}^V e_{ij} J_i^+ \quad (3.58)$$

which can be expressed in terms of elemental mass

fractions, \tilde{C}_j and elemental mass fluxes, \tilde{J}_j .

$$\rho v \tilde{C}_j^- + \tilde{J}_j^- = \rho v \tilde{C}_j^+ + \tilde{J}_j^+ \quad (3.59)$$

The above equations are the elemental surface boundary conditions and represent a significant simplification over the species surface boundary conditions since the generation terms have been eliminated.*

Energy Boundary Conditions. Starting with Equation 3.18 the energy balance at the surface will be developed in a fashion analogous to the preceding one for the species equations.

$$\rho v \frac{dH}{dy} = - \frac{d}{dy} \left[- k_f \frac{dT}{dy} + \sum_{i=1}^v h_i J_i \right] - \frac{dq_R}{dy} \quad (3.18)$$

Integrating the above equation across the char surface gives

$$\begin{aligned} \rho v (H^+ - H^-) &= \left[k_f \frac{dT}{dy} - \sum_{i=1}^v h_i J_i \right]^+ - \left[k \frac{dT}{dy} - \sum_{i=1}^v h_i J_i \right]^- \\ &\quad - q_R^+ + q_R^- \end{aligned} \quad (3.60)$$

*It should be noted that Equations 3.56 and 3.59 are both boundary conditions of the third kind since $\tilde{J} = \tilde{J} (d\tilde{C}/dy)$. The specific treatment of this difficulty is given in Chapter V.

The above equations can be placed in a more convenient form using the following equations. The equation for the total enthalpy is

$$H = h + \frac{v^2}{2g_c} \quad (3.61)$$

and, using the definition of the static enthalpy it can be written in terms of the mass fraction, C_i , and enthalpy per unit mass of i , h_i .

$$H = \sum_{i=1}^v h_i C_i + \frac{v^2}{2g_c} \quad (3.62)$$

Noting that kinetic energy terms are small compared to the enthalpy terms and can be deleted, the left hand side of Equation 3.60 can be written as

$$\rho v (H^+ - H^-) = \rho v [h_i (C_i^+ - C_i^-)] \quad (3.63)$$

The terms on the right hand side of Equation 3.60 will now be evaluated. As discussed previously and is shown in Appendix B, the bracketed terms can be expressed in terms of the total thermal conductivity.

$$\left[k_f \frac{dT}{dy} - [h_i J_i] \right] = k \frac{dT}{dy} \quad (3.64)$$

Substitution of Equations 3.63 and 3.64 into Equation 3.60 gives the following form of the energy surface balance:

$$\rho v [h_i (C_i^+ - C_i^-) = k^+ \frac{dT}{dy} \Big|_i^+ - k_b^- \frac{dT}{dy} \Big|_i^- - q_R^+ \quad (3.65)$$

where k_b is the bulk thermal conductivity of the char for which experimental values are available (Ref. 3.12). These values thus account for all modes of heat transfer in the porous media, including the radiant effect, q_R^- .

Momentum Boundary Conditions. Integration of the stagnation line y-momentum equation (Eq. 3.17) yields the following simple result:

$$p^- = p^+ \quad (3.66)$$

In summary, the derivation of the stagnation line surface boundary conditions have been presented. It should be noted that, since $u = 0$ at the interface for all x , these same boundary conditions are applicable around the body. This extension can be confirmed by performing the previous analysis with the more general two-dimensional boundary layer equations.

Ablator Response and the Quasi-steady Assumption

In the previous section boundary conditions were derived to describe the interaction between a gaseous flowfield and a moving solid-gas interface. To predict the overall heat shield requirements for a particular entry trajectory, a transient (unsteady-state) analysis can be performed. Such an analysis would involve the solution of a set of partial differential equations describing the unstead ablator response to a heat pulse determined by the trajectory. An alternate approach to this unsteady analysis is a quasi-steady analysis which is described in the following discussion.

A schematic diagram of the zones occurring in a charring ablator is given in Figure 3.3. Also shown are typical temperature and density profiles in the material. The virgin plastic decomposes in a distinct zone in a temperature range from about 700°K to 1300°K, and in this region the density decreases from that of the virgin plastic of about 35 lb/ft³ to that of the char of about 14 lb/ft³ for a nylon-phenolic resin composite.

During the heating of the material the surface is removed by chemical reactions (e.g., oxidation),

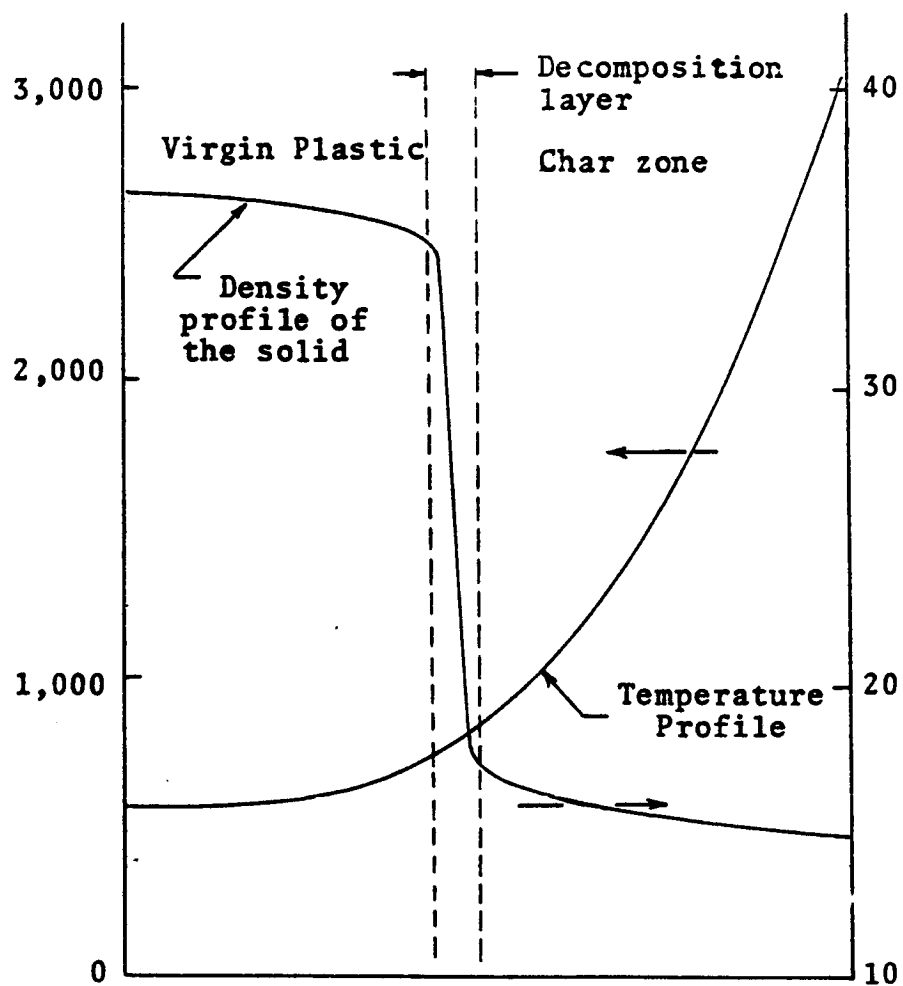


Figure 3.3. Illustration of Typical Density and Temperature Profiles in an Ablative Composite.

sublimation and erosion. As a result the total thickness of material decreases as is shown by the data in Figure 3.2. At the same time the decomposition in depth is occurring, and a char layer builds up. It is not unusual to have the rate of surface removal being equal to the rate of decomposition after an initial, transient initial period. Under these conditions a constant char layer thickness, z , and a constant surface recession velocity, v_r , are maintained after this initial period.

The previously described phenomena is referred to as a "quasi-steady state" (Refs. 3.15 and 3.16) and permits a steady state analysis of the ablator response. Assuming a quasi-steady state, an overall material balance on the ablator can be written as follows (see Figure 3.5):

$$\rho_o v_r = \rho_c v_r + \rho_g v_g \quad (3.67)$$

$$\rho_o v_r = (\rho v)_w = \text{mass injection rate wall} \quad (3.68)$$

i.e., the mass flux of virgin plastic ($\rho_o v_r$) is equal to the blowing rate, $(\rho v)_w$.

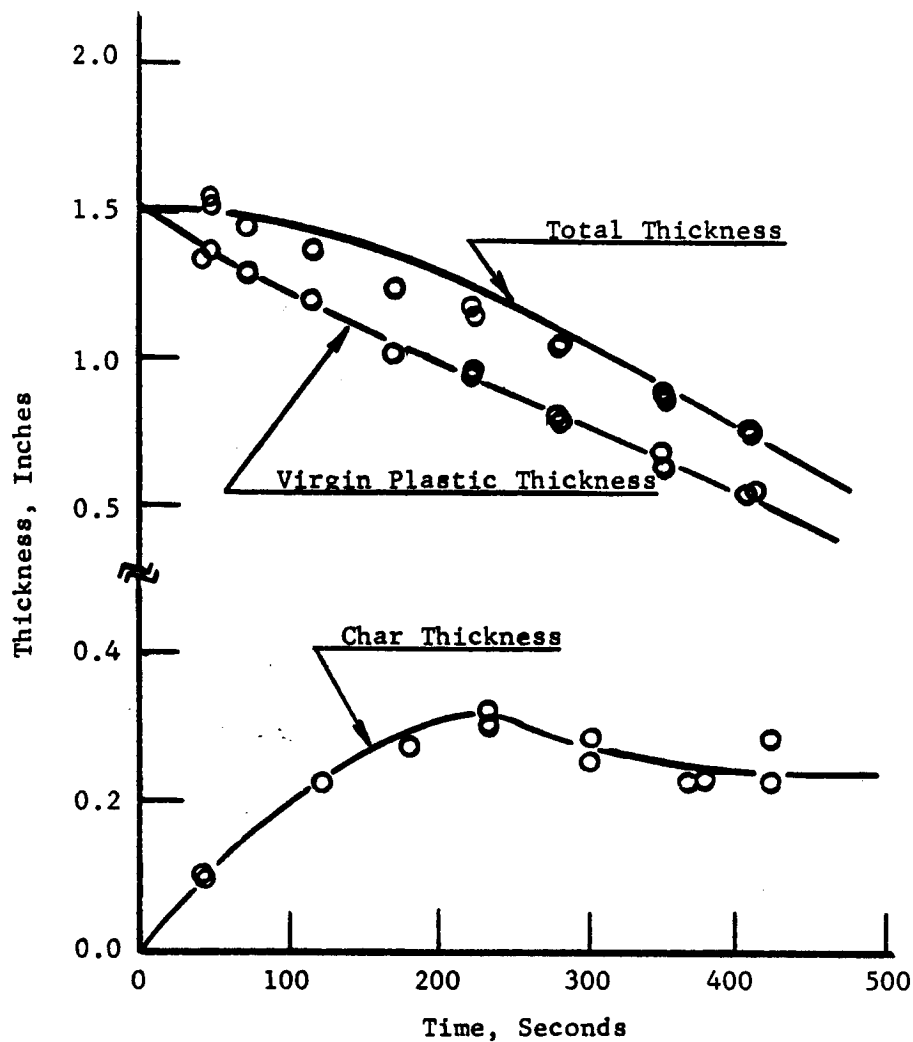


Figure 3.4. Thickness of the Char and Virgin Plastic as a Function of Time (Ref. 3.14).

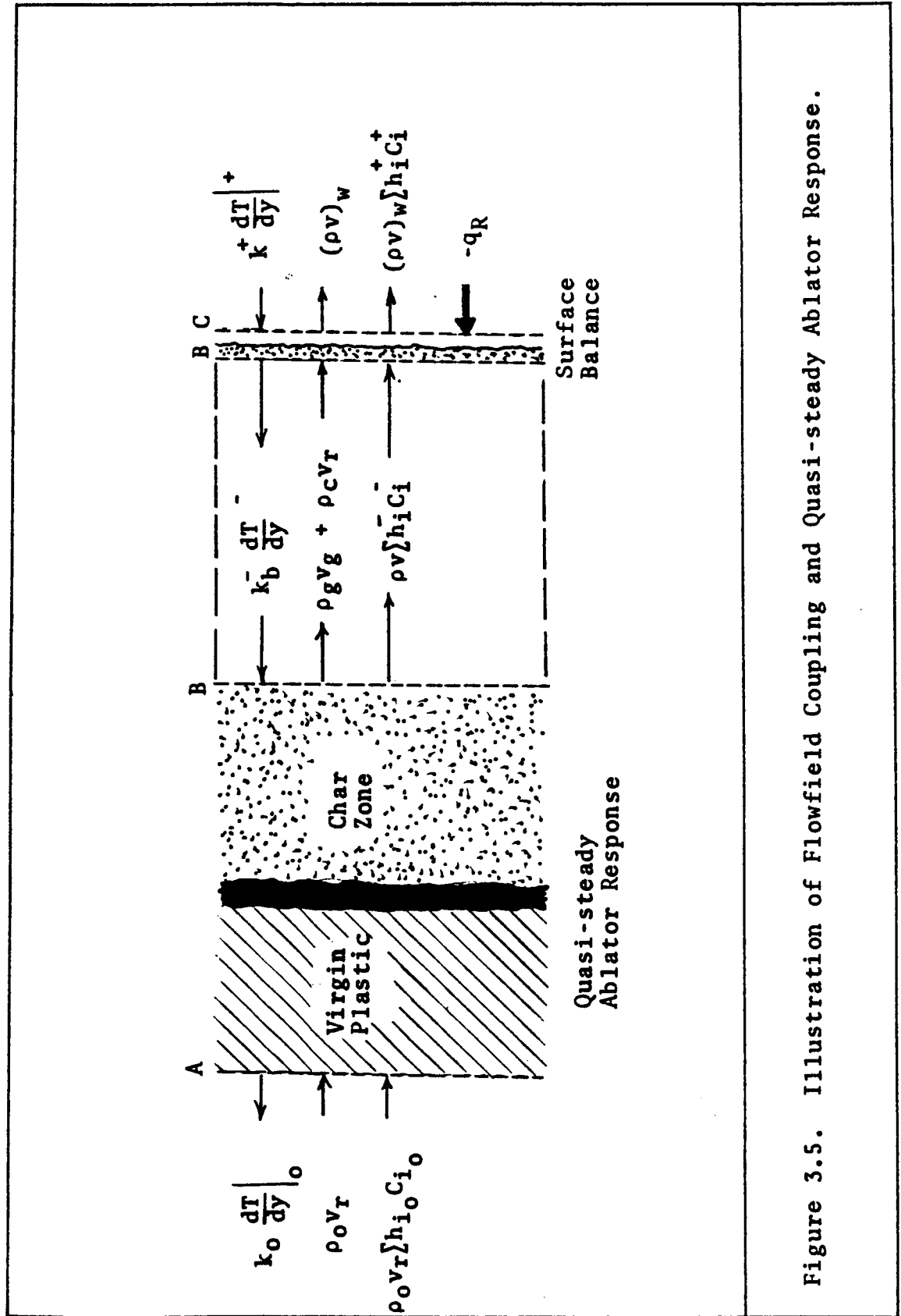


Figure 3.5. Illustration of Flowfield Coupling and Quasi-steady Ablator Response.

The overall energy balance on the ablator becomes

(See Fig. 3.5):

$$k_b \left. \frac{dT}{dy} \right|_- + \rho_o v_r \sum_{i=1}^v h_{i_o} C_{i_o} = k_o \left. \frac{dT}{dy} \right|_o + \rho v \sum_{i=1}^v h_i C_i \quad (3.69)$$

when Equation 3.69 is combined with the energy surface balance (Eq. 3.65), a useful relationship between the surface heating and the ablator response is obtained:

$$q_T = \Delta H_{\text{ablation}} (\rho v)_w + k_o \left. \frac{dT}{dy} \right|_o \quad (3.70)$$

where

$$q_T = q_R + k^+ \left. \frac{dT}{dy} \right|_+ = \text{total heat input to ablator surface} \quad (3.71)$$

and

$$\Delta H_{\text{ablation}} = \sum_{i=1}^v h_i^+ C_i^+ - \sum_{i=1}^v h_{i_o} C_{i_o} \quad (3.72)$$

[heat of ablation]

For chemical equilibrium, the heat of ablation can be determined from a specified temperature in the virgin plastic and the surface temperature of the ablator

which is equal to the sublimation temperature of char. For a given ablator, the sublimation temperature is a function of the flowfield pressure which in turn is determined by the altitude and velocity of the entering vehicle. Therefore, given a pressure at the ablator surface, a fixed relationship (Eq. 3.70) exists between the mass injection rate and total surface heating. This relationship is given for a phenolic-nylon ablator in Figure 3.6 for several surface pressures and the corresponding temperatures. In general, the heat conducted into the virgin plastic is less than 1% of the total heat absorbed by the ablator. Although not specifically included in the results of Figure 3.6 its addition would not change the results shown here.

Shock Boundary Conditions

From the shock geometry and the Rankine-Hugoniot equations (Ref. 3.13) the shock boundary conditions can be determined. In Reference 3.1, these equations are given in rectangular coordinates as shown below.

Continuity:

$$\rho_{\infty} V_{\infty} = \rho_s V_s \quad (3.73)$$

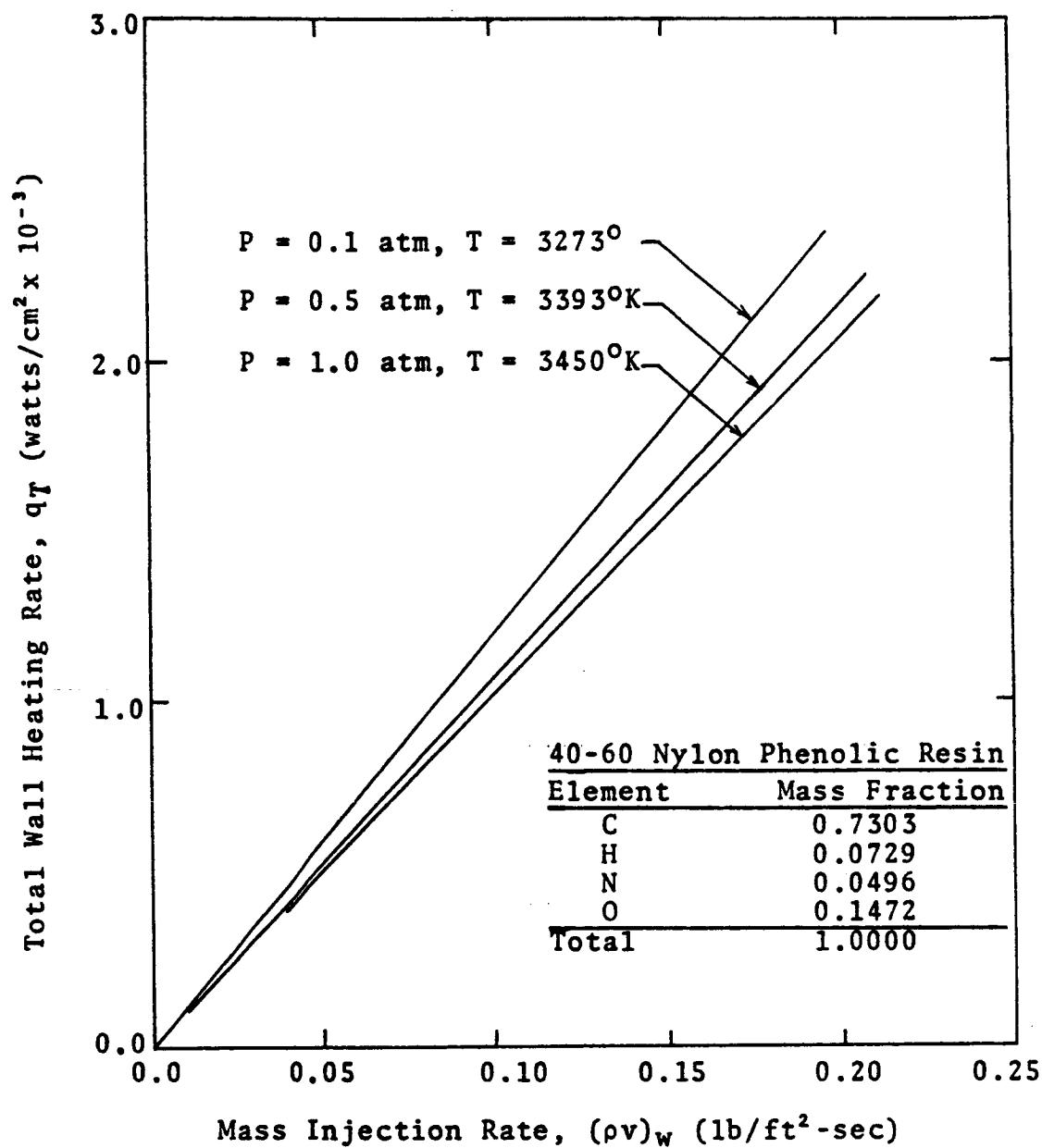


Figure 3.6. Equilibrium Mass Injection Rates Versus Wall Heating Rates for Various Surface Pressures and Corresponding Temperatures.

Momentum:

$$\text{(normal)} \quad \rho_{\infty} V_{\infty}^2 + P_{\infty} = \rho_s V_s^2 + P_s \quad (3.74)$$

$$\text{(tangential)} \quad V_{\infty} = V_s \quad (3.75)$$

Energy:

$$\frac{1}{2} V_{\infty}^2 + h_{\infty} = \frac{1}{2} V_s^2 + h_s \quad (3.76)$$

Upon transforming to curvilinear coordinates and non-dimensionalizing using dimensionless groups given in Table 3.1, the Rankine-Hugoniot equations can be written as (Ref. 3.11):

$$v_s = \sin \varnothing \sin \epsilon - \bar{\rho} \cos \varnothing \cos \epsilon \quad (3.77)$$

$$u_s = \sin \varnothing \cos \epsilon + \bar{\rho} \cos \varnothing \sin \epsilon \quad (3.78)$$

$$P_s = (1 - \bar{\rho}) \cos^2 \varnothing \quad (3.79)$$

$$h_s = (1 - \bar{\rho}^2) \cos^2 \varnothing = 1 - (u_s^2 + v_s^2) \quad (3.80)$$

For a stagnation line solution, the shock boundary conditions are determined by evaluating the above equations at $y = \delta$ and $x = 0$, with the following results:

$$v = v_s = -\bar{\rho} \quad (3.81)$$

$$u = u_s = 0 \quad (3.82)$$

$$P = P_s = 1 - \bar{\rho} \quad (3.83)$$

$$h = h_s = 1 - \bar{\rho} = 1 - v_s^2 \quad (3.84)$$

Assuming that pure air in chemical equilibrium exists at the shock, the edge boundary conditions for the species equations are thus available from an equilibrium calculation.

$$C_i = C_{i,s} = f(P_s, h_s) \quad (3.85)$$

Nondimensionalization and Transformation of the Flowfield Equations

As a matter of convenience, the final forms of the previously given flowfield equations (Eqs. 2.5, 3.14, 3.17, 3.21, and 3.40), can be nondimensionalized, using the dimensionless groups defined in Table 3.1 to yield the following set of equations:*

Continuity:

$$2f' \left(\frac{\partial u}{\partial x} \right)_s = - \frac{1}{\bar{\rho}} \frac{d}{dy} (\rho v) \quad (3.86)$$

For the remainder of this chapter, all dimensional quantities will be labeled with the symbol, () as employed in Table 3.1.

TABLE 3.1.

DIMENSIONLESS GROUPS USED FOR NONDIMENSIONALIZATION
OF THE GOVERNING TRANSPORT EQUATIONS

$$\begin{aligned}
 u &= \frac{\dot{u}^*}{\dot{U}_\infty} & v &= \frac{\dot{v}}{\dot{U}_\infty} & p &= \frac{\dot{p}}{\dot{\rho}_{s,0} \dot{U}_\infty^2} & \rho &= \frac{\dot{\rho}}{\dot{\rho}_{s,0}} \\
 x &= \frac{\dot{x}}{\dot{r}_w} & y &= \frac{\dot{y}}{\dot{r}_w} & \mu &= \frac{\dot{\mu}}{\dot{\mu}_{s,0}} & T &= \frac{\dot{T}}{\dot{T}_{s,0}} \\
 h &= \frac{\dot{h} \dot{g}_c}{\frac{1}{2} \dot{U}_\infty^2} & c_p &= \frac{\dot{c}_p \dot{T}_{s,0} \dot{g}_c}{\frac{1}{2} \dot{U}_\infty^2} & k &= \frac{\dot{k} \dot{T}_{s,0} \dot{g}_c}{\dot{R} \dot{\rho}_{s,0} \dot{U}_\infty^3} \\
 J_i &= \frac{\dot{J}_i}{\dot{\rho}_{s,0} \dot{U}_\infty} & \omega_i &= \frac{\dot{r}_w \dot{\omega}_i}{\dot{\rho}_{s,0} \dot{U}_\infty} & \frac{dq_R}{dy} &= \frac{\frac{dq_R}{dy} \dot{r}_w}{\dot{\rho}_{s,0} \dot{U}_\infty^3} \\
 Re_s &= \frac{\dot{\rho}_{s,0} \dot{U}_\infty \dot{r}_w}{\dot{\mu}_{s,0}} & D &= \frac{\dot{D}^{**}}{\dot{r}_w \dot{U}_\infty} & Vi &= \frac{\dot{V}_i}{\dot{U}_\infty}
 \end{aligned}$$

* (·) designates dimensional quantities.

**This nondimensionalization of diffusion coefficient is used for all forms (multicomponent, binary, and effective).

Species Continuity:

$$\rho v \frac{dC_i}{dy} = - \frac{dJ_i}{dy} + \omega_i \quad i = 1, 2, \dots, v \quad (3.87)$$

Elemental Continuity:

$$\rho v \frac{d\tilde{C}_j}{dy} = - \frac{d\tilde{J}_j}{dy} \quad i = 1, 2, \dots, \quad (3.88)$$

Stefan-Maxwell:

$$\frac{dY_i}{dy} = \sum_{j=1}^v \frac{Y_i Y_j}{\Delta_{ij}} (V_j - V_i) \quad i = 1, 2, \dots, v-1 \quad (3.89)$$

x-Momentum:

$$\frac{1}{Re_s} \frac{d}{dy} \left(u \frac{df'}{dy} \right) - \rho v \frac{df'}{dy} - \rho \left(\frac{\partial u}{\partial x} \right)_s (f')^2 \frac{2\bar{\rho}(1 - \bar{\rho})}{(\partial u / \partial x)_s} = 0 \quad (3.90)$$

Y-Momentum:

$$\frac{dP}{dy} = 0 \quad (3.91)$$

Energy:

$$\frac{\rho v c_p}{2} \frac{dT}{dy} = \frac{d}{dy} \left(k \frac{dT}{dy} \right) - \rho v^2 \frac{dv}{dy} - \frac{dq_R}{dy} \quad (3.92)$$

These equations can now be transformed using the Dorodnitsyn transformation. This transformation is employed to reduce the effects of the large variations in density and is written as follows:

$$\eta = \frac{\int_0^y \rho dy}{\int_0^{\delta} \rho dy} = \frac{\int_0^y \rho dy}{\tilde{\delta}} \quad (3.93)$$

which yields upon differentiation,

$$\frac{d}{dy} = \frac{\rho}{\tilde{\delta}} \frac{d}{d\eta} \quad (3.94)$$

Transforming Equations 3.86 through 3.92 by means of Equation 3.94 gives*

Global Continuity:

$$2 f' \left(\frac{\partial u}{\partial x} \right)_s = - \frac{1}{\tilde{\delta}} \frac{d}{d\eta} (\rho v) \quad (3.95)$$

Species Continuity:

$$\rho v \frac{dC_i}{d\eta} = - \frac{dJ_i}{d\eta} + \frac{\omega_i \tilde{\delta}}{\rho} \quad i = 1, 2, \dots, v \quad (3.96)$$

*In the transformed equations, the quantity f' is defined as $\rho f' / \tilde{\delta}$.

Elemental Continuity:

$$\rho v \frac{d\tilde{C}_j}{d\eta} = - \frac{d\tilde{J}_j}{d\eta} \quad j = 1, 2, \dots, \ell \quad (3.97)$$

Stefan-Maxwell:

$$\frac{dY_i}{d\eta} = \frac{\tilde{\delta}}{\rho} \sum_{j=1}^v \frac{Y_i Y_j}{\tilde{\phi}_{ij}} (V_j - V_i) \quad i = 1, 2, \dots, v-1 \quad (3.98)$$

x-Momentum:

$$\begin{aligned} \frac{d}{d\eta} \left(\rho \mu \frac{df'}{d\eta} \right) - \rho v \operatorname{Re}_s \tilde{\delta} \frac{df'}{d\eta} + \frac{\operatorname{Re}_s \frac{2\bar{\rho}(1-\bar{\rho})}{\rho} - \rho \frac{\partial u}{\partial x}_s^2 (f')^2}{\rho \left(\frac{\partial u}{\partial x} \right)_s} \\ = 0 \end{aligned} \quad (3.99)$$

y-Momentum:

$$\frac{dP}{d\eta} = 0 \quad (3.100)$$

Energy:

$$\frac{1}{2} \rho v c_p \frac{dT}{d\eta} - \frac{d}{d\eta} \left(\frac{k\rho}{\tilde{\delta}} \frac{dT}{d\eta} \right) - \rho v^2 \frac{dv}{d\eta} - \frac{dq_R}{d\eta} \quad (3.101)$$

The above set of coupled, first and second order, ordinary differential equations are the final form of the stagnation line thin-shock equations. From these equations the temperature, pressure, composition, and velocity profiles for a multicomponent reacting, and radiating chemical system can be determined. The specific way that these equations are solved with the boundary conditions is given in the discussion of numerical implementation in Chapter V.

Summary

The necessary flowfield equations and boundary conditions required for a coupled radiation analysis of stagnation region heating of ablating thermal protection systems have been presented. These equations have been further developed to a formulation which is more convenient for numerical implementation. Before discussing the details of numerical solutions, it is important that the transport, thermodynamic, and radiative properties which determine the coefficients and sources terms (in the case of radiation) of the equations be properly assessed. Therefore, the chapter to follow will contain a detailed evaluation of these properties. It will then be appropriate in Chapter V to pursue the numerical solution of these equations on a digital computer.

REFERENCES

- 3.1. Engel, C. D., D. D. Esch, R. C. Farmer, and R. W. Pike, "Formulation, Derivation, and Development of the Analysis of the Interaction of Ablating Protection Systems and Stagnation Region Heating," NASA CR-66931 (January 1, 1970).
- 3.2. Ho, H. T. and R. F. Probstein, "The Compressible Viscous Shock Layer in Rarified Hypersonic Flow," in Rarified Gas Dynamics, ed. by L. Talbot, Academic Press, New York (1961).
- 3.3. Alekseyev, B. V., "Boundary Layer and Chemical Reactions," NASA TT F-549, (July 1969).
- 3.4. Shvab, V. A., "Connection Between Temperature and Velocity Fields in a Gas Flare," In the Collection: Study of Combustion Process in Natural Fuel, (Moscow-Leningrad: Gosenergoizdat, 1948), Ref. in Alekseyev, op. cit.
- 3.5. Zeldovich, Y. B., "On the Theory of Combustion of Initially Unmixed Systems," Zh. Tekh. Fiz., Vol. 19, No. 10, pp. 1199-1210, (1944). Trans. as NASA TM-1296 (June, 1950).
- 3.6. Engel, C. D. and R. C. Farmer, "Stagnation Line Momentum and Energy Equations," Louisiana State University, NASA-RFL-TR 70-2 (September, 1970).
- 3.7. Smith, G. L., J. T. Suttles, E. M. Sullivan, and R. A. Graves, Jr., "Viscous Radiating Flow Field on an Ablating Blunt Body," AIAA Paper No. 70-218 presented at AIAA 8th Aerospace Sciences Meeting, New York (January 19-21, 1970).
- 3.8. Rigdon, W. S., R. B. Dirling, and M. Thomas, "Stagnation Point Heat Transfer During Hypervelocity Atmospheric Entry," NASA CR-1462 (February, 1970).

- 3.9. Wilson, K. H., "Stagnation Point Analysis of Coupled Viscous-Radiating Flow with Massive Blowing," NASA CR-1548, (June, 1970).
- 3.10. Davis, R. T., "Hypersonic Flow of a Chemically Reacting Binary Mixtures Past a Blunt Body," AIAA Paper No. 70-805 presented AIAA 3rd Fluid and Plasma Dynamics Conference, Los Angeles (June 29-July 1, 1970).
- 3.11. Spradley, L. W. and C. D. Engel, "Formulation of a Method for Predicting Couple Convective and Radiative Heat Transfer About a Blunt Body," NASA CR-61200 (April, 1968).
- 3.12. Wilson, G. R., Thermophysical Properties of Six Charring Ablators from 140°K to 700°K and Two Chars from 800 to 3000°K, NASA TN D-2991, (October, 1965).
- 3.13. Hayes, W. D. and R. F. Probstein, Hypersonic Flow Theory, 2nd Edition, Academic Press, New York, 1966, Vol. 1.
- 3.14. Peters, R. W. and Wadlin, K. L., "The Effect of Resin Composition and Fillers on the Performance of a Molded Charring Ablator," NASA TN D-2024 (December, 1963).
- 3.15. Swarm, R. T., C. M. Pittman and J. C. Smith, "One-dimensional Numerical Analysis of the Transient Response of Thermal Protection Systems," NASA TN D-2976 (September, 1965).
- 3.16. Stroud, C. W., "A Study of the Reaction-Plane Approximation in Ablation Analysis," NASA TN D-4817 (October, 1968).

CHAPTER IV

TRANSPORT, THERMODYNAMIC, AND RADIATIVE PROPERTIES

Theoretical Predictions of High Temperature Gas Properties

The reliability of the flowfield calculations in the current study is highly dependent on the values used for the various transport, thermodynamic, and radiative properties. With this in mind, it is desirable to attain the ultimate in accuracy; however, some complications do exist. There is very little data in the temperature range of interest in this work, and the data that does exist is subject to some scrutiny due to experimental difficulties at these higher temperatures. Therefore, it becomes necessary to rely heavily on rigorous kinetic theory and statistical thermodynamics for the estimation of these properties.

Transport Properties

Generally, investigators in this area have resorted to the classical Chapman-Enskog kinetic theory relations for estimation of the required transport properties. The modification of these relationships to

account for polyatomic, reacting mixtures results in very cumbersome equations. In some cases, as will be shown, there are simplifications which can be applied without substantial loss in accuracy. At this point, it becomes desirable to optimize between accuracy and computation time. A wide variety of methods for estimating these properties has been developed in just this manner. In this section, a formulation is provided from which an optimum method to accurately compute high temperature transport properties with reasonable computational convenience is developed.

At the lower temperatures where ionization has not yet begun to occur, the classical first order Chapman-Enskog kinetic theory relations have been found to be reasonably accurate. However, for partially and fully ionized gases, more rigorous expressions are required. An evaluation of these methods is given by Ahtye in Reference 4.1. On the basis of the available data, the estimations obtained from higher order kinetic theory analyses are quite good. Several such comparisons are given by Ahtye in the previously mentioned technical note. In the discussion to follow, the sources of theoretical estimates for the required properties of viscosity, thermal conductivity and binary diffusion

coefficients are given and the methods of computer implementation for each of these properties are discussed.

Viscosity: For computer implementation the data obtained from theoretical predictions was curve fitted to a second order polynomial.

$$\mu_i = a_i + b_i T + c_i T^2 \quad (4.1)$$

Data for air species was taken from Yan, et al. (Ref. 4.2). The estimated viscosities of the ionized species, N^+ , O^+ , and e^- , were obtained from the air mixture properties reported by Yos (Ref. 4.6). The procedure for arriving at these estimates will be subsequently discussed. Figure 4.1 shows a comparison of this data and the resulting curve-fits. Viscosity predictions for the ablation products were taken from a number of sources (Refs. 4.3-4.5). The data and corresponding correlations for each of these species are given in Figure 4.2. No data was available for the species, C_2H , C_3H , and C_4H . Therefore, on the basis of molecular weight, C_2H was assumed to have the transport properties of CN ; C_3H and C_4H were assumed to have the same properties as C_3 .

The relationship employed for the prediction of mixture viscosity was the commonly used Buddenberg-Wilke correlation (Ref. 4.6).

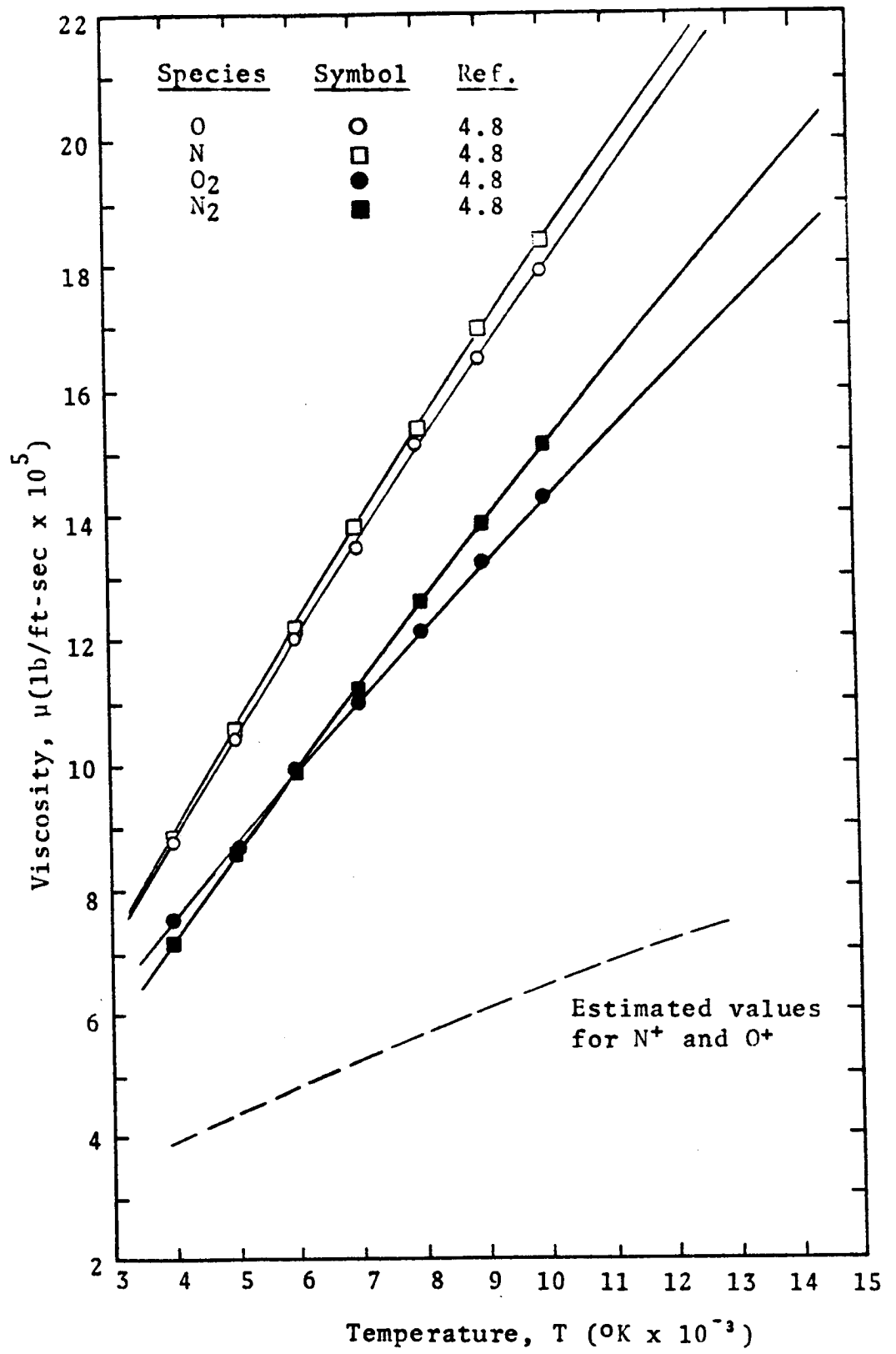


Figure 4.1 Viscosity of Air Species at 1.0 Atm.

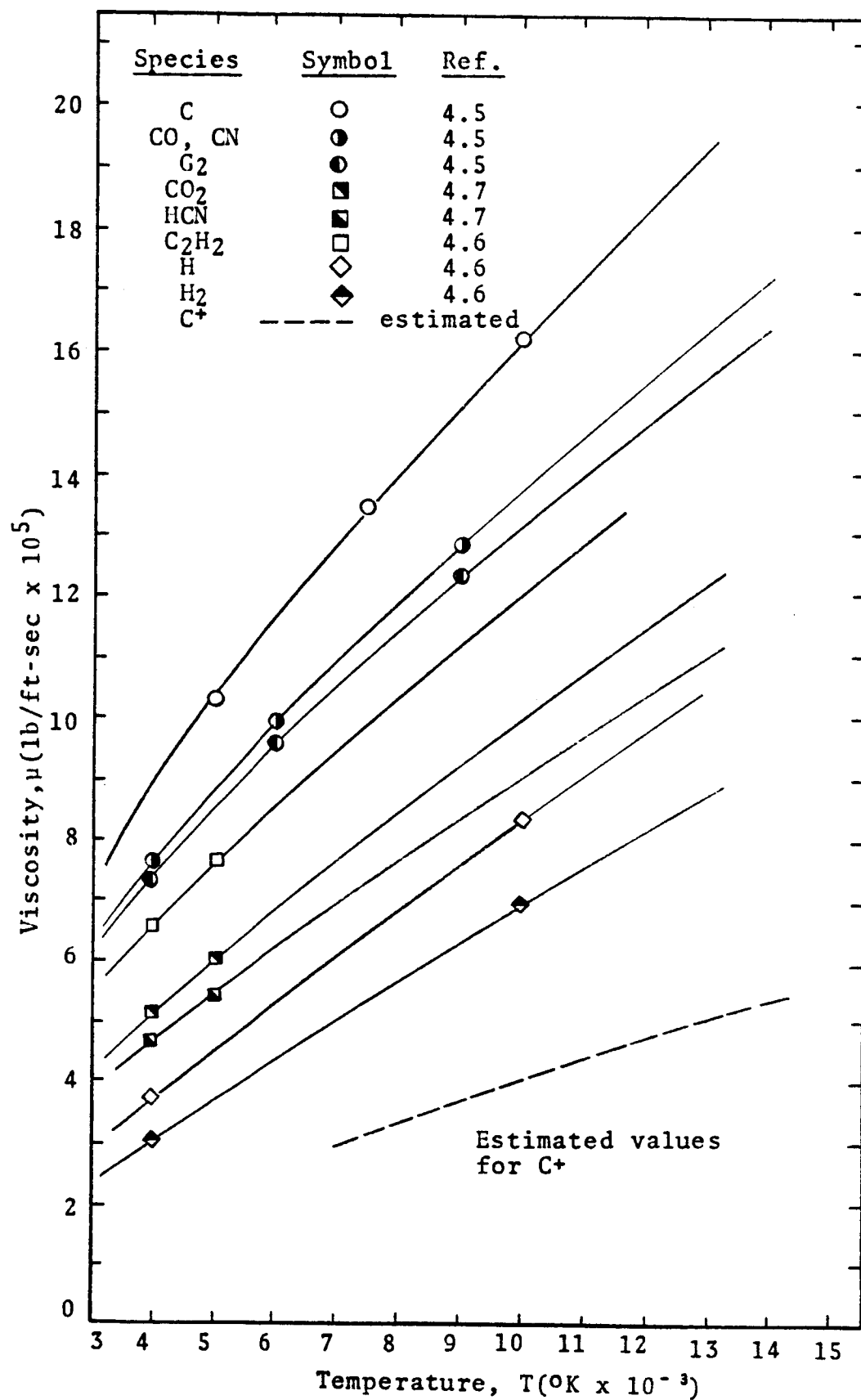


Figure 4.2. Viscosity of Ablation Products at 1 atm.

$$\mu = \sum_{i=1}^v \frac{Y_i \mu_i}{\sum_{j=1}^v Y_j \phi_{ij}} \quad (4.2)$$

where

$$\phi_{ij} = \frac{1}{\sqrt{8}} \left(1 + \frac{M_i}{M_j} \right)^{-1/2} \left[1 + \left(\frac{\mu_i}{\mu_j} \right)^{1/2} \left(\frac{M_j}{M_i} \right)^{1/4} \right]^2 \quad (4.3)$$

The results for air viscosity using this correlation are presented in Figure 4.3 and compared with those obtained from more rigorous procedures. The excellent agreement obtained for the sub-ionization temperatures (less than 9000°K at 1.0 atm) demonstrates the capabilities of the Buddenberg-Wilke correlation in predicting gas mixture properties. The viscosity and frozen thermal conductivity predictions of Yos (Ref. 4.7) and of Lee and Bobbitt (Ref. 4.8) were obtained from a more rigorous formulation than those of Hansen (Ref. 4.9). For temperatures exceeding 9000°K agreement with the results of Yos (Ref. 4.7) was accomplished by adjusting the values of the properties of N^+ , O^+ and e^- . In this manner, the properties of these species were estimated. It was further assumed that C^+ would exhibit similar behavior and could therefore be represented by the same

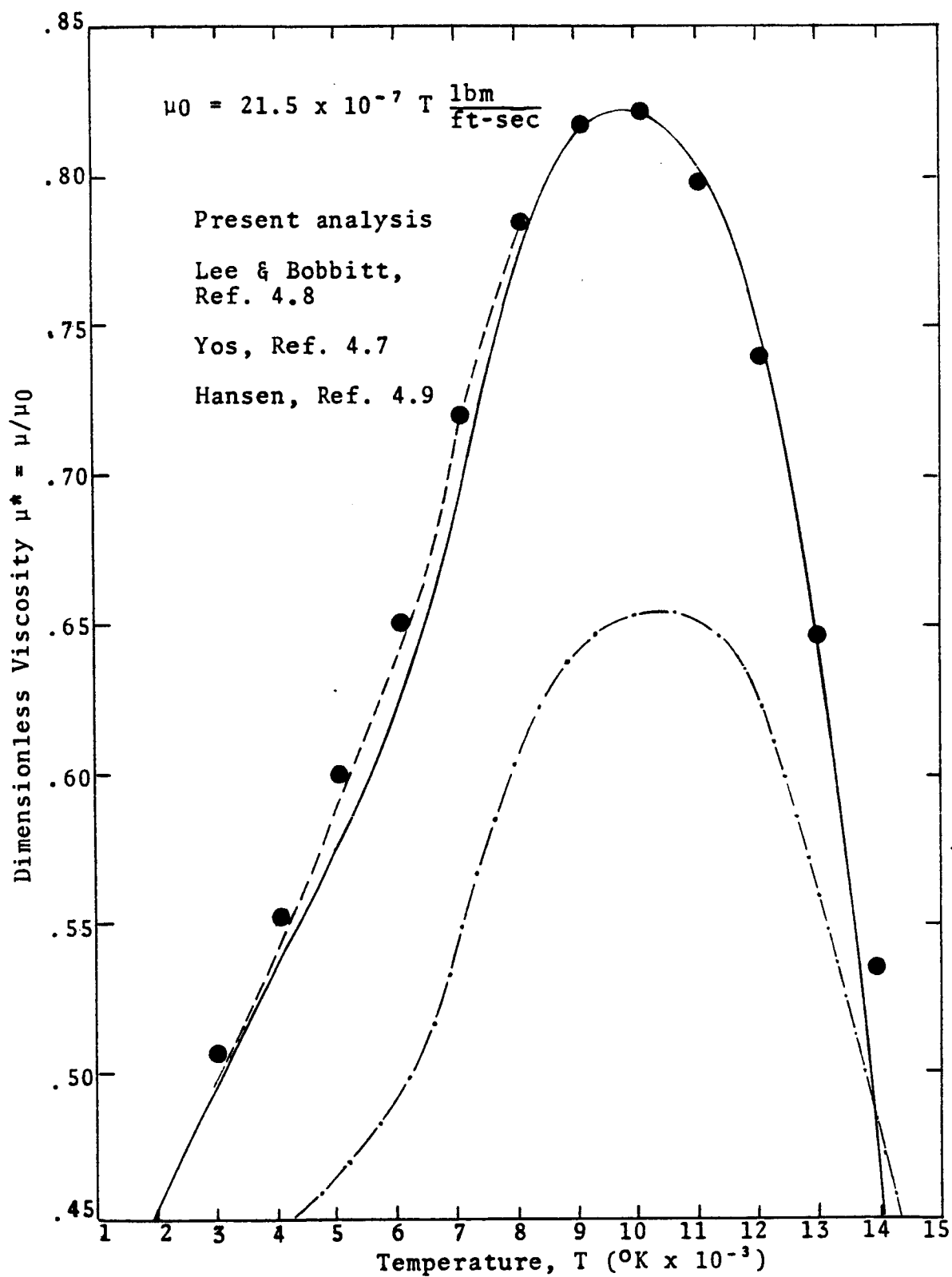


Figure 4.3. Viscosity of Air at One Atmosphere.

properties as the previously discussed ionized components. A summary of the empirical constants required for Equation 4.1 is given in Table 4.1.

Thermal Conductivity: As with the viscosity data, theoretical predictions of frozen thermal conductivities of air species were obtained from Reference 4.2. The resulting data is given in Figure 4.4. Examination of the data revealed that a linear fit would be satisfactory for accurate correlation:

$$k_i = a_i + b_i T \quad (4.4)$$

Corresponding data for the ablation products were collected from References 4.3, 4.4, and 4.5 and are shown in Figure 4.5. As with viscosity, the thermal conductivities of the ionized species were determined from air mixture properties of Yos (Ref. 4.7). A summary of the coefficients required for Equation 4.4 is given in Table 4.2. Mixture thermal conductivity was calculated in the same manner as mixture viscosity:

$$k_f = \frac{\sum_{i=1}^v Y_i k_i}{\sum_{j=1}^v Y_i \phi_{ij}} \quad (4.5)$$

TABLE 4.1
EMPIRICAL CONSTANTS FOR VISCOSITY CORRELATION

$$\mu_i = a_i + b_i T + c_i T^2 \quad \frac{\text{lbm}}{\text{ft-sec}}$$

Species	$a \times 10^5$	$b \times 10^7$	$c \times 10^{12}$	Temperature Range ($^{\circ}\text{K}$)
O ₂	1.693	0.1496	-0.2276	2,000-10,000
N ₂	0.970	0.1613	-0.1916	2,000-10,000
O	1.519	0.1875	-0.2228	2,000-10,000
N	0.253	0.2206	-0.3737	2,000-10,000
O ⁺	0.0	0.0500	-0.1000	8,000-15,000
N ⁺	0.0	0.0500	-0.1000	8,000-15,000
e ⁻	0.0	0.0500	-0.1000	8,000-15,000
C	1.997	0.1772	-0.3378	5,000-10,000
H	0.294	0.0889	-0.0811	4,000-10,000
H ₂	-0.079	0.0791	-0.0886	4,000-10,000
CO	2.404	0.1363	-0.2184	4,000- 9,000
C ₃	2.019	0.1179	-0.1655	1,000- 5,000
CN	2.404	0.1363	-0.2184	4,000- 9,000
C ₂ H	2.404	0.1363	-0.2184	4,000- 9,000
C ₂ H ₂	1.396	0.0842	-0.6939	1,000- 5,000
C ₃ H	2.019	0.1179	-0.1655	1,000- 5,000
C ₄ H	2.019	0.1179	-0.1655	1,000- 5,000
HCN	1.378	0.0965	-0.0948	1,000- 5,000
C ₂	1.931	0.1393	-0.2575	4,000- 9,000
C ⁺	0.0	0.0500	-0.1000	8,000-15,000

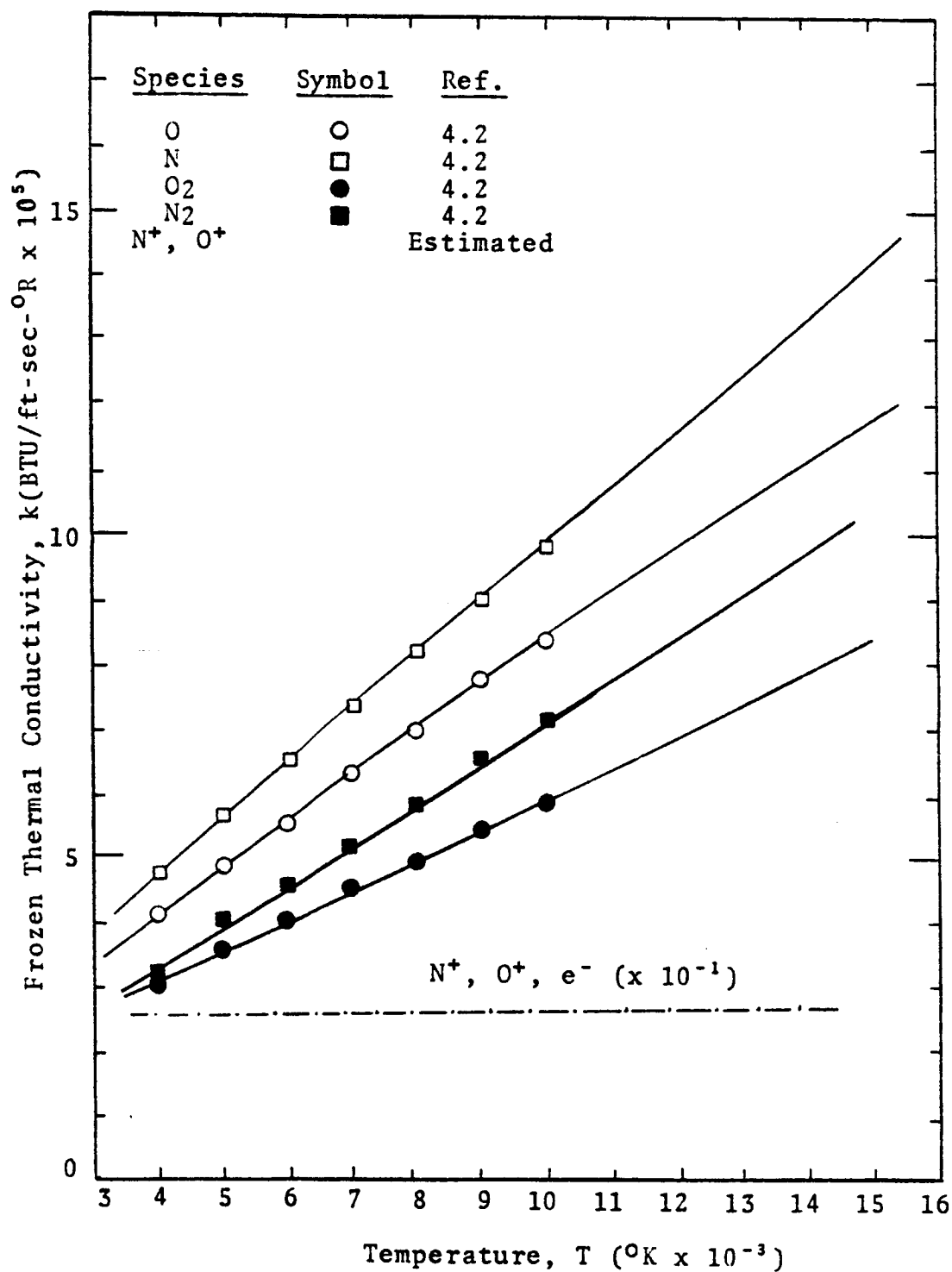


Figure 4.4. Frozen Thermal Conductivity of Air Species at 1 atm.

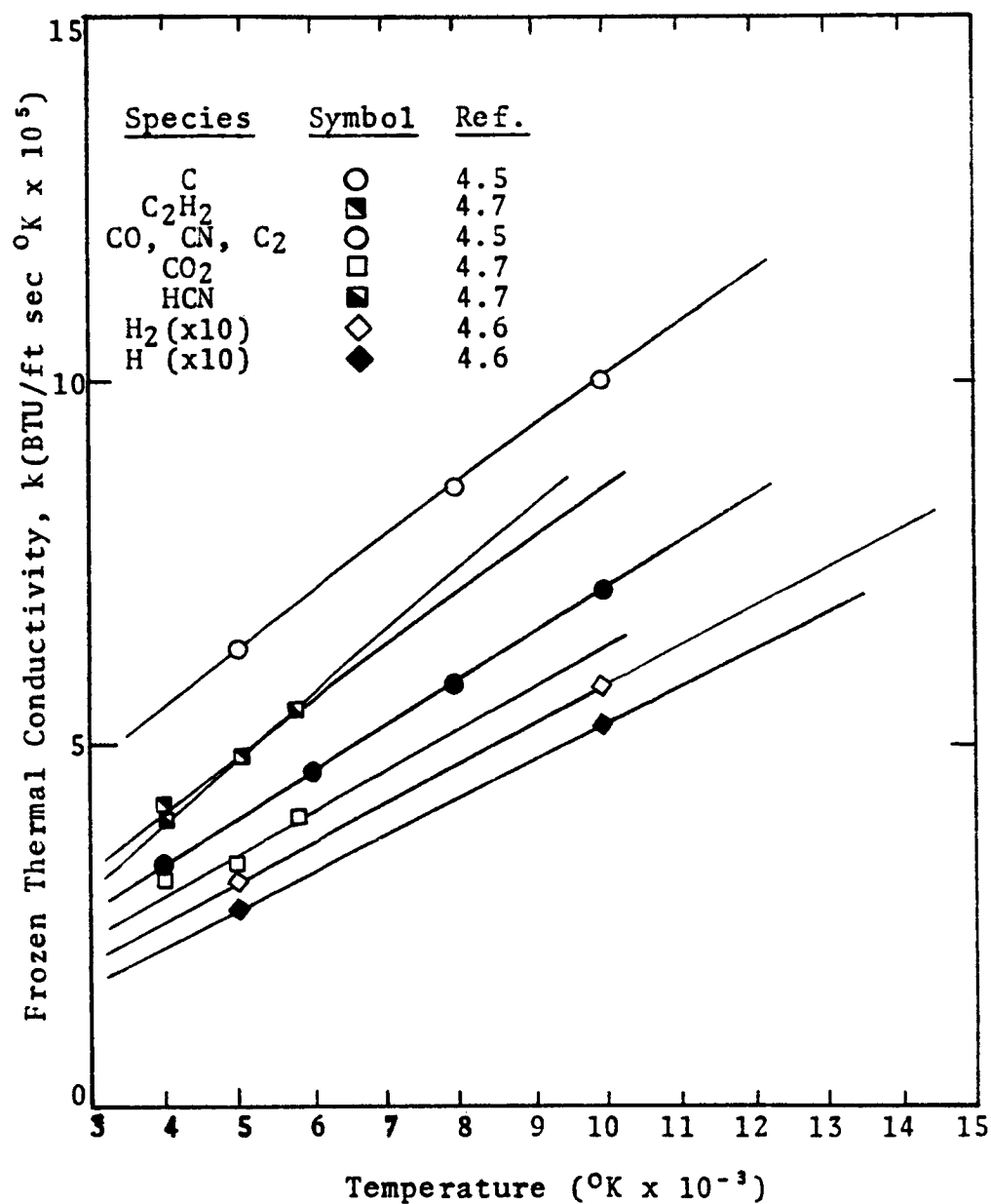


Figure 4.5. Frozen Thermal Conductivity of Ablation Products at 1 atm.

TABLE 4.2
EMPIRICAL CONSTANTS FOR THERMAL CONDUCTIVITY CORRELATION

$$k_i = a + bT \text{ (BTU/ft-sec-}^{\circ}\text{R)}$$

Species	$a \times 10^5$	$b \times 10^2$	Temperature Range ($^{\circ}\text{K}$)
O ₂	1.019	0.4901	2,000-10,000
N ₂	0.654	0.6457	2,000-10,000
O	1.250	0.7092	2,000-10,000
N	1.281	0.8593	2,000-10,000
O ⁺	26.0	0.0	8,000-15,000
N ⁺	26.0	0.0	8,000-15,000
e ⁻	26.0	0.0	8,000-15,000
C	2.506	0.7479	5,000-10,000
H	2.496	5.129	4,000-10,000
H ₂	3.211	5.344	4,000-10,000
CO	0.859	0.6233	1,000- 5,000
C ₃	0.630	0.5804	1,000- 5,000
CN	0.859	0.6233	2,000-10,000
C ₂ H	1.126	0.7439	1,000- 5,000
C ₂ H ₂	1.126	0.7439	1,000- 5,000
C ₃ H	0.630	0.5804	1,000- 5,000
C ₄ H	0.630	0.5804	1,000- 5,000
HCN	0.486	0.8714	1,000- 5,000
C ₂	0.859	0.6233	1,000- 5,000
C ⁺	26.0	0.0	8,000-15,000

where k_f is the frozen mixture thermal conductivity and Φ_{ij} is defined by Equation 4.3. The predicted results of this relationship are given in Figure 4.6 and are compared with the more rigorous predictions.

As shown in Appendix A, the total thermal conductivity is written as:

$$k = k_f + k_r \quad (4.6)$$

where k_f is given by Equation 4.5 and k_r is given by the following relationship:

$$k_r = \rho \sum_{i=1}^v D_i h_i \frac{\partial C_i}{\partial T} \quad (4.7)$$

For binary diffusion, Equation 4.7 can be written as

$$k_r = \rho \mathcal{D}_{12} \sum_{i=1}^v h_i \frac{\partial C_i}{\partial T} \quad (4.8)$$

Experimental measurements of a pure nitrogen system have shown that the results of Yos (Ref. 4.7) may be somewhat low for the prediction of the total conductivity of high temperature air.* The comparison

*This discrepancy occurs in the calculation of the reacting thermal conductivity (k_r) and does not reflect upon the accuracy of the theoretical predictions of μ and k_f in Reference 4.7.

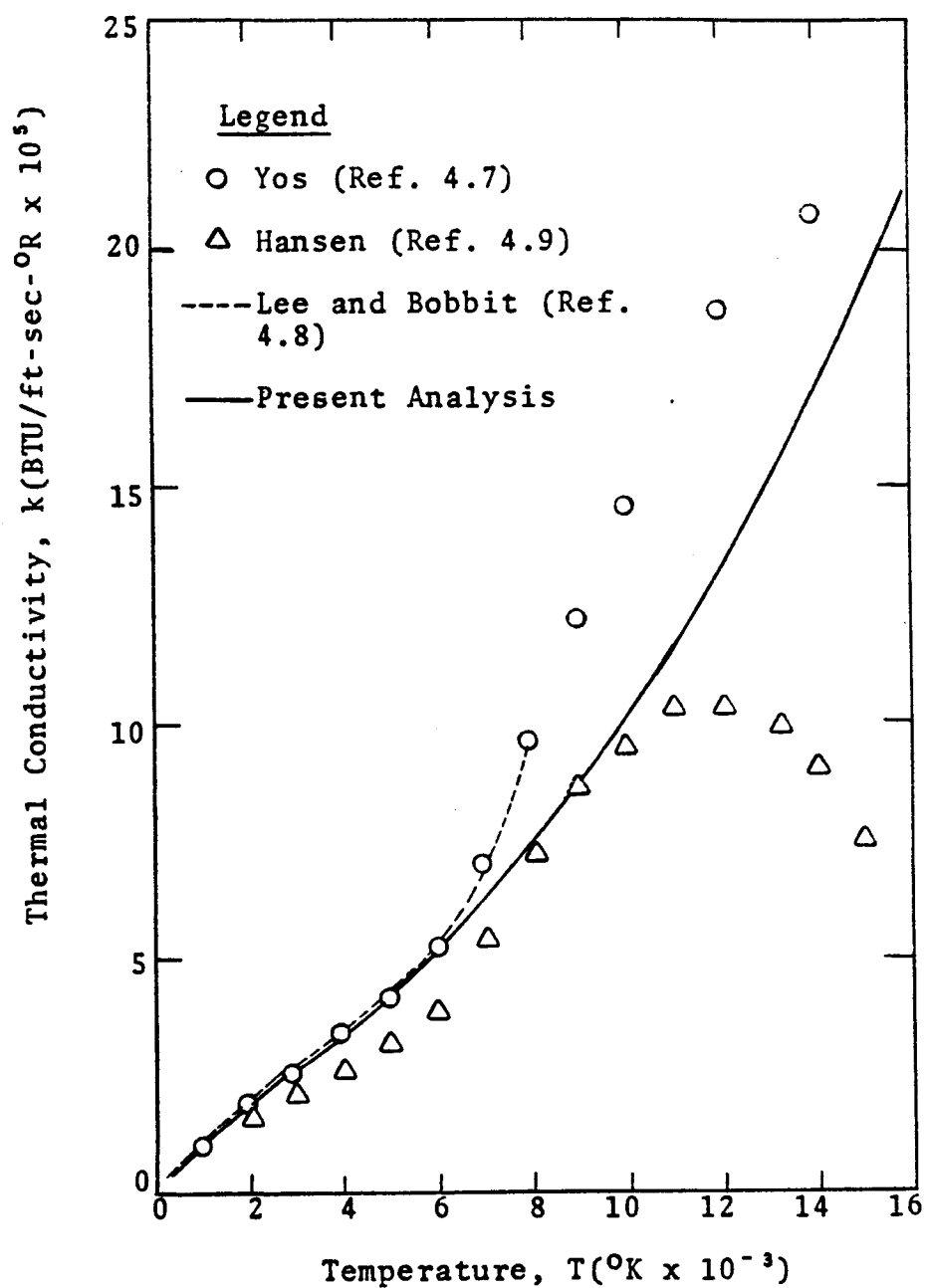


Figure 4.6. Comparison of Predictions for Frozen Thermal Conductivity of Air at 1 atm.

which includes also the results of Hansen (Ref. 4.9) is given in Figure 4.7. Upon considering the results of Figure 4.7, it was decided that an intermediate profile of total thermal conductivity would be estimated. This result was accomplished by assuming a binary diffusion coefficient, D_{12} , given by the following relationship,

$$D_{12} = \frac{AT^{1.659}}{P} \quad \text{cm}^2/\text{sec} \quad (4.9)$$

where

$$A = 1.22 \times 10^{-5} + 3.11 \times 10^{-9}T \quad (4.10)$$

The constants employed in Equation 4.10 were determined from the predicted thermal conductivity values of Lee and Bobbitt (Ref. 4.8) for temperatures less than 8000°K. These constants were then used for the higher temperature predictions. The results of this correlation are given in Figure 4.8.

Binary Diffusion Coefficients: In view of the multiplicity of binary interactions required it was decided that the following Chapman-Enskog equation for the prediction of this property would be used (Ref. 4.11):

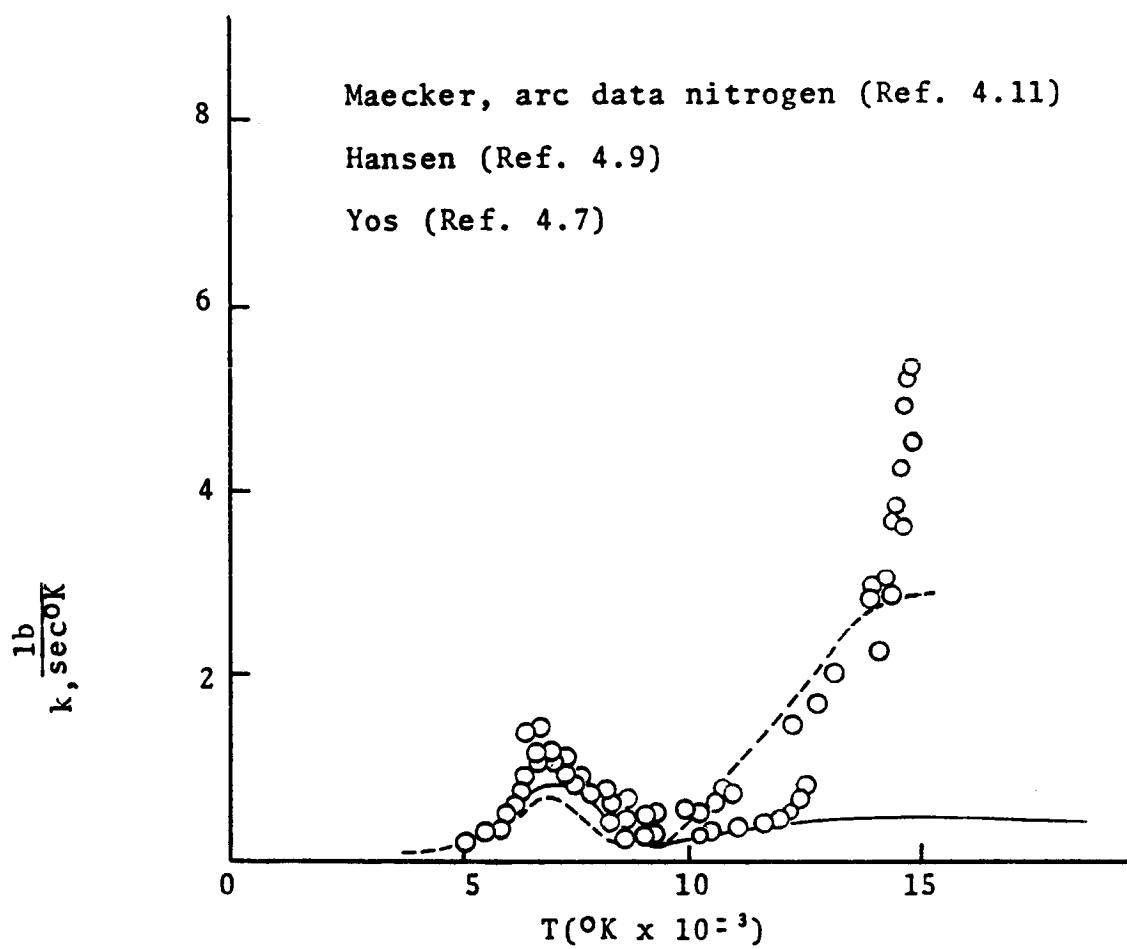


Figure 4.7. Total Thermal Conductivity of Air at One Atmosphere.

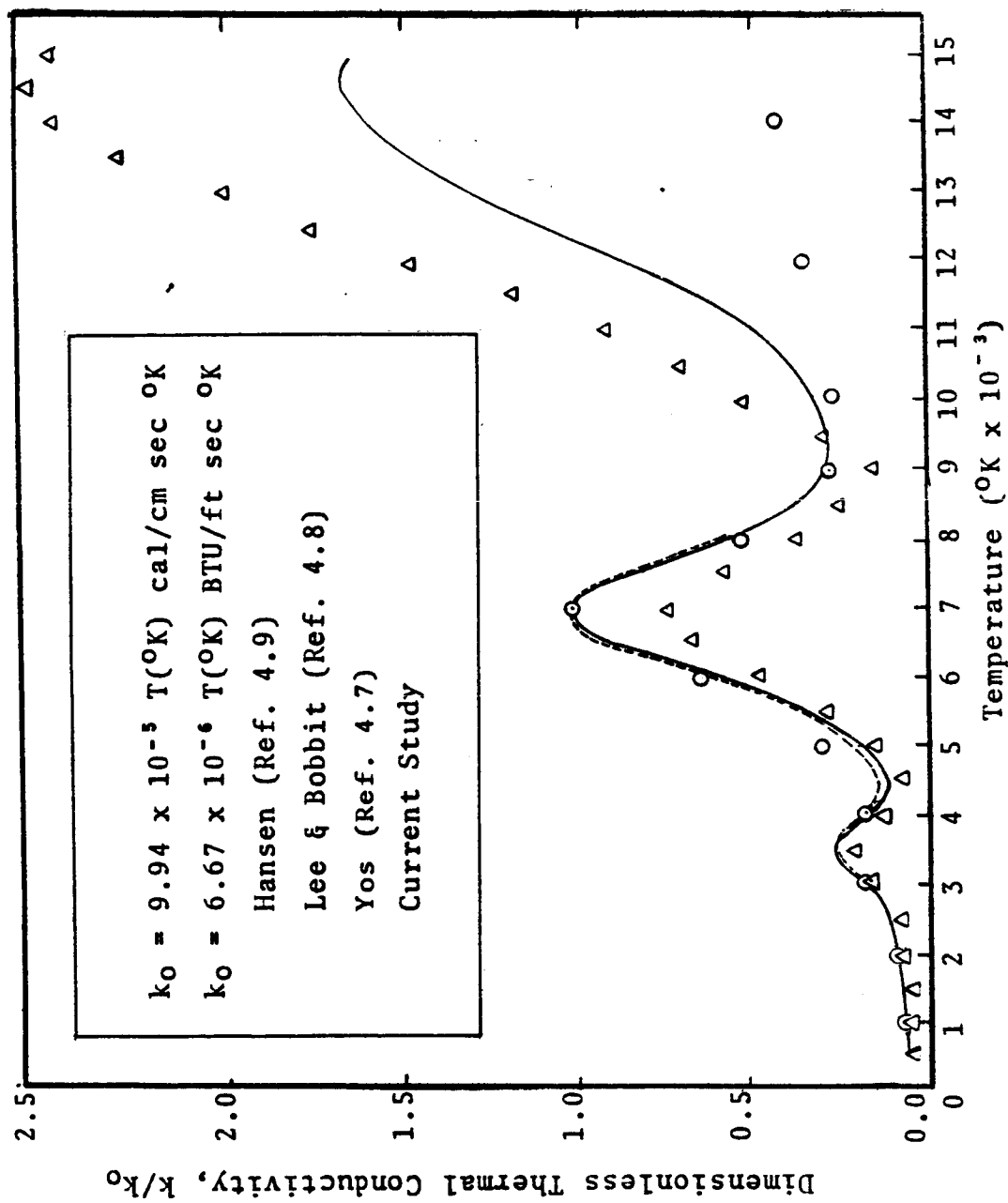


Figure 4.8. Comparison of Several Predictions of the Reacting Thermal Conductivity of Air at 1.0 Atmosphere Pressure.

$$\mathcal{Q}_{ij} = 28.28 \times 10^{-7} T^{3/2} \left(\frac{M_i + M_j}{2M_i M_j} \right)^{1/2} / P \sigma_{ij}^2 \Omega_{ij}^{(1,1)} \text{ ft}^2/\text{sec} \quad (4.11)$$

where $\sigma_{ij} = \frac{1}{2}(\sigma_i + \sigma_j)$, the quantities σ_i and σ_j being the collision diameters of the interacting species. The quantity, $\Omega_{ij}^{(1,1)}$ is the Lennard-Jones collision integral for diffusion as determined by the following empirical equation,

$$\Omega_{i,j}^{(1,1)} = 1.061 (T_{ij}^*)^{-1.56} \quad (4.12)$$

These constants were obtained from a curve-fit of the Lennard-Jones potential as reported by Hirschfelder in Reference 4.11 for $10 \leq T_{ij}^* \leq 1000$ which includes all species and temperatures considered in the current study. The quantity T_{ij}^* is computed as follows,

$$T_{ij}^* = \frac{T}{\epsilon_{ij}/k_c} \quad (4.13)$$

where $\epsilon_{ij} = \sqrt{\epsilon_i \epsilon_j}$, ϵ_i and ϵ_j being the characteristic interaction energies of species i and j .

Values for the collision parameters, σ_i and ϵ_i/k_c , for O_2 , N_2 , C , H , H_2 , CO , CN , C_2H_2 , HCN , and C_2 , were obtained from Svehla (Ref. 4.5). Since no data was available for C_3 , C_2H , C_3H , and C_4H , it was necessary to develop correlations based upon similar species. In Appendix C, the following correlations structure are developed for the prediction of the collision parameters of the above light hydrocarbon species.

Collision Diameter:

$$\sigma_i = 2.69 + 0.0514 M_i \quad (4.14)$$

Interaction Energy (C_n molecules):

$$\epsilon_i/k = -17.0 + 4.02 M_i \quad (4.15)$$

Interaction Energy (C_nH_n molecules):

$$\epsilon_i/k_c = -105. + 12.4 M_i \quad (4.16)$$

The collision parameters O , N , O^+ , N^+ and e^- were estimated from the theoretically determined binary diffusion coefficients reported by Yun, Wiessman, and Mason (Ref. 4.2) and by Yos (Ref. 4.7). The method of estimating these parameters from the rigorously determined theoretical data is also given in Appendix C.

The behavior of C^+ was then assumed to be similar to that of N^+ . A summary of the collision parameters employed in the present study is given in Table 4.3.

Thermodynamic Properties

Thermodynamic data is widely available (Refs. 4.12-4.17) for many substances relative to their values at absolute zero. Generally this data appears in the form of the thermodynamic functions, $(H_T^{\circ} - H_0^{\circ})/RT$ and $(F_T^{\circ} - H_0^{\circ})/RT$ where the superscript ($^{\circ}$) denotes the quantity at standard state (the pure component at one atmosphere pressure). The properties H_T° and F_T° computed from these functions will hereafter be referred to as "standard" properties. In the discussion to follow the required polynomial forms for curve-fits of this data are derived.

At constant pressure the following thermodynamic relations exist:

$$dH^{\circ} = C_p^{\circ} dT \quad (4.17)$$

$$dS^{\circ} = \frac{C_p^{\circ} dT}{T} \quad (4.18)$$

TABLE 4.3
COLLISION PARAMETERS EMPLOYED IN THE CURRENT STUDY

Species	M_i	σ_i	ϵ_i/k
O ₂	32.000	3.467	106.7
N ₂	28.016	3.798	71.4
O	16.000	7.990	106.7
N	14.008	7.940	71.4
O ⁺	16.000	14.220	106.7
N ⁺	14.008	14.930	71.4
e ⁻	5.486×10^{-4}	14.930	71.4
C	12.001	3.385	30.6
H	1.008	2.708	37.0
H ₂	2.016	2.827	59.7
C ₃	36.033	4.450	128.0
CN	26.019	3.856	75.0
C ₂ H	25.030	3.880	205.0
C ₂ H ₂	26.038	4.033	231.8
C ₃ H	37.041	4.600	356.0
C ₆ H	49.052	5.210	504.0
HCN	27.027	3.630	469.1
C ₂	24.022	3.913	78.8
C ⁺	12.011	15.000	30.6

Standard heat capacity data can be conveniently fitted to the following polynomial form:

$$C_p^0 = a_1 + a_2T + a_3T^2 + a_4T^3 + a_5T^4 \quad (4.19)$$

Substituting this relation into Equation 4.18 and integrating gives:

$$S_T^0 = a_1 \ln T + a_2T + \frac{a_3T^2}{2} + \frac{a_4T^3}{3} + \frac{a_5T^4}{4} + a_7 \quad (4.20)$$

where a_7 is an integration constant. The use of the indefinite integral here is necessary since the polynomial formulation yields an indeterminate expression at absolute zero; however, this does not present any difficulties at temperatures other than absolute zero.

The derivative of the standard free energy of a substance can be defined in terms of standard enthalpy and entropy as

$$dF^0 = dH^0 - d(TS^0) = dH^0 - Tds^0 - s_T^0dT \quad (4.21)$$

From Equations 4.17 and 4.18 it is noted

$$dH^0 = TdS^0 \quad (4.22)$$

therefore

$$dF^0 = - S_T^0 dT \quad (4.28)$$

Integrating this expression in temperature from absolute zero with S_T^0 defined by Equation 4.20 yields the following,

$$F_T^0 - F_0^0 = [a_1(\ln T - 1)T + \frac{a_2 T^2}{2} + \frac{a_3 T^3}{3} + \frac{a_4 T^4}{4} + \frac{a_5 T^5}{5} + a_7 T] \quad (4.24)$$

In general, standard free energy data is tabulated in non-dimensional form. Performing this nondimensionalization with the quantity RT and noting that $F_0^0 = H_0^0$ gives

$$\frac{F_T^0 - H_0^0}{RT} = A_1(1 - \ln T) - \frac{A_2 T}{2} - \frac{A_3 T^2}{6} - \frac{A_4 T^3}{12} - \frac{A_5 T^4}{20} - A_7 \quad (4.25)$$

where $A_1 = a_1/R$, $a_2 = a_2/R$, ..., $A_5 = a_5/R$ and $A_7 = a_7/R$. From Equations 4.17 and 4.18 the comparable polynomial expression for standard enthalpy can be derived.

$$\frac{H_T^0 - H_0^0}{RT} = A_1 + \frac{A_2 T}{2} + \frac{A_3 T^2}{3} + \frac{A_4 T^3}{4} + \frac{A_5 T^4}{5} \quad (4.26)$$

We have thus derived polynomial expressions for the thermodynamic functions of standard, heat capacity, entropy, enthalpy, and free energy relative to 0°K. In order to determine absolute values of enthalpy and free energy from these functions it is necessary to specify a reference state from which the enthalpy (and free energy) at absolute zero can be determined. It is convenient to select the elements at 298.16°K and one atmosphere pressure for the reference state, since this is widely used.

The reference state is established by defining the absolute enthalpy (H_T^0) of the elements equal to zero at 298.16°K. The enthalpy of an element at absolute zero (H_0^0) is then equal to the change in enthalpy from the reference temperature to absolute zero, or simply $(H_{298.16}^0 - H_0^0)$. For a compound the absolute enthalpy at the reference temperature is no longer equal to zero, but is equal to the heat of formation of the particular compound from the reference elements. Therefore, in order to determine the enthalpy of a compound at absolute zero from the tabulated enthalpy function it is necessary to correct for the heat of formation:

$$H_0^0 = - (H_{298.16}^0 - H_0^0) + (\Delta H_f)_{298.16} \quad (4.27)$$

where the quantity, $(H_{298.16}^{\circ} - H_0^{\circ})$ is available from the tabulated values of the enthalpy function. In non-dimensional form, this equation becomes

$$\frac{H_0^{\circ}}{RT} = \frac{(\Delta H_f)_{298.16} - (H_{298.16}^{\circ} - H_0^{\circ})}{RT} \quad (4.28)$$

Having defined a reference state, it is a simple matter to determine the thermodynamic properties from the thermodynamic functions as follows:

$$\frac{F_T^{\circ}}{RT} = A_1 (1 - \ln T) - \frac{A_2}{2} - \frac{A_3 T^2}{6} - \frac{A_4 T^3}{12} - \frac{A_5 T^4}{20} + \frac{A_6}{T} - A_7 \quad (4.29)$$

$$\frac{H_T^{\circ}}{RT} = A_1 + \frac{A_2}{2} T + \frac{A_3}{3} T^2 + \frac{A_4}{4} T^3 + \frac{A_5}{5} T^4 + \frac{A_6}{T} \quad (4.30)$$

where

$$A_6 = H_0^{\circ}/R = [(\Delta H_f)_{298.16} - (H_{298.16}^{\circ} - H_0^{\circ})] R \quad (4.31)$$

Thermodynamic data for the species of interest were fitted to the previously discussed polynomials by the method described in Appendix D. The resulting

coefficients (A_1, A_2, \dots, A_7) give predictions of free energy and enthalpy which reproduced the theoretical data to four significant figures. The maximum error in the entropy and heat capacity correlation was 2.12%. To further test the applicability of these results a free minimization technique,* using these correlations, was performed to determine the compositions which were then used with the enthalpy correlation to predict the total heat capacity of air by the following equation:

$$C_p = \sum Y_i C_{p_i}^0 + \sum H_i \frac{\partial Y_i}{\partial T} \quad (4.32)$$

The predicted results were then compared with those of other investigators as shown in Figure 4.9. Excellent agreement was obtained.

Radiation Properties

The radiative flux divergence (dq_R/dy) appearing in Equation 3.6 is defined as follows (Ref. 4.20):

$$\frac{dq_R}{dy} = \int_0^\infty \int_0^{4\pi} \alpha(y, \nu) [B(y, \nu) - I(y, \nu, \Omega)] d\Omega d\nu \quad (4.33)$$

where q_R = the radiative flux in the normal direction from the body,

$\alpha(y, \nu)$ = volumetric absorption coefficient,

*Described in Appendix E.

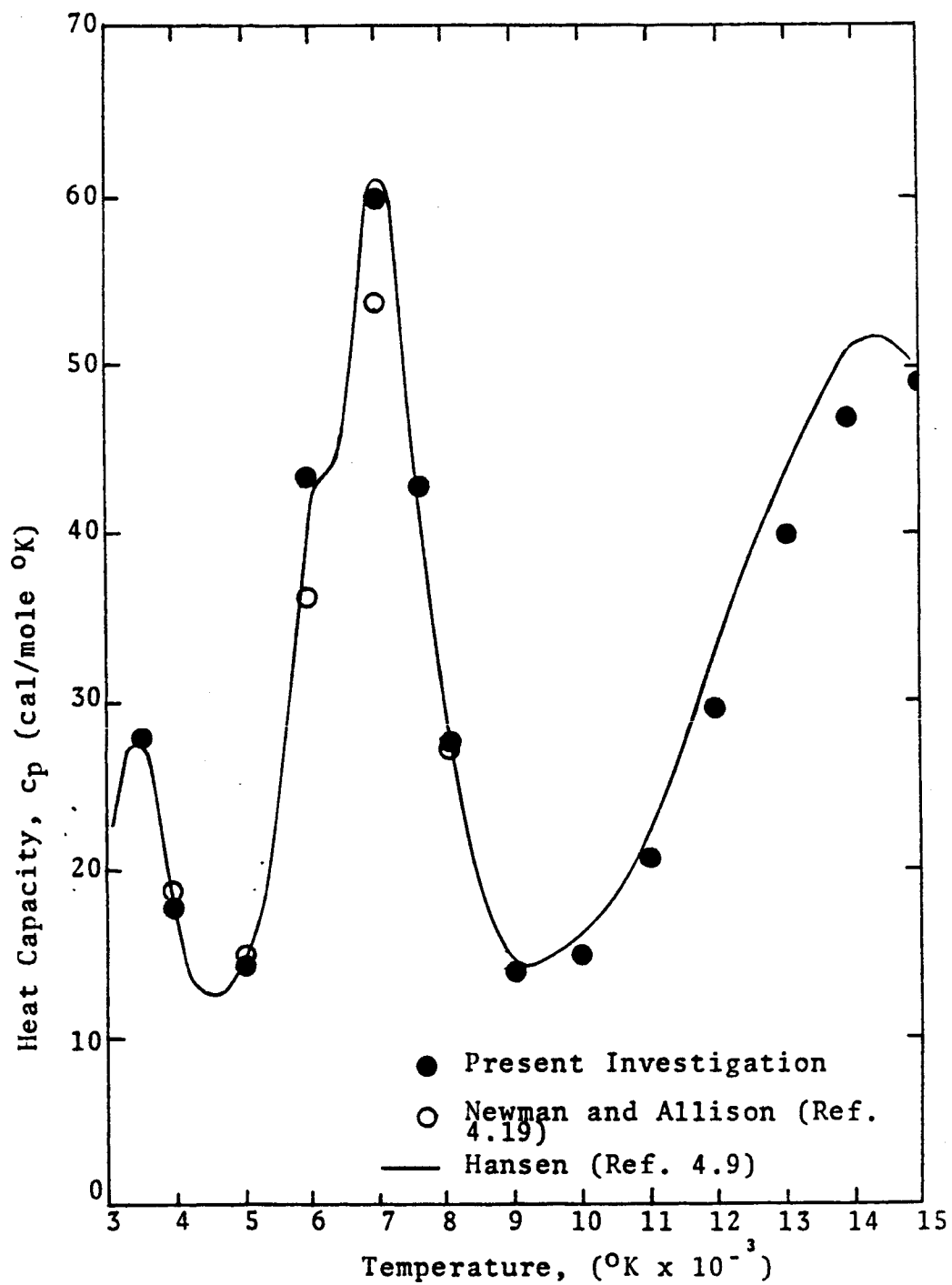


Figure 4.9. Comparison of Mixture Reacting Heat Capacity for Air and One Atmosphere.

$B(y, \nu)$ = Plankian radiation intensity,

$I(y, \nu, \Omega)$ = radiation intensity,

$d\Omega$ = solid angle about the unit vector $\bar{\Omega}$,

ν = frequency.

Given temperature and species distributions, the above integral can be evaluated theoretically. However, due to the discontinuous nature of the absorption coefficients numerical integration, in practice, is a formidable task. Typical absorption coefficient distributions are given in Figures 4.10 and 4.11 to illustrate the extent of this adversity (Ref. 4.24).

To overcome the numerical difficulties associated with the integration of distributions such as those given in Figures 4.10 and 4.11, the frequency range is arbitrarily sub-divided into regions (bands) with which the discontinuous variations are averaged. Continuum radiation bands are used to represent wider regions of continuous radiation while line bands are used to model the effects of the various discontinuous (line) contributions (see Figures 4.10 and 4.11). As in the numerical integration of continuous functions, the use of more bands leads to more accurate representation of the radiative process. In developing radiation models for computer implementation, some compromise must be made between the execution time and the number of bands.

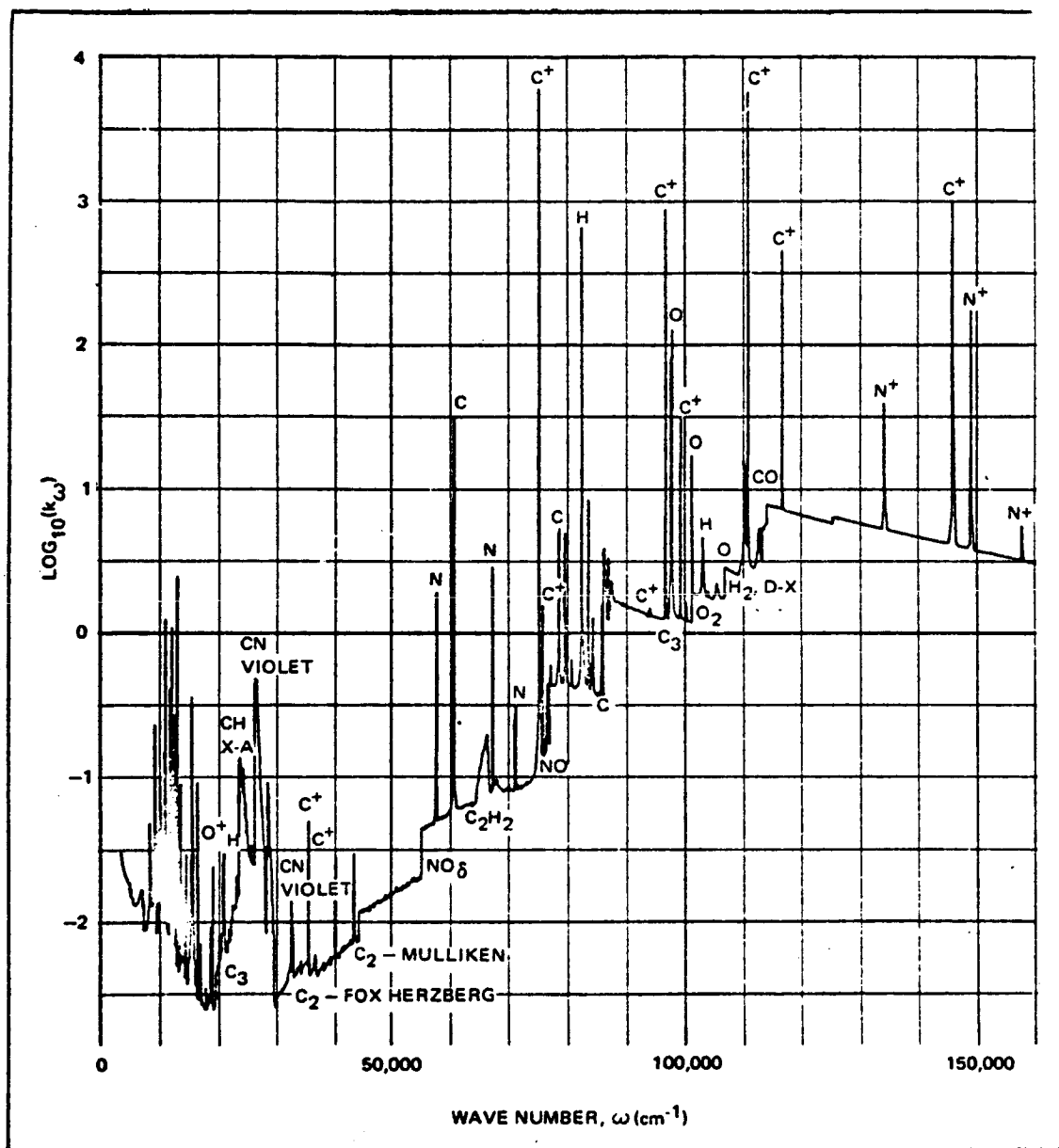
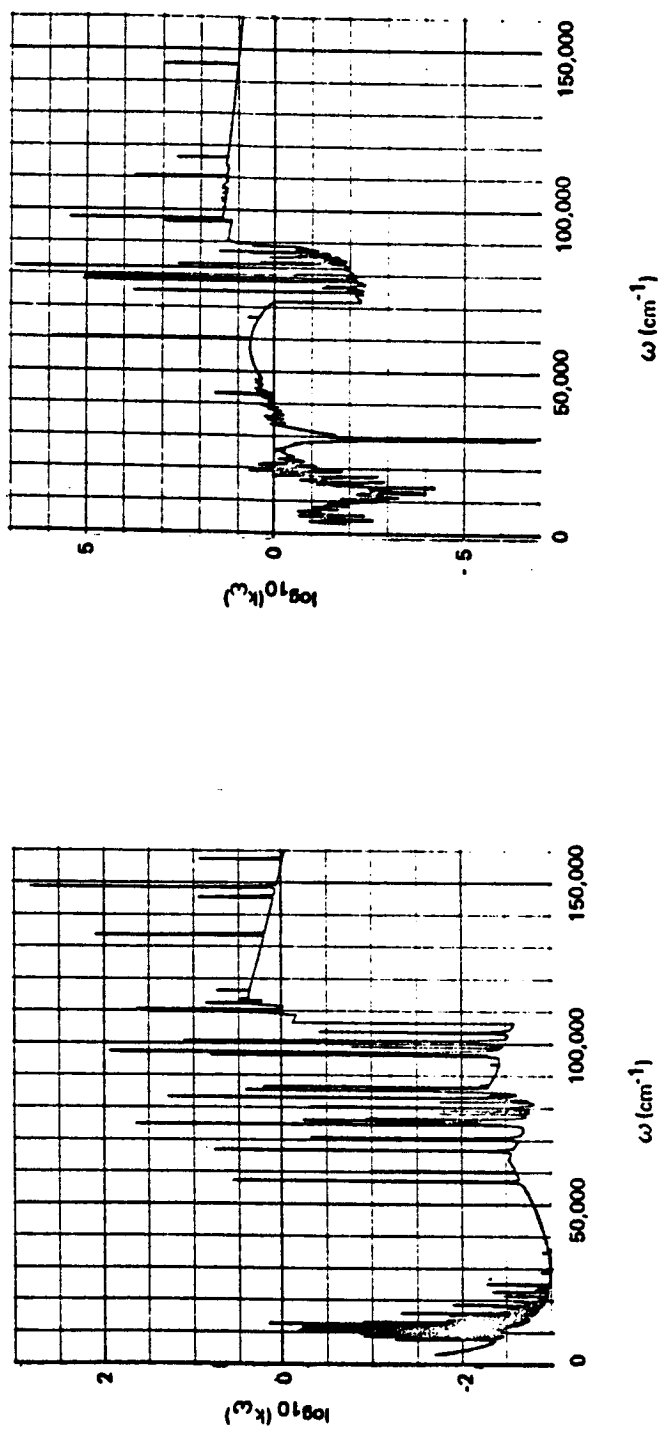


Figure 4.10. Spectral Absorption Coefficient of Air-Carbon Phenolic Ablation Products Mixture for $P = 1$ and $T = 16,000^\circ\text{K}$ (Ref. 4.24).



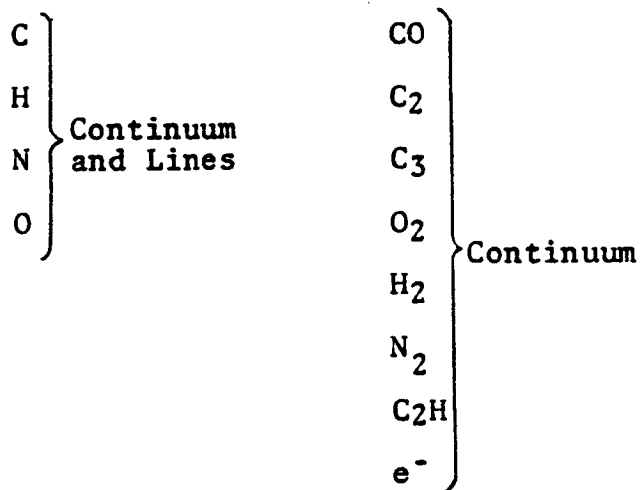
$T = 5,000^\circ\text{K}$, $CA = 1.0$

$T = 15,000^\circ\text{K}$, $CA = 0$

Figure 4.11. Typical Variation of k_ω Across the Shock Layer with Ablation Productions Injection (Ref. 4.24).

The radiation model used in the present work is a revision (Engel, Ref. 4.21) of a coupled line and continuum model originally developed by Wilson (Ref. 4.20). The program (LRAD3) provides a useful tool for evaluating the radiation flux and the radiative flux divergence across a slab of gas containing both air and ablation species.

The existing program contains twelve continuum frequency bands and nine line bands. A comparison with a more detailed model (RATRAP) in Reference 4.22, revealed that the existing analysis predicted total heat flux values within 5%. The following species are considered in the program used in the current study.



The program LRAD 3 was included in reduced form (air species only) in a program called VISRAD I which was developed by Spradley and Engel (Ref. 4.23). Figure 4.12 presents a comparison of dimensionless radiative heating rates as a function of free-stream velocity by several investigators. For this no mass injection case the comparison is quite reasonable. All investigators reported on this figure have line and continuum radiation calculations for air at stagnation line. Although this case does not contain the effects of ablation species, it is a standard for comparison of computational techniques.

Summary

Through the development of correlations from rigorously determined theoretical data an efficient means of predicting the high temperature transport and thermodynamic properties of ablation products and air species has been established. In so doing, the theoretically accurate properties can be well approximated without resorting to the more rigorous calculation procedures normally required for their prediction. These estimates are of course limited to the capabilities of the rigorous theoretical predictions. But, in the absence of sufficient experimental data, the rigorous

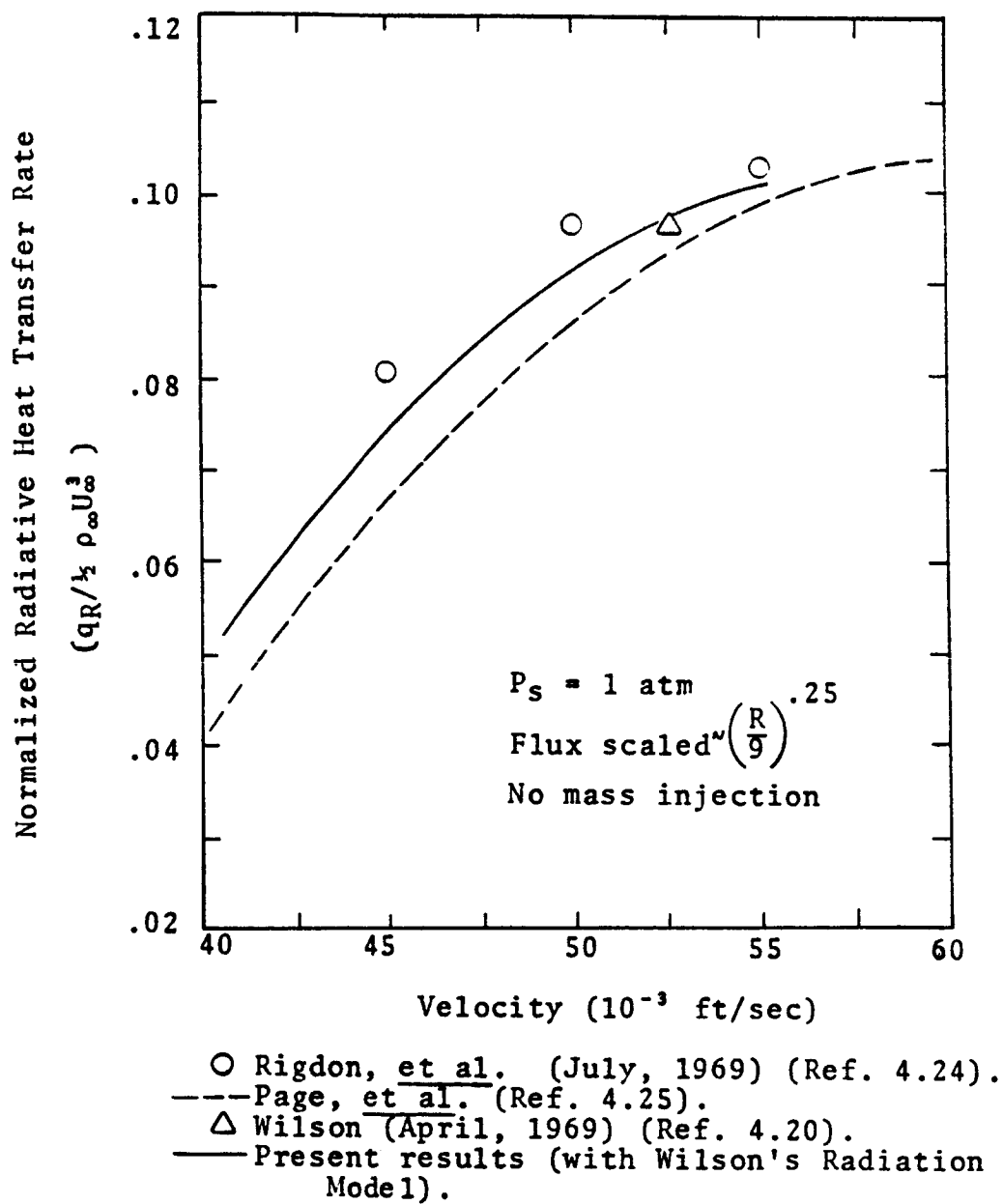


Figure 4.12. Comparison of Dimensionless Radiative Heating Rates (Ref. 4.21).

theoretical predictions as well as the correlations presented in this chapter represent the best available means of predicting transport and thermodynamic properties of the reacting gas mixtures encountered in the radiative heating of entry vehicles.

Finally, the radiative transport model employed in this study has shown excellent agreement with the predictions of models employed by other investigators and represents a well-balanced compromise between accuracy and computational convenience.

REFERENCES

- 4.1. Ahtye, W. F., "A Critical Evaluation of Methods for Calculating Transport Coefficients of Partially and Fully Ionized Gases," NASA TN D-2611, 1965.
- 4.2. Yun, Kwank-Sik, S. Weissman and E. A. Mason, "High-Temperature Transport Properties of Dissociating Nitrogen and Dissociating Oxygen," Phys. Fluids 5, 672 (1962).
- 4.3. Lasher, L. E., "The Effect of Carbon Gas Injection (Graphite Ablation) on the Stagnation-Point Compressible Boundary Layer," Masters Thesis, Cornell University, Ithaca, New York (1965).
- 4.4. Vanderslice, J. F., et.al., "High-Temperature Transport Properties of Dissociating Hydrogen," Phys. Fluids 5, 155 (1962).
- 4.5. Svehla, R. A., "Estimated Viscosities and Thermal Conductivities of Gases at High Temperatures," NASA TR R-132 (1962).
- 4.6. Buddenberg, J. W. and C. R. Wilke, Ind. Eng. Chem., 41, 1345-1347 (1949).
- 4.7. Yos, J. M., "Transport Properties of Nitrogen, Hydrogen, Oxygen, and Air to 30,000°K," AVCO RAD Technical Memorandum 63-7, (1963) as cited by Hoshizaki, op. cit.
- 4.8. Lee, J. S. and P. J. Bobbitt, "Transport Properties at High Temperatures of CO₂-N₂-O₂-Ar Gas Mixtures for Planetary Entry Applications."
- 4.9. Hansen, C. F., "Approximations for the Thermodynamic Properties of High Temperature Air," NASA TR R-50. 1959.

- 4.10. Maecker, H. "Thermal and Electrical Conductivity of Nitrogen Up to 15,000°K by Arc Measurements. Presented at meeting on Properties of Gases at High Temperatures. AGARD, Aachen, September 21-23, 1959.
- 4.11. Hirschfelder, J. O., Curtiss, C. F. and Bird, R. B., Molecular Theory of Gases and Liquids, 2nd printing, corrected with notes added, John Wiley and Sons, Inc., New York (1964).
- 4.12. Browne, W. G., "Thermodynamic Properties of Some Atoms and Atomic Ions," General Electric Co. MSVD Engr. Physics Tech. Memo. No. 2 (May 14, 1962).
- 4.13. Browne, W. G., "Thermodynamic Properties of Some Diatoms and Diatomic Ions," General Electric Co. MSVD Engr. Physics Tech. Memo. No. 8, (May 14, 1962).
- 4.14. Browne, W. G., "Thermodynamic Properties of the Species CN, C₂, C₃, C₂N₂ and C⁻," General Electric Co. MSVD Engr. Physics Tech. Memo. No. 9, (May 14, 1962).
- 4.15. Browne, W. G., "Thermodynamic Properties of Some Ablation Products from Plastic Heat Shields in Air," General Electric Co. MSVD Engr. Physics Tech. Memo. No. 11, (March 15, 1964).
- 4.16. Gurvich, A. B., et.al., "Thermodynamic Properties of Individual Substances," Vols. 1-3, Foreign Technology Division, Wright Patterson Air Force Base, Ohio, AD 659 659, AD 659 660 and AD 659 679 (May, 1967).
- 4.17. Stull, D. R., et. al., JANAF Thermochemical Tables. The Dow Chem. Co., Midland, Michigan (Dec. 31, 1960-Sept. 30, 1962).
- 4.18. Browne, H. N., M. W. Williams and D. R. Cruise, "Theoretical Computation of Equilibrium Compositions, Thermodynamic Properties and Performance Characteristics of Propellant Systems," U.S. Naval Ordnance Test Station NAVWEPS, Rept. 7043, June 1960.

- 4.19. Newman, P. A. and D. O. Allison, "Direct Calculations of Specific Heats and Related Thermodynamic Properties of Arbitrary Gas Mixtures with Tabulated Results," NASA TN D-3540 (1966).
- 4.20. Wilson, K. H., "Stagnation Point Analysis of Coupled Viscous-Radiating Flow with Massive Blowing," LMSC-687209, April 1969.
- 4.21. Engel, D. C., "Ablation and Radiation Coupled Viscous Hypersonic Shock Layers," Ph.D. Dissertation, Louisiana State University, Baton Rouge, Louisiana (1971).
- 4.22. Wilson, K. H. and H. Hoshizaki, "Effect of Ablation Product Absorption and Line Transitions on Shock Layer Radiative Transport," NASA CR-1264, 1969.
- 4.23. Spradley, L. W. and C. D. Engel, "A Computer Program for Predicting Coupled Convective and Radiative Heat Transfer to a Blunt Body During Superorbital Reentry," LMSC/HREC A791350, Lockheed Missiles and Space Company, Huntsville, Ala., May, 1968.
- 4.24. Rigdon, W. S., R. B. Dirling and M. Thomas, "Stagnation Point Heat Transfer During Hypervelocity Atmospheric Entry," NASA CR-1462, 1970.
- 4.25. Page, W. A., et al., "Radiative Transport in Inviscid Nonadiabatic Stagnation-Region Shock Layers," AIAA Paper No. 68-784, AIAA 3rd Thermophysics Conference, June 1968.

CHAPTER V

NUMERICAL IMPLEMENTATION OF THIN
SHOCK LAYER EQUATIONS

Introduction

In the previous chapters the thin shock layer equations have been developed in a form which is convenient for numerical implementation. In addition, convenient models have been developed for predictions of the necessary thermodynamic, transport, and radiative properties. This chapter will consist of a detailed description of the numerical implementation of the previously developed flowfield equations and property models to obtain a fully coupled analysis of stagnation region heating of ablative thermal protection systems.

The method of presentation will be to first outline the overall analysis with a general description of the logical process. Secondly, each of the major subprograms related to the numerical solution of the conservation equations will be separately discussed in detail. The discussion will then be concluded with a review of the computational experience with the overall analysis.

Coupled Stagnation Line Analysis With Binary Diffusion

A simplified flow diagram of the overall stagnation line analysis (SLAB)** as developed in this study is given in Figure 5.1. The major input data consist of free-stream velocity (U_∞), a free-stream density (ρ_∞), body radius (R), wall temperature (T_w), and mass injection rate (RVW), initial estimates of T , ρ , and ρu profiles and the transformed shock standoff distance $\tilde{\delta}$.* Also included are initial estimates of the injected gas compositions which have elemental ratios consistent with the selected ablator. The initialization phase consists primarily of determining the shock temperature (T_s), the normal velocity at the shock (v_s) and the pressure (P_s) from the Rankine-Hugoniot Equations (Eqs. 3.81-3.84) using the specified values of free-stream velocity (U_∞) and density (ρ_∞).

From the specified ρ and ρu profiles and the specified, transformed stand-off distance $\tilde{\delta}$, the momentum equation (Eq. 3.99) is solved to obtain an estimate of the velocity profile (MOMTM). Using the computed velocity profile and the assumed temperature and density profiles, the elemental continuity equations (Eq. 3.88) are then solved (ELEMNT). The chemical equilibrium calculation (CHEMEQ) is then performed to determine the species

*A more detailed description of these and other input parameters is given in Appendix F.

**Developed in collaboration with C. D. Engel (Ref. 5.6).

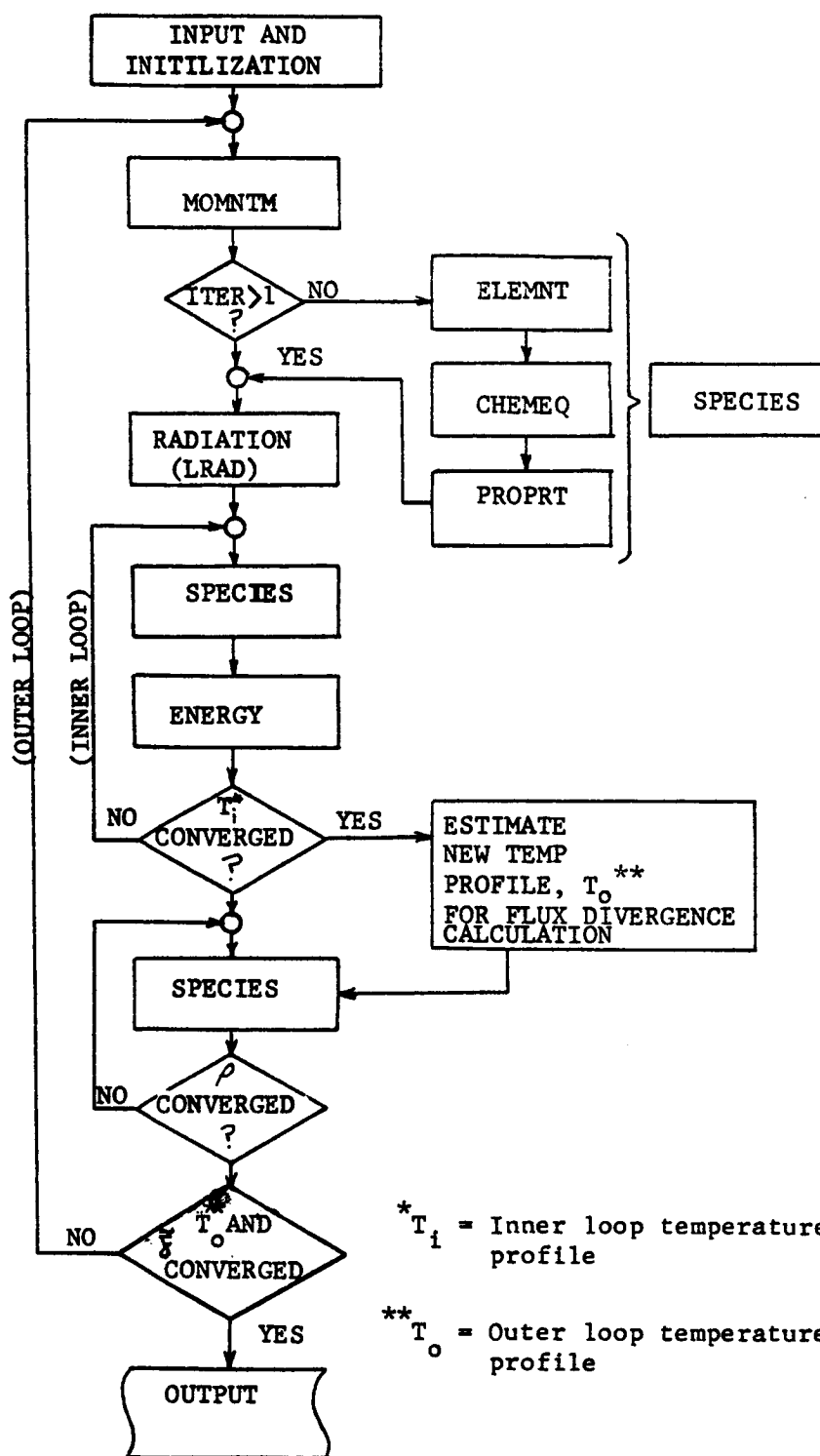


Figure 5.1. Simplified Flow Diagram for Stagnation Line Heating Analysis with Binary Diffusion (SLAB).

composition profiles. The reacting gas properties are then determined (PROPRT) along with the radiative flux divergence ($dq_R/d\eta$) from LRAD. From the flux divergence and the gas properties, the temperature profile is determined (ENERGY). The computed temperature profile is used with the previous density and velocity profiles to obtain revised thermodynamic and transport property distributions which are in turn used to compute a new temperature profile. This process is repeated until convergence is achieved. From the final temperature profile and the initial temperature profile (on which the radiative flux divergence was based), a new profile is estimated for the next cycle through the outer loop (See Figure 5.1). The density profile is then updated to correspond to the revised temperature distribution and the last computed velocity distribution. The outer loop is repeated until the momentum and energy solutions and the shock standoff distance have simultaneously converged.

Numerical Solution of the Conservation Equations:

The basic conservation equations (Eqs. 3.97, 3.99 and 3.100) can be reduced to the form:

$$\frac{d^2W}{d\eta^2} + a_1 \frac{dW}{d\eta} + a_2 W = a_3 \quad (5.1)$$

Using three point, variable step size, finite-difference approximation at $(s-2)^*$ points across the flowfield, the numerical form of the equations becomes

$$\bar{A} \cdot W = B$$

where \bar{A} is a tridiagonal matrix of order $(s-2)$. This form lends itself to numerical solution by a tridiagonal matrix inversion algorithm (Ref. 5.1). The specific treatment of the basic conservation equations is the subject of the following discussion.

Elemental Continuity Equations: Assuming binary diffusion, the elemental continuity equations (Eqs. 3.97) can be expressed in the following form,

$$\frac{d^2 C_j}{d\eta^2} + a_1 \frac{dC_j}{d\eta} = 0 \quad j=1, 2, \dots, \ell \quad (5.3)$$

where

$$a_1 = 2 \frac{d \ln \rho}{d\eta} + \frac{d \ln \Delta_{12}}{d\eta} - \frac{v \tilde{\delta}}{\rho \Delta_{12}} \quad (5.4)$$

The shock boundary conditions (of the first kind) for the elemental continuity equations are the elemental composition of air ($C_{N,s} = 0.774$ and $C_{O,s} = 0.226$).

*Point 1 is at the wall and point s is at the shock. Finite differencing is required only at the intermediate points, since the extreme values established as boundary conditions.

The boundary conditions at the wall can be obtained from Equations 3.59 as follows:

$$\rho v \tilde{C}_j^+ + \tilde{J}_j^+ = \rho v \tilde{C}_j^- + \tilde{J}_j^- = \tilde{I}_j = \left[\begin{array}{l} \text{total mass flux} \\ \text{of element } j \text{ at} \\ \text{the wall} \end{array} \right] \quad (5.5)$$

where the quantity I_j is determined from the product of the elemental composition of the ablator (\tilde{C}_j^-) and the mass injection rate (ρv) wall. Assuming binary diffusion:*

$$\tilde{J}_j = - \frac{\rho^2 \mathcal{D}_{12}}{\delta} \frac{d\tilde{C}_j}{dn} \quad (5.6)$$

Equation 5.5 can be written as

$$\rho v \tilde{C}_j - \rho^2 \frac{\mathcal{D}_{12}}{\delta} \frac{d\tilde{C}_j}{dn} = \tilde{I}_j \quad (5.7)$$

A boundary condition of the third kind is thus obtained for each of the elemental continuity equations. The treatment of this type of boundary condition will be subsequently discussed.

The binary diffusion coefficient appearing in the previous equations is determined from the following form of the Chapman-Enskog Equation (Eq. 2.32),

$$\mathcal{D}_{12} = A T^{1.656} / P \quad (\text{ft}^2/\text{sec}) \quad (5.8)$$

*Equation 5.6 is obtained from the Dorodnitsn transformation of Equation 3.23.

where,

$$A = \frac{26.65 \times 10^{-7} \sqrt{\frac{M_i + M_j}{2M_i M_j}}}{\sigma_{ij}^2 (\epsilon_{ij}/k_c)^{0.156}}$$

The quantity A, which is independent of temperature and pressure, is thus defined as the characteristic diffusion parameter, since it is a function only of the selected collision data. Typical elemental composition profiles of carbon as a function of the characteristic diffusion parameter are given in Figure 5.2.

Assuming velocity, density, and temperature profiles, the elemental continuity equation can be solved in the following manner. First, finite-differencing the third order wall boundary condition gives

$$(\rho v C_i)_1 - \frac{(\rho \Delta)_{12}}{\delta} \left(\frac{\tilde{C}_{j,2} - \tilde{C}_{j,1}}{\eta_2 - \eta_1} \right) = \tilde{I}_j \quad (5.9)$$

Rearranging and noting that $\eta_1 = 0$ yields

$$B_1 \tilde{C}_{i,1} + C_1 \tilde{C}_{i,2} = \tilde{I}_j \quad (5.10)$$

where

$$B_1 = 1 + \frac{(\rho \Delta)_{12}/v}{\delta \eta_2} \quad (5.11)$$

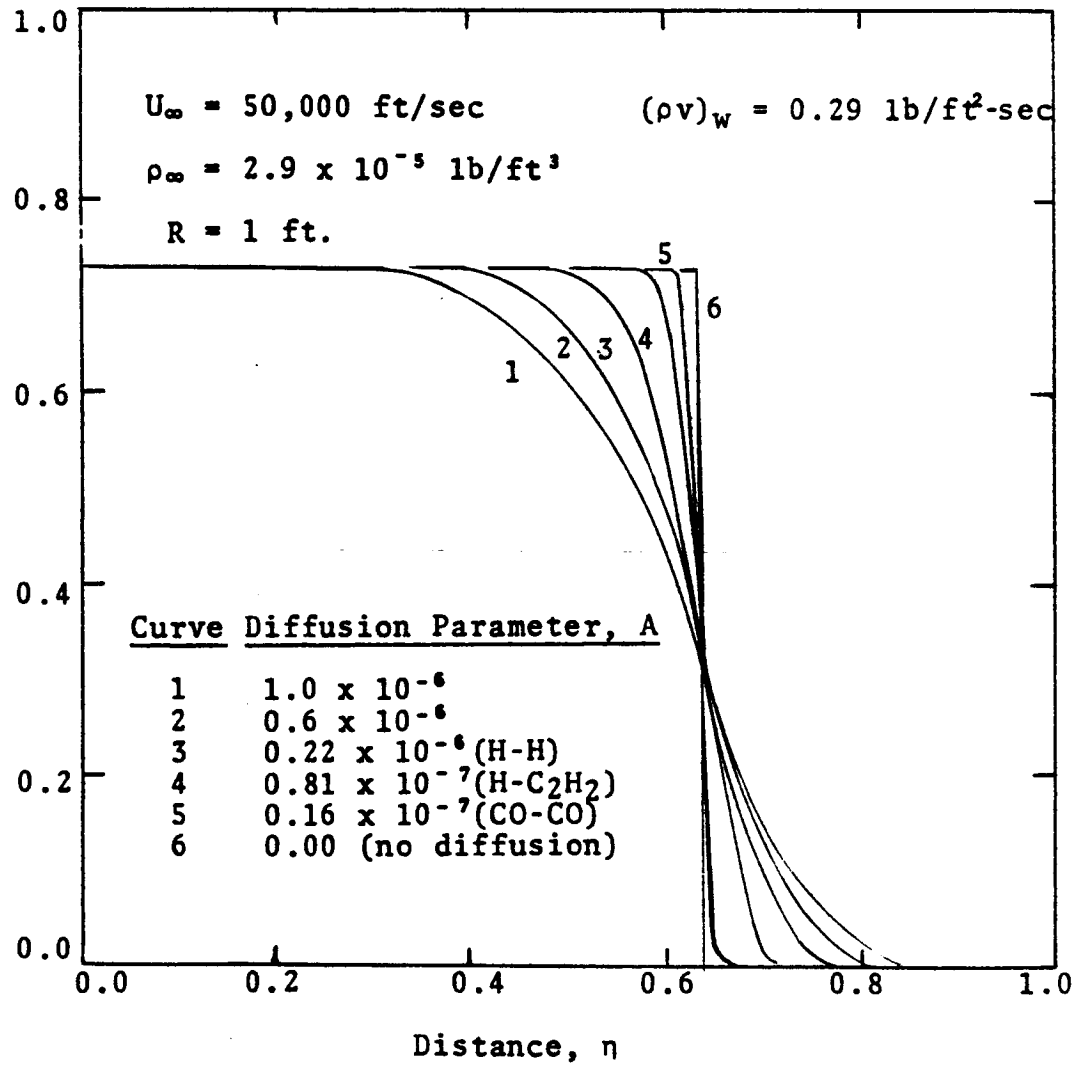


Figure 5.2. Composition Profiles of Elemental Carbon With Various Characteristic Diffusion Parameters.

and

$$C_1 = - \frac{(\rho \omega)_{12}/v)_1}{\delta \eta_2} \quad (5.12)$$

Equation 5.10 is in a form that will fit into the tridiagonal matrix scheme as will be discussed.

At each subsequent grid point in the flowfield, the derivative terms are then approximated by the following variable step-size finite-difference equations (Ref. 5.8),

$$\frac{dW}{d\eta}_n = F_n^1 W_{n+1} + G_n^1 W_n + H_n^1 W_{n-1} \quad (5.13)$$

and

$$\frac{d^2W}{d\eta^2} = F_n^2 W_{n+1} + G_n^2 W_n + H_n^2 W_{n-1} \quad (5.14)$$

where

$$F_n^1 = \Delta \eta_{n-1} / \Delta \eta_n (\Delta \eta_n + \Delta \eta_{n-1}) \quad (5.15)$$

$$G_n^1 = (\Delta \eta_n - \Delta \eta_{n-1}) / (\Delta \eta_n \Delta \eta_{n-1}) \quad (5.16)$$

$$H_n^1 = -\Delta \eta_n / \Delta \eta_{n-1} (\Delta \eta_n + \Delta \eta_{n-1}) \quad (5.17)$$

$$F_n^2 = 2 / \Delta \eta_n (\Delta \eta_n + \Delta \eta_{n-1}) \quad (5.18)$$

$$G_n^2 = -2 / \Delta \eta_n \Delta \eta_{n-1} \quad (5.19)$$

$$H_n^2 = 2 / \Delta \eta_{n-1} (\Delta \eta_n + \Delta \eta_{n-1}) \quad (5.20)$$

In finite-differenced form, the transformed elemental continuity equations (Eqs. 5.3) thus become

$$\begin{aligned} (H_n^2 + a_{1,n}H_n^1) \tilde{C}_{j,n-1} + (G_n^2 + a_{1,n}G_n^1) \tilde{C}_{j,n} \\ + (F_n^2 + a_{1,n}F_n^2) \tilde{C}_{j,n+1} = 0 \end{aligned} \quad (5.21)$$

which is of the form:

$$A_n \tilde{C}_{j,n-1} + B_n \tilde{C}_{j,n} + C_n \tilde{C}_{j,n+1} = 0$$

Performing this operation at each finite-difference station to $n = s-1$, yields the following matrix form (see Figure 5.3)

$$\begin{bmatrix} B_1 & C_1 & & & & & \\ A_2 & B_2 & C_2 & & & & \\ & A_3 & B_3 & C_3 & & & \\ & & \cdot & \cdot & \cdot & & \\ & & & \cdot & \cdot & \cdot & \\ & & & & \cdot & \cdot & \cdot \\ & & & & & A_{s-2} & B_{s-2} & C_{s-2} \\ & & & & & & A_{s-1} & B_{s-1} \end{bmatrix} \cdot \begin{bmatrix} \tilde{C}_{j,1} \\ \tilde{C}_{j,2} \\ \tilde{C}_{j,3} \\ \cdot \\ \cdot \\ \cdot \\ \tilde{C}_{j,s-2} \\ \tilde{C}_{j,s-1} \end{bmatrix} = \begin{bmatrix} -\tilde{I}_j \\ o \\ o \\ \cdot \\ \cdot \\ \cdot \\ o \\ C_{s-1} \tilde{C}_{j,s} \end{bmatrix} \quad (5.22)$$

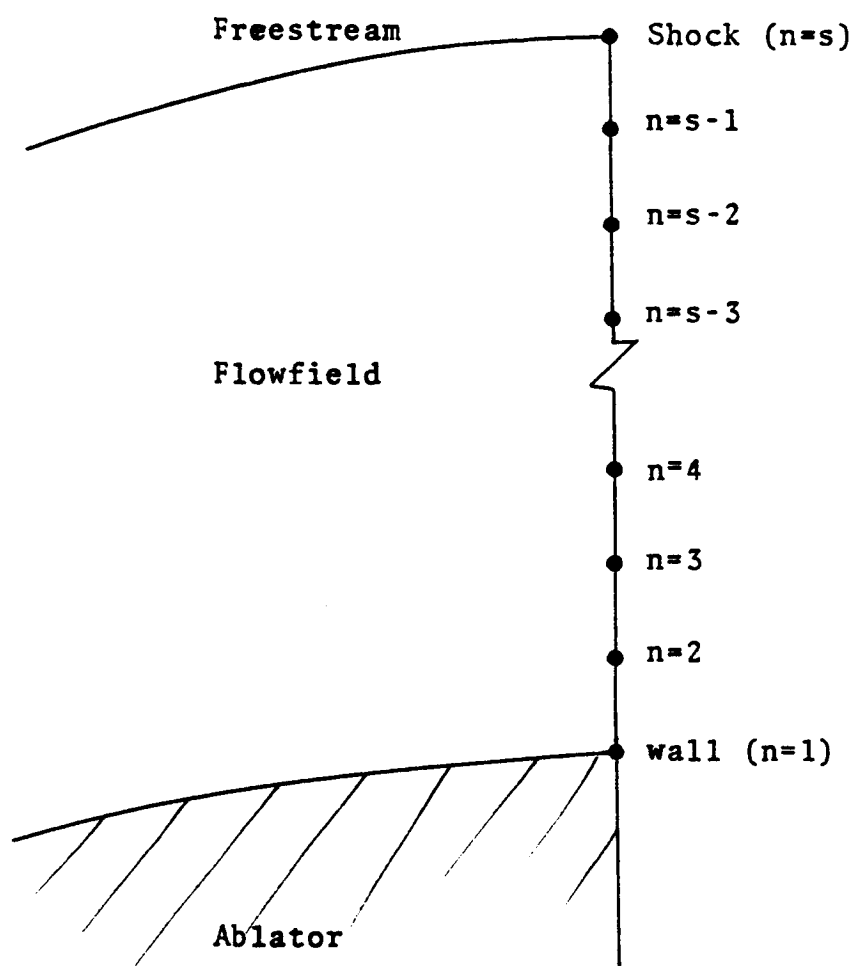


Figure 5.3. Illustration of One-dimensional Finite-difference Network.

Equation 5.22 was solved by the tridiagonal inversion algorithm program given by Conte (Ref. 5.1) and implemented in the Fortran Subprogram TRID appearing in the overall listing given in Appendix F.

The variable stepsize distribution employed in this analysis was determined from the temperature distribution, with the maximum size being $\Delta\eta = 0.04$. Generally, 55-60 steps are generated between $\eta = 0.0$ and $\eta = 1.0$. The convergence of the numerical solution of Equation 5.22 was verified by reducing the stepsize and comparing the resulting solutions. Such a comparison is given in Table 5.1. The maximum difference detected by this comparison was 0.0063. It was therefore concluded that the numerical procedure was convergent. The numerical procedure discussed in this section was implemented in the Fortran subroutine ELEMNT, a listing of which appears in the overall program listing given in Appendix F.

Momentum Equation: The solution of the momentum equation (Eq. 3.99) follows essentially the same procedure as the previously discussed elemental solution. The major difference is that the momentum equation is non-linear. The solution technique, developed by Engel (Ref. 5.2) is given in the following discussion.

TABLE 5.1

COMPARISON OF ELEMENTAL CARBON DISTRIBUTION
FOR ETA DISTRIBUTIONS OF 59 AND 126
STEPS

η^*	$\tilde{C}_C (s = 59)$	$\tilde{C}_C (s = 126)$
0.000	0.6921	0.6909
0.045	0.6762	0.6742
0.080	0.6485	0.6459
0.100	0.6228	0.6199
0.140	0.5410	0.5392
0.180	0.4211	0.4229
0.220	0.2914	0.2977
0.260	0.1859	0.1915
0.300	0.1108	0.1136
0.350	0.0511	0.0517
0.380	0.0290	0.0293
0.440	0.0066	0.0068
0.500	0.0007	0.0009
0.540	0.0001	0.0001
0.560	0.0000	0.0000
1.000	0.0000	0.0000

*Selected points

Integration of Equation 3.95, gives

$$\rho v = -2 \left(\frac{\partial u}{\partial x} \right)_s \delta f \quad (5.23)$$

which can be used to eliminate ρv in the momentum equation (Eq. 3.99). This substitution yields the following third order nonlinear ordinary differential equation,

$$\begin{aligned} (\rho u f'')' + 2 \text{Re}_s \tilde{\delta}^2 \left(\frac{\partial u}{\partial x} \right)_s f f'' + \\ \frac{\text{Re}_s \tilde{\delta}^2}{(\partial u / \partial x)_s} \left[\frac{2\bar{\rho}(1-\bar{\rho})}{\bar{\rho}} \left(\frac{\partial u}{\partial x} \right)_s^2 \right] (f')^2 = 0 \end{aligned} \quad (5.24)$$

The boundary conditions for these equations are established in the development to follow. From Equation 3.27 and L'Hospital's rule gives:

$$\lim_{x \rightarrow 0} f' = \lim_{x \rightarrow 0} \frac{(\partial u / \partial x)}{(\partial u / \partial x)_s} = \frac{u}{u_s} \quad (5.25)$$

At $x = 0$ and $\eta = 1$, $u = u_s$, therefore $f' = 1$. Similarly, at $x = 0$ and $\eta = 0$, $u = 0$, therefore $f' = 0$. A third boundary condition is obtained by evaluating Equation 5.23 at the wall*

$$f = f_w = \frac{(\rho v)_w}{2\tilde{\delta}} \quad (5.26)$$

*For a concentric shock, it can be shown from Equation 3.78 that $(\partial u / \partial x)_s = 1$.

The momentum equation (Eq. 5.24) can be reduced to a first and a second order equation by defining

$$\zeta = \frac{f'}{\tilde{\delta}} \quad (5.27)$$

Substitution of Equation 5.27 into 5.24 and noting that $(\partial u / \partial x)_s = 1$ for a concentric shock gives,

$$\begin{aligned} (\rho u) \zeta'' + [2 \operatorname{Re}_s \tilde{\delta}^2 f + (\rho u)'] \zeta - \operatorname{Re}_s \tilde{\delta}^3 \zeta^2 \\ = \frac{-2 \operatorname{Re}_s \tilde{\delta} \bar{\rho} (1 - \bar{\rho})}{\rho} \end{aligned} \quad (5.28)$$

The resulting boundary conditions for Equation 5.28 are:

$$\zeta = \zeta_1 = 0 \quad \text{at } \eta = 0 \quad (5.29)$$

$$\zeta = \zeta_2 = 1/\tilde{\delta} \quad \text{at } \eta = 1 \quad (5.30)$$

In order to obtain a linear second order equation of the form of Equation 5.1, it is necessary to linearize Equation 5.28. The nonlinear term (ζ^2) is therefore quasilinearized in the manner of Lee (Ref. 5.3):

$$(\zeta^2)^{k+1} = (\zeta)^k + 2 \zeta^k (\zeta^{k+1} - \zeta^k) \quad (5.31)$$

where k is the iteration number. Substitution of Equation 5.31 into the non-linear equation (Eq. 5.28) gives the following linear second order, ordinary differential equation:

$$\begin{aligned} \zeta'' + \left[\frac{2 \operatorname{Re}_s \delta^2}{\rho \mu} f^k + \frac{(\rho \mu)'}{\rho \mu} \right] \zeta' - \frac{2 \operatorname{Re}_s \delta^3}{\rho \mu} \zeta \\ = - 2 \operatorname{Re}_s \tilde{\delta} \left[\bar{\rho} \frac{(1 - \bar{\rho})}{\rho \mu} + \frac{\tilde{\delta}^2}{2 \rho \mu} \zeta^{2(k)} \right] \end{aligned} \quad (5.32)$$

where the superscript k is used to designate values computed from the previous iteration. Equation 5.32 is now of the form of Equation 5.1 and can therefore be finite-differenced by Equation 5.13 through 5.20 to obtain the following form:

$$A_n \zeta_{n-1} + B_n \zeta_n + C_n \zeta_{n+1} = D_n \quad (5.33)$$

where

$$A_n = H_n^2 + \alpha_n H_n' \quad (5.34)$$

$$B_n = G_n^2 + \alpha_n H_n' + \beta_n \quad (5.35)$$

$$C_n = F_n^2 + \alpha_n F_n' \quad (5.36)$$

$$D_n = - \frac{2 \operatorname{Re}_s \tilde{\delta}}{\rho_n \mu_n} \left[\bar{\rho} (1 - \bar{\rho}) + \tilde{\delta}^2 \zeta_n^{2(k)} \right] \quad (5.37)$$

$$\alpha_n = \frac{2 \operatorname{Re}_s \tilde{\delta}^2 f_n^k}{(\rho \mu)_n} + \frac{(\rho \mu)_n'}{(\rho \mu)_n} \quad (5.38)$$

and

$$\beta_n = - 2 \operatorname{Re}_s \tilde{\delta}^3 \quad (5.39)$$

Finite-differencing at each station yields the following matrix equation,

$$\begin{bmatrix} B_2 & C_2 & & & \\ A_3 & B_3 & C_3 & & \\ & A_4 & B_4 & C_4 & \\ & & \cdot & \cdot & \cdot \\ & & & \cdot & \cdot & \cdot \\ & & & & A_{s-1} & B_{s-1} \end{bmatrix} \begin{bmatrix} \zeta_2 \\ \zeta_3 \\ \cdot \\ \cdot \\ \cdot \\ \zeta_{s-1} \end{bmatrix} = \begin{bmatrix} D_2 - A_2 \zeta_1 \\ D_3 \\ \cdot \\ \cdot \\ \cdot \\ D_{s-1} - C_{s-1} \zeta_s \end{bmatrix} \quad (5.40)$$

which can be solved by the previously discussed tridiagonal matrix inversion subroutine (TRID).

The f profile is then determined by integration of Equation 5.27,

$$f = \tilde{\delta} \int_{\eta=0}^{\eta=1} \zeta \, d\eta + f_w \quad (5.41)$$

Using a simple trapezoidal scheme (QUAD).

The transformed stand off distance, $\tilde{\delta}$, is computed from f_s (Equation 5.41 evaluated at $\eta=1$) and Equation 5.23 evaluated at $\eta=1$.

$$\tilde{\delta} = - \frac{(\rho v)_s}{2f_s} \quad (5.42)$$

This computed value of $\tilde{\delta}$ is then compared to the assumed value and a new value estimated. The calculation is repeated until convergence of $\tilde{\delta}$ is achieved ($\Delta\tilde{\delta} \leq 0.001$). The actual standoff distance is then computed as

$$\delta = \tilde{\delta} \int_0^1 \rho \, d\eta \quad (5.43)$$

Again, using the simple trapezoidal scheme (QUAD). Numerical convergence of the momentum solution was verified in the same manner as the elemental equations. In Figure 5.4 a comparison is given of the results of this method to those obtained by Howe and Vegas (Ref. 5.9). The agreement is seen to be quite good.

Energy Equation: The energy equation (Eq. 5.101) is second order and linear in temperature and therefore does not require quasilinearization. Finite-differencing Equation 3.101 using the difference approximations of Equations 5.13 and 5.14 gives,

$$A_n T_{n-1} + B_n T_n + C_n T_{n+1} = D_n \quad (5.44)$$

where

$$A_n = H_n^2 + \alpha_n H_n^1 \quad (5.45)$$

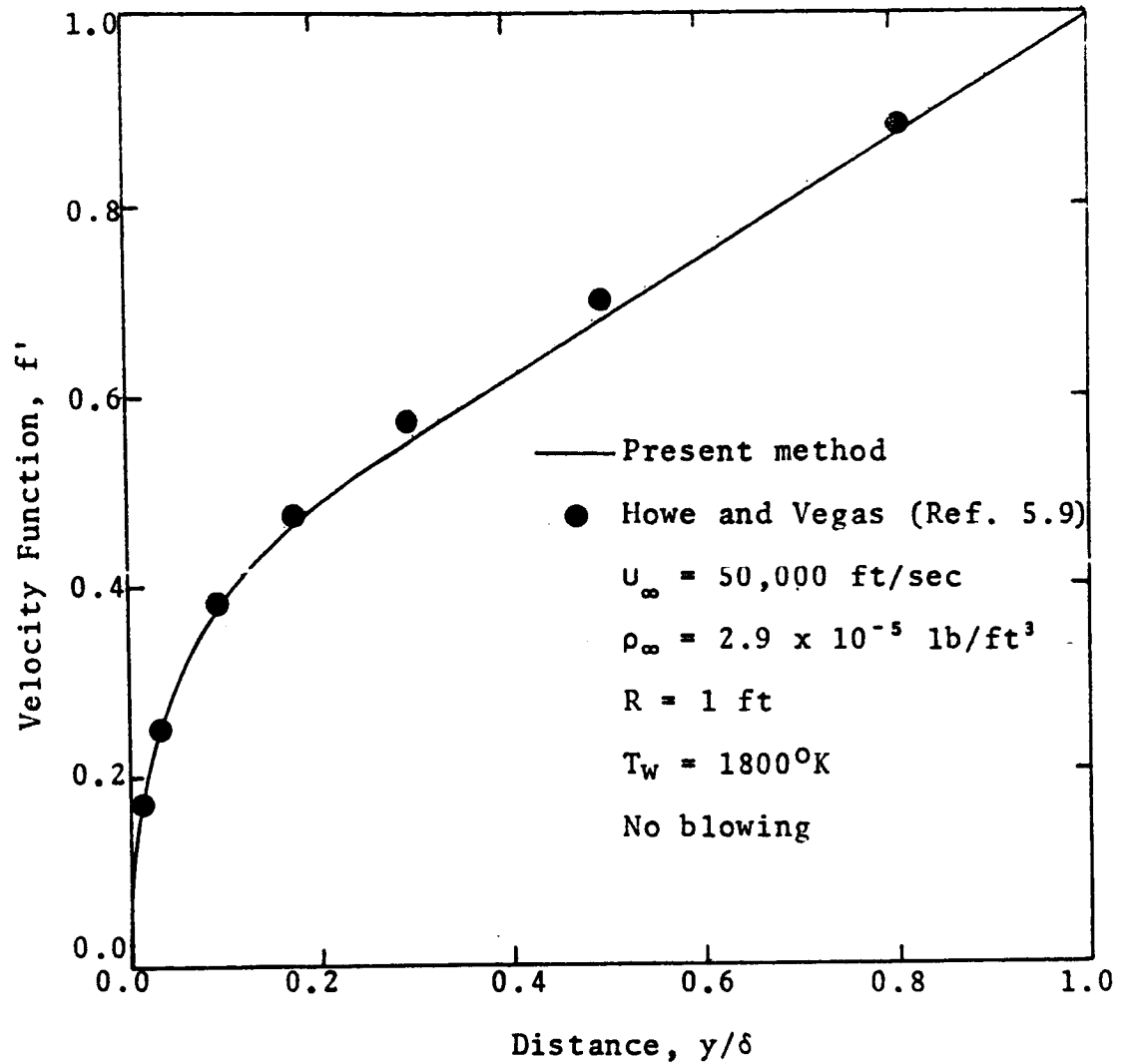


Figure 5.4. Comparison of Stagnation Line Momentum Equation Solutions (Ref. 5.2).

$$B_n = G_n^2 + \alpha_n G_n^1 \quad (5.46)$$

$$C_n = F_n^2 + \alpha_n F_n^1 \quad (5.47)$$

$$D_n = \frac{\tilde{\delta}}{\rho_n k_n} \left[\rho_n v_n^2 \left(\frac{dv}{d\eta} \right)_n + \left(\frac{dq_R}{d\eta} \right)_n \right] \quad (5.48)$$

and

$$\alpha_n = - \frac{\tilde{\delta}}{2\rho_n k_n} \left[\rho_n v_n C_{p_n} - 2 \left(\frac{d(\rho k)}{d\eta} \right)_n \right] \quad (5.49)$$

In Chapter III, it was noted that the wall boundary condition for the energy equation is simply the equilibrium sublimation temperature (T_w) of the ablator. The sublimation temperature of the phenolic-nylon ablator* employed in this study was 3450°K ($\pm 25^\circ\text{K}$) at one atmosphere pressure. The shock temperature (T_s) was determined from the Rankine-Hugoniot Equations (Eqs. 3.81-3.84).

By applying the finite-differential formulation of the energy equation (Eq. 5.44) at each station across the flowfield, the following matrix equation results,

$$4 \begin{bmatrix} B_2 & C_2 & & & & \\ A_3 & B_3 & C_3 & & & \\ & A_4 & B_4 & C_4 & & \\ & & \cdot & \vdots & \vdots & \\ & & & \vdots & \vdots & \cdot \\ & & & & A_{s-1} & B_{s-1} \end{bmatrix} \cdot \begin{bmatrix} T_2 \\ T_3 \\ T_4 \\ \vdots \\ \vdots \\ T_{s-1} \end{bmatrix} = \begin{bmatrix} D_2 - A_2 T_1 \\ D_3 \\ D_4 \\ \vdots \\ \vdots \\ D_{s-1} - C_{s-1} T_s \end{bmatrix} \quad (5.50)$$

*The elemental composition of this ablator was $C_c = 0.7303$, $C_H = 0.0729$, $C_N = 0.0729$, $C_O = 0.0496$, and $C_O = 0.1472$.

As with the previous solutions of tridiagonal matrices, Equation 5.50 was solved by the algorithm given by Conte (Ref. 5.1) and programmed in the Fortran subprogram, TRID. In the same manner as the elemental and momentum solutions, numerical convergence of the energy equation was demonstrated for $\Delta T/T_s \leq 0.05$ from one grid point to the next.

Overall Analysis

The previously discussed numerical solutions were incorporated with the chemical equilibrium calculations (CHEMEQ),* the properties package (PROPRT), and the radiative heating analysis (LRAD), in a Fortran program designated as SLAB (Stagnation Line Analysis with Binary Diffusion). A simplified flow diagram of this overall analysis was given in Figure 5.1.

Verification of the Overall Analysis: As previously shown, each of the subprograms used in this program were independently tested both for numerical convergence and agreement with other investigators. In order to test the overall analysis, a comparison was made between the dimensionless radiative heating rates predicted by the SLAB program and the predictions of other investigators. For these no mass injection cases

*Presented and verified in Appendix E.

which are shown in Figure 5.5, the comparison is quite favorable. It should be noted that the results of Rigdon, et al., are based on the most rigorous radiation analysis of those presented and that the predictions of SLAB are in excellent agreement with these results.

Computational Experience with the Overall Analysis:

Computer running time presented the major difficulty in the current study. The radiation calculation alone required approximately 2.5 minutes for a sweep of the finite difference grid;* the chemical equilibrium calculation correspondingly required approximately 1.0 minutes. The remaining calculations required a total of approximately 0.5 minutes. A single pass through the outer loop (See Figure 5.1) required one radiation (LRAD) calculation and 12-15 chemical equilibrium calculations (CHEMEQ), thus requiring a total of 15-18 minutes for each major (outer loop) iteration. Depending upon the initial estimates, the overall solution required from 3 to 20 major iterations. In terms of execution time this amounted to about 6.0 hours.**

*For approximately 59 finite-difference stations.

**It is felt that the execution time could possibly be reduced by as much as one-sixth of that presently required. A discussion of the proposed modifications is included in Chapter VII on Conclusions and Recommendations.

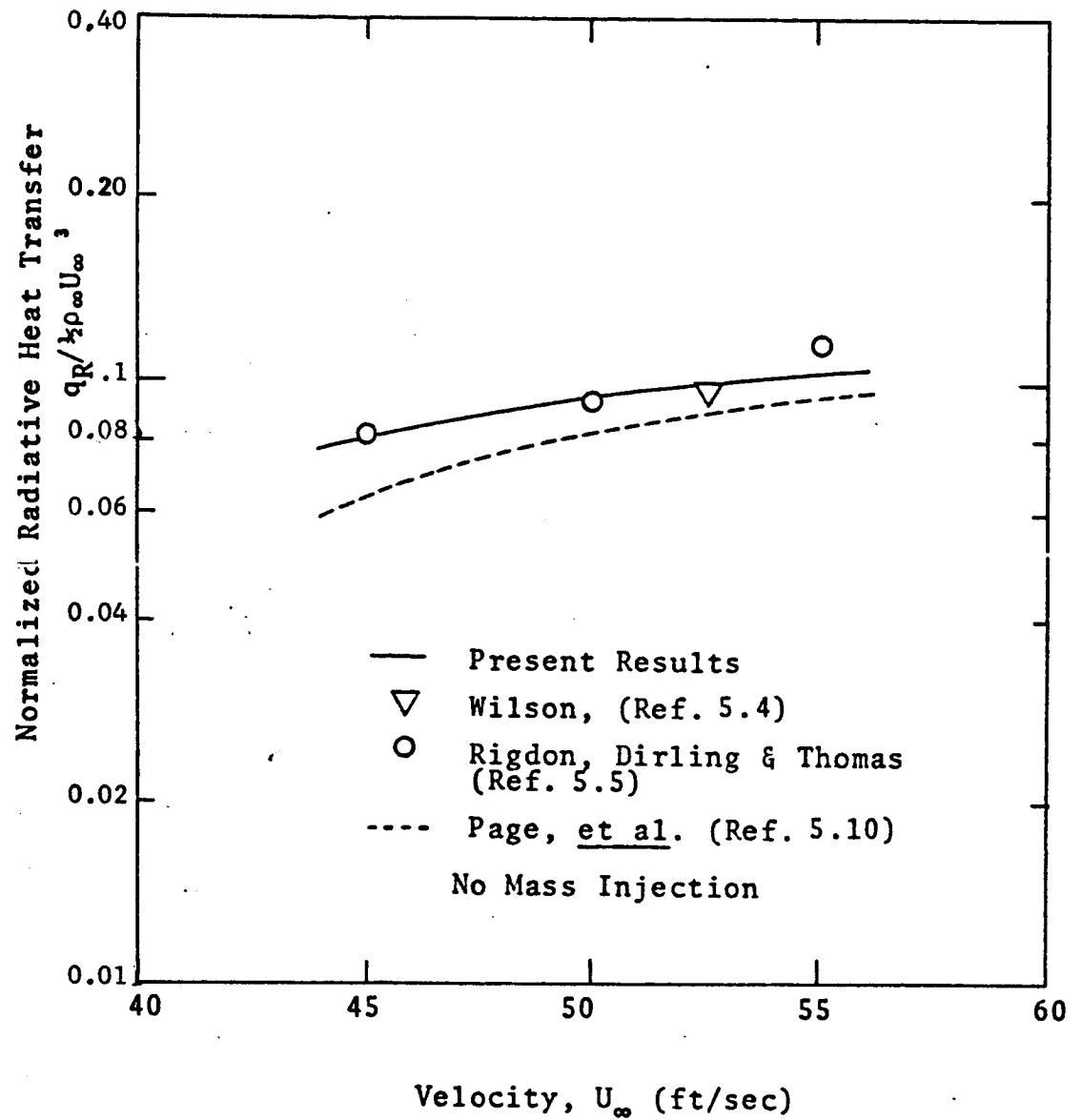


Figure 5.5. Comparison of Dimensionless Radiative Heating Rates ($P_s = 1.0$ atm, $R = 9$ ft.).

The above mentioned run times are of course dependent upon the number of steps employed in the numerical analysis. In fact, a direct proportionality was observed. Therefore, it is desirable to minimize the number of steps considered. In the current study it was found that the converged solutions could be obtained with 55-59 steps using an optimum, variable-stepsize distribution. It is felt that this number of steps represents the minimum possible for the flight conditions investigated.

Another source of difficulty encountered in this study is the extreme sensitivity and nonlinearity of the radiative flux divergence. The extent of this problem is illustrated in Figure 5.6, which demonstrates the pervasive effect of a small, localized variation in the temperature distribution upon the flux divergence profile. The sharp ridge appearing in the flux divergence at the stagnation point was typical of the cases studied.* Furthermore, the irregular behavior of the flux divergence in the region of the stagnation point did not cease until the temperature profile was nearly converged. Because of these adversities in the radiative flux divergence, it was very tedious to

*It should be pointed out that this phenomena is also observed in the results of Wilson (Ref. 5.4) and Rigdon, et al. (Ref. 5.5).

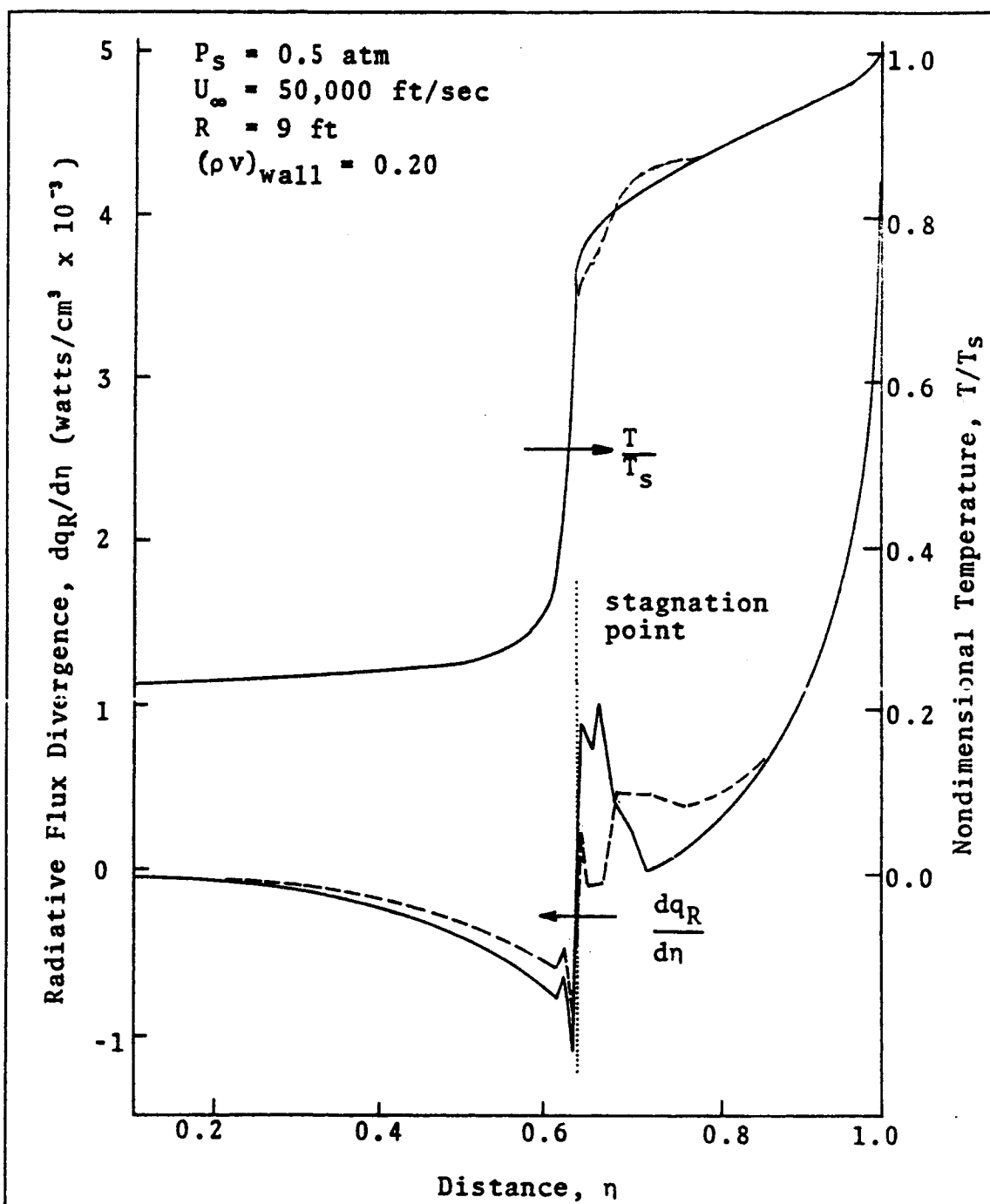


Figure 5.6. Illustration of the Effect of Temperature Variations Upon Radiative Flux Divergence.

achieve convergence. The best results were obtained by weighting the estimated temperature profiles by means of the following relationship

$$T_{\text{new}} = 0.65 T_{\text{calc}} + 0.35 T_{\text{old}} \quad (5.51)$$

where T_{calc} is the computed temperature distribution based upon a flux divergence profile computed from T_{old} . On occasion it was observed that if T_{new} differed significantly (>10%) from T_{old} , a divergence would occur in the numerical solution from which it could not recover. Therefore, a maximum of 8% variation was permitted in the temperature change from iteration to iteration.

The initial estimates for each case were obtained from the analysis by Engel (VISRAD III, Ref. 5.6). The analysis includes mass injection of ablation products with radiation coupling, but assumes air properties throughout the shock layer and a step-function representation of the elemental distribution. For low blowing cases, VISRAD was found to agree quite well with the SLAB analysis. However, for large blowing some differences were noted in the temperature profile.

The typical progress of the SLAB analysis from iteration to iteration is given in Figure 5.7 to 5.11. As the solution was approached (Fig. 5.8) instability

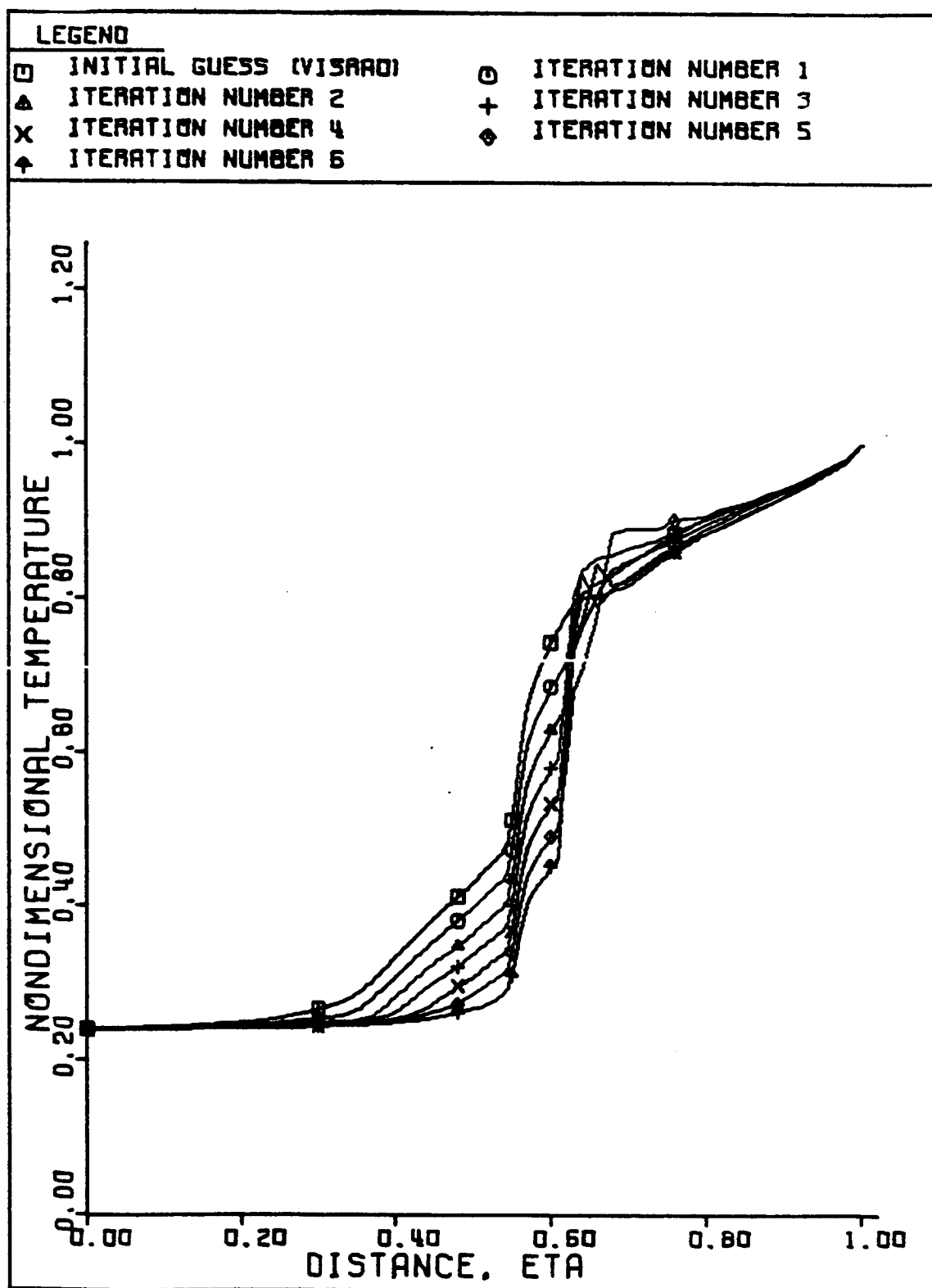


Figure 5.7. Variation in Temperature Profiles From Iteration to Iteration.

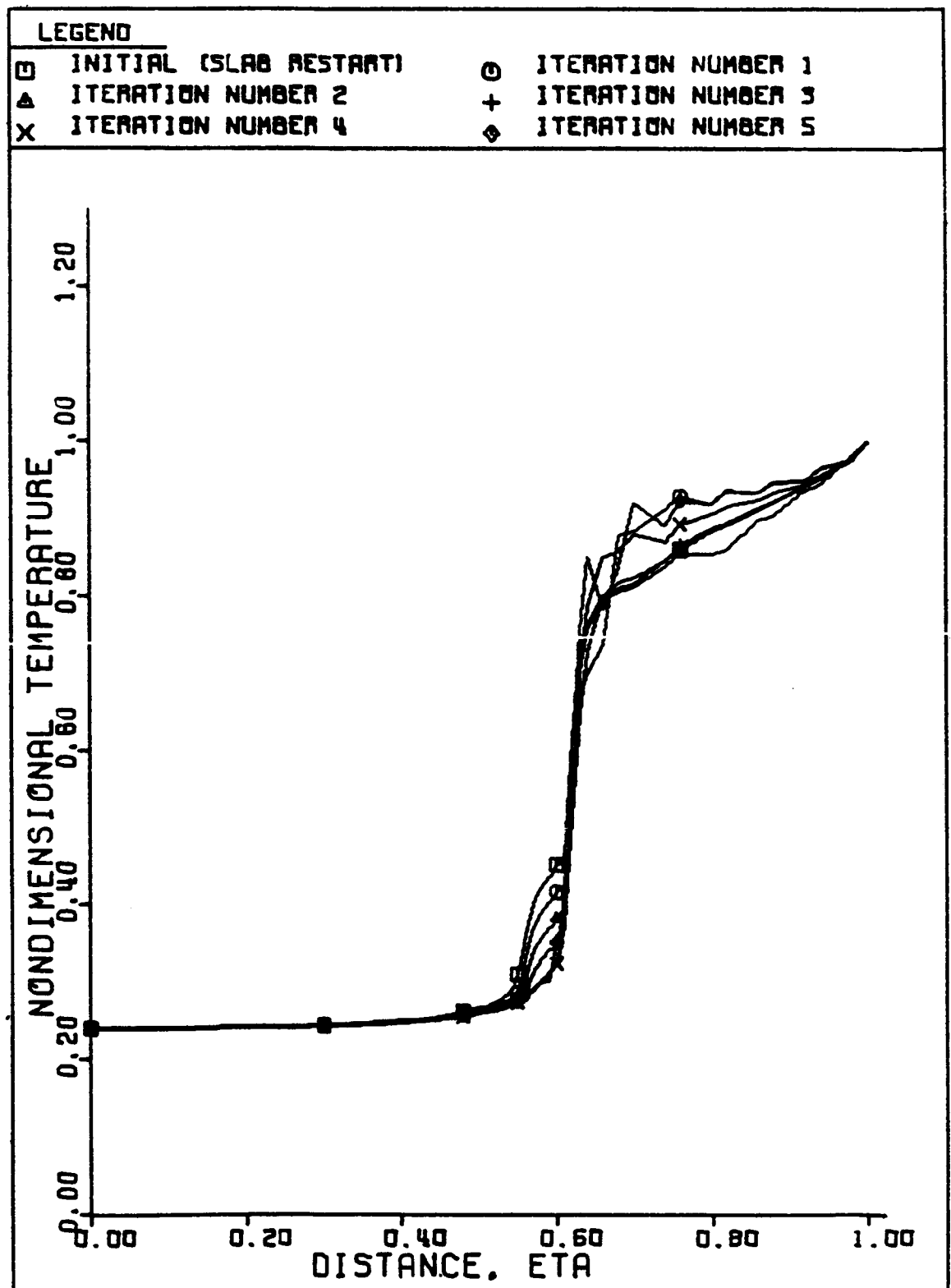


Figure 5.8. Variation in Temperature Profiles From Iteration to Iteration.

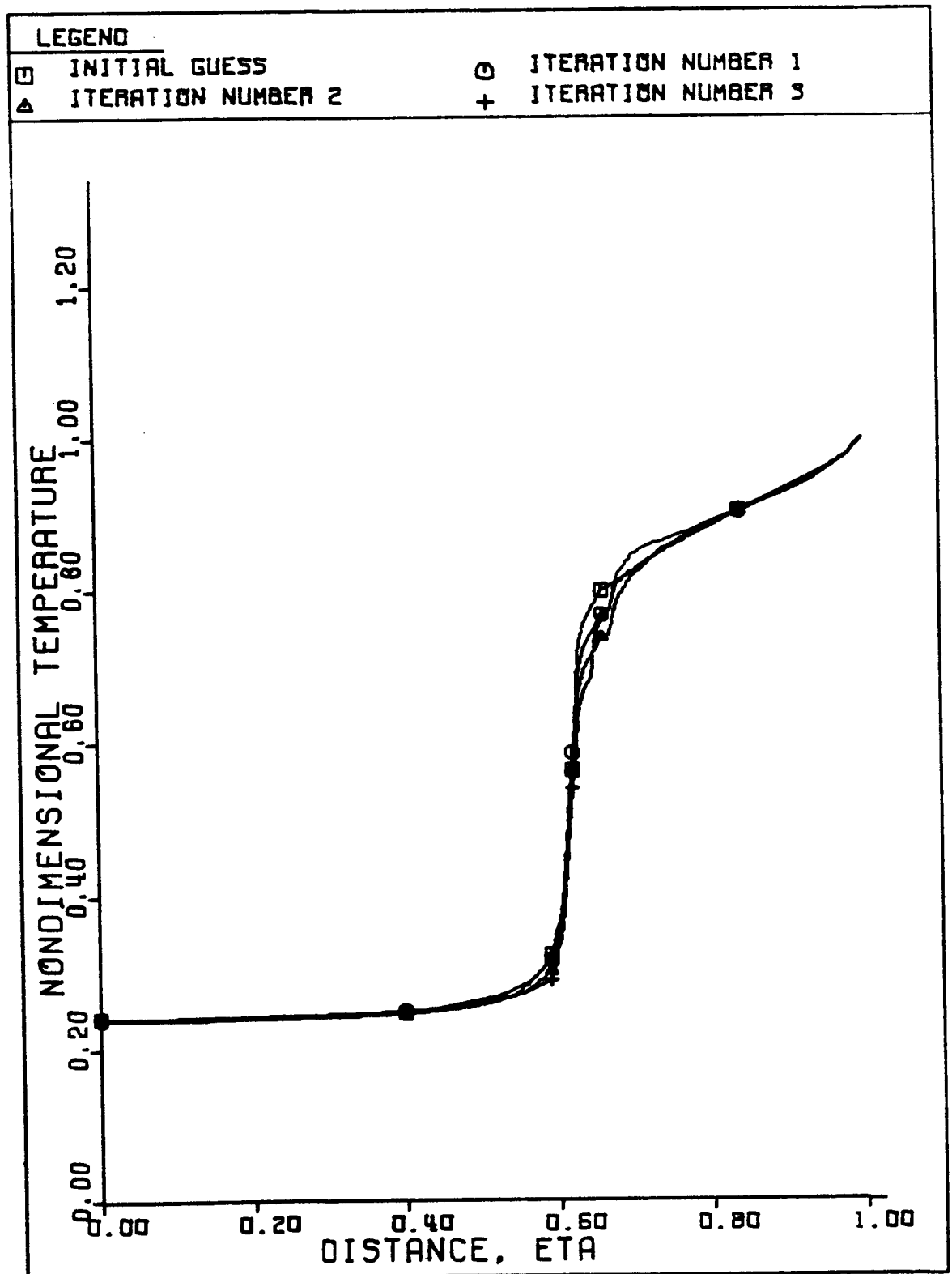


Figure 5.9. Variation in Temperature Profiles From Iteration to Iteration.

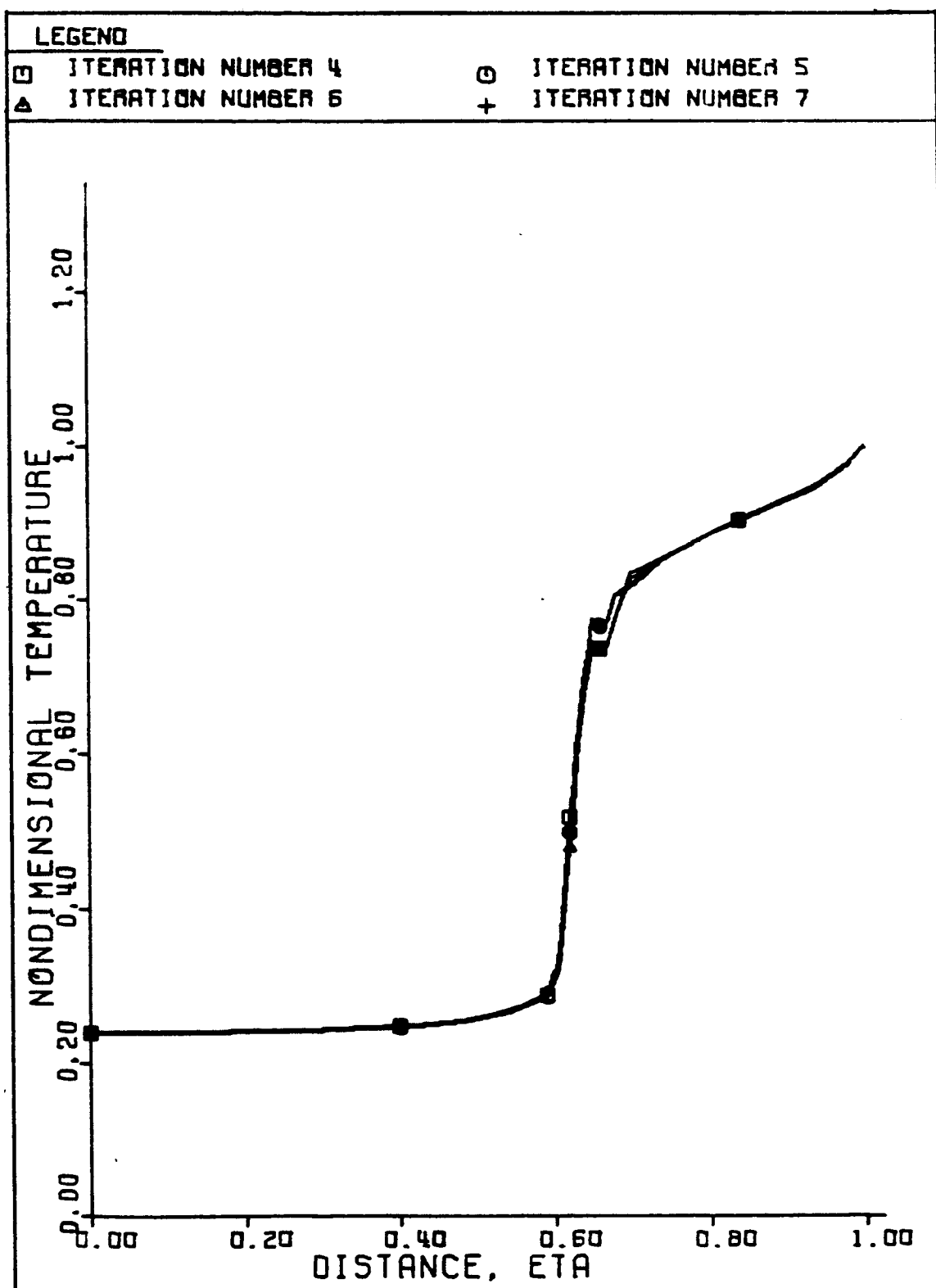


Figure 5.10. Variation in Temperature Profiles From Iteration to Iteration.

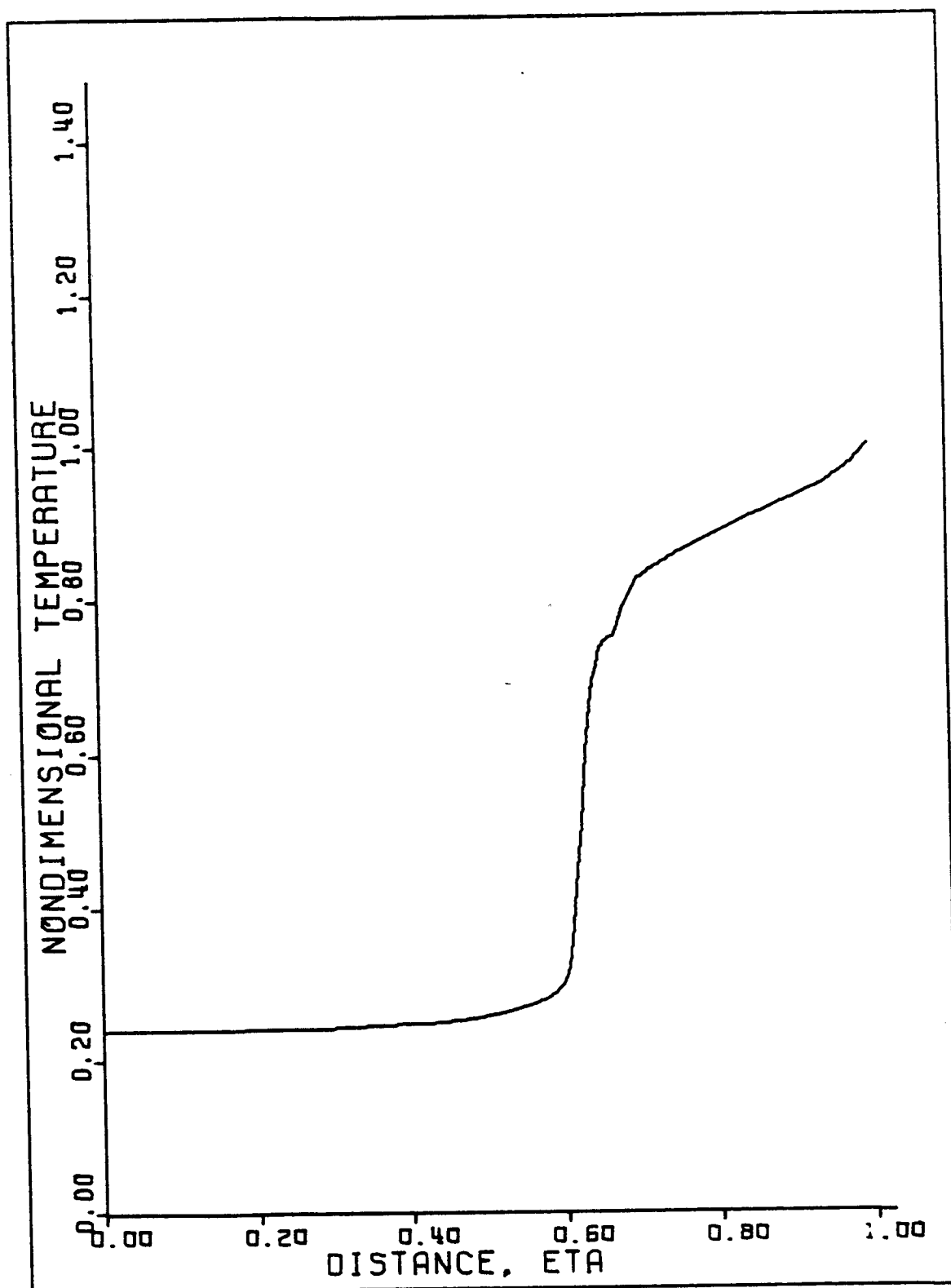


Figure 5.11. Converged Temperature Profile.

began to occur in the higher temperature region. Therefore, the stepsize distribution was revised to conform to the new profile. The program was then restarted from the third iteration of Figure 5.8. The resulting progress to convergence is seen in Figures 5.9, 5.10, and 5.11.

Stagnation Region Heating Analysis with Multicomponent Diffusion

Because of the extensive time requirements of the overall stagnation line analysis (~6.0 hours) fully coupled multicomponent diffusion calculations were not performed. Instead, a partial coupling was obtained by using the temperature and velocity profiles computed from the corresponding binary (SLAB) analysis. The resulting species distributions were then used with the given temperature profile in a radiative heating analysis (LRAD). The resulting values of wall heating rates and radiative flux divergence profiles were then compared with those obtained from the corresponding SLAB analysis. The details of the multicomponent diffusion analysis (SLAM) are given in the following discussion.

Species Solution with Multicomponent Diffusion:

Because the Stefan-Maxwell Equations (Eqs. 3.98) are implicit in the mass flux (J_i), there exists no direct

method by which a simultaneous solution with the elemental continuity equations (Eqs. 3.97) can be obtained. Without further simplification of the Stefan-Maxwell equations (e.g., the bifurcation approximation), it is therefore necessary to resort to an iterative numerical method such as that developed in the current study. In the following development it is shown that the elemental mass fluxes (\tilde{J}_j) can be rigorously expressed in terms of an effective elemental diffusion coefficient (\tilde{D}_j).

Effective Elemental Diffusion Coefficients: It was shown in Chapter II that a rigorous multicomponent expression for the species mass fluxes (J_i), could be written as follows:

$$J_i = - \rho D_i \frac{dC_i}{dy} \quad (5.52)$$

where D_i is an effective species diffusion coefficient which can be computed from Equation 2.22. A Shvab-Zeldovitch transformation of Equation 5.52 yields

$$\tilde{J}_j = - \rho \tilde{M}_j \sum_i \frac{A_{ij} D_i}{M_i} \frac{dC_i}{dy} \quad (5.53)$$

By defining:

$$\tilde{D}_j = \frac{\tilde{M}_j \sum \frac{A_{ij} D_i}{M_i} \frac{dC_i}{dy}}{\frac{d\tilde{C}_j}{dy}} = \begin{array}{l} \text{effective elemental} \\ \text{diffusion coefficient} \\ \text{of element "j"} \end{array} \quad (5.54)$$

Equation 5.53 can be written as:

$$\tilde{J}_j = - \rho \tilde{D}_j \frac{d\tilde{C}_j}{dy} \quad (5.55)$$

Upon performing a Dorodnitzn transformation (Eq. 3.93), Equation 5.55 can be substituted into the transformed elemental continuity equations (Eqs. 3.97) to give the following results,

$$\frac{d^2 C_j}{d\eta^2} + a_1 \frac{dC_j}{d\eta} = 0 \quad j = 1, 2, \dots, \ell \quad (5.56)$$

where

$$a_1 = 2 \frac{d \ln \rho}{d\eta} + \frac{d \ln \tilde{D}_j}{d\eta} - \frac{v \tilde{\delta}}{\rho \tilde{D}_j} \quad (5.57)$$

With the exception of the diffusion coefficients, the previous equations are identical to the binary elemental formulations (Eqs. 5.3 and 5.4). As with the binary formulations, the following wall boundary conditions exist:

$$\rho v \tilde{C}_j - \frac{\rho^2 \tilde{D}_j}{\tilde{\delta}} \frac{d\tilde{C}}{d\eta} = \tilde{I}_j \quad (5.58)$$

The shock boundary conditions were again expressed as the equilibrium composition of air at the shock temperature (T_s).

Assuming effective elemental diffusion coefficient profiles, the corresponding elemental distributions can be determined in the same manner as with the previously discussed binary diffusion analysis. From the elemental distributions and the temperature profiles the equilibrium species compositions can be determined.

From the Stefan-Maxwell Equations (Eqs. 3.98):

$$\frac{\rho}{\delta} \frac{dY_i}{d\eta} = \sum_{\substack{j=1 \\ j \neq i}}^v \frac{Y_i Y_j}{ij} (V_j - V_i) \quad i=1, 2, \dots, v-1 \quad (3.98)$$

and the sum of the mass fluxes based upon the assumption of a mass averaged velocity (Eq. 2.13, $\sum \rho_i V_i = 0$), the diffusion velocities corresponding to the estimated species distribution can be determined. A solution of the following matrix is thus required at each finite-difference station in the flowfield.

$$\begin{bmatrix}
 -\sum_{j \neq 1} \frac{Y_j}{\Delta_{1j}} & \frac{Y_2}{\Delta_{12}} & \cdots & \frac{Y_{v-1}}{\Delta_{1,v-1}} & \frac{Y_v}{\Delta_{1v}} \\
 \frac{Y_1}{\Delta_{21}} & -\sum_{j \neq 2} \frac{Y_j}{\Delta_{2j}} & \cdots & \frac{Y_{v-1}}{\Delta_{2,v-1}} & \frac{Y_2}{\Delta_{2v}} \\
 \cdot & \cdot & & \cdot & \cdot \\
 \cdot & \cdot & & \cdot & \cdot \\
 \cdot & \cdot & & \cdot & \cdot \\
 \frac{Y_1}{\Delta_{v-1}} & \frac{Y_2}{\Delta_{v-1,2}} & \cdots & -\sum_{j \neq v-1} \frac{Y_j}{\Delta_{v-1,j}} & \frac{Y_v}{\Delta_{v-1,v}} \\
 \rho_1 & \rho_2 & \cdots & \rho_{v-1} & \rho_v
 \end{bmatrix}
 \begin{bmatrix}
 V_1 \\
 V_2 \\
 \cdot \\
 \cdot \\
 \cdot \\
 V_{v-1} \\
 V_v
 \end{bmatrix}
 =
 \begin{bmatrix}
 \frac{\rho}{\delta Y_1} \frac{dY_1}{d\eta} \\
 \frac{\rho}{\delta Y_2} \frac{dY_2}{d\eta} \\
 \cdot \\
 \cdot \\
 \cdot \\
 \frac{\rho}{\delta Y_{v-1}} \frac{Y_{v-1}}{d\eta} \\
 0
 \end{bmatrix} \quad (5.59)$$

The solution to this set of equations was implemented in the Fortran Subprogram, MCD, a listing of which appears in Appendix C. The analysis employed in MCD was verified by a comparison with results obtained from an analytical solution reported by Toor (Ref. 5.7).^{*} This comparison is given in Figure 5.12 and reveals excellent agreement between the numerical and analytical predictions. The figure also demonstrates the capability of the current analysis to predict the cross-effects discussed with reference to Figure 2.1 from which the analytical values were taken.

^{*}Also given in Figure 2.1.

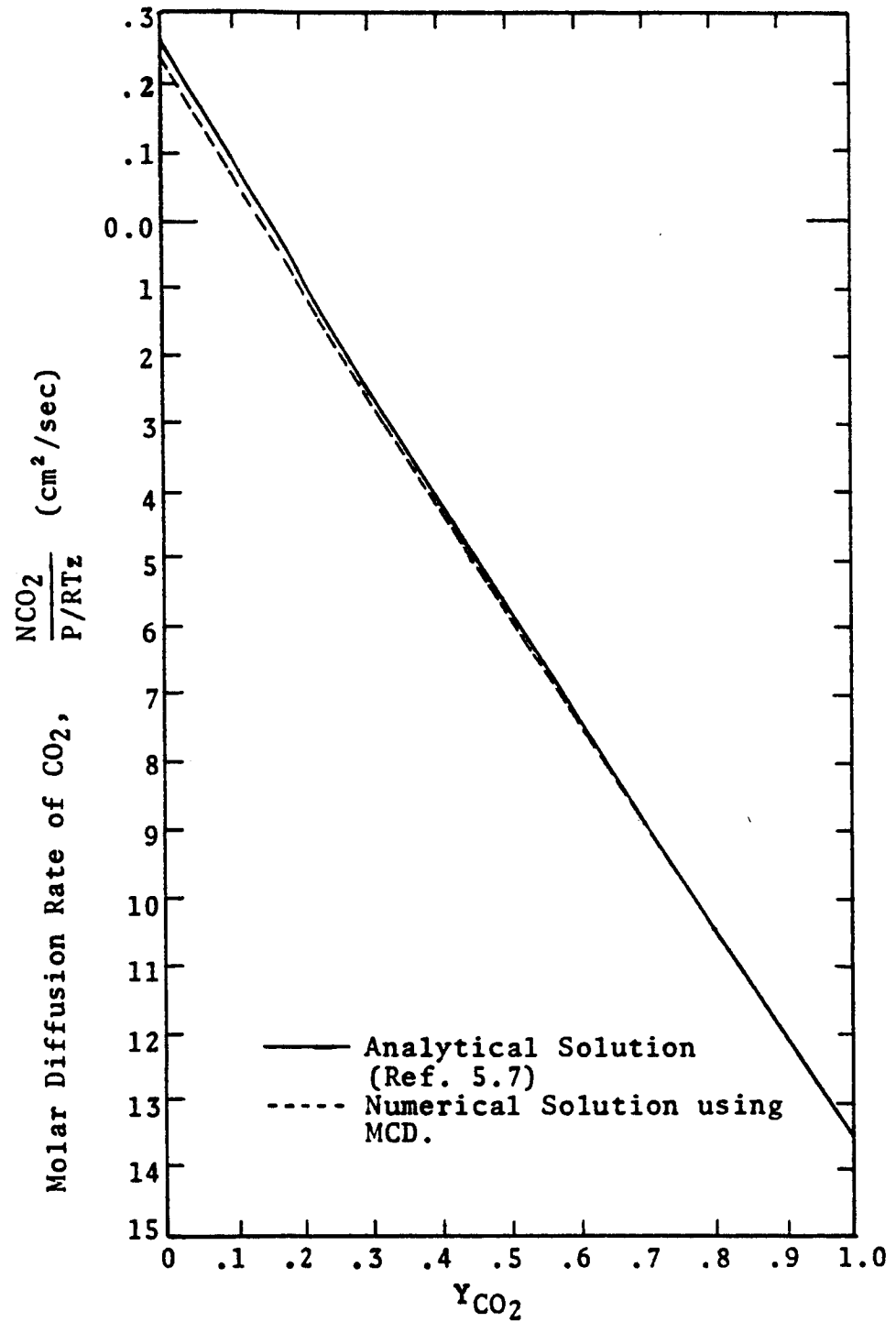


Figure 5.12. Diffusion Rates of CO₂ As a Function of Y_{CO₂} (Ref. 5.7).

The species mass fluxes are determined in MCD from the following relationship,

$$J_i = \rho_i V_i \quad (5.60)$$

Using the Shvab-Zeldovitch transformation (Eq. 3.21), the elemental mass fluxes are then computed in the subprogram EFLUX:

$$\tilde{J}_j = M_j \sum_{i=1}^V \frac{A_{ij} J_i}{M_i} \quad (3.21)$$

An estimate of the effective elemental diffusion coefficients is then obtained from the Dorodnitsyn transform of Equation 5.55:

$$\tilde{D}_{j\text{calc}} = - \frac{\tilde{\delta} \tilde{J}_j}{\rho^2 \frac{dC_j}{d\eta}} \quad (5.61)$$

The elemental continuity equations (Eqs. 5.56) are again solved using a revised estimate of the diffusion coefficients from the following relationship (DIJ):

$$\tilde{D}_j(\eta)_{\text{new}} = 0.7 \left(- \frac{\tilde{\delta} \tilde{J}_j(\eta)}{\rho^2 \frac{dC_j(\eta)}{d\eta}} \right) + 0.3 \tilde{D}_j(\eta)_{\text{old}} \quad (5.62)$$

This iterative procedure is thus repeated until all of the elemental mass fractions from one iteration to the next agree within 1%. The density profile is then

updated and above process repeated. When the density profile has converged to 5%, the overall multicomponent diffusion analysis is said to be converged. A simplified flow-diagram of the previously described iterative procedure is given in Figure 5.13.

Electron Diffusion: In the current study, the ambipolar diffusion has been assumed to describe the diffusion behavior of the electron. This assumption implies that the electron diffuses at the same rate as the parent dissociated atom, or that throughout the flowfield the density of electrons (ρ_{e^-}) is equal to the total density of the ionized atoms (e.g., O^+ , N^+ , and C^+):

$$\rho_{e^-} = \rho_C + \rho_{N^+} + \rho_{O^+} \quad (5.63)$$

For the purpose of the chemical equilibrium calculation (see Appendix E), the electron has been treated as an elemental component of the undissociated molecules.* For example, N is said to be composed of two "elements": N^+ and e^- . The basic "elements" are then C^+ , H, O^+ , N^+ and e^- (neglecting hydrogen ionization). Assuming ambipolar diffusion, the elemental composition of electrons at any point in the flowfield

*The assumption is a standard procedure in dealing with equilibrium studies of dissociated gases (Refs. 5.4 and 5.5).

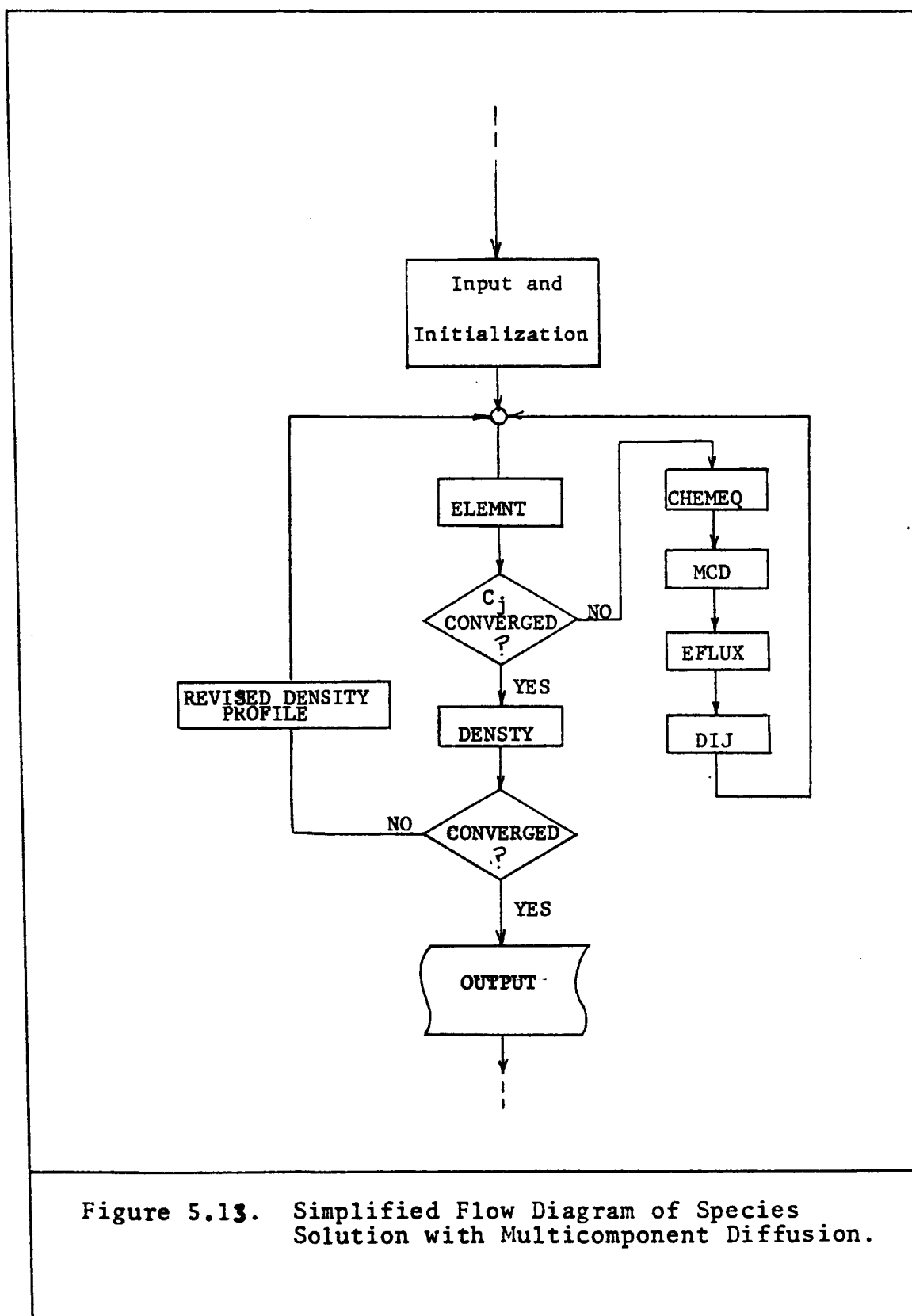


Figure 5.13. Simplified Flow Diagram of Species Solution with Multicomponent Diffusion.

is therefore related to the elemental compositions of C^+ , O^+ , and N^+ by the following equation:

$$\tilde{C}_{e^-} = \left[\frac{\tilde{C}_{C^+}}{\tilde{M}_{C^+}} + \frac{\tilde{C}_{O^+}}{\tilde{M}_{O^+}} + \frac{\tilde{C}_{N^+}}{\tilde{M}_{N^+}} \right] \tilde{M}_{e^-} \quad (5.64)$$

Numerical Difficulties: It has been noted that as the elemental diffusion effects become small (i.e., as $|\tilde{J}_j|$ becomes much less than ρv), the use of Equation 5.61 leads to erratic predictions of the elemental diffusion coefficients (\tilde{D}_j). These irregularities, occurring in the convection dominated regions, are frequently sufficient in magnitude to prevent convergence of the overall solution. This problem is partially overcome by setting the elemental diffusion coefficients equal to a small number (10^{-6}) for all values outside of the diffusion zone. The diffusion zones of each element are specified as the regions in which

$$\tilde{J}_j / \rho v \geq 0.01 \quad j=1, 2, \dots, \ell \quad (5.65)$$

The establishment of this diffusion region results in discontinuities in the diffusion coefficient profiles at the extremities of the zone. These discontinuities are amplified by the derivative term $(d \ln \tilde{D}_j / d \eta)$ appearing in the elemental continuity equations

(Eqs. 5.56 and 5.57) and quite often make convergence difficult to achieve. Since the predicted coefficients have been observed to be relatively constant across the diffusion zone, it was felt that the derivative term ($d\ln D_j/d\eta$) could be neglected without significant losses in accuracy. In Figure 5.14, a comparison is given between typical elemental profiles computed with and without the $d\ln D_j/d\eta$ term, and with the corresponding binary diffusion profile. From these results, the error in heating rate arising from the omission of the derivative term was found to be negligible in comparison to the corresponding binary diffusion results.

Summary

The details of the numerical implementation of each of the conservation equations have been given. The resulting Fortran subprograms have been individually tested and found to be functioning properly. These numerical solutions have been combined with the transport, thermodynamic, and radiation property models, discussed and verified in previous chapters, in a Fortran computer program (SLAB) which has been shown to yield heating rate predictions which are in excellent agreement with similar existing analyses. In addition, an implicit multi-component diffusion analysis (SLAM) has been developed and verified by comparison with analytical results.

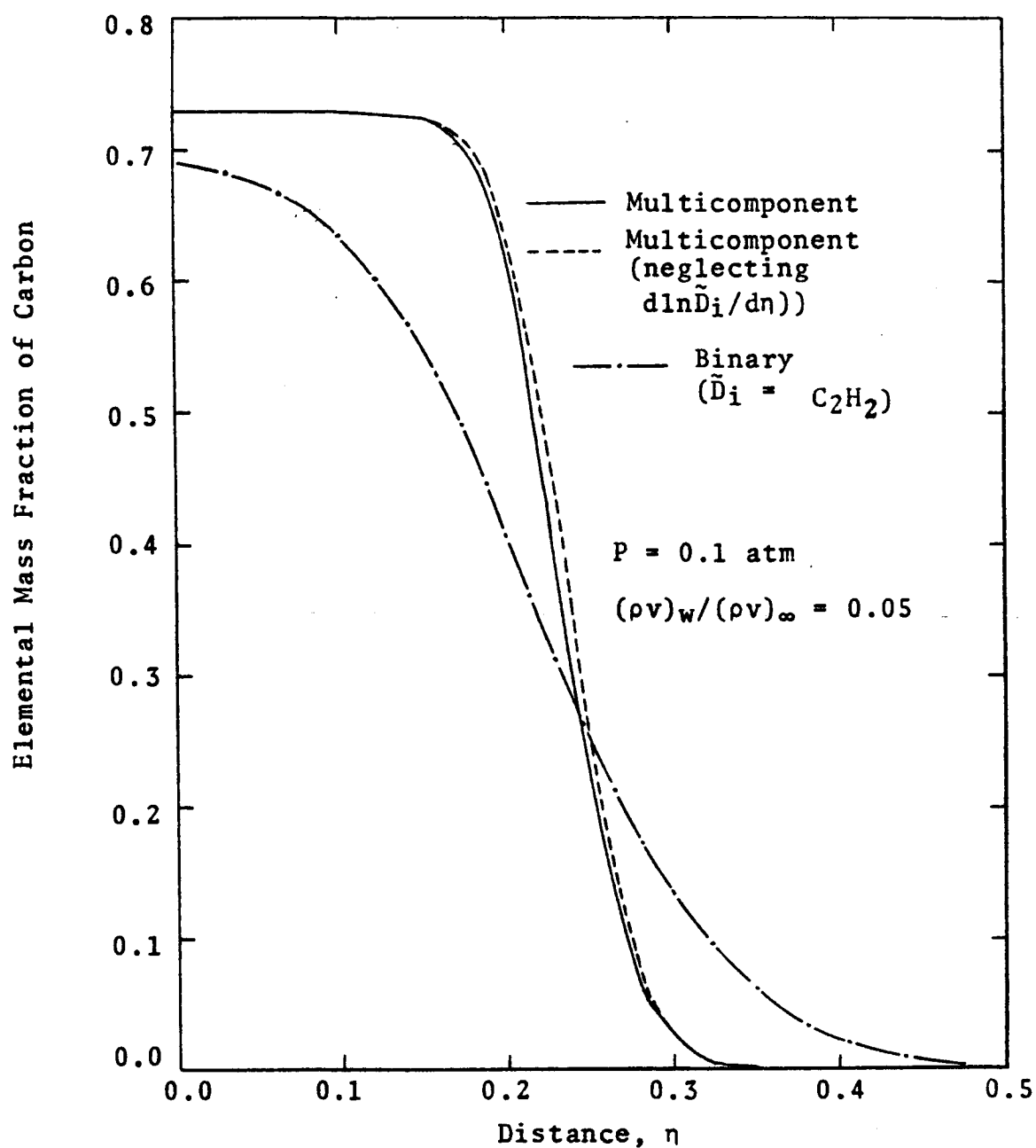


Figure 5.14. Comparisons of Numerical Results With and Without $d\ln\bar{D}_i/d\eta$.

These analyses provide the necessary tools for an accurate assessment of the transport phenomena occurring in the multicomponent, reacting flowfields surrounding and interacting with ablative thermal protection systems. In the following chapter, the results of the current study of a phenolic-nylon ablator, exposed to a high velocity entry condition, are presented.

REFERENCES

- 5.1. Conte, S. D. Elementary Numerical Analysis, McGraw-Hill Book Co., New York (1965).
- 5.2. Engel, C. D. "Stagnation Line Momentum and Energy Solutions," Louisiana State University, Department of Chemical Engineering, NASA-RFL-TR 70-2 (September, 1970).
- 5.3. Lee, E. S. Quasilinearization and Invariant Imbedding, Academic Press, New York (1968).
- 5.4. Wilson, K. H. "Stagnation Point Analysis of Coupled Viscous-Radiating Flow With Massive Blowing," NASA CR-1548 (June, 1970).
- 5.5. Rigdon, W. S., R. B. Dirling, and M. Thomas, "Stagnation Point Heat Transfer During Hypervelocity Atmospheric Entry," NASA CR-1462 (February, 1970).
- 5.6. Engel, C. D. "Ablation and Radiation Coupled Viscous Hypersonic Shock Layers. Ph.D. Dissertation, Louisiana State University (1971).
- 5.7. Toor, H. L. "Diffusion in Three-Component Gas Mixture," AIChE Journal, Vol. 6, No. 3, (September, 1960), pp. 516-524.
- 5.8. Davis, R. T. "Numerical Solution of the Hypersonic Viscous Shock Layer Equations," AIAA Journal, Vol. 8, No. 5 (May, 1970).
- 5.9. Howe, J. T. and J. R. Vegas, "Solutions of the Ionized Radiating Shock Layer, Including Reabsorption and Foreign Species Effects and Stagnation Region Heat Transfer," NASA TR R-159, 1963.
- 5.10. Page, W. A., et al., "Radiative Transport in Inviscid Nonadiabatic Stagnation-Region Shock Layers," AIAA Paper No. 68-784, AIAA 3rd Thermophysics Conference, June 1968.

CHAPTER VI

RESULTS OF STAGNATION REGION HEATING ANALYSES

Typical trajectories for earth entry from space origins are shown in Figure 6.1. As discussed in Chapter I, the increase in entry velocities over lunar return missions is such that radiation heating becomes the governing factor in the design of thermal protection systems. Because of the tremendous success and the corresponding advanced state of technology associated with charring ablators of the Apollo shape, it is indeed desirable to fully explore the possibilities of employing the same type of heat protection system for return missions from planetary flight.

Several studies have been made of the effectiveness of charring ablators in blocking the radiation heat transfer during high velocity re-entry (Refs. 6.1-6.4). It has been shown from these studies that ablation product absorption is effective in reducing the radiation heat flux to the vehicle surface. However, in an effort to simplify the required calculations these

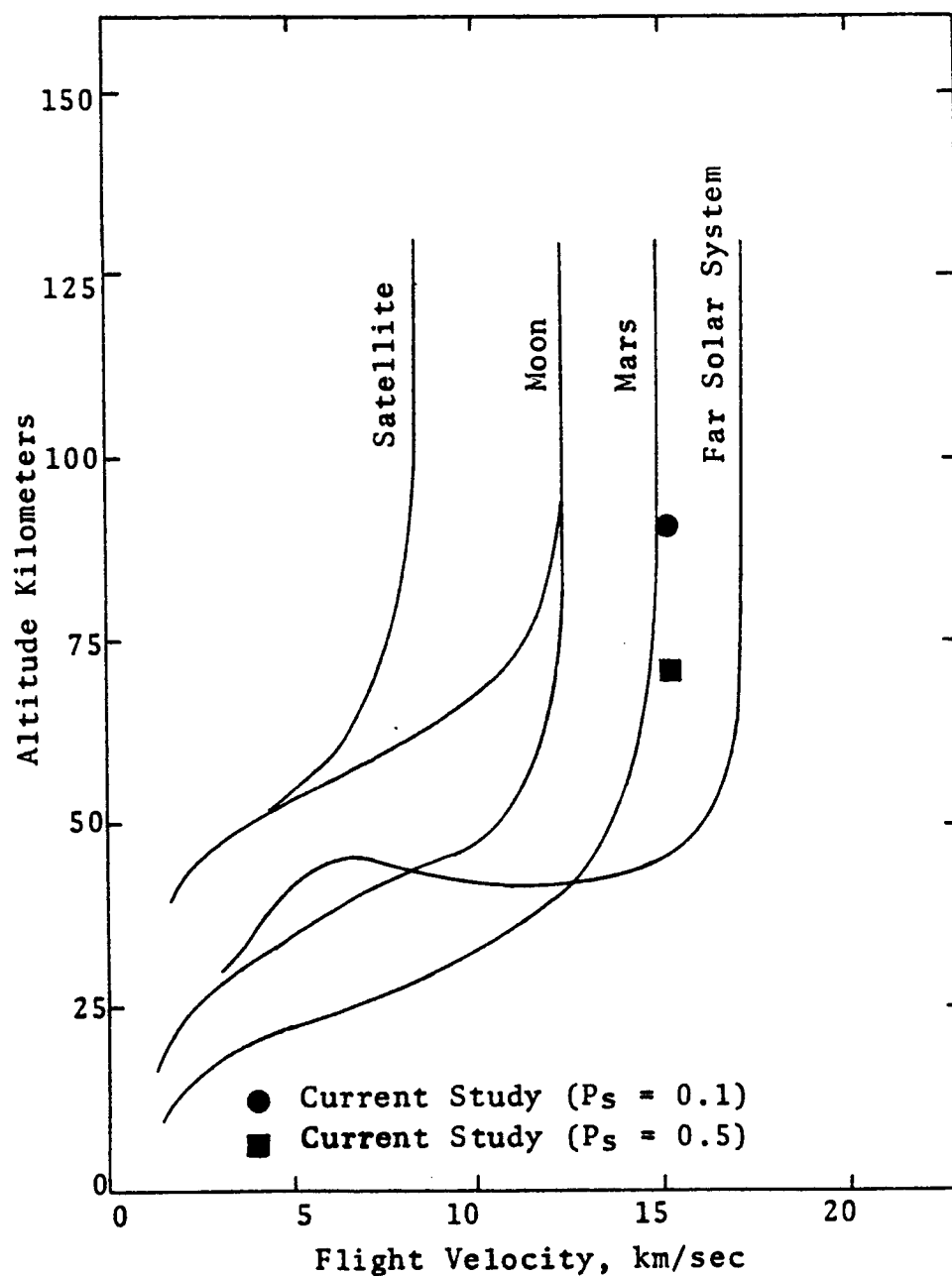


Figure 6.1. Typical Trajectories for Earth Entry From Space Origins (Ref. 6.5).

investigators have all neglected the effects of multi-component diffusion. In most cases, air transport and thermodynamic properties have also been assumed for the injected ablation products. Furthermore, with the exception of a single case for a pure graphite ablator (Ref. 6.2), the previously mentioned studies have concentrated on a specific carbon-phenolic ablator.

The reasoning for the selection of ablators with high carbon content is based upon the fact that atomic carbon is an excellent absorber of radiant energy. However, as observed by Rigdon (Ref. 6.2), the pure graphite ablator was found to be less effective in reducing radiant heating effects than the carbon-phenolic blend. Two observations can be made from this result. First, the increase in heating (relative to the carbon-phenolic ablator) is most likely attributable to re-radiation by the atomic carbon which occurs as the temperature is increased by the absorption process. Secondly, this analysis by Rigdon includes air thermodynamic and transport properties for the ablation products. The use of the correct properties could significantly affect the results of this analysis.

The foregoing discussion leads directly to the objectives of the current study. First of all, what are the effects on heating rate predictions of assuming a computationally more simple binary diffusion model (or no diffusion as in Ref. 6.3) as opposed to a rigorous multicomponent diffusion analysis? Secondly, what are the effects of assuming simplified (air) transport and thermodynamic properties for the injected ablation products? Finally, how do other ablators compare to carbon-phenolic and graphite in reducing radiation heating of high-velocity entry vehicles? The indications are that an optimum blend of ablation products exists.

In this study, a rigorous computer analysis (SLAB)* was developed to accurately determine the effectiveness of given ablative materials in reducing radiation heating of entry vehicles. The analysis, which has been described and verified in the previous chapters, includes a capability for assessing the effects of multicomponent diffusion. In addition, property models have been included to describe the actual

*Listing and input description are presented in Appendix F.

transport and thermodynamic properties for the ablation product and air mixtures encountered in these investigations. This computer analysis, thus provides the necessary tool for answering the above questions relating to the design of ablative thermal protection systems.

The results presented in this chapter are based upon a 40% nylon-60% phenolic resin ablator. The elemental composition of this ablator is compared to that of the previously studied carbon-phenolic ablator in Table 6.1. A body radius of 9.0 feet and an entry velocity of 50,000 feet per second (15.24 km/sec) have also been selected for the current study. In addition two altitudes have been chosen which yield shock layer pressures (P_s) of 0.1 and 0.5 atmospheres.* At an entry velocity of 50,000 ft/sec, a shock pressure of 0.1 atmosphere represents an approximate point in the trajectory where radiation coupling first begins to occur. Shock calculations for this trajectory have shown that the maximum heating occurs near a shock pressure of 0.5 atmospheres. These flight conditions are compared in Figure 6.1 to typical trajectories for earth entry from space origins.

*Determined from Rankine Hugoniot Equations (Eqs. 3.73-3.76) and selected values of free stream velocity (U_∞) and free stream density (ρ_∞ corresponding to altitude).

TABLE 6.1

COMPARISON OF ELEMENTAL COMPOSITION (MASS PERCENT) OF
PHENOLIC-NYLON AND CARBON-PHENOLIC ABLATORS

<u>Element</u>	<u>Phenolic-Nylon</u>	<u>Carbon-Phenolic</u>
C	73.03	92.07
H	7.29	2.16
N	4.96	0.86
O	<u>14.72</u>	<u>4.91</u>
Total	100.00	100.00

A summary of the major flowfield parameters and wall heating results for all cases considered is given in Table 6.2.** As shown in Table 6.2, results have been obtained for the above flight conditions with several variations in transport and thermodynamic properties and in diffusion models. Following a presentation of the ablator-coupled reference cases (i.e., those computed with multicomponent diffusion and exact transport and thermodynamic properties and which are coupled to the ablator response), the effects of these variations will be assessed.

Coupled Ablator-Flowfield Analyses

In order to perform flowfield analyses which are coupled with ablator performance, it is necessary to employ a trial and error solution of the flowfield behavior and the ablator response.* The solution can be accomplished by varying mass injection rates until convergence of wall heating rates is achieved. Due to the excessive computer time requirements (minimum of six hours per case), this procedure was not employed using the SLAB analysis. Instead, parametric studies performed by Engel (Ref. 6.6) with a simplified analysis

*A discussion of ablator response was presented in Chapter III.

**Graphical results corresponding to each of these cases are given in Appendix H.

TABLE 6.2
SUMMARY OF MAJOR FLOWFIELD PARAMETERS AND CORRESPONDING HEATING RATE PREDICTIONS

Case Number	ρ_{∞} (lb/ft ³)	U_{∞} (ft/sec)	$(\rho v)_w$	T_s (°K)	P_s (atm)	Diffu- sion Model	Injectant Properties				Wall Heating Rates (watts/cm ²)**	
							cp	μ	k	δ (cm)	qc	qr
1*	3.57×10^{-5}	45,000	0.0	14,011	1.0	Binary	--	--	--	10.57	179	5981
2*	2.89×10^{-5}	50,000	0.0	15,044	1.0	Binary	--	--	--	9.48	213	7916
3*	2.41×10^{-5}	55,000	0.0	16,231	1.0	Binary	--	--	--	8.57	255	9588
4	2.85×10^{-6}	50,000	0.05	12,998	0.1	MCD	PN	PN	PN	10.85	120	340
5	2.85×10^{-6}	50,000	0.05	12,998	0.1	Binary	PN	PN	PN	10.85	120	397
6	1.45×10^{-5}	50,000	0.20	14,382	0.5	MCD	PN	PN	PN	13.93	0.3	2022
7	1.45×10^{-5}	50,000	0.20	14,382	0.5	Binary	PN	PN	PN	13.93	0.3	2064
8	2.85×10^{-6}	50,000	0.05	12,998	0.1	Binary	Air	PN	Air	11.38	44	372
9	1.45×10^{-5}	50,000	0.20	14,382	0.5	Binary	PN	PN	Air	13.90	1.2	2104
10	1.45×10^{-5}	50,000	0.20	14,382	0.5	Binary	Air	PN	Air	15.95	0.5	1964

*Cases run to verify overall analysis. These results are presented in Figure 5.4.

**Excluding surface re-radiation.

(VISRAD) were used to obtain an estimate of the ablator-coupled solutions. The VISRAD analysis predicted mass injection rates $[(\rho v)_w/(\rho v)_\infty]$, for the coupled solutions of approximately 0.05 and 0.20 respectively for pressures (P_s) of 0.1 and 0.5 atmospheres. These values were then input to the SLAB program and more accurate heating rates determined. It should be noted that the net radiant heat flux to the ablator surface must include re-radiation from the char (q_{RR}). For these results q_{RR} was determined from the Stefan-Boltzmann Equation:*

$$q_{RR} = \epsilon \sigma T^4 \quad (6.1)$$

where

$$\sigma = 5.6697 \times 10^{-8} \text{ watts/m}^2\text{°K}^4$$

$$\epsilon = 0.66 \text{ (Ref. 6.8)}$$

The total heating of the ablator surface is then, *

$$q_T = q_C + q_R - q_{RR} \quad (6.2)$$

*It is recognized that an approximation has been introduced by handling the re-radiation effect in the above manner. A rigorous approach would require that the appropriate part of the radiation contribution from the ablator surface be included throughout the flowfield in the calculation of the radiation flux divergence. However almost all of the energy re-radiated by the surface occurs below the frequency range of the flowfield. Consequently, the gas is optically thin with respect to this radiation, and this energy is not absorbed. An assessment of the effect of the small amount of energy in the frequency range that is absorbed is given by Engel (Ref. 6.6) which shows that this effect is of no consequence.

The total wall heating rates and the corresponding mass injection rates for the 0.1 and 0.5 atmosphere cases were then compared to the ablator response curves. These results are shown in Figure 6.2 and clearly show that the ablator-coupled solution is well approximated by the assumed mass injection rates. In addition, excellent agreement with the VISRAD analysis is observed. In the following discussion, the results of this rigorous analysis of a phenolic-nylon ablator will be more closely examined and a comparison made with the carbon-phenolic ablator.

The Effects of Simplifications in Property Models Upon Radiation Heating Prediction

Using phenolic nylon and air mixture properties for the injected gases, analyses were performed for each of the reference cases assuming both binary and multi-component diffusion. The analysis of the effects of viscosity, thermal conductivity and heat capacity models were performed assuming binary diffusion. The results of these investigations are presented in the following section.

Heating Rate Comparison for Binary and Multi-component Diffusion: Davy, et al. (Ref. 6.8), reported that for systems with large variations in molecular size,

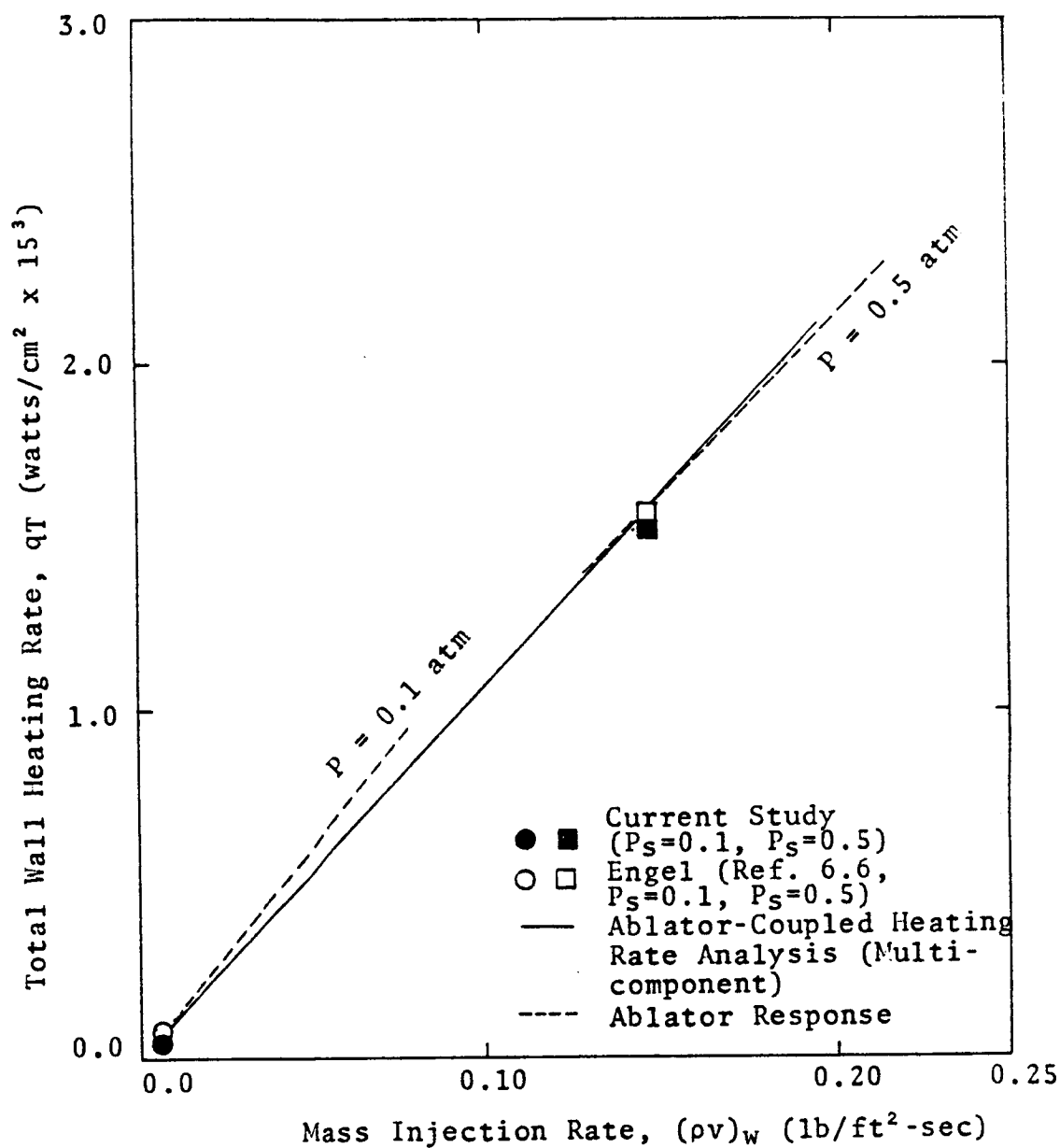


Figure 6.2. Ablator-Coupled Heating Rate Predictions for Phenolic-Nylon Ablator.

a binary coefficient characteristic of a large-small molecular interaction yielded the best results in predicting the multicomponent behavior. Therefore, the binary diffusion coefficient selected for the following comparison to multicomponent analyses was $H-C_2H_2$ (as computed from Equation 4.11). The heating rates and flight conditions pertinent to this comparison are presented in Table 6.3, and in Figure 6.3 the computed elemental distributions for the low and high blowing cases are shown for binary and multicomponent solutions. Referring to Table 6.3 the assumption of binary diffusion resulted in predictions of radiation heating rates which were in error by 16.8% in the case of low mass injection (Fig. 6.5A) and 2.1% for the high blowing case (Fig. 6.5B). The first observation to be made concerning these results is that the binary diffusion model selected for this comparison substantially over-predicts the diffusion velocities predicted by the more rigorous multicomponent analysis. It is further observed that the thickness of the diffusion zone is considerably less for the higher blowing rate. Although this effect can be partially attributed to the pressure differences, the principle cause is felt to be the differences in

TABLE 6.3
COMPARISON OF HEATING RATE PREDICTIONS FOR BINARY AND MULTICOMPONENT ANALYSES

Case Number	ρ_{∞} (lb/ft ³)	U_{∞} (ft/sec)	$\frac{(\rho v)_w}{(\rho v)_{\infty}}$	T_s (°K)	P_s (atm)	Diffusion Model	Injectant Properties c_p μ k	δ (cm)	Wall Heating, Rates (watts/cm ²) Convective Radiative
4	2.85×10^{-6}	50,000	0.05	12,998	0.1	MCD*	PN** PN	10.85	120 340
5	2.85×10^{-6}	50,000	0.05	12,998	0.1	Binary	PN PN	10.85	120 397
6	1.45×10^{-5}	50,000	0.20	14,382	0.5	MCD	PN PN	13.93	0.3 2022
7	1.45×10^{-5}	50,000	0.20	14,382	0.5	Binary	PN PN	13.93	0.3 2064

*(MCD) Multicomponent diffusion

** (PN) Phenolic Nylon

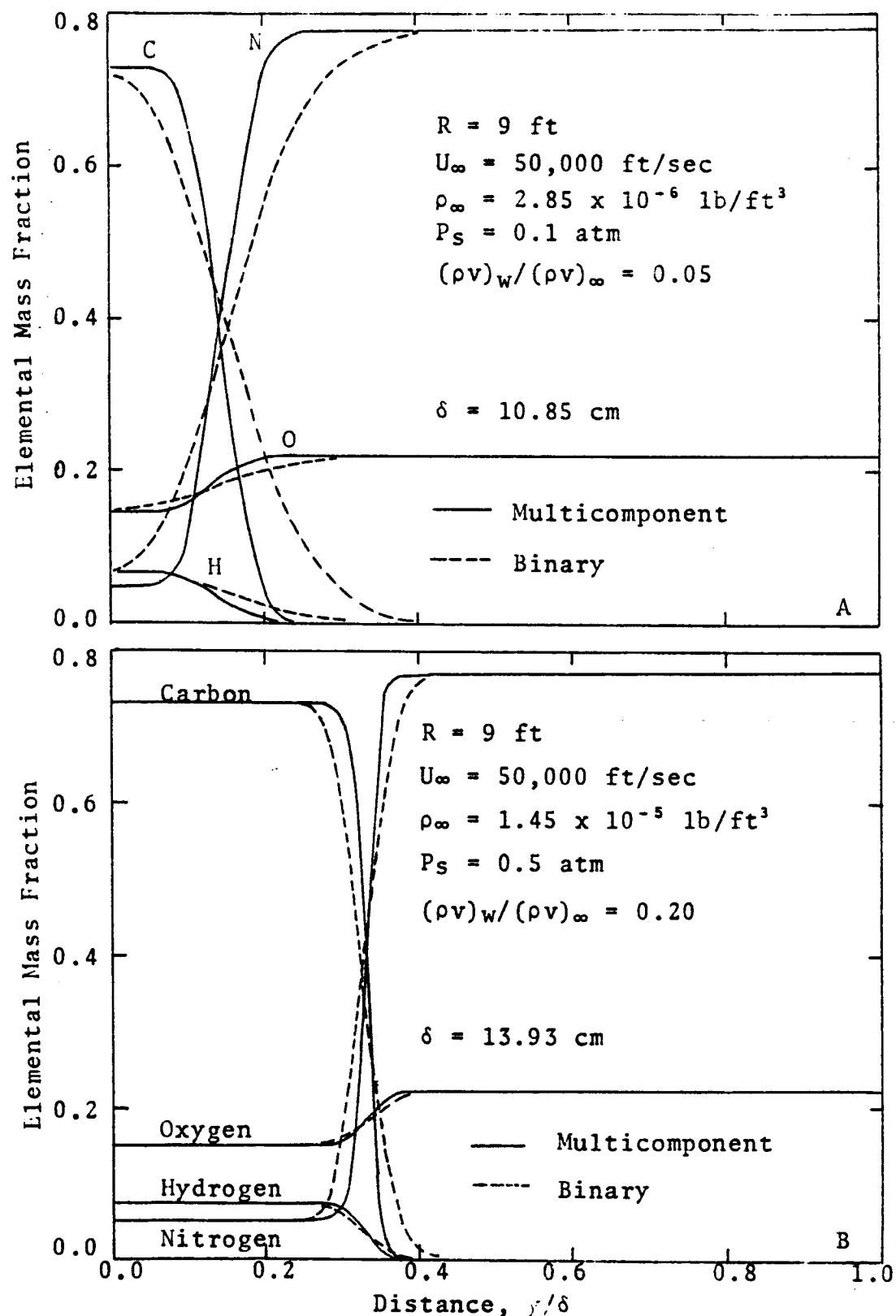


Figure 6.3. Comparison of Elemental Profiles Obtained From Binary and Multicomponent Diffusion Calculations.

the corresponding velocity profile. It has been observed that for higher blowing rates, the velocity profile changes more abruptly through the stagnation region, thereby reducing the zone in which the diffusion velocities contribute to the total mass flux.

The species mass fractions corresponding to the previously given elemental solutions are presented in Figures 6.4, 6.5, 6.6 and 6.7. These figures include comparisons between binary and multicomponent behavior for the principle species. For the low blowing case presented in Figures 6.4 and 6.5, considerable differences in the predicted compositions are observed. In contrast, the differences predicted for the high blowing case are quite small (Figs. 6.6 and 6.7).

From these observations, it can be concluded that for the high blowing rate case, the choice of diffusion models has very little influence upon the wall heating rates. From the low blowing rate case it is concluded that a more precise description of the diffusion process is needed for accurate heating rate predictions. This result contradicts the

*A more precise description could be obtained by performing uncoupled studies with the multicomponent diffusion analysis developed in this study.

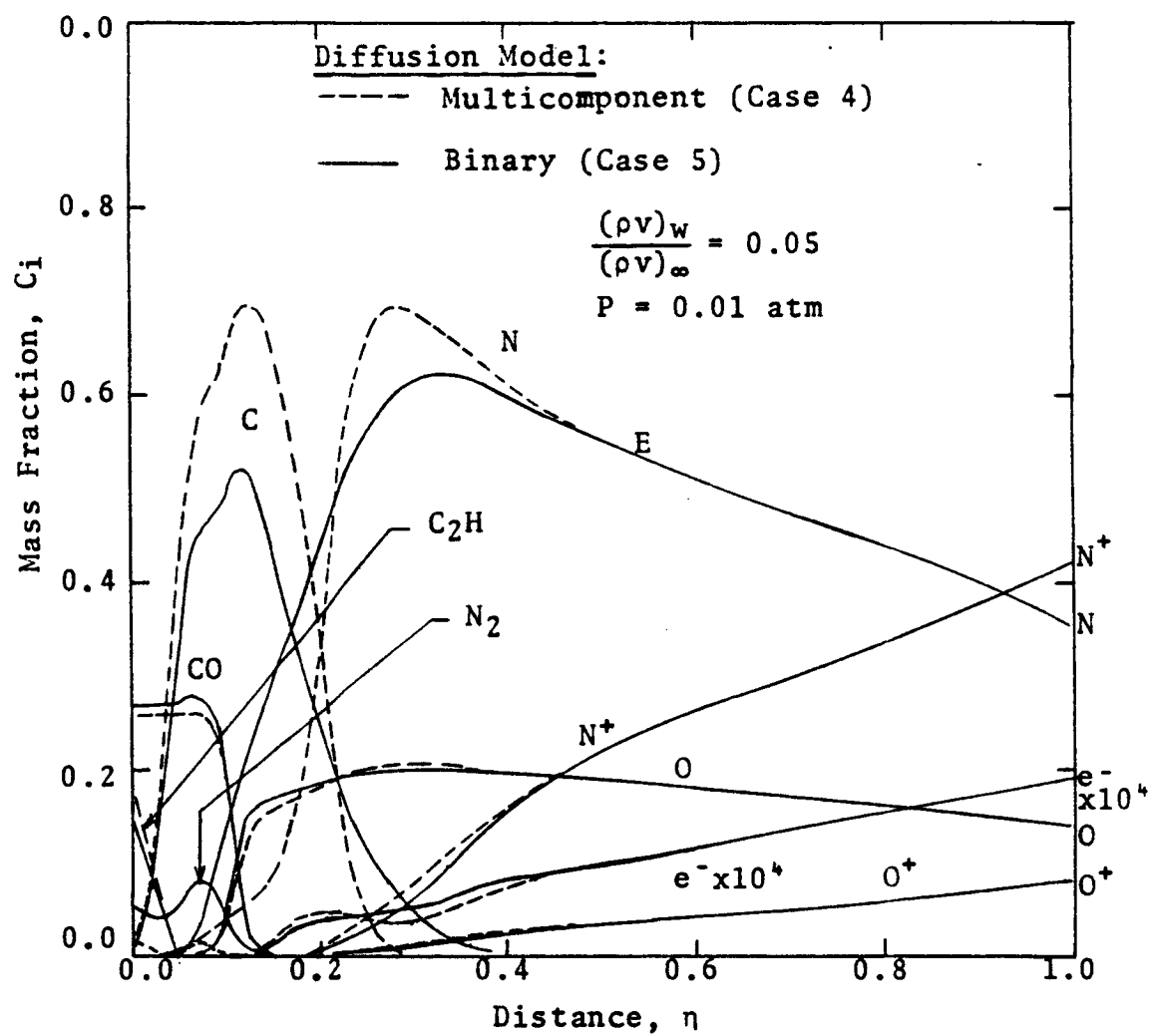


Figure 6.4. Composition Profiles For Air and Major Ablation Species.

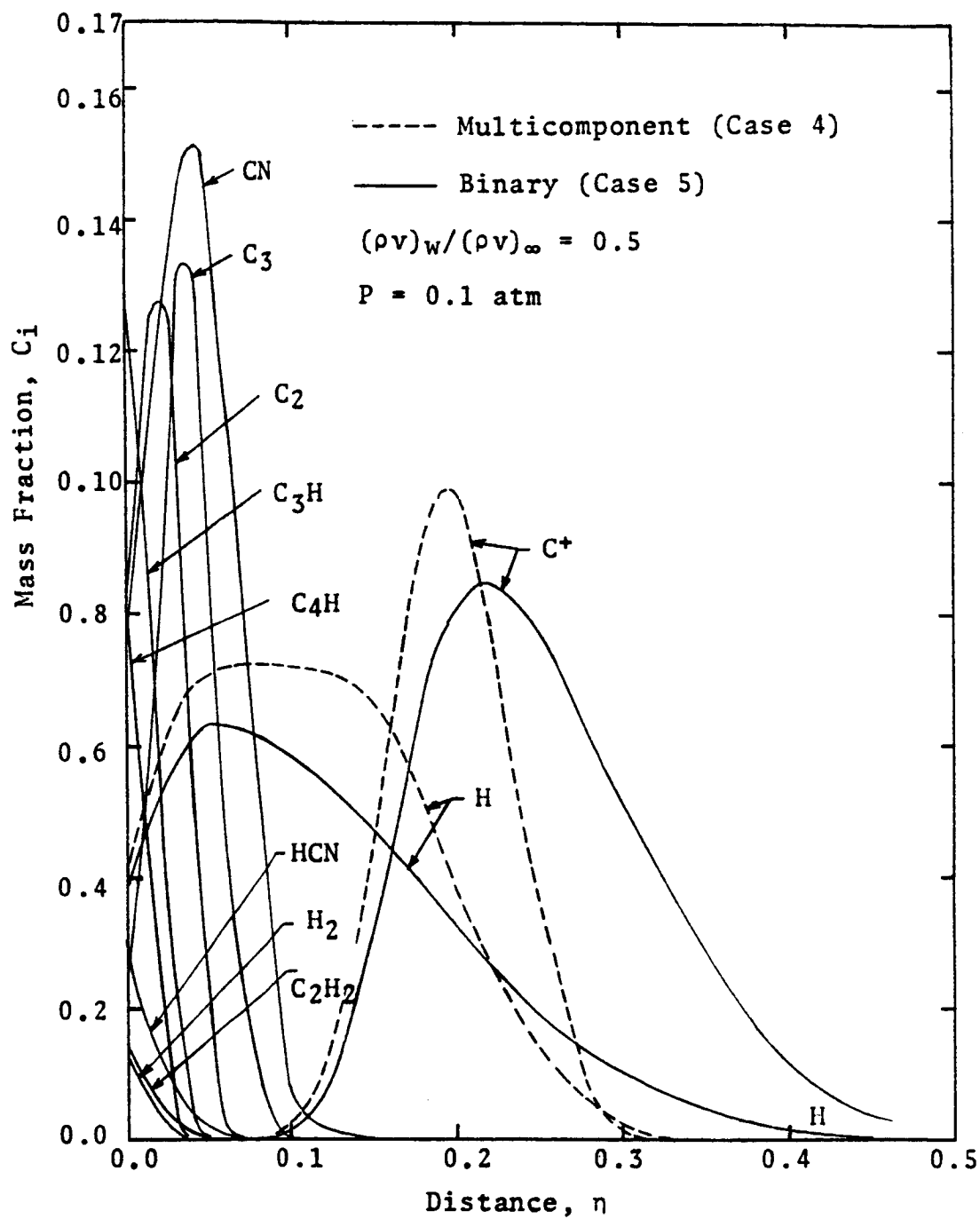


Figure 6.5. Composition Profiles for Minor Ablation Species.

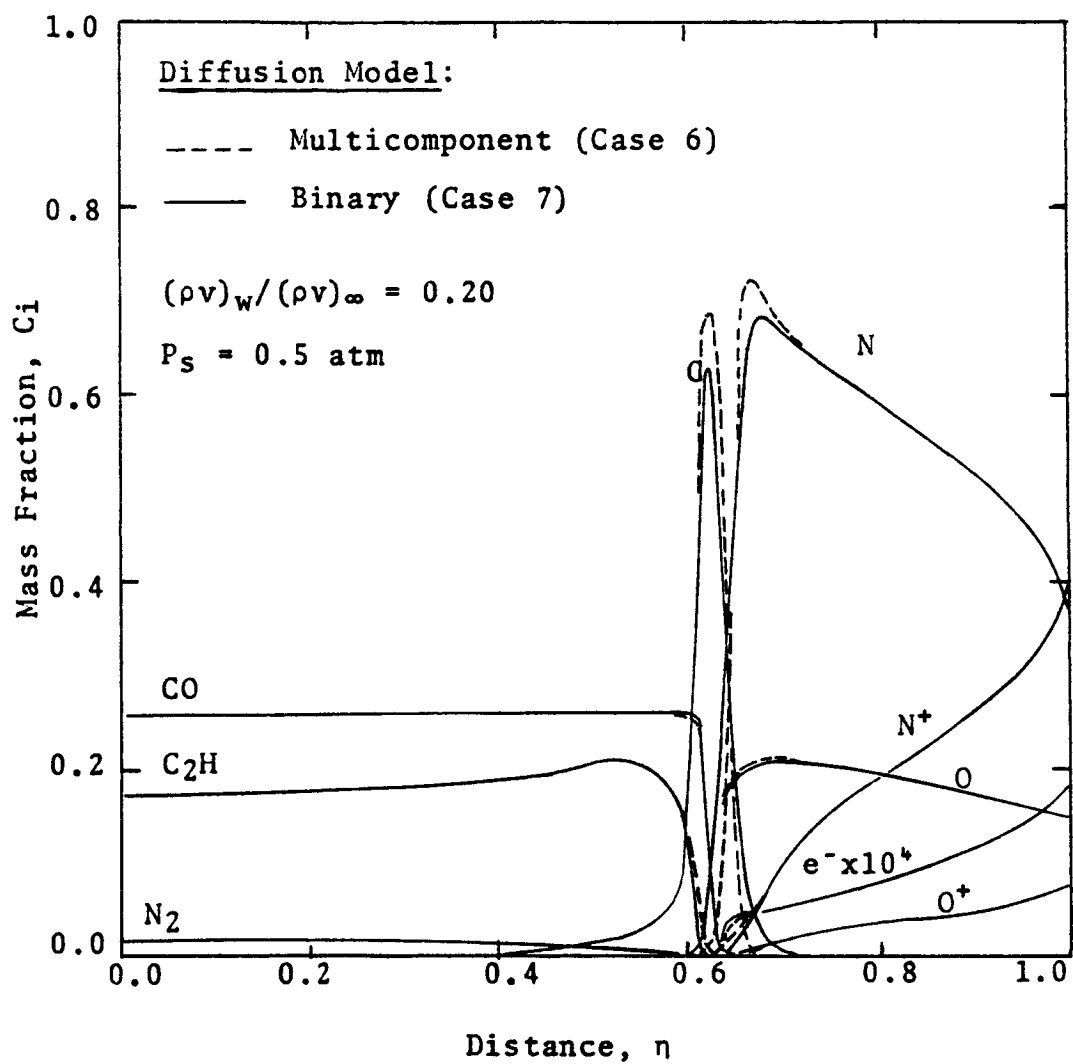


Figure 6.6. Composition Profiles for Air and Major Ablation Species.

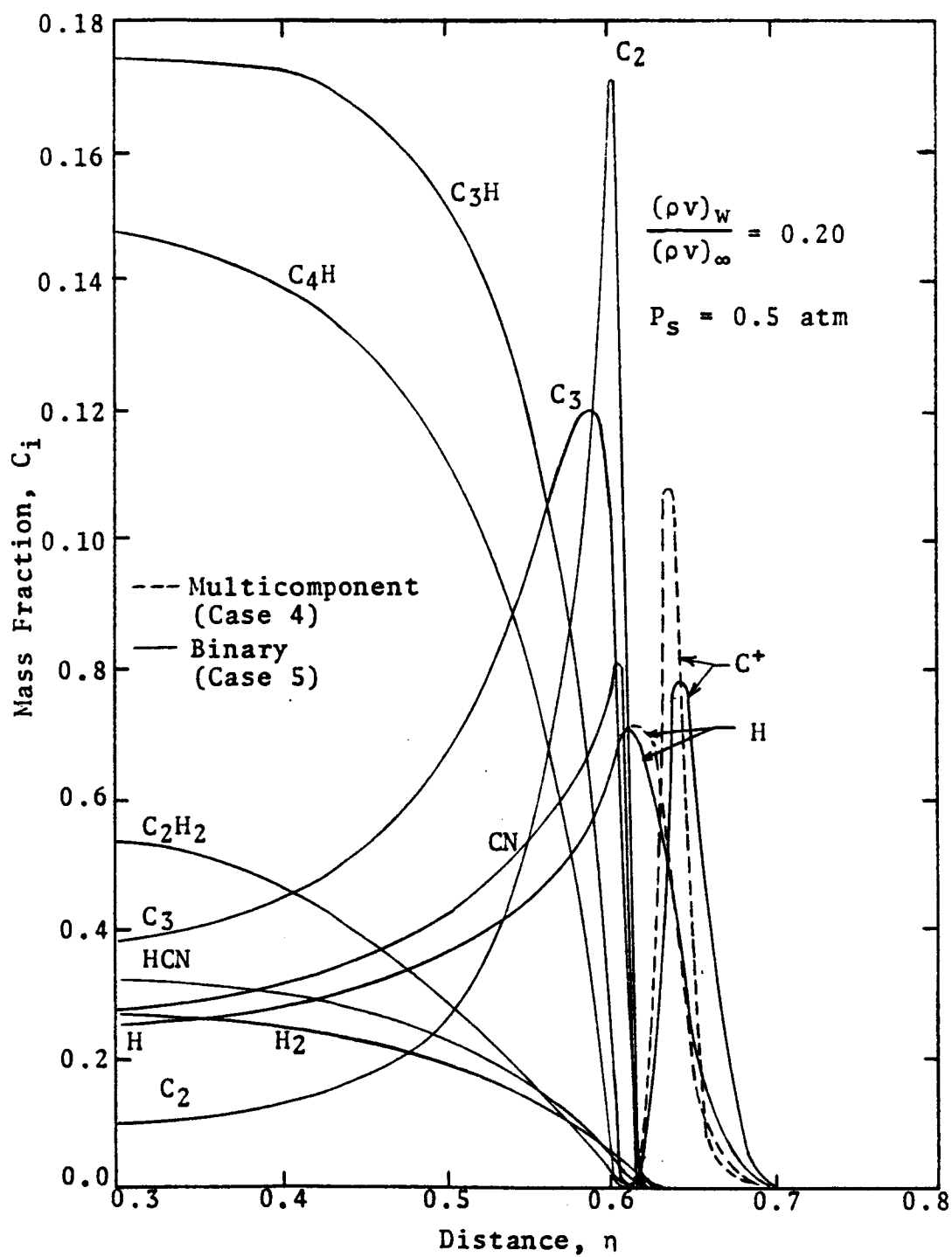


Figure 6.7. Composition Profiles for Minor Ablation Species.

observation by Rigdon, "that the choice of binary diffusion was not critical" (Ref. 6.2). However, the statement is applicable for high blowing situations such as those on which his statement was based.

It is noted that for the low blowing and correspondingly low pressure case (0.1 atm), the error in radiative heating is of little consequence since the heating rate itself is an order of magnitude less than the heating rate observed for the 0.5 atmosphere case. Recalling Figure 6.2 it is noted that as the heating rate increases to higher and more significant values the mass injection rate correspondingly advances. The ablator thus responds in such a manner as to decrease the inaccuracies in heating rate predictions which are brought about by the simplified diffusion model.

Comparisons of Heating Rate Predictions
Using Ablation Product-Air and Pure Air
Transport and Thermodynamic Properties

In the previous section it was noted that for large blowing rates, the selected binary diffusion coefficient gave a good approximation of the diffusion process. In spite of the differences (16.8%) in heating rate predictions encountered for the low blowing rate

case, it is felt that this model is suitable for studies of the effects of assuming different transport and thermodynamic property models. Therefore, for computational convenience, the same binary coefficient was employed for the results of this section. Also, a preliminary analysis revealed that the effect of using air viscosity was negligible (less than 1.0%) with respect to heating rate predictions. Nevertheless, this property was computed in all cases to correspond to the actual composition of the air and ablation product mixture.

Comparisons were made at both the high and low blowing conditions to determine effect on heating rates of assuming air heat capacity and thermal conductivities for the injected ablation products. For the high blowing case, the effect of using only the thermal conductivity of air and maintaining the proper value for the remaining ablation product thermodynamic and transport properties was also examined. All of these results are summarized in Table 6.4. In Figure 6.8 and 6.9 comparisons are made between the temperature and radiative flux divergence profiles resulting from these assumptions for the high and low blowing cases.

TABLE 6.4
COMPARISON OF HEATING RATE PREDICTIONS OBTAINED BY ASSUMING AIR PROPERTIES FOR
INJECTED SPECIES

Case Number	ρ_{∞} (#/ft ³)	U_{∞} (ft/sec)	$\frac{(\rho v)_w}{(\rho v)_{\infty}}$	T_s (°K)	P_s (atm)	Diffusion Model	Injectant Properties			δ (cm)	Wall Heating Rate	
							C_p	μ	k		Convective	Radiative
5	2.85×10^{-6}	50,000	0.05	12,998	0.1	Binary	PN*	PN	PN	10.85	120	397
8	2.85×10^{-6}	50,000	0.05	12,998	0.1	Binary	Air	PN	Air	11.38	44	372
7	1.45×10^{-5}	50,000	0.20	14,382	0.5	Binary	PN	PN	PN	13.93	0.3	2064
9	1.45×10^{-5}	50,000	0.20	14,382	0.5	Binary	PN	PN	Air	13.90	1.2	2104
10	1.45×10^{-5}	50,000	0.20	14,382	0.5	Binary	Air	PN	Air	15.95	0.5	1964

*Phenolic Nylon

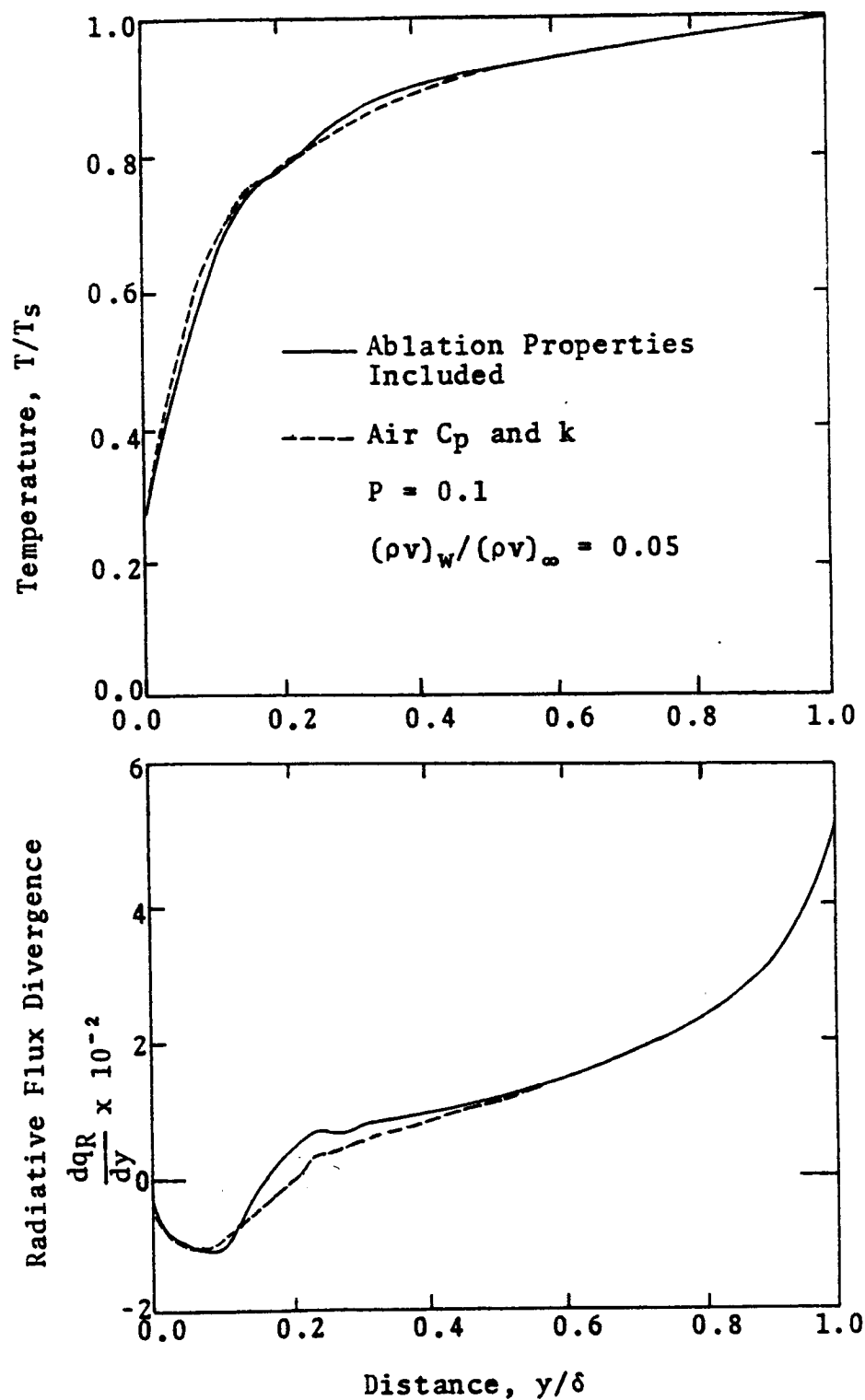


Figure 6.8. Temperature and Flux Divergence Profiles for Various Property Models.

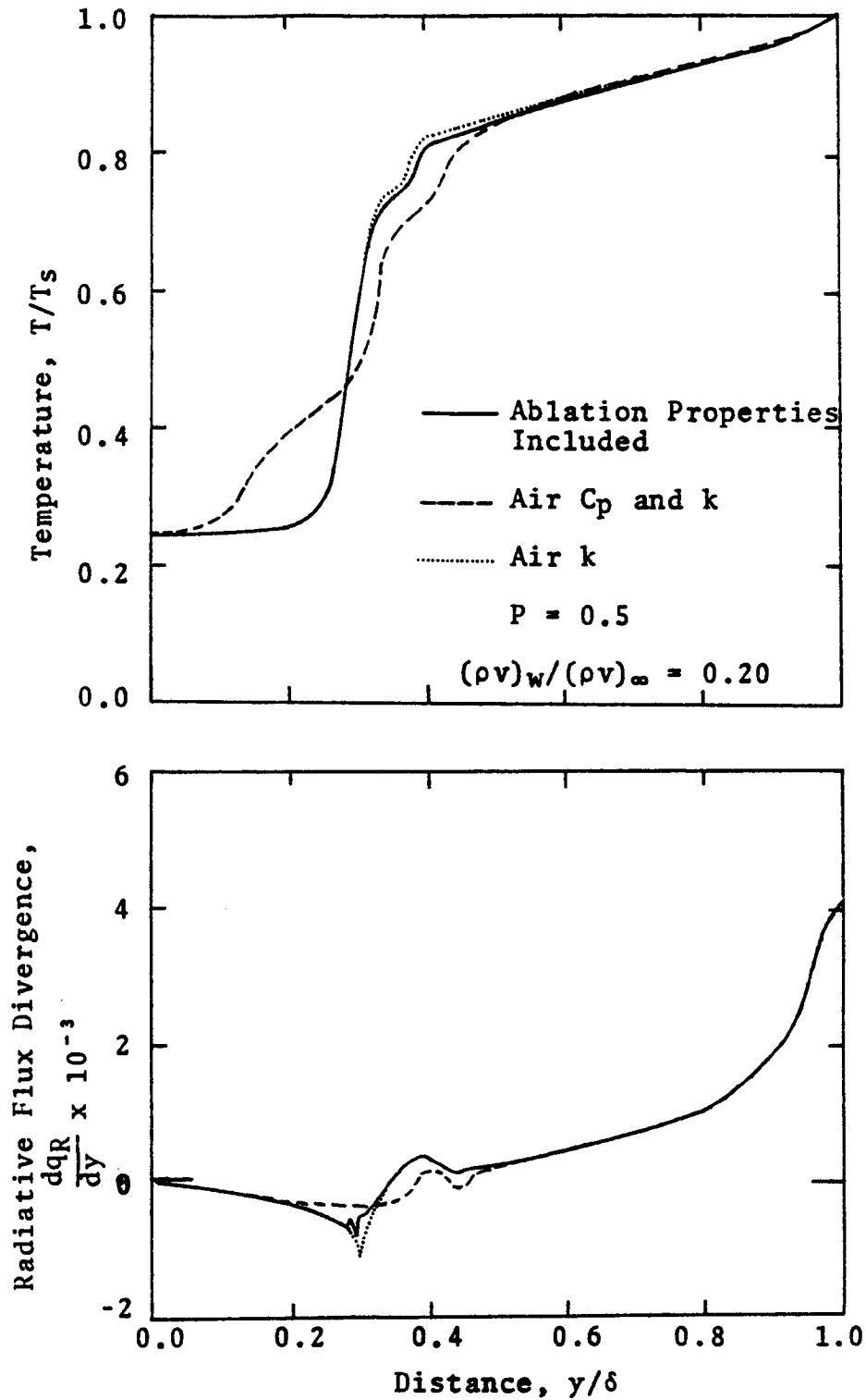


Figure 6.9. Temperature and Flux Divergence Profiles for Various Property Models.

For the low pressure, low mass injection case (Fig. 6.8), the radiative heating was under-predicted by 4.8% by using the air properties. Although the air properties resulted in an increase of approximately 120% in wall temperature gradient, the predicted convective heating rate was reduced by 63.3%. In comparison to the total heating this error only amounts to 14.7%. In Figure 6.10, the ratios of the properties of phenolic nylon and air mixtures to the corresponding properties of pure air are given for the cases considered. From this figure, it is noted that at the wall temperature of 3450°K , the actual thermal conductivity is approximately six times the corresponding pure air property, thus explaining the observed variation in convective heating rates.

For the higher blowing case (Fig. 6.9), very little change is observed in the temperature and flux divergence profiles as a result of using air thermal conductivity for the injected gases. The result is attributed to the fact that the conduction effects are restricted to a thin region around the stagnation point. The variation in predicted radiative heating rates resulting from this assumption was only 1.9%.

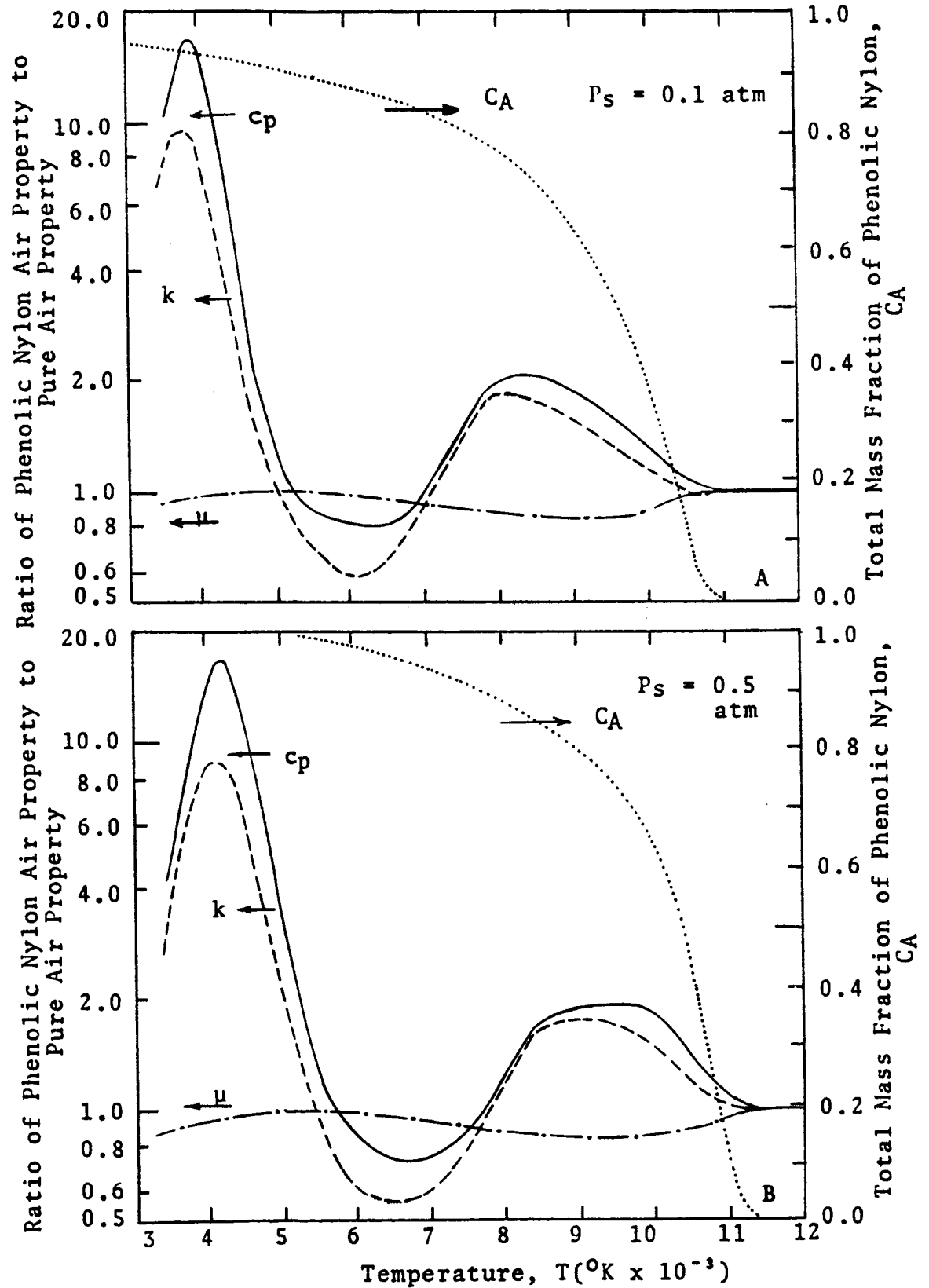


Figure 6.10. Comparison Between Phenolic Nylon and Air Mixture Properties to Those of Pure Air.

In comparing the effect of using air heat capacity for the ablation products, it is noted that extensive differences* appear in both the temperature and radiative flux divergence profiles. In spite of these observations, the predicted radiation heating rates varied only by 4.8%.

In this case the assumption of air properties resulted in an increase in shock stand-off distance from 13.93 cm to 15.95 cm (a 14.5% increase). This effect accounts for the fact that while the outer temperatures for the air properties case were generally lower (tending toward lower heating rates), the zone of more intense radiation (the high temperature air) was more extensive. Since these effects have confounded the results, a general conclusion concerning the importance of assuming the correct heat capacity for the injected species cannot be made. However, for both of the cases considered, the reduction of temperature which occurs in the ablation layer when the proper heat capacity is included, is attributed to the resulting increase in heat capacity. In fact, as shown in

*It should be pointed out that the flux divergence profile appearing in Figure 6.11 has been scaled down by a factor of ten as compared to the low pressure case shown in Figure 6.10.

Figure 6.10, the heat capacity of phenolic-nylon at the wall temperature (3450°K) is approximately 17 times greater than air for the same temperature. Due to the extensive variations in temperature and flux divergence that were observed in this comparison (Fig. 6.9), it is concluded that the use of air heat capacity for injected species can contribute to significant errors in heating rate predictions.

The Effectiveness of Phenolic Nylon
Ablators in Reducing Radiative Heat
Transfer to the Wall

In the following discussion an attempt will be made to compare the performance of the phenolic-nylon ablator examined in this analysis with the performance of carbon-phenolic ablators reported in References 6.1 to 6.4. However, little agreement has been reported in comparisons among investigations of the carbon-phenolic ablator. It is felt that the apparent lack of agreement is due to two major causes: (1) ill-suited comparisons (e.g., values obtained from widely varying flight conditions and body geometry) and (2) oversimplified radiation models. Consequently, an effort was made to select and compare only data from consistent flight conditions and body radii. As a consequence, no comparisons were available

for the low pressure ($P_s = 0.1$) case. However, several values were reported in the range of the higher pressure ($P_s = 0.5$) case. A comparison among these results is shown in Figure 6.11. The value reported by Smith, et al. (Ref. 6.4) is considered to be somewhat in error due to the fact that line radiation contributions from atomic carbon and hydrogen were excluded in that analysis. Similarly, the results of Wilson (Ref. 6.1) include only continuum radiation. In comparing the performance of the phenolic-nylon ablator examined in the current study to that of the carbon-phenolic ablator it is desirable for an ablator-coupled mass injection rate to be also used for the latter system. Unfortunately this information is not available. However it is reasonable to assume that the ablator response for these two systems is similar; therefore a comparison can be made at the mass injection rate of 20%. On the basis of this comparison it appears that the phenolic-nylon ablator is approximately 5% less effective than the carbon phenolic ablator.*

*Under the imposed flight conditions.

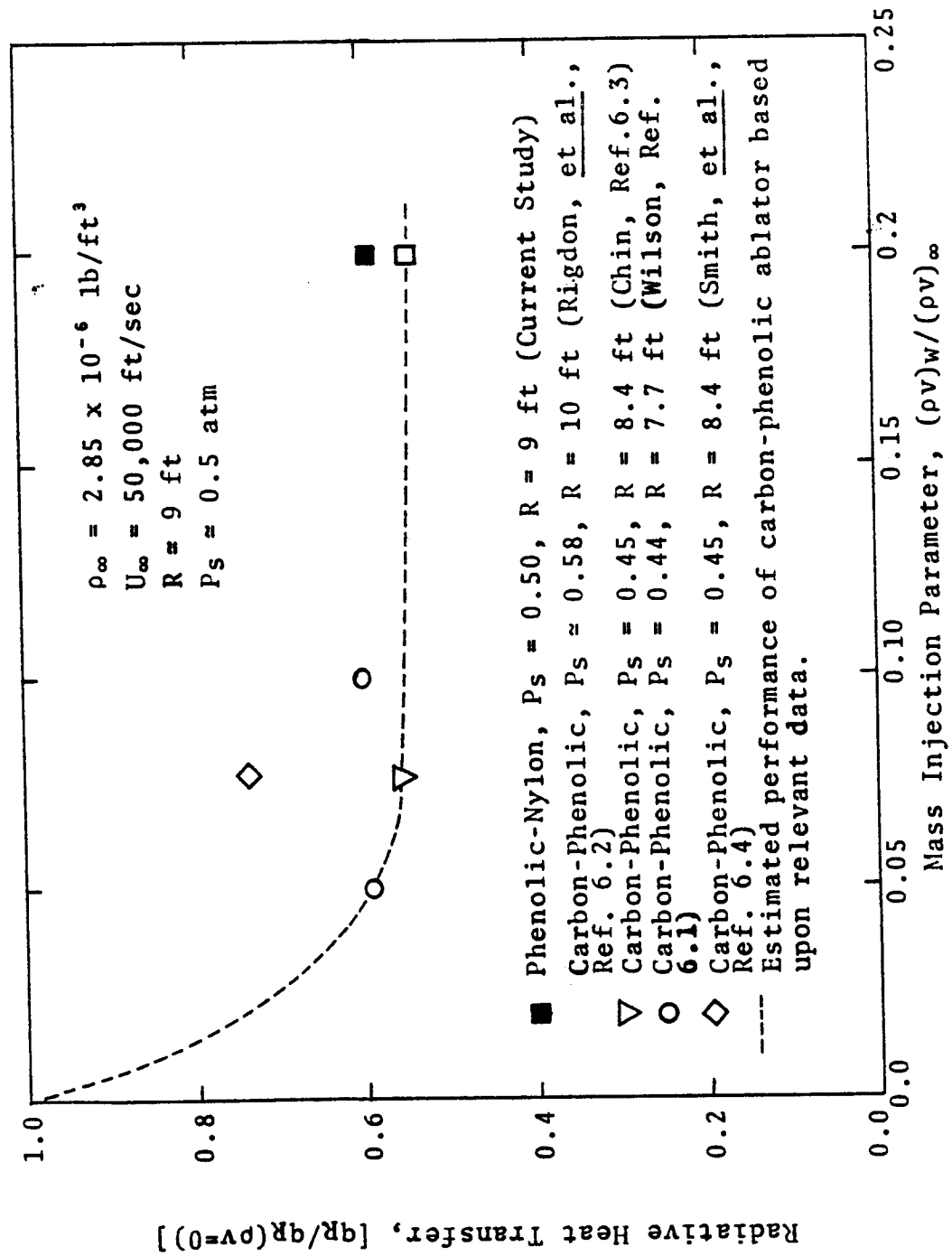


Figure 6.11. Comparison Between Effectiveness of Phenolic-Nylon and Carbon-Phenolic Ablators.

Further Observations

Irregularities in predicted temperature profiles:

Since the intermediate plateaus in the temperature profiles are present for all cases considered, their presence is attributed to radiation phenomena. Further evidence of the radiation origins of this behavior is the fact that the plateaus are less pronounced for the low pressure cases where radiation is substantially less. Upon examining the species distribution corresponding to these cases (Figs. 6.5, 6.6, 6.7 and 6.8) it is observed that the spacial location of the large peak in atomic corresponds exactly to the location of the intermediate temperature plateaus. The local increase in the absorption of the ablation layer due to the presence of this species is thus considered cause of the intermediate plateaus in the temperature distributions.

Thermal Diffusion Effects: Throughout the preceding heating rate analysis, the contributions of thermal diffusion have been neglected. Due to the extremely high values of the radiation heat transport, large variations (as much as a factor of six) in thermal conductivities were observed to have only slight

effects upon the radiation heat flux (a maximum of 4.8%). Furthermore, in the process of examining the effects of binary and multicomponent diffusion on radiation heating predictions, large variations in the diffusive behavior were observed. In spite of these variations a relatively small effect upon the heating rate was detected. It is well known from irreversible thermodynamics that the cross effects--in this case the Soret and Dufour effects--are small with respect to the principle transport mechanisms. It would therefore appear that the thermal diffusion effects are indeed negligible. To further substantiate this reasoning, a posteriori assessment was made of the contribution to the mass fluxes resulting from the large temperature gradients encountered.* A conservative estimate revealed that the maximum Soret effect is at least an order of magnitude less than the significant species mass fluxes. On the basis of the foregoing observations, it is therefore concluded that the neglect of thermal diffusion effects is an appropriate assumption in the current analysis.

*See Appendix I.

Incomplete Radiation Data: An examination of the molar compositions corresponding to the species distributions presented in Figures 6,5-6.8 reveals that the ablation species included in the radiation model (LRAD)* represent a large percentage of those actually present. Overall, the minimum total molar percentage of the included species was 81.5% (Case 6). Furthermore, this percentage was seen to increase up to the stagnation point where a value of 93.7% was observed. From the flux divergence profile given in Figure H-4 it is noted that the major portion of the radiative absorption in the ablation layer occurs in the region immediately behind the stagnation point where the excluded species are present in the lowest concentration.

Summary

An investigation of the performance of a phenolic-nylon ablator has been made for flight conditions characteristics of return from planetary flight. The conclusions and recommendations arising from the results of this study are presented in the following chapter.

*The excluded species, for which no radiation data exists are C^+ , CN, C_2H_2 , C_3H , C_4H , and HCN.

REFERENCES

- 6.1. Wilson, K. H., "Stagnation Point Analysis of Coupled Viscous-Radiating Flow With Massive Blowing," NASA CR-1548 (June, 1970).
- 6.2. Rigdon, W. S., R. B. Dirling and M. Thomas, "Stagnation Point Heat Transfer During Hypervelocity Atmospheric Entry," NASA CR-1462 (February, 1970).
- 6.3. Chin, J. H., "Radiation Transport for Stagnation Flow Including the Effects of Lines and Ablation Layer," AIAA Paper No. 68-644, (June, 1968).
- 6.4. Smith, G. L., J. T. Suttles, E. M. Sullivan, and R. A. Graves, Jr., "Viscous Radiating Flow Field on an Ablating Blunt Body," AIAA Paper No. 70-218 presented at AIAA 8th Aerospace Sciences Meeting, New York (January 19-21, 1970).
- 6.5. Howe, J. T. and Y. S. Sheaffer, "Role of Charge Separation and Pressure Diffusion in the Gascap of Entry Objects," AIAA Journal, Vol. 7, No. 10 (October, 1969), p. 1971-1977.
- 6.6. Engel, C. D., "Ablation and Radiation Coupled Viscous Hypersonic Shock Layers," Ph.D. Dissertation, Louisiana State University, Baton Rouge, Louisiana (1971).
- 6.7. Davy, W. C., R. A. Craig and G. C. Lyle, "An Evaluation of Approximations Used in the Analysis of Chemically Reacting, Stagnation Point Boundary Layers with Wall Injection," in Proceedings of the 1970 Heat Transfer and Fluid Mechanics Institute, ed. by Turgut Sarpkaya, (Stanford University Press: Stanford, California) 1970, p. 222-237.
- 6.8. Pope, R. B., "Measurement of the Total Surface Emittance of Charring Ablators," AIAA Journal, Vol. 5, No. 12, (1967), pp. 2285-2287.

CHAPTER VII

CONCLUSIONS AND RECOMMENDATIONS

Conclusions

Based upon the results of this research the following conclusions are drawn:

1. The binary diffusion can yield accurate heating rate predictions at all blowing rates provided the appropriate binary coefficient is employed.
2. For low mass injection, the choice of the appropriate binary diffusion coefficient is critical in determining the proper wall heating rate.
3. For large mass injection rates ($>20\%$), typical of those occurring during peak heating, the principal transport mechanisms (i.e., diffusion, conduction, and viscous transport) contribute very little ($<5\%$) to the heat transfer process.
4. For low mass injection (≤ 0.05) characteristic of low heating rates, thermal conduction significantly contributes to the heat transfer process.
5. Since heat capacity affects temperatures throughout the flowfield, this thermodynamic property

must be properly determined or significant errors in heat rate predictions will be computed.

6. For the flight conditions examined the 40% nylon-60% phenolic resin ablator is slightly less effective in blocking radiative heating (~5%) than the carbon-phenolic ablator which it was compared.

Recommendation for Design Calculations

Transport Properties: It has been observed in this study that for the higher heating rates (~20%) and correspondingly higher mass injection rates, the flowfield is inviscid except for a thin region at the stagnation point. Consequently, these heating rate predictions were insensitive to variations in transport properties (including diffusion coefficients). Although heating rates were affected by variations in transport properties at the low mass injection conditions, it was noted that the corresponding heating rates were an order of magnitude less than those anticipated during peak heating. Inaccuracies in heating predictions at these conditions are therefore of little consequence in determining overall surface removal for the entire trajectory. It is therefore recommended that for computational convenience simplified transport

models (i.e., air) be employed in design calculations relating to re-entry from planetary missions.

Heat Capacity: In this study heat capacity has been observed to affect temperature profiles throughout the flowfield. Therefore, it is recommended that this property be properly determined for the existing chemical system.

Recommendations for the Improvement of the SLAB Program

The major difficulty in the use of the SLAB program is that of maintaining the proper stepsize distribution. Although a stepsize control subroutine is employed in this analysis, it is quite common for the temperature profile to shift from one iteration to the next to such an extent that the current stepsize distribution is inadequate and has to be changed by hand. If this change is not made then instability occurs and the solution wanders off into oblivion. To circumvent this difficulty it is recommended that more steps be used in the analysis. For fear of further extending the required computer time, the addition of more steps was not attempted. In retrospect, it is felt that the overall analysis would be shorter since little or no time would be spent in recovering from instabilities.

An examination of the typical results obtained from this analysis reveals that the elemental profiles are constant over a large portion (80-90%) of the flowfield. In view of this fact, considerable time could be saved by internally establishing during the first iteration a table of equilibrium compositions of pure air and of the pure ablation products. In subsequent iterations it would then only be necessary to perform equilibrium calculations in the diffusion zone. In this manner, the computer time possibly could be reduced by as much as sixty to eighty percent.

NOMENCLATURE

<u>Symbol</u>	<u>Description</u>	<u>Units</u>
A_{ij}	Element ratio (defined in Appendix A)	
C_d	Drag coefficient	none
C_f	Friction factor	none
C_h	Heat transfer coefficient	none
C_p	Total heat capacity (defined by Equation 3.41)	FL/MT
C_{pf}	Frozen heat capacity, $C_i C_{pi}$	FL/MT
C_{pi}	Heat capacity of species i	FL/MT
C_i	Mass fraction of species i	none
C_j	Mass fraction of element j	none
C_p	Total molar heat capacity (Eq. 4.32)	FL/mole T
C_{pi}	Molar heat capacity of species i	FL/mole T
\bar{D}	Reference diffusion coefficient (Eq. 2.23)	L^2/t
D_{ij}	Binary diffusion coefficient	L^2/t
\tilde{D}_j	Effective elemental diffusion coefficient	L^2/t
D_i	Effective diffusion coefficient	L^2/t
D_i^T	Thermal diffusion coefficient	M/Lt

<u>Symbol</u>	<u>Description</u>	<u>Units</u>
D_{ij}	Multicomponent diffusion coefficient	L^2/t
e_{ij}	Mass fraction of element j in compound i (Appendix A)	none
f'	Velocity function $\left(\frac{df}{dn}\right)$	none
F_i	Diffusion factors (Eq. 2.23)	none
g_c	Gravitational constant	ML/Ft^2
H	Total enthalpy, $H = h + \frac{v^2}{2g_c}$	FL/M
h	Static enthalpy, $h - C_i h_i$	FL/M
h_i	Enthalpy of species i	FL/M
H_T^0	Molar enthalpy at temperature T	$FL/mole$
I_j	Total mass flux of element j	M/L^2t
J_i	Diffusive mass flux of species i	M/L^2t
\tilde{J}_j	Diffusive mass flux of element j	M/L^2t
k	Total thermal conductivity (Eq. 3.42)	F/tT
k_f	Frozen thermal conductivity (Eq. 4.5)	F/tT
k_b	Bulk thermal conductivity (of char)	F/tT
ℓ	Number of elements	none
m	Mass	M
m_i	Mass of particle i	M
M	Molecular weight	$M/mole$
M_i	Molecular weight of species i	$M/mole$

<u>Symbol</u>	<u>Description</u>	<u>Units</u>
\tilde{M}_j	Atomic weight of element i	M/mole
n	Number density	particles/ L^3
P	Pressure	F/L^2
P_r	Prandtl number, $C_p\mu/k$	none
q_r	Radiative heat flux	F/Lt
q_r^+	Total radiative heat flux at the wall	F/Lt
R	Principal body radius	L
R	Ideal gas constant	$F/mole\ T$
r_i	Homogeneous reaction term	M/TL^3
Re_s	Reynolds number, $\rho_s U_\infty R/\mu_s$	
s_i	Sublimation rate	M/TL^3
S_i	Surface mass generation	M/TL^3
T	Temperature	T
T_{ij}^*	Reduced temperature (Eq. 4.13)	none
u	Tangential velocity	L/t
v	Normal velocity	L/t
U_∞	Normal free stream velocity	L/t
Y_i	Mole fraction of species i	none
δ	Shock standoff distance	L
$\bar{\delta}$	Transformed standoff distance (Eq. 3.93)	none
ϵ	Difference between body and shock angles (See Fig. 3.1)	radians

<u>Symbol</u>	<u>Description</u>	<u>Units</u>
η	Dorodnitzn variable	none
θ	Body angle (See Fig. 3.1)	radians
κ	Local body curvature	1/L
$\tilde{\kappa}$	$1+\kappa y$	none
μ_i	Viscosity of species i	M/Lt
μ	Mixture viscosity	M/Lt
v	Number of species	none
ρ	Density	M/L ³
ρ_i	Partial density of species i	M/L ³
ρ_g	Density of the gas phase	M/L ³
ρ_o	Density of the virgin plastic	M/L ³
$\bar{\rho}$	Density ratio across the shock	none
σ	Collision diameter	L
k_c	Stefan-Boltzmann constant 5.6697×10^{-8} watts/m ² °K ⁴	F/tLT ⁴
ϕ	Shock angle	Radians
$\omega_{i(1,1)}$	Chemical generation term	M/L ³ t
Ω_{ij}	Collision integral for diffusion coefficients	none
<u>Subscripts</u>		
i	Species i	
w	Wall quantities	
o	Stagnation line quantities	

<u>Symbol</u>	<u>Description</u>	<u>Units</u>
---------------	--------------------	--------------

∞	Free-stream conditions	
S	Quantities immediately behind shock	

Superscripts

0	Standard state quantity
-	Evaluated on char side of ablator interface
+	Evaluated on flowfield side of ablator interface

APPENDIX A

TRANSFORMATION OF SPECIES CONTINUITY EQUATIONS TO ELEMENTAL CONTINUITY EQUATIONS

The elemental mass distribution within a single chemical component can be easily determined from the atomic weights of the elements present, M_j ; the molecular weight of the compound, M_i ; and the chemical formula. For example, the weight fractions of H in H_2O is 2/18 and O is 16/18. Mathematically this is expressed as follows:

$$e_{ij} = \frac{A_{ij}\tilde{M}_j}{M_i} = \left(\begin{array}{l} \text{the mass of element } j \text{ per unit} \\ \text{mass of compound } i \end{array} \right) \quad (A-1)$$

where A_{ij} is simply the moles of element j per mole of compound i . In the above example $A_{H_2O,H} = 2$ and $A_{H_2O,O} = 1$.

The elemental mass distribution within a mixture of chemical species can be determined from the species mass distribution by multiplying each component mass fraction by the corresponding elemental distribution and summing over all species as follows:

$$\tilde{C}_j = \sum_{i=1}^V e_{ij}C_i = (\text{mass fraction of element } j) \quad (A-2)$$

where C_i is the mass fraction of component i and v is the number of species.

The elemental continuity equations can be derived from the species continuity equations (Eqs. 3.15) in the previous manner. The latter equations are written as follows:

$$\rho v \frac{dC_i}{dy} = - \frac{dJ_i}{dy} + \omega_i \quad (\text{A-3})$$

Multiplication of each equation by the corresponding elemental distributions and summing over the species gives:

$$\rho v \frac{d\tilde{C}_j}{dy} = - \frac{d}{dy} \sum_{i=1}^v e_{ij} J_i + \sum_{i=1}^v e_{ij} \omega_i \quad j=1, \dots, \quad (\text{A-4})$$

where v is the total number of elements.

It is convenient to define \tilde{J}_j , an elemental mass diffusion flux as follows:

$$\tilde{J}_j = \sum_{i=1}^v e_{ij} J_i = \tilde{M} \sum_{i=1}^v \frac{A_{ij} J_i}{M_i} \quad (\text{A-5})$$

Substituting Equation A-5 into Equation A-4, and noting that the total mass of any element is unchanged due to chemical reactions the elemental continuity equation can be written as follows:

$$\rho v \frac{d\tilde{C}_j}{dy} = - \frac{d\tilde{J}_j}{dy} \quad (\text{A-6})$$

With the exception of the generation term, Equation A-6, is now of the same form as Equation A-3, the species continuity equation.

When the mass flux J_i appearing in Equation A-3 can be represented with binary diffusion (Fick's Law, Eq. 3.22), the elemental flux can be determined in the following manner. From Equation 3.22 and the definition of Equation A-5,

$$\tilde{J}_j = \sum_{i=1}^v e_{ij} - \rho \mathcal{D}_{12} \frac{dC_i}{dy} \quad (\text{A-7})$$

or,

$$\tilde{J}_j = - \rho \mathcal{D}_{12} \frac{d}{dy} \sum_{i=1}^v e_{ij} C_i \quad (\text{A-8})$$

Substituting Equation A-2 gives

$$\tilde{J}_j = - \rho \mathcal{D}_{12} \frac{d\tilde{C}_j}{dy} \quad (\text{A-9})$$

This relationship can be substituted directly into the Elemental Continuity Equations (Eqs. A-6) to describe the elemental distribution of a gaseous chemical system having a common diffusion coefficient (\mathcal{D}_{12}).

APPENDIX B

DERIVATION OF TOTAL THERMAL CONDUCTIVITY AND HEAT CAPACITY EXPRESSIONS

In this appendix, the expressions describing the total thermal conductivity and the total heat capacity are derived from a rearrangement of the energy equation (Eq. 3.39). The development of these expressions is performed to demonstrate that the additional mechanisms (as opposed to the frozen properties) due to the existence of chemical reactions. It is shown that these effects are accounted for by terms contained in the energy equation which are not normally associated with these properties. The energy equation can be expressed as follows (Eq. 3.39):

$$\begin{aligned} \rho v C_p \frac{dT}{dy} = & \frac{d}{dy} \left(k_f \frac{dT}{dy} \right) - \rho v \sum_{i=1}^v h_i \frac{dC_i}{dy} - \rho v^2 \frac{dv}{dy} \\ & - \frac{d}{dy} \sum_{i=1}^v h_i J_i - \frac{dq_R}{dy} \end{aligned} \quad (B-1)$$

The mass flux (J_i) can be exactly represented by the following relationship:

$$J_i = - \rho D_i \frac{dC_i}{dy} \quad (B-2)$$

where D_i , is an effective diffusion coefficient as described in Chapter II. Substituting Equation B-2 into the energy equation (Eq. B-1) and rearranging the following relationship is obtained.

$$\rho v C_{pf} \frac{dT}{dy} + \sum_{i=1}^v h_i \frac{dC_i}{dy} = \frac{d}{dy} k_f + \rho \sum_{i=1}^v D_i h_i \frac{dC_i}{dy} - \rho v^2 \frac{dv}{dy} - \frac{dq_R}{dy} \quad (B-3)$$

For chemical equilibrium $C_i = C_i(T, P, \tilde{C}_1, \dots, \tilde{C}_\ell)$, therefore we can write

$$\frac{dC_i}{dy} = \frac{\partial C_i}{\partial T} \frac{dT}{dy} + \frac{\partial C_i}{\partial P} \frac{dP}{dy} + \sum_{j=1}^{\ell} \frac{\partial C_i}{\partial \tilde{C}_j} \frac{d\tilde{C}_j}{dy} \quad (B-4)$$

Since $dP/dy = 0$ (Eq. 3.17), then

$$\frac{dC_i}{dy} = \frac{\partial C_i}{\partial T} \frac{dT}{dy} + \sum_{j=1}^{\ell} \frac{\partial C_i}{\partial \tilde{C}_j} \frac{d\tilde{C}_j}{dy} \quad (B-5)$$

Substitution of this equation into Equation B-3 gives,

$$\begin{aligned}
 \rho v \left[c_{pf} + \sum_{i=1}^v h_i \frac{\partial C_i}{\partial T} \right] \frac{dT}{dy} + \rho v \sum_{i=1}^v h_i \sum_{j=1}^v \frac{\partial C_i}{\partial \tilde{C}_j} \frac{d\tilde{C}_j}{dy} = \\
 \frac{d}{dy} \left[k_f + \rho \sum_{i=1}^v D_i h_i \frac{\partial C_i}{\partial T} \right] \frac{dT}{dy} + \frac{d}{dy} \sum_{i=1}^v D_i h_i \sum_{j=1}^v \frac{\partial C_i}{\partial \tilde{C}_j} \frac{d\tilde{C}_j}{dy} \\
 - \rho v^2 \frac{dv}{dy} - \frac{dq_R}{dy} \quad (B-6)
 \end{aligned}$$

Due to the computational difficulties of determining the partial derivatives of concentration with respect to elemental concentration ($\partial C_i / \partial \tilde{C}_j$), previous investigators have neglected the additional terms containing these quantities. On the basis of a posteriori analysis, Wilson (Ref. 3.9) reported that only a slight contribution of these terms to the overall heat transport could be detected. Considering Wilson's observation, and the extent of the computational difficulties, the additional terms were neglected in the current analysis. Equation B-6 can then be written as,

$$\rho v C_p \frac{dT}{dy} = \frac{d}{dy} k \frac{dT}{dy} - \rho v^2 \frac{dv}{dy} - \frac{dq_R}{dy} \quad (B-7)$$

$$\text{where } c_p = c_{pf} + \sum_i h_i \frac{\partial C_i}{\partial T} = \begin{matrix} \text{total heat} \\ \text{capacity} \end{matrix} \quad (\text{B-8})$$

$$\text{and } k = k_f + \rho \sum D_i h_i \frac{\partial C_i}{\partial T} = \begin{matrix} \text{total thermal} \\ \text{conductivity} \end{matrix} \quad (\text{B-9})$$

It is observed that the total heat capacity (Eq. B-8) thus includes the effects of chemical heats of reaction as an additional mechanism for energy absorption. Furthermore, it is noted that the total thermal conductivity (Eq. B-9) accounts for an additional transport of energy through the diffusion of high energy molecules into regions of lower energy.

APPENDIX C

ESTIMATION OF COLLISION PARAMETERS FOR BINARY DIFFUSION COEFFICIENTS

The methods employed for the estimation of the ablation products (C_3 , C_2H , C_3H , C_4H , and C^+) and air species (O , N , O^+ , N , e^-) collision parameters are described in this appendix. A literature survey indicated that such data was unavailable for these species. Therefore, in the case of the ablation products, correlations were developed based upon similar types of species. For the air species, rigorous theoretical binary diffusion coefficients were reported from estimates of these parameters could be obtained.

Ablation Species (C_3 , C_2H , C_3H , C_4H , and C^+)

In Figures C-1 and C-2 the collision parameters of species similar to those of interest are plotted against molecular weight. In the case of the collision diameter σ (Figure C-1), excellent agreement is noted. From the data, the following correlation was obtained:

$$\sigma_i = 2.69 + 0.0514 M_i \quad (C-1)$$

This relationship was used to estimate the collision diameters of C_3 , C_2H , C_3H and C_4H .

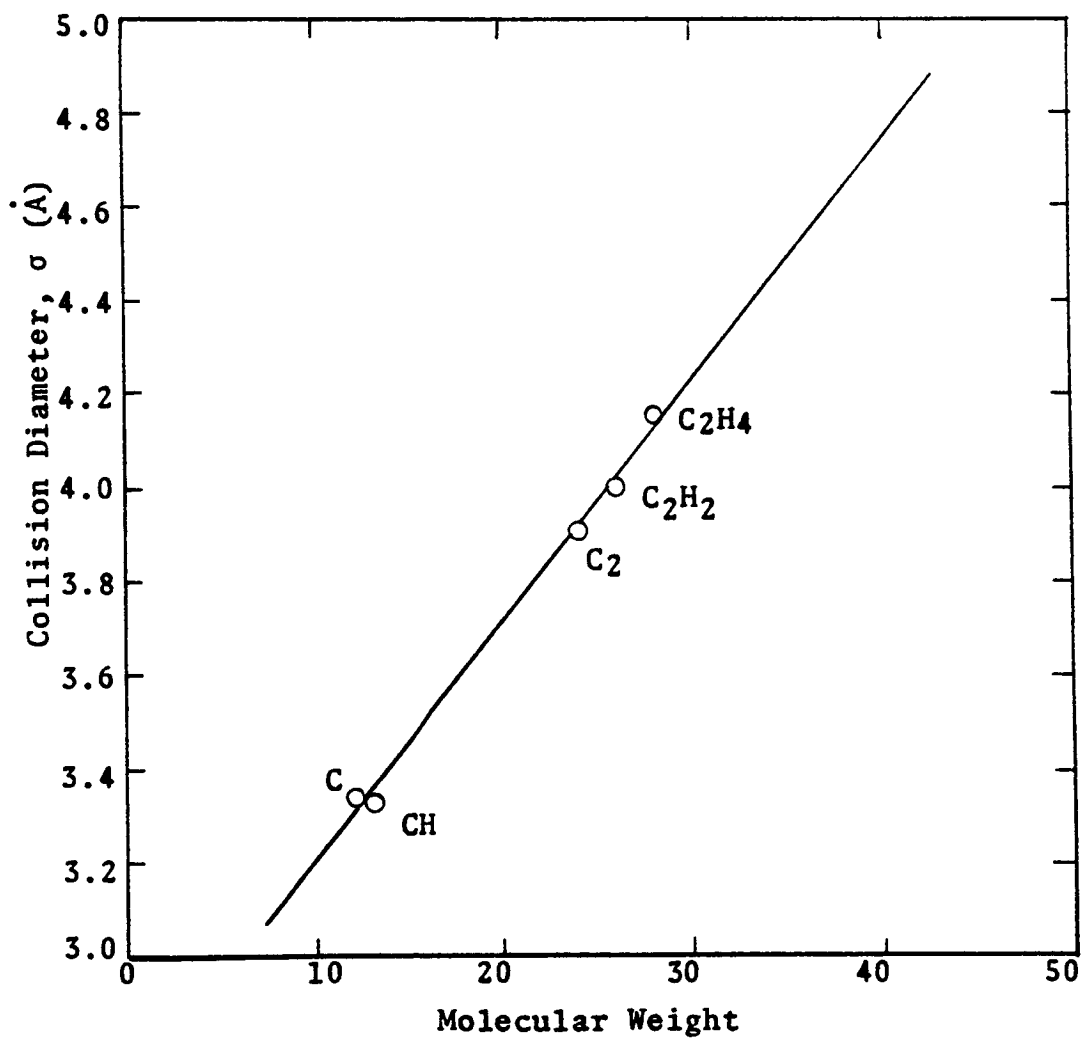


Figure C-1. Collision Diameter of Light Hydrocarbon Versus Molecular Weight (Ref. 4.5).

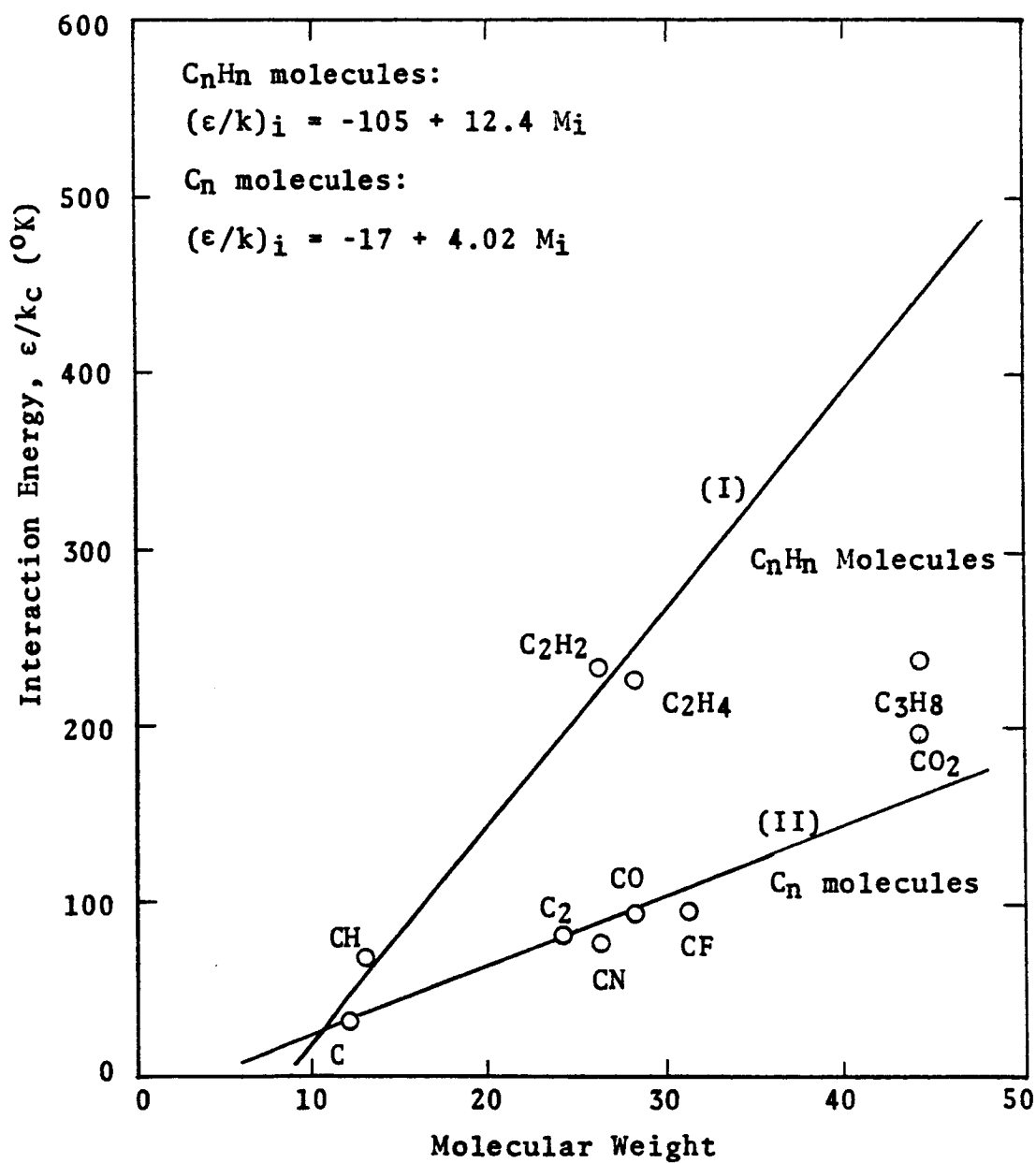


Figure C-2. Interaction Energy of Light Hydrocarbons Versus Molecular Weight (Ref. 4.5).

The correlations of interaction energy ϵ_i/k_C (Figure C-2) were obtained by grouping the C_nH_n compounds and the C_n compounds. The interaction energies of similar polyatomic molecules are also given to further support the validity of the C_n correlation (Curve II). The resulting correlations are given as follows:

C_nH_n Molecules (C_2H , C_3H , and C_4H):

$$\epsilon_i/k_C = -105 + 12.4 M_i$$

C_n Molecules (C_3):

$$\epsilon_i/k_C = -17 + 4.02 M_i$$

Air Species (O , N , O^+ , N^+ and e^-)

The collision parameters for the high temperature air species were estimated from the binary diffusion coefficients reported by Yun, Wiessman, and Mason (Ref. 4.2) and Yos (Ref. 4.7). Some difficulty was encountered in attempting to simultaneously satisfy the theoretical data. Therefore, the correlations shown in Figure C-3 were obtained by arbitrarily weighting each interaction according to the frequency of its occurrence over the temperature range of interest (3000-14000°K). In this manner a nearly exact fit was obtained for the most frequent interactions (atom-atom) while the least accurate fit was obtained for least frequent (ion-ion). The resulting

correlations are shown in Figure C-3. The corresponding binary collision parameters are reported in Table 4.3. The electron (e^-) was assumed to exhibit the same diffusion characteristics as the parent dissociated atoms (N^+ , O^+).

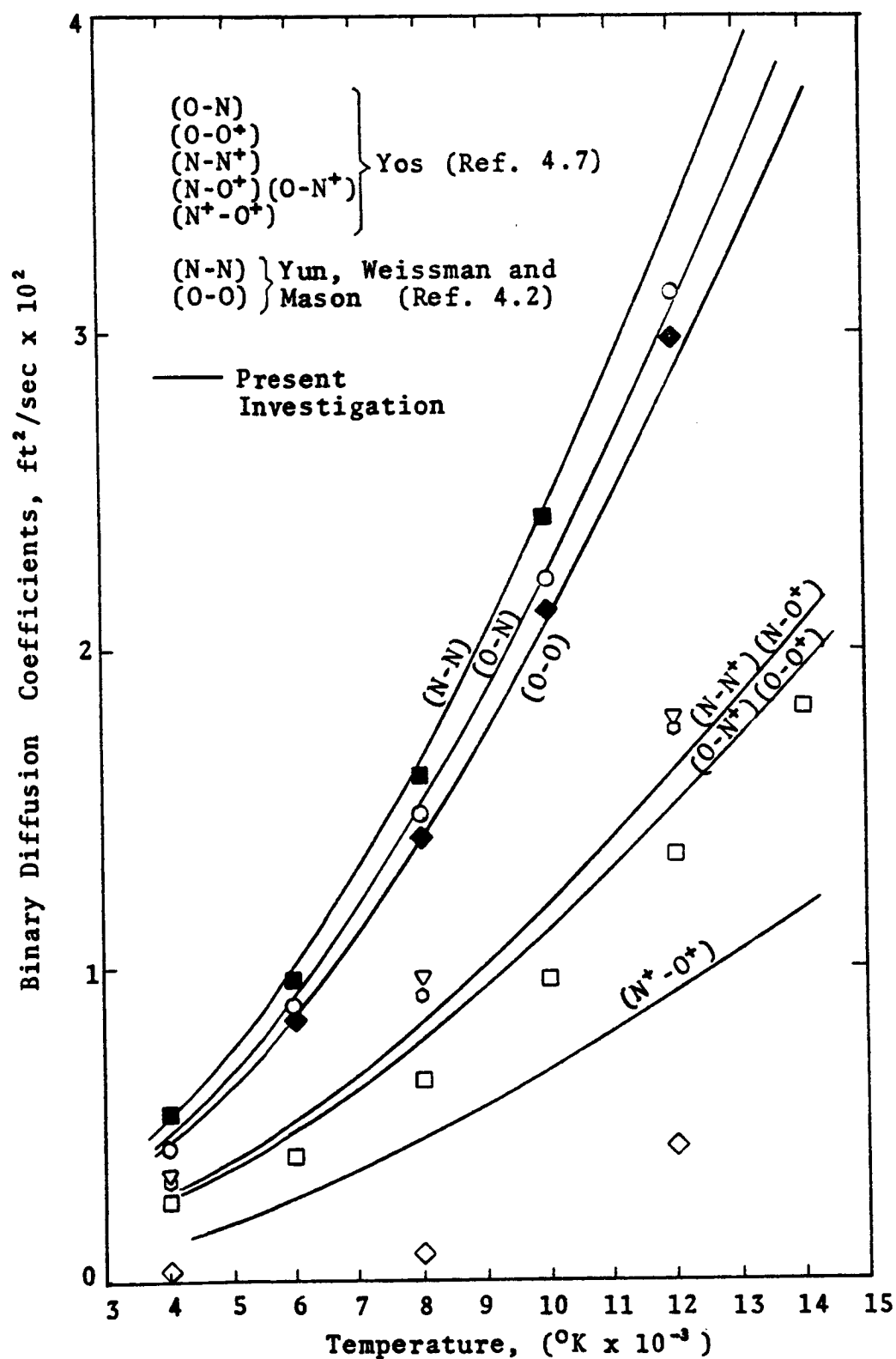


Figure C-3. Binary Diffusion Coefficients for the Constituents of Air at Atmospheric Pressure.

APPENDIX D

DETERMINATION OF POLYNOMIAL COEFFICIENTS FOR THERMODYNAMIC PROPERTIES

There are several procedures for obtaining the polynomial constants as required for the equations given in Table D-1. McBride, et al. (Ref. D-1), used a least squares technique which was simultaneously applied to all four of the thermodynamic functions. For the purpose of this study, the emphasis was placed upon the free energy fit rather than the properties in general. In the following paragraphs the procedure for determining these constants is explained.

From tabulated enthalpy functions as given in several reports (Refs. 4.12-4.17), the following polynomial was curve fit using a simple least squares analysis.

$$\frac{H_T^O - H_O^O}{RT} = B_1 + B_2T + B_3T^2 + B_4T^3 + B_5T^4 \quad (D-1)$$

From Equation 4.22 the constants A_1 through A_5 were determined as shown below:

$$A_1 = B_1$$

$$A_2 = 2B_2$$

TABLE D-1

A SUMMARY OF RELATED POLYNOMIAL EQUATIONS FOR
STANDARD THERMODYNAMIC PROPERTIES

Specific Heat

$$\frac{C_p^0}{R} = A_1 + A_2T + A_3T^2 + A_4T^3 + A_5T^4 \quad (A)$$

Enthalpy

$$\frac{H_T^0}{RT} = A_1 + \frac{A_2}{2}T + \frac{A_3}{3}T^2 + \frac{A_4}{4}T^3 + \frac{A_5}{5}T^4 + \frac{A_6}{T} \quad (B)$$

Entropy

$$\frac{S_T^0}{R} = A_1 \ln T + A_2T + \frac{A_3}{2}T^2 + \frac{A_4}{3}T^3 + \frac{A_5}{4} + A_7 \quad (C)$$

Free Energy

$$\begin{aligned} \frac{F_T^0}{RT} = A_1(1 - \ln T) - \frac{A_2}{2}T - \frac{A_3}{6}T^2 - \frac{A_4}{12}T^3 - \frac{A_5}{20}T^4 \\ + \frac{A_6}{T} - A_7 \end{aligned} \quad (D)$$

$$A_3 = 3B_3$$

$$A_4 = 4B_4$$

$$A_5 = 5B_5$$

The constant, A_6 , was computed separately from Equation 4.27:

$$A_6 = H_0^0 / R = (\Delta H_f)_{T_{\text{ref}}} - (H_T^0 - H_0^0)_{T_{\text{ref}}} / R \quad (4.27)$$

where $(\Delta H)_{T_{\text{ref}}}$ = heat of formation at the reference temperature (298.16°K).

$(H_T^0 - H_0^0)_{T_{\text{ref}}}$ = Enthalpy (relative to absolute zero) at the reference temperature.

The value of A_7 was determined as the constant difference between the tabulated free energy data and the remaining terms of the free energy polynomial as computed from the previously determined constants.

$$A_7 = A_1(1 - \ln T) - \frac{A_2}{2} - \frac{A_3 T^2}{6} - \frac{A_4 T^4}{12} - \frac{A_5 T^5}{20} - \frac{F_T^0 - H_0^0}{RT} \quad (D-2)$$

In this report constants were evaluated at two temperature ranges for all species of interest and are listed in Table D-2. The ranges considered were 1000-7000°K and 5000-18000°K. The overlapping and extension of temperature ranges was necessary to overcome accuracy limitations at the extremes of the fit. The constants used for C_3H , C_4H , and HCN were taken from Duff (Ref. D-2) and are valid to 6000°K. Above this temperature these species do not exist in significant quantities at pressures of interest in the study.

TABLE D-2
POLYNOMIAL COEFFICIENTS FOR THERMODYNAMIC PROPERTY CORRELATIONS

Species	A1	A2	A3	A4	A5	A6	A7	T*
C+	0.2609E 01	-0.1393E-03	0.5959E-07	-0.1037E-10	0.6345E-15	0.2168E 06	0.3709E 01	L
	0.2528E 01	0.4869E-05	-0.7026E-08	0.1134E-11	-0.3476E-16	0.2168E 06	0.4139E 01	H
H	0.2500E 01	-0.8243E-06	0.6421E-09	-0.1720E-12	0.1457E-16	0.2547E 05	-0.4612E 01	L
	0.3934E 01	-0.1776E-02	0.6013E-06	-0.7819E-10	0.3482E-14	0.2547E 05	-0.8598E 01	H
N+	0.2727E 01	-0.2820E-03	0.1105E-06	-0.1551E-10	0.7847E-15	0.2254E 06	0.3645E 01	L
	0.2499E 01	-0.3725E-05	0.1147E-07	-0.1102E-11	0.3078E-16	0.2254E 06	0.4950E 01	H
O+	0.2491E 01	0.2762E-04	-0.1881E-07	0.3807E-11	-0.1028E-15	0.1879E 06	0.4424E 01	L
	0.2944E 01	-0.4108E-03	0.9156E-07	-0.5848E-11	0.1190E-15	0.1879E 06	0.1750E 01	H
E-	0.2500E 01	0.3440E-06	-0.1954E-09	0.3937E-13	-0.2573E-17	-0.7450E 03	-0.1173E 02	L
	0.2508E 01	-0.6332E-05	0.1364E-08	-0.1094E-12	0.2934E-17	-0.7450E 03	-0.1208E 02	H
C	0.2612E 01	-0.2030E-03	0.1095E-06	-0.1695E-10	0.8590E-15	0.8542E 05	0.4144E 01	L
	0.2141E 01	0.3219E-03	-0.5498E-07	0.3604E-11	-0.5564E-16	0.8542E 05	0.6874E 01	H
CN	0.3411E 01	0.4897E-03	0.1005E-06	-0.3473E-10	0.2361E-14	0.4745E 05	0.4746E 01	L
	0.3473E 01	0.7337E-03	-0.9088E-07	0.4847E-11	-0.1018E-15	0.5420E 05	0.4152E 01	H
CO	0.3254E 01	0.9698E-03	-0.2647E-06	0.3037E-10	-0.1177E-14	-0.1434E 05	0.4875E 01	L
	0.3366E 01	0.8027E-03	-0.1968E-06	0.1940E-10	-0.5549E-15	-0.1434E 05	0.4263E 01	H
C2	0.4443E 01	-0.2885E-03	0.3036E-06	-0.6244E-10	0.3915E-14	0.9787E 05	-0.1090E 01	L
	0.4026E 01	0.4857E-03	-0.7026E-07	0.4666E-11	-0.1142E-15	0.9787E 05	0.1090E 01	H
C2H	0.3485E 01	0.3563E-02	-0.1237E-05	0.1866E-09	-0.1013E-13	0.5809E 05	0.4784E 01	L
	0.5307E 01	0.8966E-03	-0.1378E-06	0.9251E-11	-0.2278E-15	0.5809E 05	-0.5288E 01	H

*Temperature Range L = 1000-6000°K, H = 6000-15,000°K

(continued)

TABLE D-2 (continued)

Species	A1	A2	A3	A4	A5	A6	A7	T*
C2H2	0.3891E 01	0.5717E-02	-0.1957E-05	0.2931E-09	-0.1585E-13	0.2590E 05	0.6520E 00	L
	0.6789E 01	0.1503E-02	-0.2295E-06	0.1534E-10	-0.3763E-15	0.2590E 05	-0.1539E 02	H
C3	0.4002E 01	0.3541E-02	-0.1318E-05	0.2064E-09	-0.1144E-13	0.9423E 05	0.2020E 01	L
	0.2213E 02	-0.1759E-01	0.5565E-05	-0.6758E-09	0.2825E-13	0.9423E 05	-0.1021E 03	H
C3H	0.3965E 01	0.6200E-02	-0.2265E-05	0.3717E-09	-0.2262E-13	0.6283E 05	0.3467E 01	L
	0.3965E 01	0.6200E-02	-0.2265E-05	0.3717E-09	-0.2262E-13	0.6283E 05	0.3467E 01	H
C4H	0.5874E 01	0.7403E-02	-0.2729E-05	0.4437E-09	-0.2637E-13	0.7605E 05	-0.4010E 01	L
	0.5874E 01	0.7403E-02	-0.2729E-05	0.4437E-09	-0.2637E-13	0.7605E 05	-0.4010E 01	H
HCN	0.3654E 01	0.3444E-02	-0.1258E-05	0.2169E-09	-0.1430E-13	0.1442E 05	0.2373E 01	L
	0.3654E 01	0.3444E-02	-0.1258E-05	0.2169E-09	-0.1430E-13	0.1442E 05	0.2373E 01	H
H2	0.3358E 01	0.2794E-03	0.9372E-07	-0.2948E-10	0.2141E-14	-0.1018E 04	-0.3548E 01	L
	0.3363E 01	0.4656E-03	-0.5127E-07	0.2802E-11	-0.4905E-16	-0.1018E 04	-0.3716E 01	H
N	0.2474E 01	0.9097E-04	-0.7814E-07	0.2218E-10	-0.1489E-14	0.5609E 05	0.4300E 01	L
	0.2746E 01	-0.3909E-03	0.1338E-06	-0.1191E-10	0.3369E-15	0.5609E 05	0.2872E 01	H
O	0.2670E 01	-0.1970E-03	0.7193E-07	-0.8901E-11	0.4002E-15	0.2915E 05	0.4504E 01	L
	0.2548E 01	-0.5952E-04	0.2701E-07	-0.2798E-11	0.9380E-16	0.2915E 05	0.5049E 01	H
N2	0.3221E 01	0.9878E-03	-0.2907E-06	0.3938E-10	-0.2000E-14	-0.1043E 04	0.4326E 01	L
	0.3727E 01	0.4684E-03	-0.1140E-06	0.1154E-10	-0.3293E-15	-0.1043E 04	0.1294E 01	H
O2	0.3316E 01	0.1151E-02	-0.3726E-06	0.6186E-10	-0.3666E-14	-0.1044E 04	0.5393E 01	L
	0.3721E 01	0.4254E-03	-0.2835E-07	0.6050E-12	-0.5186E-17	-0.1044E 04	0.3254E 01	H

*Temperature Range L = 1000-6000°K, H = 6000-15,000°K

REFERENCES

- D-1. McBride, G. J., et al., "Thermodynamic Properties to 6000°K for 210 Substances Involving the First Eighteen Elements," NASA SP-3001 (1963).
- D-2. Duff, R. E. and S. H. Bauer, "Equilibrium Composition of the C/H System at Elevated Temperatures," Jour. Chem. Physics, Vol. 36, 1754 (1962).

APPENDIX E

DETERMINATION OF EQUILIBRIUM COMPOSITIONS

A free energy minimization approach was used in the current study to determine equilibrium species compositions. The minimization technique employed in the analysis is the method of undetermined multipliers and was originally presented by White, Johnson, and Dantzig (Ref. E-1). The present analysis, a subroutine (CHEMEQ) was developed through an extensive modification of a program based upon the above method and reported by Stroud and Brinkley (Ref. E-2). Prior to being used in both the SLAB and the SLAM programs, this subroutine was carefully tested and found to be predicting compositions which were in full agreement with other investigators. In Figure E-1, a comparison with other investigators is shown for the prediction of equilibrium air compositions. Excellent agreement is observed. Further verifications is noted in Figure 4.9 in a comparison of predicted values of reacting heat capacity (Eq. 4.32).

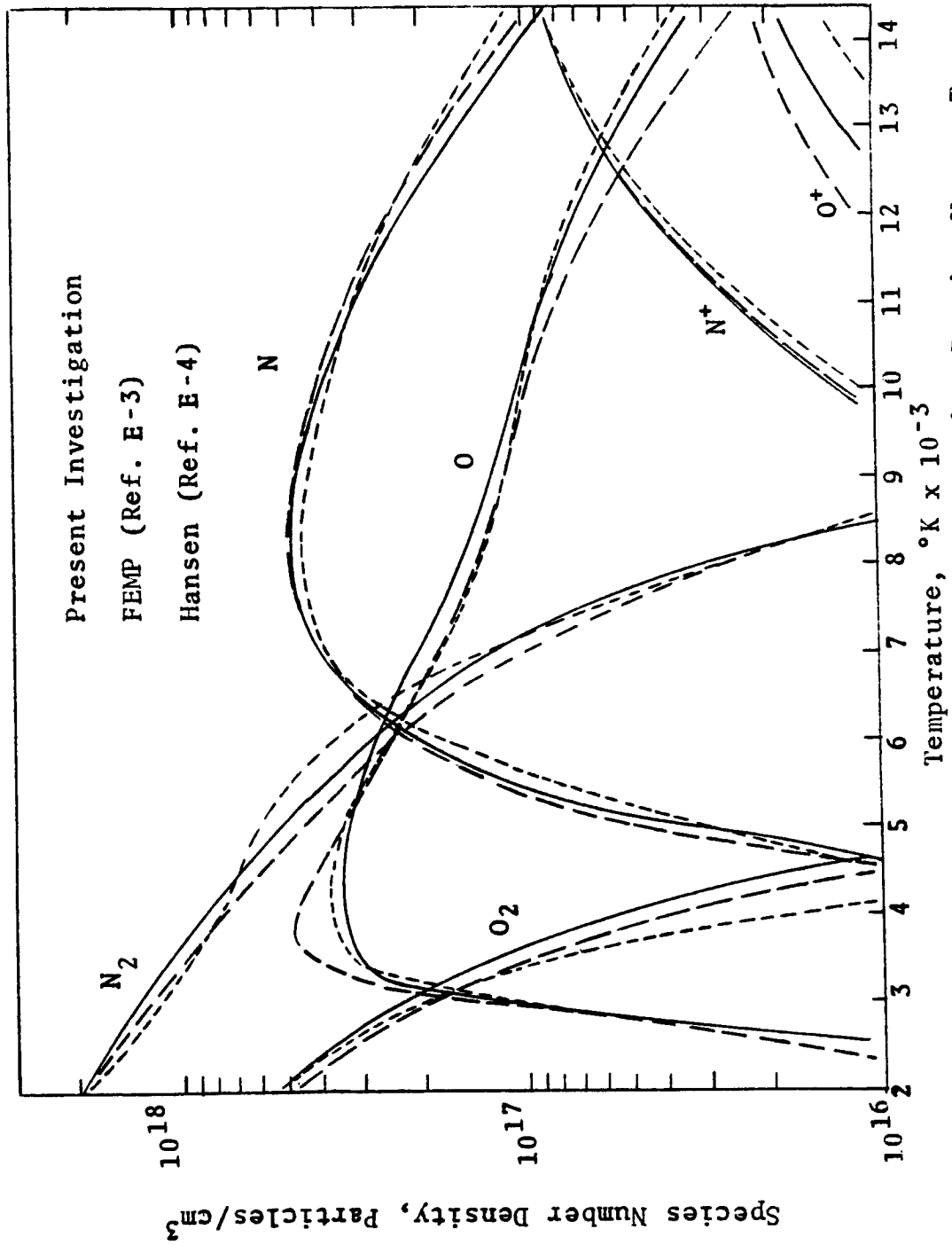


Figure E-1. Comparison of Species Number Density Versus Temperature Using Several Methods (P=1.0 atm).

REFERENCES

- E-1. White, W. B., S. M. Johnson, and G. B. Dantzig, "Chemical Equilibrium in Complex Mixtures," J. Chem. Phys., vol. 28, no. 5, May 1958, pp. 751-755.
- E-2. Stroud, C. W. and K. L. Brinkley, "Chemical Equilibrium of Ablation Materials Including Condensed Species," NASA TN D-5391 (August, 1969).
- E-3. Browne, H. N., M. W. Williams and D. R. Cruise, "Theoretical Computation of Equilibrium Compositions, Thermodynamic Properties and Performance Characteristics of Propellant Systems," U.S. Naval Ordnance Test Station NAVWEPS, Rept. 7043, June 1970.
- E-4. Hansen, C. F., "Approximations for the Thermodynamic Properties of High Temperature Air," NASA TR R-50, 1959.

APPENDIX F

COMPUTER PROGRAM FOR A VISCOUS COUPLED STAGNATION LINE HEATING ANALYSIS

The program (SLAB) described in this appendix consists of a numerical solution of the viscous thin shock layer equations presented in Chapter III. A general description of the overall logic and the details of the numerical solutions are given in Chapter V. The program represents the efforts of many individuals over a considerable amount of time. Several of the major subroutines are modifications of previously developed programs dating back as far as 1954. The overall analysis is a modification of a program (VISRAD) primarily developed by Engel (Ref. 5.6). Specifically, the modifications include a solution of the elemental continuity equations with binary diffusion and the addition of a general properties package for the prediction of ablation product transport and thermodynamic properties. A brief description of each of the subprograms included in this code is presented in Table F-1. In the following section, a detailed input guide

is given. A complete listing will then follow which includes a sample data package and the corresponding final solution.

Input Guide

The following chart shows the format of the card input.

<u>Card</u>	<u>Variables</u>	<u>Format</u>
1	TITLE	18A4
2	KEEP, NETA, IRAD, ITYPE, MAXM, MAXE, MAXD, LT, IPHI, FPRCT, TPRCT, IDEBUG	9I5, 2E12.0, 2X, I1
3	UINF, RINF, R, TWK, HTOTAL, RVW	5E12.0
4	DELTA, DTIL, RZB, RE, PDTIL	5E12.0
5	T(I)	6E12.0
6A	RHØ(I)	6E12.0
6B	RM(I)	6E12.0
7	DEPS	E12.0
8	ETA(I)	6E12.0
9	NDBUG, TOL	I5, 5X, E10.4
10	CWALL(J)	5E15.8

The meaning of these program variables are as follows:

<u>Variable</u>	<u>Description</u>
TITLE	Title for identification of the problem.
KEEP	Indicator to determine if the temperature profile from the previous case is to be kept as a guess for the current case. KEEP = 0 Temperature not kept KEEP = 1 Temperature kept
NETA	The number of points to be used in the shock layer profile. If NETA = 0, a set of 51 equally spaced points will be used.
IRAD	A variable used to specify the type of solution. IRAD = 1 Convective solution only = 2 Uncoupled radiation solution = 3 Coupled radiation solution
ITYPE	A variable used to specify the type of radiation model to be used. ITYPE = 0 Line and continuum radiation model = 1 Emission radiation model
MAXM	Maximum number of iterations allowed in the internal momentum loop. If MAXM = 0, it is internally set = 15.
MAXE	Maximum number of iterations allowed in the energy equation and in the overall momentum-energy loop. If MAXE = 0, it is internally set = 15.
MAXD	Maximum number of iterations allowed in the external momentum loop. If MAXD = 0, it is internally set = 15.

<u>Variable</u>	<u>Description</u>
LT	Indicator to determine if a temperature guess and if ρ and $\rho\mu$ guesses are to be read in. LT = 0 Cards 5 and 6 are not read. = 1 Card 5 but not card 6 is read. = 2 Cards 5 and 6 are read.
IPHI	Indicator to determine if the shock curvature is to be input. IPHI = 0 $d/d = 0$ is internally set. = 1 Card 7 is required for input.
FPRCT	Convergence tolerance for each point in the f' profile. If FPRCT = 0.0 it is internally set = .005.
TPRCT	Convergence tolerance for each point in the T profile. If TPRCT = 0.0 it is internally set = .005.
IDEBUG	A switch to allow intermediate printout to be obtained at each iteration IDEBUG = 0 No print. = 1 Print is given.
UNIF	The freestream flight velocity (U_∞) in feet/sec.
RINF	The freestream density (ρ_∞) in slugs/ft ³ .
R	Principal body radius in feet.
TWK	Wall temperature in degrees Kelvin.
HTOTAL	Total freestream enthalpy in ft ² /sec ² . If HTOTAL = 0.0, it is set to $U_\infty^2/2$. (Freestream static enthalpy is assumed negligible).
RVW	Mass injection rate $(\rho v)_w/(\rho U)_\infty$.
DELTA	An initial guess for the shock standoff distance δ/R . If DELTA = 0.0, a guess is supplied by program.

<u>Variable</u>	<u>Description</u>
DTIL	A guess for the transformed standoff distance δ/R . The program will also supply this value if DTIL = 0.0.
RZB	The density ratio across the shock $\bar{\rho} = \rho / \rho_\delta$. If RZB is input as 0.0, the code will determine a value.
RE	The Reynolds number for the problem, $Re_s = U_\infty R \rho_\delta / \mu_\delta$. This quantity is determined by the program if RE is input as 0.0.
PDTIL	Convergence tolerance placed on $\tilde{\delta}$ for total solution convergence. If PDTIL = 0.0, it is internally set = .001.
T(I), I=1, NETA	An initial guess for the dimensionless shock layer temperature profile (T/T_δ). If LT > 0, this profile is supplied by the user.
RHØ(I), I=1, NETA	An initial guess for the dimensionless shock layer density profile (ρ/ρ_δ). If LT = 2, this profile is supplied by the user.
RM(I), I=1, NETA	An initial guess for the dimensionless shock layer $\rho\mu$ profile ($\rho\mu/\rho_\delta \mu_\delta$). If LT = 2, this profile is supplied by the user.
DEPS	The stagnation line shock curvature ($d\epsilon/d\eta$). If IPHI = 0 then $d\epsilon/d\eta = 0.0$ is internally set. If IPHI = 1, card 7 is read and $d\epsilon/d$ is supplied by the user.
ETA(I), I=1, NETA	The grid shock layer points at which the solution profiles are to be computed. If NETA = 0, $\Delta\eta$ is set to 0.02 and ETA(I) is computed by the program.
NDEBUG	Debug option to output intermediate print from chemical equilibrium calculation. NDEBUG = 0 No output. NDEBUG = 1 Output given.

<u>Variable</u>	<u>Description</u>
TOL	Convergence criteria for CHEMEQ. If TOL is input as 0.0, the code will set to 0.001.
CWALL(J), J=1,NSP	Wall mass fractions (NSP = 20) species included in order are, <div style="margin-left: 40px;"> J = 1 = O₂ 6 = N⁺ 11 = CO 16 = C₃H 2 = N₂ 7 = E⁻ 12 = C₃ 17 = C₄H 3 = O 8 = C 13 = CN 18 = HCN 4 = N 9 = H 14 = C₂H 19 = C₂ 5 = O⁺ 10 = H₂ 15 = C₂H₂ 20 = C⁺ </div>

TABLE F-1

DESCRIPTION OF SLAB SUBPROGRAMS

Subprogram	Driver program	Description	Additional Sub- programs Required
MAIN			INPUT, INIT, MOMTM, ERROR, ENERGY, OUTPUT and MULTI
INPUT		Reads in all necessary data and prints out key parameters	none
INIT		Initialization program: Performs shock calculation to determine shock temperature (TD), density ratio (RZB), velocity (VD), and pressure (PD). Estimates shock standoff distance x (DELTA, DTIL). Converts wall and shock compositions to elemental basis. Sets up elemental diffusion coefficient profile.	GAS
MOMTM		Numerical solution to momentum equation as described in Chapter V.	TRID

TABLE F-1 (continued)

Subprogram	Description	Additional Sub- programs Required
ENERGY	Numerical solution of energy equation as described in Chapter V. Serves as driver program for subroutines required for species solution (ELEMNT, CHEMEQ, and PROPRT).	GAS, ELEMNT, CHEMEQ, PROPRT, ELPROF, STPSZE, and TRID
ELEMNT	Numerical solution of elemental continuity equations as described in Chapter V.	FGH, FGHZ, TRID
CHEMEQ	Free energy minimization program for determining equilibrium species compositions. An extensive modification of a program reported by Stroud and Brinkley (Ref. F-1). For further details refer to Appendix E.	ALTERY, THERMO, and NATINV
ALTERY	Adjusts assumed compositions such that desired elemental ratios are obtained. An auxiliary subprogram for CHEMEQ.	none
THERMO	Computes the free energy of the species. Auxiliary program for CHEMEQ.	none

TABLE F-1 (continued)

Subprogram	Description	Additional Sub- programs Required
PROPRT	Calculation of thermodynamic and transport properties by methods described in Chapter IV.	none
GAS	Thermodynamic and transport properties of air, Hansen (Ref. F-2).	none
EFLUX	Correlation developed by Engel (Ref. F-3) for estimation of air radiation properties emission only.	none
LRAD	Driver program for radiation calculation.	TRANS
TRANS	Coupled line and continuum radiation calculation. A modification by Engel (Ref. F-4) of an analysis developed by Wilson (Ref. F-5).	SND, ZHV, BUGPR
SND	Converts mass fractions to number densities. Auxiliary program for TRANS.	none
STPSZE	Adjusts stepsize distribution based on temperature profile.	none

TABLE F-1 (continued)

Subprogram	Description	Additional Sub-program Required
MATINV	Matrix inversion and solution to simultaneous linear equations (Ref. F-1).	none
FGH, FGH2	Three point difference formulas for first and second derivatives (Eqs. 5.15-5.20).	none
TRID	Solution to simultaneous linear equations with tri-diagonal coefficient matrix.	none
QUAD	Trapezoidal rule integration program.	none
OUTPUT	Prints out intermediate and final solutions (See Table F-3). Also punches intermediate and converged solutions for use in restarting.	TRANS, EFLUX, TRANSZ
ERROR	Prints out a diagnostic message when energy and/or momentum solutions fail to converge.	none
ELPROF	Prints out intermediate solutions to elemental continuity equations.	none

TABLE F-1 (continued)

Subprogram	Description	Additional Sub-program Required
MULTI	Punches out data package for multicomponent diffusion analysis (SLAM).	none
BLOCK DATA	Data package containing the following information: Optional initial guesses for ρ , $\rho\mu$, and T profiles; Alphameric labels for species identification; molecular weights; coefficients for individual viscosity and thermal conductivity curve fits (Discussed in Chapter IV); polynomial coefficients for thermodynamic properties (Chapter IV); atomic weights of the elements; and the matrix of elemental ratios (A_{ij} 's, See Appendix A) for the species considered.	none

REFERENCES

- F-1. Stroud, C. W. and K. L. Brinkley, "Chemical Equilibrium of Ablation Materials Including Condensed Species," NASA TN D-5391 (August, 1969).
- F-2. Hansen, C. F., "Approximations for the Thermodynamic Properties of High Temperature Air," NASA TR R-50, 1959.
- F-3. Engel, C. D., and L. W. Spradley, Radiation Absorption Effects on Heating Loads Encountered During Hyperbolic Entry, JSR, Vol. 6, No. 6, pp. 764-766, June 1969.
- F-4. Engel, C. D. "Ablation and Radiation Coupled Viscous Hypersonic Shock Layers," Ph.D. Dissertation, Louisiana State University, Baton Rouge, Louisiana (1971).
- F-5. Wilson, K. H., "Stagnation Point Analysis of Coupled Viscous-Radiating Flow with Massive Blowing," NASA CR-1548 (June, 1970).

[illegible]

```
C MAIN 370  
C ** ERROR EXIT IF MOMENTUM ITERATION DOES NOT CONVERGE **  
C  
C CALL ERPROR ( 1 )  
C  
C 1500 CONTINUE  
C  
C ** SOLVE ENERGY EQUATION **  
C  
C CALL ENERGY  
C ** INTERMEDIATE PRINTOUT OF TEMPERATURE ITERATION **  
C  
C IF( IDEBUG.GT. 0 )          CALL OUTPUT(2)  
C  
C ** CHECK FOR CONVERGENCE OF TEMPERATURE ITERATION **  
C  
C  
C IF( ECONV ) GO TO 2500  
C  
C ** ERROR EXIT IF TEMPERATURE ITERATION DOES NOT CONVERGE **  
C  
C CALL ERROR ( 2 )  
C  
C 2500 CONTINUE  
C  
C ** CHECK SIMULTANEOUS MOMENTUM AND ENERGY CONVERGENCE **  
C  
C IF( IEM.EQ.2.OR.IEM.EQ.4) GOTO1600  
C IF( IEM.GT.MAXD) GO TO 3000  
C IF(.NOT.MCONV) GO TO 1000  
C IF(.NOT.FCONV) GO TO 1000  
C IF(.NOT.DCONV) GO TO 1000  
C ** PRINT ALL OUTPUT **  
C  
C CALL OUTPUT ( 1 )  
C CALL MULTI
```



```

C
C
C
C
C
SUBROUTINE INPUT
** ROUTINE TO READ AND PRINT ALL INPUT DATA **

COMMON /CONV/ FPRCT,TPRCT,DDAMP,TDAMP,PTIL
COMMON /DEL/ DELTA,DTIL,DTILS
COMMON /FRSTRM/ U INF, RINF, UINF2, R, RE, LXI, ITM, IEM, NETA
COMMON /MAIM/KEEP,MAXE,MAXM,MAXD,IDEBUG,MCONV,ECONV,DCONV,LT,IAB
COMMON /PROP1/PI(60),RHO(60), T(60),AMW(50),C (20,60),CC(5,60)
COMMON /PROP2/ MU(60),RM(60), AK(60)
COMMON /PROP3/ CPS(20,60),HS(20,60),CP (60),HM(60)
COMMON /RFLUX/ E(60),IRAD,ITYPE
COMMON /RH/ DUD,DPHI,TD,RZB,PD,HD,HTOTAL
COMMON /WALL/RVW,PRW,TWOLD,FLUX(20),CWALL(20),ECWALL(5)
COMMON /YL/ETA(60),YOND(60)

C
C
COMMON/EQ1/AI(20), BI(20), CI(20), DI(20), EI(20), FI(20), GI(20),
X   AII(20),BII(20),CII(20),DII(20),EII(20),FII(20),GII(20)
COMMON/EQ2/AA(20,5),ICODE(20)
COMMON/EQ3/IA(20,5)
COMMON/ID/SP(20),EL(5)
COMMON/WT/SMW(20),AWT(5)
COMMON/NUMBER/NSP,NNS,NE,NC
COMMON/SP1/SS,TOL,NDRUG

REAL MU,MUDZ
LOGICAL MCONV,ECONV,DCONV
DIMENSION TITLE(18)
DATA END /'END ' /
IF ( TITLE ( 1 ) .EQ. END ) STOP

** INPUT FORMATS **
INPU 1C
INPU 2C
INPU 3C
INPU 4C
INPU 5C
INPU 6C
INPU 7C
INPU 8C
INPU 9C
INPU 10C
INPU 11C
INPU 12C
INPU 13C
INPU 14C
INPU 15C
INPU 16C
INPU 17C
INPU 18C
INPU 19C
INPU 20C
INPU 21C
INPU 22C
INPU 23C
INPU 24C
INPU 25C
INPU 26C
INPU 27C
INPU 28C
INPU 29C
INPU 30C
INPU 31C
INPU 32C
INPU 33C
INPU 34C
INPU 35C
INPU 36C

```

```
C
      100 FORMAT (18A4)
      101 FORMAT (9I5,2E12.0,2X,I1)
      102 FURMAT ( 6E12.0 )
      103 FORMAT(A4,6X, E1C.4,2CX,5F5.0,F10.5)
      104 FORMAT(7E10.4)
      105 FORMAT(A4,E16.8)
      106 FORMAT(6E10.4,I3)
      107 FORMAT(I5, 5X,E10.4,I5)
      108 FORMAT(5E15.8)

C
      ** OUTPUT FORMATS **

C
      200 FORMAT ( 1H1 , 18A4 //// )
      201 FORMAT ( 12H0 INPUT DATA /// )
      202 FORMAT ( 9H0KEEP = I5
          1 / 9H NETA = I5
          2 / 9H MAXM = I5
          3 / 9H MAXE = I5
          4 / 9H MAXD = I5
          5 / 9H FPRCT = IPE15.6
          6 / 9H TPRCT = E15.6
          7 / 9H LT = I5
          8 / 9H IDEBUG = I5
          9 / 9H IPHI = I5 )
      204 FORMAT ( 9HCUNF = IPE15.6
          1 / 9H RINF = E15.6
          2 / 9H R = E15.6
          3 / 9H TW = E15.6
          4 / 9H HTOTAL = E15.6
          5 / 9H RVW = E15.6
          6 / 9H PDTIL = E15.6 //)

C
      206 FORMAT ( 2CHCINITIAL T PROFILE / ( 1H , 12F10.5 ) )
      207 FORMAT ( 2CHCINITIAL RHO PROFILE/ ( 1H , 12F10.5 ) )
      208 FORMAT ( 2CHCINITIAL RM PROFILE/ ( 1H , 12F10.5 ) )
```

```

210 FORMAT(32H * CONVECTIVE CALCULATION ONLY * )
211 FORMAT(36H * UNCOUPLED RADIATION CALCULATION * )
212 FORMAT(34H * COUPLED RADIATION CALCULATION * )
213 FORMAT(36H * CONTINUUM AND LINE CALCULATION * )
214 FORMAT(19H * EMISSION MODEL * )
216 FORMAT (16H SPECIES INPUTS
1 /16H NO. ELEMENTS = 15
2 /25X,5(15,2X,A4) )
218 FORMAT (16H NO. SPECIES = 15)
220 FORMAT (25X,5(15,2X,A4))
222 FORMAT (16H NO. SOLIDS = 15)
C CARD 1 -----
READ (5,100) TITLE
IF ( TITLE ( 1 ) .EQ. END ) STOP
WRITE ( 6,200 ) TITLE
C
C
C ** INPUT OPTION PARAMETERS **
C
C ** IRAD = 1 NO RADIATION CALCULATED
C IRAD = 2 UNCOUPLED SOLUTION
C IRAD = 3 COUPLED SOLUTION **
C ** ITYPE=C SPECTRAL MODEL WITH LINES
C ITYPE=1 EMISSION MODEL
C
C KETA = NETA
C CARD 2 -----
READ (5,101)KEEP,NETA,IRAD,ITYPE,MAXM,MAXE,MAXD,LT,IPHI,
1 FPRCT,IPRCT,IDEBUG
NETA = NETA
IF(KETA .EQ. C) KEEP = 0
IF(KEEP. GT. C) NETA = KETA
ODAMP = C.5
TDAMP = C.6
INPU 740
INPU 750
INPU 760
INPU 770
INPU 780
INPU 790
INPU 800
INPU 810
INPU 820
INPU 830
INPU 840
INPU 850
INPU 860
INPU 870
INPU 875
INPU 880
INPU 890
INPU 900
INPU 910
INPU 920
INPU 930
INPU 940
INPU 950
INPU 960
INPU 970
INPU 980
INPU 990
INPU1000
INPU1010
INPU1020
INPU1030
INPU1040
INPU1050
INPU1060
INPU1070
INPU1080

```

```

INPUT090
INPUT100
INPUT110
INPUT120
INPUT130
INPUT140
INPUT150
INPUT160
INPUT170
INPUT180
INPUT190
INPUT200
INPUT210
INPUT220
INPUT230
INPUT240
INPUT250
INPUT260
INPUT270
INPUT280
INPUT290
INPUT300
INPUT310
INPUT320
INPUT330
INPUT340
INPUT350
INPUT360
INPUT370
INPUT380
INPUT390
INPUT400
INPUT410
INPUT420
INPUT430
INPUT440

IF(MAXM.EQ.0) MAXM=15
IF(MAXE.EQ.0) MAXE=20
IF(MAXD.EQ.0) MAXD=15
IF(FPRCT.EQ.0.0) FPRCT=.005
IF(TPRCT.EQ.0.0) TPRCT=C.005
IF ( NETA.EQ.0 ) NETA = 51
IF (IRAD.EQ.0) IRAD =1

C
WRITE ( 6,201 )
WRITE (6,202)KEEP,NETA,MAXM,MAXE,MAXD,FPRCT,TPRCT,LT,IDEBUG
1
C
** FREE-STREAM FLIGHT CONDITIONS **
C CARD 3 -----
READ(5,102) U INF,R INF,R,TWK,HTOTAL,RVW
UINF2=UINF**2
IF(KEEP.GT.0) TWOLD = T(1)
T(1)=TWK

C
IF(HTOTAL.EQ.0.0) HTOTAL=UINF2/2.0

C
** INITIAL SHOCK QUANTITY ESTIMATES **
C CARD 4 -----
READ(5,102) DELTA,DTIL,RZB,RE,PDITIL
IF(PDITIL.EQ.0.0) PDITIL = .001
WRITE(6,204) U INF,R INF,R,TWK,HTOTAL,RVW,PDITIL
IF (IRAD.EQ.1) WRITE (6,210)
IF (IRAD.EQ.2) WRITE (6,211)
IF (IRAD.EQ.3) WRITE (5,212)
IF(IRAD.EQ.1) GO TO 300
IF( ITYPE.EQ.0) WRITE(5,213)
IF( ITYPE.EQ.1) WRITE(6,214)

300 CONTINUE

C
** INPUT INITIAL TEMPERATURE PROFILE **
C CARD 5 -----

```

```

IF(LT,50,0) GO TO 2800
READ ( 5,102 ) ( T ( I ) , I = 1 , NETA )
WRITE ( 6,206 ) ( T ( I ) , I = 1 , NETA )
T(1) = TWK
2800 CONTINUE
C ** INPUT RHO AND (RHO)(MU) PROFILES **
C CARD 6 -----
IF(LT,LT,2) GO TO 2900
READ(5,102) (RHO(I),I=1,NETA)
READ(5,102) (RM (I),I=1,NETA)
WRITE(6,207)(RHO(I),I=1,NETA)
WRITE(6,208)(RM (I),I=1,NETA)
2900 CONTINUE
C ** SHOCK SHAPE (DEPS/DXI) **
C
C
IF (IPHI,NE,0) GO TO 2550
DEPS = 0.0
GO TO 2570
2550 CONTINUE
C CARD 7 -----
READ(5,102) DEPS
2570 CONTINUE
DPHI = 1. -DEPS
WRITE(6,217) DEPS
217 FORMAT(SHCDEPS/DXI /(1H,12F10.5) )
C
C
IF ( META,GT,0 ) GO TO 1000
IF(KEEP,GT,0) GO TO 1500
C
C
C ** FIXED GRID SIZE ON ETA **
DETA = 0.02
ETA ( 1 ) = 0.0
DO 500 I = 2 , 51

```

INPU1450
 INPU1460
 INPU1470
 INPU1480
 INPU1490
 INPU1500
 INPU1510
 INPU1520
 INPU1530
 INPU1540
 INPU1550
 INPU1560
 INPU1570
 INPU1580
 INPU1590
 INPU1600
 INPU1610
 INPU1620
 INPU1630
 INPU1640
 INPU1650
 INPU1660
 INPU1670
 INPU1680
 INPU1690
 INPU1700
 INPU1710
 INPU1720
 INPU1730
 INPU1740
 INPU1750
 INPU1760
 INPU1770
 INPU1780
 INPU1790
 INPU1800

```

      ETA ( I ) = FTA ( I-1 ) + DELTA
500  CONTINUE
C
      GO TO 1500
C
1000  CONTINUE
C
      ** INPUT ETA POINTS **
C CARD 8 -----
      READ ( 5,102 ) ( ETA ( I ) , I = 1 , NETA )
C
1500  CONTINUE
C
C-----READ SPECIES PARAMETER CARDS.....
C CARD 9 -----
      READ 107,NDEBUG,TOL
C
      IAB = 1
      IF (TOL.LE.0.0) TOL = .001
      NDEBUG=OPTIONAL OUTPUT VARIABLE
      NC = NUMBER OF GASEOUS COMPONENTS
C CARD 10 -----
      READ 108,(CWall(I),I=1,NSP)
      WRITE(6,216) NE,(I,EL(I),I=1,NE)
      WRITE(6,218) NSP
      JJ = 1
      KK = JJ+4
30  WRITE(6,220) (I,SP(I),I=JJ,KK)
      IF(KK+5.GT.NSP) GO TO 35
      JJ = JJ+5
      KK = JJ +4
      GO TO 30
35  KD = NSP -KK
      IF(KD.LE.0) GO TO 45
      KK = KK +KD
      JJ = JJ +5

```

INPUT1810
 INPUT1820
 INPUT1830
 INPUT1840
 INPUT1850
 INPUT1860
 INPUT1870
 INPUT1880
 INPUT1890
 INPUT1900
 INPUT1910
 INPUT1920
 INPUT1930
 INPUT1940
 INPUT1950
 INPUT1960
 INPUT1970
 INPUT1980
 INPUT1990
 INPUT2000
 INPUT2010
 INPUT2020
 INPUT2030
 INPUT2040
 INPUT2050
 INPUT2060
 INPUT2070
 INPUT2080
 INPUT2090
 INPUT2100
 INPUT2110
 INPUT2120
 INPUT2130
 INPUT2140
 INPUT2150
 INPUT2160

```

4  GO TO 30
45 CONTINUE
  WRITE(6,222) NNS
  PRINT 305
305 FORMAT(/, 'SPECIES', NAME, 9X, 'SMW',
1, 'WALL MASS FRACTION', /)
  DO 10 I=1, NSP
10  PRINT 302, SP(I), SMW(I), CWALL(I)
302  FORMAT(1X, A4, 1F13.3, E12.4)
  IF(NDEBUG.EQ.0) GOTO 9999
  PRINT 309
309  FORMAT(/, 'SPECIES', 35X, 'THERMO-CONSTANTS A-G', 29X, 'RANGE')
  DO 11 I=1, NSP
  PRINT 303, SP(I), AI(I), BI(I), CI(I), DI(I), EI(I), FI(I), GI(I)
11  PRINT 304, AI(I), BI(I), CI(I), DI(I), EI(I), FI(I), GI(I)
303  FORMAT(/, 1X, A4, 7E12.4, ' LOW RANGE')
304  FORMAT( 5X, 7E12.4, ' HIGH RANGE')
  PRINT 307
307  FORMAT(/, 25X, ' AA(I,J) MATRIX', /)
  DO 12 J=1, NE
12  PRINT 306, (IA(I,J), I=1, NSP)
306  FORMAT(5X, 20I5)
9999 CONTINUE
C
  RETURN
  END

```

```

INPU2170
INPU2180
INPU2190
INPU2200
INPU2210
INPU2220
INPU2230
INPU2240
INPU2250
INPU2260
INPU2270
INPU2280
INPU2290
INPU2300
INPU2310
INPU2320
INPU2330
INPU2340
INPU2350
INPU2360
INPU2370
INPU2380
INPU2390
INPU2400
INPU2410
INPU2420

```

```

C
C
C
C
C
C
SUBROUTINE INIT
** ROUTINE TO COMPUTE NECESSARY INITIAL QUANTITIES

COMMON /CONV/ FPRCT,TPRCT,DDAMP,TDAMP,PDIL
COMMON /DEL/ DELTA,DTIL,DTILS
COMMON/EQ2/AA(20,5),ICODE(20)
COMMON/EQ3/IA(20,5)
COMMON /FRSTRM/ U INF, RINF, UINF2, R, RE, LXI, ITM, IEM, NETA
COMMON/GUESS/TG1(60),TG2(60)
COMMON /MAIM/KEEP,MAXE,MAXM,MAXD,IDEBUG,MCONV,ECONV,DCONV,LT,IAB
COMMON /NON/RDZ,MUDZ,RMDZ,AKNF,HNF,CPNF
COMMON/NUMBER/NSP,NNS,NE,NC
COMMON/PROP1/PI(60),RHO(60), T(60),AMW(60),C (20,60),EC(5,60)
COMMON/PROP2/ MU(60),RM(60), AK(60)
COMMON/PROP3/CPS(20,60),HS(20,60),CP (60),HM(60)
COMMON/VECTOR/ CA(60),CB(60),CC(60),B(60)
COMMON /VEL/ F(60),FC(60),Z(60),V(60)
COMMON /RFLUX/ E(60),IRAD,ITYPE
COMMON /RH/ DUD,DPHI,TD,RZB,PD,HD,HTOTAL
COMMON/SP2/BR,S(20),CSHOCK(5)
COMMON/WALL/RVW,PRW,TWOLD,FLUX(20),CWALL(20),ECWALL(5)
COMMON/WT/SMW(20),AWT(5)
COMMON /YL/ETA(60),YOND(60)
COMMON /DIF/ D(5,60)
REAL MU,MUDZ

C
C
LOGICAL MCONV,ECONV,DCONV

MCONV = .FALSE.
ECONV = .FALSE.
DCONV = .FALSE.
DO 900 I=1,60
DO 900 J=1,NSP

```

```

INIT 10
INIT 20
INIT 30
INIT 40
INIT 50
INIT 60
INIT 70
INIT 80
INIT 90
INIT 100
INIT 110
INIT 120
INIT 130
INIT 140
INIT 150
INIT 160
INIT 170
INIT 180
INIT 190
INIT 200
INIT 210
INIT 220
INIT 230
INIT 240
INIT 250
INIT 260
INIT 270
INIT 280
INIT 290
INIT 300
INIT 310
INIT 320
INIT 330
INIT 340
INIT 350
INIT 360

```



```

C 997 CONTINUE
DC 995 I=1, NETA
PI(1) = PD
E(1) = 0.0
CONTINUE
** RANKIN-HUGONIOT RELATIONS **
C
C      VD = -RZB
      TW = T(1)
      T(1) = T(1)/TD
C
C      ** STAGNATION POINT LIMIT QUANTITIES **
C
C      DUD = DPHI + RZB*(1.-DPHI)
C      VONDIMENSIONALIZING FACTORS
      AKNF = 1.8*778.28*TD      *RZB/(R*RINF*UINF*UINF2)
      CPNF = 1.8*778.28*32.172*TD *2. /UINF2
C
C      GUESSED F AND Z PROFILES
C
C      IF(KEEP.GT. 0) GO TO 9
      N = NETA-2
      FD = RZB/(2.*DUD*DTIL)
      FW = -RVW*FD
      F(1) = FW
      DO 2 K=2, NETA
      F(K) = (FD-FW)*ETA(K) + FW
2 CONTINUE
      DO 3 I=1, N
      Z(I) = ETA(I+1)/DTIL
3 CONTINUE
C      GUESSED T PROFILES
      IF(KEEP.GT.0)GOTO9
      IF(LT.GT.0) GO TO 11
      IF(RVW.GT.0.0)GOTO7
INIT 739
INIT 740
INIT 750
INIT 760
INIT 770
INIT 780
INIT 790
INIT 800
INIT 810
INIT 820
INIT 830
INIT 840
INIT 850
INIT 860
INIT 870
INIT 880
INIT 890
INIT 900
INIT 910
INIT 920
INIT 930
INIT 940
INIT 950
INIT 960
INIT 970
INIT 980
INIT 990
INIT1000
INIT1010
INIT1020
INIT1030
INIT1040
INIT1050
INIT1060
INIT1070
INIT1080

```

```

C NO BLOWING T PROFILE
  TWG1 = .1033
  DO6K = 2,NETA
  TP = TG1(K) + (T(1) - TWG1)
  T(K) = TP - (T(1) - TWG1) * ETA(K)
6 CONTINUE
  GO TO 11
7 CONTINUE
  TWG2 = .3325
C BLOWING T PROFILE
  DO8K = 2,NETA
  TP = TG2(K) + (T(1) - TWG2)
  T(K) = TP - (T(1) - TWG2) * ETA(K)
8 CONTINUE
  GO TO 11
9 CONTINUE
  DO 10 K=2,NETA
  TP = T(K) + T(1) - TWOLD
  T(K) = TP - (T(1) - TWOLD) * ETA(K)
  WRITE(6,100) T(K),ETA(K)
10 CONTINUE
11 CONTINUE
C
C ** INITIALIZE SHOCK LAYER PARAMETERS FOR VARIABLE STEP SIZE
  DO 81C I=NETA,60
    ETA(I)=1.0
    T(I) = 1.0
    E(I) = 0.0
    PI(I) = PD
    MU(I)=1.0
    CP(I) = CP(NETA)
    AK(I) = AK(NETA)
    V(I) = VD
    F(I) = FD
    FC(I)=FD
  DO 31C J=1,NSP

```

```

INIT1092
INIT1100
INIT1110
INIT1120
INIT1130
INIT1140
INIT1150
INIT1160
INIT1170
INIT1180
INIT1190
INIT1200
INIT1210
INIT1220
INIT1230
INIT1240
INIT1250
INIT1260
INIT1270
INIT1280
INIT1290
INIT1300
INIT1310
INIT1320
INIT1330
INIT1340
INIT1350
INIT1360
INIT1370
INIT1380
INIT1390
INIT1400
INIT1410
INIT1420
INIT1430
INIT1440

```

```

C(J,I) = C(J,NETA)
HS(J,I)=1.0
810 CONTINUE
1000 CONTINUE
C
D022I=1,NSP
C(I,I) = CWALL(I)
221 CONTINUE
C-----CALCULATE AMW(N)
C
WAMW = 0.0
DO 25 J=1,NSP
25 WAMW = WAMW + CWALL(J)/SMW(J)
WAMW = 1./WAMW
26 AMW(I)= WAMW
C
C-----FLOAT AA(I,J) MATRIX....
C
D030I=1,NSP
D030J=1,NE
30 AA(I,J)=IA(I,J)
C
IF(ITYPE.EQ.C)CALL RADIN
C-----CONVERT WALL AND SHOCK COMPOSITIONS TO AN ELEMENTAL BASIS.....
C
D033I=1,NE
EC(J,I)=0.0
EC(J,NETA)=C.C
D033I=1,NSP
FAC=AA(I,J)*AWT(J)/SMW(I)
EC(J,I)=EC(J,I) + FAC*C(I,I)
33 EC(J,NETA)=EC(J,NETA) + FAC*C(I,NETA)
331 ECWALL(J)=EC(J,I)
C
D034N=NETA,60
INIT1450
INIT1460
INIT1470
INIT1480
INIT1490
INIT1500
INIT1510
INIT1520
INIT1530
INIT1540
INIT1550
INIT1560
INIT1570
INIT1580
INIT1590
INIT1600
INIT1610
INIT1620
INIT1630
INIT1640
INIT1650
INIT1660
INIT1670
INIT1680
INIT1690
INIT1700
INIT1710
INIT1720
INIT1730
INIT1740
INIT1750
INIT1760
INIT1770
INIT1780
INIT1790
INIT1800

```

```

DO34J=1,NE
34 EC(J,N)=EC(J,NETA)
C
C-----INITIALIZE ELEMENTAL DIFFUSION COEFFICIENTS.....
C
DO35N=1,NETA
TT=T(N)*TD
DO35J=1,NE
35 D(J,N)=0.8128E-07*(TT**1.659)/(PI(N)*R*JINF)
C
C
DTILS = .01
IF(IDEBUG.EQ. 0) RETURN
WRITE(6,4000) VD,DUD,PD
WRITE(6,4000) DELTA,DTIL,RZB,RE
4000 FORMAT(1H0,6E15.6)
203 FORMAT(6E12.0)
100 FORMAT(1X,9E14.6)
RETURN
END
INIT1810
INIT1820
INIT1830
INIT1840
INIT1850
INIT1860
INIT1870
INIT1880
INIT1890
INIT1900
INIT1910
INIT1920
INIT1930
INIT1940
INIT1950
INIT1960
INIT1970
INIT1980
INIT1990
INIT2000

```

```

SUBROUTINE MOMTM
C -----THIS SUBROUTINE SOLVES THE MOMENTUM EQUATION AS A
C SECOND ORDER EQUATION AND A FIRST ORDER EQUATION -----
C
COMMON /CONV/ =PRCT,TPRCT,DDAMP,TDAMP,PDIL
COMMON /DEL/ DELTA,DTIL,DTILS
COMMON /FRSTRM/ U INF, RINF, UINF2, R, RE, LXI, ITM, IEM, NETA
COMMON /MAIM/KEEP,MAXE,MAXM,MAXD,IDEBUG,MCONV,ECONV,DCONV,LT,IAB
COMMON /NON/RDZ,MUDZ,RMDZ,AKNF,HNF,CPNF
COMMON/PROPI/PI(60),RHO(60), T(60),AMW(50),C (20,60),EC(5,60)
COMMON/PROP2/ MU(60),RM(60), AK(60)
COMMON/PROP3/CP3(20,60),HS(20,60),CP (60),HM(60)
COMMON /RFLUX/ E(60),IRAD,ITYPE
COMMON /RH/ DUD,DPHI,TD,RZB,PD,HD,HTOTAL
COMMON/VECTOR/ CA(60),CB(60),CC(60),B(60)
COMMON /VEL/ F(60),FC(60),Z(60),V(60)
COMMON/WALL/RVW,PRW,TWOLD,FLUX(20),CWALL(20),ECWALL(5)
COMMON /YL/ETA(60),YOND(60)
LOGICAL MCONV,ECONV,DCONV

C----- INITIALIZED QUANTITIES -----
C
MCONV = .FALSE.
ITM = 1
N = NETA -2
L = NETA-1
AA3 = RZB*(1,-RZB)*DPHI**2/DUD
IF(IEM,GT,3) DTIL=.5*(DTIL+DTILS2)

C
C
C-----Z +A1*Z'+A2*Z=A3
C COMPUTE A1,A2,A3
C 14 CONTINUE
C----- BOUNDARY CONDITIONS -----
C
MOMT 10
MOMT 20
MOMT 30
MOMT 40
MOMT 50
MOMT 60
MOMT 70
MOMT 80
MOMT 90
MOMT 100
MOMT 110
MOMT 120
MOMT 130
MOMT 140
MOMT 150
MOMT 160
MOMT 170
MOMT 180
MOMT 190
MOMT 200
MOMT 210
MOMT 220
MOMT 230
MOMT 240
MOMT 250
MOMT 260
MOMT 270
MOMT 280
MOMT 290
MOMT 300
MOMT 310
MOMT 320
MOMT 330
MOMT 340
MOMT 350
MOMT 360

```

```

      RED = RE*DTIL
      RED2 = 2.*RED*DTIL*DUD
      DTIL2 = DTIL*DTIL
      FD = RZ8/(2.*DUD*DTIL)
      FW = -RVW*FD
      F(1) = FW
      B(L) = 1./DTIL
      ITER = 1
15  CONTINUE
      II = 1
      DO 20 I=1,N
        DET=ETA(I+1)-ETA(I)
        DETN=ETA(I+2)-ETA(I+1)
        D1 = DETN*(DETN+DET)
        D2 = DETN*DET
        D3 = DET*(DETN+DET)
        RMP = DET*RM(I+2)/D1 + (DETN-DET)*RM(I+1)/D2 - DETN*RM(I)/D3
        A1 = (RED2*F(I+1) +RMP)/RM(I+1)
        A2 = -RED2*DTIL*Z(I)/RM(I+1)
        A3 = -2.*RED*( AA3/(RHO(I+1)*RM(I+1))
1          +DTIL2 *DUD*Z(I)**2/(2.*RM(I+1)) )
      C-----CA*Z(N-1)+CB*Z(N)+CC*Z(N+1)=B
      C  COMPUTE CA,CB,CC
      CA(11) =(2.-A1*DETN)/D3
      CB(1)=A1*(DETN-DET)/D2-2./D2+A2
      CC(1)=(2.+A1*DET)/D1
      B(1)=A3
      II = I
20  CONTINUE
      B(N)=B(N)-CC(N)/DTIL
      CALL TRID (N)
      C-----INTEGRATE FIRST ORDER EQUATION-----
      FC(1)=FW

```

MOMT 370
 MOMT 380
 MOMT 390
 MOMT 400
 MOMT 410
 MOMT 420
 MOMT 430
 MOMT 440
 MOMT 450
 MOMT 460
 MOMT 470
 MOMT 480
 MOMT 490
 MOMT 500
 MOMT 510
 MOMT 520
 MOMT 530
 MOMT 540
 MOMT 550
 MOMT 560
 MOMT 570
 MOMT 580
 MOMT 590
 MOMT 600
 MOMT 610
 MOMT 620
 MOMT 630
 MOMT 640
 MOMT 650
 MOMT 660
 MOMT 670
 MOMT 680
 MOMT 690
 MOMT 700
 MOMT 710
 MOMT 720

```

SUM=FW+ (B(1)+FW)*(ETA(2)-ETA(1))*DTIL/2.
FC(2)=SUM
DO 30 K=3, NETA
SUM=SUM+DTIL*(B(K-1)+B(K-2))*(ETA(K) -ETA(K-1))/2.
30 FC(K) = SUM
C
C-----CHECK FOR CONVERGENCE
C
DO 40 K=2, NETA
PRCT=ABS((FC(K)-F(K))/F(K))
IF (PRCT.GT.FPRCT) GO TO 50
40 CONTINUE
GO TO 90
50 CONTINUE
ITER=ITER+1
DO 60 K=1, NETA
60 F(K)=FC(K)
DO 65 I=1, N
65 Z(I)=B(I)
IF(ITER.GE.MAXM ) GO TO 90
GO TO 15
90 CONTINUE
C
C----- COMPUTE NEW DTIL -----
C
DTILC = (FD-FW)*DTIL/(F(NETA)-FW)
PRCT = ABS((DTIL-DTILC)/DTIL)
IF(ITEM.GT.MAXM) GO TO 160
ITEM = ITEM +1
IF(PRCT.LE.PDTIL) GO TO 150
DTIL = DTIL +DDAMP*(DTILC-DTIL)
GO TO 14
150 CONTINUE
DTIL = DTIL+ DDAMP*(DTILC -DTIL)
MCONV = .TRUE.
C

```

MOMT 730
MOMT 740
MOMT 750
MOMT 760
MOMT 770
MOMT 780
MOMT 790
MOMT 800
MOMT 810
MOMT 820
MOMT 830
MOMT 840
MOMT 850
MOMT 860
MOMT 870
MOMT 880
MOMT 890
MOMT 900
MOMT 910
MOMT 920
MOMT 930
MOMT 940
MOMT 950
MOMT 960
MOMT 970
MOMT 980
MOMT 990
MOMT1000
MOMT1010
MOMT1020
MOMT1030
MOMT1040
MOMT1050
MOMT1060
MOMT1070
MOMT1080


```

C CHECK MOMENTUM-ENERGY CONVERGENCE
  PRCT = ABS((DTIL-DTILS)/DTILS)
  IF (PRCT.LE.PDTIL) DCONV = .TRUE.
160 CONTINUE
C
  DO 170 K=1,NETA
170  V(K) = -FC(K)*DTIL*2./RHO(K)
      DTILS2 = DTILS
C DEBUG OUTPUT
      IF (IDBUG.EQ. 0) RETURN
      WRITE(6,102) ITER,ITM
      WRITE(6,100) DTIL,DTILC
      DO 120 K=1,NETA
      VS=-FC(K)*DTIL*UINF*2./RHO(K)
      WRITE(6,100) ETA(K),F(K),FC(K), RHO(K),RM(K),VS ,V(K)
120 CONTINUE
      DO 121 I=1,N
      U=B(I)*DTIL
      WRITE(6,100) ETA(I+1),Z(I),B(I),U
121 CONTINUE
100 FORMAT(1X,9E14.6)
102 FORMAT(10X,2I3/)
      RETURN
      END
MOMT1090
MOMT1100
MOMT1110
MOMT1120
MOMT1130
MOMT1140
MOMT1150
MOMT1160
MOMT1170
MOMT1180
MOMT1190
MOMT1200
MOMT1210
MOMT1220
MOMT1230
MOMT1240
MOMT1250
MOMT1260
MOMT1270
MOMT1280
MOMT1290
MOMT1300
MOMT1310
MOMT1320

```

```

SUBROUTINE ENERGY
C-----THIS SUBROUTINE SOLVES THE ENERGY EQUATION
C    IN A GLOBALLY IMPLICIT MANNER-----
C
COMMON /CONV/ FPRCT,IPRCT,DDAMP,TDAMP,PTIL
COMMON /DEL/ DELTA,DTIL,DTILS
COMMON /FRSTRM/ U INF, RINF, UINF2, R, RE, LXI, ITM, IEM, NETA
COMMON /MAIM/KEEP,MAXE,MAXM,MAXD,IDEBUG,MCONV,ECONV,DCONV,LT,IAB
COMMON /NON/RDZ,MUDZ,RMDZ,AKNF,HNF,CPNF
COMMON/NUMBER/NSP,NNS,NE,NC
COMMON/PROP1/PI(60),RHO(60), T(60),AMW(50),C (20,60),EC(5,60)
COMMON/PROP2/ MU(60),RM(60), AK(60)
COMMON/PROP3/CPS(20,60),HS(20,60),CP (60),HM(60)
COMMON /RFLUX/ E(60),IRAD,ITYPE
COMMON /RH/ DUD,DPHI,TD,RZB,PD,HD,HTOTAL
COMMON/SP2/BR,S(20),CSHOCK(5)
COMMON/VECTOR/ CA(60),CB(60),CC(60),B(60)
COMMON /VEL/ F(60),FC(60),Z(60),V(60)
COMMON/WALL/RVW,PRW,TWOLD,FLUX(20),CWALL(20),ECWALL(5)
COMMON /YL/ETA(60),YOND(60)
COMMON /OLD/ TOLD(60),EOLD(60),RHOS(60)
DIMENSION RHOLD(60)
REAL MU,MUDZ
LOGICAL MCONV,ECONV,DCONV
C-----INITIALIZED QUANTITIES-----
C
ECONV = .FALSE.
DTILN = DTIL
IF(IEM,GE, 2) DTIL= DTILN+.45*(DTILS -DTILN)
DTILS = DTILN
NF=NETA
N=NETA-2
ITER = 0
EPRCT=.5
ENER 10
ENER 20
ENER 30
ENER 40
ENER 50
ENER 60
ENER 70
ENER 80
ENER 90
ENER 100
ENER 110
ENER 120
ENER 130
ENER 140
ENER 150
ENER 160
ENER 170
ENER 180
ENER 190
ENER 200
ENER 210
ENER 220
ENER 230
ENER 240
ENER 250
ENER 260
ENER 270
ENER 280
ENER 290
ENER 300
ENER 310
ENER 320
ENER 330
ENER 340
ENER 350
ENER 360

```

```

      DG 3 I=1,NETA
      EOLD(I)=E(I)
      RHOS(I)=RHO(I)
      TOLD(I) = T(I)
      C
      IF(ITYPE.NE.C.OR.IRAD.NE.3)GOTO7
      CALL GAS(1)
      IF(RVM.LE.0.0)NSP=7
      CALL ELEMNT
      CALL CHEMEQ(1,NF)
      CALL PROPRT(NSP,1,NF)
      C
      7 CONTINUE
      IF(IRAD.EQ.3.AND.ITYPE.EQ.1) CALL EFLUX
      IF(IRAD.EQ.3.AND.ITYPE.EQ.0)CALL LRAD
      C
      IF(IEM.EQ.1)GOTO9
      DOBI=1,NETA
      E(I)=EPRCT*E(I) + (1.-EPRCT)*EOLD(I)
      8 CONTINUE
      9 C
      10 CONTINUE
      NS = NSP
      CALL GAS(1)
      C
      CALL ELEMNT
      CALL CHEMEQ(1,NETA)
      CALL PROPRT(NSP,1,NETA)
      C
      11 CONTINUE
      C
      C-----T..+A1*T.=A2
      C COMPUTE A1 AND A2
      C
      II = 1

```

ENER 370
ENER 380
ENER 390
ENER 400
ENER 410
ENER 430
ENER 440
ENER 460
ENER 470
ENER 480
ENER 490
ENER 500
ENER 510
ENER 520
ENER 530
ENER 540
ENER 550
ENER 560
ENER 570
ENER 580
ENER 590
ENER 600
ENER 610
ENER 620
ENER 630
ENER 660
ENER 670
ENER 680
ENER 690
ENER 710
ENER 720
ENER 730
ENER 740
ENER 750
ENER 760
ENER 770

```

00 20 I=1,N
DET=ETA(I+1)-ETA(I)
DETN=ETA(I+2)-ETA(I+1)
C1= DET/(DETN*(DETN+DET))
C2=(DETN-DET)/(DETN*DET)
C3=DETN/(DET*(DETN+DET))
COEF=DTIL/(2.*RHO(I+1)*AK(I+1))
C
C-----A1-----
C
TARM1=RHO(I+1)*V(I+1)*CP(I+1)
TARM2=0.0
TARM3=C1*RHO(I+2)*AK(I+2)+C2*RHO(I+1)*AK(I+1)
1 -C3*RHO(I)*AK(I)
A1=-COEF*(TARM1+TARM2-TARM3)
C
C-----A2-----
C
TERM1=0.0
IF(I.GE.N) NS=7
IF(IEM.LT.IAB) NS=7
DO 16 J=1,NS
TERM1=TERM1+HS(J,I+1)*(C1*C(J,I+2)+C2*C(J,I+1)
1 -C3*C(J,I))
16 CONTINUE
TERM1 = 0.0
TERM2=2.*V(I+1)*(C1*V(I+2)+C2*V(I+1)-C3*V(I))
TERM3=0.0
A2=COEF*(RHO(I+1)*V(I+1)*(TERM1+TERM2)
1 +TERM3+2.*DTIL*(I+1)/RHO(I+1) )
C
C-----CA*T(N-1)+CB*T(N)+CC*T(N+1)=B
C
CA(I1) = C3*(-A1+2./DETN)
CB(I1) =C2* A1 -2./(DETN*DET)
CC(I1) = C1*(A1+2./DET)
ENER 780
ENER 790
ENER 800
ENER 810
ENER 820
ENER 830
ENER 840
ENER 850
ENER 860
ENER 870
ENER 880
ENER 890
ENER 900
ENER 910
ENER 920
ENER 930
ENER 940
ENER 950
ENER 960
ENER 970
ENER 980
ENER 990
ENER1000
ENER1010
ENER1020
ENER1030
ENER1040
ENER1050
ENER1060
ENER1070
ENER1080
ENER1090
ENER1100
ENER1110
ENER1120
ENER1130

```

```

IF (I.EQ.1) BC=CA(1)*T(1)
H(I)=A2-BC
BC=0.0
II = I
20 CONTINUE
H(N)=A2-CC(N)
CALL TRID (N)
C
C-----CHECK FOR CONVERGENCE
C
DO 30 I=1,N
IF(B(I).LT.T(1))GOTO30
PRCT=ABS(B(I)-T(I+1))/T(I+1)
IF (PRCT.GT.TPRCT) GO TO 40
30 CONTINUE
GO TO 90
40 ITER=ITER+1
DO 50 I=1,N
II=I+1
T(II) = T(II) +TDAMP*(B(I)-T(II))
IF(T(II).GT.1.0) T(II) = .99999
IF(T(II).LT.T(1)) T(II)=1.000001*T(1)
50 CONTINUE
IF(ITER.GE.MAXE ) GOTO 90
GO TO 10
90 CONTINUE
IF(ITER.LT.MAXE) ECONV=.TRUE.
IF(IEM.EQ.2.OR.IEM.EQ.4) CALL STPSZ
C
C
TMCH=.08
DO 91 I=1,N
II = I+1
T(II) = T(II) +.35*(TOLD(II) -T(II))
PRCT=(T(II)-TOLD(II))/TOLD(II)
IF(ABS(PRCT).GT.TMCH)T(II)=TOLD(II)+TMCH*PRCT*TOLD(II)/ABS(PRCT)
ENER1140
ENER1150
ENER1160
ENER1170
ENER1180
ENER1190
ENER1200
ENER1210
ENER1220
ENER1230
ENER1240
ENER1250
ENER1260
ENER1270
ENER1280
ENER1290
ENER1300
ENER1310
ENER1320
ENER1330
ENER1340
ENER1350
ENER1360
ENER1370
ENER1380
ENER1390
ENER1400
ENER1410
ENER1420
ENER1430
ENER1440
ENER1450
ENER1460
ENER1470
ENER1480
ENER1490

```

```

91 CONTINUE
ITER = 0
915 ITER = ITER + 1
IF(ITER.GT.5)GOTO9251
DO921=1,NETA
RHOLD(I)=RHO(I)
CALL ELEMNT
CALL CHEMEQ(1,NETA)
CALL PROPRT (NSP,1,NETA)
DO9251=1,NETA
ERR=ABS(RHOLD(I)-RHO(I))/RHO(I)
IF(ERR.GT..01)GOTO915
925 CONTINUE
9251 CONTINUE
C
C-----NEW GUESS FOR DENSITY PROFILE.....
C
IF(IEM.EQ.1)GOTO927
DO9261=1,NETA
926 RHO(I)=RHO(I)*.7 + RHOS(I)*.3
927 CONTINUE
IF(IDEBUG.GT.0) CALL ELPROF
93 CONTINUE
DTIL = DTILN
C DEBUG OUTPUT
IF(IDEBUG.EQ. 0) RETURN
WRITE(6,102) ITER
DO 95 K=1,NETA
TK = T(K) *TD
WRITE (6,100) ETA(K),TK,E(K)
95 CONTINUE
100 FORMAT(1X,9E14.6)
102 FORMAT(10X,13/)
RETURN
END
ENER1500
ENER1530
ENER1540
ENER1550
ENER1560
ENER1570
ENER1580
ENER1590
ENER1600
ENER1610
ENER1620
ENER1630
ENER1640
ENER1650
ENER1660
ENER1670
ENER1680
ENER1690
ENER1700
ENER1710
ENER1720
ENER1730
ENER1740
ENER1750
ENER1760
ENER1770
ENER1780
ENER1790
ENER1800
ENER1810
ENER1820
ENER1830
ENER1840
ENER1850
ENER1860

```

```

SUBROUTINE ELEMNT
COMMON/NUMBER/NS,NNS,NE,NC
COMMON /MCD1/JS(20, 60),JE(5, 60)
COMMON/PRCP1/PI( 60),RO( 60),TT( 60),AMW( 60),C (20, 60),CC(5, 60)
COMMON /FRSTRM/ U INF, RINF, UINF2,RAD, RE, LXI, ITM, IEM, NETA
COMMON /VECTOR/SUB( 60),DIAG( 60),SUP( 60),B( 60)
COMMON /SCE/ NCHECK,ITER
COMMON/SP1/SS,TOL,NDEBUG
COMMON /DIF/D(5, 60)
COMMON /YL/ ET( 60),YOND( 60)
COMMON /VEL/FF( 60),FC( 60),ZZ( 60),VV( 60)
COMMON /DEL/ DELTA,DTIL,DTILS
COMMON/WALL/RVW,PRW,TWOLD,FLUX(20),CWALL(20),ECWALL(5)
DIMENSION TEF(5, 60)
DIMENSION XM(5)
REAL JS, JE
NCHECK=0
NM1=NETA-1
IF(RVW.LE.0.0) GO TO 200
DO15J=1,NE
15 XM(J)=RO(1)*VV(1)*ECWALL(J)
M=1
C
150 DO180J=1,NE
DIAG(1)= 1.0 + ET(2)*DTIL*VV(1)/(RO(1)*D(J,1))
SUP(1)=-1.0
B(1)=DTIL*XM(J)*ET(2)/(RO(1)*RO(1)*D(J,1))
154 DO155K=2,NETA
N=M-1+K
CALL FGH(N,F1,G1,H1)
CALL FGH2(N,F2,G2,H2)
DLVRO=F1*RO(N+1)/RO(N) + G1 + H1*RO(N-1)/RO(N)
DLNDJ=F1*D(J,N+1)/D(J,N) + G1 + H1*D(J,N-1)/D(J,N)
PETA=-DTIL*VV(N)/(RO(N)*D(J,N)) + 2.*DLNRO + DLNDJ
SUB(K-1)= PETA*H1 + H2
DIAG(K)= PETA*G1 + G2
ELEM 10
ELEM 20
ELEM 30
ELEM 40
ELEM 50
ELEM 60
ELEM 70
ELEM 80
ELEM 90
ELEM 100
ELEM 110
ELEM 120
ELEM 130
ELEM 140
ELEM 150
ELEM 160
ELEM 170
ELEM 180
ELEM 185
ELEM 190
ELEM 200
ELEM 210
ELEM 220
ELEM 230
ELEM 240
ELEM 250
ELEM 260
ELEM 270
ELEM 280
ELEM 290
ELEM 300
ELEM 310
ELEM 320
ELEM 330
ELEM 340
ELEM 350

```

```

      SUP(K)= PETA*F1 + F2
      B(K)=0.0
      IF(N.GE.(NETA-1))GOTO160
155  CONTINUE
160  B(K)=-SUP(K)*CC(J,NETA)
      CALL TRID(K)
      DU173L=1,K
      COLD=CC(J,M-1+L)
      CC(J,M-1+L)=B(L)
      ERR=ABS(CC(J,M-1+L) -COLD)
      IF(ERR.GE..01)NCHECK=NC+1
170  CONTINUE
180  CONTINUE
      RETURN
200  CONTINUE
      DO210 J=1,NE
      DO210 N=1,NM1
      CC(J,N)=CC(J,NETA)
210  CONTINUE
      RETURN
      END
ELEM 360
ELEM 370
ELEM 380
ELEM 390
ELEM 400
ELEM 410
ELEM 420
ELEM 430
ELEM 440
ELEM 450
ELEM 460
ELEM 470
ELEM 480
ELEM 490
ELEM 500
ELEM 510
ELEM 520
ELEM 530
ELEM 540
ELEM 550
ELEM 560

```



```

C * * * * * SUBROUTINE CHEMEO( NI,NF)
C * * * * *
C * * * * * THIS SUBPROGRAM IS A REVISION OF A PROGRAM ORIGINALLY REPORTED
C * * * * * IN NASA-TN-D-5391 (AUGUST 1969). THE PROGRAM COMPUTES FOR A
C * * * * * PRESSURE ARRAY,PP(N),TEMPERATURE ARRAY,TT(N), AND AN ARRAY
C * * * * * OF ELEMENTAL MASS FRACTIONS-CC(I,N), THE EQUILIBRIUM SPECIES
C * * * * * MASS FRACTIONS AT EACH POINT-N REPRESENTED BY THE GIVEN ARRAYS.
C * * * * * THE EQUILIBRIUM COMPOSITIONS ARE STORED IN THE MATRIX CE(I,N).
C * * * * *
C * * * * * DONALD D. ESCH
C * * * * * LOUISIANA STATE UNIVERSITY
C * * * * * AUGUST 7. 1970
C * * * * *
C * * * * * IN = INITIAL POINT FOR EQUILIBRIUM CALCULATIONS.
C * * * * * NF = FINAL POINT.
C * * * * *
C * * * * * COMMON/WALL/RVW,PRW,TWOLD,FLUX(20),CWAL-(20),ECWALL(5)
C * * * * * COMMON/SP1/SS,TOL,NDBG
C * * * * * COMMON/EQ1/AI(20),BI(20),CI(20),DI(20),EI(20),FI(20),GI(20),
C * * * * * HII(20),BII(20),CII(20),DII(20),EII(20),FII(20),GII(20)
C * * * * * X
C * * * * * COMMON/EQ2/AA(20,5),ICODE(20)
C * * * * * COMMON/THERM1/C(20),FORT(20)
C * * * * * COMMON/ID/SP(20),EL(5)
C * * * * * COMMON/NUMBER/NS ,NNS,MM,NC
C * * * * * COMMON/WT/XMW(20),AWT(5)
C * * * * * COMMON /RH/ DUD,DPHI,YD,RZB,PD,HD,HTOTAL
C * * * * * COMMON /DY/ DYDT(20,60)
C * * * * * COMMON/PROPI/PP(60),RO(60),TT(60),AMW(60),CE(20,60),CC(5,60)
C * * * * * DIMENSION R( 7, 7),B( 7,1),YINT(20),FY(20),PI(7),FSUM(20),YSUM(20)
C * * * * * 1 ,X(20),DELT(20),XLAM(20)
C * * * * * DIMENSION E(5),BB(5),Y(20)
C * * * * * CONTINUE
C * * * * *
CHEM 17
CHEM 20
CHEM 30
CHEM 40
CHEM 50
CHEM 60
CHEM 70
CHEM 80
CHEM 90
CHEM 100
CHEM 110
CHEM 120
CHEM 130
CHEM 140
CHEM 150
CHEM 160
CHEM 170
CHEM 180
CHEM 190
CHEM 200
CHEM 210
CHEM 220
CHEM 230
CHEM 240
CHEM 250
CHEM 260
CHEM 270
CHEM 280
CHEM 290
CHEM 300
CHEM 310
CHEM 320
CHEM 330
CHEM 340
CHEM 350
CHEM 360

```

```

CHEM 370
CHEM 380
CHEM 390
CHEM 400
CHEM 410
CHEM 420
CHEM 430
CHEM 440
CHEM 450
CHEM 460
CHEM 470
CHEM 480
CHEM 490
CHEM 500
CHEM 510
CHEM 520
CHEM 530
CHEM 540
CHEM 550
CHEM 560
CHEM 570
CHEM 580
CHEM 590
CHEM 600
CHEM 610
CHEM 620
CHEM 630
CHEM 640
CHEM 650
CHEM 660
CHEM 670
CHEM 680
CHEM 690
CHEM 700
CHEM 710
CHEM 720

MA=1
C-----INITIAL GUESS FOR EQUILIBRIUM CALCULATIONS....
DO10I=1,NS
10 Y(I) = CWall(I)*AMW(NI)/XMW(I)
C-----COMPUTE THE SIZE OF THE MATRIX
NA=MM+1
NS=NUMBER OF SPECIES....
CRIT=CRITERIA FOR CONVERGENCE.
DT=25.
DT=200.
CRIT=TOL
XBETA=CRIT
BETA=0.
LL=NS+1
TOLD=C.C
THE REMAINDER OF THE PROGRAM COMPUTES EQUILIBRIUM COMPOSITIONS
CORRESPONDING TO THE ELEMENTAL MASS FRACTIONS IN THE CC-ARRAY
FROM POINT N = NI TO POINT N = NF.
DO50CCN=NI,NF
KT=1
T = TT(N)*TD
P=PP(N)
RTOLD=C.C
SUM=0.0
DO15I=1,MM
15 SUM=SUM + CC(I,N)
DO20 I=1,MM
```

```

      IF (CC(I,N).LT.1.(E-10)CC(I,N)=1.0E-10
      E(I)=CC(I,N)/SUM
      C
      CALL ALTERY(E,Y,TOLD)
      C
      TINC=ABS(T-TOLD)
      IF (TINC.LE.50.)GOTO1750
      NT=1
      DO25 J=1,MM
      BB(J)=0.0
      DO 25 I=1,NS
      BB(J)=BB(J)+AA(I,J)*Y(I)
      C
      CALL THERMO(T,P)
      C
      C-----THERMO SUBPROGRAM CALCULATES F/RT FOR EACH COMPONENT.....
      C
      C-----SET-UP THE R-MATRIX AND THE B-VECTOR.....
      C
      40  YBAR=0.
      DO50 I=1,NS
      50  YBAR=YBAR+Y(I)
      C
      C      YBAR IS THE TOTAL NUMBER OF MOLES OF GAS SPECIES
      C
      C-----CALCULATE THE FREE ENERGY PARAMETER OF THE GAS SPECIES
      C
      DO60 I=1,NS
      FAC=Y(I)/YBAR
      IF (FAC.LT.1.E-73)FAC=1.E-73
      60  FY(I)=Y(I)*(C(I)+ALOG(FAC))
      C
      C-----PRODCEED TO CONSTRUCT THE R MATRIX
      C

```

CHEM 730
CHEM 740
CHEM 750
CHEM 760
CHEM 770
CHEM 780
CHEM 790
CHEM 800
CHEM 810
CHEM 820
CHEM 830
CHEM 840
CHEM 850
CHEM 860
CHEM 870
CHEM 880
CHEM 890
CHEM 900
CHEM 910
CHEM 920
CHEM 930
CHEM 940
CHEM 950
CHEM 960
CHEM 970
CHEM 980
CHEM 990
CHEM1000
CHEM1010
CHEM1020
CHEM1030
CHEM1040
CHEM1050
CHEM1060
CHEM1070
CHEM1080

```

C-----INITIALIZE TO ZERO....
C
DO75J=1,NA
DO75K=1,NA
75 R(J,K)=0.0
C
DO90J=1,MM
DO90K=J,MM
SUM=0.
DO80I=1,NS
80 SUM=SUM+AA(I,J)*AA(I,K)*Y(I)
R(J,K)=SUM
90 R(K,J)=SUM
C
DO 103 K=1,MM
SUM=0.
DO 101 I=1,NS
101 SUM=SUM+AA(I,K)*Y(I)
R(K,NA)=SUM
R(NA,K)=SUM
103 CONTINUE
C
C -----PROCEED TO CALCULATE THE VECTOR B.
C
DO140J=1,MM
SUM=0.
DO130I=1,NS
130 SUM=SUM+AA(I,J)*FY(I)
140 B(J,I)=SUM+BB(J)
C
SUM=0.
DO150I=1,NS
150 SUM=SUM+FY(I)
B(NA,I)=SUM
C
C-----MATRIX INVERSION IS CALLED TO PROVIDE THE SOLUTION FOR
CHEM1190
CHEM1100
CHEM1110
CHEM1120
CHEM1130
CHEM1140
CHEM1150
CHEM1160
CHEM1170
CHEM1180
CHEM1190
CHEM1200
CHEM1210
CHEM1220
CHEM1230
CHEM1240
CHEM1250
CHEM1260
CHEM1270
CHEM1280
CHEM1290
CHEM1300
CHEM1310
CHEM1320
CHEM1330
CHEM1340
CHEM1350
CHEM1360
CHEM1370
CHEM1380
CHEM1390
CHEM1400
CHEM1410
CHEM1420
CHEM1430
CHEM1440

```

```

C      THE LINEARIZED EQUATIONS. THE SOLUTION OF THE EQUATIONS
C      GIVES THE LAGRANGIAN MULTIPLIERS NEEDED TO COMPUTE THE MOLES
C      OF EACH GAS SPECIES.
C
C      CALL MATINV(R,NA,B,NA,NMAX)
C      CONTINUE
C
C      DO160I=1,NA
C
C      PI(I)=LAGRANGINA MULTIPLIERS
C
C      160 PI(I)=B(I,1)
C      U=PI(NA)
C      XBAR=U*YBAR
C
C      C-----COMPUTE THE MOLES OF EACH SPECIE....
C
C      DO170I=1,NS
C      170 FSUM(I)=-FY(I)+(Y(I)/YBAR)*XBAR
C      DO200I=1,NS
C      PSUM=0.
C      DO180J=1,MM
C      180 PSUM=PSUM+PI(J)*AA(I,J)
C      YSUM(I)=PSUM*Y(I)
C      200 X(I)=FSUM(I)+YSUM(I)
C
C      C-----CHECK IF CONVERGENCE CRITERIA HAS BEEN MET. IF SO, GO TO 300
C
C      BETA=0.0
C      DO215I=1,NS
C      DELT(I)=X(I)-Y(I)
C      215 BETA=BETA+ABS(DELT(I))
C      IF(BETA.GT.BETOLD)GOTO216
C      IF(BETA.LT.XBETA)GOTO300
C      216 CONTINUE
C
CHEM1450
CHEM1460
CHEM1470
CHEM1480
CHEM1490
CHEM1500
CHEM1510
CHEM1520
CHEM1530
CHEM1540
CHEM1550
CHEM1560
CHEM1570
CHEM1580
CHEM1590
CHEM1600
CHEM1610
CHEM1620
CHEM1630
CHEM1640
CHEM1650
CHEM1660
CHEM1670
CHEM1680
CHEM1690
CHEM1700
CHEM1710
CHEM1720
CHEM1730
CHEM1740
CHEM1750
CHEM1760
CHEM1770
CHEM1780
CHEM1790
CHEM1800

```

```

CHEM1810
CHEM1820
CHEM1830
CHEM1840
CHEM1850
CHEM1860
CHEM1870
CHEM1880
CHEM1890
CHEM1900
CHEM1910
CHEM1920
CHEM1930
CHEM1940
CHEM1950
CHEM1960
CHEM1970
CHEM1980
CHEM1990
CHEM2000
CHEM2010
CHEM2020
CHEM2030
CHEM2040
CHEM2050
CHEM2060
CHEM2070
CHEM2080
CHEM2090
CHEM2100
CHEM2110
CHEM2120
CHEM2130
CHEM2140
CHEM2150
CHEM2160

C-----COMPUTE THE CONVERGENCE PARAMETER XLAMB
C
      XLAMB=1.
      DO210 I=1,NS
      IF(A3S(DEL(I)).LT.1.0E-20)DEL(I)=0.0
      IF(DEL(I).GE.0.)GOTO210
      IF(X(I).GT.0.)GOTO210
      XLAM(I)=-Y(I)/DEL(I)
      XLAMB=AMIN1(XLAMB,XLAM(I))
      XLAMB=.99*XLAMB
210  CONTINUE
      XLAM1=XLAMB
      IF(XLAM1.EQ.0.)XLAM1=1.0E-5
      DEBAR=0.
      DO220 I=1,NS
      DEBAR=DEBAR+DEL(I)
220  DEBAR=DEBAR+DEL(I)
C
C-----DETERMINE THE SIZE OF THE UNIT VECTOR XLAMB.
C      APPLY THE CORRECTIONS TO OBTAIN A NEW SET OF ESTIMATES FOR THE
C      NEXT ITERATION. WHEN THE VALUE OF XLAMB IS VERY SMALL SET THE
C      VALUES OF Y(I) EQUAL TO X(I) TO AVOID USING THE SAME VALUES OF
C      Y(I) AS WAS USED IN THE PREVIOUS ITERATION
C
C-----DETERMINE THE FREE ENERGY GRADIENT. IF POSITIVE REDUCE XLAMBDA
C      DFDL=FREE ENERGY GRADIENT
C
230  DFDL=C.
      DO280 I=1,NS
      FAC=(Y(I)+XLAMB*DEL(I))/(YBAR+XLAMB*DEBAR)
      IF(FAC.LT.1.E-73)FAC=1.E-73
      DERP=(DEL(I)*YBAR-DEBAR*Y(I))/(YBAR+XLAMB*DEBAR)
      DFDL=DFDL+DEL(I)*(C(I)+ALOG(FAC)) + DERP
      DFDL=DFDL+DEL(I)*(C(I)+ALOG(FAC))
      IF(DFDL.LT.0.000)GOTO300
      XLAMB=.8*XLAMB

```

```

      IF (XLAMBD.GT.1.0E-08)GOTO230
C
C-----THE VALUE OF XLAMBD THAT ASSURES CONVERGENCE HAS BEEN FOUND
C
      300 DO350I=1,NS
      IF (XLAMBD.GT.1.0E-6)GOTO230C
      IF (DFDL.LT.0.)GOTO230C
      IF (XLAM1.LT.1.0E-6)XLAM1=1.0E-6
C
C-----CALCULATE THE NEW COMPOSITION FOR THE NEXT ITERATION
C
      Y(I)=Y(I)+XLAM1*DELT(I)*.1
      GOTO340
      330 Y(I)=Y(I)+XLAMBD*DELT(I)
      340 IF (Y(I).LT.0.)Y(I)=1.0E-73
      350 CONTINUE
C
      532 NT=NT+1
      BETOLD=BETA
      TOLD=T
C
C-----IF THE NUMBER OF ITERATIONS EXCEED 900 STOP COMPUTATIONS
C
      IF (NT.GT.900)GOTO6000
      GOTO40
      800 CONTINUE
C
C-----CONVERT Y(I) TO MOLE FRACTIONS.....
C
      CONVERT EQUILIBRIUM MOLE FRACTIONS TO MASS FRACTIONS AND STORE
      THESE VALUES IN THE CE-MATRIX. AMW(N) IS THE AVERAGE MOLECULAR
      WEIGHT AT THE POINT. N.
      SUMY=0.0
      DO900I=1,NS
      900 SUMY=SUMY+Y(I)

```

CHEM2170
 CHEM2180
 CHEM2190
 CHEM2200
 CHEM2210
 CHEM2220
 CHEM2230
 CHEM2240
 CHEM2250
 CHEM2260
 CHEM2270
 CHEM2280
 CHEM2290
 CHEM2300
 CHEM2310
 CHEM2320
 CHEM2330
 CHEM2340
 CHEM2350
 CHEM2360
 CHEM2370
 CHEM2380
 CHEM2390
 CHEM2400
 CHEM2410
 CHEM2420
 CHEM2430
 CHEM2440
 CHEM2450
 CHEM2460
 CHEM2470
 CHEM2480
 CHEM2490
 CHEM2500
 CHEM2510
 CHEM2520

```

CHEM2530
CHEM2540
CHEM2550
CHEM2560
CHEM2570
CHEM2580
CHEM2590
CHEM2600
CHEM2610
CHEM2620
CHEM2630
CHEM2640
CHEM2650
CHEM2660
CHEM2670
CHEM2680
CHEM2690
CHEM2700
CHEM2710
CHEM2720
CHEM2730
CHEM2740
CHEM2750
CHEM2760
CHEM2770
CHEM2780
CHEM2790
CHEM2800
CHEM2810
CHEM2820
CHEM2830
CHEM2840
CHEM2850
CHEM2860
CHEM2870
CHEM2880

      IF(KT.GT.1)GOTO1500
      AMW(N) = 0.C
      DO1000I=1,NS
      Y(I)=Y(I)/SUMY
1000  AMW(N) = AMW(N) + Y(I)*XMW(I)
      DO1005I=1,NS
1005  CE(I,N) = Y(I)*XMW(I)/AMW(N)
      GOTO1800
C
C-----COMPUTE THE PARTIAL DERIVATIVE OF THE MOLE FRACTION, DYDT...
C
1500  AMPLUS=0.0
      DO1525I=1,NS
      Y(I)=Y(I)/SUMY
1525  AMPLUS=AMPLUS + Y(I)*XMW(I)
      DO1550I=1,NS
      DYDT(I,N)=0.0
      IF(Y(I).LT.1.0E-10)GOTO1550
      YY=Y(I)*AMW(N)/AMPLUS - CE(I,N)*AMW(N)/XMW(I)
      DYDT(I,N)=YY/DT
1550  CONTINUE
      GOTO3300
C
C-----IF THE TEMPERATURE CHANGE IS LESS THAN 50 DEGREES FROM LAST
C      F. E. M. CALCULATION ASSUME CURRENT VALUES AS EQUAL TO LAST
C      VALUES...
C
1750  DO1760I=1,NS
      CE(I,N)=CE(I,N-1)
1760  DYDT(I,N)=DYDT(I,N-1)
      AMW(N)=AMW(N-1)
1800  CONTINUE
C
C      OPTIONAL OUTPUT OF POSITION , TEMPERATURE AND EQUILIBRIUM
C      COMPOSITIONS.
C

```



```

      IF(NDEBUG,LT,2)GOTO3000
      PRINT 2000,P,T,NT
2000 FORMAT(/,,' P = ',F5.3,' T(UK) = ',F6.0,SX,'NUMBER OF ITERATIONS
      X='13,/,11X,'Y(I)',12X,'C(I,N)',/)
      PRINT 2005,(SP(I),Y(I),CE(I,N),I=1,NS)
2005 FORMAT(1X,A4,2E18.8)
C
3000 CONTINUE
      KT=2
      T=T+DT
      IF(TINCR.GT.50.)GOTO22
3300 XBETA=CRIT
5000 CONTINUE
8000 CONTINUE
      RETURN
6000 PRINT6001
6001 FORMAT(' NUMBER OF ITERATIONS EXCEEDED 900, PROGRAM TERMINATING')
      RETURN
      END
CHEM2890
CHEM2900
CHEM2910
CHEM2920
CHEM2930
CHEM2940
CHEM2950
CHEM2960
CHEM2970
CHEM2980
CHEM2990
CHEM3000
CHEM3010
CHEM3020
CHEM3030
CHEM3040
CHEM3050
CHEM3060
CHEM3070

```

```

SUBROUTINE ALTEPY(E,Y,TOLD)
COMMON/WT/SMW(20),AWT(5)
COMMON/NUMBER/NSP,NNS,NE,NC
COMMON/EQ2/AA(20,5),ICODE(20)
COMMON/ELSP/LSP(5)
COMMON /SP1/SS,TOL,NDBG
DIMENSION E(5),Y(20),B(5),EOLD(5)
DATA EOLD/5*0.0/

C-----CHECK TO SEE IF ELEMENTAL COMPOSITION HAS CHANGED SIGNIFICANTLY.
C IF NOT, THEN RETURN....
C
CHANGE=0.0
DO5J=1,NE
CHANGE=CHANGE+ABS(EOLD(J))-E(J))
5 EOLD(J)=E(J)
IF(CHARGE.LT.1.0E-3)RETURN
IF(NDBG.GT.1)PRINT101
101 FORMAT(' INITIAL GUESS ON MOLE FRACTIONS UPDATED')

C-----ASSUME ALL SPECIES HAVE THE SAME COMPOSITION.....
C
C-----COMPUTE GRAM-ATOMS OF EACH ELEMENT FROM KNOWN ELEMENTAL CPMPPOS
C DISTRIBUTION AND THE MAXIMUM POSSIBLE MOLECULAR WEIGHT.....
C
DO20J=1,NE
IF(E(J).GT.1.0E-8)GOTO20
DO15I=1,NSP
IF(AA(I,J).LE.0.0)GOTO15
Y(I)=1.0E-12
15 CONTINUE
20 E(J)=E(J)*100./AWT(J)

C-----CALCULATE FOR EACH ELEMENT, THE NUMBER OF G-ATOMS BASED ON THE
C FIRST GUESS. ADJUST THE COMPOSITION OF EACH ELEMENT-SPECIE AS

```

ALTE 10
 ALTE 20
 ALTE 30
 ALTE 40
 ALTE 50
 ALTE 60
 ALTE 70
 ALTE 80
 ALTE 90
 ALTE 100
 ALTE 110
 ALTE 120
 ALTE 130
 ALTE 140
 ALTE 150
 ALTE 160
 ALTE 170
 ALTE 180
 ALTE 190
 ALTE 200
 ALTE 210
 ALTE 220
 ALTE 230
 ALTE 240
 ALTE 250
 ALTE 260
 ALTE 270
 ALTE 280
 ALTE 290
 ALTE 300
 ALTE 310
 ALTE 320
 ALTE 330
 ALTE 340
 ALTE 350
 ALTE 360

ALTE 370
 ALTE 380
 ALTE 390
 ALTE 400
 ALTE 410
 ALTE 420
 ALTE 430
 ALTE 440
 ALTE 450
 ALTE 460
 ALTE 470

```

C
C      REQUIRED.....
      DO30J=1,NE
      B(J)=0.0
      DO30I=1,NSP
      B(J)=B(J)+AA(I,J)*Y(I)
      DO40J=1,NE
      Y(LSP(J))=Y(LSP(J)) + (E(J)-B(J))
      TOLD=0.0
      RETURN
      END
30
40

```

```

C
C
C-----SUBROUTINE THERMC CALCULATES THE FREE ENERGY FUNCTION FOR EACH
C          CHEMICAL SPECIE.
C
C
C          COMMON/NUMBER/NO ,NNS,NE,NC
C          COMMON/EQ1/AI(20), BI(20), CI(20), DI(20), EI(20), FI(20), GI(20),
C          X      AII(20),BII(20),CII(20),DII(20),EII(20),FII(20),GII(20)
C          COMMON/EQ2/AA(20,5),ICODE(20)
C          COMMON/THERM1/C(20),FORT(20)
C
C          T=TEMPERATURE IN OK
C
C          T1=T
C          T2=T1*T
C          T3=T2*T
C          T4=T3*T
C          T5=T4*T
C
C
C-----CALCULATE THE FREE ENERGY FUNCTION FORT(I)
C
C          FORT(I)=FREE ENERGY FUNCTION
C
C          DO 41 I=1,NQ
C          IF(T.GT,6000.) )GOTO6205
C          FORT(I)=AI(I)*(1.-ALOG(T))-BI(I)*T/2.-CI(I)*T2/6.-DI(I)*T3/12.
C          ,      -EI(I)*T4/20.,+FI(I)/T-GI(I)
C          IF(ICODE(I).EQ.1)GOTO41
C          C(I)=FORT(I)+ALOG(P)
C          GOTO41
C
C          6205 FORT(I)=AII(I)*(1.-ALOG(T))-BII(I)*T/2.-CII(I)*T2/6.-DII(I)*T3/12.
C          ,      -EII(I)*T4/20.,+FII(I)/T-GII(I)
C          1  IF(ICODE(I).EQ.1)GOTO41

```

```

THER 10
THER 20
THER 30
THER 40
THER 50
THER 60
THER 70
THER 80
THER 90
THER 100
THER 110
THER 120
THER 130
THER 140
THER 150
THER 160
THER 170
THER 180
THER 190
THER 200
THER 210
THER 220
THER 230
THER 240
THER 250
THER 260
THER 270
THER 280
THER 290
THER 300
THER 310
THER 320
THER 330
THER 340
THER 350
THER 360

```

THIR 370
THIR 380
THIR 390
THIR 400

C(I)=FORT(I)+ALOG(P)
41 CONTINUE
RETURN
END


```

      REAL K1,K2
      DATA R /1.98716/

      T72 = .7628
      TOLD=0.0
      DO20 N=NI,NF
      T1=TT(N)*TD
      DO30 J=1,5
      C(J,N)=C.8128E-07*(T1**1.659)/(PI(N)*RAD*UINF)
      PO(N) = R7R *PI(N)*AMW(N)/T1
      IF (ABS(T1-TOLD).LE.150.) GOTO150
      AA=.130E-7 + 3.35E-12*T1
      D12=AA*929.*(T1**1.659)/PI(N)
      T2=T1*T1
      T3=T2*T1
      T4=T3*T1
      T5=T4*T1
      DO90 I=1,NSP
      IF (T1.GT.6000.) GOTO150
      CP(I,N)=( AI(I)+ BI(I)*T1+ CI(I)*T2+ DI(I)*T3+ EI(I)*T4)*R
      H(I,N)=( AI(I)*T1+ BI(I)*T2/2.+ CI(I)*T3/3.+ DI(I)*T4/4.
      + EI(I)*T5/5.+ FI(I))*R
      X
      GOTO60
50  CP(I,N)=(AI1(I)+BI1(I)*T1+CI1(I)*T2+DI1(I)*T3+EI1(I)*T4)*R
      H(I,N)=(AI1(I)*T1+BI1(I)*T2/2.+CI1(I)*T3/3.+DI1(I)*T4/4.
      +EI1(I)*T5/5.+FI1(I))*R
      X
60  Y(I)=C(I,N)*AMW(N)/SMW(I)
      VIS(I)=(V1(I) + V2(I)*T1 + V3(I)*T2)*1.0E-C5
      TC(I)=(K1(I)+K2(I)*T1)*1.0E-4/.662
      CONTINUE
90
C-----CALCULATE PHI(I,J) PARAMETERS FOR MIXTURE PROPERTIES.....
C
      DO95 I=1,NSP
      DO95 J=1,NSP
      VI312=SQRT(VIS(I)/VIS(J))

```

```

PROP 370
PROP 380
PROP 390
PROP 400
PROP 410
PROP 420
PROP 430
PROP 440
PROP 450
PROP 460
PROP 470
PROP 480
PROP 490
PROP 500
PROP 510
PROP 520
PROP 530
PROP 540
PROP 550
PROP 560
PROP 570
PROP 580
PROP 590
PROP 600
PROP 610
PROP 620
PROP 630
PROP 640
PROP 650
PROP 660
PROP 670
PROP 680
PROP 690
PROP 700
PROP 710
PROP 720

```

```

          SMW14=(SMW(J)/SMW(I))**.25
          PHI(I,J)=.254*(1.+VIS12*SMW14)**2)/SQRT(1.+SMW(I)/SMW(J))
    95  CONTINUE
C-----CALCULATION OF MIXTURE PROPERTIES....
C
      DO100I=1,NSP
      YPHI(I)=0.0
      DO100J=1,NSP
    100  YPHI(I)=YPHI(I) + Y(J)*PHI(I,J)
      VISM(N)=0.0
      HM(N)=0.0
      TCF=0.0
      CPF=0.0
      CPR=C.0
      SUMY=C.0
      DO120I=1,NSP
      IF(Y(I).LT.1.E-5) GO TO 120
      HM(N)=HM(N)+Y(I)*H(I,N)
      SUMY=SUMY+Y(I)
      CPF=CPF + Y(I)*CP(I,N)
      CPR=CPR + H(I,N)*DYDT(I,N)
      VISM(N)=VISM(N)+Y(I)*VIS(I)/YPHI(I)
      TCF=TCF + Y(I)*TC(I)/YPHI(I)
    120  CONTINUE
      CPM(N)=CPF + CPR
      TCR=RG(N)*D12*CPR/(AMW(N)*62.4)
      TCM(N)=TCF + TCR
      PR=VISM(N)*CPM(N)*14.88/(TCM(N)*AMW(N))
      TOLD=1
      GO10200
    130  CONTINUE
      DO160I=1,NSP
      CP(I,N)=CP(I,N-1)
      H(I,N)=H(I,N-1)
      VISM(N)=VISM(N-1)

```

PROP 730
 PROP 740
 PROP 750
 PROP 760
 PROP 770
 PROP 780
 PROP 790
 PROP 800
 PROP 810
 PROP 820
 PROP 830
 PROP 840
 PROP 850
 PROP 860
 PROP 870
 PROP 880
 PROP 890
 PROP 900
 PROP 910
 PROP 920
 PROP 930
 PROP 940
 PROP 950
 PROP 960
 PROP 970
 PROP 980
 PROP 990
 PROP1000
 PROP1010
 PROP1020
 PROP1030
 PROP1040
 PROP1050
 PROP1060
 PROP1070
 PROP1080
 PROP1090


```

TCM(N)=TCM(N-1)
CPM(N)=CPM(N-1)
200 CONTINUE
C
C----- NONDIMENSIONALIZE QUANTITIES -----
C
MUDZ=VISM(NF)
DO 250 I=NI,NF
  TI=TT(I)*TD
  VISM(I) = VISM(I)/MUDZ
  TCM(I) = TCM(I)*AKNF*6.715E-2
  RO(I) = RO(I)/(RDZ*32.174)
  RM(I)=RO(I)*VISM(I)
  CPM(I)=CPM(I)*CPNF/AMW(I)
DO 250 K=1,NSP
  CP(K,I) = CP(K,I)*CPNF/SMW(K)
  H(K,I) = H(K,I)*HNF*1.89/SMW(K)
250 CONTINUE
  RETURN
  END
PROP1100
PROP1110
PROP1120
PROP1130
PROP1140
PROP1150
PROP1160
PROP1190
PROP1200
PROP1210
PROP1220
PROP1230
PROP1240
PROP1250
PROP1280
PROP1290
PROP1300
PROP1310
PROP1320
PROP1330

```



```

COMMON /R4/ DUD,DPHI,TD,RZH,PD,HD,HTOTAL
COMMON/WALL/RVW,PRW,TWOLD,FLUX(20),CWALL(20),ECWALL(5)
REAL MU,MUDZ
LOGICAL MCONV,GCONV,SCONV
DATA GASC /49721.7/

C
C
DO 2000 I=KODE,NETA
  T = TI(I) * TD
  P = PI(I)

C
C THE FOLLOWING PART OF PROGRAM USES PRESSURE IN ATMOSPHERES
C AND TEMPERATURE IN DEG K
C
C
ITER=0

C
C ** TEMPERATURE - ENTHALPY ITERATION **

CONTINUE
ITER=ITER+1
IF(T.LT.100.) T=100.
A1=11390./T
A2=18990./T
A3=2270./T
A4=3390./T
A5=228./T
A6=326./T
A7=22300./T
A8=48600./T
A9=27700./T
A10=41500./T
A11=38600./T
A12=58200./T
A13=70.6/T
A14=188.9/T
A15=22100./T

```

GAS 370
 GAS 380
 GAS 390
 GAS 400
 GAS 410
 GAS 420
 GAS 430
 GAS 440
 GAS 450
 GAS 460
 GAS 470
 GAS 480
 GAS 490
 GAS 500
 GAS 510
 GAS 520
 GAS 530
 GAS 540
 GAS 550
 GAS 560
 GAS 570
 GAS 580
 GAS 590
 GAS 600
 GAS 610
 GAS 620
 GAS 630
 GAS 640
 GAS 650
 GAS 660
 GAS 670
 GAS 680
 GAS 690
 GAS 700
 GAS 710
 GAS 720

```

A16=47000./T
A17=67900./T
A18=2270./(4.*T)
A19=TANH(A18)
A20=3390./(4.*T)
A21=TANH(A20)
TT=1./T
TSQ=T**2
TSQRT=T**0.5
A22=112.2222/T
A23=T/59000.
A24=T/113200.
A25=T/75400.
AA1=EXP(-A1)
AA2=EXP(-A2)
AA3=EXP(A3)
AA4=EXP(A4)
AA5=EXP(-A5)
AA6=EXP(-A6)
AA7=EXP(-A7)
AA8=EXP(-A8)
AA9=EXP(-A9)
AA10=EXP(-A10)
AA11=EXP(-A11)
AA12=EXP(-A12)
AA13=EXP(-A13)
AA14=EXP(-A14)
AA15=EXP(-A15)
AA16=EXP(-A16)
AA17=EXP(-A17)

C CALCULATING ENERGIES PER COMPONENT OF GAS MIXTURE ABOVE
C REFERENCE ENERGIES.
  E1=2.5+((2.*AA1*A1+AA2*A2)/(3.+2.*AA1+AA2))+(A3/(AA3-1.))
  E2=2.5+ (A4/(AA4-1.))
  E3=1.5+((3.*AA5*A5+AA6*A6+5.*AA7*A7+AA8*A8)/(5.+3.*AA5+AA6+5.*AA7+
1AA9))
GAS 730
GAS 740
GAS 750
GAS 760
GAS 770
GAS 780
GAS 790
GAS 800
GAS 810
GAS 820
GAS 830
GAS 840
GAS 850
GAS 860
GAS 870
GAS 880
GAS 890
GAS 900
GAS 910
GAS 920
GAS 930
GAS 940
GAS 950
GAS 960
GAS 970
GAS 980
GAS 990
GAS 1000
GAS 1010
GAS 1020
GAS 1030
GAS 1040
GAS 1050
GAS 1060
GAS 1070
GAS 1080

```

```

E4=1.5+((1.0.* AA9*AA9+6.*AA10*(AA10)/(4.+10.*AA9+6.*AA10))
E5=1.5+((1.0.*AA11*AA11+5.*AA12*AA12)/(4.+10.*AA11+5.*AA12))
E6=1.5+((3.*AA13*AA13+5.*AA14*AA14+5.*AA15*AA15+AA16*AA16+5.*AA17*AA17)
1/(1.+3.*AA13+5.*AA14+5.*AA15+AA16+5.*AA17))
E7=1.5
C TOTAL ENERGY PER COMPONENT OF GAS MIXTURE
EN1=E1
EN2=E1
EN3=E3+29500./T
EN4=E4+56600./T
EN5=E5+187500./T
EN6=E6+225400./T
EN7=E7
C LOGS OF PARTITION FUNCTIONS
TL1=ALOG(T)*3.5
TL2=ALOG(T)*2.5
EQ1=TL1+.11+ALOG((3.+2.*AA1+AA2)/(1.-(1.0/AA3)))
EQ2=TL1-.42-ALOG((1.-(1.0/AA4)))
EQ3=TL2+.5+ALOG((5.+3.*AA5+AA6+5.*AA7+AA8))
EQ4=TL2+.3+ALOG((4.+10.*AA9+6.*AA10))
EQ5=TL2+.5+ALOG((4.+10.*AA11+6.*AA12))
EQ6=TL2+.3+ALOG((1.+3.*AA13+5.*AA14+5.*AA15+AA16+5.*AA17))
EQ7=TL2-14.24
C EQUILIBRIUM CONSTANTS FOR CHEMICAL REACTIONS
EK1=-59000./T+2.*EQ3-EQ1
EK2=-113200./T+2.*EQ4-EQ2
EK3=-158000./T+EQ5+EQ7-EQ3
EK4=-168800./T+EQ6+EQ7-EQ4
CCC=-79.9
YC(PK1-1.0,CCC) PK1=-79.9
IF(EK2,LE,CCC) EK2=-79.9
IF(EK3,LE,CCC) EK3=-79.9
IF(EK4,LE,CCC) EK4=-79.9
XK1=EXP(EK1)
XK2=EXP(EK2)
XK3=EXP(EK3)
GAS 1090
GAS 1100
GAS 1110
GAS 1120
GAS 1130
GAS 1140
GAS 1150
GAS 1160
GAS 1170
GAS 1180
GAS 1190
GAS 1200
GAS 1210
GAS 1220
GAS 1230
GAS 1240
GAS 1250
GAS 1260
GAS 1270
GAS 1280
GAS 1290
GAS 1300
GAS 1310
GAS 1320
GAS 1330
GAS 1340
GAS 1350
GAS 1360
GAS 1370
GAS 1380
GAS 1390
GAS 1400
GAS 1410
GAS 1420
GAS 1430
GAS 1440

```

```

XK4=FXP(EK4)
XK34=.2*XK3+.2*XK4
EE1=(-0.8+(.64+.8*(1.+(4.*P)/XK1))**.5)/(2.*(1.+4.*P/XK1))
EE2=(-0.4+(.16+3.84*(1.+(4.*P)/XK2))**.5)/(2.*(1.+4.*P/XK2))
EE3=1./((1.+P/XK34)**.5)
C COMPRESSIBILITY (Z) DIMENSIONLESS
Z=1.+EE1+EE2+2.*EE3
C COMPONENT MOL FRACTIONS IN AIR
X1=(.2-EE1)/Z
X2=(.8-EE2)/Z
X3=(2.*EE1-.4*EE3)/Z
X4=(2.*EE2-1.6*EE3)/Z
X5=.4*EE3/Z
X6=1.6*EE3/Z
X7=2.*EE3/Z
IF(X1.LE.0.) X1=1.E-20
IF(X2.LE.0.) X2=1.E-20
IF(X3.LE.0.) X3=1.E-20
IF(X4.LE.0.) X4=1.E-20
IF(X5.LE.0.) X5=1.E-20
IF(X6.LE.0.) X6=1.E-20
IF(X7.LE.0.) X7=1.E-20
C ENERGY PER MOL OF INITIALLY UNDISSOCIATED AIR-DIMENSIONLESS
ER=7*(X1*EN1+X2*EN2+X3*EN3+X4*EN4+X5*EN5+X6*EN6+X7*EN7)
C ENTHALPY PER INITIAL MOL OF AIR-DIMENSIONLESS
HR=ER+Z
C ENTHALPY PER INITIAL MOL OF AIR (H) IN BTU/LB
H=HR*T*.12348
IF(KODE.LT.NETA) GO TO 1000
HRATO=.5*(H-HD)/H
AHR=ABS(HRATO)
IF(AHR.LE.0.001) GO TO 999
IF(ITER.GT.1) GO TO 203
TP=T
HP=HRATO
T=T*(1.-HRATO)
GAS 1450
GAS 1460
GAS 1470
GAS 1480
GAS 1490
GAS 1500
GAS 1510
GAS 1520
GAS 1530
GAS 1540
GAS 1550
GAS 1560
GAS 1570
GAS 1580
GAS 1590
GAS 1600
GAS 1610
GAS 1620
GAS 1630
GAS 1640
GAS 1650
GAS 1660
GAS 1670
GAS 1680
GAS 1690
GAS 1700
GAS 1710
GAS 1720
GAS 1730
GAS 1740
GAS 1750
GAS 1760
GAS 1770
GAS 1780
GAS 1790
GAS 1800

```

```

GAS 1810
GAS 1820
GAS 1830
GAS 1840
GAS 1850
GAS 1860
GAS 1870
GAS 1880
GAS 1890
GAS 1900
GAS 1910
GAS 1920
GAS 1930
GAS 1940
GAS 1950
GAS 1960
GAS 1970
GAS 1980
GAS 1990
GAS 2000
GAS 2010
GAS 2020
GAS 2030
GAS 2040
GAS 2050
GAS 2060
GAS 2070
GAS 2080
GAS 2090
GAS 2100
GAS 2110
GAS 2120
GAS 2130
GAS 2140
GAS 2150
GAS 2160

IF(ITER .LT. 15) GO TO 900
203 CONTINUE
TS=T*(1.-HRATO)
IF(HRATO*HP .LT.C.C) TS=.5*(T+TP)
TP=T
T=TS
HP=HRATO
IF(ITER .LT. 15) GO TO 900
WRITE(6,200) T,H,HT
200 FORMAT(39H1TEMPERATURE-ENTHALPY DID NOT CONVERGE /3E15.6)
C CALL OUTPUT(4)
STOP
999 CONTINUE
TD = T
C
1000 CONTINUE
C ENTROPY PER INITIAL MOL OF AIR-DIMENSIONLESS
D1=EQ1+E1+1.
D2=EQ2+E2+1.
D3=EQ3+E3+1.
D4=EQ4+E4+1.
D5=EQ5+E5+1.
D6=EQ6+E6+1.
D7=EQ7+E7+1.
C TOTAL ENTROPY
SR=Z*(X1*D1+X2*D2+X3*D3+X4*D4+X5*D5+X6*D6+X7*D7)-Z*(X1*ALOG(X1) +
1X2*ALOG(X2)+X3*ALOG(X3)+X4*ALOG(X4)+X5*ALOG(X5)+X6*ALOG(X6)+X7*
2ALOG(X7))-7*ALOG(P)
C ENTROPY PER INITIAL MOL OF AIR (S) IN BTU/LB-DEG R
S =SR*.7686
C SPECIFIC HEAT AT CONSTANT VOLUME-CV
FF1=3.+2.*AA1+AA2
CV1=2.5+((2.*AA1+AA1*AA1+AA2*AA2)/FF1)-((2.*AA1*AA1+AA2*AA2)/FF1)**GAS 2130
12.)+(1.25*AA3*AA3)/((2.*AA1)+(1.-AA1*AA1)**2)) GAS 2140
CV2=2.5+((.25*AA4*AA4)/((2.*AA1)+(1.-AA1*AA1)**2)) GAS 2150
CV3=1.5+((3.*AA5*AA5+AA6*AA6+AA7*AA7+AA8*AA8)/(5.+3.*AAAS 2160

```

```

15+AA6+5.*AA7+AA8))-((E3-1.5)**2.)
CV4=1.5+((1C.*AA9*AA9+6.*AA1C*AA1C*AA1C)/(4.+10.*AA9+6.*AA1C))
1-((E4-1.5)**2.)
CV5=1.5+((1C.*AA11*AA11*AA11+6.*AA12*AA12*AA12)/(4.+10.*AA11+6.*AA12))
1-((E5-1.5)**2.)
CV6=1.5+((3.*AA13*AA13*AA13+5.*AA14*AA14*AA14+5.*AA15*AA15*AA16*AA16GAS 2170
1*AA16+5.*AA17*AA17**2.)/(1.+3.*AA13+5.*AA14+5.*AA15+AA16+5.*AA17))-((GAS 2180
2E6-1.5)**2.)
CV7=1.5
GAS 2190
GAS 2200
GAS 2210
GAS 2220
GAS 2230
GAS 2240
GAS 2250
GAS 2260
GAS 2270
GAS 2280
GAS 2290
GAS 2300
GAS 2310
GAS 2320
GAS 2330
GAS 2340
GAS 2350
GAS 2360
GAS 2370
GAS 2380
GAS 2390
GAS 2400
GAS 2410
GAS 2420
GAS 2430
GAS 2440
GAS 2450
GAS 2460
GAS 2470
GAS 2480
GAS 2490
GAS 2500
GAS 2510
GAS 2520
C LOGARITHMIC DERIVATIVES
CK1=TT*(59000./T+2.*E3-E1)
CK2=TT*(113200./T+2.*E4-E1)
CK3=TT*(158000./T+E5+E7-E3)
CK4=TT*(168000./T+E6+E7-E4)
CK34=.2*CK3+.8*CK4
PK1= CK1+TT
PK2= CK2+TT
PK3= CK3+TT
PK4= CK4+TT
PK34=C.2*PK3+C.8*PK4
C PARTIAL DERIVATIVES REQUIRED FOR CP
DE1P=(PK1*EE1*(1.+EE1))*(.2-EE1))/(.8*(.5-EE1))
DE2P=(PK2*EE2*(1.2+EE2))*(.8-EE2))/(.4*(4.8-EE2))
DE3P=.5*PK34*EE3*(1.-EE3**2)
DZX1P=-DE1P
DZX2P=-DE2P
DZX3P=2.*DE1P-.4*DE3P
DZX4P=2.*DE2P-1.6*DE3P
DZX5P=.4*DE3P
DZX6P=1.6*DE3P
DZX7P=2.*DE3P
C EQUATION FOR SPECIFIC HEAT AT CONSTANT PRESSURE
CPF=Z*(X1*(CV1+1.)+X2*(CV2+1.)+X3*(CV3+1.)+X4*(CV4+1.)+X5*(CV5+1.
1)+X6*(CV6+1.)+X7*(CV7+1.))
CPF = CPF + T*(DZX1P*(EN1+1.)+DZX2P*(EN2+1.)+DZX3P*(EN3+1.)+DZX4P*(EN4+1.)+DZX5P*(EN5+1.)+DZX6P*(EN6+1.)+DZX7P*(EN7+1.))GAS 2530

```



```

4)
  CPF = CPP
  C SPECIFIC HEAT AT CONSTANT PRESSURE (CP) IN BTU/LB-DEG R
    CP=CPR*.0066
  CPF = CPF*.0066
  C DENSITY (DEN) IN LB/FT**3
    DEN=22.03703*P/(Z*T)
  C **TRANSPORT PROPERTIES**
  C COLLISION CROSS SECTIONS
    S2=31.4*1.E-16*(1.+(112./T))
    SI2=(S2/3.1415927)**.5
    SI4=(1.11676-(.01490* ALOG(1.-(1.-A23) **.5))-(.23654* ALOG
      1(1.-(1.-A24)**.5))-(.11582* ALOG(1.-(1.-A25)**.5)))*1.0E-8
    S4=3.1415927*(SI4)**2
    SI24=(SI2+SI4)/2.
    S24=3.1415927*(SI24)**2
    S47=9.40*1.0E-14/TSQRT
    FI=ALOG(1.042*1.0E-7*TSQ*(P*X7) **(-.5))
    S7=8.55644*1.CE-6*(1./TSQ)*FI
    SIP4=(1.11676-(.0149*ALOG(1.-(1.-2.*A23)**.5))-(.23654*ALOG(1.-(1.
      1-2.*A24)**.5))-(.11582* ALOG(1.-(1.-2.*A25)**.5)))*1.0E-8
    SP4=3.145927*(SIP4)**2
    SIP24=(SI2+SIP4)/2.
    SP24=3.145927*SIP24**2
  C COMPONENT MOL FRACTIONS FOR INDEPENDENT REACTIONS
    F1=1.+FE1
    F2=1.2+EE2
    F3=1.+EE3
    X10D=(.2-EE1)/F1
    X20D=.3/F1
    X30D=2.*EE1/F1
    X2ND=(.8-EE2)/F2
    X3ND=.4/F2
    X4ND=2.*EE2/F2
    X4I=(1.-EE3)/F3
    X6I=EE3/F3
  GAS 2530
  GAS 2540
  GAS 2550
  GAS 2560
  GAS 2570
  GAS 2580
  GAS 2590
  GAS 2600
  GAS 2610
  GAS 2620
  GAS 2630
  GAS 2640
  GAS 2650
  GAS 2660
  GAS 2670
  GAS 2680
  GAS 2690
  GAS 2700
  GAS 2710
  GAS 2720
  GAS 2730
  GAS 2740
  GAS 2750
  GAS 2760
  GAS 2770
  GAS 2780
  GAS 2790
  GAS 2800
  GAS 2810
  GAS 2820
  GAS 2830
  GAS 2840
  GAS 2850
  GAS 2860
  GAS 2870
  GAS 2880

```

```

C MEAN FREE PATH RATIOS
SS1=S24/S2
SS2=S4/S2
SS3=S7/S2
SS4=S47/S2
FP10D=X10D+X20D*.9660918 +X30D*SS1*.8164966
FP20D=X10D*1.032796+X20D+X30D*SS1*.8528029
FP30D=X10D*1.154701*SS1+X2ND*SS1*1.128152+X30D*SS2
FP2ND=X2ND+X4ND*SS1*.8164966+X3ND*SS1*.8528029
FP3ND=X2ND*SS1*1.128152+X4ND*SS2*.9660918+X3ND*SS2
FP4ND=X2ND*SS1*1.154701+X4ND*SS2+X3ND*SS2*1.032796
FP4I=X4I*SS2+X6I*SS2
FP6I=X4I*SS2+X6I*SS3
FP7I=X4I*SS4*1.414186+X6I*SS3*1.414186+X6I*SS3
C VISCOSTITES OF THE COMPONENTS FOR THE DIFFERENT REACTIONS
V10D=1.054093*X10D*1./FP10D
V20D=.9860133*X20D*1./FP20D
V30D=.745356*X30D*1./FP30D
V2ND=.9860133*X2ND*1./FP2ND
V3ND=.745356*X3ND*1./FP3ND
V4ND=.6972167*X4ND*1./FP4ND
V4I=.6972167*X4I*1./FP4I
V6I=.6972167*X6I*1./FP6I
V7I=.4367848*1.0E-2*X6I*1./FP7I
VR0D=V10D+V20D+V30D
VRND=V2ND+V3ND+V4ND
VRI=V4I+V6I+V7I
F4=EE2/(.2-EE1+EE2)
F5=2.*EE3/(.8-EE2+2.*EE3)
VR=VR0D+(F4*(VRND-VR0D))+(F5*(VRI-VRND))
C TOTAL VISCOSITY (V) IN LB/FT-SEC
V=VR*.9841838*1.0E-6*TSQRT/(1.+A22)
C CONDUCTIVITY DUE TO MOLECULAR COLLISIONS FOR DIFFERENT REACTIONS
G1=.2105263*CV1+.4736842
G2=.2105263*CV2+.4736842
G3=.2105263*CV3+.4736842
GAS 289C
GAS 2900
GAS 2910
GAS 2920
GAS 2930
GAS 2940
GAS 2950
GAS 2960
GAS 2970
GAS 2980
GAS 2990
GAS 3000
GAS 3010
GAS 3020
GAS 3030
GAS 3040
GAS 3050
GAS 3060
GAS 3070
GAS 3080
GAS 3090
GAS 3100
GAS 3110
GAS 3120
GAS 3130
GAS 3140
GAS 3150
GAS 3160
GAS 3170
GAS 3180
GAS 3190
GAS 3200
GAS 3210
GAS 3220
GAS 3230
GAS 3240

```

```

G4=.2105363*CV4+.4736842      GAS 3250
G5=.2105363*CV6+.4736842      GAS 3260
G6=.2105363*CV7+.4736842      GAS 3270
XKNOD=(V10D*.9*G1)+(V20D*1.028571*G2)+(V30D*1.8*G3)      GAS 3280
XKNND=(V2ND*1.028571*G2)+(V3ND*1.8*G3)+(V4ND*2.057143*G4)      GAS 3290
XKNI=(V4I*2.057143*G4)+(V6I*2.057143*G5)+(V7I*52416.0*G6)      GAS 3300
XKN=XKNOD+(F4*(XKNND-XKNOD))+(F5*(XKNI-XKNND))      GAS 3310
C CONDUCTIVITY DUE TO CHEMICAL REACTIONS FOR THE DIFFERENT REACTIONS      GAS 3320
XKROD=(.178637*(T*PK1)**2)/((SP24/(1.732051*S2))*((X30D+2.*X10D)      GAS 3330
1**2)/(X30D*X10D)+(4.*X20D/X30D))+(X20D/(1.414214*X10D)))      GAS 3340
XKRND=(.178637*(T*PK2)**2)/((SP24/(1.732051*S2))*((X4ND+2.*X2ND)      GAS 3350
1**2)/(X4ND*X2ND))+(X3ND/X2ND))+(SP4*2.*X3ND/(S2*X4ND)))      GAS 3360
XKR1=(.178637*(T*PK34)**2)/((.5*SP4/S2)+(.4347826*1.0E-2*S47/S2))      GAS 3370
1*((X4I+X6I)**2)/(X4I*X6I))      GAS 3380
XKOD=XKNOD+XKROD      GAS 3390
XKNND=XKNND+XKRND      GAS 3400
XKI=XKNI+XKR1      GAS 3410
XKR=XKOD+(F4*(XKND-XKOD))+(F5*(XKI-XKND))      GAS 3420
C TOTAL THERMAL CONDUCTIVITY (XK) IN BTU/FT-SEC-DEG R      GAS 3430
XK=XKR*((.3206522*1.0E-6*TSQRT)/(1.+A22))      GAS 3440
C PRANDTL NUMBER (PR) DIMENSIONLESS      GAS 3450
PRN = .2105263 * CPR * VR / XKR      GAS 3460
IF(1.EQ. 1) PRW = PRN      GAS 3470
C FORM REQUIRED BY CALL STATEMENT      GAS 3480
C      GAS 3490
C      GAS 3500
C      ** RHO UNITS SLUGS/FT**3      GAS 3510
C      ** MU UNITS LBM/FT-SEC      GAS 3520
C      ** RM UNITS LBF**2 SEC**3/FT**6      GAS 3530
C      MU (I) = V      GAS 3540
C      RHO(I)=DEN/32.174.      GAS 3550
C      RM(I)=RHO(I)*MU(I )/32.174      GAS 3560
C      AK(I) = XK      GAS 3570
C      CPT(I) = CPF      GAS 3580
C *** CALCULATE THE MEAN MOLECULAR WT. ***      GAS 3590
C      REAL = 25050.*S *Z / SR      GAS 3600

```

```

      AMW(I)= GASC / REAL
C MASS FRACTIONS
      C(1,I) = X1      *32.CC/AMW(I)
      C(2,I) = X2      *28.CC/AMW(I)
      C(3,I) = X3      *16.CC/AMW(I)
      C(4,I) = X4      *14.CC/AMW(I)
      C(5,I) = X5      *14.CC/AMW(I)
      C(6,I) = X6      *16.CC/AMW(I)
      C(7,I) = X7      /(1820.*AMW(I))
C SPECIES ENTHALPY PER INITIAL MOLE OF AIR IN BTU/LB OF I
      HS(1,I) = (Z*X1*EN1/C(1,I) +Z)*T*.12348
      HS(2,I) = (Z*X2*EN2/C(2,I) +Z)*T*.12348
      HS(3,I) = (Z*X3*EN3/C(3,I) +Z)*T*.12348
      HS(4,I) = (Z*X4*EN4/C(4,I) +Z)*T*.12348
      HS(5,I) = (Z*X5*EN5/C(5,I) +Z)*T*.12348
      HS(6,I) = (Z*X6*EN6/C(6,I) +Z)*T*.12348
      HS(7,I) = (Z*X7*EN7/C(7,I) +Z)*T*.12348
2000 CONTINUE
      MUDZ= MU(NETA)
      RDZ= RHO(NETA)
      RMDZ= RM(NETA)
C
C
C
C
C
C
      DO 4C I=KODE,NETA
C
C
C
C
C
C
      ** NONDIMENSIONALIZE RHO AND MU **
C
      RHO(I) = RHO(I)/RDZ
      MU(I) = MU(I)/MUDZ
      RM(I) =RM(I)/RMDZ
      AK(I) = AK(I)*AKNF
      CPT(I) = CPT(I)*CPNF
C NONDIMENSIONAL SPECIES ENTHALPY
      HS(1,I) = HS(1,I)*HNF
      HS(2,I) = HS(2,I)*HNF
      HS(3,I) = HS(3,I)*HNF
      HS(4,I) = HS(4,I)*HNF
      HS(5,I) = HS(5,I)*HNF
      HS(6,I) = HS(6,I)*HNF
      HS(7,I) = HS(7,I)*HNF

```

GAS 3970
 GAS 3980
 GAS 3990
 GAS 4000
 GAS 4010
 GAS 4020
 GAS 4030
 GAS 4040
 GAS 4050
 GAS 4060

HS(4,1) = HS(4,1)*HNF
 HS(5,1) = HS(5,1)*HNF
 HS(6,1) = HS(6,1)*HNF
 HS(7,1) = HS(7,1)*HNF

C
 C

40 CONTINUE
 100 FORMAT(1X,9E14.6)
 RETURN
 END

```

SUBROUTINE EFLUX
COMMON /EPSTRM/ U INF, RINF, UINF2, R, RE, LX1, ITM, IEM, NETA
COMMON /R4/ DUD,DFHI,TD,RZB,PD,HD,HTUTAL
COMMON /RFLUX/ F(60),IRAD,ITYPE
COMMON/PROPI/PI(60),RHO(60), T(60),AMW(50),C (20,60),CC(5,60)
DIMENSION EOLD(60)
DO 100 I=1,NETA
IF(IEM.GT.1) EOLD(I) = E(I)
PL = ALOG10(PI(I) )
TSI= T(I)*TD
TS = 1100. * PL +13800.
IF (TS -TSI ) 300,200,200
200 EP = 10.**(.0005 *TSI +1.15*PL -3.15 )
GO TO 350
300 EP = 10.**((1.875 *PL + 3.903)
C **** EP HAS UNITS OF WATTS/CM**3 ***
C
350 E(I) =(EP*R/( RINF *UINF2 *U INF) ) * 20866.0
400 E(I) =E(I) *RZB
C IF(IEM.GT.1) E(I) = .6 *E(I) +.4 *EOLD(I)
C
C **** E IS NONDIMENSIONAL ***
C
100 CONTINUE
RETURN
END
EFLU 10
EFLU 20
EFLU 30
EFLU 40
EFLU 50
EFLU 60
EFLU 70
EFLU 80
EFLU 90
EFLU 100
EFLU 110
EFLU 120
EFLU 130
EFLU 140
EFLU 150
EFLU 160
EFLU 170
EFLU 180
EFLU 190
EFLU 200
EFLU 210
EFLU 220
EFLU 230
EFLU 240
EFLU 250
EFLU 260

```

```

C
C-----THIS IS A MODIFIED VERSION OF SUBROUTINE TRANS FROM K WILSON
C TRANS IS DOCUMENTED IN LMSC-687209 APRIL 69 -----
C
COMMON /ZPI/ ZPO(6), ZPN(6), ZPH(2), ZPC(7)
COMMON /FINV/ NHVL,NIHVC,FHVC(12),DJ(9),HVJ(9),ZKZ
COMMON /SFLUX/ QRI(3)
COMMON /TRN/ NUT(60), FMC(12,60), FPC(12,60),
1 FM(9,60), FP(9,60), LINES
COMMON /YL/ETA(60), YD(60)
COMMON /PROPI/P (60), R(60), T(60),AMW(50),C (20,60),EC(5,60)
COMMON /FRSTRM/ U INF, RINF, UINF2,XL , RE, LXI, ITM, IEM, NES
COMMON /DEL/ W(1),DTIL,DTILS
COMMON /NON/RDZ,MUDZ,RMDZ,AKNF,HNF,CPNF
COMMON /MAIM/KEEP,MAXE,MAXM,MAXD, IDG,MCONV,ECONV,DCONV,LT,IAB
COMMON /RFLUX/ E(60),IRAD,ITYPE
COMMON /RH/ DUD,DPHI,TD,RZB,PD,HD,HTOTAL
COMMON /WT/SMW(20),AWT(5)
COMMON /TEST/ETZ(60),IEZ
COMMON /NUMDEN/ SNDD2(60), SNDN2(60), SNDD(60), SNDN(60),
1 SNDE(60), SNDC(60),
2 SNDE(60), SNDC(60),
3 SNDE(60), SNDC(60),
COMMON /DBUG/ QLC(60), QCL(60), QLL(60), DQN(60), QCC(60),
1 BEEC(12,60), FMUC(12,60), FM(12,60),
2 EP(12,60), TAUC(12,60), BEEL(9,60),
3 QCCP(12), WMM(9,60), GMM(9,60),
4 FEM(9,60), XLMM(9,60), QLCP(9),
5 QCLP(9), QLLP(9), DELTA, IY, IYY,
6 WPP(9,60), GPP(9,60), EEP(9,60),
7 XLFF(9,60), FG(9,4), GP(9,4),
8 WN(9,4), FMUL(9,60), SSM(9,4,60),
9 GGM(9,4,60), ETAM(9,4,60), SBM(9,4,60),
A TAUL(9,60)
COMMON /SPEC/ MF, XNOL

```

```

TRAN 10
TRAN 20
TRAN 30
TRAN 40
TRAN 50
TRAN 60
TRAN 70
TRAN 80
TRAN 90
TRAN 100
TRAN 110
TRAN 120
TRAN 130
TRAN 140
TRAN 150
TRAN 160
TRAN 170
TRAN 180
TRAN 190
TRAN 200
TRAN 210
TRAN 220
TRAN 230
TRAN 240
TRAN 250
TRAN 260
TRAN 270
TRAN 280
TRAN 290
TRAN 300
TRAN 310
TRAN 320
TRAN 330
TRAN 340
TRAN 350
TRAN 360

```

```

C **      C
C **      DIMENSION  XKT(F()),      DQ(60)
C **      BAND AVERAGE ABSORPTION CROSS SECTION (EQ.A2)  **
C **
C **      SIGMA(ZH,ZA,ZB,ZG)= ((5.0E+03*T1*ZG*ZKZ)/RE) * (EXP(ZDL/T1)
1      *ZH*(ZA+ZB*(ZH**2)/3.0) +
2      T1 * (ZA+2.0*ZB*T12) -T1*EXP((ZH-ZHVP)/T1)
3      *(ZA+ZB*(ZHVP-ZH)**2) -T1*EXP((ZH-ZHVP)/T1)
4      *2.0*ZB*T1*(ZHVP-ZH+T1))
C **      SIGMA2(ZH,ZG,ZE,ZY)=7.26E-16*T1*ZG*EXP((-ZE+ZY+ZDL)/T1)/ZH**3
C **      GAMMA(ZX)=(1.0+(1.5707963*ZX)**1.25)**(-0.4)
C **      XLAMB(ZX)=(1.0+ZX*EXP(-ZX))/SORT(1.0+6.283185 *ZX)
C **
C **      W(GROUP)/D CORRELATION (EQ.88)  **
C **
C **      PHI1(ZX)=(ATAN(1.570796 *ZX)/1.570796 )
C **
C **      FLUX DIVERGENCE OVERLAPPING FUNCTION (EQ.92)  **
C **
C **      PHI2(ZX)=EXP(-ZX)
C **
C **      DO 400 I=1,NES
400  T(I)= T(I)*TD
C **      ZHVP=5.0
C **      Y1=0.0
C **      CONVER = 3.1(375E+23 *R (I) *RDZ
C **      SNDE(NES) = CONVER * C( 7,NES)/SMW(7)
C **      XNE=SNDE(NES)
C **      FNF=(4.71E-6 * XNE**((2.0/7.0))/((T(NES)/11606.)*(1.0/7.0))
C **      ZDL=AMIN1(0.20,FNF)
C **
C **      DEBUG PRINT  **
C **
C **      IF (IDG.NE.0) CALL HUGPR (1)
C **      DFLTA=W(1) * XL * 37.48**6
C **      CALL HUGPR (2)

```

TRAN 370
 TRAN 380
 TRAN 390
 TRAN 400
 TRAN 410
 TRAN 420
 TRAN 430
 TRAN 440
 TRAN 450
 TRAN 460
 TRAN 470
 TRAN 480
 TRAN 490
 TRAN 500
 TRAN 510
 TRAN 520
 TRAN 530
 TRAN 540
 TRAN 550
 TRAN 560
 TRAN 570
 TRAN 580
 TRAN 590
 TRAN 600
 TRAN 610
 TRAN 620
 TRAN 630
 TRAN 640
 TRAN 650
 TRAN 660
 TRAN 670
 TRAN 680
 TRAN 690
 TRAN 700
 TRAN 710
 TRAN 720


```

6001 CONTINUE
DO 91 L=1,NES
  XKT(L)=T(L)/11606.
  T1=XKT(L)
  CALL SND(L)
C
C ** PARTITION FUNCTIONS FOR H, C, N, O **
C
C 94 IF(T(L).GT.15000.) GO TO 6
C
C ** LOW TEMPERATURE **
C
SUMH=2.0
SUMC=9.0 + 5.0 * EXP(-1.264/T1) + EXP(-2.684/T1) +
1 5.0 * EXP(-4.183/T1)
SUMN=4.0 + 10.0 * EXP(-2.384/T1) + 6.0 * EXP(-3.576/T1)
SUMO= 9.0 + 5.0 * EXP(-1.975/T1)
GO TO 7
C
C ** HIGH TEMPERATURE **
C
6 SUMH=2.0
SUMC=2.71818 + 6.40677 * T(L)/1.0E4 -3.45466 * (T(L)/1.0E4)**2
SUMN=5.938216 - 0.225593 * T(L)/1.0E3 + 0.015408 * (T(L)/1.0E3)**2
SUMO=11.79563 -0.317964 * T(L)/1.0E3 + 0.013765 * (T(L)/1.0E3)**2
7 CONTINUE
T12=T1**2
GH = 6.4904
DO 5 K=1,12
  GF=FHVC(K)/T1
  GHM=GH
  GH=EXP(-GF) * GF * (3**2 + 3.0 *GF +6.0 + 6.0/GF)
C
C ** PLANK MEAN ABSORPTION COEFFICIENT FOR BAND INTERVALS (EQ. A3) **
C
C 95 GFEC(K,L)=5.04E3 * (T12**2) * (GHM-GH)
C

```

```

TRAN 730
TRAN 740
TRAN 750
TRAN 760
TRAN 770
TRAN 780
TRAN 790
TRAN 800
TRAN 810
TRAN 820
TRAN 830
TRAN 840
TRAN 850
TRAN 860
TRAN 870
TRAN 880
TRAN 890
TRAN 900
TRAN 910
TRAN 920
TRAN 930
TRAN 940
TRAN 950
TRAN 960
TRAN 970
TRAN 980
TRAN 990
TRAN1000
TRAN1010
TRAN1020
TRAN1030
TRAN1040
TRAN1050
TRAN1060
TRAN1070
TRAN1080

```

```

C C ** RE=REFC(K,L)
C C ** ABSORPTION CROSS SECTIONS **
C C SPECIES --
C C N N2 CO
C C O O2
C C C C2 C2H
C C H H2 C3
C C

SGH=0.
SGN=0.
SGC=0.
SGO=0.
SGCO=0.
SGC2=0.
SGO2=0.
SGN2=0.
SGH2=0.
SGC3=0.
SGC2H = 0.0
GO TO (581,582,583,584,585,586,587,588,589,590,591,592),K
581 SG1=SIGMA(2.4,1.0,0.0,1.0) * EXP(-13.56/T1)
SGC=SIGMA(3.78, 0.3, 0.0488, 1.33) * EXP(-11.26/T1)
SGN=SIGMA(4.22, 4.24, 0.0426, 4.5) * EXP(-14.54/T1)
SGO=SIGMA(4.22, 0.24, 0.0426, .8888889) * EXP(-13.61/T1)
GO TO 38
582 ZZHV=5.5
SGC2=8.0E-18 * EXP(-0.5/T1) + 3.0E-18
SGC3=4.0E-18
583 CALL ZHV(ZZHV,ZZO,ZZN,ZZI,ZZC)
SGC=SIGMA2(ZZHV, 1.33, 11.26, 3.78) * ZZC + SGC
SGN=SIGMA2 (ZZHV,4.50, 14.54, 4.22) * ZZN
SGO=SIGMA2 (ZZHV, .889, 13.61, 4.22) * ZZU
SGH=SIGMA2 (ZZHV, 1.00, 13.56, 2.40)
GO TO 38
583 ZZHV=6.5

```

TRAN1090
 TRAN1100
 TRAN1110
 TRAN1120
 TRAN1130
 TRAN1140
 TRAN1150
 TRAN1160
 TRAN1170
 TRAN1180
 TRAN1190
 TRAN1200
 TRAN1210
 TRAN1220
 TRAN1230
 TRAN1240
 TRAN1250
 TRAN1260
 TRAN1270
 TRAN1280
 TRAN1290
 TRAN1300
 TRAN1310
 TRAN1320
 TRAN1330
 TRAN1340
 TRAN1350
 TRAN1360
 TRAN1370
 TRAN1380
 TRAN1390
 TRAN1400
 TRAN1410
 TRAN1420
 TRAN1430
 TRAN1440

```

SGC2=1.0E-18
SGC0=3.0E-18 * EXP(-0.7/T1)
GO TO 593

584 ZHV=7.5
SGC=5.0E-17 * EXP(-4.18/T1)/SUMC
SGC0=1.9E-17 * EXP(-0.5/T1)
SG02=6.0E-19
SGC2H = 1.3E-18
GO TO 593

585 ZHV=8.5
SGC=5.0E-17 * EXP(-4.18/T1)/SUMC +
1 2.2E-17 * EXP(-2.68/T1)/SUMC
SGC0=2.5E-17
SG02=2.0E-19
SGC2H = 8.5E-19
GO TO 593

586 ZHV=9.5
SGC=5.0E-17 * EXP(-4.18/T1)/SUMC +
1 2.2E-17 * EXP(-2.68/T1)/SUMC
SGC0=5.0E-18
SG02=1.0E-18
GO TO 593

587 SGN=3.2E-18 *T1 *EXP(-10.2/T1)/SUMN
SG02=6.0E-19
ZZHV=10.4
CALL ZHV(ZZHV,ZZC,ZZN,ZZI,ZZC)
586 SGC=(8.5E-17 *EXP(-1.26/T1) + 2.2E-17 * EXP(-2.75/T1)
1 + 5.0E-17 * EXP(-4.18/T1))/SUMC
GO TO 594

588 ZHV=10.9
CALL ZHV(ZZHV,ZZC,ZZN,ZZI,ZZC)
SGN=(5.1E-17 *EXP(-3.5/T1))/SUMN
GO TO 596

589 ZHV=11.6
CALL ZHV(ZZHV,ZZC,ZZN,ZZI,ZZC)
SGN2=1.0E-18

```

```

TRAN1450
TRAN1460
TRAN1470
TRAN1480
TRAN1490
TRAN1500
TRAN1510
TRAN1520
TRAN1530
TRAN1540
TRAN1550
TRAN1560
TRAN1570
TRAN1580
TRAN1590
TRAN1600
TRAN1610
TRAN1620
TRAN1630
TRAN1640
TRAN1650
TRAN1660
TRAN1670
TRAN1680
TRAN1690
TRAN1700
TRAN1710
TRAN1720
TRAN1730
TRAN1740
TRAN1750
TRAN1760
TRAN1770
TRAN1780
TRAN1790
TRAN1800

```

```

TRAN181C
598 SGN=(5.16E-17 * EXP(-3.50/T1))/SUMN
SGC=(9.9E-17 + 8.5E-17 * EXP(-1.26/T1) +2.2E-17 * EXP(-2.75/T1))
1 + 5.0E-17 * EXP(-4.18/T1))/SUMC
IF (K.LT.11) GO TO 594
GO TO 38
590 ZZHV=12.7
CALL ZHV (ZZHV,ZZO,ZZN,ZZI,ZZC)
SGN2=2.0E-18
SGH2 = 2.7E-17
599 SGN=(6.4E-17 * EXP(-2.30/T1) + 5.16E-17 * EXP(-3.50/T1))/SUMN
1 + SGN
GO TO 598
591 SGH=1.18E-17/SUMH
SGO=3.6E-17/SUMO
SGN2=1.0E-17
SGH2 = 2.7E-17
GO TO 599
592 SGN=3.6E-17/SUMN
SGN2=1.0E-18
GO TO 599
38 CONTINUE
FMUC(K,L)= SNDH(L)*SGH + SNDL(L)*SGC + SNDN(L)*SGN + SNDD(L)*SGO
1 + XMOL * (SNDN2(L)*SGN2 + SNDD2(L)*SGO2 +
2 SNDC2(L)*SGC2 + SNDH2(L)*SGH2 + SNDDC(L)*SGCD +
3 SNDC3(L)*SGC3 + SNDDC2H(L)*SGC2H )
IF (L.GT.1) GO TO 8
TAUC(K,L)=0.
GO TO 5
8 TAUC(K,L)=TAUC(K,L-1)+(YD(L)-YD(L-1))*
1 (FMUC(K,L-1)+FMUC(K,L)) * DELTA
5 CONTINUE
IF (LINES.EQ.0) GO TO 91
C ** FRACTIONAL POPULATION STATES FOR H, N, O, C **
CALL ZP (T1,SUMN,SUMO,SUMH,SUMC)
TRAN182C
TRAN183C
TRAN184C
TRAN185C
TRAN186C
TRAN187C
TRAN188C
TRAN189C
TRAN190C
TRAN191C
TRAN192C
TRAN193C
TRAN194C
TRAN195C
TRAN196C
TRAN197C
TRAN198C
TRAN199C
TRAN200C
TRAN201C
TRAN202C
TRAN203C
TRAN204C
TRAN205C
TRAN206C
TRAN207C
TRAN208C
TRAN209C
TRAN210C
TRAN211C
TRAN212C
TRAN213C
TRAN214C
TRAN215C
TRAN216C

```

```

C **      CALCULATION OF PARAMETERS FOR 9 LINE GROUPES      **
C      WN -- NUMBER OF LINES
C      FG -- EFFECTIVE F-NUMBER
C      GP -- EFFECTIVE HALF-WIDTH
C
C GROUP 1
  FG(1,2)=(1.02 * ZPC(5) + .795 * ZPC(6) + 0.114 * ZPC(7))
  1 /WN(1,2)
  GP(1,2)=(8.16E-11 * SQR(ZPC(5)) + 1.25E-10 * SQR(ZPC(6))
  1 +2.55E-10 * SQR(ZPC(7)))**2 / (FG(1,2)* WN(1,2)**2)
  FG(1,3)=(1.040 * ZPN(4) + 1.29 * ZPN(5) + 0.00 * ZPN(6))
  1 /WN(1,3)
  GP(1,3)=(6.65E-11 * SQR(ZPN(4)) + 1.71E-10 * SQR(ZPN(5))
  1 + 0.00E-10 * SQR(ZPN(6)))**2 / (FG(1,3) * WN(1,3)**2)
  FG(1,4)=(1.00 * ZPO(5) + .978 * ZPO(6)) / WN(1,4)
  GP(1,4)=(3.90E-11 * SQR(ZPO(5)) + 9.58E-11 * SQR(ZPO(6)))**2
  1 / (FG(1,4) * WN(1,4)**2)
  FMUL(1,L)=FMUC(1,L)
C GROUP 2
  FG(2,1)=0.805 * ZPH(2) / WN(2,1)
  GP(2,1)=2.37E-10 * 2.37E-10 * ZPH(2) / (FG(2,1) * WN(2,1)**2)
  FG(2,2)=(0.00E-2 * ZPC(5) + 6.71E-2 * ZPC(6)) / WN(2,2)
  GP(2,2)=(0.00E-12 * SQR(ZPC(5)) + 7.15E-11 * SQR(ZPC(6)))**2
  1 / (FG(2,2) * WN(2,2)**2)
  FG(2,3)=(0.047 * ZPN(4) + 2.85E-2 * ZPN(5)) / WN(2,3)
  GP(2,3)=(1.11E-10 * SQR(ZPN(4)) + 6.37E-11 * SQR(ZPN(5)))**2
  1 / (FG(2,3) * WN(2,3)**2)
  FG(2,4)=(0.0217 * ZPO(4) + 8.25E-2 * ZPO(5)) / WN(2,4)
  GP(2,4)=(2.61E-11 * SQR(ZPO(4)) + 7.19E-11 * SQR(ZPO(5)))**2
  1 / (FG(2,4) * WN(2,4)**2)
  FMUL(2,L)=FMUC(1,L)
C GROUP 3
  FG(3,2)=(7.29E-2 * ZPC(2) + 6.76E-2 * ZPC(3)) / WN(3,2)
  GP(3,2)=(9.08E-12 * SQR(ZPC(2)) + 8.75E-12 * SQR(ZPC(3)))**2
  1 / (FG(3,2) * WN(3,2)**2)
  FMUL(3,L)=FMUC(2,L)

```

TRAN2170
 TRAN2180
 TRAN2190
 TRAN2200
 TRAN2210
 TRAN2220
 TRAN2230
 TRAN2240
 TRAN2250
 TRAN2260
 TRAN2270
 TRAN2280
 TRAN2290
 TRAN2300
 TRAN2310
 TRAN2320
 TRAN2330
 TRAN2340
 TRAN2350
 TRAN2360
 TRAN2370
 TRAN2380
 TRAN2390
 TRAN2400
 TRAN2410
 TRAN2420
 TRAN2430
 TRAN2440
 TRAN2450
 TRAN2460
 TRAN2470
 TRAN2480
 TRAN2490
 TRAN2500
 TRAN2510
 TRAN2520

```

C GROUP 4
  FG(4,2)=(1.05 * ZPC(1) + 1.10E-2 * ZPC(2) + 0.150 * ZPC(3))
  1 /WN(4,2)
  GP(4,2)=(9.57E-12 * SQR(ZPC(1)) + 4.86E-12 * SQR(ZPC(2))
  1 + 5.93E-10 * SQR(ZPC(3)))**2/(FG(4,2) * WN(4,2))**2
  FG(4,3)=( 7.40E-2 * ZPN(2) + 6.34E-2 * ZPN(3))/WN(4,3)
  GP(4,3)=(8.22E-12 * SQR(ZPN(2)) + 7.50E-12 * SQR(ZPN(3)))**2
  1 /((FG(4,3) * WN(4,3))**2)
  FMUL(4,L)=FMUC(4,L)
C GROUP 5
  FG(5,2)=(0.329 * ZPC(1) + 0.118 * ZPC(2) + 0.226 * ZPC(4))
  1 /WN(5,2)
  GP(5,2)=(3.65E-11 * SQR(ZPC(1)) + 5.77E-10 * SQR(ZPC(2))
  1 + 6.56E-11 * SQR(ZPC(4)))**2/(FG(5,2) * WN(5,2))**2
  FG(5,3)=0.108 * ZPN(3)/WN(5,3)
  GP(5,3)=3.09E-11 * 3.09E-11 * ZPN(3)/(FG(5,3) * WN(5,3))**2
  FG(5,4)=4.71E-2 * ZPO(1)/WN(5,4)
  GP(5,4)=5.08E-12 * 5.08E-12 * ZPO(1)/(FG(5,4) * WN(5,4))**2
  FMUL(5,L)=FMUC(6,L)
C GROUP 6
  FG(6,1)=0.416 * ZPH(1)/WN(6,1)
  GP(6,1)=3.02E-11 * 3.02E-11 * ZPH(1)/(FG(6,1) * WN(6,1))**2
  FG(6,2)=8.65E-2 * ZPC(1)/WN(6,2)
  GP(6,2)=2.35E-10 * 2.35E-10 * ZPC(1)/(FG(6,2) * WN(6,2))**2
  FG(6,3)=(0.184 * ZPN(1) + 0.290 * ZPN(2) + 8.52E-2 * ZPN(3))
  1 /WN(6,3)
  GP(6,3)=(1.07E-11 * SQR(ZPN(1)) + 4.28E-11 * SQR(ZPN(2))
  1 + 2.09E-10 * SQR(ZPN(3)))**2/(FG(6,3) * WN(6,3))**2
  FG(6,4)=(0.120 * ZPO(2) + 0.151 * ZPO(3))/WN(6,4)
  GP(6,4)=(8.85E-12 * SQR(ZPO(2)) + 9.93E-12 * SQR(ZPO(3)))**2
  1 /((FG(6,4) * WN(6,4))**2)
  FMUL(6,L)=FMUC(7,L)
C GROUP 7
  FG(7,2)=(4.51E-2 * ZPC(1) + 0.705 * ZPC(2))/WN(7,2)
  GP(7,2)=(5.07E-10 * SQR(ZPC(1)) + 2.10E-10 * SQR(ZPC(2)))**2
  1 /((FG(7,2) * WN(7,2))**2)

```

TRAN2530
 TRAN2540
 TRAN2550
 TRAN2560
 TRAN2570
 TRAN2580
 TRAN2590
 TRAN2600
 TRAN2610
 TRAN2620
 TRAN2630
 TRAN2640
 TRAN2650
 TRAN2660
 TRAN2670
 TRAN2680
 TRAN2690
 TRAN2700
 TRAN2710
 TRAN2720
 TRAN2730
 TRAN2740
 TRAN2750
 TRAN2760
 TRAN2770
 TRAN2780
 TRAN2790
 TRAN2800
 TRAN2810
 TRAN2820
 TRAN2830
 TRAN2840
 TRAN2850
 TRAN2860
 TRAN2870
 TRAN2880

```

TRAN2890
TRAN2900
TRAN2910
TRAN2920
TRAN2930
TRAN2940
TRAN2950
TRAN2960
TRAN2970
TRAN2980
TRAN2990
TRAN3000
TRAN3010
TRAN3020
TRAN3030
TRAN3040
TRAN3050
TRAN3060
TRAN3070
TRAN3080
TRAN3090
TRAN3100
TRAN3110
TRAN3120
TRAN3130
TRAN3140
TRAN3150
TRAN3160
TRAN3170
TRAN3180
TRAN3190
TRAN3200
TRAN3210
TRAN3220
TRAN3230
TRAN3240

      FG(7,3)=(0.454 * ZPN(1) + 9.66E-2 * ZPN(2)
1      + 0.173 * ZPN(3))/WN(7,3)
      GP(7,3)=(2.71E-12 * Sqrt(ZPN(1)) + 2.34E-10 * Sqrt(ZPN(2))
1      + 2.46E-11 * Sqrt(ZPN(3)))**2/(FG(7,3) * WN(7,3)**2)
      FG(7,4)=4.23E-2 * ZPO(3)/WN(7,4)
      GP(7,4)=2.52E-11 * 2.52E-11 * ZPO(3)/(FG(7,4) * WN(7,4)**2)
      FMUL(7,L)=FMUC(9,L)

C      GROUP 8
      FG(8,1)=0.108 * ZPH(1)/WN(8,1)
      GP(8,1)=1.32E-10 * 1.32E-10 * ZPH(1)
1      /(FG(8,1) * WN(8,1)**2)
      FG(8,2)=(0.379 * ZPC(1) + 1.05 * ZPC(3))/WN(8,2)
      GP(8,2)=(1.95E-11 * Sqrt(ZPC(1)) + 1.27E-10 * Sqrt(ZPC(3)))**2
1      /(FG(8,2) * WN(8,2)**2)
      FG(8,3)=(0.155 * ZPN(1) + 0.142*ZPN(2) + 3.75E-2 * ZPN(3))
1      /WN(8,3)
      GP(8,3)=(2.98E-11 * Sqrt(ZPN(1)) + 7.08E-11 * Sqrt(ZPN(2))
1      + 1.33E-10 * Sqrt(ZPN(3)))**2/(FG(8,3) * WN(8,3)**2)
      FG(8,4)=(0.146 * ZPO(1) + 8.61E-2*ZPO(2)
1      + 9.33E-2 * ZPO(3))/WN(8,4)
      GP(8,4)=(1.97E-10 * Sqrt(ZPO(1)) + 1.80E-11 * Sqrt(ZPO(2))
1      + 8.13E-11 * Sqrt(ZPO(3)))**2/(FG(8,4) * WN(8,4)**2)
      FMUL(8,L)=FMUC(10,L)

C      GROUP 9
      FG(9,2)=2.95 * ZPC(2)/WN(9,2)
      GP(9,2)=5.85E-12 * 5.85E-12 * ZPC(2)/(FG(9,2) * WN(9,2)**2)
      FG(9,3)=(0.224 * ZPN(1) + 2.92E-2 * ZPN(2))/WN(9,3)
      GP(9,3)=(3.41E-10 * Sqrt(ZPN(1)) + 1.48E-10 * Sqrt(ZPN(2)))**2
1      /(FG(9,3) * WN(9,3)**2)
      FG(9,4)=(5.24E-2 * ZPO(1) + 7.22E-2 * ZPO(2)
1      + 6.74E-2 * ZPO(3))/WN(9,4)
      GP(9,4)=(5.76E-12 * Sqrt(ZPO(1)) + 7.20E-11 * Sqrt(ZPO(2))
1      + 8.05E-11 * Sqrt(ZPO(3)))**2/(FG(9,4) * WN(9,4)**2)
      FMUL(9,L)=FMUC(11,L)

C
C      ** PLANCK FUNCTION **

```

```

C
DO 9 J=1,NHVL
  BEEL(J,L)=S.04F3 * HVJ(J)**3 / (EXP(HVJ(J)/T1) - 1.0)
C
C ** INDUCED EMISSION FACTOR (EQ 81) **
C
SSM(J,1,L)=1.10E-16*SNDH (L)*(1.0-EXP(-HVJ(J)/T1)) * FG(J,1)
SSM(J,2,L)=1.10E-16*SNDH (L)*(1.0-EXP(-HVJ(J)/T1)) * FG(J,2)
SSM(J,3,L)=1.10E-16*SNDH (L)*(1.0-EXP(-HVJ(J)/T1)) * FG(J,3)
SSM(J,4,L)=1.10E-16*SNDH (L)*(1.0-EXP(-HVJ(J)/T1)) * FG(J,4)
DO 10 M=1,4
  GGM(J,M,L)=GP(J,M) * SNDE(L) * (T(L)/1.0E4)**0.25
  1 + 1.0E-6
  IF(L.GT.1) GO TO 11
  ETAM(J,M,1)=0.
  SBM (J,M,1)=0.
  GO TO 10
11 ETAM(J,M,L)=ETAM(J,M,L-1)+ (YD(L)-YD(L-1))
  1 * (SSM(J,M,L-1) * GGM(J,M,L-1) + SSM(J,M,L) * GGM(J,M,L))
  2 * DELTA/3.14159265
  SBM(J,M,L)=SBM(J,M,L-1) + (YD(L)-YD(L-1))
  1 * (SSM(J,M,L-1)+SSM(J,M,L)) * DELTA
10 CONTINUE
  IF (L.GT.1) GO TO 12
  TAUL(J,1)=0.
  GO TO 9
12 TAUL(J,L)=TAUL(J,L-1) + (YD(L)-YD(L-1))
  1 * (FMUL(J,L-1)+FMUL(J,L)) * DELTA
  2 CONTINUE
  IF (IDG.NE.99) GO TO 91
  CALL RUGPR (7)
C
91 CONTINUE
  IF Z=16Z+1
  1Z(16Z)=1.0
C

```

TRAN3250

TRAN3260

TRAN3270

TRAN3280

TRAN3290

TRAN3300

TRAN3310

TRAN3320

TRAN3330

TRAN3340

TRAN3350

TRAN3360

TRAN3370

TRAN3380

TRAN3390

TRAN3400

TRAN3410

TRAN3420

TRAN3430

TRAN3440

TRAN3450

TRAN3460

TRAN3470

TRAN3480

TRAN3490

TRAN3500

TRAN3510

TRAN3520

TRAN3530

TRAN3540

TRAN3550

TRAN3560

TRAN3570

TRAN3580

TRAN3590

TRAN3600


```

C **      CONTINUUM - CONTINUUM FLUX DIVERGENCE CALCULATION **
C
      DO 300 K=1,IEZ
      DO 31 LK=1,NES
      I=LK
      NUT(K)=I
      IF (ABS(ETZ(K)-ETA(LK)) - 1.0E-5) 300,300,31
      31 CONTINUE
      300 CONTINUE
      DO 1612 J=1,9
      QCLP(J)=0.
      QLCP(J)=0.
      QLLP(J)=0.
      DO 1612 L=1,NES
      FM(J,L)=0.
      1612 FP(J,L)=0.
      DO 1613 L=1,IEZ
      QCL(L)=0.
      QLC(L)=0.
      1613 QLL(L)=0.
      DO 49 IYY=1,IEZ
      IY=NUT(IYY)
      DO 20 K=1,12
      FMC(K,IY)=0.
      FPC(K,IY)=0.
      IF (IY.EQ.1) GO TO 44
      DO 43 L=1,IY
      C **      MINUS EMISSIVITY FUNCTION (EQ 47) *
      C
      EM(K,L)=1.0 - EXP(TAUC(K,L)-TAUC(K,IY))
      IF (L.EQ.1) GO TO 40
      C **      MINUS CONTINUUM FLUX (EQ 46) **
      C
      FMC(K,IY)=FMC(K,IY) - (EM(K,L)-EM(K,L-1))
      C
      TRAN3610
      TRAN3620
      TRAN3630
      TRAN3640
      TRAN3650
      TRAN3660
      TRAN3670
      TRAN3680
      TRAN3690
      TRAN3700
      TRAN3710
      TRAN3720
      TRAN3730
      TRAN3740
      TRAN3750
      TRAN3760
      TRAN3770
      TRAN3780
      TRAN3790
      TRAN3800
      TRAN3810
      TRAN3820
      TRAN3830
      TRAN3840
      TRAN3850
      TRAN3860
      TRAN3870
      TRAN3880
      TRAN3890
      TRAN3900
      TRAN3910
      TRAN3920
      TRAN3930
      TRAN3940
      TRAN3950
      TRAN3960

```

```

TRAN3970
TRAN3980
TRAN3990
TRAN4000
TRAN4010
TRAN4020
TRAN4030
TRAN4040
TRAN4050
TRAN4060
TRAN4070
TRAN4080
TRAN4090
TRAN4100
TRAN4110
TRAN4120
TRAN4130
TRAN4140
TRAN4150
TRAN4160
TRAN4170
TRAN4180
TRAN4190
TRAN4200
TRAN4210
TRAN4220
TRAN4230
TRAN4240
TRAN4250
TRAN4260
TRAN4270
TRAN4280
TRAN4290
TRAN4300
TRAN4310
TRAN4320

1      * (BEEC(K,L-1))+BEEC(K,L))/2.
40 CONTINUE
44 IF (IY.EQ.NES ) GO TO 41
DO 42 L=IY,NES
C
C ** POSITIVE EMISSIVITY FUNCTION (EQ 47) **
C
EP(K,L)=1.0 - EXP(TAUC(K,IY)-TAUC(K,L))
IF (L.EQ.IY) GO TO 42
C
C ** POSITIVE EMISSIVITY CONTINUUM FLUX (EQ 46) **
C
FPC(K,IY)=FPC(K,IY) + (EP(K,L)-EP(K,L-1))
1      * (BEEC(K,L-1))+BEEC(K,L))/2.
42 CONTINUE
C
C ** POSITIVE EMISSIVITY CONTINUUM FLUX DIVERGENCE (EQ 51) **
C
41 QCCP(K)=6.2831853 * FMUC(K,IY) *
1      (FMC(K,IY) + FPC(K,IY) - 2.0 * BEEC(K,IY))
FMC(K,IY)=FMC(K,IY) * 3.14159265
FPC(K,IY)=FPC(K,IY) * 3.14159265
20 CONTINUE
C
C ** DEBUG PRINT **
C
IF (IDG.NE.99) GO TO 21
CALL BUGPR (3)
21 QCC(IY)=0.
DO 24 K=1,12
C
C ** LINE AND CROSS TERM FLUX DIVERGENCE CALCULATION **
C
24 QCC(IY)=QCC(IY) + QCCP(K)
IF (LINES.EQ.0) GO TO 1014
C

```

```

C **      INTEGRATION FROM 1 TO IY **
C
IF (IY.EQ.1) GO TO 68
DO 65 J=1,9
DO 66 L=1,IY
WIM=0.
SUM1=0.
SUM2=0.
DO 67 M=1,4
DIF=ETAM(J,M,IY) - ETAM(J,M,L)
DIFSBM = SBM(J,M,IY)-SBM(J,M,L)
IF (ABS(DIFSBM).LT.1.E-10) DIFSBM = 1.E-10
BETAM=DIF / ( DIFSBM ) * 3.14159265
IF (L.EQ.IY) BETAM=GGM(J,M,L)
IF (ABS(DIF).GT.1.E-10) GO TO 9001
TM = 1.E-10
GO TO 9002
9001 CONTINUE
TM=DIF/2.0/BETAM**2
9002 RRM=DIF/2.0/GGM(J,M,IY)**2
WWM=6.2831853 * WN(J,M) * BETAM * GAMMA(TM) * TM
SUM1=SUM1 + GAMMA(TM) * WN(J,M) * SSM(J,M,IY)
SUM2=SUM2 + XLAMB(RRM) * WN(J,M) * SSM(J,M,IY)
67 WIM=WIM + WWM
ALPHAM=WIM/DJ(J)
C **      OVERLAPPING LINE CALCULATIONS **
C
C **      GROUP EQUIVALENT WIDTHS (EQ.88) **
C
WWM(J,L)=DJ(J) * PHI1(ALPHAM) * EXP(TAUL(J,L)-TAUL(J,IY))
C
C **      GROUP GAMMA -- LINE TRANSPORT FUNCTION (EQ.92) **
C
GWM(J,L)=PHI2(ALPHAM) * SUM1

```

TRAN4339
 TRAN4340
 TRAN4350
 TRAN4360
 TRAN4370
 TRAN4380
 TRAN4390
 TRAN4400
 TRAN4410
 TRAN4420
 TRAN4430
 TRAN4440
 TRAN4450
 TRAN4460
 TRAN4470
 TRAN4480
 TRAN4490
 TRAN4500
 TRAN4510
 TRAN4520
 TRAN4530
 TRAN4540
 TRAN4550
 TRAN4560
 TRAN4570
 TRAN4580
 TRAN4590
 TRAN4600
 TRAN4610
 TRAN4620
 TRAN4630
 TRAN4640
 TRAN4650
 TRAN4660
 TRAN4670
 TRAN4680

```
C C C ** MINUS EMISSIVITY FUNCTION FOR LINES (EQ.47) **
C C C
TRAN4690
TRAN4700
TRAN4710
TRAN4720
TRAN4730
TRAN4740
TRAN4750
TRAN4760
TRAN4770
TRAN4780
TRAN4790
TRAN4800
TRAN4810
TRAN4820
TRAN4830
TRAN4840
TRAN4850
TRAN4860
TRAN4870
TRAN4880
TRAN4890
TRAN4900
TRAN4910
TRAN4920
TRAN4930
TRAN4940
TRAN4950
TRAN4960
TRAN4970
TRAN4980
TRAN4990
TRAN5000
TRAN5010
TRAN5020
TRAN5030
TRAN5040
C C C
EEM(J,L)=1.0 - EXP(TAUL(J,L)-TAUL(J,IY))
66 XLMM(J,L)=PHI2(ALPHAM) * SUM2
65 CONTINUE
IF (IDG.EQ.99) CALL BUGPR(1)
IF (IDG.EQ.99) CALL BUGPR (4)
68 IF (IY.EQ.NES) GO TO 72
C C C ** INTEGRATION FROM IY TO NES **
C C C
DO 69 J=1,9
DO 70 L=IY,NES
WIP=0.
SUM1=0.
SUM2=0.
DO 71 M=1,4
DIF=ETAM(J,M,L) - ETAM(J,M,IY)
DIFSBM = SBM(J,M,L)-SBM(J,M,IY)
IF(ABS(DIFSBM).LT.1.E-10) DIFSBM = 1.E-10
BETAP=DIF / ( DIFSBM ) * 3.14159265
IF (L.EQ.IY) BETAP=GGM(J,M,L)
IF(ABS(DIF).GT.1.E-10) GO TO 90C3
TP = 1.E-10
GO TO 90C4
90C3 CONTINUE
TP=DIF/2./BETAP**2
90C4 RRP=DIF/2.0/GGM(J,M,IY)**2
WWP=6.2831853 * WN(J,M) * RETAP * GAMMA(TP) * TP
SUM1=SUM1 + GAMMA(TP) * WN(J,M) * SSM(J,M,IY)
SUM2=SUM2 + XLAMB(RRP) * WN(J,M) * SSM(J,M,IY)
71 WIP=WIP+WWP
ALPHAF=WIP/DJ(J)
WPP(J,L)=DJ(J) * PHI1(ALPHAF) * EXP(TAUL(J,IY)-TAUL(J,-))
GPP(J,L)=PHI2(ALPHAF) * SUM1
```

```

C ** POSITIVE EMISSIVITY FUNCTION FOR LINES (EQ.47) **
C
C
      EEP(J,L)=1.0 - EXP(TAUL(J,IY)-TAUL(J,L))
70 XLPP(J,L)=PHI2(ALPHAP) * SUM2
69 CONTINUE
C
C ** DEBUG PRINT **
C   IF (IDG.EQ.99) CALL BUGPR (5)
C
72 DO 80 J=1,9
   ASM1=0.
   ASM2=0.
   FM(J,IY)=0.
   IF (IY.EQ.1) GO TO 81
   DO 82 L=2,IY
   FM(J,IY)=FM(J,IY) - (WMM(J,L)-WMM(J,L-1))
1   * (BEEL(J,L-1)+BEEL(J,L)) * 1.5707963
   IF (L.EQ.IY) GO TO 82
   ASM1=ASM1 - (EEM(J,L)-EEM(J,L-1))
1   * (BEEL(J,L-1) * XLMM(J,L-1) + BEEL(J,L) * XLMM(J,-1))/2.
   ASM2=ASM2 - (XLMM(J,L)-XLMM(J,L-1))
1   * (BEEL(J,L-1) * EXP(TAUL(J,L-1)-TAUL(J,IY)) + BEEL(J,L)
2   * EXP(TAUL(J,L)-TAUL(J,IY)))/2.
82 CONTINUE
81 ASP1=0.
   ASP2=0.
   IYP=IY+1
   IF (IY.EQ.NES) GO TO 83
   DO 84 L=IYP,NES
   FP(J,IY)=FP(J,IY) + (WPP(J,L)-WPP(J,L-1))
1   * (BEEL(J,L-1)+BEEL(J,L)) * 1.5707963
   IF (L.EQ.IYP) GO TO 84
   ASP1=ASP1 + (EEP(J,L)-EEP(J,L-1))
1   * (BEEL(J,L-1) * XLPP(J,L-1) + BEEL(J,L) * XLPP(J,L))/2.
   ASP2=ASP2 + (XLPP(J,L)-XLPP(J,L-1)) *

```

TRAN5050
TRAN5060
TRAN5070
TRAN5080
TRAN5090
TRAN5100
TRAN5110
TRAN5120
TRAN5130
TRAN5140
TRAN5150
TRAN5160
TRAN5170
TRAN5180
TRAN5190
TRAN5200
TRAN5210
TRAN5220
TRAN5230
TRAN5240
TRAN5250
TRAN5260
TRAN5270
TRAN5280
TRAN5290
TRAN5300
TRAN5310
TRAN5320
TRAN5330
TRAN5340
TRAN5350
TRAN5360
TRAN5370
TRAN5380
TRAN5390
TRAN5400

```

1      (BEEL(J,L-1) * EXP(TAUL(J,IY)-TAUL(J,L-1)) + BEEL(J,L)
2      * EXP(TAUL(J,IY)-TAUL(J,L)))/2.0
84 CONTINUE
83 QCLP(J)=2.0 * FMUL(J,IY) * (FM(J,IY)+FP(J,IY))
SUMS=1.0
SUMT=0.
DO 86 M=1.4
86 SUMT=SUMT + SSM(J,M,IY) * WN(J,M)
ATM1=0.
IF (IY.NE.1) ATM1=(BEEL(J,IY-1)+BEEL(J,IY))/2.0 * EEM(J,IY-1)
1      * XLMM(J,IY-1)
ATP1=0.
IF (IY.NE.NES) ATP1=(BEEL(J,IY+1)+BEEL(J,IY))/2.0 * EEP(J,IY+1)
1      * XLPP(J,IY+1)
QCLP(J)=6.2831853 * SUMS * (ASM1+ASPI+ATM1+ATP1)
IF (IY.EQ.1) ATM2=-BEEL(J,IY) * SUMT
IF (IY.NE.1) ATM2=(BEEL(J,IY-1)-BEEL(J,IY)) * GMM(J,IY-1)
1      - BEEL(J,IY-1) * XLMM(J,IY-1)
IF (IY.EQ.NES) ATP2=-BEEL(J,IY) * SUMT
IF (IY.NE.NES) ATP2=(BEEL(J,IY+1)-BEEL(J,IY)) * GPP(J,IY+1)
1      - BEEL(J,IY+1) * XLPP(J,IY+1)
QLLP(J)=6.2831853 * SUMS*(-ASM2-ASP2+ATM2+ATP2)
80 CONTINUE
QCL(IY)=0.
QLC(IY)=0.
QLL(IY)=0.
DO 85 J=1.9
QCL(IY)=QCL(IY) + QCLP(J)
QLC(IY)=QLC(IY) + QCLP(J)
QLL(IY)=QLL(IY) + QLLP(J)
85 CONTINUE
1014 QGN(IY)=-((QCC(IY)+QCL(IY)+QLC(IY)+QLL(IY))
C
C **      DEBUG PRINT **
C
C      IF (IDG.EQ.0) GO TO 40

```

TRANS410
 TRANS420
 TRANS430
 TRANS440
 TRANS450
 TRANS460
 TRANS470
 TRANS480
 TRANS490
 TRANS500
 TRANS510
 TRANS520
 TRANS530
 TRANS540
 TRANS550
 TRANS560
 TRANS570
 TRANS580
 TRANS590
 TRANS600
 TRANS610
 TRANS620
 TRANS630
 TRANS640
 TRANS650
 TRANS660
 TRANS670
 TRANS680
 TRANS690
 TRANS700
 TRANS710
 TRANS720
 TRANS730
 TRANS740
 TRANS750
 TRANS760

```

CALL BUGPR(6)
49 CONTINUE
  IEZ=IEZ-1
  DQ(1)=DQN(1)
  L=2
  DO 1 N=2,NES
    DO 2 I=2,IEZ
      NP=I
      IF (ETZ(I).GT.ETA(N)) GO TO 3
2 CONTINUE
3 NN=NP-1
  AA=0.0
  ZB=(DQN(NN)-DQN(NP)) / (ETZ(NN)-ETZ(NP))
  CC=DQN(NN) - ZB * ETZ(NN)
  DQ(N)=AA * ETA(N)**2 + ZB * ETA(N) + CC
  GO TO 1
4 DQ(N)=DQN(NN)
1 CONTINUE
C
C ** NON-DIMENSIONALIZE E(I) **
DO 250 I=1,NES
  T(I) = T(I)/TD
250 E(I) = ((DQ(I)*XL) / (RINF*UINF**3)) * 20.866 * C * RZB
      RETURN
      END

```

TRAN5770
 TRAN5780
 TRAN5790
 TRAN5800
 TRAN5810
 TRAN5820
 TRAN5830
 TRAN5840
 TRAN5850
 TRAN5860
 TRAN5870
 TRAN5880
 TRAN5890
 TRAN5900
 TRAN5910
 TRAN5920
 TRAN5930
 TRAN5940
 TRAN5950
 TRAN5960
 TRAN5970
 TRAN5980
 TRAN5990
 TRAN6000
 TRAN6010

```

SUBROUTINE SND(I)
COMMON/PROPI/PI(60),RHO(60),T(60),AMW(50),C(20,60),EC(5,60)
COMMON /R=LUX/ E(60),IRAD,ITYPE
COMMON /NON/RDZ,MUDZ,RMDZ,AKNF,HNF,CPNF
COMMON/WT/SMW(20),AWT(5)
COMMON /NUMDEN/ SNO2(60), SOND2(60), SNO2(60), SOND(60),
1          SNDE(60), SOND(60),
2          SNDC2(60), SOND2H(60)
3          SOND3(60),SONDC2H(60)
** CALCULATE SPECIE NUMBER DENSITIES BASED ON MOLE FRACTIONS **
CONVER = 3.10375E+23 *RHO(I) *RDZ

SNO2(I) = CONVER * C( 1,I)/SMW( 1)
SOND2(I) = CONVER * C( 2,I)/SMW( 2)
SNO( I) = CONVER * C( 3,I)/SMW( 3)
SON( I) = CONVER * C( 4,I)/SMW( 4)
SNDE (I) = CONVER * C( 7,I)/SMW( 7)
SNDC (I) = CONVER * C( 8,I)/SMW( 8)
SONH (I) = CONVER * C( 9,I)/SMW( 9)
SONDH2(I) = CONVER * C(10,I)/SMW(10)
SONDCO(I) = CONVER * C(11,I)/SMW(11)
SONDC3(I) = CONVER * C(12,I)/SMW(12)
SONDC2(I) = CONVER * C(19,I)/SMW(19)
SONDC2H(I)= CONVER * C(14,I)/SMW(14)
RETURN
END

```

C
C
C

SND(10
SND(20
SND(30
SND(40
SND(50
SND(60
SND(70
SND(80
SND(90
SND(100
SND(110
SND(120
SND(130
SND(140
SND(150
SND(160
SND(170
SND(180
SND(190
SND(200
SND(210
SND(220
SND(230
SND(240
SND(250
SND(260
SND(270


```

SUBROUTINE LRAD
** THIS IS A DRIVER PROGRAM FOR SUBROUTINE TRANS WHICH CALCULATES **LRAD 10
THE RADIATIVE FLUX DIVERGENCE THROUGH A ONE-DIMENSIONAL SLAB LRAD 20
FOR A GIVEN TEMPERATURE AND SPECIES DISTRIBUTION LRAD 30
COMMON /SFLUX/ QRI(3) LRAD 40
COMMON /TRN/ NUT(60), FMC(12,60), FPC(12,60), LRAD 50
COMMON /FM(9,60), FP(9,60), LINES LRAD 60
COMMON /TEST/ETZ(60), IEZ LRAD 70
COMMON /YL/ETA(60), YOND(60) LRAD 80
COMMON /PROPI/PI(60), RHO(60), T(60), AMW(60), C(20,60), EC(5,60) LRAD 90
COMMON /FRSTRM/ U INF, RINF, UINF2, R, RE, LXI, ITM, IEM, NETA LRAD 100
COMMON /DEL/ DELTA, DTIL, DTILS LRAD 110
COMMON /NON/RDZ, MUDZ, RMDZ, AKNF, HNF, CPNF LRAD 120
COMMON /MAIM/KEEP, MAXE, MAXM, MAXD, IDG, MCONV, ECONV, DCONV, LT, IAB LRAD 130
COMMON /RFLUX/ E(60), IRAD, ITYPE LRAD 140
COMMON /NUMDEN/ SNDQ2(60), SNDN2(60), SNDQ(60), SNDN(60), SDC(60), LRAD 150
COMMON /SNDH(60), SDC2(60), SDC2H(60), SDC3(60), SDC3H(60) LRAD 160
COMMON /SPEC/ MF, XMOL LRAD 170
** NETA = NUMBER OF ETA POINTS LRAD 180
MF = 1 IF SPECIE MOLE FRACTIONS ARE INPUT AND NUMBER DENSITY LRAD 190
TO BE COMPUTED LRAD 200
NS = 1 IF SPECIE NUMBER DENSITIES ARE INPUT LRAD 210
LINES= 1 IF LINE CALCULATION IS TO BE DONE LRAD 220
IDG = 1 IF ONLY CONTINUUM CALCULATION IS TO BE DONE LRAD 230
1 PRINT IS GIVEN FOR EACH ETA LRAD 240
99 COMPLETE PRINT LRAD 250
LRAD 260
LRAD 270
LRAD 280
LRAD 290
LRAD 300
LRAD 310
LRAD 320
LRAD 330
LRAD 340
LRAD 350
LRAD 360

```

```

C **      R      = BODY RADIUS (FT)
C      DELTA = NONDIMENSIONAL STAND-OFF DISTANCE
C      DTIL  = TRANSFORMED STAND-OFF DISTANCE
C      XMOL  = 1.0 FOR RUN WITH MOLECULES
C           0.0 FOR RUN WITHOUT MOLECULES
C
C      XMOL = 0.0
C      XMOL = 1.0
C
C      ** DETERMINE ETZ POINTS
C      N2 = NETA-2
C      K = 0
C      IEZ = 0
C      DO 20 I=1,N2.2
C      K=K+1
C      ETZ(K) = ETA(I)
C      ETZ(K+1) = ETA(NEGA-1)
C      ETZ(K+2) = ETA(NEGA)
C      IEZ = K + 1
C
C      ** COMPUTE THE Y COORDINATE **
C      YOND(1) = 0.0
C      SUM = 0.0
C      DO 30 K=2,NEGA
C      DELTA = ETA(K) -ETA(K-1)
C      SUM = SUM +DELTA*(1./RHO(K) +1./RHO(K-1) )/2.0
C      YOND(K) = DTIL *SUM
C      CONTINUE
C      DELTA = YOND(NEGA)
C      DO 40 K=1,NEGA
C      YOND(K) = YOND(K)/YOND(NEGA)
C      CONTINUE
C
C      LINES= 1
C      IDG3 = IDG
C      IDG = 0

```

LRAD 370
 -RAD 380
 LRAD 390
 LRAD 400
 LRAD 410
 LRAD 420
 LRAD 430
 LRAD 440
 LRAD 450
 LRAD 460
 LRAD 470
 LRAD 480
 LRAD 490
 LRAD 500
 LRAD 510
 LRAD 520
 LRAD 530
 LRAD 540
 LRAD 550
 LRAD 560
 LRAD 570
 LRAD 580
 LRAD 590
 LRAD 600
 LRAD 610
 LRAD 620
 LRAD 630
 LRAD 640
 -RAD 650
 LRAD 660
 LRAD 670
 LRAD 680
 -RAD 690
 -RAD 700
 LRAD 710
 -RAD 720

LRAD 730
 LRAD 740
 LRAD 750
 LRAD 760
 LRAD 770
 LRAD 780
 LRAD 790
 LRAD 800
 LRAD 810
 LRAD 820
 LRAD 830
 LRAD 840
 LRAD 850
 LRAD 860
 LRAD 870
 LRAD 880
 LRAD 890
 LRAD 900
 LRAD 910
 LRAD 920

```

CALL TRANS(1)
IDG= IDGS

C  ** INDEX IS NUMBER GIVEN SPECIE FOR USE IN STORING ARRAYS **
C
C  1 = O2
C  2 = N2
C  3 = O
C  4 = N
C  5 = E-
C  6 = C
C  7 = H
C  8 = C2
C  9 = H2
C 10 = CO
C 11 = C3
C 12 = C2H

RETURN
END

```

```

C
C
C
SUBROUTINE ZP(T1,SUMN,SUM0,SUMH,SUMC)
** FRACTIONAL POPULATION STATES FOR N, O, H, C **
COMMON /ZPI/ ZP0(6), ZPN(6),ZPH(2), ZPC(7)
ZPH(1)=2.0/SUMH
ZPH(2)=8.0 * EXP(-10.20/T1)/SUMH
ZPC(1)=9.0/SUMC
ZPC(2)=5.0 * EXP(-1.264/T1)/SUMC
ZPC(3)=EXP(-2.684/T1)/SUMC
ZPC(4)=5.0 * EXP(-4.183/T1)/SUMC
ZPC(5)=12.0 * EXP(-7.532/T1)/SUMC
ZPC(6)=36.0*EXP(-8.722/T1)/SUMC
ZPC(7)=60.0 * EXP(-9.724/T1)/SUMC
ZPN(1)=4.0/SUMN
ZPN(2)=10.0* EXP(-2.384/T1)/SUMN
ZPN(3)=6.0 * EXP(-3.576/T1)/SUMN
ZPN(4)=18.0 * EXP(-10.452/T1)/SUMN
ZPN(5)=54.0 * EXP(-11.877/T1)/SUMN
ZPN(6)=90.0 * EXP(-13.002/T1)/SUMN
ZP0(1)=9.0/SUM0
ZP0(2)=5.0 * EXP(-1.967/T1)/SUM0
ZP0(3)=EXP(-4.188/T1)/SUM0
ZP0(4)=8.0 * EXP(-9.283/T1)/SUM0
ZP0(5)=24.0 * EXP(-10.830/T1)/SUM0
ZP0(6)=40.0 * EXP(-12.077/T1)/SUM0
RETURN
END
C
ZP(T 10
ZP(T 20
ZP(T 30
ZP(T 40
ZP(T 50
ZP(T 60
ZP(T 70
ZP(T 80
ZP(T 90
ZP(T 100
ZP(T 110
ZP(T 120
ZP(T 130
ZP(T 140
ZP(T 150
ZP(T 160
ZP(T 170
ZP(T 180
ZP(T 190
ZP(T 200
ZP(T 210
ZP(T 220
ZP(T 230
ZP(T 240
ZP(T 250
ZP(T 260
ZP(T 270
ZP(T 280
ZP(T 290
ZP(T 295

```

```

SUBROUTINE TRANS2
COMMON /SFLUX/ QRI(3)
COMMON /YL/ETA(60),YOND(60)
COMMON /FRSTRM/ U INF, RINF, UINF2, R, RE, LXI, ITM, IEM, NES
COMMON /TRN/      NUT(60), FMC(12,60), FPC(12,60),
1      FM(9,60), FP(9,60), LINES
COMMON /FINV/ NHVL,NIHVC,FHVC(12),DJ(9),HVJ(9),ZKZ
COMMON /TEST/ETZ(60),IEZ
COMMON /NUMDEN/ SND02(60), SNDN2(60), SND0(60), SNDN(60),
1      SNDE(60), SNDC(60),
2      SNDE(60), SNDC(60),
3      SNDC3(60),SNDCH(60)
COMMON /SPEC/ MF, XMOL
DIMENSION ETOUT(3)
NETA=NES
ETOUT(1)=0.0
ETOUT(2)=0.5
ETOUT(3)=1.0
NOUT=3

C
C   OUTPUT FLUX
C
WRITE (6,600)
WRITE (6,603) (ETA(I),SNDN2(I),SND02(I),SNDN(I),SND0(I),
1      SNDE(I), SNDH(I),
2      SNDC(I),SNDC2(I),SNDH2(I),SNDH2(I),SND0(I),SND02(I),SND03(I),
3      SNDC2H(I),
I=1,NETA)
C *
C   CONTINUUM CONTRIBUTION TO THE SPECTRAL FLUX **
C
WRITE (6,4103)
DO 8040 K=1,NOUT
DO 8041 LK=1,NES
NUT(K)=LK
IF (ABS(ETOUT(K)-ETA(LK)) - 1.0E-05) 8040,8040,8041
8041 CONTINUE
8041 CONTINUE

```

TRAN 10
 TRAN 20
 TRAN 30
 TRAN 40
 TRAN 50
 TRAN 60
 TRAN 70
 TRAN 80
 TRAN 90
 TRAN 100
 TRAN 110
 TRAN 120
 TRAN 130
 TRAN 140
 TRAN 150
 TRAN 160
 TRAN 170
 TRAN 180
 TRAN 190
 TRAN 200
 TRAN 210
 TRAN 220
 TRAN 230
 TRAN 240
 TRAN 250
 TRAN 260
 TRAN 270
 TRAN 280
 TRAN 290
 TRAN 300
 TRAN 310
 TRAN 320
 TRAN 330
 TRAN 340
 TRAN 350
 TRAN 360

```

L1=NUT(1)
L2=NUT(2)
L3=NUT(3)
WRITE (6,8037) (ETOUT(IL),IL=1,3)
FM1=0.0
FP1=0.0
FM2=0.0
FP2=0.0
FM3=0.0
FP3=0.0
DO 4104 KL=1,NIHVC
WRITE (6,8042) KL, FHV(KL), FMC(KL,L1), FPC(KL,L1),
1 FMC(KL,L2), FPC(KL,L2), FMC(KL,L3), FPC(KL,L3)
FM1=FM1 + FMC(KL,L1)
FP1=FP1 + FPC(KL,L1)
FM2=FM2 + FMC(KL,L2)
FP2=FP2 + FPC(KL,L2)
FM3=FM3 + FMC(KL,L3)
FP3=FP3 + FPC(KL,L3)
4104 CONTINUE
WRITE (6,8045) FM1, FP1, FM2, FP2, FM3, FP3
QRI(1)=FM1+FP1
QRI(2)=FM2+FP2
QRI(3)=FM3+FP3
C
C * * LINE CONTRIBUTION TO THE SPECTRAL FLUX **
C
IF (LINES.EQ.0) RETURN
WRITE (6,8035)
WRITE (6,8037) (ETOUT(IL),IL=1,3)
FM1=0.0
FP1=0.0
FM2=0.0
FP2=0.0
FM3=0.0
FP3=0.0
TRAN 370
TRAN 380
TRAN 390
TRAN 400
TRAN 410
TRAN 420
TRAN 430
TRAN 440
TRAN 450
TRAN 460
TRAN 470
TRAN 480
TRAN 490
TRAN 500
TRAN 510
TRAN 520
TRAN 530
TRAN 540
TRAN 550
TRAN 560
TRAN 570
TRAN 580
TRAN 590
TRAN 600
TRAN 610
TRAN 620
TRAN 630
TRAN 640
TRAN 650
TRAN 660
TRAN 670
TRAN 680
TRAN 690
TRAN 700
TRAN 710
TRAN 720

```

```

C ** TOTAL FLUX CALCULATION **
C
C
      DO 8043 KL=1,NHVL
      WRITE (6,8042) KL, HVJ(KL), FM(KL,L1), FP(KL,L1),
1      FM(KL,L2), FP(KL,L2), FM(KL,L3), FP(KL,L3)
      FM1=FM1 + FM(KL,L1)
      FP1=FP1 + FP(KL,L1)
      FM2=FM2 + FM(KL,L2)
      FP2=FP2 + FP(KL,L2)
      FM3=FM3 + FM(KL,L3)
      FP3=FP3 + FP(KL,L3)
8043 CONTINUE
      WRITE (6,8045) FM1, FP1, FM2, FP2, FM3, FP3
      QRI(1)=QRI(1) + FM1 + FP1
      QRI(2)=QRI(2) + FM2 + FP2
      QRI(3)=QRI(3) + FM3 + FP3
C
      600 FORMAT (1H1,33HNUMBER DENSITIES (PARTICLES/CM3) ///5X,3HETA, 8X,
1      2HN2, 8X,2HO2, 8X,1HN, 8X,1HO, 9X, 2HE-,8X,
2      1HH,8X,1HC, 8X,2HC2, 8X,2HH2, 8X,2HCO, 8X,2HC3,8X,3HC2H///)
      603 FORMAT (1P13E10.2)
      4103 FORMAT (44H1CONTINUUM CONTRIBUTION TO THE SPECTRAL FLUX)
      8035 FORMAT (39HC1INE CONTRIBUTION TO THE SPECTRAL FLUX)
      8037 FORMAT (/22X,SHETA =F7.3,13X,SHETA =F7.3,13X,SHETA =F7.3//3X,1HI,
1      3X,3HNU,8X,6HQM1NUS,7X,5HOP1US,8X,6HQM1NUS,7X,5HOP-US,8X,
2      6HQM1NUS,7X,5HOP1US/)
      8042 FORMAT (14,F8.3,1P8E13.3)
      8045 FORMAT (12HC1OTAL FLUX ,1P8E13.3)
      RETURN
      END
TRAN 730
TRAN 740
TRAN 750
TRAN 760
TRAN 770
TRAN 780
TRAN 790
TRAN 800
TRAN 810
TRAN 820
TRAN 830
TRAN 840
TRAN 850
TRAN 860
TRAN 870
TRAN 880
TRAN 890
TRAN 900
TRAN 910
TRAN 920
TRAN 930
TRAN 940
TRAN 950
TRAN 960
TRAN 970
TRAN 980
TRAN 990
TRAN1000
TRAN1010
TRAN1020
TRAN1030

```

```

SUBROUTINE BUGPR (IDGSW)
COMMON /FSTRM/ U INF, RINF, UINF2, R, RE, LXI, ITM, IEM, NES
COMMON /YL/ETA(60), YD(60)
COMMON /TRN/ NUT(60), FMC(12,60), FPC(12,60),
1 FM(9,60), FP(9,60), LINES
COMMON /DBG/ QLC(60), QCL(60), QLL(60), DQN(60), QCC(60),
1 BEEC(12,60), FMUC(12,60), EM(12,60),
2 EP(12,60), TAUC(12,60), BEEL(9,60),
3 QCCP(12), WMM(9,60), GMM(9,60),
4 EEM(9,60), XLMM(9,60), QLCP(9),
5 QCLP(9), QLLP(9), DELTA, IY, IYY,
6 WPP(9,60), GPP(9,60), EEP(9,60),
7 XLPP(9,60), FG(9,4), GP(9,4),
8 WN(9,4), FMUL(9,60), SSM(9,4,60),
9 GGM(9,4,60), ETAM(9,4,60), SBM(9,4,60),
A TAU(9,60)
GO TO (10,20,30,40,50,60,70), IDGSW
10 WRITE (6,194)
194 FORMAT (1H1)
RETURN
20 WRITE (6,7182) DELTA
7182 FORMAT (7HODELTA=1PE14.7,3H CM)
RETURN
30 WRITE (6,190) IY, YD(1Y)
190 FORMAT (4H1Y=13,2X,3HYD=1PE12.5//2X,1HK,2X,1HL,7X,3HETA,13X,2HYD,BUGP 250
1 13X,2HMU,11X,3HTAU,14X,1HE,11X,3HBE//)
DO 22 K=1,12
IF (1Y.EQ.1) GO TO 23
WRITE (6,191) (K, L,
1 FM(K,L), BEEC(K,L), L=1,IY)
191 FORMAT (2I3,1P6E15.5)
WRITE (6,192)
192 FORMAT (//)
23 IF (1Y.EQ.NES) GO TO 22
WRITE (6,191) (K, L,
1 TAUC(K,L), EP(K,L), BEEC(K,L), L=1,IY,NES)
BUGP 10
BUGP 20
BUGP 30
BUGP 40
BUGP 50
BUGP 60
BUGP 70
BUGP 80
BUGP 90
BUGP 100
BUGP 110
BUGP 120
BUGP 130
BUGP 140
BUGP 150
BUGP 160
BUGP 170
BUGP 180
BUGP 190
BUGP 200
BUGP 210
BUGP 220
BUGP 230
BUGP 240
BUGP 250
BUGP 260
BUGP 270
BUGP 280
BUGP 290
BUGP 300
BUGP 310
BUGP 320
BUGP 330
BUGP 340
BUGP 350
BUGP 360

```



```

22 WRITE (6,193) FMC(K,IY), FPC(K,IY), QCCP(K)      BUGP 370
193 FORMAT (5HOFIM=1PE12.5,2X,4HFIP=E12.5,2X,5H0CCP=E12.5)  BUGP 380
RETURN      BUGP 390
40 WRITE (6,195) IY, YD(IY), ((J, L, YD(L),      BUGP 400
      1 WMM(J,L), GMM(J,L), XLMM(J,L), EEM(J,L),      BUGP 410
      2 BEEL(J,L), L=1,IY), J=1,9)      BUGP 420
195 FORMAT (4H0IY=13,2X,3HYI=1PE12.5//2X,1HJ,2X,1HL,7X,2HYD,12X,3HMMM,BUGP 430
      1 12X,3HMMM,11X,4HXLMM,13X,3HEEM,13X,3HEE//((2I3,6E16.5))      BUGP 440
RETURN      BUGP 450
50 WRITE (6,196) IY, YD(IY), ((J, L, YD(L),      BUGP 460
      1 WPP(J,L), GPP(J,L), XLPP(J,L), EEP(J,L),      BUGP 470
      2 BEEL(J,L), L=1,IY, NES), J=1,9)      BUGP 480
196 FORMAT (4H0IY=13,2X,3HYI=1PE12.5//2X,1HJ,2X,1HL,7X,2HYD,13X,3HPPP,BUGP 490
      1 2X,3HPPP,11X,4HXLPP,13X,3HEEP,13X,3HEE//((2I3,6E16.5))      BUGP 500
RETURN      BUGP 510
60 WRITE (6,198) IY, ETA(IY), YD(IY)      BUGP 520
198 FORMAT (4H0IY=13,2X,4HETA=1PE12.5,2X,3HYI=E12.5//2X,1HJ,5X,3HQQC,      BUGP 530
      1 11X,3HFMC,11X,3HFPC,11X,3HQLC,11X,3HQLC,11X,3HQLC,12X,2HFM,12X,      BUGP 540
      2 2HFP,11X,3HDQN//)      BUGP 550
WRITE (6,199) (J, QCCP(J), FMC(J,IY), FPC(J,IY),      BUGP 560
      1 QCLP(J), QCLP(J), QCLP(J), FM(J,IY),FP(J,IY),      BUGP 570
      2 J=1,9)      BUGP 580
199 FORMAT (13,1P8E14.5)      BUGP 590
WRITE (6,8069) (J, QCCP(J), FMC(J,IY), FPC(J,IY), J=10,12)BUGP 600
8069 FORMAT (13,1P3E14.5)      BUGP 610
WRITE (6,200) QCC(IY), QCL(IY), QCL(IY), QLL(IY),      BUGP 620
      1 DQN(IY)      BUGP 630
200 FORMAT (1HG,2X,1PE14.5,23X,3E14.5,28X,E14.5)      BUGP 640
RETURN      BUGP 650
70 WRITE (6,197) L, ETA(L), YD(L), ((J, M, WN(J,M),      BUGP 660
      1 FG(J,M), GP(J,M), FMUL(J,L), TAU(L,J,L),      BUGP 670
      2 SSM(J,M,L), GGM(J,M,L), ETAM(J,M,L), SBM(J,M,L),BUGP 680
      3 M=1,4),J=1,9)      BUGP 690
197 FORMAT (3HOL=13,2X,4HETA=1PE12.5,2X,3HYD=E12.5//2X,1HJ,2X,1HM,7X,      BUGP 700
      1 14N,13X,1HF,13X,1HG,11X,3HFMU,11X,3HTAU,11X,3HSSM,11X,3HGGM,10X,      BUGP 710
      2 4HETAM,11X,3HSSM//((2I3,9E14.5))      BUGP 720

```

3USP 730
BUGP 749

DETURN
END

```

C
C
C
C
C
C
SUBROUTINE ZHV(HV,ZO,ZN,ZI,ZC)
** THIS SUBROUTINE CALCULATES THE QUANTUM MECHANICAL CORRECTION
   FACTORS GIVEN A FREQUENCY (HV) **
X= HV
X2 =X*X
X3 =X2*X
X4 =X3*X
X5 =X4*X
X6 =X5*X
X7 =X6*X
IF (X -9.82) 1,1.2
1  Z0 = .9999795
   1  +6.677328 E-03*X3
   2  -7.708637 E-05*X6
   GO TO 3
2  Z0 = (X/9.82)**3
3  IF (X -8.35) 4,4.5
4  ZN = 1.000148
   1  -9.779458 E-02*X3
   2  +4.515535E-04*X6
   GO TO 6
5  ZN = (X/8.35)**3
6  Y = X/4.0
   IF (Y-6.6) 9,9.10
9  Y2 =Y*Y
   Y3 =Y2*Y
   Y4 =Y3*Y
   Y5 =Y4*Y
   Y6 =Y5*Y
   Y7 =Y6*Y
   ZI = 1.000379
   1  -1.702948E-02*Y2
   GO TO 11
   +2.824548 E-02*X2
   +8.058070 E-04*X5
   - .3155480*X
   -3.644585 E-03*X4
   +2.668133 E-06*X7
   + .1680359 *X2
   -5.609353 E-03*X5
   - .4183535 *X
   +3.354635 E-02*X4
   -1.403585 E-05*X7
   - .2964767 *Y
   +3.279554 E-03*Y4
   +7.505242 E-02*Y2
   -2.128469 E-04*Y5
ZHV( 10
ZHV( 20
ZHV( 30
ZHV( 40
ZHV( 50
ZHV( 60
ZHV( 70
ZHV( 80
ZHV( 90
ZHV( 100
ZHV( 110
ZHV( 120
ZHV( 130
ZHV( 140
ZHV( 150
ZHV( 160
ZHV( 170
ZHV( 180
ZHV( 190
ZHV( 200
ZHV( 210
ZHV( 220
ZHV( 230
ZHV( 240
ZHV( 250
ZHV( 260
ZHV( 270
ZHV( 280
ZHV( 290
ZHV( 300
ZHV( 310
ZHV( 320
ZHV( 330
ZHV( 340
ZHV( 350
ZHV( 360

```

```

10  ZI = (Y/6.6)**3
11  IF (X-7.37) 12,12,13
12  ZC = .9974367
    1  -1.393917 E-02*X3
    2  +2.812126 E-05*X6
      GO TO 14
13  ZC = (X/7.37)**3
14  RETURN
    END

      - .4341812 *X
      +4.338545 E-03*X4
      -3.883530 E-07*X7
      +8.531314 E-02*X2
      -5.426425 E-04*X5

ZHV( 370
ZHV( 380
ZHV( 390
ZHV( 400
ZHV( 410
ZHV( 420
ZHV( 430
ZHV( 440
ZHV( 450

```

```

SUBROUTINE RADIN
COMMON /DHUG/ QLC(60), QCL(60), QLL(60), DON(60), QCC(60),
1 REEC(12,60), FMUC(12,60), EM(12,60),
2 EP(12,60), TAUC(12,60), BEEL(9,60),
3 QCCP(12), WMM(9,60), GMM(9,60),
4 EEM(9,60), XLMM(9,60), QLCP(9),
5 QCLP(9), DELTA, IY, IYY,
6 WPP(9,60), GPP(9,60), EEP(9,60),
7 XLPP(9,60), FG(9,4), GP(9,4),
8 WN(9,4), FMUL(9,60), SSM(9,4,60),
9 GGM(9,4,60), ETAM(9,4,60), SBM(9,4,60),
A TAU(9,60)

C ** GROUP 1 **
WN(1,1)=0.
FG(1,1)=0.
GP(1,1)=0.
WN(1,2)=18.
WN(1,3)=15.
WN(1,4)=5.

C ** GROUP 2 **
WN(2,1)=3.0
WN(2,2)=5.0
WN(2,3)=11.0
WN(2,4)=10.

C ** GROUP 3 **
WN(3,1)=0.
FG(3,1)=0.
GP(3,1)=0.
WN(3,2)=2.0
WN(3,3)=0.
FG(3,3)=0.
GP(3,3)=0.
WN(3,4)=0.
FG(3,4)=0.
GP(3,4)=0.

C ** GROUP 4 **

```

RADI 10
RADI 20
RADI 30
RADI 40
RADI 50
RADI 60
RADI 70
RADI 80
RADI 90
RADI 100
RADI 110
RADI 120
RADI 130
RADI 140
RADI 150
RADI 160
RADI 170
RADI 180
RADI 190
RADI 200
RADI 210
RADI 220
RADI 230
RADI 240
RADI 250
RADI 260
RADI 270
RADI 280
RADI 290
RADI 300
RADI 310
RADI 320
RADI 330
RADI 340
RADI 350
RADI 360

```

WN(4,1)=0.
FG(4,1)=0.
GP(4,1)=0.
WN(4,2)=8.0
WN(4,3)=2.0
WN(4,4)=0.
FG(4,4)=0.
GP(4,4)=0.
C ** GROUP 5 **
WN(5,1)=0.
FG(5,1)=0.
GP(5,1)=0.
WN(5,2)=14.
WN(5,3)=4.0
WN(5,4)=1.0
C ** GROUP 6 **
WN(6,1)=1.0
WN(6,2)=4.0
WN(6,3)=13.0
WN(6,4)=2.0
C ** GROUP 7 **
WN(7,1)=0.
FG(7,1)=0.
GP(7,1)=0.
WN(7,2)=6.0
WN(7,3)=14.0
WN(7,4)=3.0
C ** GROUP 8 **
WN(8,1)=2.0
WN(8,2)=2.0
WN(8,3)=11.
WN(8,4)=15.
C ** GROUP 9 **
WN(9,1)=0.
FG(9,1)=0.
GP(9,1)=0.

RADI 370
RADI 380
RADI 390
RADI 400
RADI 410
RADI 420
RADI 430
RADI 440
RADI 450
RADI 460
RADI 470
RADI 480
RADI 490
RADI 500
RADI 510
RADI 520
RADI 530
RADI 540
RADI 550
RADI 560
RADI 570
RADI 580
RADI 590
RADI 600
RADI 610
RADI 620
RADI 630
RADI 640
RADI 650
RADI 660
RADI 670
RADI 680
RADI 690
RADI 700
RADI 710
RADI 720

```

```
RADI 733  
RADI 740  
RADI 750  
RADI 760  
RADI 770
```

```
WN(9,2)=1.0  
WN(9,3)=11.  
WN(9,4)=10.  
RETURN  
END
```

```

SUBROUTINE STPSIZE
** ROUTINE TO ADJUST STEP SIZE AS NEEDED
   TO MAINTAIN ACCURACY **

COMMON /DEL/ DELTA,CTIL,DILS
COMMON /FRSTRM/ U INF, RINF, UINF2, R, RE, LXI, ITM, IEM, NETA
COMMON /PROP1/PI(60),RHO(60),G(60),AMW(50),C(20,60),EC(5,60)
COMMON /PROP2/ MU(60),RM(60), AK(60)
COMMON /PROP3/CP(60),HS(20,60),CP(60),HM(60)
COMMON /RH/ DUD,DPHI,TD,RZB,PD,HD,HTOTAL
COMMON /RFLUX/ E(60),IRAD,ITYPE
COMMON /VEL/ F(60),FC(60),Z(60),V(60)
COMMON /WALL/RVW,PRW,TWOLD,FLUX(20),CWALL(20),ECWALL(5)
COMMON /YL/ETA(60),YOND(60)
COMMON /OLD/ TOLD(60),EOLD(60),RHOS(60)

N=2
CONTINUE
I2=2
IF (NETA.GE. 59) GO TO 5

DO 2 I=N,NETA
L=I
CHECK = ABS(G(I)-G(I-1))
IF (CHECK .GT. .05) GO TO 3
CONTINUE
GO TO 5

CONTINUE
M = NETA - L + 1
DO 4 I=1,M
K = NETA - I + 1

```

STPS 1:
 STPS 20
 STPS 30
 STPS 40
 STPS 50
 STPS 60
 STPS 70
 STPS 80
 STPS 90
 STPS 100
 STPS 110
 STPS 120
 STPS 130
 STPS 140
 STPS 150
 STPS 160
 STPS 170
 STPS 180
 STPS 190
 STPS 200
 STPS 210
 STPS 220
 STPS 230
 STPS 240
 STPS 250
 STPS 260
 STPS 270
 STPS 280
 STPS 290
 STPS 300
 STPS 310
 STPS 320
 STPS 330
 STPS 340
 STPS 350
 STPS 360


```

      G(K+1) = G(K)
      F(K+1) = F(K)
      DO100JJ=1,5
      EC(JJ,K+1)=EC(JJ,K)
      TOLD(K+1)=TOLD(K)
      RHOS(K+1)=RHOS(K)
      RHO(K+1) = RHO(K)
      RM (K+1) = RM (K)
      IF(IRAD.EQ. 3) E(K+1) = E(K)
      ETA(K+1) = ETA(K)
      CONTINUE
4
C
      G(L) = (G(L-1) + G(L+1)) / 2.0
      F(L) = (F(L-1)+F(L+1))/2.
      DO101JJ=1,5
      EC(JJ,L)=(EC(JJ,L-1)+EC(JJ,L+1))/2.
      TOLD(L)=(TOLD(L-1)+TOLD(L+1))/2.0
      RHOS(L)=(RHOS(L-1)+RHOS(L+1))/2.0
      RHO(L) = (RHO(L-1) +RHO(L+1))/2.
      RM (L) = (RM (L-1) +RM (L+1))/2.
      IF(IRAD.EQ. 3) E(L) =(E(L-1)+ E(L+1))/2.0
      ETA(L) = (ETA(L-1) + ETA(L+1) )/2.0
      NETA = NETA + 1
      N=L
C
      IF( NETA .LT. 59) GO TO 1
C
      CONTINUE
5
C
      IF(I2.GE. NETA) GO TO 10
      DO 6 I=12,NETA,2
      L=I
      IF (L.EQ.NETA) GO TO 6
      IF(ETA(I).EQ. 0.98) GO TO 6
      CHECK =ABS(G(I+1) - G(I-1) )
      IF(CHECK .LT. 0.005) GO TO 7

```

STPS 370
STPS 380
STPS 390
STPS 400
STPS 410
STPS 420
STPS 430
STPS 440
STPS 450
STPS 460
STPS 470
STPS 480
STPS 490
STPS 500
STPS 510
STPS 520
STPS 530
STPS 540
STPS 550
STPS 560
STPS 570
STPS 580
STPS 590
STPS 600
STPS 610
STPS 620
STPS 630
STPS 640
STPS 650
STPS 660
STPS 670
STPS 680
STPS 690
STPS 700
STPS 710
STPS 720

```

6      CONTINUE
C
7      GO TO 10
CONTINUE
I2=L+1
IF (ETA(L+1)-ETA(L-1)).GT. .04) GO TO 5
C
DO 8 I=L,NETA
G(I) = G(I+1)
F(I) = F(I+1)
DO 102 JJ=1,5
102  EC(JJ,I)=EC(JJ,I+1)
TOLD(I)=TOLD(I+1)
RHOS(I)=RHOS(I+1)
RHO(I) = RHO(I+1)
RM (I) = RM (I+1)
IF (IRAD.EQ. 3) E(I) =E(I+1)
ETA(I)=ETA(I+1)
CONTINUE
C
NETA=NETA-1
IF (NETA .GT. 1) GO TO 5
C
10     CONTINUE
NN = NETA-2
DO 20 I=1,NN
20     Z(I) = ETA(I+1)/DTIL
CONTINUE
RETURN
END

```

STPS 730
STPS 740
STPS 750
STPS 760
STPS 770
STPS 780
STPS 790
STPS 800
STPS 810
STPS 820
STPS 830
STPS 840
STPS 850
STPS 860
STPS 870
STPS 880
STPS 890
STPS 900
STPS 910
STPS 920
STPS 930
STPS 940
STPS 950
STPS 960
STPS 970
STPS 980
STPS 990
STPS1000
STPS1010
STPS1020

```

C C C SUBROUTINE MATINV(A,N,B,M,NMAX)
C C C
C C C MATRIX INVERSION WITH ACCOMPANYING SOLUTION OF LINEAR EQUATIONS
C C C DIMENSION A(7,7),B(7,1),IPIVOT(7),INDEX(7,2)
C C C EQUIVALENCE (IROW,JROW), (ICOLUM,JCOLUM), (AMAX,T,SWAP)
C C C
C C C INITIALIZATION
C C C
C C C   5 ISCALE=0
C C C   6 R1=10.0**18
C C C   7 R2=1.0/R1
C C C  10 DETERM=1.0
C C C  15 DO 20 J=1,N
C C C  20 IPIVOT(J)=0
C C C  30 DO 550 I=1,N
C C C
C C C SEARCH FOR PIVOT ELEMENT
C C C
C C C   40 AMAX=0.0
C C C   45 DO 105 J=1,N
C C C   50 IF (IPIVOT(J)-1)60,105,60
C C C   60 DO 100 K=1,N
C C C   70 IF (IPIVOT(K)-1)80,100,740
C C C   80 IF (ABS(AMAX)-ABS(A(J,K)))85,100,100
C C C   85 IROW=J
C C C   90 ICOLUM=K
C C C   95 AMAX=A(J,K)
C C C  100 CONTINUE
C C C  105 CONTINUE
C C C   IF (AMAX)110,100,110
C C C  106 DETERM=D.0
C C C   ISCALE=0
C C C   GO TO 740
C C C  110 IPIVOT(ICOLUM)=IPIVOT(ICOLUM)+1

```

```

C      INTERCHANGE ROWS TO PUT PIVOT ELEMENT ON DIAGONAL
C
130 IF (IROW-ICOLU)140,260,140
140 DETERM=-DETERM
150 DO 200 L=1,N
160 SWAP=A(IROW,L)
170 A(IROW,L)=A(ICOLU,L)
200 A(ICOLU,L)=SWAP
205 IF(M)260,260,210
210 DO 250 L=1,M
220 SWAP=B(IROW,L)
230 B(IROW,L)=B(ICOLU,L)
250 B(ICOLU,L)=SWAP
260 INDEX(I,1)=IROW
270 INDEX(I,2)=ICOLU
310 PIVOT=A(ICOLU,ICOLU)

C      SCALE THE DETERMINANT
C
1000 PIVOTI=PIVOT
1005 IF(ABS(DETERM)-R1)1030,1010,1010
1010 DETERM=DETERM/R1
      ISCALE=ISCALE+1
1020 IF(ABS(DETERM)-R1)1060,1020,1020
      DETERM=DETERM/R1
      ISCALE=ISCALE+1
      GO TO 1060
1030 IF(ABS(DETERM)-R2)1040,1040,1060
1040 DETERM=DETERM*R1
      ISCALE=ISCALE-1
1050 IF(ABS(DETERM)-R2)1050,1050,1060
      DETERM=DETERM*R1
      ISCALE=ISCALE-1
1060 IF(ABS(PIVOTI)-R1)1070,1070,1070
1070 PIVOTI=PIVOTI/R1
      ISCALE=ISCALE+1

```

MATI 370
MATI 380
MATI 390
MATI 400
MATI 410
MATI 420
MATI 430
MATI 440
MATI 450
MATI 460
MATI 470
MATI 480
MATI 490
MATI 500
MATI 510
MATI 520
MATI 530
MATI 540
MATI 550
MATI 560
MATI 570
MATI 580
MATI 590
MATI 600
MATI 610
MATI 620
MATI 630
MATI 640
MATI 650
MATI 660
MATI 670
MATI 680
MATI 690
MATI 700
MATI 710
MATI 720

```

1080 IF (ABS(PIVOTI)-R1)320,1080,1080
1090 PIVOTI=PIVOTI/R1
1100 ISCALE=ISCALE+1
1110 GO TO 320
1090 IF (ABS(PIVOTI)-R2)2000,2000,320
2000 PIVOTI=PIVOTI*R1
1120 ISCALE=ISCALE-1
1090 IF (ABS(PIVOTI)-R2)2010,2010,320
2010 PIVOTI=PIVOTI*R1
1130 ISCALE=ISCALE-1
320 DETERM=DETERM*PIVOTI
C
C
C
330 A(ICOL,ICOL)=1.0
340 DO 350 L=1,N
350 A(ICOL,L)=A(ICOL,L)/PIVOT
355 IF(M) 380,380,360
360 DO 370 L=1,M
370 B(ICOL,L)=B(ICOL,L)/PIVOT
C
C
C
380 DO 550 L1=1,N
390 IF (L1-ICOL)400,550,400
400 T=A(L1,ICOL)
420 A(L1,ICOL)=0.0
430 DO 450 L=1,N
450 A(L1,L)=A(L1,L)-A(ICOL,L)*T
455 IF(M) 550,550,460
460 DO 500 L=1,M
500 B(L1,L)=B(L1,L)-B(ICOL,L)*T
550 CONTINUE
C
C
C
INTERCHANGE COLUMNS
600 DO 710 I=1,N

```

```

MATI 730
MATI 740
MATI 750
MATI 760
MATI 770
MATI 780
MATI 790
MATI 800
MATI 810
MATI 820
MATI 830
MATI 840
MATI 850
MATI 860
MATI 870
MATI 880
MATI 890
MATI 900
MATI 910
MATI 920
MATI 930
MATI 940
MATI 950
MATI 960
MATI 970
MATI 980
MATI 990
MATI 1000
MATI 1010
MATI 1020
MATI 1030
MATI 1040
MATI 1050
MATI 1060
MATI 1070
MATI 1080

```

MAT11090
 MAT11100
 MAT11110
 MAT11120
 MAT11130
 MAT11140
 MAT11150
 MAT11160
 MAT11170
 MAT11180
 MAT11190
 MAT11200
 MAT11210

C
 610 L=N+1-I
 620 IF (INDEX(L,1)-INDEX(L,2))630,710,630
 630 JROW=INDEX(L,1)
 640 JCOLUMN=INDEX(L,2)
 650 DO 705 K=1,N
 660 SWAP=A(K,JROW)
 670 A(K,JROW)=A(K,JCOLUMN)
 700 A(K,JCOLUMN)=SWAP
 705 CONTINUE
 710 CONTINUE
 740 RETURN
 END

```

C ** SUBROUTINE FGH(N,F,G,H)
C ** ** FIRST DERIVATIVE
C-----EVALUATES COEFFICIENTS FOR THREE POINT DIFFERENCE APPROXIMATION
C OF DAVIS (AIAA JR. VOL. 8, NO. 5, MAY 1970).
COMMON /YL/ETA(60),YOND(60)
DN=ETA(N+1)-ETA(N)
DNM1=ETA(N)-ETA(N-1)
DEL=DN+DNM1
D1=DN*DEL
D2=DN*DNM1
D3=DNM1*DEL
F=DNM1/D1
G=(DN-DNM1)/D2
H=-DN/D3
RETURN
END

```

FGH(10
FGH(20
FGH(30
FGH(40
FGH(50
FGH(60
FGH(70
FGH(80
FGH(90
FGH(100
FGH(110
FGH(120
FGH(130
FGH(140
FGH(150
FGH(160

```

C      **      SUBROUTINE FGH2(N,F,G,H)
C      **      SECOND DERIVATIVE
C-----EVALUATES COEFFICIENTS FOR THREE POINT DIFFERENCE APPROXIMATION
C      OF DAVIS (AIAA JK. VOL. 8, NO. 5, MAY 1970).
COMMON /YL/ETA(60),YOND(60)
DN=ETA(N+1)-ETA(N)
DNM1=ETA(N)-ETA(N-1)
F=2./((DN*(DN+DNM1))
G=-2./((DN*DNM1)
H=2./((DNM1*(DN+DNM1))
RETURN
END

```

FGH2	10
FGH2	20
FGH2	30
FGH2	40
FGH2	50
FGH2	60
FGH2	70
FGH2	80
FGH2	90
FGH2	100
FGH2	110
FGH2	120


```

SUBROUTINE TRID (M)
C*** TRID --TRIDIAGONAL EQUATION SOLVER OBTAINED FROM CONTE P-184 ***
C SUBROUTINE SOLVES AX = B FOR THE VECTOR X (WHERE A IS TRIDIAGONAL)
C M = ORDER OF SYSTEM
C SUP = SUPER DIAGONAL OF A
C SUB = SUB DIAGONAL OF A
C DIAG = MAIN DIAGONAL OF A
C B = CONSTANT VECTOR
C SUP AND DIAG ARE DESTROYED
C SOLUTION VECTOR IS RETURNED IN B
C
COMMON/VECTOR/ SUB(60),DIAG(60),SUP(60),B(60)
C
N = M
NN = N - 1
SUP(1) = SUP(1)/DIAG(1)
B(1) = B(1)/DIAG(1)
DO 10 I=2,N
  II = I - 1
  C-----DECOMPOSE A TO FORM A = LU WHERE L IS LOWER TRIANGULAR,
  C AND U IS UPPER TRIANGULAR -----
  DIAG(I) = DIAG(I) - SUP(II)*SUB(II)
  IF(I.EQ. N) GO TO 10
  SUP(I) = SUP(II) / DIAG(II)
  C-----COMPUTE Z WHERE LZ = B
  10 B(I) = (B(I) - SUP(II) *B(II))/ DIAG(I)
  C-----COMPUTE X BY BACK SUBSTITUTION WHERE UX = Z
  DO 20 K =1,NN
    I = N - K
    20 B(I) = B(I) -SUP(I) *B(I+1)
  RETURN
END

```

TRID 10
TRID 20
TRID 30
TRID 40
TRID 50
TRID 60
TRID 70
TRID 80
TRID 90
TRID 100
TRID 110
TRID 120
TRID 130
TRID 140
TRID 150
TRID 160
TRID 170
TRID 180
TRID 190
TRID 200
TRID 210
TRID 220
TRID 230
TRID 240
TRID 250
TRID 260
TRID 270
TRID 280
TRID 290
TRID 300
TRID 310
TRID 320

QU 10
QU 20
QU 30
QU 40
QU 50
QU 60
QU 70
QU 80
QU 90

```

FUNCTION QUAD (X,FX,I)
**  TRAPEZOIDAL QUADRATURE FUNCTION **
DIMENSION X(60),FX(60)
DX=X(I)-X(I-1)
QUAD = (DX/2.0) * (FX(I) + FX(I-1) )
RETURN
END

```

C
C
C

```

SUBROUTINE OUTPUT(N)
** ROUTINE TO PRINT SHOCK LAYER SOLUTION **

COMMON/ID/SP(20),EL(5)
COMMON/CONV/ FPRCT,TPRCT,DDAMP,TDAMP,PDIL
COMMON/DEL/ DELTA,DTIL,DTILS
COMMON/FRSTRM/ U INF, RINF, UINF2, R , RE, LXI, ITM, IEM, NETA
COMMON/MAIM/KEEP,MAXE,MAXM,MAXD,IDEBUG,MCONV,ECONV,DCONV,LT,IAB
COMMON/NON/RDZ,MUDZ,RMDZ,AKNF,HNF,CPNF
COMMON/NUMBER/NSP,NNS,NE,NC
COMMON/PROPI/PI(60),RHO(60), T(60),AMW(60),C (20,60),EC(5,60)
COMMON/PROP2/ MU(60),RM(60), AK(60)
COMMON/PROP3/CPS(20,60),HS(20,60),CP (60),HM(60)
COMMON/RFLUX/ E(60),IRAD,ITYPE
COMMON/RH/ DUD,DPhi,TD,RZB,PD,HD,HTOTAL
COMMON/SFLUX/QRI(3)
COMMON/VECTOR/ CA(60),CB(60),CC(60),B(60)
COMMON/VEL/ F(60),FC(60),Z(60),V(60)
COMMON/WALL/RVW,PRW,TWOLD,FLUX(20),CWALL(20),ECWALL(5)
COMMON/YL/ETA(60),YOND(60)
COMMON/DY/ DYDT(20,60)
DIMENSION BOUT(60),DQR(30)
REAL MU,MUDZ
DATA HEAD1/'WALL',HEAD2/,HEAD3/'SHOC'/

** COMPUTE RADIATION FLUX IF UNCOUPLED PROBLEM **

IF(ITYPE,NE,0)GOTO20
IF(IRAD,EO,2 ,AND, N,NE, 2) CALL TRANS(1)
IF (IRAD,NE,1) CALL TRANS2
IF (IRAD,EO,2,AND,ITYPE,EO,1) CALL EFLUX
WRITE(6,243)

```

```

OUTPUT 10
OUTPUT 20
OUTPUT 30
OUTPUT 40
OUTPUT 50
OUTPUT 60
OUTPUT 70
OUTPUT 80
OUTPUT 90
OUTPUT 100
OUTPUT 110
OUTPUT 120
OUTPUT 130
OUTPUT 140
OUTPUT 150
OUTPUT 160
OUTPUT 170
OUTPUT 180
OUTPUT 190
OUTPUT 200
OUTPUT 210
OUTPUT 220
OUTPUT 230
OUTPUT 240
OUTPUT 250
OUTPUT 260
OUTPUT 270
OUTPUT 280
OUTPUT 290
OUTPUT 300
OUTPUT 310
OUTPUT 320
OUTPUT 330
OUTPUT 340
OUTPUT 350
OUTPUT 360

```

```

203 FORMAT(1H1)
C
C      ** COMPUTE Y COORDINATE **
C
      YOND(1) = 0.0
      SUM = 0.0
      DO 40 K=2, NETA
        DELTA = ETA(K) - ETA(K-1)
        SUM = SUM + DELTA * (1. / RHO(K) + 1. / RHO(K-1)) / 2.
        YOND(K) = DTIL * SUM
      40 CONTINUE
      DELTA = YOND(NEGA)
      DO 50 K=1, NETA
        YOND(K) = YOND(K) / DELTA
      50 CONTINUE
C
C      ** COMPUTE CONVECTIVE HEATING RATE **
C
C      WATTS/CM**3
      QC = -AK(1) * RINF * UINF * UINF2 * (T(2) - T(1)) /
      1 (.88 * 778.28 * YOND(2) * DELTA * RZB)
C BTU/FT**2-SEC
      QCP = QC * .88
C
C      ** COMPUTE RADIATIVE FLUX TO SURFACE **
C
      QR = 0.0
      IF (IRAD .EQ. 1) GO TO 445
      DO 1100 K=2, NETA
        QR = QR + QUAD(YOND, E, K)
      1100 CONTINUE
C WATTS/CM**2
      QP = -QR * RINF * UINF2 * UINF * DELTA / (.85 * RZB)
      IF (ITYPE .EQ. 0) QR = -QRI(1)
      445 CONTINUE
C BTU/FT**2-SEC

```

OUTPUT 370
 OUTPUT 380
 OUTPUT 390
 OUTPUT 400
 OUTPUT 410
 OUTPUT 420
 OUTPUT 430
 OUTPUT 440
 OUTPUT 450
 OUTPUT 460
 OUTPUT 470
 OUTPUT 480
 OUTPUT 490
 OUTPUT 500
 OUTPUT 510
 OUTPUT 520
 OUTPUT 530
 OUTPUT 540
 OUTPUT 550
 OUTPUT 560
 OUTPUT 570
 OUTPUT 580
 OUTPUT 590
 OUTPUT 600
 OUTPUT 610
 OUTPUT 620
 OUTPUT 630
 OUTPUT 640
 OUTPUT 650
 OUTPUT 660
 OUTPUT 670
 OUTPUT 680
 OUTPUT 690
 OUTPUT 700
 OUTPUT 710
 OUTPUT 720

```

QRP=QR*1.38
QTOTAL=QC+QR
QUTP=QTOTAL*.88
QCZ=QC
QRZ=QR
QTZ=QTOTAL
QCRAT = 1.0
IF(QC.LT.0.0) QCRAT= QC/QCZ
QRRAT = 1.0
IF(QR.LT. 0.0) QRRAT = QR/QRZ
QTRAT=1.0

** DIMENSIONALIZE RHO,MU,P.AND E **

DO 450 I = 1 , NETA
  RHO(I)=RHO(I)*RDZ
  MU (I)=MU(I)*MUDZ
  RM (I)=RM(I)*RMDZ
  AK(I) = AK(I)/AKNF
  E(I) = E(I) * RINF      * UINF2 * UINF / (20866.0 * R *RZB)
  CP(I) = CP(I)/CPNF
450 CONTINUE

** CORRELATION FORMULAS FOR OUTPUT **

QKR=16000.0*SQRT(RINF)*((UINF/10000.0)**3.25
QKR=-QKR/SQRT(R)
HIS=HTOTAL/(32.174*778.0)
SRENU=0.763*(PRW      )**0.4 * (RM(NEGA)/RM(1)  )**0.4
PS=PD*2116.0
RS=RHO(NEGA)
DUEDX=(1.0/R)*SQRT(2.0*PS/RS)
SDUEDX=SQRT(DUEDX      )
SRMPR=SQRT(RM(1      ))**32.174/PRW
QFR=-SRENU*SRMPR*SDUEDX*HIS
QRT=-495000.0*PINF**1.93*(UINF/10000.0)**14*R

C
C
C
450
C
C
C

```

```

OUTP 730
OUTP 740
OUTP 750
OUTP 760
OUTP 770
OUTP 780
OUTP 790
OUTP 800
OUTP 810
OUTP 820
OUTP 830
OUTP 840
OUTP 850
OUTP 860
OUTP 870
OUTP 880
OUTP 890
OUTP 900
OUTP 910
OUTP 920
OUTP 930
OUTP 940
OUTP 950
OUTP 960
OUTP 970
OUTP 980
OUTP 990
OUTP1000
OUTP1010
OUTP1020
OUTP1030
OUTP1040
OUTP1050
OUTP1060
OUTP1070
OUTP1080

```

```

      QT=QRT+QKP
      RLAMBA=QRP/(RINF*UINF**3/(2.*778.28))

      GO TO (1,2,3,4), N

      1  WRITE(6,201) IEM
      201 FORMAT(23H SOLUTION CONVERGED IN ,I3.11H ITERATIONS //)
      GO TO 4

      2  WRITE (6,202) IEM
      202 FORMAT(1H0,37H INTERMEDIATE PRINT AT ITERATION NO. ,I4,/)
      GO TO 4

      3  CONTINUE

      4  CONTINUE

      ** PRINT SHOCK QUANTITIES AND HEATING RATE **

      XID=0.0
      WRITE(6,204) XID,DELTA,DITL
      204 FORMAT(1H0,7H XI = ,F9.4, 9X,9H DELTA = ,1PE14.6,10X,7HDITL = ,
      1  E15.6)

      EPSOT = 0.0
      WRITE (6,210) EPSOT,QC,QCP
      210 FORMAT ( 1HC,7H EPS = ,F9.4,9X,5H QC = E15.6,2X,13H(WATTS/CM**2),
      1  2X,1H=,E15.6,2X,17H(BTU/FT**2 - SEC) )
      WRITE(6,212) RZB,QR,QRP
      212 FORMAT ( 1HC,6H RZB =,F9.4,10X,5H QR = E15.6,2X,13H(WATTS/CM**2),
      1  2X,1H=,E15.6,2X,17H(BTU/FT**2 - SEC) )
      WRITE(6,213) RVW,QKP,QFR
      213 FORMAT(1HC,6H RVW= ,F9.4,10X,6H QKP = E14.6,12X,6H QFR = E15.6)
      WRITE (6,214) QRT,QI,RLAMBA
      214 FORMAT (1H ,25X,6H QRT =E14.6,12X,6H QT = E15.6,8X,
      1  9HLAMBA = ,E15.6)

```

OUTP109A
 OUTP1100
 OUTP1110
 OUTP1120
 OUTP1130
 OUTP1140
 OUTP1150
 OUTP1160
 OUTP1170
 OUTP1180
 OUTP1190
 OUTP1200
 OUTP1210
 OUTP1220
 OUTP1230
 OUTP1240
 OUTP1250
 OUTP1260
 OUTP1270
 OUTP1280
 OUTP1290
 OUTP1300
 OUTP1310
 OUTP1320
 OUTP1330
 OUTP1340
 OUTP1350
 OUTP1360
 OUTP1370
 OUTP1380
 OUTP1390
 OUTP1400
 OUTP1410
 OUTP1420
 OUTP1430
 OUTP1440

```

C
      WRITE(6,215) QTCIAL,QTOIP
      FORMAT(1H0,16HTCTIAL HEATING = E15.6,2X,13H(WATTS/CM**2),
      1 2X,1H=E15.6,2X,17H(BTU/FT**2 - SEC)
      )
      WRITE(6,216) QCRAT,QRRAT,QTRAT
      FORMAT(21HCHEATING DISTRIBUTION ,
      1 5X,5H QC/QCZ = E14.6,2X,8HQR/QRZ = E14.6,2X,
      1 8HQT/QTZ = E14.6 ,///)
C
      ** PRINT Y/D , F AND T PROFILES **
C
C
      WRITE(6,205)
      FORMAT(1H0,7X, 4H ETA, 5X, 4HY/DZ, 8X, 2HF., 8X, 3H RV, 8X ,
      1 4HT/TD, 4X ,13H E(WATTS/CM3),4X,2H V, 7X,12H V (FT/SEC) ,
      2 5X,2H G,6X,12H H (STATIC) , //)
      FP = 0.0
      NS=NSP
C
      DO 100 I=1,NETA
C COMPUTE ENTHALPIES
      IF(IEM,LT,IAB) NS=7
      HSTAT = 0.0
      DO 99 J=1,NS
      HSTAT = HSTAT + HS(J,I)*C(J,I)
      G = HSTAT + V(I)**2
C
      HEAD=HEAD2
      IF(I.EQ. 1) HEAD=HEAD1
      IF (I.EQ. NETA) HEAD=HEAD3
      YDZ = YOND(I)
      IF(I.EQ. NETA) FP =1.0
      RV = -FC(I)*DTIL*2.
      VS = V(I) *UINF
      WRITE(6,208) HEAD,ETA(I),YDZ,FP,RV,T(I),E(I),V(I),VS,G,HSTAT
      FORMAT(1H ,A4, F6.3,1P1E12.3)
      IF(I,LT,NETA-1) FP = Z(I)*DTIL
      208
      OUTPUT1450
      OUTPUT1460
      OUTPUT1470
      OUTPUT1480
      OUTPUT1490
      OUTPUT1500
      OUTPUT1510
      OUTPUT1520
      OUTPUT1530
      OUTPUT1540
      OUTPUT1550
      OUTPUT1560
      OUTPUT1570
      OUTPUT1580
      OUTPUT1590
      OUTPUT1600
      OUTPUT1610
      OUTPUT1620
      OUTPUT1630
      OUTPUT1640
      OUTPUT1650
      OUTPUT1660
      OUTPUT1670
      OUTPUT1680
      OUTPUT1690
      OUTPUT1700
      OUTPUT1710
      OUTPUT1720
      OUTPUT1730
      OUTPUT1740
      OUTPUT1750
      OUTPUT1760
      OUTPUT1770
      OUTPUT1780
      OUTPUT1790
      OUTPUT1800

```

```

C      100 CONTINUE
C
C      ** WRITE OUT SHOCK LAYER GAS PROPERTIES **
C
C      WRITE(6,44)
C      FORMAT(1H1,48X,28H-SHOCK LAYER GAS PROPERTIES- )
C
C      44
C
C      WRITE(6,206)
C      FORMAT(1H0,3X,3HETA,8X,4H Y/D,12X,2HP ,12X,2H T,11X,3HRHD,11X,2HMU,
C      1      , 12X, 3HRMU,11X,2H K)
C
C      206
C
C      WRITE(6,207)
C      FORMAT(1H ,27X,6H(ATM.),6X,13H (DEG.KEL.) ,12H(SLUGS/FT3) .2X,
C      1      28H(LBM/FT-SEC) (LBF2-SEC3/FT6) .16H (BTU/FT-SEC-R) ,//))
C
C      DO 101 I=1,NETA
C
C      TS = T(I)*TD
C      WRITE(6,8)ETA(I),YOND(I),PI(I),TS ,RHO(I),MU(I),RM (I),AK(I)
C
C      3 FORMAT(1H F7.4,1P8E14.4)
C      9 FORMAT(1H F7.4,1P7E14.4)
C
C      101 CONTINUE
C
C      ** WRITE SPECIES MASS FRACTIONS **
C
C      WRITE(6,230)
C      FORMAT(1H1,48X,26H-SPECIES MASS FRACTIONS- )
C      WRITE(6,231)
C      231 FORMAT(1H ,14X,3H O2,11X,2HN2,11X,3H O ,11X,3H N ,11X,3H O+,
C      1      11X,3H N+,11X,3H E-,//)
C
C      DO 102 I=1,NETA
C      WRITE(6,8) ETA(I),C(1,I),C(2,I),C(3,I),C(4,I),C(5,I),
C      1      C(6,I),C(7,I)
C
C      102 CONTINUE

```



```

      WRITE(5,230)
      WRITE(5,233) (SP(I),I=8,15)
233  FORMAT(2X,4H ETA,1X,8(10X,A4)//)
      WRITE(6,8) (ETA(I), (C(J,I),J= 8,15),I=1,NETA)
      WRITE(6,230)
      WRITE(6,234) (SP(I),I=16,20)
234  FORMAT(2X,4H ETA,7X,3H CP,5(11X,A4),8X,4H AMW,/)
      WRITE(6,9) (ETA(I),CP(I),(C(J,I),J=16,20),AMW(I),I=1,NETA)
C NONDIMENSIONALIZE
DO1001I=1,NETA
  RHO(I) = RHO(I)/RDZ
  RM(I) = RM(I)/RMDZ
  E(I) = ((E(I)*R)/(RINF*UINF**3))*20866.0*RZB
  CP(I) = CP(I)*CPNF
1001 AK(I) = AK(I)*AKNF
      WRITE(7,217) (T (I),I=1,NETA)
      WRITE (7,217) (RHO(I),I=1,NETA)
      WRITE (7,217) (RM (I),I=1,NETA)
      WRITE(7,217) (ETA(I),I=1,NETA)
217  FORMAT(6E12.5)
1000 CONTINUE
C
      RETURN
C
      END

```

```

OUTPUT2170
OUTPUT2180
OUTPUT2190
OUTPUT2200
OUTPUT2210
OUTPUT2220
OUTPUT2230
OUTPUT2240
OUTPUT2250
OUTPUT2260
OUTPUT2270
OUTPUT2280
OUTPUT2290
OUTPUT2300
OUTPUT2310
OUTPUT2320
OUTPUT2330
OUTPUT2340
OUTPUT2350
OUTPUT2360
OUTPUT2370
OUTPUT2380
OUTPUT2390
OUTPUT2400
OUTPUT2410

```

```

C      SUBROUTINE ERROR ( N )
C
C      IF(N .EQ. 1 ) WRITE(6,1 )
C
C      IF(N .EQ. 2 ) WRITE(6,2 )
C
C      IF(N .EQ. 3) WRITE(6,3)
C
C      RETURN
C
C      FORMAT(36H1 MOMENTUM EQUATION DID NOT CONVERGE )
C      FORMAT(34H1 ENERGY EQUATION DID NOT CONVERGE )
C      FORMAT(54H MOMENTUM AND ENERGY FAILED TO CONVERGE SIMULTANEOUSLY )
C
C      END

```

```

SUBROUTINE ELPROF
COMMON /FRSTRM/ U INF, RINF, UINF2, R , RE, LXI, ITM, IEM, NT
COMMON /VEL/ F(60),FC(60),Z(60),VV(60)
COMMON /YL/ ET(60),YOND(60)
COMMON/PROPI/PI(60),RO(60),TT(60),AMW(60),C (20,60),CC(5,60)
DOUBLE PRECISION NAME(9)
DATA NAME/' CARBON ','HYDROGEN','NITROGEN',' OXYGEN ','ELECTRON',
      , T(OK) ','VELOCITY',' Y/D ',' DENSITY'/
1 PRINT 103
PRINT 100,NAME
DO5N=1,NT
5 PRINT 101,ET(N),(CC(I,N),I=1,5),TT(N),VV(N),YOND(N),RO(N)
RETURN
100 FORMAT( 5X,'ETA',3X,9(2X,A8,2X))
101 FORMAT(F10.4,1X,9E12.4)
103 FORMAT(15X,14(' '),ELEMENTAL MASS FRACTIONS',15(' '))
END

```

```

ELPR 10
ELPR 20
ELPR 30
ELPR 40
ELPR 50
ELPR 60
ELPR 70
ELPR 80
ELPR 90
ELPR 100
ELPR 110
ELPR 120
ELPR 130
ELPR 140
ELPR 150
ELPR 160
ELPR 170

```

```

SUBROUTINE MULTI
COMMON /DEL/ DELTA,DTIL,DTILS
COMMON /FRSTRM/ U INF, RINF, UINF2,RAD, RE, LXI, ITM, IEM,NETA
COMMON /RH/ DUD,DPHI,TD,RZB,PD,HD,HTOTAL
COMMON /YL/ ET( 60),YOND( 60)
COMMON /VEL/ F( 60),FC( 60),ZZ( 60),VV( 60)
COMMON/PROPI/PI( 60),RO( 60),TT( 60),AMW( 60),C (20, 60),CC(5, 60)MULT 10
COMMON/NUMBER/NSP,NNS,NE,NCMULT 20

PUNCHES DATA PKG. FOR MULTICOMPONENT DIFFUSION ANALYSISMULT 30
MULT 40
MULT 50
MULT 60
MULT 70
MULT 80
MULT 90
MULT 100
MULT 110
MULT 120
MULT 130
MULT 140
MULT 150
MULT 160
MULT 170
MULT 180
MULT 190
MULT 200
MULT 210
MULT 220
MULT 230
MULT 240
MULT 250
MULT 260
MULT 270
MULT 280
MULT 290
MULT 300
MULT 310
MULT 320
MULT 330

M=7
TOL=.01
RINF=RINF*32.164
DO10N=1,NETA
TT(N)=TT(N)*TD
VV(N)=VV(N)*UINF

WRITE(M,100)NETA,NSP,NE,NSP
WRITE(M,101)TOL,UINF,DTIL,RAD,RINF,RZB,DELTA

WRITE(M,102)( ET(N),N=1,NETA)
WRITE(M,102)(YOND(N),N=1,NETA)
WRITE(M,102)( TT(N),N=1,NETA)
WRITE(M,102)( PI(N),N=1,NETA)
WRITE(M,102)( VV(N),N=1,NETA)
WRITE(M,102)( RO(N),N=1,NETA)

RETURN
100 FORMAT(5X,21S,5X,2I5)
101 FORMAT(8E10.4)
102 FORMAT(6E12.4)
END

```

```

BLOCK DATA
COMMON/FINV/ N4VL,NIHVC,FHVC(12),DJ(9),HVJ(9),ZKZ
COMMON /FRSTRM/ U INF, RINF, UINF2, R , RE, LXI, ITM, IEM, NETA
COMMON/GUESS/TG1(6C),TG2(6C)
COMMON/PROPI/PI(6C),RHO(6C), T(6C),AMW(50),C (20,60),EC(5,60)
COMMON/PROP2/ MU(6C),RM(60), AK(60)
COMMON/PROP3/CPS(20,60),HS(20,60),CP (60),HM(60)
COMMON/NUMBER/NSP,NNS,NE,NC
COMMON/ELSP/LSP(5)
COMMON/ID/SP(20),EL(5)
COMMON/WT/SMW(20),AWT(5)
COMMON /BLOCK1/V1(20),V2(20),V3(20)
COMMON/BLOCK3/K1(20),K2(20)
COMMON/EQ1/AI(20),BI(20),CI(20),DI(20),EI(20),FI(20),GI(20),
X      AII(20),BII(20),CII(20),DII(20),EII(20),FII(20),GII(20)
COMMON/EQ2/AA(20,5),ICODE(20)
COMMON/EQ3/IA(20,5)
REAL K1,K2
DATA NETA/0/
DATA RHO /25,1,14,3,8,85,6,50,4,37,3,01,2,49,2,17,1,90,1,67,1,46,
1      1,29,1,16,1,08,1,03,1,00,4,4*1,0/
DATA RM /10,0,7,71,5,89,5,10,4,18,3,54,3,31,3,10,2,83,2,48,2,09,
1      1,72,1,42,1,22,1,09,1,02,4,4*1,0/
DATA TG1 / .1033,.,2294,.,3531,.,4719,.,5777,.,6531,.,6867,.,7034,.,7145,
1 .7236,.,7321,.,7401,.,7479,.,7554,.,7628,.,7699,.,7769,.,7836,.,7902,
2 .7967,.,8030,.,8092,.,8153,.,8213,.,8272,.,8331,.,8389,.,8447,.,8504,
3 .8562,.,8619,.,8676,.,8734,.,8791,.,8850,.,8908,.,8968,.,9028,.,9089,
4 .9151,.,9215,.,9280,.,9347,.,9417,.,9488,.,9563,.,9641,.,9723,.,9809,
5 .9901,10*1,0/
DATA TG2 / .3325,.,3325,.,3325,.,3325,.,3325,.,3325,.,3325,.,3326,.,3328,
1 .3331,.,3336,.,3344,.,3357,.,3378,.,3408,.,3452,.,3515,.,3601,.,3718,
2 .3873,.,4076,.,4335,.,4665,.,5075,.,5560,.,6054,.,6487,.,6857,.,7161,
3 .7404,.,7595,.,7749,.,7878,.,7993,.,8100,.,8203,.,8302,.,8399,.,8496,
4 .8594,.,8693,.,8797,.,8904,.,9019,.,9142,.,9278,.,9476,.,9609,.,9757,
5 .9877,10*1,0/
DATA 10
DATA 20
DATA 30
DATA 40
DATA 50
DATA 60
DATA 70
DATA 80
DATA 90
DATA 100
DATA 110
DATA 120
DATA 130
DATA 140
DATA 150
DATA 160
DATA 170
DATA 180
DATA 190
DATA 200
DATA 210
DATA 220
DATA 230
DATA 240
DATA 250
DATA 260
DATA 270
DATA 280
DATA 290
DATA 300
DATA 310
DATA 320
DATA 330
DATA 340
DATA 350
DATA 360

```

```

DATA NSP,NNS,NE,NC/20,0,5,20/
DATA SP/ '02 ' 'N2 ' ' ' 'O ' ' ' 'N ' ' ' 'O+ ' '
1 'N+ ' ' 'E- ' ' 'C ' ' 'H ' ' 'H2 ' '
2 'CO ' ' 'C3-G ' ' 'CN ' ' 'C2H ' ' 'C2H2 ' '
3 'C3H ' ' 'C4H ' ' 'HCN ' ' 'C2 ' ' 'C+ ' /
DATA SMW/32,000, 28,016, 16,000, 14,008, 16,000,
1 14,008, 5,486E-4, 12,011, 1,008, 2,016,
2 28,011, 36,033, 26,019, 25,030, 26,038,
3 37,041, 49,052, 27,027, 24,022, 12,011/
DATA V1/0,1693E 01,0,9704E 00,0,1519E 01,0,2534E 00,0,0
1 0,0 .0,0 .0,1997E 01,0,2941E 00,-,7944E-01,
2 0,2404E 01,0,2019E 01,0,2404E 01,0,2404E 01,0,1396E 01,
3 0,2019E 01,0,2019E 01,0,1378E 01,0,1931E 01,0,0 /
DATA V2/0,1496E-02,0,1613E-02,0,1875E-02,0,2206E-02,0,5000E-03,
1 0,5000E-03,0,5000E-03,0,1772E-02,0,8893E-03,0,7907E-03,
2 0,1363E-02,0,1179E-02,0,1363E-02,0,1363E-02,0,8423E-03,
3 0,1179E-02,0,1179E-02,0,9651E-03,0,1393E-02,0,5000E-03/
DATA V3/-,2276E-07,-,1916E-07,-,2228E-07,-,3737E-07,-,1000E-07,
1 -,1000E-07,-,1000E-07,-,3379E-07,-,8111E-08,-,8864E-08,
2 -,2184E-07,-,1655E-07,-,2184E-07,-,2184E-07,-,6939E-08,
3 -,1655E-07,-,1655E-07,-,9481E-08,-,2575E-07,-,1000E-07/
DATA AI/0,3316E 01,0,3221E 01,0,2670E 01,0,2474E 01,0,2491E 01,
1 0,2727E 01,0,2500E 01,0,2612E 01,0,2500E 01,0,3358E 01,
2 0,3254E 01,0,4002E 01,0,3411E 01,0,3485E 01,0,3891E 01,
3 0,3965E 01,0,5374E 01,0,3654E 01,0,4443E 01,0,2609E 01/
DATA BI/0,1151E-02,0,9878E-03,-,1970E-03,0,9037E-04,0,2762E-04,
1 -,2820E-03,0,3440E-06,-,2030E-03,-,8243E-06,0,2794E-03,
2 0,9698E-03,0,3541E-02,0,4897E-03,0,3563E-02,0,5717E-02,
3 0,6200E-02,0,7403E-02,0,3444E-02,-,2386E-03,-,1393E-03/

```

```

DATA C1/-0.3726E-06,-0.2907E-06,0.0.7193E-07,-0.7814E-07,-0.1881E-07, DATA 730
1 0.1105E-06,-0.1954E-09,0.0.1095E-06,0.6421E-09,0.9372E-07, DATA 740
2 -0.2647E-06,-0.1318E-05,0.0.1705E-06,-0.1237E-05,-0.1957E-05, DATA 750
3 -0.2265E-05,-0.2729E-05,-0.1258E-05,0.0.3036E-06,0.5959E-07/ DATA 760
DATA 770
DATA 780
DATA 790
DATA 800
DATA 810
DATA 820
DATA 830
DATA 840
DATA 850
DATA 860
DATA 870
DATA 880
DATA 890
DATA 900
DATA 910
DATA 920
DATA 930
DATA 940
DATA 950
DATA 960
DATA 970
DATA 980
DATA 990
DATA1000
DATA1010
DATA1020
DATA1030
DATA1040
DATA1050
DATA1060
DATA1070
DATA1080

DATA DI/0.6186E-10,0.3938E-10,-0.8901E-11,0.2218E-10,0.3807E-11,
1 -0.1651E-10,0.3937E-13,-0.1695E-10,-0.1720E-12,-0.2948E-10,
2 0.3037E-10,0.2064E-09,-0.3473E-10,0.1866E-09,0.2931E-09,
3 0.3717E-09,0.4437E-09,0.2169E-09,-0.6244E-10,-0.1037E-10/

DATA EI/-0.3666E-14,-0.2000E-14,0.4002E-15,-0.1489E-14,-0.1028E-15,
1 0.7847E-15,-0.2573E-17,0.8590E-15,0.1457E-16,0.2141E-14,
2 -0.1177E-14,-0.1144E-13,0.2361E-14,-0.1013E-13,-0.1585E-13,
3 -0.2262E-13,-0.2537E-13,-0.1430E-13,0.3915E-14,0.6345E-15/

DATA FI/-0.1044E 04,-0.1043E 04,0.2915E 05,0.5609E 05,0.1879E 06,
1 0.2254E 06,-0.7450E 03,0.8542E 05,0.2547E 05,-0.1018E 04,
2 -0.1434E 05,0.9423E 05,0.4745E 05,0.5809E 05,0.2590E 05,
3 0.6283E 05,0.7605E 05,0.1442E 05,0.9787E 05,0.2168E 06/

DATA GI/0.5393E 01,0.4326E 01,0.4504E 01,0.4300E 01,0.4424E 01,
1 0.3645E 01,-0.1173E 02,0.4144E 01,-0.4612E 00,-0.3548E 01,
2 0.4875E 01,0.2020E 01,0.4746E 01,0.4784E 01,0.6520E 00,
3 0.3467E 01,-0.4010E 01,0.2373E 01,-0.1090E 01,0.3709E 01/

DATA HI/0.3721E 01,0.3727E 01,0.2548E 01,0.2746E 01,0.2944E 01,
1 0.2499E 01,0.2508E 01,0.2141E 01,0.3934E 01,0.3363E 01,
2 0.3366E 01,0.2213E 02,0.3473E 01,0.5307E 01,0.6789E 01,
3 0.3965E 01,0.5874E 01,0.3654E 01,0.4026E 01,0.2528E 01/

DATA IJ/0.4254E-03,0.4084E-03,-0.5952E-04,-0.3909E-03,-0.4108E-03,
1 -0.3725E-05,-0.6332E-05,0.3219E-03,-0.1776E-02,0.4656E-03,
2 0.8027E-03,-0.1759E-01,0.7337E-03,0.8966E-03,0.1503E-02,
3 0.6200E-02,0.7403E-02,0.3444E-02,0.4857E-03,0.4869E-05/

DATA CII/-0.2835E-07,-0.1140E-06,0.2701E-07,0.1338E-06,0.9156E-07,

```

```

1      0.1147E-07,0.1364E-08,-.5498E-07,0.6013E-06,-.5127E-07, DATA1090
2      -.1968E-06,0.5565E-05,-.9088E-07,-.1378E-06,-.2295E-06, DATA1100
3      -.2265E-05,-.2729E-05,-.1258E-05,-.7026E-07,-.7026E-08/ DATA1110
C
DATA DI1/0.6050E-12,0.1154E-10,-.2798E-11,-.1191E-10,-.5848E-11, DATA1120
1      -.1102E-11,-.1094E-12,0.3604E-11,-.7819E-10,0.2802E-11, DATA1130
2      0.1940E-10,-.6758E-09,0.4847E-11,0.9251E-11,0.1534E-10, DATA1140
3      0.3717E-09,0.4437E-09,0.2169E-09,0.4666E-11,0.1134E-11/ DATA1150
C
DATA EI1/-0.5186E-17,-.3293E-15,0.9380E-16,0.3369E-15,0.1190E-15, DATA1160
1      0.3078E-16,0.2934E-17,-.5564E-16,0.3482E-14,-.4905E-16, DATA1170
2      -.5549E-15,0.2825E-13,-.1018E-15,-.2278E-15,-.3763E-15, DATA1180
3      -.2262E-13,-.2637E-13,-.1430E-13,-.1142E-15,-.3476E-16/ DATA1190
C
DATA FI1/-0.1044E 04,-.1043E 04,0.2915E 05,0.5609E 05,0.1879E 06, DATA1200
1      0.2254E 06,-.7450E 03,0.8542E 05,0.2547E 05,-.1018E 04, DATA1210
2      -.1434E 05,0.9423E 05,0.5420E 05,0.5809E 05,0.2590E 05, DATA1220
3      0.6283E 05,0.7605E 05,0.1442E 05,0.9787E 05,0.2168E 06/ DATA1230
C
DATA GI1/0.3254E 01,0.1294E 01,0.5049E 01,0.2872E 01,0.1750E 01, DATA1240
1      0.4950E 01,-.1208E 02,0.6874E 01,-.8598E 01,-.3716E 01, DATA1250
2      0.4263E 01,-.1021E 03,0.4152E 01,-.5288E 01,-.1539E 02, DATA1260
3      0.3467E 01,-.4010E 01,0.2373E 01,0.1090E 01,0.4139E 01/ DATA1270
C
DATA KI1/0.1019E 01,0.6541E 00,0.1250E 01,0.1281E 01,2.6000E 01, DATA1280
1      2.6000E 01,2.6000E 01,0.2506E 01,0.2496E 01,0.3211E 01, DATA1290
2      0.8589E 00,0.6304E 00,0.8589E 00,0.1126E 01,0.1126E 01, DATA1300
3      0.6304E 00,0.6304E 00,0.4855E 00,0.8589E 00,0.1000E-04/ DATA1310
C
DATA K2/0.4401E-03,0.6457E-03,0.7092E-03,0.8593E-03,0.0000E-03, DATA1320
1      0.0000E-03,0.0000E-03,0.7479E-03,0.5129E-02,0.5344E-02, DATA1330
2      0.6233E-03,0.5804E-03,0.6233E-03,0.7439E-03,0.7439E-03, DATA1340
3      0.5804E-03,0.5804E-03,0.8714E-03,0.6233E-03,0.7350E-03/ DATA1350
C
DATA ICODE/20*0/ DATA1360
DATA1370
DATA1380
DATA1390
DATA1400
DATA1410
DATA1420
DATA1430
DATA1440

```



```

DATA FL/ 'C', 'H', 'N', 'O', 'E' /
DATA AWT/ 12.011, 1.008, 14.008, 16.000, 5.486E-4 /

DATA IA/ 0.0,0.0,0.0,0.0,1.0,0.0,1.3,1.2,2.3,4.1,2.1,
H      0.0,0.0,0.0,0.0,1.2,0.0,0.1,2.1,1.1,0.0,
N      0.2,0.1,0.1,0.0,0.0,0.0,1.0,0.0,0.1,0.0,
O      2.0,1.0,1.0,0.0,0.1,0.0,0.0,0.0,0.0,0.0,
E      2.2,1.1,0.0,1.1,0.0,2.3,2.2,2.3,4.2,2.2,0/

DATA LSP/20.9,6.5,7/
DATA NHVL /9/, NIHVC /12/
DATA FHVC /5.0, 6.0, 7.0, 8.0, 9.0, 10.0, 10.8, 11.1,
1 12.0, 13.4, 14.3, 20.0/
DATA DJ /0.6, 2.2, 1.5, 1.65, 1.4, 1.0, 1.2, 1.4, 1.0/
DATA HVJ /1.3, 2.7, 5.75, 7.57, 9.1, 10.4, 11.4, 12.7, 13.9/
DATA ZKZ /7.26E-16/
END

```

```

DATA1450
DATA1460
DATA1470
DATA1480
DATA1490
DATA1500
DATA1510
DATA1520
DATA1530
DATA1540
DATA1550
DATA1560
DATA1570
DATA1580
DATA1590
DATA1600
DATA1610

```


0.53750E-01	0.62500E-01	0.71250E-01	0.80000E-01	0.85000E-01	0.92500E-01	
0.10000E 00	0.11000E 00	0.12000E 00	0.13000E 00	0.14000E 00	0.15000E 00	
0.16000E 00	0.17000E 00	0.18000E 00	0.20000E 00	0.21000E 00	0.22000E 00	
0.23000E 00	0.24000E 00	0.26000E 00	0.28000E 00	0.30000E 00	0.33000E 00	
0.35000E 00	0.38000E 00	0.42000E 00	0.44000E 00	0.48000E 00	0.50000E 00	
0.54000E 00	0.56000E 00	0.58000E 00	0.62000E 00	0.64000E 00	0.68000E 00	
0.70000E 00	0.74000E 00	0.76000E 00	0.80000E 00	0.82000E 00	0.86000E 00	
0.88000E 00	0.92000E 00	0.94000E 00	0.98000E 00	0.10000E 01		
1.0E-10	.02389		1.0E-10	2.0E-05		1.0E-10
1.0E-10	1.0E-10		.00157	.01708		.03277
.25780	.01767		.00310	.15000		.08216
.20370	.15890		.04710	.00413		1.0E-10

NO. SPECIES =	20	1	C	2	H	3	N	4	O	5	E
		1	O2	2	N2	3	C	4	N	5	O+
		6	N+	7	E-	8	C	9	H	10	H2
		11	CO	12	C3-G	13	CN	14	C2H	15	C2H2
		16	C3H	17	C4H	18	HCN	19	C2	20	C+

NO. SOLIDS = 0

SPECIES NAME SMW WALL MASS FRACTION

O2	32.000	0.1000E-09
N2	28.016	0.2389E-01
O	16.000	0.1000E-09
N	14.008	0.2000E-04
O+	16.000	0.1000E-09
N+	14.008	0.1000E-09
E-	0.001	0.1000E-09
C	12.011	0.1570E-02
H	1.008	0.1708E-01
H2	2.016	0.3277E-01
CO	28.011	0.2578E 00
C3-G	36.033	0.1767E-01
CN	26.019	0.3100E-02
C2H	25.030	0.1500E 00
C2H2	26.038	0.8216E-01
C3H	37.041	0.2037E 00
C4H	49.052	0.1589E 00
HCN	27.027	0.4710E-01
C2	24.022	0.4130E-02
C+	12.011	0.1000E-09

DENSITY RATIO REYNOLDS NO.
0.536357E-01 0.311032E 06

DELTA DTIL
0.418359E-01 0.106019E 00

0.05 BLOWING CASE 0.1 ATMOSPHERE

INPUT DATA

KEEP = 0
 META = 59
 MAXM = 15
 MAXE = 15
 MAXD = 15
 FPRCT = 4.999999E-03
 TPRCT = 4.995999E-03
 LT = 2
 IDEBUG = 0
 IPHI = 0
 UNIF = 5.000000E 04
 RINF = 8.849997E-08
 R = 9.000000E 00
 TW = 3.450000E 03
 MTOTAL = 1.250000E 09
 RVW = 5.000000E-02
 OXI = 0.0
 PDIL = 9.999999E-04

 * COUPLED RADIATION CALCULATION *
 * CONTINUUM AND LINE CALCULATION *

INITIAL T PROFILE
 0.26543 0.26995 0.27470 0.27972 0.28505 0.28855 0.29220 0.29600 0.29998 0.30413 0.30846 0.31771
 0.33187 0.34731 0.36387 0.38144 0.39192 0.40829 0.42539 0.44927 0.47403 0.49951 0.52554 0.55146
 0.57621 0.59891 0.61933 0.65350 0.66844 0.68234 0.69555 0.70835 0.73310 0.75734 0.78036 0.81150
 0.82929 0.85139 0.87347 0.88234 0.89646 0.90210 0.91165 0.91591 0.92002 0.92797 0.93172 0.93903
 0.94263 0.94959 0.95309 0.96002 0.96350 0.97049 0.97411 0.98153 0.98559 0.99414 1.00000
 INITIAL RHO PROFILE
 5.29860 5.01820 4.74330 4.47480 4.21300 4.05410 3.89980 3.75070 3.60770 3.47220 3.34450 3.11500
 2.85320 2.65140 2.48940 2.34840 2.27230 2.16120 2.05330 1.91540 1.78730 1.67720 1.59020 1.52470
 1.47570 1.43970 1.41460 1.39230 1.39030 1.39310 1.39940 1.40800 1.42930 1.45020 1.46840 1.46600
 1.49000 1.48370 1.45650 1.43810 1.39700 1.37810 1.34240 1.32570 1.30980 1.27990 1.26340 1.23660
 1.22530 1.20030 1.18760 1.16360 1.15140 1.12810 1.11610 1.09190 1.07920 1.05250 1.03510
 INITIAL RM PROFILE
 3.43370 3.27700 3.12140 3.13190 2.97060 2.87070 2.89750 2.79580 2.69610 2.71120 2.61370 2.55200
 2.44190 2.36900 2.32130 2.28730 2.21830 2.24740 2.22290 2.14020 2.03820 2.03820 2.04960
 2.03790 2.03080 2.02790 2.04140 2.05520 2.07350 2.09510 2.11830 2.16720 2.20920 2.23930 2.24980
 2.23330 2.17910 2.07450 2.04930 1.89950 1.67440 1.75350 1.73200 1.71150 1.59370 1.57580 1.54270
 1.45710 1.42740 1.41220 1.36650 1.29270 1.26660 1.19530 1.16930 1.05260 1.03510

DEPS/OXI

0.0

SPECIES INPUTS

NO. ELEMENTS = 5

NUMBER DENSITIES (PARTICLES/CM³)

ETA	N2	O2	N	C	E-	H	C	C2	H2	CC	C3	C2H
0.0	9.67E 15	5.05E 02	2.49E 13	1.95E 10	3.41E 13	1.00E 17	2.91E 15	2.59E 15	1.71E 16	4.80E 16	5.51E 15	1.61E 16
5.00E-03	6.78E 15	7.41E 02	3.32E 13	2.86E 10	3.51E 13	1.03E 17	4.12E 15	3.40E 15	1.33F 16	2.65E 16	6.08E 15	1.48E 16
1.00E-02	7.91E 15	1.11E 03	4.43E 13	4.17E 10	3.13F 13	1.06E 17	5.78E 15	4.38E 15	1.02E 16	2.50F 16	6.51E 15	1.32E 16
1.50E-02	7.07E 15	1.71E 03	5.91E 13	6.18E 10	2.83E 13	1.07E 17	8.04E 15	5.49E 15	7.56F 15	2.36E 16	6.66F 15	1.13E 16
2.00E-02	6.31E 15	2.76E 03	7.91E 13	9.40E 10	3.06E 13	1.07E 17	1.10E 16	6.63E 15	5.48F 15	2.21E 16	6.43E 15	9.18E 15
2.31E-02	5.89E 15	3.64E 03	9.54E 13	1.24E 11	2.97E 13	1.06E 17	1.33E 16	7.30E 15	4.43E 15	2.13E 16	6.00E 15	7.81E 15
2.62E-02	5.42E 15	4.42E 03	1.16E 14	1.67E 11	2.90E 13	1.05E 17	1.59E 16	7.86E 15	3.53E 15	2.04E 16	5.51E 15	6.45E 15
2.94E-02	5.20E 15	5.08E 03	1.41E 14	2.28E 11	2.73E 13	1.04E 17	1.88E 16	8.23E 15	2.79E 15	1.96E 16	4.81E 15	5.15E 15
3.25E-02	4.95E 15	1.24E 04	1.73E 14	3.17E 11	2.66E 13	1.02E 17	2.19E 16	8.41E 15	2.18E 15	1.88E 16	4.01E 15	4.97E 15
3.56E-02	4.70E 15	1.98E 04	2.15E 14	4.52E 11	2.62E 13	1.00E 17	2.52E 16	8.29E 15	1.69E 15	1.81E 16	3.17E 15	2.94E 15
3.87E-02	4.65E 15	3.36E 04	2.65E 14	6.61E 11	2.54E 13	9.76E 16	2.85E 16	7.89E 15	1.29E 15	1.74E 16	2.36E 15	2.08E 15
4.50E-02	4.62E 15	1.07E 05	4.35F 14	1.52E 12	2.44E 13	9.26E 16	3.47E 16	6.35E 15	7.46F 14	1.62E 16	1.30E 15	9.17E 14
5.37E-02	4.89E 15	7.33E 05	8.88E 14	5.66E 12	2.20E 13	8.56E 16	4.07E 16	3.71E 15	3.40E 14	1.48E 16	2.61E 14	2.28E 14
6.25E-02	5.11E 15	5.95E 06	1.78E 15	2.27E 13	2.40E 13	7.93E 16	4.33E 16	1.82E 15	1.59E 14	1.37E 16	4.46E 13	4.86E 13
7.12E-02	4.92E 15	4.82E 07	3.30E 15	8.93E 13	3.06E 13	7.36E 16	4.35E 16	8.32E 14	7.63E 14	1.27E 16	8.35E 12	1.00E 13
8.00E-02	4.15E 15	3.52E 08	5.52E 15	3.28E 14	4.76E 13	6.82E 16	4.25E 16	3.78E 14	2.64E 13	1.16E 16	1.48E 12	2.15E 12
8.50E-02	3.52E 15	9.97E 08	6.97E 15	6.44E 14	6.16E 13	6.53E 16	4.17E 16	2.46E 14	2.64E 13	1.09E 16	5.82E 11	9.41E 11
9.25E-02	2.44E 15	4.96E 09	9.20E 15	1.60E 15	1.02E 14	6.09E 16	4.06E 16	1.31E 14	1.52E 13	9.22E 15	1.42E 11	2.78E 11
1.00E-01	1.48E 15	1.26E 10	1.13E 16	2.99E 15	1.48E 14	5.63E 16	3.98E 16	7.23E 13	8.65E 12	7.13E 15	4.29E 10	8.67E 10
1.10E-01	5.67E 14	2.48E 10	1.25E 16	5.71E 15	2.87E 14	5.06E 16	3.66E 16	3.35E 13	4.17E 12	3.55E 15	8.00E 09	1.90E 10
1.20E-01	2.09E 14	2.46E 10	1.89E 16	7.33E 15	5.93E 14	4.58E 16	3.67E 16	1.57E 13	2.13E 12	1.27E 15	1.57E 09	4.44E 09
1.30E-01	7.84E 13	1.67E 10	1.3CE 16	7.71E 15	9.19E 14	4.20E 16	3.40E 16	7.49E 12	1.17E 12	1.41E 14	3.34E 08	1.14E 09
1.40E-01	3.45E 13	1.05E 10	1.32E 16	7.63E 15	1.51E 15	3.87E 16	3.09E 16	3.75E 12	6.95E 11	1.45E 14	8.10E 07	3.35E 08
1.50E-01	1.72E 13	7.32E 09	1.34E 16	7.62E 15	2.25E 15	3.58E 16	2.79E 16	1.98E 12	4.37E 11	5.65E 13	2.24E 07	1.10E 08
1.60E-01	9.59E 12	5.18E 09	1.36E 16	7.21E 15	3.12E 15	3.32E 16	2.49E 16	1.09E 12	2.90E 11	2.46E 13	6.98E 06	4.06E 07
1.70E-01	5.96E 12	3.04E 09	1.40E 16	6.87E 15	5.00E 15	3.08E 16	2.20E 16	6.31E 11	2.01E 11	1.19E 13	2.43E 06	1.65E 07
1.80E-01	4.08E 12	3.04E 09	1.44E 16	6.72E 15	6.04E 15	2.86E 16	1.93E 16	3.79E 11	1.46E 11	6.38E 12	9.32E 05	7.36E 06
2.00E-01	2.45E 12	2.17E 09	1.54E 16	6.71E 15	7.29E 15	2.33E 16	1.30E 16	1.03E 11	8.48E 10	2.35E 12	1.81E 05	1.85E 06
2.10E-01	2.08E 12	1.94E 09	1.61E 16	6.71E 15	7.81E 15	2.18E 16	1.15E 16	5.11E 10	4.45E 10	1.13E 12	4.73F 04	6.01E 05
2.20E-01	1.88E 12	1.86E 09	1.58E 16	6.81E 15	8.21E 15	2.04E 16	1.01E 16	5.11E 10	8.54E 10	8.54E 10	2.67E 04	3.70E 05
2.30E-01	1.70E 12	1.71E 09	1.77E 16	6.82E 15	8.59E 15	2.00E 16	9.00E 15	3.74E 10	3.72E 10	6.70E 11	1.56E 04	2.37E 05
2.40E-01	1.74E 12	1.67E 09	1.87E 16	6.82E 15	8.90E 15	1.90E 16	9.00E 15	3.74E 10	2.58E 10	4.47E 11	6.05E 03	1.03E 05
2.60E-01	1.78E 12	1.67E 09	2.06E 16	7.22E 15	9.37E 15	1.39E 16	7.11E 15	1.14E 10	1.73E 10	3.04E 11	2.29E 03	4.41E 04
2.80E-01	1.85E 12	1.71E 09	2.31E 16	7.57E 15	9.11E 15	1.16E 16	4.35E 15	6.84E 09	1.17E 10	2.35E 11	1.03E 03	2.11E 04
3.00E-01	2.13E 12	1.87E 09	2.57E 16	8.04E 15	9.14E 15	8.27E 15	2.84E 15	2.71E 09	5.60E 09	1.44E 11	2.43E 02	5.57E 03
3.30E-01	2.40E 12	2.04E 09	2.91E 16	8.52E 15	9.33E 15	6.24E 15	2.00E 15	1.27E 09	3.06E 09	9.35E 10	7.45E 01	1.87E 03
3.80E-01	2.14E 12	1.95E 09	3.18E 16	9.66E 15	9.88E 15	3.69E 15	1.06E 15	3.23F 08	9.99E 08	4.16E 10	8.92F 00	2.56E 02
4.20E-01	1.64E 12	1.74F 09	3.13E 16	8.92E 15	1.09E 16	1.48E 15	3.74E 14	3.50E 07	1.46E 08	1.12E 10	2.92E-01	9.83E 00
4.40E-01	1.42E 12	1.60E 09	3.05E 16	8.76E 15	1.14E 16	8.18E 14	1.96E 14	9.01E 06	4.27E 07	5.12E 09	3.52E-02	1.32E 00
4.80E-01	1.06E 12	1.35E 09	2.88E 16	8.35E 15	1.24E 16	2.10E 14	4.58E 13	4.50F 05	2.62E 06	9.66E 08	3.54E-04	1.56E-02
5.00E-01	9.35E 11	1.26E 09	2.80E 16	8.16E 15	1.28E 16	7.60E 13	1.64E 13	5.59E 04	3.51E 04	3.12F 08	3.91E-05	6.58E-04
5.40E-01	7.52E 11	1.11E 09	2.64E 16	7.81E 15	1.35E 16	1.34E 13	2.65E 12	1.38E 03	9.91F 03	4.16E 07	4.22E-06	7.12E-07
5.60E-01	6.82E 11	1.04F 09	2.57E 16	7.66E 15	1.38E 16	1.32E 13	2.55E 12	1.24E 03	9.50E 03	3.92E 07	4.17E-06	7.03E-07
5.80E-01	6.20E 11	9.83E 08	2.51E 16	7.50E 15	1.41E 16	1.30E 13	2.46E 12	1.13F 03	9.41F 03	3.54E 07	4.11E-06	6.95E-07
6.20E-01	5.11E 11	8.76E 08	2.35E 16	7.32E 15	1.46E 16	1.28E 13	2.29E 12	9.24E 02	8.41E 03	2.88E 07	4.04E-06	6.80E-07
6.40E-01	4.66E 11	8.30E 08	2.32E 16	7.08E 15	1.48E 16	1.26E 13	2.21E 12	8.44E 02	8.09E 03	2.62E 07	3.99E-06	6.73E-07
6.80E-01	3.91E 11	7.45E 08	2.21E 16	6.82E 15	1.53E 16	1.24E 13	2.07E 12	7.06E 02	7.52E 03	2.18E 07	3.91E-06	6.59E-07
7.00E-01	3.63E 11	7.08E 08	2.21E 16	6.68E 15	1.55E 16	1.22E 13	2.00E 12	6.55E 02	7.26E 03	2.01E 07	3.87E-06	6.52E-07
7.40E-01	3.01E 11	6.34E 08	2.05E 16	6.43E 15	1.60E 16	1.20E 13	1.87E 12	5.44E 02	6.75E 03	1.66E 07	3.79E-06	6.39E-07
7.60E-01	2.80E 11	6.03E 08	1.95E 16	6.30E 15	1.62E 16	1.19E 13	1.69E 12	4.19E 02	6.06F 03	1.54E 07	3.75E-06	6.32E-07
8.00E-01	2.32E 11	5.35E 08	1.84E 16	6.05E 15	1.66E 16	1.16E 13	1.63E 12	3.85E 02	5.85E 03	1.18E 07	3.68E-06	6.20E-07
8.20E-01	2.15E 11	5.11E 08	1.84E 16	5.92E 15	1.69E 16	1.15E 13	1.63E 12	3.85E 02	5.85E 03	1.18E 07	3.68E-06	6.13E-07
8.60E-01	1.77E 11	4.55E 08	1.74E 16	5.68E 15	1.73E 16	1.13E 13	1.52E 12	3.21E 02	5.44E 03	9.66E 06	3.57E-06	6.01E-07
8.80E-01	1.63E 11	4.31E 08	1.69E 16	5.55E 15	1.75E 16	1.12E 13	1.47E 12	2.98E 02	5.25E 03	8.93E 06	3.53E-06	5.94E-07
9.20E-01	1.33E 11	3.79E 08	1.56E 16	5.30E 15	1.79E 16	1.09E 13	1.36E 12	2.43E 02	4.85E 03	7.23E 06	3.45E-06	5.82E-07
9.40E-01	1.14E 11	3.52E 08	1.53E 16	5.16E 15	1.81E 16	1.08E 13	1.30E 12	2.16E 02	4.64E 03	6.40E 06	3.41E-06	5.75E-07
9.80E-01	9.51E 10	3.05E 08	1.42E 16	4.87E 15	1.86E 16	1.05E 13	1.19E 12	1.76E 02	4.26E 03	5.19E 06	3.34E-06	5.61E-07
1.00E 00	7.92E 10	2.74E 08	1.35E 16	4.68E 15	1.89E 16	1.04E 13	1.12E 12	1.48E 02	4.00E 03	4.33E 06	3.27E-06	5.51E-07

CONTINUUM CONTRIBUTION TO THE SPECTRAL FLUX

ETA = 0.0				ETA = 0.500				ETA = 1.000			
I	HNU	QMINUS	QPLUS	QMINUS	QPLUS	QMINUS	QPLUS	QMINUS	QPLUS	QMINUS	QPLUS
1	5.000	0.0	6.212E 01	5.235E-03	1.080E-04	6.213E 01	0.0	6.213E 01	0.0	6.213E 01	0.0
2	6.000	0.0	2.742E 00	8.535E-03	1.085E-04	2.802E 00	0.0	2.802E 00	0.0	2.802E 00	0.0
3	7.000	0.0	1.647E 00	6.654E-02	1.670E-05	1.666E 00	0.0	1.666E 00	0.0	1.666E 00	0.0
4	8.000	0.0	3.153E 00	1.031E-01	2.914E-02	3.457E 00	0.0	3.457E 00	0.0	3.457E 00	0.0
5	9.000	0.0	2.917E 00	1.673E-01	2.084E-01	4.413E 00	0.0	4.413E 00	0.0	4.413E 00	0.0
6	10.000	0.0	1.783E 00	2.689E-01	3.025E-01	1.943E 00	0.0	1.943E 00	0.0	1.943E 00	0.0
7	10.800	0.0	7.986E 00	4.026E-03	5.030E-04	8.806E 00	0.0	8.806E 00	0.0	8.806E 00	0.0
8	11.100	0.0	1.995E 01	1.961E-04	5.030E-04	2.381E 01	0.0	2.381E 01	0.0	2.381E 01	0.0
9	12.000	0.0	1.576E 01	3.315E-21	1.331E-04	5.376E 01	0.0	5.376E 01	0.0	5.376E 01	0.0
10	13.400	0.0	2.887E 01	2.872E-01	1.110E-04	1.369E 02	0.0	1.369E 02	0.0	1.369E 02	0.0
11	14.300	0.0	2.614E 00	2.559E-01	1.114E-04	5.529E 01	0.0	5.529E 01	0.0	5.529E 01	0.0
12	20.000	0.0	5.394E 00	3.498E 00	1.707E-05	1.040E 02	0.0	1.040E 02	0.0	1.040E 02	0.0
TOTAL FLUX		0.0	1.549E 02	4.665E 00	5.416E-01	4.589E 02	0.0	4.589E 02	0.0	4.589E 02	0.0

LINE CONTRIBUTION TO THE SPECTRAL FLUX

ETA = 0.0				ETA = 0.500				ETA = 1.000			
I	HNU	QMINUS	QPLUS	QMINUS	QPLUS	QMINUS	QPLUS	QMINUS	QPLUS	QMINUS	QPLUS
1	1.300	0.0	7.021E 01	0.0	0.0	7.379E 01	0.0	7.379E 01	0.0	7.379E 01	0.0
2	2.700	0.0	1.869E 01	0.0	0.0	1.853E 01	0.0	1.853E 01	0.0	1.853E 01	0.0
3	5.750	0.0	3.855E 00	0.0	0.0	8.118E 00	0.0	8.118E 00	0.0	8.118E 00	0.0
4	7.570	0.0	4.061E 01	0.0	0.0	9.114E 01	0.0	9.114E 01	0.0	9.114E 01	0.0
5	9.100	0.0	3.835E 01	0.0	0.0	8.659E 01	0.0	8.659E 01	0.0	8.659E 01	0.0
6	10.400	0.0	6.289E 01	0.0	0.0	1.448E 02	0.0	1.448E 02	0.0	1.448E 02	0.0
7	11.400	0.0	7.452E 00	0.0	0.0	1.045E 02	0.0	1.045E 02	0.0	1.045E 02	0.0
8	12.700	0.0	1.019E-01	0.0	0.0	5.175E 01	0.0	5.175E 01	0.0	5.175E 01	0.0
9	13.900	0.0	-3.010E-01	0.0	0.0	3.123E 01	0.0	3.123E 01	0.0	3.123E 01	0.0
TOTAL FLUX		0.0	2.419E 02	0.0	0.0	6.105E 02	0.0	6.105E 02	0.0	6.105E 02	0.0

SOLUTION CONVERGED IN 3 ITERATIONS

Reproduced from
best available copy.

XI = 0.0 DELTA = 3.046145E-02 CTIL = 5.383645E-02
 EPS = 0.0 QC = -0.119654E C3 (WATTS/CM**2) = -0.105296E 03 (BTU/FT**2 - SEC)
 RD = 0.0536 QR = -0.350790E C3 (WATTS/CM**2) = -0.349182E 03 (BTU/FT**2 - SEC)
 RVW = 0.0500 OKR = -0.296567E C3 CFR = -0.134537E 03
 ORY = -0.294690E C3 CT = -0.591265E 03 LAMBDA = -0.491320E-01
 TOTAL HEATING = -0.516452E C3 (WATTS/CM**2) = -0.454478E 03 (BTU/FT**2 - SEC)
 HEATING DISTRIBUTION UC/QCZ = 0.100000E 01 QR/QRZ = 0.100000E 01 QT/QTZ = 0.100000E 01

ETA	Y/DZ	F*	RV	T/TO	E(WATTS/CM3)	V	V (FT/SEC)	G	H (STATIC)
WALL 0.0	0.0	0.0	2.683E-03	2.654E-01	-5.902E 01	5.121E-04	2.501E C1	2.427E-01	2.427E-01
0.005	1.336E-03	2.717E-03	2.682E-03	2.710E-01	-5.512E 01	5.431E-04	2.715E C1	2.565E-01	2.565E-01
0.010	2.754E-03	5.699E-03	2.680E-03	2.709E-01	-5.122E 01	5.769E-04	2.885E C1	2.718E-01	2.718E-01
0.015	4.264E-03	8.816E-03	2.678E-03	2.831E-01	-5.018E 01	6.141E-04	3.070E C1	2.849E-01	2.849E-01
0.020	5.874E-03	1.210E-02	2.676E-03	2.857E-01	-5.018E 01	6.549E-04	3.275E C1	3.144E-01	3.144E-01
0.025	6.735E-03	1.430E-02	2.666E-03	2.940E-01	-5.022E 01	6.825E-04	3.412E C1	3.270E-01	3.270E-01
0.026	8.043E-03	1.657E-02	2.661E-03	2.985E-01	-5.130E 01	7.115E-04	3.558E C1	3.459E-01	3.459E-01
0.029	9.200E-03	1.891E-02	2.655E-03	3.032E-01	-5.376E 01	7.419E-04	3.710E C1	3.602E-01	3.602E-01
0.032	1.041E-02	2.159E-02	2.648E-03	3.082E-01	-5.621E 01	7.734E-04	3.867E C1	3.749E-01	3.749E-01
0.036	1.167E-02	2.394E-02	2.640E-03	3.134E-01	-5.975E 01	8.055E-04	4.024E C1	3.946E-01	3.946E-01
0.039	1.299E-02	2.636E-02	2.632E-03	3.188E-01	-6.329E 01	8.377E-04	4.189E C1	4.088E-01	4.088E-01
0.045	1.578E-02	3.221E-02	2.612E-03	3.304E-01	-7.094E 01	8.997E-04	4.458E C1	4.397E-01	4.397E-01
0.054	2.003E-02	4.008E-02	2.578E-03	3.483E-01	-8.164E 01	9.734E-04	4.867E C1	4.695E-01	4.695E-01
0.063	2.465E-02	4.937E-02	2.535E-03	3.678E-01	-8.811E 01	1.031E-03	5.153E C1	4.883E-01	4.883E-01
0.071	2.959E-02	5.906E-02	2.484E-03	3.884E-01	-9.457E 01	1.078E-03	5.390E C1	5.022E-01	5.022E-01
0.080	3.484E-02	6.963E-02	2.424E-03	4.100E-01	-9.769E 01	1.118E-03	5.590E C1	5.161E-01	5.161E-01
0.085	3.798E-02	7.493E-02	2.385E-03	4.227E-01	-9.947E 01	1.137E-03	5.686E C1	5.250E-01	5.250E-01
0.092	4.291E-02	8.408E-02	2.321E-03	4.266E-01	-1.011E 02	1.167E-03	5.834E C1	5.447E-01	5.447E-01
0.100	4.813E-02	9.356E-02	2.249E-03	4.338E-01	-1.028E 02	1.199E-03	5.936E C1	5.717E-01	5.717E-01
0.110	5.561E-02	1.048E-01	2.141E-03	4.944E-01	-1.057E 02	1.236E-03	6.175E C1	6.146E-01	6.146E-01
0.120	6.369E-02	1.266E-01	2.010E-03	5.271E-01	-1.086E 02	1.250E-03	6.251E C1	6.486E-01	6.486E-01
0.130	7.231E-02	1.348E-01	1.882E-03	5.601E-01	-1.124E 02	1.232E-03	6.159E C1	6.663E-01	6.663E-01
0.140	8.138E-02	1.453E-01	1.729E-03	5.915E-01	-1.163E 02	1.184E-03	5.922E C1	6.759E-01	6.759E-01
0.150	9.081E-02	1.635E-01	1.560E-03	6.205E-01	-1.159E 02	1.111E-03	5.555E C1	6.829E-01	6.829E-01
0.160	1.006E-01	1.786E-01	1.376E-03	6.468E-01	-1.156E 02	1.012E-03	5.060E C1	6.885E-01	6.885E-01
0.170	1.105E-01	1.934E-01	1.176E-03	6.594E-01	-1.066E 02	8.871E-04	4.437E C1	6.922E-01	6.922E-01
0.180	1.207E-01	2.081E-01	9.595E-04	6.880E-01	-9.756E 01	7.382E-04	1.631E C1	6.935E-01	6.935E-01
0.200	1.412E-01	2.368E-01	4.805E-04	7.204E-01	-8.049E 01	3.760E-04	1.840E C1	6.663E-01	6.663E-01
0.210	1.514E-01	2.503E-01	2.184E-04	7.329E-01	-7.196E 01	1.709E-04	4.544E C0	6.790E-01	6.790E-01
0.220	1.616E-01	2.632E-01	5.801E-05	7.432E-01	-6.586E 01	4.519E-05	2.279E C0	6.667E-01	6.667E-01
0.230	1.717E-01	2.753E-01	3.478E-04	7.521E-01	-6.957E 00	2.687E-04	1.343E C1	6.597E-01	6.597E-01
0.240	1.816E-01	2.869E-01	6.504E-04	7.601E-01	-4.542E 00	4.969E-04	2.465E C1	6.466E-01	6.466E-01
0.260	2.011E-01	3.076E-01	1.290E-03	7.744E-01	3.154E 01	9.608E-04	6.404E C1	6.296E-01	6.296E-01
0.280	2.207E-01	3.267E-01	1.973E-03	7.888E-01	4.901E 01	1.436E-03	7.181E C1	6.153E-01	6.153E-01
0.300	2.387E-01	3.448E-01	2.696E-03	8.021E-01	6.648E 01	1.890E-03	9.450E C1	6.060E-01	6.060E-01
0.330	2.459E-01	3.717E-01	3.253E-03	8.240E-01	6.300E 01	2.587E-03	1.294E C2	6.075E-01	6.075E-01

0.350	2.840E-01	4.901E-01	-4.673E-03	8.382E-01	6.068E 01	-3.094E-03	-1.547E 02	0.145E-01	6.145E-01
0.380	3.111E-01	4.186E-01	-5.979E-03	8.574E-01	6.968E 01	-4.961E-03	-1.981E 02	0.316E-01	6.316E-01
0.420	3.481E-01	4.586E-01	-7.868E-03	8.782E-01	8.168E 01	-5.350E-03	-2.875E 02	0.60CE-01	6.60CE-01
0.440	3.670E-01	4.784E-01	-8.876E-03	8.867E-01	8.304E 01	-5.138E-03	-3.069E 02	0.724E-01	6.724E-01
0.480	4.057E-01	5.175E-01	-1.102E-02	9.055E-01	8.576E 01	-7.897E-03	-3.948E 02	7.033E-01	7.033E-01
0.500	4.256E-01	5.368E-01	-1.216E-02	9.059E-01	8.912E 01	-8.844E-03	-4.422E 02	7.142E-01	7.142E-01
0.540	4.660E-01	5.748E-01	-1.455E-02	9.149E-01	9.583E 01	-1.088E-02	-5.438E 02	7.384E-01	7.384E-01
0.560	4.866E-01	5.939E-01	-1.581E-02	9.189E-01	1.028E 02	-1.196E-02	-5.982E 02	7.478E-01	7.478E-01
0.580	5.075E-01	6.127E-01	-1.711E-02	9.227E-01	1.082E 02	-1.310E-02	-6.50E 02	7.570E-01	7.569E-01
0.620	5.499E-01	6.504E-01	-1.982E-02	9.302E-01	1.217E 02	-1.553E-02	-7.761E 02	7.782E-01	7.782E-01
0.640	5.715E-01	6.691E-01	-2.124E-02	9.337E-01	1.285E 02	-1.682E-02	-8.412E 02	7.885E-01	7.885E-01
0.680	6.152E-01	7.063E-01	-2.421E-02	9.406E-01	1.434E 02	-1.957E-02	-9.786E 02	8.058E-01	8.058E-01
0.700	6.375E-01	7.249E-01	-2.575E-02	9.441E-01	1.509E 02	-2.104E-02	-1.052E 03	8.191E-01	8.187E-01
0.740	6.826E-01	7.621E-01	-2.895E-02	9.568E-01	1.684E 02	-2.414E-02	-1.207E 03	8.366E-01	8.360E-01
0.760	7.055E-01	7.803E-01	-3.405E-02	9.669E-01	1.987E 02	-2.579E-02	-1.200E 03	8.461E-01	8.454E-01
0.800	7.521E-01	8.175E-01	-3.583E-02	9.710E-01	2.095E 02	-3.114E-02	-1.484E 03	8.690E-01	8.681E-01
0.820	7.757E-01	8.359E-01	-3.951E-02	9.746E-01	2.379E 02	-3.503E-02	-1.557E 03	8.787E-01	8.777E-01
0.860	8.237E-01	8.725E-01	-4.140E-02	9.746E-01	2.521E 02	-3.711E-02	-1.752E 03	8.974E-01	8.961E-01
0.880	8.480E-01	8.900E-01	-4.532E-02	9.819E-01	2.998E 02	-4.152E-02	-1.856E 03	9.117E-01	9.103E-01
0.920	8.975E-01	9.275E-01	-4.733E-02	9.859E-01	3.237E 02	-4.52E-02	-2.076E 03	9.324E-01	9.307E-01
0.940	9.226E-01	9.457E-01	-5.148E-02	9.942E-01	4.540E 02	-4.388E-02	-2.194E 03	9.437E-01	9.417E-01
0.980	9.739E-01	9.822E-01	-5.362E-02	1.000E 00	5.191E 02	-4.893E-02	-2.446E 03	9.739E-01	9.715E-01
SHOC 1.000	1.000E 00	1.000E 00	-5.362E-02	1.000E 00	5.191E 02	-5.181E-02	-2.591E 03	9.907E-01	9.880E-01

-SHOCK LAYER GAS PROPERTIES-

ETA	Y/D	P (ATM.)	T (DEG.KEL.)	RHC (SLUGS/FT ³)	MU (LRM/FT-SEC)	KMU (LBF2-SEC3/FT6)	K (BTU/FT-SEC-R)
0.0	0.0	9.8952E-02	3.450E 03	8.7212E-06	6.2556E-05	1.3527E-11	3.8267E-04
0.0050	1.3361E-03	9.8952E-02	3.4525E 04	8.2500E-06	6.2556E-05	1.2759E-11	3.8267E-04
0.0100	2.7445E-03	9.8952E-02	3.5499E 01	7.7395E-06	6.2556E-05	1.2004E-11	3.8267E-04
0.0150	4.2637E-03	9.8952E-02	3.7696E 03	7.2646E-06	6.2556E-05	1.2039E-11	4.2309E-04
0.0200	5.8737E-03	9.8952E-02	3.7651E 03	6.8022E-06	6.2556E-05	1.1276E-11	4.2309E-04
0.0231	6.9354E-03	9.8952E-02	3.8214E 03	6.5203E-06	6.2556E-05	1.0811E-11	4.2309E-04
0.0262	8.0435E-03	9.8952E-02	3.8802E 03	6.2460E-06	6.2556E-05	1.0939E-11	4.2309E-04
0.0294	9.2004E-03	9.8952E-02	3.9416E 03	5.9811E-06	6.2556E-05	1.0478E-11	4.2309E-04
0.0325	1.0409E-02	9.8952E-02	4.0056E 03	5.7278E-06	6.2556E-05	1.0010E-11	4.2309E-04
0.0356	1.1670E-02	9.8952E-02	4.0731E 03	5.4877E-06	6.2556E-05	1.0141E-11	3.7100E-04
0.0387	1.2985E-02	9.8952E-02	4.1436E 03	5.2641E-06	6.2556E-05	9.7313E-12	3.7100E-04
0.0420	1.4379E-02	9.8952E-02	4.2947E 03	4.8727E-06	6.2556E-05	9.5494E-12	2.8910E-04
0.0450	1.5779E-02	9.8952E-02	4.5275E 03	4.4519E-06	6.2556E-05	9.2034E-12	2.8910E-04
0.0537	2.0034E-02	9.8952E-02	4.7861E 03	4.1346E-06	6.2556E-05	8.7229E-12	2.1251E-04
0.0625	2.4648E-02	9.8952E-02	5.0481E 03	3.8650E-06	6.2556E-05	8.1444E-12	2.1251E-04
0.0712	2.9586E-02	9.8952E-02	5.3287E 03	3.6587E-06	6.2556E-05	8.7427E-12	2.4077E-04
0.0800	3.4839E-02	9.8952E-02	5.6366E 03	3.5372E-06	6.2556E-05	8.6809E-12	2.6056E-04
0.0850	3.7983E-02	9.8952E-02	5.7524E 03	3.3518E-06	6.2556E-05	8.5767E-12	3.1488E-04
0.0925	4.2913E-02	9.8952E-02	5.7524E 03	3.1560E-06	6.2556E-05	8.4464E-12	3.4489E-04
0.1000	4.8132E-02	9.8952E-02	6.0284E 03	2.9054E-06	6.2556E-05	8.2583E-12	3.3272E-04
0.1100	5.3609E-02	9.8952E-02	6.4263E 03	2.6999E-06	6.2556E-05	8.1066E-12	2.7099E-04
0.1200	5.9292E-02	9.8952E-02	6.8516E 03	2.5519E-06	6.2556E-05	8.0098E-12	2.4735E-04
0.1300	6.5145E-02	9.8952E-02	7.2800E 03	2.4161E-06	6.2556E-05	7.9264E-12	2.5767E-04
0.1400	7.1179E-02	9.8952E-02	7.6888E 03	2.2936E-06	6.2556E-05	7.8386E-12	2.8295E-04
0.1500	7.7401E-02	9.8952E-02	8.0658E 03	2.1850E-06	6.2556E-05	7.7503E-12	3.1451E-04
0.1600	8.3813E-02	9.8952E-02	8.4055E 03	2.0900E-06	6.2556E-05	7.6790E-12	3.4726E-04
0.1700	9.0355E-02	9.8952E-02	8.7066E 03	2.0050E-06	6.2556E-05	7.6210E-12	3.7753E-04
0.1800	9.7009E-02	9.8952E-02	8.9666E 03	1.9315E-06	6.2556E-05	7.5710E-12	4.2441E-04
0.2000	1.0533E-01	9.8952E-02	9.3666E 03	1.8055E-06	6.2556E-05	7.4249E-12	4.4250E-04
0.2100	1.1195E-01	9.8952E-02	9.5263E 03	1.7222E-06	6.2556E-05	7.3107E-12	4.2500E-04
0.2200	1.1612E-01	9.8952E-02	9.6602E 03	1.6602E-06	6.2556E-05	7.2328E-12	4.7200E-04
0.2300	1.1707E-01	9.8952E-02	9.7763E 03	1.6155E-06	6.2556E-05	7.1711E-12	4.7200E-04
0.2400	1.1646E-01	9.8952E-02	9.8799E 03	1.5848E-06	6.2556E-05	7.1200E-12	5.1623E-04
0.2600	1.0111E-01	9.8952E-02	1.0065E 04	1.5668E-06	6.2556E-05	7.0855E-12	5.5904E-04
0.2800	2.2010E-01	9.8952E-02	1.0253E 04	1.4670E-06	6.2556E-05	6.9845E-12	6.1000E-04
0.3000	2.3865E-01	9.8952E-02	1.0425E 04	1.3745E-06	6.2556E-05	6.8484E-12	7.1500E-04
0.3300	2.6593E-01	9.8952E-02	1.0711E 04	1.2511E-06	6.2556E-05	6.6847E-12	7.9213E-04
0.3500	2.8395E-01	9.8952E-02	1.1144E 04	1.1048E-06	6.2556E-05	6.4742E-12	9.0566E-04
0.3800	3.1113E-01	9.8952E-02	1.1415E 04	1.0038E-06	6.2556E-05	6.1896E-12	1.0349E-03
0.4200	3.4809E-01	9.8952E-02	1.1526E 04	9.0348E-06	6.2556E-05	6.0594E-12	1.0349E-03
0.4800	4.0573E-01	9.8952E-02	1.1704E 04	8.2979E-06	6.2556E-05	7.4129E-12	1.1640E-03
0.5000	4.2556E-01	9.8952E-02	1.1775E 04	7.6790E-06	6.2556E-05	7.3107E-12	1.1640E-03
0.5400	4.6602E-01	9.8952E-02	1.1892E 04	6.7694E-06	6.2556E-05	6.8484E-12	1.2379E-03
0.5600	4.8664E-01	9.8952E-02	1.1944E 04	6.1817E-06	6.2556E-05	6.7694E-12	1.2379E-03
0.5800	5.0750E-01	9.8952E-02	1.1944E 04	5.7511E-06	6.2556E-05	6.6934E-12	1.2379E-03
0.6200	5.4991E-01	9.8952E-02	1.2091E 04	5.1106E-06	6.2556E-05	6.2584E-12	1.3176E-03
0.6400	5.7146E-01	9.8952E-02	1.2137E 04	4.6089E-06	6.2556E-05	6.1910E-12	1.3176E-03
0.6800	6.1525E-01	9.8952E-02	1.2271E 04	3.9455E-06	6.2556E-05	6.0680E-12	1.3176E-03
0.7000	6.3748E-01	9.8952E-02	1.2271E 04	3.6243E-06	6.2556E-05	5.7413E-12	1.3551E-03
0.7400	6.8263E-01	9.8952E-02	1.2359E 04	1.9847E-06	6.2556E-05	5.6297E-12	1.3551E-03
0.8000	7.5555E-01	9.8952E-02	1.2402E 04	1.6426E-06	6.2556E-05	5.5718E-12	1.3551E-03
0.8600	8.2365E-01	9.8952E-02	1.2490E 04	1.2577E-06	6.2556E-05	5.1706E-12	1.4100E-03
0.8800	8.4800E-01	9.8952E-02	1.2533E 04	1.19059E-06	6.2556E-05	5.1179E-12	1.4100E-03
0.9200	8.9746E-01	9.8952E-02	1.2622E 04	1.0862E-06	6.2556E-05	5.0175E-12	1.4100E-03
0.9400	9.2243E-01	9.8952E-02	1.2676E 04	1.0359E-06	6.2556E-05	4.7340E-12	1.4199E-03
0.9800	9.7386E-01	9.8952E-02	1.2814E 04	1.7894E-06	6.2556E-05	4.5850E-12	1.4199E-03
1.0000	1.0000E 00	9.8952E-02	1.2922E 04	1.7452E-06	6.2556E-05	4.1874E-12	1.4283E-03
		9.8952E-02	1.2998E 04	1.7105E-06	6.2556E-05	4.1165E-12	1.4263E-03

Reproduced from
Best available copy.

-SPECIES MASS FRACTIONS-						
C2	N2	C	N	O4	N4	E-
0.0	5.3704E-02	9.7359E-08	9.4364E-05	1.6573E-20	5.7159E-18	1.1314E-09
0.0050	5.1156E-02	1.5970E-07	1.3280E-04	2.6218E-20	1.3441E-17	2.1749E-09
0.0100	4.8352E-02	2.4557E-07	1.8692E-04	4.9059E-19	1.2624E-16	3.3392E-09
0.0150	4.5496E-02	3.8634E-07	2.6386E-04	2.3591E-18	4.1715E-16	3.6559E-09
0.0200	4.2861E-02	6.2240E-07	3.7479E-04	1.1942E-17	2.8704E-15	2.8928E-09
0.0231	4.1461E-02	8.5259E-07	4.6941E-04	2.2395E-17	5.2652E-15	4.1721E-09
0.0262	4.0359E-02	1.1661E-06	5.9160E-04	5.7082E-17	7.2221E-15	3.8580E-09
0.0294	3.9648E-02	1.6782E-06	7.5115E-04	1.7987E-16	1.2808E-14	4.0366E-09
0.0325	3.9431E-02	2.4208E-06	9.6228E-04	5.3856E-16	1.0175E-13	4.1105E-09
0.0356	3.9214E-02	3.5704E-06	1.2461E-03	1.1370E-15	2.6442E-13	4.3428E-09
0.0387	3.8998E-06	5.3899E-06	1.6316E-03	2.0150E-15	6.9529E-13	4.7269E-09
0.0450	4.0907E-02	1.3192E-05	2.8856E-03	4.6768E-14	5.6237E-12	4.7745E-09
0.0500	4.5545E-02	5.2489E-05	6.6316E-03	1.2864E-12	7.4431E-11	5.4184E-09
0.0537	5.7248E-02	2.2285E-02	1.4753E-02	2.9941E-11	1.4547E-09	1.1180E-08
0.0625	7.0820E-02	2.2285E-02	1.4753E-02	2.9941E-11	1.4547E-09	1.1180E-08
0.0712	7.9228E-02	9.3031E-04	3.0095E-02	5.4085E-10	1.4506E-08	2.0264E-08
0.0800	7.7234E-02	3.5971E-03	5.5072E-02	6.3197E-09	9.7814E-08	2.9042E-08
0.0850	7.0910E-02	7.4518E-03	7.3718E-02	2.6223E-08	2.5310E-07	4.9659E-08
0.0925	5.5671E-02	2.0463E-02	1.0648E-01	1.7193E-07	9.6502E-07	7.6269E-08
0.1000	4.9158E-02	4.2220E-02	1.4572E-01	8.1270E-07	2.7933E-06	1.6178E-07
0.1100	1.8157E-02	9.4512E-02	1.8491E-01	5.1888E-06	1.1259E-05	3.2861E-07
0.1200	7.6614E-03	1.3775E-01	2.1560E-01	2.0274E-05	1.1579E-04	6.0581E-07
0.1300	9.4479E-07	1.5779E-01	2.4216E-01	5.5900E-05	1.5795E-04	1.0055E-06
0.1400	5.2169E-07	1.6625E-01	2.6813E-01	1.1266E-04	2.9735E-04	1.5169E-06
0.1500	3.8362E-07	1.7090E-01	2.9487E-01	2.5501E-04	6.6205E-04	2.1039E-06
0.1600	2.9703E-07	1.7438E-01	3.2266E-01	4.5400E-04	1.3286E-03	2.7091E-06
0.1700	2.2666E-07	1.7746E-01	3.5115E-01	7.3798E-04	2.3666E-03	3.2794E-06
0.1800	2.0771E-07	1.8308E-01	3.8004E-01	1.1093E-03	3.9397E-03	4.1328E-06
0.2000	1.7154E-07	1.8549E-01	4.3762E-01	2.0640E-03	8.5246E-03	4.4153E-06
0.2100	1.6191E-07	1.8849E-01	4.6470E-01	2.6450E-03	1.1568E-02	4.6048E-06
0.2200	1.5606E-07	1.9089E-01	4.9027E-01	3.2535E-03	1.5042E-02	4.7266E-06
0.2300	1.5138E-07	1.9306E-01	5.1402E-01	3.9284E-03	1.8924E-02	4.7995E-06
0.2400	1.4833E-07	1.9506E-01	5.3568E-01	4.6120E-03	2.3226E-02	4.8780E-06
0.2500	1.4334E-07	1.9827E-01	5.7224E-01	6.2084E-03	3.3179E-02	5.0119E-06
0.2600	1.3620E-07	2.0289E-01	5.8666E-01	8.2090E-03	4.5937E-02	5.1650E-06
0.3000	1.2899E-07	2.0139E-01	6.1653E-01	1.0444E-02	6.0325E-02	5.6937E-06
0.3300	1.1339E-07	2.0096E-01	6.2614E-01	1.4686E-02	8.7667E-02	6.1708E-06
0.3500	1.0294E-07	1.9971E-01	6.2451E-01	1.7848E-02	1.0788E-01	6.5959E-06
0.3800	8.8844E-08	1.9697E-01	6.1442E-01	2.2650E-02	1.3805E-01	8.1434E-06
0.4200	7.4146E-08	1.9268E-01	5.9414E-01	2.8517E-02	1.7365E-01	8.6977E-06
0.4400	6.8216E-08	1.9051E-01	5.8316E-01	3.1144E-02	1.8908E-01	9.7089E-06
0.4500	5.9376E-08	1.8641E-01	5.6198E-01	3.5657E-02	2.1429E-01	1.0141E-05
0.5000	5.9595E-08	1.8462E-01	5.5272E-01	3.7532E-02	2.2445E-01	1.0908E-05
0.5400	5.0573E-08	1.8141E-01	5.3605E-01	4.0794E-02	2.4159E-01	1.1265E-05
0.5600	4.8285E-08	1.7991E-01	5.2634E-01	4.2295E-02	2.4931E-01	1.1613E-05
0.5800	4.6151E-08	1.7842E-01	5.2078E-01	4.3786E-02	2.5686E-01	1.1613E-05
0.6200	4.2116E-08	1.7553E-01	5.0618E-01	4.6678E-02	2.7147E-01	1.2286E-05
0.6400	4.0463E-08	1.7374E-01	4.9664E-01	4.8257E-02	2.7901E-01	1.2637E-05
0.7000	3.7044E-08	1.6944E-01	4.7708E-01	5.2766E-02	2.9304E-01	1.3285E-05
0.7400	3.5612E-08	1.5842E-01	4.6304E-01	5.7232E-02	3.1401E-01	1.4290E-05
0.8000	3.1319E-08	1.3454E-01	4.5946E-01	6.0582E-02	3.3653E-01	1.5174E-05
0.8200	2.7446E-08	1.0704E-01	4.4112E-01	6.2391E-02	3.4414E-01	1.5679E-05
0.8600	2.4951E-08	8.4701E-02	4.1874E-01	6.5740E-02	3.5889E-01	1.6372E-05
0.8800	2.3881E-08	7.9216E-02	4.1076E-01	6.7707E-02	3.6686E-01	1.6752E-05
0.9200	2.1468E-08	6.5767E-02	3.9463E-01	7.1539E-02	3.8299E-01	1.7516E-05
0.9400	2.0221E-08	5.8997E-02	3.8585E-01	7.3636E-02	3.9176E-01	1.7933E-05
0.9800	1.8004E-08	4.8613E-02	3.6725E-01	7.8447E-02	4.1036E-01	1.8426E-05
1.0000	1.6495E-08	4.2239E-02	3.5440E-01	8.1751E-02	4.2322E-01	1.9443E-05

ETA	C	H	H2	-SPECIES MASS FRACTIONS- CO	C3-G	CN	C2+	L2+2
0.0	1.3358E-02	3.6629E-02	1.3630E-02	2.0899E-01	8.1634E-02	7.7916E-02	1.6518E-01	1.6737E-02
0.0500	2.0124E-02	4.2237E-02	1.1259E-02	2.6320E-01	9.6442E-02	9.9449E-02	1.6232E-01	1.2200E-02
0.1000	3.0151E-02	4.5927E-02	9.1136E-03	2.6944E-01	1.1071E-01	1.0148E-01	1.5478E-01	6.5183E-03
0.1500	4.4806E-02	4.9203E-02	7.2311E-03	2.6976E-01	1.2214E-01	1.1354E-01	1.4209E-01	5.6484E-03
0.2000	6.5743E-02	5.2557E-02	5.5810E-03	2.7006E-01	1.2759E-01	1.2506E-01	1.2427E-01	3.5179E-03
0.2500	8.2861E-02	5.4433E-02	4.6965E-03	2.7021E-01	1.2651E-01	1.3170E-01	1.1087E-01	2.5177E-03
0.3000	1.0357E-01	5.6289E-02	3.9068E-03	2.7044E-01	1.2128E-01	1.3772E-01	9.6194E-02	1.7400E-03
0.3500	1.2810E-01	5.7936E-02	3.2196E-03	2.7068E-01	1.1175E-01	1.4291E-01	6.6847E-02	1.1580E-03
0.4000	1.5642E-01	5.9377E-02	2.6275E-03	2.7074E-01	9.6357E-02	1.4709E-01	6.5548E-02	7.3822E-04
0.4500	1.8820E-01	6.0608E-02	2.1133E-03	2.7122E-01	8.2116E-02	1.5003E-01	5.1027E-02	4.4922E-04
0.5000	2.2248E-01	6.1594E-02	1.6918E-03	2.7122E-01	6.4660E-02	1.5152E-01	3.8012E-02	2.6002E-04
0.5500	2.5247E-01	6.2477E-02	1.0508E-03	2.7221E-01	3.3177E-03	1.4927E-01	1.8390E-02	7.5654E-05
0.6000	3.7461E-01	6.3414E-02	5.2727E-04	2.7329E-01	8.6567E-03	1.3358E-01	5.0918E-03	1.0044E-05
0.6500	4.2557E-01	6.3118E-02	2.6740E-04	2.7433E-01	1.8009E-03	1.0760E-01	1.1866E-03	1.1592E-06
0.7000	4.5281E-01	6.2448E-02	1.3974E-04	2.7461E-01	3.3619E-04	7.9377E-02	2.6605E-04	1.1345E-07
0.7500	4.6649E-01	6.1576E-02	7.5076E-05	2.7165E-01	6.3918E-05	5.4423E-02	6.1583E-05	1.6503E-08
0.8000	4.7145E-01	6.1005E-02	5.3514E-05	2.6598E-01	2.5532E-05	4.2605E-02	2.7541E-05	5.2746E-09
0.8500	4.7970E-01	6.0058E-02	3.2565E-05	2.4513E-01	6.7527E-06	2.8177E-02	4.5105E-06	9.9070E-10
0.9000	4.9553E-01	5.8981E-02	1.9588E-05	2.0883E-01	1.9475E-06	6.0546E-03	2.7393E-06	1.9300E-10
1.0000	5.1736E-01	5.7329E-02	1.0194E-05	1.2027E-01	3.9182E-07	3.1128E-03	6.3457E-07	2.3625E-11
1.2000	5.2656E-01	5.5393E-02	5.4643E-06	4.8028E-02	7.9836E-08	1.5373E-03	1.5396E-07	3.1457E-12
1.3000	5.1251E-01	5.3196E-02	3.1062E-06	1.6840E-02	1.7488E-08	7.7627E-04	4.0722E-08	4.9072E-13
1.4000	4.9444E-01	5.0769E-02	1.8769E-06	6.3107E-03	4.2958E-09	4.2409E-04	1.2309E-08	9.4066E-14
1.5000	4.4904E-01	4.8139E-02	1.2287E-06	2.6681E-03	1.2917E-09	2.5211E-04	4.2572E-09	2.2164E-14
1.6000	4.0955E-01	4.5338E-02	8.3343E-07	1.3723E-03	4.1101E-10	1.6154E-04	1.6539E-09	6.1965E-15
1.7000	3.6826E-01	4.2398E-02	5.8818E-07	6.7698E-04	1.6137E-10	1.1051E-04	7.1091E-10	2.0082E-15
1.8000	3.2716E-01	3.9362E-02	4.2440E-07	3.9481E-04	6.6458E-11	7.9668E-05	3.3146E-10	7.3300E-16
2.0000	2.5109E-01	3.3153E-02	2.4214E-07	1.6987E-04	1.4505E-11	4.7416E-05	8.9304E-11	1.3286E-16
2.1000	2.1783E-01	3.0142E-02	1.8575E-07	1.0200E-05	7.3445E-12	3.8022E-05	4.9501E-11	6.2104E-17
2.2000	1.8805E-01	2.7236E-02	1.4265E-07	6.8290E-05	3.8705E-12	2.5610E-05	2.8309E-11	3.0328E-17
2.3000	1.6159E-01	2.4474E-02	1.1074E-07	6.6525E-05	2.0956E-12	2.5610E-05	1.6508E-11	1.5218E-17
2.4000	1.3622E-01	2.1877E-02	8.5286E-08	5.6942E-05	1.1480E-12	2.1202E-05	9.7613E-12	7.2059E-18
2.6000	9.9656E-02	1.7223E-02	5.0035E-08	3.0363E-05	3.4468E-13	1.4222E-05	3.3252E-12	1.9696E-18
2.8000	6.9954E-02	1.3306E-02	2.8061E-08	1.7477E-05	9.4731E-14	9.3141E-06	1.6501E-12	4.4945E-19
3.0000	4.8340E-02	1.0081E-02	1.5152E-08	1.0080E-05	2.5429E-14	5.9034E-06	3.2074E-13	9.8286E-20
3.2000	2.6435E-02	6.3873E-03	5.4432E-09	4.0074E-06	2.8628E-15	2.6680E-06	4.4528E-14	7.3761E-21
3.4000	1.7094E-02	4.5299E-03	2.5382E-09	2.1029E-06	6.1207E-16	1.5052E-06	1.0713E-14	8.3776E-22
3.6000	8.4331E-03	2.5242E-03	7.0431E-10	7.7791E-07	5.2829E-17	6.0664E-07	1.0448E-15	9.6144E-23
4.0000	2.9170E-03	5.9270E-04	9.5558E-11	1.9570E-07	1.5218E-18	1.6517E-07	3.6702E-17	1.1049E-23
4.2000	1.5306E-03	3.4889E-04	2.7606E-11	8.9546E-08	1.8112E-19	7.7861E-08	4.8277E-18	1.2682E-24
4.4000	3.7643E-04	1.4694E-04	1.7964E-12	1.7779E-08	2.0804E-21	1.6065E-08	6.2439E-20	1.4309E-25
4.6000	1.4690E-04	3.6614E-05	2.5951E-13	6.0959E-09	2.3204E-22	5.5874E-09	4.3207E-21	1.6004E-26
4.8000	2.4231E-05	1.0344E-05	7.4234E-15	9.0485E-10	2.5651E-23	8.4761E-10	4.7750E-22	1.7763E-27
5.0000	2.3626E-05	1.0344E-05	7.7714E-15	8.2641E-10	2.5664E-23	7.8111E-10	4.7786E-22	1.7763E-27
5.2000	2.3049E-05	1.0344E-05	7.5560E-15	7.5700E-10	2.5663E-23	7.2149E-10	4.7786E-22	1.7763E-27
5.4000	2.1948E-05	1.0343E-05	7.1277E-15	6.3025E-10	2.5662E-23	6.1150E-10	4.7786E-22	1.7763E-27
5.6000	2.1452E-05	1.0343E-05	6.9514E-15	5.8886E-10	2.5661E-23	5.7331E-10	4.7786E-22	1.7763E-27
5.8000	2.0469E-05	1.0343E-05	6.5472E-15	4.9468E-10	2.5660E-23	4.8957E-10	4.7777E-22	1.7759E-27
6.0000	2.0014E-05	1.0343E-05	6.4308E-15	4.6400E-10	2.5659E-23	4.6075E-10	4.7777E-22	1.7759E-27
6.2000	1.9699E-05	1.0343E-05	6.1026E-15	3.9955E-10	2.5658E-23	3.9357E-10	4.7777E-22	1.7759E-27
6.4000	1.8672E-05	1.0342E-05	5.9607E-15	3.6712E-10	2.5657E-23	3.7061E-10	4.7777E-22	1.7759E-27
6.6000	1.7800E-05	1.0342E-05	5.6559E-15	3.0898E-10	2.5656E-23	3.1557E-10	4.7777E-22	1.7759E-27
6.8000	1.7395E-05	1.0342E-05	5.5255E-15	2.9020E-10	2.5655E-23	2.9731E-10	4.7777E-22	1.7759E-27
7.0000	1.6557E-05	1.0342E-05	5.2410E-15	2.4353E-10	2.5654E-23	2.5228E-10	4.7766E-22	1.7759E-27
7.2000	1.6156E-05	1.0342E-05	5.1139E-15	2.2785E-10	2.5653E-23	2.3653E-10	4.7766E-22	1.7759E-27
7.4000	1.5301E-05	1.0342E-05	4.8318E-15	1.8888E-10	2.5652E-23	1.9812E-10	4.7766E-22	1.7759E-27
7.6000	1.4844E-05	1.0342E-05	4.6812E-15	1.6944E-10	2.5651E-23	1.7812E-10	4.7766E-22	1.7759E-27
7.8000	1.3903E-05	1.0341E-05	4.4058E-15	1.4047E-10	2.5650E-23	1.4911E-10	4.7766E-22	1.7759E-27
8.0000	1.3355E-05	1.0341E-05	4.2144E-15	1.2187E-10	2.5649E-23	1.3020E-10	4.7766E-22	1.7759E-27

-SPECIES MASS FRACTIONS-									
ETA	CP	CJM	C4H	HCN	C2	C+	AMW		
0.0	6.0950E 00	1.3016E-01	8.4212E-02	1.1046E-02	2.4706E-02	1.4319E-11	1.2861E CA		
0.0500	6.3209E 00	1.1452E-01	7.0180E-02	2.6259E-02	3.4577E-02	1.2240E-11	1.2405L C1		
0.1000	6.5821E 00	9.6704E-02	5.5544E-02	2.1609E-02	4.7611E-02	1.3096E-10	1.1928E C1		
0.1500	6.9703E 00	7.7417E-02	4.1067E-02	1.7131E-02	6.4040E-02	9.4347E-10	1.1450E C1		
0.2000	7.2726E 00	5.7659E-02	2.7789E-02	1.3455E-02	8.3347E-02	3.2759E-09	1.0974E C1		
0.2312	7.4735E 00	4.6165E-02	2.0570E-02	1.1295E-02	9.6172E-02	5.7085E-09	1.0679E C1		
0.2625	7.6356E 00	3.5379E-02	1.4450E-02	9.3564E-03	1.0872E-01	1.3792E-08	1.0396L C1		
0.2937	7.7230E 00	2.5894E-02	9.5617E-03	7.6372E-03	1.1990E-01	2.8704E-08	1.0110E C1		
0.3250	7.7426E 00	1.7988E-02	5.9112E-03	6.1413E-03	1.2847E-01	6.1184E-08	5.8426E C0		
0.3562	5.9582E 00	1.1777E-02	3.3823E-03	4.8610E-03	1.3315E-01	1.3328E-07	9.5918E 00		
0.3875	6.1013E 00	7.2325E-03	1.7798E-03	3.7867E-03	1.3291E-01	2.6783E-07	5.3635E C0		
0.4500	4.9066E 00	2.2318E-03	3.7895E-04	2.1917E-03	1.1703E-01	7.0954E-07	8.9894E C0		
0.5375	2.7115E 00	2.9142E-04	2.6048E-05	9.2597E-04	7.5438E-02	6.8666E-06	8.6644E 00		
0.7125	2.0286E 00	2.9711E-05	1.2919E-06	3.6037E-04	3.9911E-02	3.4500E-05	8.5110E 00		
0.8000	2.2636E 00	2.9798E-07	1.7741E-09	4.7501E-05	9.4058E-03	2.9899E-04	8.3945E C0		
0.8500	2.6283E 00	6.5591E-06	5.8836E-10	2.6109E-05	6.2715E-03	4.7527E-04	8.3648E 00		
0.9250	3.2314E 00	1.3879E-06	5.3721E-11	1.0246E-05	3.4206E-03	9.2476E-04	8.2960E 00		
1.0000	3.5329E 00	2.1489E-09	2.7311E-12	3.9382E-06	1.9950E-03	1.4847E-03	8.1798E 00		
1.1000	3.1121E 00	2.5225E-10	2.4875E-13	9.6192E-07	9.8277E-04	3.3208E-03	8.0165E C0		
1.2000	2.0291E 00	2.8604E-11	1.6214E-14	2.3330E-07	4.8564E-04	6.9120E-03	7.9337E C0		
1.3000	1.5628E 00	3.7094E-12	1.1305E-15	6.2735E-08	2.4114E-04	1.2864E-02	7.9652E 00		
1.4000	1.5696E 00	5.6934E-13	1.0417E-16	1.9817E-08	1.2534E-04	2.1380E-02	8.0527E 00		
1.5000	1.7534E 00	1.1840E-13	1.2666E-17	7.3211E-09	8.8784E-05	3.2132E-02	8.1618E C0		
1.6000	1.9932E 00	2.8182E-14	1.9574E-18	3.1000E-09	3.9042E-05	4.4215E-02	8.2836E 00		
1.7000	2.2302E 00	7.6177E-15	3.7107E-19	1.4782E-09	2.3848E-05	5.6330E-02	8.4196E 00		
1.8000	2.4294E 00	4.8866E-15	8.4247E-20	7.7663E-10	1.4841E-05	6.7143E-02	8.5733E C0		
2.0000	2.6766E 00	3.4423E-16	6.9606E-21	2.7485E-10	6.3484E-06	8.1977E-02	8.9527E C0		
2.1000	2.7442E 00	1.4326E-16	1.3189E-21	1.7645E-10	4.2762E-06	8.4197E-02	9.1695E 00		
2.2000	2.6762E 00	0.2864E-17	1.1947E-22	1.1742E-10	2.9230E-06	8.4873E-02	9.4023E 00		
2.3000	2.8136E 00	2.8579E-17	1.0975E-23	7.7924E-11	2.0156E-06	8.3663E-02	9.6447E C0		
2.4000	2.7433E 00	1.3194E-17	1.0688E-29	5.4938E-11	1.3932E-06	6.1018E-02	9.8916E C0		
2.6000	2.8893E 00	2.8656E-18	1.0318E-25	2.5849E-11	6.5898E-07	7.2950E-02	1.0378E 01		
2.8000	3.0025E 00	5.2941E-19	1.0562E-26	1.1201E-11	2.9410E-07	6.3392E-02	1.0811E 01		
3.0000	3.1516E 00	9.9135E-20	1.1252E-27	4.7039E-12	1.2841E-07	5.2686E-02	1.1187E 01		
3.3000	3.5038E 00	5.3013E-21	1.2390E-28	1.0496E-12	3.2604E-08	3.7578E-02	1.1563E 01		
3.5000	3.7672E 00	6.0195E-22	1.4068E-29	3.5195E-13	1.2231E-08	2.8306E-02	1.1709E 01		
4.0000	4.6299E 00	9.9095E-23	1.6149E-30	6.1213E-14	2.5582E-09	1.6865E-02	1.1791E 01		
4.2000	4.6595E 00	9.1125E-25	2.1297E-32	1.6810E-15	2.5817E-10	7.0326E-03	1.1724E C1		
4.4000	5.1339E 00	1.1259E-25	2.8225E-31	1.0935E-15	6.6012E-11	1.9706E-03	1.1650E 01		
4.6000	5.1339E 00	1.0346E-25	2.4180E-33	4.8892E-17	3.5570E-12	1.0960E-03	1.1460E 01		
5.0000	5.4525E 00	1.1539E-26	2.6969E-34	6.0020E-18	4.7465E-13	4.2878E-04	1.1369E 01		
5.4000	5.4525E 00	1.2763E-27	2.9830E-35	1.4047E-19	1.2955E-14	7.9442E-05	1.1191E C1		
5.6000	5.4922E 00	1.2763E-27	2.9828E-35	1.0191E-19	1.1891E-14	6.0046E-05	1.1117E 01		
6.0000	5.5310E 00	1.2762E-27	2.9827E-35	9.3350E-20	1.0928E-14	6.0621E-05	1.1039E 01		
6.2000	5.8168E 00	1.2762E-27	2.9826E-35	4.8203E-20	9.1762E-15	8.1720E-05	1.0891E 01		
6.4000	5.6573E 00	1.2761E-27	2.9825E-35	4.8203E-20	8.5923E-15	8.2213E-05	1.0816E 01		
6.6000	5.9322E 00	1.2761E-27	2.9824E-35	4.4202E-20	7.2744E-15	4.3193E-05	1.0679E 01		
7.0000	5.9980E 00	1.2760E-27	2.9822E-35	2.1430E-20	6.8335E-15	4.3646E-05	1.0606E 01		
7.4000	6.0736E 00	1.2760E-27	2.9821E-35	2.1437E-20	5.7969E-15	8.4559E-05	1.0474E 01		
7.6000	6.1149E 00	1.2759E-27	2.9820E-35	2.1436E-20	4.5288E-15	8.4983E-05	1.0404E C1		
8.0000	6.2664E 00	1.2759E-27	2.9819E-35	2.1435E-20	4.6190E-15	8.5833E-05	1.0273E 01		
8.2000	6.3088E 00	1.2758E-27	2.9818E-35	2.1434E-20	4.4555E-15	8.6255E-05	1.0204E 01		
8.6000	6.3295E 00	1.2758E-27	2.9816E-35	2.1433E-20	3.6698E-15	8.7089E-05	1.0074E 01		
8.8000	6.3295E 00	1.2757E-27	2.9815E-35	2.1432E-20	3.4388E-15	8.7467E-05	1.0004E C1		
9.0000	6.4177E 00	1.2757E-27	2.9814E-35	2.1432E-20	2.8702E-15	8.8359E-05	9.5667E 00		
9.2000	6.4657E 00	1.2756E-27	2.9813E-35	2.1432E-22	2.5852E-15	8.8795E 00	9.7934E 00		
9.4000	6.3927E 00	1.2756E-27	2.9812E-35	2.1431E-22	2.1576E-15	8.9675E-05	5.6394E 00		
10.0000	6.4620E 00	1.2755E-27	2.9811E-35	2.1430E-22	1.8810E-15	9.0281E-05	5.5363E 00		

APPENDIX G

COMPUTER PROGRAM FOR MULTICOMPONENT
DIFFUSION ANALYSIS

The program (SLAM) presented in this appendix consists of the interactive numerical solution of the elemental continuity equations (Eqs. 3.97) with effective multicomponent diffusion coefficients as determined by the Stefan-Maxwell Equations (Eqs. 3.98) and equilibrium compositions. A general description of the overall logic and the details of the numerical solutions is given in Chapter V.

A brief description of each of the sub-programs included in this code is presented in Table G-1. In the following section, a detailed input guide is given. A complete listing will then follow which includes a sample data package and the corresponding final solution.

Input Guide

The following chart shows the format of the card input.

<u>Card</u>	<u>Variables</u>	<u>Format</u>
1	TITLE	20A4
2	NDEBUG, NETA, NSP, NE	3I5, 5X, I5
3	TOL, UINF, DTIL, RAD, RINF, RZB, DELTA	8E10.4
4	ET(N)	6E12.8
5	YOND(N)	6E12.8
6	TT(N)	6E12.8
7	PI(N)	6E12.8
8	VV(N)	6E12.8
9	RO(N)	6E12.8

The meaning of these program variables are as follows:

<u>Variable</u>	<u>Description</u>
TITLE	Title for identification of the problem.
NDEBUG	Debug option NDEBUG = 0 only results NDEBUG = 1 includes intermediate computations
NETA	Length of input stepsize distribution.
NSP	Number of species.
NE	Number of elements.

<u>Variable</u>	<u>Description</u>
TOL	Convergence criteria for chemical equilibrium calculation. Recommended value is 0.001.
UINF	Freestream velocity (ft/sec).
DTIL	Transformed standoff distance.
RAD	Body radius (ft).
RINF	Freestream Density (lb/ft ³)
RZB	Density ratio across shock.
DELTA	Nondimensional standoff distance, δ .
ET(N)	Stepsize distribution, η .
YOND(N)	y/δ , distribution.
TT(N)	Temperature distribution(^o K).
PI(N)	Pressure distribution (atm).
W(N)	Velocity distribution (ft/sec).
RO(N)	Density distribution (ρ/ρ_s).

TABLE G-1
DESCRIPTION OF SLAM SUBPROGRAMS

Subprogram	Driver Program	Description	Additional Subprograms Required
MAIN			INPUT, STPZE, INIT, ELEMNT, CHEMEQ, DENSITY, DELTAY, MCD, EFLUX, DIJ, REDUCE, OUTPUT, COMP, PROFIL, PLOTIT, LRAD4.
INPUT STPZE	Data input.		none
INPUT STPZE	Increases number of steps such that the maximum change in temperature from one point to the next.		SPACE
SPACE	Transfers tabular data from one stepsize distribution to another.		INTRPL
INTRPL	Interpolation scheme.		none
INIT	Initialization routine--for further details see listing.		SG13

TABLE G-1 (continued)

Subprogram	Description	Additional Subprograms Required
SG13	Curve smoothing program.	none
ELEMNT	Solves elemental equations as described in Chapter V.	FGH, FGH2, TRID
FGH, FGH2	Three point difference formulas for first and second derivatives.	none
TRID	Solution to simultaneous linear equations with tri-diagonal coefficient matrix.	none
OUTPUT	Prints out elemental profiles.	none
CHEMEQ	Determines equilibrium compositions. See Appendix E.	ALTERY, THERMO, MATINV
ALTERY	Adjusts assumed compositions such that desired elemental ratios are obtained.	none
THERMO	Computes the free energy of the species.	none
MATINV	Matrix inversion and simultaneous solution of linear equation set.	none

TABLE G-1 (continued)

Subprogram	Description	Additional Subprograms Required
DENSTY	Computes density profiles from equilibrium compositions.	none
PROFIL	Prints out composition profile.	none
DELTAY	Determines derivatives of mole fractions for MCD.	FGH
MCD	Solves Stefan-Maxwell equations as described in Chapter V.	MATINV
EFLUX	Computes elemental mass fluxes from species mass fluxes.	none
DIJ	Estimates new effective elemental diffusion coefficient.	none
COMP	Converts from mole fraction to mass fraction or the reverse.	none
LRAD4	Punches data package for LRAD4 radiation program described in Reference 5.6.	none

```

C      * * * * * M A I N * * * * *
C      **          FLOW FIELD ANALYSIS WITH EQUILIBRIUM CHEMISTRY
C      **          AND MULTICOMPONENT DIFFUSION.  11/20/79
C      * * * * *
C      COMMON/NUMBER/NSF,NNS,NE,NC
C      COMMON /SCF/ NCHECK,ITER
C      COMMON /FPSTRM/ U INF, RINF, UINF2,RAD, RE, LXI, ITM, IEM,NETA
C      COMMON/SP1/SS,TOL,NDHUG
C      ND=0
C      ITER=0
C      ITYPE=2
C      CALL INPUT
C      CALL STPZE(NETA)
C      CALL INIT
C      CALL ELEMNT
C      CALL CHEMEQ(1,NETA)
C      CALL DENSTY(ND)
C      CALL ELEMNT
C      CALL CHEMEQ(1,NETA)
C      CALL DENSTY(ND)
C      CONTINUE
C      ITER=ITER + 1
C      CALL FLEMNT
C           IF(NDBG,GT,0)CALL OUTPUT
C           IF(ITFF,EQ,1)NCHECK=99
C           IF(NCHECK,LE,0,AND,ITER,GT,1)GOTO150
C      CALL CHEMEQ(1,NETA)
C           IF(NDBG,GT,0)CALL PROF IL(ITYPE)
C      CALL DELTAY(NETA,NSF)
C      CALL MCD
C      CALL EFFLUX
C      CALL DTJ
C      GOTO100

```

```

C-----ELEMENTAL PROFILES HAVE CONVERGED FOR THE GIVEN DENSITY PROFILE...
C
C      150  CONTINUE
C
C-----CHECK FOR DENSITY CONVERGENCE.....
C
C      CALL DENSTY(ND)
C      IF (ND.GT.C)GOTO100
C
C-----IF DENSITY PROFILE HAS CONVERGED, PRINT OUT SOLUTION.....
C
C      CALL REDUCE(NETA)
C      CALL OUTPUT
C      CALL PROFIL(ITYPE)
C      CALL COMP(ITYPE,NSP,NETA)
C      CALL PROFIL(ITYPE)
C
C      CALL LRAD4
C      STOP
C      END

```

MAIN 370
 MAIN 380
 MAIN 390
 MAIN 400
 MAIN 410
 MAIN 420
 MAIN 430
 MAIN 440
 MAIN 450
 MAIN 460
 MAIN 470
 MAIN 480
 MAIN 490
 MAIN 500
 MAIN 510
 MAIN 520
 MAIN 530
 MAIN 540
 MAIN 550
 MAIN 560

```

C
SUBROUTINE INPUT
COMMON/PROPI/PI(20),PO(200),IT(200),AMW(200),C(20,200),CC(5,200)
COMMON/NUMBER/NSP,NNS,NE,NC
COMMON/TITL/TITLE(20)
COMMON/WT/SMW(20),AWT(5)
COMMON/SP1/SS,TOL,NDBG
COMMON/ID/SP(20),EL(5)
COMMON/EQ1/AI(20),BI(20),CI(20),DI(20),EI(20),FI(20),GI(20),
X      AII(20),BII(20),CII(20),DII(20),EII(20),FII(20),GII(20)
COMMON/EQ2/AA(20,5)
COMMON/EQ3/IA(20,5)
COMMON/BLOCK2/ SIG(20),EOK(20)
COMMON /FRSTRM/ U INF, RINF, UINF2,RAD, RE, LXI, ITM, IEM,NETA
COMMON /VEL/ F(200),FC(200),ZZ(200),VV(200)
COMMON /YL/ ET(200),YOND(200)
COMMON /DEL/ DELTA,DTIL,DTILS
COMMON /RH/ DUD,DPHI,TD,RZB,PD,HD,HTOTAL
DOUBLE PRECISION NAME(7),PARM(8)
DATA NAME/' SPECIES',' SMW ',' SIGMA ',' EOK ',' CWall ','
X  ' CSHOCK ',' A(I,J) ' /
DATA PARM/' NETA ',' NSP ',' UINF ',' DTIL ',' RAD ','
X      ' RINF ',' RZB ',' DELTA ' /

C-----READ IN TITLE CARD.....
C
C      READ 99,TITLE
C
C-----READ IN PARAMETER CARDS.....
C
C      READ 101,NDBG,NETA,NSP, NE
C      READ 102,TOL,UINF,DTIL,RAD,RINF,RZB,DELTA
C
C-----READ IN PROFILES.....
C
C      READ 103,(ET(I),I=1,NETA)

```

DENS 160
 INPU 10
 INPU 20
 INPU 30
 INPU 40
 INPU 50
 INPU 60
 INPU 70
 INPU 80
 INPU 90
 INPU 100
 INPU 110
 INPU 120
 INPU 130
 INPU 140
 INPU 150
 INPU 160
 INPU 170
 INPU 180
 INPU 190
 INPU 200
 INPU 210
 INPU 220
 INPU 230
 INPU 240
 INPU 250
 INPU 260
 INPU 270
 INPU 280
 INPU 290
 INPU 300
 INPU 310
 INPU 320
 INPU 330
 INPU 340
 INPU 350

```

360 READ 102,(YOND(I),I=1,NETA)
370 INPU 360
380 READ 102,(TT(I),I=1,NETA)
390 INPU 380
400 READ 102,(PI(I),I=1,NETA)
410 INPU 400
420 READ 102,(VV(I),I=1,NETA)
430 INPU 420
440 DO5N=1,NETA
450 PRINT 206,ST(N),YOND(N),TT(N),PI(N),VV(N),RO(N)
460 INPU 440
470 FORMAT(2F8.4,4E12.4)
480 INPU 460
490 C-----READ IN SPECIES CARDS.....
500 C
510 DO10CI=1,NSP
520 READ 101,SP(I),SMW(I),SIG(I),EOK(I),C(I,1),C(I,NETA)
530 X,
540 (IA(I,J),J=1,NE)
550 READ 103,AII(I),BII(I),CH(I),DII(I),EII(I),FII(I),GII(I)
560 INPU 510
570 READ 103,AI (I),BI (I),CI (I),DI (I),EI (I),FI (I),GI (I)
580 INPU 520
590 CONTINUE
600 INPU 530
610 C-----LIST INPUT DATA....
620 C
630 PRINT99,TITLE
640 PRINT 205, PARM
650 PRINT 201,NETA,NSP,UINF,DTIL,RAD,RINF,RZB,DELTA
660 PRINT 205,NAME
670 DO30CI=1,NSP
680 PRINT 212,SP(I),SMW(I),SIG(I),EOK(I),C(I,1),C(I,NETA)
690 X,
700 (IA(I,J),J=1,NE)
710 PRINT200
720 DO40CI=1,NSP
730 PRINT203,SP(I),AI (I),BI (I),CI (I),DI (I),EI (I),FI (I),GI (I)
740 PRINT204,
750 AII(I),BII(I),CH(I),DII(I),EII(I),FII(I),GII(I)
760 RETURN
770 FORMAT(21A4)
780 DO50CI=1,NSP
790 PRINT 205,ST(N),YOND(N),TT(N),PI(N),VV(N),RO(N)
800 INPU 740
810 FORMAT(3I5,5X,5I1)
820 INPU 760
830 PRINT 206,ST(N),YOND(N),TT(N),PI(N),VV(N),RO(N)
840 INPU 780
850 FORMAT(1X,A4,5F10.5,5X,5I1)
860 INPU 800
870 PRINT 205,NAME
880 INPU 820
890 FORMAT(6E12.8)
900 INPU 840

```

```

103 FORMAT(7F10.4)
104 FORMAT(1X,A4,F10.5,I5)
105 FORMAT(8F10.4)
200 FORMAT(1H1,' SPECIES',35X,'THERMO-CONSTANTS A-G',29X,'RANGE')
201 FORMAT(2(4X,I2.4X),7F10.3)
202 FORMAT(2X,A4,2X,2F10.3,F10.1,2F10.5,5X,5I1)
203 FORMAT(1X,A4,7F12.4,' LOW RANGE')
204 FORMAT(5X,7F12.4,' HIGH RANGE')
205 FORMAT(/,8(1X,A8,1X))
      END
INPU 720
INPU 730
INPU 740
INPU 750
INPU 760
INPU 770
INPU 780
INPU 790
INPU 800
INPU 810

```



```

C
SUBROUTINE STPZF(NETA)
COMMON/NUMBER/NSP,NNS,NE,NC
COMMON/PROPI/PI(200),RO(200),TT(200),AMW(200),C(20,200),CC(5,200)
COMMON /VEL/ F(200),FC(200),ZZ(200),VV(200)
COMMON /STPZ/ EN(200),NPT
COMMON /YL/ ET(200),YOND(200)
DIMENSION DUM(200)

C-----SET UP THE ETA DISTRIBUTION....
C
EN(1)=0.0
N=2
NU=2
TMAX=75.0
DELT=ABS(TT(NO)-TT(NJ-1))
NSTEP=DELT/TMAX + 1.0
I=0
DELETA=(ET(NO)-ET(NO-1))/NSTEP
EN(N)=EN(N-1) + DELETA
I=I+1
N=N+1
IF(I.LT.NSTEP)GOTO15
NO=NO+1
IF(NO.LE.NETA)GOTO10
N=N+1
EN(N)=1.0
NPT=N
PRINT 99
99  FORMAT(/,20X,' REVISED ETA DISTRIBUTION.....',/)
PRINT 101, (EN(I),I=1,NPT)
101  FORMAT(10E12.4)
CALL SPACE(EN,NPT,ET,TT,NETA)
CALL SPACE(EN,NPT,ET,PI,NETA)
CALL SPACE(EN,NPT,ET,RO,NETA)
CALL SPACE(EN,NPT,ET,VV,NETA)

```

INPU 320
 STPZ 10
 STPZ 20
 STPZ 30
 STPZ 40
 STPZ 50
 STPZ 60
 STPZ 70
 STPZ 80
 STPZ 90
 STPZ 100
 STPZ 110
 STPZ 120
 STPZ 130
 STPZ 140
 STPZ 150
 STPZ 160
 STPZ 170
 STPZ 180
 STPZ 190
 STPZ 200
 STPZ 210
 STPZ 220
 STPZ 230
 STPZ 240
 STPZ 250
 STPZ 260
 STPZ 270
 STPZ 280
 STPZ 290
 STPZ 300
 STPZ 310
 STPZ 320
 STPZ 330
 STPZ 340
 STPZ 350

```

C          CALL      SPACE(EN,NPT,ET,YOND,NETA)
STPZ 360
STPZ 370
STPZ 380
STPZ 390
STPZ 400
STPZ 410
STPZ 420
STPZ 430
STPZ 440
STPZ 450
STPZ 460
STPZ 470
STPZ 480
STPZ 490
STPZ 500
STPZ 510
STPZ 520
STPZ 530
STPZ 540
STPZ 550
STPZ 560
STPZ 570
STPZ 580
STPZ 590
STPZ 600
STPZ 610
STPZ 620
STPZ 630
STPZ 640
STPZ 650
STPZ 660
STPZ 670
STPZ 680
STPZ 690
STPZ 700
STPZ 710

45      DO45N=1,NETA
      DUM(N)=ET(N)
      DO46N=1,NPT
46      ET(N)=EN(N)
      DO47N=1,NETA
47      EN(N)=DUM(N)
      N=NETA
      NETA=NPT
      NPT=N

C
      DO50I=1,NSP
50      C(I,NETA)=C(I,NPT)
C
      DO60N=2,NETA
      IF(TT(N).GT.TT(N-1))GOTO60C
      TT(N)=TT(N-1)*.5 + TT(N+1)*.5
60      CONTINUE
      PRINT 100,NETA
100     FORMAT(///' NETA=',I3)
      RETURN

C
C * * * * *
C      ENTRY REDUCE(NETA)
C * * * * *
C
C          CALL      SPACE(EN,NPT,ET,TT,NETA)
          CALL      SPACE(EN,NPT,ET,PI,NETA)
          CALL      SPACE(EN,NPT,ET,RO,NETA)
          CALL      SPACE(EN,NPT,ET,VV,NETA)
          CALL      SPACE(EN,NPT,ET,AMW,NETA)
          CALL      SPACE(EN,NPT,ET,YOND,NETA)

C          DO75J=1,NE
          DO76N=1,NETA

```

```

7      DUM(N)=CC(J,N)
      CALL SPACE(EN,NPT,ET,DUM,NETA)
      DO75N=1,NPT
75     CC(J,N)=DUM(N)
      C
      DO80I=1,NSP
      DO78N=1,NETA
78     DUM(N)=C(I,N)
      CALL SPACE(EN,NPT,ET,DUM,NETA)
      DO80N=1,NPT
80     C(I,N)=DUM(N)
      C
      DO85N=1,NETA
85     DUM(N)=ET(N)
      DO86N=1,NPT
86     ET(N)=EN(N)
      DO87N=1,NETA
87     EN(N)=DUM(N)
      C
      N=NETA
      NETA=NPT
      NPT=N
      C
      RETURN
      C
      END

```

STPZ 720
 STPZ 730
 STPZ 740
 STPZ 750
 STPZ 760
 STPZ 770
 STPZ 780
 STPZ 790
 STPZ 800
 STPZ 810
 STPZ 820
 STPZ 830
 STPZ 840
 STPZ 850
 STPZ 860
 STPZ 870
 STPZ 880
 STPZ 890
 STPZ 900
 STPZ 910
 STPZ 920
 STPZ 930
 STPZ 940
 STPZ 950
 STPZ 960
 STPZ 970

SP 1
SP 20
SP 30
SP 40
SP 50
SP 60
SP 70
SP 80
SP 90
SP 100

```

SUBROUTINE SPACE(XNEW,NEW,X,Y,NOLD)
DIMENSION XNEW(200),X(200),Y(200),DUM(200)
DO 10 N=1,NEW
X=XNEW(N)
CALL INTPL(XN,X,Y,NOLD,YN)
DUM(N)=YN
DO 20 N=1,NEW
Y(N)=DUM(N)
RETURN
END

```

10

20

```

C
C
C-----THIS PROGRAM PERFORMS LAGRANGIAN INTERPOLATION
C WITH NON-EQUAL STEP SIZE BETWEEN POINTS
C F=DEPENDENT VARIABLE
C X=INDEPENDENT VARIABLE
C VAR=VALUE OF X FOR WHICH CORRESPONDING VALUE OF
C F IS DESIRED BY INTERPOLATION
C IMAX=NUMBER OF POINTS IN ARRAY X OR F
C SOM=VALUE OF INTERPOLATED DEPENDENT VARIABLE
C NPTS=NUMBER OF POINTS USED FOR INTERPOLATION
C
C      DIMENSION X(100),F(100),XN(300),FN(300)
C      NPTS=7
C      XUP=1.E30
C      DO 611 I=1,IMAX
C      T=VAR-X(I)
C      IF(T.GE.0.C)GO TO 609
C      T=-T
C      IF(T.GE.0.XUP)GO TO 611
C      IP=1
C      XUP=T
C      CONTINUE
C      IN=1
C      NPP=NPTS+1
C      DO 613 I=1,NPP
C      FN(I)=F(IP)
C      XN(I)=X(IP)
C      IF(IN.GT.0)GO TO 615
C      IQ=IP-I
C      GO TO 615
C      IQ=IP+I
C      IF(IMAX.GE.IQ)GO TO 615
C      IP=IP-1
C      GO TO 613

```

SP 110
INTR 10
INTR 20
INTR 30
INTR 40
INTR 50
INTR 60
INTR 70
INTR 80
INTR 90
INTR 100
INTR 110
INTR 120
INTR 130
INTR 140
INTR 150
INTR 160
INTR 170
INTR 180
INTR 190
INTR 200
INTR 210
INTR 220
INTR 230
INTR 240
INTR 250
INTR 260
INTR 270
INTR 280
INTR 290
INTR 300
INTR 310
INTR 320
INTR 330
INTR 340
INTR 350

```

615 IF(IQ,GT,0)GO TO 617
616 IP=IP+1
    GO TO 618
617 IP=IQ
    IN=-IN
618 CONTINUE
    SOM=0.0
    FACT=1.0
    DO620 J=1,NPTS
    SOM=SOM+FACT*FN(1)
    DO619 I=J,NPTS
        IQ=I-J+1
        FN(IQ)=(FN(IQ+1)-FN(IQ))/(XN(I+1)-XN(IQ))
619 FACT=FACT*(VAR-XN(J))
620 RETURN
    END
INTR 360
INTR 370
INTR 380
INTR 390
INTR 400
INTR 410
INTR 420
INTR 430
INTR 440
INTR 450
INTR 460
INTR 470
INTR 480
INTR 490
INTR 500
INTR 510

```

```
C
SUBROUTINE INIT
COMMON/NUMBER/NSF,NIS,NE,NC
COMMON/PROPI/PI(200),RO(200),TT(200),AMW(200),C(20,200),CC(5,200)
COMMON/WT/SMW(20),AWT(5)
COMMON/WALL/ECWALL(5)
COMMON/EQ2/AA(20,5)
COMMON/RH/DUD,DPHI,TD,RZB,PD,HD,HTOTAL
COMMON/FRSTRM/UINF,RINF,UINF2,RAD,RE,LXI,ITM,IEM,NETA
COMMON/EQ3/IA(20,5)
COMMON/VEL/F(200),FC(200),ZZ(200),VV(200)
COMMON/DIF/D(5,200)
COMMON/MCD1/JS(20,200),JE(5,200)
COMMON/YL/ET(200),YOND(200)
DIMENSION DUM(200)
REAL JS, JE
TD=1.0
RHOD=RINF/RZB
FACT=RHOD*.7604

C-----FIRST NE SPECIES ARE ELEMENTS.....
C
DO5J=1,NE
5 AWT(J)=SMW(J)
C
C-----SMOOTH AND NON-DIMENSIONALIZE VELOCITY PROFILE, GUESS INITIAL
C
AMW-PROFILE....
C
CALL SG13(ET,VV,DUM,NETA,IER)
DO25N=1,NETA
VV(N)=DUM(N)/UINF
AMW(N)=RO(N)*FACT*TT(N)/PI(N)
25 DUM(N)=TT(N)
C
C-----SMOOTH TEMPERATURE PROFILE.....
C
```

```

      CALL SG12(ET,DUP,TT,NETA,IER)
      C-----FLOAT AA(I,J) MATFIX.....
      C
      DO3CI=1,NSP
      DO3CJ=1,NE
      30  AA(I,J)=IA(I,J)
      C
      C-----CONVERT WALL AND SHOCK COMPOSITIONS TO AN ELEMENTAL BASIS.....
      C
      DO35N=1,NETA
      DO35J=1,5
      35  CC(J,N)=0.0
      DO24J=1,NE
      DO23I=1,NSP
      FAC=AA(I,J)*AWT(J)/SMW(I)
      CC(J,I)=CC(J,I) + FAC*CC(I,I)
      23  CC(J,NETA)=CC(J,NETA) + FAC*CC(I,NETA)
      24  ECWALL(J)=CC(J,I)
      C
      C-----ESTIMATE INITIAL ELEMENTAL DIFFUSION COEFFICIENTS.....
      C
      READ(99,A
      999  FORMAT(E10.4)
      DO5CJ=1,NE
      DO5CN=1,NETA
      JF(J,N)=C.0
      50  D(J,N)=A*(TT(N)**1.659)/(PI(N)*UINF*HRAD)
      RETURN
      END

```

```

INIT 360
INIT 370
INIT 380
INIT 390
INIT 400
INIT 410
INIT 420
INIT 430
INIT 440
INIT 450
INIT 460
INIT 470
INIT 480
INIT 490
INIT 500
INIT 510
INIT 520
INIT 530
INIT 540
INIT 550
INIT 560
INIT 570
INIT 580
INIT 590
INIT 600
INIT 610
INIT 620
INIT 630
INIT 640
INIT 650

```


SUBROUTINE SG13(X,Y,Z,NDIM,IER)

SUBROUTINE SG 13

PURPOSE

TO COMPUTE A VECTOR OF SMOOTHED FUNCTION VALUES GIVEN
VECTORS OF ARGUMENT VALUES AND CORRESPONDING FUNCTION
VALUES

USAGE

CALL SG13(X,Y,Z,NDIM,IER)

DESCRIPTION OF PARAMETERS

X - GIVEN VECTOR OF ARGUMENT VALUES (DIMENSION NDIM)
Y - GIVEN VECTOR OF FUNCTION VL
Y - GIVEN VECTOR OF FUNCTION VALUES CORRESPONDING TO X
(DIMENSION NDIM)
Z - RESULTING VECTOR OF SMOOTHED FUNCTION VALUES
(DIMENSION NDIM)
NDIM - DIMENSION OF VECTORS X,Y,AND Z
IER - RESULTING ERROR PARAMETER
IER = -1 - NDIM IS LESS THAN 3
IER = 0 - NO ERROR

REMARKS

(1) IF IER=-1 THERE HAS BEEN NO COMPUTATION.
(2) Z CAN HAVE THE SAME STORAGE ALLOCATION AS X OR Y. IF
X OR Y IS DISTINCT FROM Z, THEN IT IS NOT DESTROYED.
SUBROUTINES AND SUBPROGRAMS REQUIRED

NONE

METHOD

EXCEPT AT THE ENDPOINTS X(1) AND X(NDIM), EACH SMOOTHED
VALUE Z(I) IS OBTAINED BY EVALUATING AT X(I) THE LEAST-
SQUARES POLYNOMIAL OF DEGREE 1 RELEVANT TO THE 3 SUCCESSIVE

SG13 11
SG13 20
SG13 30
SG13 40
SG13 50
SG13 60
SG13 70
SG13 80
SG13 90
SG13 100
SG13 110
SG13 120
SG13 130
SG13 140
SG13 150
SG13 160
SG13 170
SG13 180
SG13 190
SG13 200
SG13 210
SG13 220
SG13 230
SG13 240
SG13 250
SG13 260
SG13 270
SG13 280
SG13 290
SG13 300
SG13 310
SG13 320
SG13 330
SG13 340
SG13 350
SG13 360

```

C          POINTS (X(I+K),Y(I+K),
C          POINTS (X(I+K),Y(I+K)) K =-1,0,1.(SEE HILDEBRAND,F.P.,
C          INTRODUCTION TO NUMERICAL ANALYSIS, MC GRAW-HILL, NEW YORK/
C          TORONTO/LONDON, 1956, PP. 258-311.)
C          SG13 370
C          SG13 380
C          SG13 390
C          SG13 400
C          SG13 410
C          SG13 420
C          SG13 430
C          SG13 440
C          SG13 450
C          SG13 460
C          SG13 470
C          SG13 480
C          SG13 490
C          SG13 500
C          SG13 510
C          SG13 520
C          SG13 530
C          SG13 540
C          SG13 550
C          SG13 560
C          SG13 570
C          SG13 580
C          SG13 590
C          SG13 600
C          SG13 610
C          SG13 620
C          SG13 630
C          SG13 640
C          SG13 650
C          SG13 660
C          SG13 670
C          SG13 680
C          SG13 690
C          SG13 700
C          SG13 710
C          SG13 720

          POINTS (X(I+K),Y(I+K),
          POINTS (X(I+K),Y(I+K)) K =-1,0,1.(SEE HILDEBRAND,F.P.,
          INTRODUCTION TO NUMERICAL ANALYSIS, MC GRAW-HILL, NEW YORK/
          TORONTO/LONDON, 1956, PP. 258-311.)

          DIMENSION X(1),Y(1), Z(1)

          TEST OF DIMENSION
          IF(NDIM-3)7,1,1

          START LOOP
          1 DO 6 I=3,NDIM
             XM=.3333333*(X(I-2)+X(I-1)+X(I))
             YM=.3333333*(Y(I-2)+Y(I-1)+Y(I))
             T1=X(I-2)-XM
             T2=X(I-1)-XM
             T3=X(I)-XM
             XM=T1*T1+T2*T2+T3*T3
             IF(XM)3,3,2
          2   XM=(T1*(Y(I-2)-YM)+T2*(Y(I-1)-YM)+T3*(Y(I)-YM))/XM
          C
          C          CHECK FIRST POINT
          3 IF(I-3)4,4,5
          4 H=XM*T1+YM
          5 Z(I-2)=H
          6 H=XM*T2+YM
          C          END OF LOOP
          C
          C          UPDATE LAST TWO COMPONENTS
          Z(NDIM-1)=H
          ICP=C
          IER=1
          Z(NDIM)=XM*T3+YM
          RETURN
          C

```

SG13 730
SG13 740
SG13 750
SG13 760

C ERROR EXIT IN CASE NDIM IS LESS THAN 3
7 IER=-1
 RETURN
 END

DATA 10
DATA 20
DATA 30
DATA 40

BLOCK DATA
COMMON/ID/SP(20),FL(5)
DATA SP(2)*, /
END

```

C
SUBROUTINE ELEMNT
COMMON /JALL/ECWALL(5)
COMMON/WT/SMW(20),AWT(5)
COMMON/NUMBER/NS,NNS,NE,NCC
COMMON /MCD1/JS(20,200),JE(5,200)
COMMON/PROPI/PI(200),RO(200),TT(200),AMW(200),C(20,200),CC(5,200)ELEM 50
COMMON /FRSTPM/ U INF, RINF, UINF2,RAD, RE, LXI, ITM, IEM, NETA 60
COMMON /VECTOR/SUB(200),DIAG(200),SUP(200),B(200) 70
COMMON /SCE/ NCHECK,ITER 80
COMMON/SPI/SS,TOL,NDEBUG 90
COMMON /DIF/D(5,200) 100
COMMON /YL/ ET(200),YOND(200) 110
COMMON /VFL/FF(200),FC(200),ZZ(200),VV(200) 120
COMMON /DEL/ DELTA,DTIL,DTILS 130
COMMON/FUNCTN/DROV(200),X(200) 140
DIMENSION TEF(5,200) 150
DIMENSION XM(5) 160
REAL JS, JE 170
M=1 180
NCHECK=0 190
NM1=NETA-1 200
DO15J=1,NE 210
15 XM(J)=RO(1)*VV(1)*ECWALL(J) 220
C-----SOLVE ELEMENTAL SPECIES EQUATIONS IN A GLOBALLY IMPLICIT MATTER...ELEM 230
C 240
C 250
157 DO180J=1,NE 260
DIAG(1)=DTIL*VV(1)*ET(2)/(RO(1)*D(J,1)) + 1.0 270
SUP(1)=-1.0 280
R(1)=XM(J)*DTIL*ET(2)/(RO(1)*RO(1)*D(J,1)) 290
C 300
154 DO195K=2,NETA 310
NM=1+K 320
CALL FGH(N,F1,G1,H1) 330
CALL FGH2(N,F2,G2,H2) 340
ELEM 350

```

```

155  Q11FD=FI*RO(N+1)/RO(N) + G1 + H1*PO(N-1)/RO(N)
160  PETA=-OTIL*VV(N)/(RO(N)*D(J,N)) + 2.*DLNRO
      SUB(K-1)= PETA*H1 + H2
      DIAG(K)= PETA*G1 + G2
      SUP(K)= PETA*F1 + F2
      H(K)=C.C
      IF(N.GE.(NETA-1))GOTO160
170  155 CONTINUE
180  B(K)=-SUP(K)*CC(J,NETA)
      CALL TRID(K)
      DO170L=1,K
      ERR=ABS(B(L)-CC(J,M-1+L))
      IF(ERR.GT..025)NCHECK=NCHECK+1
190  CC(J,M-1+L)=B(L)
200  170 CONTINUE
210  IF(NE.LT.5)GOTO1100
220  CC(5,N)=(CC(1,N)/AWT(1) + CC(3,N)/AWT(3) + CC(4,N)/AWT(4))*AWT(5)
230  190 CONTINUE
240  RETURN
250  END
ELEM 360
ELEM 370
ELEM 380
ELEM 390
ELEM 400
ELEM 410
ELEM 420
ELEM 430
ELEM 440
ELEM 450
ELEM 460
ELEM 470
ELEM 480
ELEM 490
ELEM 500
ELEM 510
ELEM 520
ELEM 530
ELEM 540
ELEM 550

```

```

C
C SUBROUTINE FGH(N,F,G,H)
C ** ** = FIRST DERIVATIVE ** ** **
C-----EVALUATES COEFFICIENTS FOR THREE POINT DIFFERENCE APPROXIMATION
C OF DAVIS (AIAA JR. VOL. 8, NO. 5, MAY 1970).
C COMMON /YL/ FT(200),YOND(200)
DN=ET (N+1)-ET (N)
DNM1=ET (N)-ET (N-1)
DEL=DN+DNM1
D1=DN*DEL
D2=DN*DNM1
D3=DNM1*DEL
F=DNM1/D1
G=(DN-DNM1)/D2
H=-DN/D3
RETURN
END
ELEM 560
FGH( 10
FGH( 20
FGH( 30
FGH( 40
FGH( 50
FGH( 60
FGH( 70
FGH( 80
FGH( 90
FGH( 100
FGH( 110
FGH( 120
FGH( 130
FGH( 140
FGH( 150
FGH( 160

```

```

C ** SUBROUTINE FGH2(N,F,G,H)
C ** SECOND DERIVATIVE
C-----F EVALUATES COEFFICIENTS FOR THREE POINT DIFFERENCE APPROXIMATION
C OF DAVIS (AIAA JR. VOL. 8, NO. 5, MAY 1970).
COMMON /YL/ ET(200),YOND(200)
DN=ET (N+1)-ET (N)
DNM1=ET (N)-ET (N-1)
F=2./ (DN*(DN+DNM1))
G=-2./ (DN*DNM1)
H=2./ (DNM1*(DN+DNM1))
RETURN
END

```

FGH2	10
FGH2	20
FGH2	30
FGH2	40
FGH2	50
FGH2	60
FGH2	70
FGH2	80
FGH2	90
FGH2	100
FGH2	110
FGH2	120


```

C
C*** SUBROUTINE TRID (N)
C      TRID --TRIDIAGONAL EQUATION SOLVER  OBTAINED FROM CONTE P-184 ***
C      SUBROUTINE SOLVES AX = B FOR THE VECTOR X (WHERE A IS TRIDIAGONAL)
C      M = ORDER OF SYSTEM
C      SUP = SUPER DIAGONAL OF A
C      SUB = SUB DIAGONAL OF A
C      DIAG = MAIN DIAGONAL OF A
C      B = CONSTANT VECTOR
C      SUP AND DIAG ARE DESTROYED
C      SOLUTION VECTOR IS RETURNED IN B
C
COMMON /VECTOR/SUB(200),DIAG(200),SUP(200),B(200)
C
N = M
NN = N -1
SUP(1) = SUP(1)/DIAG(1)
B(1) = B(1)/DIAG(1)
DO 10 I=2,N
  II = I -1
  C-----DECOMPOSE A TO FORM A = LU WHERE L IS LOWER TRIANGULAR,
  C      AND U IS UPPER TRIANGULAR -----
  DIAG(I) = DIAG(I) - SUP(II)*SUB(II)
  IF (I.EQ. N) GO TO 10
  SUP(I) = SUP(I) / DIAG(I)
  C-----COMPUTE Z WHERE LZ = B
  10  B(I) = (B(I) - SUB(II) *B(II))/ DIAG(I)
  C-----COMPUTE X BY BACK SUBSTITUTION WHERE UX = Z
  DO 20 K =1,NN
    I = N - K
    B(I) = B(I) -SUP(I) *B(I+1)
  RETURN
END

```

```

FGH2 130
TRID 10
TRID 20
TRID 30
TRID 40
TRID 50
TRID 60
TRID 70
TRID 80
TRID 90
TRID 100
TRID 110
TRID 120
TRID 130
TRID 140
TRID 150
TRID 160
TRID 170
TRID 180
TRID 190
TRID 200
TRID 210
TRID 220
TRID 230
TRID 240
TRID 250
TRID 260
TRID 270
TRID 280
TRID 290
TRID 300
TRID 310
TRID 320

```

```

C
SUBROUTINE OUTPUT
COMMON /FRSTRM/ U INF, RINF, RINF2, R, RE, LXI, ITM, IEM, NT
COMMON /VEL/ F(200),FC(200),ZZ(200),VV(200)
COMMON /YL/ ET(200),YOND(200)
COMMON /PROP1/PI(200),RO(200),TT(200),AMW(200),C(20,200),CC(5,200)
COMMON /SCE/ NCHECK,ITER
DOUBLE PRECISION NAME(9)
DATA NAME/' CARBON ','HYDROGEN','NITROGEN',' OXYGEN ','ELECTRON',
, T(CK) ',','VELOCITY',' Y/D ',',', DENSITY'/
1 IF(NCHECK.GT.C)PRINT 104,ITER
IF(NCHECK.LE.C)PRINT 102,ITER
PRINT 103
PRINT 100,NAME
DO5N=1,NT
PRINT 101,ET(N),(CC(1,N),I=1,5),TT(N),VV(N),YOND(N),RO(N)
RETURN
100 FORMAT( 5X,'ETA',3X,9(2X,AR,2X))
101 FORMAT(F10.4,1X,9E12.4)
102 FORMAT(1H,1X,'MULTICOMPONENT SOLUTION CONVERGED IN ',I2,' ITERATION',
XONS'/)
103 FORMAT(15X,14(' '),ELEMENTAL MASS FRACTIONS',15(' '))
104 FORMAT('///',' ITERATION NUMBER ',I2)
END
TRID 330
OUTP 10
OUTP 20
OUTP 30
OUTP 40
OUTP 50
OUTP 60
OUTP 70
OUTP 80
OUTP 90
OUTP 100
OUTP 110
OUTP 120
OUTP 130
OUTP 140
OUTP 150
OUTP 160
OUTP 170
OUTP 180
OUTP 190
OUTP 200
OUTP 210
OUTP 220
OUTP 230

```

[illegible]

```

C-----INITIAL GUESS FOR EQUILIBRIUM CALCULATIONS.....
C
      DO10I=1,NS
      IF(CE(I,NI).LE.0.0)CE(I,NI)=1.0E-10
      Y(I) = CE(I,NI)*AMW(NI)/XMW(I)
C
C-----COMPUTE THE SIZE OF THE MATRIX
C
      NA=MM+1
C
      NS=NUMBER OF SPECIES.....
C
      CRIT=CRITERIA FOR CONVERGENCE.
C
      CRIT=1.0E-4
      CRIT=.001
      XBETA=CRIT
      BETA=0.
      LL=NS+1
      TOLD=0.0
C
C      THE REMAINDER OF THE PROGRAM COMPUTES EQUILIBRIUM COMPOSITIONS
C      CORRESPONDING TO THE ELEMENTAL MASS FRACTIONS IN THE CC-ARRAY
C      FROM POINT N = NI TO POINT N = NF.
C
      DO5000N=NI,NF
      T = TT(N)*TD
      P=PP(N)
      NT=1
      RETOLD=.0
      SUM=0.0
      DO15I=1,MM
      SUM=SUM + CC(I,N)
      DO20 I=1,MM
      IF(CC(I,N).LT.1.0E-10)CC(I,N)=1.0E-10
      E(I)=CC(I,N)/SUM

```

CHEM 360
CHEM 370
CHEM 380
CHEM 390
CHEM 400
CHEM 410
CHEM 420
CHEM 430
CHEM 440
CHEM 450
CHEM 460
CHEM 470
CHEM 480
CHEM 490
CHEM 500
CHEM 510
CHEM 520
CHEM 530
CHEM 540
CHEM 550
CHEM 560
CHEM 570
CHEM 580
CHEM 590
CHEM 600
CHEM 610
CHEM 620
CHEM 630
CHEM 640
CHEM 650
CHEM 660
CHEM 670
CHEM 680
CHEM 690
CHEM 700
CHEM 710

```

C      CALL ALTERY(F,Y,TOLD)
C
C      IF (A3S(T-TOLD).LE.50.)GOTO800
C
C      DO22I=1,NS
C      IF (Y(I).LT.1.E-8)Y(I)=1.E-8
C      22 CONTINUE
C
C      DO25 J=1,MM
C      BB(J)=0.C
C      DO 25 I=1,NS
C      25 BB(J)=BB(J)+AA(I,J)*Y(I)
C
C      CALL THERMO(T,P)
C
C-----THERMO SUBROUTINE CALCULATES THE FREE ENRGY FUNCTION,THE HEAT OF
C      FORMATION OF EVERY CHEMICAL SPECIE AT ANY TEMPERATURE T....
C
C-----SET-UP THE R-MATRIX AND THE B-VECTOR....
C
C      40 YBAR=0.
C      DO50I=1,NS
C      50 YBAR=YBAR+Y(I)
C
C      YUAK IS THE TOTAL NUMBER OF MOLES OF GAS SPECIES
C
C-----CALCULATE THE FREE ENERGY PARAMETER OF THE GAS SPECIES
C
C      DO60I=1,NS
C      FAC=Y(I)/YBAR
C      IF (FAC.LT.1.E-73)FAC=1.E-73
C      60 FY(I)=Y(I)*C(I)+ALOG(FAC)
C
CHEM 720
CHEM 730
CHEM 740
CHEM 750
CHEM 760
CHEM 770
CHEM 780
CHEM 790
CHEM 800
CHEM 810
CHEM 820
CHEM 830
CHEM 840
CHEM 850
CHEM 860
CHEM 870
CHEM 880
CHEM 890
CHEM 900
CHEM 910
CHEM 920
CHEM 930
CHEM 940
CHEM 950
CHEM 960
CHEM 970
CHEM 980
CHEM 990
CHEM1000
CHEM1010
CHEM1020
CHEM1030
CHEM1040
CHEM1050
CHEM1060
CHEM1070

```

```

C-----PROCEED TO CONSTRUCT THE R MATRIX
C
C-----INITIALIZE TO ZERO.....
C
      DO75J=1,NA
      DO75K=1,NA
      75  R(J,K)=0.0
C
      DO90J=1,MM
      DO90K=J,MM
      SUM=0.
      80  SUM=SUM+AA(I,J)*AA(I,K)*Y(I)
      90  R(J,K)=SUM
C
      DO103 K=1,MM
      SUM=0.
      DO101 I=1,NS
      101 SUM=SUM+AA(I,K)*Y(I)
      R(K,NA)=SUM
      R(NA,K)=SUM
      103 CONTINUE
C
C-----PROCEED TO CALCULATE THE VECTOR B.
C
      DO140 J=1,MM
      SUM=0.
      DO130 I=1,NS
      130 SUM=SUM+AA(I,J)*FY(I)
      140 B(J,1)=SUM+HB(J)
C
      SUM=0.
      DO150 I=1,NS
      150 SUM=SUM+FY(I)
      B(NA,1)=SUM

```

CHEM1080
CHEM1090
CHEM1100
CHEM1110
CHEM1120
CHEM1130
CHEM1140
CHEM1150
CHEM1160
CHEM1170
CHEM1180
CHEM1190
CHEM1200
CHEM1210
CHEM1220
CHEM1230
CHEM1240
CHEM1250
CHEM1260
CHEM1270
CHEM1280
CHEM1290
CHEM1300
CHEM1310
CHEM1320
CHEM1330
CHEM1340
CHEM1350
CHEM1360
CHEM1370
CHEM1380
CHEM1390
CHEM1400
CHEM1410
CHEM1420
CHEM1430

```

C-----MATRIX INVERSION IS CALLED TO PROVIDE THE SOLUTION FOR
C THE LINEARIZED EQUATIONS. THE SOLUTION OF THE EQUATIONS
C GIVES THE LAGRANGIAN MULTIPLIERS NEEDED TO COMPUTE THE MOLES
C OF EACH GAS SPECIES.
C
C      CALL MATINV(R,NA,B,MA,NMAX)
C      150 CONTINUE
C
C      DO160I=1,NA
C
C      PI(I)=LAGRANGINA MULTIPLIERS
C
C      160 PI(I)=B(I,1)
C      U=PI(NA)
C      XBAR=U*YBAR
C
C-----COMPUTE THE MOLES OF EACH SPECIE.....
C
C      DO170I=1,NS
C      FSUM(I)=-FY(I)+(Y(I)/YBAR)*XBAR
C      DO200I=1,NS
C      PSUM=0.
C      DO180J=1,MM
C      PSUM=PSUM+PI(J)*AA(I,J)
C      YSUM(I)=PSUM*Y(I)
C      200 X(I)=FSUM(I)+YSUM(I)
C
C-----CHECK IF CONVERGENCE CRITERIA HAS BEEN MET. IF SO, GO TO 800
C
C      BETA=.0
C      DO210I=1,NS
C      DELT(I)=X(I)-Y(I)
C      210 BETA=BETA+ABS(DELT(I))
C      IF (BETA,GT,HE TOLD)GOTO216

```

CHEM1440
CHEM1450
CHEM1460
CHEM1470
CHEM1480
CHEM1490
CHEM1500
CHEM1510
CHEM1520
CHEM1530
CHEM1540
CHEM1550
CHEM1560
CHEM1570
CHEM1580
CHEM1590
CHEM1600
CHEM1610
CHEM1620
CHEM1630
CHEM1640
CHEM1650
CHEM1660
CHEM1670
CHEM1680
CHEM1690
CHEM1700
CHEM1710
CHEM1720
CHEM1730
CHEM1740
CHEM1750
CHEM1760
CHEM1770
CHEM1780
CHEM1790

```

CHEM1800
CHEM1810
CHEM1820
CHEM1830
CHEM1840
CHEM1850
CHEM1860
CHEM1870
CHEM1880
CHEM1890
CHEM1900
CHEM1910
CHEM1920
CHEM1930
CHEM1940
CHEM1950
CHEM1960
CHEM1970
CHEM1980
CHEM1990
CHEM2000
CHEM2010
CHEM2020
CHEM2030
CHEM2040
CHEM2050
CHEM2060
CHEM2070
CHEM2080
CHEM2090
CHEM2100
CHEM2110
CHEM2120
CHEM2130
CHEM2140
CHEM2150

      IF (DELTA.LT.XBETA)GOTO200
210  CONTINUE
C-----COMPUTE THE CONVERGENCE PARAMENTER XLAMBDA
C
      XLAMBDA=1.
      DO210 I=1,NS
      IF (ABS(DELT(I)).LT.1.0E-20)DELT(I)=0.0
      IF (DELT(I).GE.0.)GOTO210
      IF (X(I).GT.0.)GOTO210
      XLAM(I)=-Y(I)/DELT(I)
      XLAMBDA=AMIN1(XLAMBDA,XLAM(I))
      XLAMBDA=.99*XLAMBDA
210  CONTINUE
      XLAM1=XLAMBDA
      IF (XLAM1.EQ.0.)XLAM1=1.0E-5
      DEBAR=0.
      DO220 I=1,NS
220  DEBAR=DEBAR+DELT(I)
C-----DETERMINE THE SIZE OF THE UNIT VECTOR XLAMBDA.
C      APPLY THE COPRECTIONS TO OBTAIN A NEW SET OF ESTIMATES FOR THE
C      NEXT ITERATION. WHEN THE VALUE OF XLAMBDA IS VERY SMALL SET THE
C      VALUES OF Y(I) EQUAL TO X(I) TO AVOID USING THE SAME VALUES OF
C      Y(I) AS WAS USED IN THE PREVIOUS ITERATION
C
C-----DETERMINE THE FREE ENERGY GRADIENT. IF POSITIVE REDUCE XLAMBDA
C      DFOL=FREE ENERGY GRADIENT
C
230  DFOL=0.
      DO240 I=1,NS
      FAC=(Y(I)+XLAMBDA*DELT(I))/(YBAR+XLAMBDA*DEHAP)
      IF (FAC.GT.0.)GOTO230
      XLAMBDA=.9*XLAMBDA
      GOTO230

```



```

200  DERP=(DEL(T(I)*YBAR-DEBAR*Y(I))/(YBAR+XLAMBD*DEBAR)
      IF (FAC.LT.1.E-73) FAC=1.E-73
210  DFOL=DFOL+DEL(T(I)*(C(I)+ALOG(FAC)) + DERP
      IF (DFOL.LT.0.00) GOTO 300
      XLAMBD=.8*XLAMBD
      IF (XLAMBD.GT.1.0E-08) GOTO 230
C
C-----THE VALUE OF XLAMBD THAT ASSURES CONVERGENCE HAS BEEN FOUND
C
300  DO 350 I=1,NS
      IF (XLAMBD.GT.1.E-6) GOTO 330
      IF (DFOL.LT.0.0) GOTO 330
      IF (XLAM1.LT.1.E-6) XLAM1=1.E-6
C
C-----CALCULATE THE NEW COMPOSITION FOR THE NEXT ITERATION
C
      Y(I)=Y(I)+XLAM1*DEL(T(I))*0.1
      GOTO 340
330  Y(I)=Y(I)+XLAMBD*DEL(T(I)
340  IF (Y(I).LT.0.0) Y(I)=1.E-73
350  CONTINUE
C
532  NT=NT+1
      BETOLD=BETA
      TOLD=T
C
C-----IF THE NUMBER OF ITERATIONS EXCEED 900 STOP COMPUTATIONS
C
      IF (NT.GT.900) GOTO 600
      GOTO 40
      RTT CONTINUE
C
C-----CONVERT Y(I) TO MOLE FRACTIONS.....
C
      THESE VALUES IN THE CF-MATRIX. AMW(N) IS THE AVERAGE MOLECULAR
      CONVERT EQUILIBRIUM MOLE FRACTIONS TO MASS FRACTIONS AND STORE

```

CHEM2160
 CHEM2170
 CHEM2180
 CHEM2190
 CHEM2200
 CHEM2210
 CHEM2220
 CHEM2230
 CHEM2240
 CHEM2250
 CHEM2260
 CHEM2270
 CHEM2280
 CHEM2290
 CHEM2300
 CHEM2310
 CHEM2320
 CHEM2330
 CHEM2340
 CHEM2350
 CHEM2360
 CHEM2370
 CHEM2380
 CHEM2390
 CHEM2400
 CHEM2410
 CHEM2420
 CHEM2430
 CHEM2440
 CHEM2450
 CHEM2460
 CHEM2470
 CHEM2480
 CHEM2490
 CHEM2500
 CHEM2510

```

C      WEIGHT AT THE POINT, N.
C
      SUMY=0.0
      DO900 I=1,NS
900    SUMY=SUMY+Y(I)
      AMW(N) = 0.0
      DO1000 I=1,NS
1000    Y(I)=Y(I)/SUMY
      AMW(N) = AMW(N) + Y(I)*XMW(I)
      DO1005 I=1,NS
1005    CE(I,N) = Y(I)
1005    CE(I,N) = Y(I)*XMW(I)/AMW(N)
C
C      OPTIONAL OUTPUT OF POSITION , TEMPERATURE AND EQUILIBRIUM
C      COMPOSITIONS.
C
      IF(NDRUG.LT.3)GOTO3300
      PRINT 2000,P,TT(N),NT
      PRINT 2000,P,TT(N),NT
      X=.13,/,11X,Y(I),.12X,C(I,N),/
      PRINT 2005,(SP(I),Y(I),CE(I,N),I=1,NS)
      PRINT 2005,(SP(I),Y(I),CE(I,N),I=1,NS)
      PRINT 2005,(SP(I),Y(I),CE(I,N),I=1,NS)
C
3300    XBETA=CRIT
5000    CONTINUE
      RETURN
6000    PRINT6001
6001    PRINT6001
      RETURN
      END

```

CHEM2520
CHEM2530
CHEM2540
CHEM2550
CHEM2560
CHEM2570
CHEM2580
CHEM2590
CHEM2600
CHEM2610
CHEM2620
CHEM2630
CHEM2640
CHEM2650
CHEM2660
CHEM2670
CHEM2680
CHEM2690
CHEM2700
CHEM2710
CHEM2720
CHEM2730
CHEM2740
CHEM2750
CHEM2760
CHEM2770
CHEM2780
CHEM2790
CHEM2800
CHEM2810

```

C
SUBROUTINE ALTERY(F,Y,TOLD)
COMMON/WT/SMW(20),AWT(5)
COMMON/NUMBER/NSP,NNS,NE,NC
COMMON/EQ2/AA(20,5)
COMMON /SP1/SS,TOL,NDRUG
DIMENSION E(5),Y(20),B(5),EOLD(5)
DATA EOLD/5*0.0/

C
C-----CHECK TO SEE IF ELEMENTAL COMPOSITION HAS CHANGED SIGNIFICANTLY.
C
C IF NOT, THEN RETURN.....
C
C
CHANGE=0.0
DO5J=1,NE
CHANGE=CHANGE+ABS(EOLD(J)-E(J))
EOLD(J)=E(J)
IF(CHANGE.LT.1.0E-4)RETURN
5
C
C-----ASSUME ALL SPECIES HAVE THE SAME COMPOSITION.....
C
C
C
C-----COMPUTE GRAM-ATOMS OF EACH ELEMENT FROM KNOWN ELEMENTAL CPMPOS
C
C DISTRIBUTION AND THE MAXIMUM POSSIBLE MOLECULAR WEIGHT.....
C
DO20J=1,NE
IF(E(J).GT.1.0E-8)GOTO20
DO15I=1,NSP
IF(AA(I,J).LE.0.0)GOTO15
Y(I)=1.0E-12
15 CONTINUE
20 E(J)=E(J)*100./AWT(J)
C
C-----CALCULATE FOR EACH ELEMENT, THE NUMBER OF G-ATOMS BASED ON THE
C FIRST GUESS. ADJUST THE COMPOSITION OF EACH ELEMENT-SPECIE AS
C REQUIRED.....
C
C

```

ALTE 36C
 ALTE 37C
 ALTE 38C
 ALTE 39C
 ALTE 40C
 ALTE 41C
 ALTE 42C
 ALTE 43C
 ALTE 44C

```

0030 J=1,NE
      R(J)=C,C
0031 I=1,NSP
      R(J)=B(J)+AA(I,J)*Y(I)
0040 J=1,NE
      Y(J)=Y(J)      + (E(J)-B(J))
      TOLD=C,C
      RETURN
      END
30
40
  
```


1HER 360
1HER 370
1HER 380
1HER 390
1HER 400
1HER 410
1HER 420
1HER 430

C(I)=FURT(I)+ALOG(P)
IF(T.GT.7000)GOTO41
FAC=(T-5000.)/2000.
FURT(I)=FURT(I)*FAC + FLOW*(1.0-FAC)
C(I)=C(I)*FAC + CLOW*(1.0-FAC)
41 CONTINUE
RETURN
END

```
CHEM282
MATI 10
MATI 20
MATI 30
MATI 40
MATI 50
MATI 60
MATI 70
MATI 80
MATI 90
MATI 100
MATI 110
MATI 120
MATI 130
MATI 140
MATI 150
MATI 160
MATI 170
MATI 180
MATI 190
MATI 200
MATI 210
MATI 220
MATI 230
MATI 240
MATI 250
MATI 260
MATI 270
MATI 280
MATI 290
MATI 300
MATI 310
MATI 320
MATI 330
MATI 340
MATI 350
```

SUBROUTINE MATINV(A,N,B,M,NMAX)

MATRIX INVERSION WITH ACCOMPANYING SOLUTION OF LINEAR EQUATIONS
DIMENSION A(20,20),B(20,1),IPIVOT(20),INDEX(20,2)
EQUIVALENCE (IRCW,JROW), (ICOLU,JCOLU), (AMAX,T,SWAP)

INITIALIZATION

5 ISCALE=0
6 R1=10.0**18
7 R2=1.0/R1
10 DETERM=1.0
15 DO 20 J=1,N
20 IPIVOT(J)=0
30 DO 550 I=1,N

SEARCH FOR PIVOT ELEMENT

40 AMAX=0.0
45 DO 105 J=1,N
50 IF (IPIVOT(J)-1)60,105,60
60 DO 100 K=1,N
70 IF (IPIVOT(K)-1)80,100,740
80 IF (ABS(AMAX)-ABS(A(J,K)))85,100,100
85 IPOW=J
90 ICOLU=K
95 AMAX=A(J,K)
100 CONTINUE
105 CONTINUE
IF (AMAX)110,106,110
106 DETERM=C.0
ISCALE=0
GO TO 740
110 IPIVOT(ICOLU)=IPIVOT(ICOLU)+1

```

C
C      INTERCHANGE ROWS TO PUT PIVOT ELEMENT ON DIAGONAL
C
      130 IF (IROW-ICOLU)140,260,140
      140 DETERM=-DETERM
      150 DO 200 L=1,N
      160 SWAP=A(IROW,L)
      170 A(IROW,L)=A(ICOLU,L)
      200 A(ICOLU,L)=SWAP
      205 IF(M)260,260,210
      210 DO 250 L=1,M
      220 SWAP=B(IROW,L)
      230 B(IROW,L)=B(ICOLU,L)
      250 B(ICOLU,L)=SWAP
      260 INDEX(I,1)=IROW
      270 INDEX(I,2)=ICOLU
      310 PIVOT=A(ICOLU,ICOLU)
C
C      SCALE THE DETERMINANT
C
      1000 PIVOTI=PIVOT
      1005 IF(ABS(DETERM)-R1)1030,1010,1010
      1010 DETERM=DETERM/R1
           ISCALE=ISCALE+1
      1020 IF(ABS(DETERM)-R1)1060,1020,1020
      1020 DETERM=DETERM/R1
           ISCALE=ISCALE+1
           GO TO 1060
      1030 IF(ABS(DETERM)-R2)1040,1040,1060
      1040 DETERM=DETERM*R1
           ISCALE=ISCALE-1
      1050 IF(ABS(DETERM)-R2)1050,1050,1060
      1050 DETERM=DETERM*R1
           ISCALE=ISCALE-1
      1060 IF(ABS(PIVOTI)-R1)1090,1070,1070
      1070 PIVOTI=PIVOTI/R1

```

```

MATI 361
MATI 370
MATI 380
MATI 390
MATI 400
MATI 410
MATI 420
MATI 430
MATI 440
MATI 450
MATI 460
MATI 470
MATI 480
MATI 490
MATI 500
MATI 510
MATI 520
MATI 530
MATI 540
MATI 550
MATI 560
MATI 570
MATI 580
MATI 590
MATI 600
MATI 610
MATI 620
MATI 630
MATI 640
MATI 650
MATI 660
MATI 670
MATI 680
MATI 690
MATI 700
MATI 710

```



```

1080 ISCALE=ISCALE+1
      IF (ABS(PIVOTI)-R1) 320,1080,1080
1090 PIVOTI=PIVOTI/R1
2000 ISCALE=ISCALE+1
      GO TO 320
1090 IF (ABS(PIVOTI)-R2) 2000,2000,320
2000 PIVOTI=PIVOTI*R1
      ISCALE=ISCALE-1
2010 IF (ABS(PIVOTI)-R2) 2010,2010,320
2010 PIVOTI=PIVOTI*R1
      ISCALE=ISCALE-1
320 DETERM=DETERM*PIVOTI
C
C      DIVIDE PIVOT ROW BY PIVOT ELEMENT
C
330 A(ICOLU,ICOLU)=1.0
340 DO 350 L=1,N
350 A(ICOLU,L)=A(ICOLU,L)/PIVOT
355 IF(M) 380,380,360
360 DO 370 L=1,M
370 B(ICOLU,L)=B(ICOLU,L)/PIVOT
C
C      REDUCE NON-PIVOT ROWS
C
380 DO 550 L1=1,N
390 IF(L1-ICOLU) 400,550,400
400 T=A(L1,ICOLU)
420 A(L1,ICOLU)=T.0
430 DO 450 L=1,N
450 A(L1,L)=A(L1,L)-A(ICOLU,L)*T
455 IF(M) 550,550,460
460 DO 500 L=1,M
500 B(L1,L)=B(L1,L)-B(ICOLU,L)*T
550 CONTINUE
C
C      INTERCHANGE COLUMNS
C

```

```

MATI 720
MATI 730
MATI 740
MATI 750
MATI 760
MATI 770
MATI 780
MATI 790
MATI 800
MATI 810
MATI 820
MATI 830
MATI 840
MATI 850
MATI 860
MATI 870
MATI 880
MATI 890
MATI 900
MATI 910
MATI 920
MATI 930
MATI 940
MATI 950
MATI 960
MATI 970
MATI 980
MATI 990
MATI 1000
MATI 1010
MATI 1020
MATI 1030
MATI 1040
MATI 1050
MATI 1060
MATI 1070

```

```

C
610 DO 710 I=1,N
      615 L=N+1-I
      620 IF (INDEX(L,1)-INDEX(L,2))630,710,630
      630 JROW=INDEX(L,1)
      640 JCOLUM=INDEX(L,2)
      650 DO 705 K=1,N
        660 SWAP=A(K,JROW)
        670 A(K,JROW)=A(K,JCOLUM)
        700 A(K,JCOLUM)=SWAP
      705 CONTINUE
      710 CONTINUE
      740 RETURN
      END
MAT11080
MAT11090
MAT11100
MAT11110
MAT11120
MAT11130
MAT11140
MAT11150
MAT11160
MAT11170
MAT11180
MAT11190
MAT11200
MAT11210

```

```

C
SUBROUTINE DENSITY(ND)
COMMON/PECP1/PI(200),RO(200),TT(200),AMW(200),C(20,200),CC(5,200)DENS 10
COMMON /R4/ DUC,DPHI,TD,RZB,PD,HD,HTOTALDENS 20
COMMON /FRSTPM/ U INF, RINF, UINF2,RAD, RE, LXI, ITM, IEM,NETA DENS 30
COMMON /YL/ ET(200),YOND(200)DENS 40
DIMENSION RS(200)DENS 50
DEN=RZB*.76C4/RINF DENS 60
ND=0 DENS 70
DO10N=1,NETA DENS 80
RNEW=DEN*AMW(N)*PI(N)/TT(N) DENS 90
ERR=(RNEW-RO(N))/RO(N) DENS 100
IF(ABS(ERR).GT..05)ND=ND+1 DENS 110
RO(N)=RNEW*.7 + RO(N)*.3 DENS 120
RETURN DENS 130
END DENS 140
10 DENS 150

```

```

C
SUBROUTINE PROFIL(ITYPE)
COMMON /YL/ ET(200),YOND(200)
COMMON /FRSTRM/ U INF, RINF, UINF2, R , RE, LXI, ITM, IEM, NETA
COMMON/NUMBER/NSP,NNS,NE,NC
COMMON /VEL/ F(200),FC(200),ZZ(200),VV(200)
COMMON/PROPI/PI(200),RO(200),TT(200),AMW(200),C (20,200),CC(5,200)
COMMON/ID/SP(20),EL(5)
DIMENSION TYPE(2)
DATA TYPE/'MASS','MOLE' /
PRINT 200
PRINT 201,TYPE(ITYPE),(SP(I),I=1,10)
DO10N=1,NETA
NCP=10
IF(NSP,LT,10)NCP=NSP
PRINT 202, ET(N),(C(I,N),I=1,NCP)
IF(NSP,LE,10)GOTO30
PRINT 200
PRINT 201,TYPE(ITYPE),(SP(I),I=11,NSP)
DO20N=1,NETA
PRINT 202, ET(N),(C(I,N),I=11,NSP)
RETURN
FORMAT(1H1)
FORMAT( ,EQUILIBRIUM ',A4,',FRACTIONS'/' ,ETA ',2X,10(5X,A4,3X))
FORMAT(1X,F6.4,10F12.4)
END

```

10
 20
 30
 200
 201
 202

MATI1220
 PROF 10
 PROF 20
 PROF 30
 PROF 40
 PROF 50
 PROF 60
 PROF 70
 PROF 80
 PROF 90
 PROF 100
 PROF 110
 PROF 120
 PROF 130
 PROF 140
 PROF 150
 PROF 160
 PROF 170
 PROF 180
 PROF 190
 PROF 200
 PROF 210
 PROF 220
 PROF 230
 PROF 240
 PROF 250

```

C
SUBROUTINE DELTAY(NETA,NSP)
COMMON /DELY/ DY(20,200)
COMMON /YL/ ET(200),YOND(200)
COMMON/PROPI/PI(200),RO(200),TT(200),AMW(200),C (20,200),CC(5,200)DELT 40
NM1=NETA-1
DO1CN=2,NM1
CALL FGH(N,F,G,H)
DO1CI=1,NSP
10 DY(I,N)=F*C(I,N+1) + G*C(I,N) + H*C(I,N-1)
DO2OI=1,NSP
20 DY(I,NETA)=DY(I,NM1)
DY(I,1)=DY(I,2)
RETURN
END
DELT 10
DELT 20
DELT 30
DELT 40
DELT 50
DELT 60
DELT 70
DELT 80
DELT 90
DELT 100
DELT 110
DELT 120
DELT 130
DELT 140

```

```

C      SUBROUTINE MCD
C-----SOLVES FOR FLUXES FROM STEFAN-MAXWELL EQUATION AND SPECIFIED
C      COMPOSITION PROFILES.....
COMMON /DELY/ DY(20,200)
COMMON /MCD1/JS(20,200),JE(5,200)
COMMON/NUMBER/NSP,NNS,NE,NC
COMMON/SP1/SS,TCL,NDBUG
COMMON/WT/SMW(20),AWT(5)
COMMON/ID/SP(20),EL(5)
COMMON /FRSTRM/ U INF, RINF, UINF2,RAD, RE, LXI, ITM, IEM,NETA
COMMON /BLOCK2/ SIG(20),EOK(20)
COMMON/PROPI/PI(20),RO(20),TT(200),AMW(200),Y (20,200),CC(5,200)MCD
COMMON /YL/ ET(200),YOND(200)
COMMON /DEL/ DELTA,DYIL,DYILS
COMMON /RH/ DUD,DPHI,TD,RZB,PD,HD,HTOTAL
REAL JS,JE,LAMBDA,M12
DIMENSION A(20,20),B(20,1),D(20,20),L(20)
C-----INITIALIZATION.....
NM1=NETA-1
DO2I=1,NSP
Y(I,NETA+1)=Y(I,NETA)
JS(I,NETA)=0.0
JS(I,1)=0.0
2
C-----COMPUTE FLUXES FROM POINT 2 TO POINT NETA-1 -----
DO1(CON=2,NM1
Y=TT(N)
P=PI(N)
THETA=PO(N)/DYIL
C-----DETERMINE WHICH SPECIES ARE PRESENT IN SIGNIFICANT AMOUNTS.....

```

DELT 150
 MCD 10
 MCD 20
 MCD 30
 MCD 40
 MCD 50
 MCD 60
 MCD 70
 MCD 80
 MCD 90
 MCD 100
 MCD 110
 MCD 120
 MCD 130
 MCD 140
 MCD 150
 MCD 160
 MCD 170
 MCD 180
 MCD 190
 MCD 200
 MCD 210
 MCD 220
 MCD 230
 MCD 240
 MCD 250
 MCD 260
 MCD 270
 MCD 280
 MCD 290
 MCD 300
 MCD 310
 MCD 320
 MCD 330
 MCD 340
 MCD 350

```

NS=0
DO25I=1,NSP
JS(I,N)=0.0
IF(Y(I,N).LT..1E-(5)GOTO25
NS=NS+1
L(NS)=I
25 CONTINUE
NSM1=NS-1
C
C-----COMPUTE B-VECTOR,IF GRADIENTS ARE LESS THAN 1.0E-8. SET FLUXES TO
C ZERO AND ADVANCE TO NEXT POINT IN FLOW-FIELD....
C
CALL FGH(N,F,G,H)
DO3M=1,NS
I=L(M)
B(M,1)=DY(I,N)*THETA
3 CONTINUE
B(NS,1)=0.0
C
C-----EVALUATE BINARY COEFFICIENTS, D(I,J)....
C
DO5 I=1,NSP
DO5 J=I,NSP
S2=((SIG(I)+SIG(J))*5)**2
E=SQRT(EOK(I)*EOK(J))
TS=T/E
D=1.061/TS**.156
M12=SQRT((SMW(I)+SMW(J))/(2.*SMW(I)*SMW(J)))
T32=T**.5
D(I,J)=28.28E-07*T32*M12/(P*S2*Q*UINF*RAD)
5 D(J,I)=D(I,J)
C
C-----COMPUTE A-MATRIX....
C
DO10,II=1,NSM1
I=L(II)

```

MCD 360
MCD 370
MCD 380
MCD 390
MCD 400
MCD 410
MCD 420
MCD 430
MCD 440
MCD 450
MCD 460
MCD 470
MCD 480
MCD 490
MCD 500
MCD 510
MCD 520
MCD 530
MCD 540
MCD 550
MCD 560
MCD 570
MCD 580
MCD 590
MCD 600
MCD 610
MCD 620
MCD 630
MCD 640
MCD 650
MCD 660
MCD 670
MCD 680
MCD 690
MCD 700
MCD 710

```

A(II,II)=0.0
DO1CJJ=1,NS
J=L(JJ)
IF(I.EQ.J)GOTO1C
A(II,JJ)=Y(J,N)*Y(I,N)/D(I,J)
A(II,II)=A(II,II) - A(II,JJ)
10 CONTINUE
DO45JJ=1,NS
J=L(JJ)
45 A(NS,JJ)=Y(J,N)*SMW(J)
C
CALL MATINV(A,NS ,B,1,NMAX)
C
DO50II=1,NS
I=L(II)
50 JS(I,N)=B(II,1)*Y(I,N)*SMW(I)*RO(N)/AMW(N)
100 CONTINUE
C ---
IF(NDBUG.LT.2)GOTO200
101 FORMAT(1H1,' DIFFUSION FLUXES',/,' ETA ',2X,10(5X,A4,3X))
102 FORMAT(1X,F6.4,10E12.4)
103 FORMAT(1H1)
PRINT 101,(SP(I),I=1,10)
DO11CN=1,NETA
NCP=1C
IF(NSP.LT.1C)NCP=NSP
110 PRINT 102,ET(N),(JS(I,N),I=1,NCP)
IF(NSP.LE.10)GOTO13C
PRINT 101,(SP(I),I=11,NSP)
DO12CN=1,NETA
120 PRINT 102,ET(N),(JS(I,N),I=11,NSP)
130 PRINT 103
200 RETURN
END

```

MCD 720
MCD 730
MCD 740
MCD 750
MCD 760
MCD 770
MCD 780
MCD 790
MCD 800
MCD 810
MCD 820
MCD 830
MCD 840
MCD 850
MCD 860
MCD 870
MCD 880
MCD 890
MCD 900
MCD 910
MCD 920
MCD 930
MCD 940
MCD 950
MCD 960
MCD 970
MCD 980
MCD 990
MCD 1000
MCD 1010
MCD 1020
MCD 1030
MCD 1040
MCD 1050


```

C
C      SUBROUTINE EFLUX
C-----  CONVERTS MASS FLUXES TO ELEMENTAL BASIS
C
COMMON/NUMBER/NSP,NNS,NE,NC
COMMON /FRSTRM/ U INF, RINF, UINF2, P , RE, LXI, ITM, IEM,NETA
COMMON/WT/SMW(20),AWT(5)
COMMON/EQ2/AA(20,5)
COMMON /MCD1/JS(20,200),JE(5,200)
REAL JS, JE
DO15N=1,NETA
DO10J=1,NE
JE(J,N)=0.0
DO10I=1,NSP
10  JE(J,N)=JE(J,N) + AA(I,J)*AWT(J)*JS(I,N)/SMW(I)
15  CONTINUE
RETURN
END
MCD 1060
EFLU 10
EFLU 20
EFLU 30
EFLU 40
EFLU 50
EFLU 60
EFLU 70
EFLU 80
EFLU 90
EFLU 100
EFLU 110
EFLU 120
EFLU 130
EFLU 140
EFLU 150
EFLU 160
EFLU 170
EFLU 180

```

```

C
SUBROUTINE DIJ
COMMON/SP1/SS,TOL,NDEBUG
COMMON /VEL/FF(200),FC(200),ZZ(200),VV(200)
COMMON /MCD1/JS(20,200),JE(5,200)
COMMON/NUMBER/NSP,NNS,NE,NC
COMMON /FRSTRM/ U INF, RINF, UINF2,RAD, RE, LXI, ITM, IEM,NETA
COMMON/PROPI/PI(200),RO(200),TT(200),AM(200),C(20,200),CC(5,200)
COMMON /YL/ ET(200),YOND(200)
COMMON /DEL/ DELTA,DTIL,DTILS
COMMON /DIF/D(5,200)
DIMENSION DCDE(5)
REAL*4 DCDE
REAL*4 JS,JE
NM1=NETA-1
DO10J=1,NE
  JE(J,1)=0.0
  JE(J,NETA)=0.0
  DO40N=2,NM1
    RV=RO(N)*VV(N)
    CALL FGH(N,F1,G1,H1)
    DO30J=1,NE
      DNEW = 1.0E-6
      IF (ABS(JE(J,N)/RV).LE.0.01)GOTO25
      DCDE(J) =CC(J,N+1)*F1 + CC(J,N)*G1 + CC(J,N-1)*H1
      IF (ABS(DCDE(J)).LE.1.0E-3)GOTO25
      DNEW = -JE(J,N)*DTIL/(RO(N)*RO(N)*DCDE(J))
      IF (DNEW.LE.0.0)DNEW=1.0E-6
      D(J,N)=D(J,N)*.3 + DNEW*.7
    CONTINUE
  IF (NDEBUG,LT.2)GOTO40
  PRINT 101,ET(N),(JE(J,N),DCDE(J),D(J,N),J=1,NE)
CONTINUE
RETURN
FORMAT(F6.3,5(1X,3E8.2))
101
END

```

EFLU 190
 DIJ 19
 DIJ 20
 DIJ 30
 DIJ 40
 DIJ 50
 DIJ 60
 DIJ 70
 DIJ 80
 DIJ 90
 DIJ 100
 DIJ 110
 DIJ 120
 DIJ 130
 DIJ 140
 DIJ 150
 DIJ 160
 DIJ 170
 DIJ 180
 DIJ 190
 DIJ 200
 DIJ 210
 DIJ 220
 DIJ 230
 DIJ 240
 DIJ 250
 DIJ 260
 DIJ 270
 DIJ 280
 DIJ 290
 DIJ 300
 DIJ 310
 DIJ 320
 DIJ 330
 DIJ 340
 DIJ 350

```

SUBROUTINE COMP(ITYPE,NSP,NETA)
COMMON/PROF1/PI(200),RO(200),TT(200),AMW(200),C (20,200),CC(5,200)
COMMON /WT/SMW(20),AWT(5)
IF(ITYPE.EQ.1)GOTO20
C-----CONVERT MOLE FRACTIONS TO MASS FRACTIONS.....
C
DO1CN=1,NETA
DO1CI=1,NSP
10 C(I,N)=C(I,N)*SMW(I)/AMW(N)
ITYPE=1
RETURN
C
C-----CONVERT MASS FRACTIONS TO MOLE FRACTIONS.....
C
DO3CN=1,NETA
DO3CI=1,NSP
30 C(I,N)=C(I,N)*AMW(N)/SMW(I)
ITYPE=2
RETURN
END
COMP 10
COMP 20
COMP 30
COMP 40
COMP 50
COMP 60
COMP 70
COMP 80
COMP 90
COMP 100
COMP 110
COMP 120
COMP 130
COMP 140
COMP 150
COMP 160
COMP 170
COMP 180
COMP 190
COMP 200
COMP 210

```

```

SUBROUTINE LRAD4
C
C ** PUNCH PROGRAM FOR LRAD4 DATA ** ** **
C
COMMON/TITL/TITLE(20)
COMMON/ID/SP(20),EL(5)
COMMON/WT/SMW(20),AWT(5)
COMMON /YL/ ET(200),YOND(200)
COMMON /DEL/ DELTA,DTIL,DTILS
COMMON/PROP1/PI(200),RO(200),TT(200),AMW(200),C (20,200),CC(5,200),RE, IEM, NETA
COMMON /FRSTRM/ U INF, RINF, UINF2, R , RE, LXI, ITM, IEM, NETA
DIMENSION SNAME(12),Y(200)
DATA SNAME/'O2 ','N2 ','O ','N ','E- ','C ','H2 ','C2 ','CO ','C3 ','C2H ' /
X
MF=0
NS=12
LINES=1
IDG=1
IEZ=0
XMOL=1.0
C
C-----PUNCH HEADER, CONTROL PARAMETERS, FLOW-FIELD PARAMETERS, AND
C PROFILES....
C
WRITE(6,100)TITLE
WRITE(7,100)TITLE
WRITE(6,101)NETA,MF,NS,LINES,IDG,IEZ
WRITE(7,101)NETA,MF,NS,LINES,IDG,IEZ
WRITE(6,105)R,DELTA,DTIL,XMOL
WRITE(7,105)R,DELTA,DTIL,XMOL
WRITE(6,105)(TT(I),I=1,NETA)
WRITE(7,105)(TT(I),I=1,NETA)
WRITE(6,105)(YOND(I),I=1,NETA)
WRITE(7,105)(YOND(I),I=1,NETA)
WRITE(6,105)(ET(I),I=1,NETA)
WRITE(7,105)(ET(I),I=1,NETA)

```

```

LRAD 10
-RAD 20
LRAD 30
LRAD 40
LRAD 50
LRAD 60
LRAD 70
LRAD 80
LRAD 90
LRAD 100
LRAD 110
LRAD 120
LRAD 130
LRAD 140
LRAD 150
LRAD 160
LRAD 170
-RAD 180
LRAD 190
LRAD 200
LRAD 210
LRAD 220
LRAD 230
LRAD 240
LRAD 250
LRAD 260
LRAD 270
LRAD 280
LRAD 290
LRAD 300
LRAD 310
LRAD 320
LRAD 330
LRAD 340
LRAD 350
LRAD 360

```

```

C          DO20I=1,NS
C
C-----SEARCH FOR SPECIES CORRESPONDING TO LRAD4 LISTING---THEN
C          SET INDEX TO PROPER VALUE....
C
C          L=0
C          DO15K=1,20
C            IF(SP(K).EQ.SNAME(I))L=K
C          15 CONTINUE
C            IF(L.EQ.0)GOTO20
C
C          WRITE(6,104)I,SP(L)
C          WRITE(7,104)I,SP(L)
C
C-----COMPUTE AND PUNCH NUMBER DENSITIES FOR THOSE SPECIES INCLUDED
C          IN THE LRAD4 RADIATION PROGRAM....
C
C          DO10N=1,NETA
C          10 Y(N)=(C(L,N)*AMW(N)/SMW(L))*7.336E21*PI(N)/TT(N)
C
C          WRITE(6,105)(Y(N),N=1,NETA)
C          WRITE(7,105)(Y(N),N=1,NETA)
C          20 CONTINUE
C
C          RETURN
C          100 FORMAT(20A4)
C          101 FORMAT(6I5)
C          104 FORMAT(15,2X,A4)
C          105 FORMAT(6E12.5)
C          END

```

```

LRAD 370
LRAD 380
-RAD 390
LRAD 400
LRAD 410
LRAD 420
LRAD 430
LRAD 440
LRAD 450
LRAD 460
LRAD 470
LRAD 480
LRAD 490
LRAD 500
-RAD 510
LRAD 520
LRAD 530
LRAD 540
LRAD 550
LRAD 560
-RAD 570
LRAD 580
-RAD 590
LRAD 600
-RAD 610
LRAD 620
LRAD 630
-RAD 640
LRAD 650
LRAD 660
LRAD 670

```


O+	16.00	14.22	106.7	0.0	7.2149E-C2	00010		
C.2944E	01-.4108F-C30.9156E-07-	5848E-110.1192E-150.1879E	060.1750E	01			0+	B3
0.2491E	010.2762E-04-.1881E-070.3807E-11-	1028E-150.1879E	060.4424E	01			0+	B2
E-	5.486F-4	14.93	71.4	7.5326E-10	1.770E-05	00001		
0.2508E	01-.6332E-050.1364E-03-	1094E-120.2934E-17-	7450E	03-	1208E	02	E-	B3
0.2507E	010.3440E-06-.1954E-090.3937E-13-	2573E-17-	7450E	03-	1173E	02	E-	B2
C	12.011	3.365	30.6	1.5893E-03	0.0	10001		
0.2141E	010.3219E-03-.5498E-070.3604E-11-	5564E-160.8542E	050.6874E	01			C	B3
0.2612E	01-.2030E-030.1095E-06-	1695E-100.8590E-150.8542E	050.4144E	01			C	B2
CN	26.019	3.856	75.0	1.8989E-02	0.0	10102		
0.3473E	010.7337E-03-.9088E-070.4847E-11-	1018E-150.5420E	050.4152E	01			CN	B3
0.3411E	010.4897E-030.1005E-06-	3473E-100.2361E-140.4745E	050.4746E	01			CN	B2
CO	28.011	3.690	91.7	2.5784E-01	0.0	10012		
0.3366E	010.8027E-03-.1968E-060.1940E-10-	5549E-15-	1434E	050.4263E	01		CO	B3
0.3254E	010.9698E-03-.2647E-060.3037E-10-	1177E-14-	1434E	050.4875E	01		CO	B2
C2	24.022	3.913	78.8	4.2760E-03	0.0	20002		
0.4026E	010.4857E-03-.7026E-070.4666E-11-	1142E-150.9787E	050.1090E	01			C2	B3
0.4443E	01-.2885E-030.3036E-06-	6244E-100.3915E-140.9787E	05-.1090E	01			C2	B2
C2H	25.030	3.880	205.0	1.5543E-01	0.0	21002		
0.5307E	010.8966E-03-.1378E-060.9251E-11-	2278E-150.5809E	05-.5288E	01			C2H	B3
0.3485E	010.3563E-02-.1237E-050.1856E-09-	1013E-130.5809E	050.4784E	01			C2H	B2
C2H2	26.038	4.033	231.8	8.5629E-02	0.0	22002		
0.6789E	010.1503E-02-.2295E-060.1534E-10-	3763E-150.2590E	05-.1539E	02			C2H2	B3
0.3891E	010.5717E-02-.1957E-050.2931E-09-	1585E-130.2590E	050.6520E	00			C2H2	B2
C3	36.033	4.450	128.0	2.0563E-02	0.0	30003		
0.2213F	02-.1759E-010.5565E-05-.6758E-090.2825E-130.	9423E	05-.1021E	03			C3	B3
0.4002E	010.3541E-02-.1316E-050.2064E-09-	1144E-130.9423E	050.2020E	01			C3	B2
C3H	37.041	4.600	356.0	1.7822E-01	0.0	31003		
0.3964709E1	0.620030E-2-.22655E-5.371712E-9-.2262E-13.6283285E5.	3467072E1					C3H	*D2
0.3964709E1	0.620030E-2-.22655E-5.371712E-9-.2262E-13.6283285E5.	3467072E1					C3H	*D2
C4H	49.052	5.210	504.0	1.6777E-01	0.0	41004		
0.5973679E1	0.740338E-2-.27289E-5.443720E-9-.2637E-13.7605163E5-	401004E1					C4H	*D2
0.5973679E1	0.740338E-2-.27289E-5.443720E-9-.2637E-13.7605163E5-	401004E1					C4H	*D2
HCN	27.027	3.630	569.1	4.1142E-02	0.0	11102		
0.653803E03	0.44363E-3-1.2585E-62.1692E-10-1.430E-141.442180E42.	372602E0					HCN	*M3
0.653803E03	0.44363E-3-1.2585E-62.1692E-10-1.430E-141.442180E42.	372602E0					HCN	*M2

H2	2.016	2.827	59.7	3.2934E-02	C.0	C200C	
C.3363E	010.4656E-03-	5127E-070.2802E-11-	4905E-16-	1018E	04-.3716E	01	H2
C.3358E	010.2794E-030.9372E-07-	2948E-100.2141E-14-	1018E	04-.3548E	01		
N	14.008	7.94	71.4	C.0	3.9086E-01	0C101	
0.2746E	01-.3909E-030.1338E-06-	1191E-100.3369E-150.5609E		050.2872E	01	N	B3
0.2474E	010.9097E-04-.7814E-070.2218E-10-	1489E-140.5609E		050.4300E	01	N	B2
0	16.000	7.99	106.7	C.0	1.5007E-01	C0011	
0.2548E	01-.5952E-040.2701E-07-	2798E-110.9380E-160.2915E		050.5049E	01	0	B3
0.2670E	01-.1970E-030.7193E-07-	8901E-110.4002E-150.2915E		050.4504E	01	0	B2
N2	28.616	3.798	71.4	1.8435E-02	1.360E-05	00202	
0.3727E	010.4684E-03-.1140E-060.1154E-10-	3293E-15-.1043E		040.1294E	01	N2	B3
0.3221E	010.9878E-03-.2907E-060.3938E-10-	2000E-14-.1043E		040.4326E	01	N2	B2
02	32.000	3.467	106.7	0.0	00022		
0.3721E	010.4254E-03-.2835E-070.6050E-12-	5186E-17-.1044E		040.3254E	01	02	B3
0.3316E	010.1151E-02-.3726E-060.6186E-10-	3665E-14-.1044E		040.5393E	01	02	B2
C.810E-07							

SLAB P=0.1,BLOWING RATE=C.05 7-2-585

NETA	NSP	UINF	DTIL	RAD	RINF	RZB	DELTA
59	20	0.50CE 05	0.538E-01	0.9C0E 01	0.285E-05	0.536E-01	0.395E-01
SPECIES	SMW	SIGMA	EOK	CWALL	CSHOCK	A(I,J)	
C+	12.011	15.000	30.6	0.0	0.0	10000	
H	1.008	2.708	37.0	0.01717	0.0	01000	
N+	14.008	14.930	71.4	0.0	0.38688	00100	
O+	16.000	14.220	106.7	0.0	0.07215	00010	
E-	0.001	14.930	71.4	0.00000	0.00002	00001	
C	12.011	3.385	30.6	0.00159	0.0	10001	
CN	26.019	3.856	75.0	0.01899	0.0	10102	
CO	28.011	3.690	91.7	0.25784	0.0	10012	
C2	24.022	3.913	78.8	0.00428	0.0	20002	
C2H	25.030	3.880	205.0	0.15543	0.0	21002	
C2H2	26.038	4.033	231.8	0.08563	0.0	22002	
C3	36.033	4.450	128.0	0.02056	0.0	30003	
C3H	37.041	4.600	356.0	0.17822	0.0	31003	
C4H	49.052	5.210	504.0	0.16777	0.0	41004	
HCN	27.027	3.630	569.1	0.04114	0.0	11102	
H2	2.016	2.827	59.7	0.03293	0.0	02000	
N	14.008	7.940	71.4	0.0	0.39086	00101	
O	16.000	7.990	106.7	0.0	0.15007	00011	
N2	28.016	3.798	71.4	0.01843	0.00001	00202	
O2	32.000	3.467	106.7	0.0	0.0	00022	

EQUILIBRIUM MASS FRACTIONS

CTA	C+	H	N+	N	G+	E-	C	CN	CC	C2	C2H
0.0	0.5310E-04	0.4141E-01	0.1153E-10	0.6806E-13	0.1117E-14	0.1434E-01	0.4503E-01	0.5084E-01	0.2574E-00	0.2751E-01	0.1904E-00
0.0050	0.5507E-05	0.4543E-01	0.4517E-11	0.2291E-14	0.6806E-14	0.2150E-01	0.5084E-01	0.5084E-01	0.2574E-00	0.2751E-01	0.1904E-00
0.0100	0.4959E-11	0.4937E-01	0.3971E-17	0.3793E-20	0.2720E-11	0.3280E-01	0.5644E-01	0.5644E-01	0.2574E-00	0.2751E-01	0.1904E-00
0.0150	0.4623E-06	0.5327E-01	0.1247E-14	0.5863E-17	0.2875E-16	0.4407E-01	0.6160E-01	0.6160E-01	0.2574E-00	0.2751E-01	0.1904E-00
0.0200	0.1639E-06	0.5710E-01	0.4249E-13	0.6528E-15	0.5988E-15	0.7262E-01	0.6641E-01	0.6641E-01	0.2574E-00	0.2751E-01	0.1904E-00
0.0231	0.5677E-08	0.5930E-01	0.4010E-14	0.2650E-16	0.5294E-17	0.9269E-01	0.7103E-01	0.7103E-01	0.2574E-00	0.2751E-01	0.1904E-00
0.0262	0.2411E-06	0.6153E-01	0.1581E-12	0.4010E-14	0.4866E-16	0.1167E-00	0.7103E-01	0.7103E-01	0.2574E-00	0.2751E-01	0.1904E-00
0.0294	0.6043E-09	0.6337E-01	0.3579E-15	0.2521E-17	0.7476E-12	0.1461E-00	0.7277E-01	0.7277E-01	0.2574E-00	0.2751E-01	0.1904E-00
0.0325	0.8784E-13	0.6542E-01	0.5707E-19	0.6353E-21	0.2944E-09	0.1801E-00	0.7406E-01	0.7406E-01	0.2574E-00	0.2751E-01	0.1904E-00
0.0356	0.2778E-09	0.6703E-01	0.2406E-15	0.6013E-17	0.1505E-09	0.2193E-00	0.7466E-01	0.7466E-01	0.2574E-00	0.2751E-01	0.1904E-00
0.0387	0.8870E-13	0.6840E-01	0.1321E-18	0.1764E-20	0.3763E-07	0.2622E-00	0.7514E-01	0.7514E-01	0.2574E-00	0.2751E-01	0.1904E-00
0.0450	0.2360E-06	0.7040E-01	0.4952E-12	0.6491E-14	0.3220E-07	0.3529E-00	0.7387E-01	0.7387E-01	0.2574E-00	0.2751E-01	0.1904E-00
0.0537	0.1740E-05	0.7143E-01	0.7644E-11	0.1019E-12	0.3303E-07	0.4632E-00	0.6733E-01	0.6733E-01	0.2574E-00	0.2751E-01	0.1904E-00
0.0625	0.1650E-04	0.7236E-01	0.9111E-10	0.3724E-11	0.3303E-07	0.5332E-00	0.5540E-01	0.5540E-01	0.2574E-00	0.2751E-01	0.1904E-00
0.0712	0.2092E-03	0.7241E-01	0.5357E-06	0.6346E-09	0.8921E-04	0.5717E-00	0.4080E-01	0.4080E-01	0.2574E-00	0.2751E-01	0.1904E-00
0.0800	0.4561E-03	0.7243E-01	0.5352E-07	0.6944E-08	0.1916E-07	0.5944E-00	0.2644E-01	0.2644E-01	0.2574E-00	0.2751E-01	0.1904E-00
0.0850	0.6866E-03	0.7241E-01	0.1173E-06	0.2436E-07	0.2923E-07	0.6040E-00	0.1902E-01	0.1902E-01	0.2574E-00	0.2751E-01	0.1904E-00
0.0925	0.1252E-02	0.7233E-01	0.3659E-06	0.1476E-06	0.5377E-07	0.6187E-00	0.1164E-01	0.1164E-01	0.2574E-00	0.2751E-01	0.1904E-00
0.1000	0.2260E-02	0.7219E-01	0.1017E-05	0.7616E-06	0.9851E-07	0.6386E-00	0.6425E-02	0.6425E-02	0.2574E-00	0.2751E-01	0.1904E-00
0.1100	0.4320E-02	0.7153E-01	0.4650E-05	0.4604E-05	0.2169E-06	0.6730E-00	0.2746E-02	0.2746E-02	0.2574E-00	0.2751E-01	0.1904E-00
0.1200	0.1022E-01	0.7157E-01	0.1090E-04	0.1742E-04	0.4523E-06	0.6949E-00	0.1177E-02	0.1177E-02	0.2574E-00	0.2751E-01	0.1904E-00
0.1300	0.1661E-01	0.7084E-01	0.7034E-04	0.4756E-04	0.7327E-06	0.6951E-00	0.2254E-03	0.2254E-03	0.2574E-00	0.2751E-01	0.1904E-00
0.1400	0.2403E-01	0.6947E-01	0.1715E-03	0.1067E-03	0.1250E-05	0.6798E-00	0.1259E-03	0.1259E-03	0.2574E-00	0.2751E-01	0.1904E-00
0.1500	0.4300E-01	0.6692E-01	0.3992E-03	0.3765E-03	0.1522E-05	0.6510E-00	0.8722E-03	0.8722E-03	0.2574E-00	0.2751E-01	0.1904E-00
0.1600	0.6044E-01	0.6280E-01	0.3992E-03	0.3765E-03	0.2676E-05	0.6110E-00	0.6779E-04	0.6779E-04	0.2574E-00	0.2751E-01	0.1904E-00
0.1700	0.7742E-01	0.5765E-01	0.8226E-03	0.6163E-03	0.3429E-05	0.5557E-00	0.5885E-04	0.5885E-04	0.2574E-00	0.2751E-01	0.1904E-00
0.1800	0.9103E-01	0.5162E-01	0.1828E-02	0.9413E-03	0.4087E-05	0.4498E-00	0.5427E-04	0.5427E-04	0.2574E-00	0.2751E-01	0.1904E-00
0.2000	0.9834E-01	0.3874E-01	0.5113E-02	0.2504E-02	0.4813E-05	0.3105E-00	0.4566E-04	0.4566E-04	0.2574E-00	0.2751E-01	0.1904E-00
0.2100	0.9182E-01	0.3258E-01	0.5912E-02	0.3207E-02	0.4613E-05	0.2510E-00	0.3051E-04	0.3051E-04	0.2574E-00	0.2751E-01	0.1904E-00
0.2200	0.8008E-01	0.2691E-01	0.1490E-01	0.3707E-02	0.4420E-05	0.1228E-00	0.1479E-04	0.1479E-04	0.2574E-00	0.2751E-01	0.1904E-00
0.2300	0.6545E-01	0.2185E-01	0.2135E-01	0.4186E-02	0.4133E-05	0.7853E-01	0.1479E-04	0.1479E-04	0.2574E-00	0.2751E-01	0.1904E-00
0.2400	0.4989E-01	0.1740E-01	0.2854E-01	0.5260E-02	0.3634E-05	0.2662E-01	0.5064E-05	0.5064E-05	0.2574E-00	0.2751E-01	0.1904E-00
0.2600	0.2317E-01	0.1020E-01	0.4672E-01	0.7804E-02	0.3634E-05	0.2662E-01	0.5064E-05	0.5064E-05	0.2574E-00	0.2751E-01	0.1904E-00
0.2800	0.8036E-02	0.4947E-02	0.6446E-01	0.1043E-01	0.3593E-05	0.7132E-02	0.1256E-05	0.1256E-05	0.2574E-00	0.2751E-01	0.1904E-00
0.3000	0.2435E-02	0.1531E-02	0.6000E-01	0.1279E-01	0.3840E-05	0.1894E-02	0.2596E-06	0.2596E-06	0.2574E-00	0.2751E-01	0.1904E-00
0.3300	0.2507E-03	0.1457E-03	0.1032E-01	0.1644E-01	0.4698E-05	0.1613E-03	0.1944E-07	0.1944E-07	0.2574E-00	0.2751E-01	0.1904E-00
0.3500	0.3380E-04	0.1891E-04	0.1194E-01	0.1507E-01	0.5408E-05	0.1940E-04	0.1947E-08	0.1947E-08	0.2574E-00	0.2751E-01	0.1904E-00
0.3800	0.3617E-04	0.1884E-04	0.1446E-01	0.2364E-01	0.6544E-05	0.1770E-04	0.1286E-08	0.1286E-08	0.2574E-00	0.2751E-01	0.1904E-00
0.4200	0.3665E-04	0.1877E-04	0.1756E-01	0.2864E-01	0.7935E-05	0.1603E-04	0.2172E-09	0.2172E-09	0.2574E-00	0.2751E-01	0.1904E-00
0.4400	0.3975E-04	0.1868E-04	0.1506E-01	0.3128E-01	0.8625E-05	0.1531E-04	0.5222E-09	0.5222E-09	0.2574E-00	0.2751E-01	0.1904E-00
0.4800	0.4087E-04	0.1890E-04	0.2026E-01	0.3421E-01	0.5305E-05	0.1457E-04	0.3492E-09	0.3492E-09	0.2574E-00	0.2751E-01	0.1904E-00
0.5000	0.4180E-04	0.1850E-04	0.2231E-01	0.3724E-01	0.1091E-04	0.1334E-04	0.2452E-09	0.2452E-09	0.2574E-00	0.2751E-01	0.1904E-00
0.5400	0.4289E-04	0.1852E-04	0.2406E-01	0.4066E-01	0.1091E-04	0.1334E-04	0.2452E-09	0.2452E-09	0.2574E-00	0.2751E-01	0.1904E-00
0.5600	0.4338E-04	0.1853E-04	0.2483E-01	0.4209E-01	0.1127E-04	0.1287E-04	0.2149E-09	0.2149E-09	0.2574E-00	0.2751E-01	0.1904E-00
0.5800	0.4385E-04	0.1853E-04	0.2571E-01	0.4350E-01	0.1101E-04	0.1267E-04	0.2149E-09	0.2149E-09	0.2574E-00	0.2751E-01	0.1904E-00
0.6200	0.4463E-04	0.1854E-04	0.2714E-01	0.4669E-01	0.1233E-04	0.1202E-04	0.2149E-09	0.2149E-09	0.2574E-00	0.2751E-01	0.1904E-00
0.6400	0.4463E-04	0.1854E-04	0.2714E-01	0.4669E-01	0.1233E-04	0.1202E-04	0.2149E-09	0.2149E-09	0.2574E-00	0.2751E-01	0.1904E-00
0.6800	0.4537E-04	0.1895E-04	0.2865E-01	0.4580E-01	0.1307E-04	0.1103E-04	0.2149E-09	0.2149E-09	0.2574E-00	0.2751E-01	0.1904E-00
0.7000	0.4605E-04	0.1895E-04	0.3003E-01	0.5271E-01	0.1343E-04	0.1059E-04	0.2149E-09	0.2149E-09	0.2574E-00	0.2751E-01	0.1904E-00
0.7400	0.4671E-04	0.1857E-04	0.3145E-01	0.5577E-01	0.1434E-04	0.1059E-04	0.2149E-09	0.2149E-09	0.2574E-00	0.2751E-01	0.1904E-00
0.7600	0.4671E-04	0.1857E-04	0.3145E-01	0.5577E-01	0.1434E-04	0.1059E-04	0.2149E-09	0.2149E-09	0.2574E-00	0.2751E-01	0.1904E-00
0.8000	0.4737E-04	0.1857E-04	0.3290E-01	0.5894E-01	0.1501E-04	0.1014E-04	0.1667E-09	0.1667E-09	0.2574E-00	0.2751E-01	0.1904E-00
0.8200	0.4802E-04	0.1857E-04	0.3434E-01	0.6221E-01	0.1509E-04	0.9714E-05	0.1074E-09	0.1074E-09	0.2574E-00	0.2751E-01	0.1904E-00
0.8600	0.4867E-04	0.1857E-04	0.3587E-01	0.6570E-01	0.1641E-04	0.9280E-05	0.7273E-10	0.7273E-10	0.2574E-00	0.2751E-01	0.1904E-00
0.8800	0.4867E-04	0.1899E-04	0.3587E-01	0.6570E-01	0.1641E-04	0.9280E-05	0.7273E-10	0.7273E-10	0.2574E-00	0.2751E-01	0.1904E-00
0.9200	0.4934E-04	0.1900E-04	0.3748E-01	0.6560E-01	0.1717E-04	0.8430E-05	0.7584E-10	0.7584E-10	0.2574E-00	0.2751E-01	0.1904E-00
0.9400	0.5000E-04	0.1900E-04	0.3748E-01	0.6560E-01	0.1717E-04	0.8430E-05	0.7584E-10	0.7584E-10	0.2574E-00	0.2751E-01	0.1904E-00
0.9800	0.5093E-04	0.1903E-04	0.3912E-01	0.7362E-01	0.1795E-04	0.8405E-05	0.4395E-10	0.4395E-10	0.2574E-00	0.2751E-01	0.1904E-00
1.0000	0.5148E-04	0.1904E-04	0.4231E-01	0.8180E-01	0.1944E-04	0.7634E-05	0.5947E-10	0.5947E-10	0.2574E-00	0.2751E-01	0.1904E-00

9

EQUILIBRIUM MASS FRACTIONS

FTA	C2H2	C3	C3H4	C4H	HCN	H2	N	U	N2	C2
0.0	0.197E-01	0.942E-01	0.155E-01	0.142E-01	0.153E-01	0.153E-01	0.526E-04	0.971E-07	0.161E-01	0.332E-14
0.0056	0.1457E-01	0.113E-01	0.138E-01	0.142E-01	0.153E-01	0.153E-01	0.721E-04	0.145E-01	0.145E-01	0.546E-14
0.0100	0.1035E-01	0.113E-01	0.118E-01	0.113E-01	0.123E-01	0.101E-01	0.595E-04	0.223E-01	0.111E-01	0.554E-14
0.0150	0.0660E-02	0.147E-01	0.106E-01	0.106E-01	0.106E-01	0.106E-01	0.116E-03	0.355E-01	0.102E-01	0.555E-14
0.0200	0.4365E-02	0.155E-01	0.106E-01	0.106E-01	0.106E-01	0.106E-01	0.177E-03	0.555E-01	0.102E-01	0.555E-14
0.0231	0.3185E-02	0.155E-01	0.106E-01	0.106E-01	0.106E-01	0.106E-01	0.231E-03	0.767E-01	0.102E-01	0.555E-14
0.0262	0.223E-02	0.155E-01	0.106E-01	0.106E-01	0.106E-01	0.106E-01	0.286E-03	0.106E-01	0.102E-01	0.555E-14
0.0294	0.149E-02	0.145E-01	0.106E-01	0.106E-01	0.106E-01	0.106E-01	0.358E-03	0.106E-01	0.102E-01	0.555E-14
0.0325	0.959E-03	0.131E-01	0.106E-01	0.106E-01	0.106E-01	0.106E-01	0.450E-03	0.106E-01	0.102E-01	0.555E-14
0.0356	0.574E-03	0.111E-01	0.106E-01	0.106E-01	0.106E-01	0.106E-01	0.575E-03	0.106E-01	0.102E-01	0.555E-14
0.0387	0.348E-03	0.901E-01	0.106E-01	0.106E-01	0.106E-01	0.106E-01	0.743E-03	0.106E-01	0.102E-01	0.555E-14
0.0450	0.104E-03	0.485E-01	0.106E-01	0.106E-01	0.106E-01	0.106E-01	0.129E-02	0.106E-01	0.102E-01	0.555E-14
0.0537	0.142E-04	0.131E-01	0.106E-01	0.106E-01	0.106E-01	0.106E-01	0.259E-02	0.106E-01	0.102E-01	0.555E-14
0.0625	0.167E-05	0.282E-02	0.106E-01	0.106E-01	0.106E-01	0.106E-01	0.675E-02	0.106E-01	0.102E-01	0.555E-14
0.0712	0.201E-06	0.532E-03	0.106E-01	0.106E-01	0.106E-01	0.106E-01	0.137E-01	0.106E-01	0.102E-01	0.555E-14
0.0800	0.258E-07	0.103E-03	0.106E-01	0.106E-01	0.106E-01	0.106E-01	0.237E-01	0.106E-01	0.102E-01	0.555E-14
0.0850	0.841E-08	0.416E-04	0.106E-01	0.106E-01	0.106E-01	0.106E-01	0.306E-01	0.106E-01	0.102E-01	0.555E-14
0.0925	0.164E-08	0.108E-04	0.106E-01	0.106E-01	0.106E-01	0.106E-01	0.450E-01	0.106E-01	0.102E-01	0.555E-14
0.1000	0.338E-09	0.326E-05	0.106E-01	0.106E-01	0.106E-01	0.106E-01	0.504E-01	0.106E-01	0.102E-01	0.555E-14
0.1100	0.439E-10	0.641E-06	0.106E-01	0.106E-01	0.106E-01	0.106E-01	0.544E-01	0.106E-01	0.102E-01	0.555E-14
0.1200	0.625E-11	0.136E-06	0.106E-01	0.106E-01	0.106E-01	0.106E-01	0.596E-01	0.106E-01	0.102E-01	0.555E-14
0.1300	0.877E-12	0.326E-07	0.106E-01	0.106E-01	0.106E-01	0.106E-01	0.675E-01	0.106E-01	0.102E-01	0.555E-14
0.1400	0.221E-12	0.903E-08	0.106E-01	0.106E-01	0.106E-01	0.106E-01	0.818E-01	0.106E-01	0.102E-01	0.555E-14
0.1500	0.565E-13	0.282E-08	0.106E-01	0.106E-01	0.106E-01	0.106E-01	0.105E-01	0.106E-01	0.102E-01	0.555E-14
0.1600	0.167E-13	0.105E-08	0.106E-01	0.106E-01	0.106E-01	0.106E-01	0.142E-01	0.106E-01	0.102E-01	0.555E-14
0.1700	0.556E-14	0.420E-09	0.106E-01	0.106E-01	0.106E-01	0.106E-01	0.194E-01	0.106E-01	0.102E-01	0.555E-14
0.1800	0.197E-14	0.175E-09	0.106E-01	0.106E-01	0.106E-01	0.106E-01	0.263E-01	0.106E-01	0.102E-01	0.555E-14
0.2000	0.259E-15	0.291E-10	0.106E-01	0.106E-01	0.106E-01	0.106E-01	0.306E-01	0.106E-01	0.102E-01	0.555E-14
0.2100	0.884E-16	0.106E-10	0.106E-01	0.106E-01	0.106E-01	0.106E-01	0.354E-01	0.106E-01	0.102E-01	0.555E-14
0.2200	0.276E-16	0.346E-11	0.106E-01	0.106E-01	0.106E-01	0.106E-01	0.401E-01	0.106E-01	0.102E-01	0.555E-14
0.2300	0.783E-17	0.992E-12	0.106E-01	0.106E-01	0.106E-01	0.106E-01	0.450E-01	0.106E-01	0.102E-01	0.555E-14
0.2400	0.192E-17	0.240E-12	0.106E-01	0.106E-01	0.106E-01	0.106E-01	0.504E-01	0.106E-01	0.102E-01	0.555E-14
0.2600	0.686E-19	0.814E-14	0.106E-01	0.106E-01	0.106E-01	0.106E-01	0.675E-01	0.106E-01	0.102E-01	0.555E-14
0.2800	0.224E-20	0.126E-15	0.106E-01	0.106E-01	0.106E-01	0.106E-01	0.818E-01	0.106E-01	0.102E-01	0.555E-14
0.3000	0.375E-21	0.200E-17	0.106E-01	0.106E-01	0.106E-01	0.106E-01	0.105E-01	0.106E-01	0.102E-01	0.555E-14
0.3300	0.282E-22	0.756E-21	0.106E-01	0.106E-01	0.106E-01	0.106E-01	0.142E-01	0.106E-01	0.102E-01	0.555E-14
0.3500	0.554E-22	0.871E-22	0.106E-01	0.106E-01	0.106E-01	0.106E-01	0.194E-01	0.106E-01	0.102E-01	0.555E-14
0.3600	0.360E-22	0.607E-21	0.106E-01	0.106E-01	0.106E-01	0.106E-01	0.263E-01	0.106E-01	0.102E-01	0.555E-14
0.4200	0.460E-22	0.694E-21	0.106E-01	0.106E-01	0.106E-01	0.106E-01	0.306E-01	0.106E-01	0.102E-01	0.555E-14
0.4600	0.514E-22	0.742E-21	0.106E-01	0.106E-01	0.106E-01	0.106E-01	0.354E-01	0.106E-01	0.102E-01	0.555E-14
0.4800	0.586E-22	0.797E-21	0.106E-01	0.106E-01	0.106E-01	0.106E-01	0.401E-01	0.106E-01	0.102E-01	0.555E-14
0.5000	0.673E-22	0.921E-21	0.106E-01	0.106E-01	0.106E-01	0.106E-01	0.450E-01	0.106E-01	0.102E-01	0.555E-14
0.5400	0.764E-22	0.920E-21	0.106E-01	0.106E-01	0.106E-01	0.106E-01	0.504E-01	0.106E-01	0.102E-01	0.555E-14
0.5600	0.835E-22	0.947E-21	0.106E-01	0.106E-01	0.106E-01	0.106E-01	0.544E-01	0.106E-01	0.102E-01	0.555E-14
0.5800	0.885E-22	0.976E-21	0.106E-01	0.106E-01	0.106E-01	0.106E-01	0.596E-01	0.106E-01	0.102E-01	0.555E-14
0.6200	0.100E-21	0.102E-20	0.106E-01	0.106E-01	0.106E-01	0.106E-01	0.675E-01	0.106E-01	0.102E-01	0.555E-14
0.6400	0.100E-21	0.107E-20	0.106E-01	0.106E-01	0.106E-01	0.106E-01	0.818E-01	0.106E-01	0.102E-01	0.555E-14
0.6800	0.129E-21	0.117E-20	0.106E-01	0.106E-01	0.106E-01	0.106E-01	0.105E-01	0.106E-01	0.102E-01	0.555E-14
0.7000	0.129E-21	0.117E-20	0.106E-01	0.106E-01	0.106E-01	0.106E-01	0.142E-01	0.106E-01	0.102E-01	0.555E-14
0.7400	0.140E-21	0.117E-20	0.106E-01	0.106E-01	0.106E-01	0.106E-01	0.194E-01	0.106E-01	0.102E-01	0.555E-14
0.8000	0.140E-21	0.117E-20	0.106E-01	0.106E-01	0.106E-01	0.106E-01	0.263E-01	0.106E-01	0.102E-01	0.555E-14
0.8600	0.157E-21	0.123E-20	0.106E-01	0.106E-01	0.106E-01	0.106E-01	0.306E-01	0.106E-01	0.102E-01	0.555E-14
0.9200	0.175E-21	0.124E-20	0.106E-01	0.106E-01	0.106E-01	0.106E-01	0.354E-01	0.106E-01	0.102E-01	0.555E-14
0.9600	0.609E-21	0.240E-20	0.106E-01	0.106E-01	0.106E-01	0.106E-01	0.401E-01	0.106E-01	0.102E-01	0.555E-14
0.9800	0.700E-21	0.250E-20	0.106E-01	0.106E-01	0.106E-01	0.106E-01	0.450E-01	0.106E-01	0.102E-01	0.555E-14
1.0000	0.388E-21	0.261E-20	0.106E-01	0.106E-01	0.106E-01	0.106E-01	0.504E-01	0.106E-01	0.102E-01	0.555E-14
1.0000	0.444E-22	0.439E-21	0.106E-01	0.106E-01	0.106E-01	0.106E-01	0.544E-01	0.106E-01	0.102E-01	0.555E-14

EQUILIBRIUM MOLE FRACTIONS

ETA	C+	H	N4	O+	H-	C	CN	CO	C2	C2H
0.0	0.5703E-04	0.510E	0.1025E-10	0.5351E-11	0.2531E-10	0.1465E-01	0.2153E-01	0.1145E	0.1426E-01	0.1458E-01
0.0050	0.5478E-05	0.5384E	0.3852E-11	0.4679E-14	0.1735E-09	0.2147E-01	0.2233E-01	0.1110E	0.1926E-01	0.1926E-01
0.0100	-0.4730E-11	0.5612E	0.3248E-17	-0.4152E-20	0.5631E-07	0.3134E-01	0.2485E-01	0.1055E	0.2580E-01	0.2580E-01
0.0150	0.4403E-08	0.5794E	0.9763E-15	0.4017E-17	0.5745E-12	0.4479E-01	0.2599E-01	0.1059E	0.3303E-01	0.3303E-01
0.0200	0.1602E-06	0.5925E	0.3591E-13	0.4268E-15	0.1639E-10	0.6325E-01	0.2670E-01	0.9630E-01	0.4250E-01	0.4250E-01
0.0231	0.4796E-08	0.5975E	0.2908E-14	0.1300E-16	0.1719E-12	0.7830E-01	0.2666E-01	0.7332E-01	0.4211E-01	0.4211E-01
0.0262	0.1990E-06	0.6004E	0.1110E-12	0.8866E-15	-0.1589E-11	0.9574E-01	0.2684E-01	0.7051E-01	0.3151E-01	0.3151E-01
0.0294	0.4793E-09	0.6008E	0.2441E-15	0.1501E-17	0.1298E-07	0.1159E	0.2664E-01	0.6769E-01	0.5600E-01	0.5600E-01
0.0325	0.6750E-13	0.5991E	0.3760E-19	0.3665E-21	0.4987E-05	0.1364E	0.2628E-01	0.6456E-01	0.6124E-01	0.6124E-01
0.0356	0.2070E-09	0.5951E	0.1537E-15	0.3635E-17	0.3108E-05	0.1634E	0.2575E-01	0.8239E-01	0.6250E-01	0.6250E-01
0.0387	-0.6431E-13	0.5893E	0.8169E-19	-0.9575E-21	0.5957E-03	0.1895E	0.2508E-01	0.7594E-01	0.6160E-01	0.6160E-01
0.0450	0.1650E-06	0.5759E	0.2056E-12	0.3345E-14	0.4839E-03	0.2422E	0.2341E-01	0.7591E-01	0.5137E-01	0.5137E-01
0.0537	0.1136E-05	0.5585E	0.4277E-11	0.4699E-13	0.4622E-03	0.3023E	0.2028E-01	0.7214E-01	0.3392E-01	0.3392E-01
0.0625	0.6662E-05	0.5472E	0.4558E-10	0.1774E-11	0.4590E-03	0.3385E	0.1623E-01	0.7101E-01	0.1776E-01	0.1776E-01
0.0712	0.1310E-03	0.5400E	0.5621E-08	0.2981E-09	0.1222E-03	0.3578E	0.1179E-01	0.6490E-01	0.2659E-01	0.2659E-01
0.0800	0.2825E-03	0.5346E	0.2683E-07	0.3182E-08	0.2599E-03	0.3662E	0.7571E-02	0.6718E-01	0.4186E-01	0.4186E-01
0.0850	0.4230E-03	0.5316E	0.1965E-07	0.1127E-07	0.3943E-03	0.3721E	0.5560E-02	0.6535E-01	0.2803E-01	0.2803E-01
0.0925	0.7633E-03	0.5262E	0.1918E-06	0.6766E-07	0.7189E-03	0.3777E	0.3282E-02	0.6001E-01	0.1562E-01	0.1562E-01
0.1000	0.1362E-02	0.5186E	0.5259E-06	0.3447E-06	0.1300E-02	0.3850E	0.1788E-02	0.4902E-01	0.1270E-01	0.1270E-01
0.1100	0.5919E-02	0.4936E	0.1766E-05	0.2037E-05	0.2798E-02	0.3966E	0.7470E-03	0.2755E-01	0.4365E-01	0.4365E-01
0.1200	0.5919E-02	0.4936E	0.5442E-05	0.7571E-05	0.5734E-02	0.4022E	0.3148E-03	0.1661E-01	0.2164E-01	0.2164E-01
0.1300	0.9571E-02	0.4863E	0.1340E-04	0.2037E-04	0.9242E-02	0.4005E	0.5594E-04	0.4332E-02	0.1110E-01	0.1110E-01
0.1400	0.1616E-01	0.4771E	0.3476E-04	0.4616E-04	0.1579E-01	0.3918E	0.3453E-04	0.1670E-02	0.6121E-01	0.6121E-01
0.1500	0.2499E-01	0.4633E	0.2546E-04	0.9185E-04	0.2446E-01	0.3787E	0.2340E-04	0.3734E-03	0.3000E-01	0.3000E-01
0.1600	0.3575E-01	0.4432E	0.2027E-03	0.1672E-03	0.3470E-01	0.3618E	0.1853E-04	0.3731E-03	0.2242E-01	0.2242E-01
0.1700	0.4715E-01	0.4182E	0.4659E-03	0.2817E-03	0.4572E-01	0.3392E	0.1854E-04	0.2144E-03	0.1442E-01	0.1442E-01
0.1800	0.5754E-01	0.3888E	0.5908E-03	0.4406E-03	0.5655E-01	0.3096E	0.1564E-04	0.1333E-03	0.5335E-01	0.5335E-01
0.2000	0.6868E-01	0.3224E	0.3660E-02	0.9802E-03	0.7317E-01	0.2311E	0.1471E-04	0.6169E-04	0.3605E-01	0.3605E-01
0.2100	0.6794E-01	0.2672E	0.4289E-02	0.1391E-02	0.7798E-01	0.1862E	0.1323E-04	0.4254E-04	0.2045E-01	0.2045E-01
0.2200	0.6291E-01	0.2519E	0.1609E-01	0.1928E-02	0.8025E-01	0.1422E	0.1106E-04	0.2940E-04	0.1060E-01	0.1060E-01
0.2300	0.5451E-01	0.2168E	0.1525E-01	0.2617E-02	0.8059E-01	0.1023E	0.8528E-05	0.1944E-04	0.5036E-01	0.5036E-01
0.2400	0.4391E-01	0.1825E	0.2184E-01	0.3476E-02	0.7568E-01	0.6909E-01	0.6009E-05	0.1220E-04	0.2113E-01	0.2113E-01
0.2600	0.2238E-01	0.1175E	0.3870E-01	0.5650E-02	0.7614E-01	0.5752E-01	0.2266E-05	0.3524E-04	0.2530E-01	0.2530E-01
0.2800	0.8291E-02	0.6081E-01	0.5702E-01	0.8078E-02	0.8116E-01	0.7554E-02	0.1828E-06	0.9751E-06	0.1200E-01	0.1200E-01
0.3000	0.2603E-02	0.1951E-01	0.7334E-01	0.1027E-01	0.6590E-01	0.2029E-02	0.1464E-06	0.2141E-06	0.2794E-14	0.2794E-14
0.3300	0.2672E-03	0.1851E-02	0.9429E-01	0.1315E-01	0.1096E	0.1719E-03	0.9563E-08	0.1269E-07	0.7171E-14	0.7171E-14
0.3500	0.3550E-04	0.2354E-03	0.1075E	0.1504E-01	0.1243E	0.2037E-04	0.9437E-09	0.1184E-08	0.5931E-14	0.5931E-14
0.3800	0.3701E-04	0.2257E-03	0.1269E	0.1787E-01	0.1466E	0.1816E-04	0.6073E-09	0.7130E-09	0.5600E-14	0.5600E-14
0.4200	0.3834E-04	0.2230E-03	0.1495E	0.2133E-01	0.1728E	0.1589E-04	0.3284E-09	0.3637E-09	0.2616E-14	0.2616E-14
0.4400	0.3866E-04	0.2200E-03	0.1598E	0.2295E-01	0.1847E	0.1496E-04	0.2359E-09	0.2550E-09	0.1521E-14	0.1521E-14
0.4800	0.3934E-04	0.2167E-03	0.1706E	0.2472E-01	0.1573E	0.1404E-04	0.1552E-09	0.1636E-09	0.8481E-14	0.8481E-14
0.5000	0.3982E-04	0.2135E-03	0.1812E	0.2649E-01	0.2097E	0.1311E-04	0.1073E-09	0.1016E-09	0.6111E-14	0.6111E-14
0.5400	0.3998E-04	0.2101E-03	0.1923E	0.2840E-01	0.2227E	0.1226E-04	0.1935E-10	0.1156E-10	0.4657E-14	0.4657E-14
0.5600	0.4014E-04	0.2087E-03	0.1970E	0.2924E-01	0.2283E	0.1191E-04	0.1012E-10	0.6503E-11	0.3171E-14	0.3171E-14
0.5800	0.4030E-04	0.2074E-03	0.2015E	0.3005E-01	0.2236E	0.1156E-04	0.9762E-11	0.7459E-11	0.1413E-14	0.1413E-14
0.6200	0.4043E-04	0.2045E-03	0.2108E	0.3175E-01	0.2446E	0.1089E-04	0.3386E-10	0.2394E-10	0.1234E-14	0.1234E-14
0.6400	0.4043E-04	0.2045E-03	0.2108E	0.3175E-01	0.2446E	0.1089E-04	0.3386E-10	0.2394E-10	0.1234E-14	0.1234E-14
0.6800	0.4043E-04	0.2017E-03	0.2195E	0.3340E-01	0.2549E	0.1027E-04	0.3074E-10	0.1872E-10	0.1060E-14	0.1060E-14
0.7000	0.4063E-04	0.1953E-03	0.2272E	0.3491E-01	0.2642E	0.9735E-05	0.9450E-10	0.8698E-10	0.9071E-15	0.9071E-15
0.7400	0.4070E-04	0.1969E-03	0.2350E	0.3647E-01	0.2735E	0.8644E-05	0.8644E-10	0.8626E-10	0.7276E-15	0.7276E-15
0.7600	0.4070E-04	0.1969E-03	0.2350E	0.3647E-01	0.2735E	0.8644E-05	0.8644E-10	0.8626E-10	0.7276E-15	0.7276E-15
0.8000	0.4075E-04	0.1945E-03	0.2426E	0.3806E-01	0.2827E	0.8722E-05	0.6020E-10	0.6020E-10	0.5737E-15	0.5737E-15
0.8200	0.4078E-04	0.1921E-03	0.2501E	0.3967E-01	0.2918E	0.8250E-05	0.4210E-10	0.4210E-10	0.3704E-15	0.3704E-15
0.8600	0.4079E-04	0.1897E-03	0.2578E	0.4117E-01	0.3011E	0.7778E-05	0.2814E-10	0.2340E-10	0.6752E-16	0.6752E-16
0.8800	0.4079E-04	0.1897E-03	0.2578E	0.4117E-01	0.3011E	0.7778E-05	0.2814E-10	0.2340E-10	0.6752E-16	0.6752E-16
0.9200	0.4078E-04	0.1871E-03	0.2656E	0.4319E-01	0.3108E	0.7305E-05	0.2897E-10	0.2422E-10	0.6367E-16	0.6367E-16
0.9400	0.4075E-04	0.1846E-03	0.2734E	0.4504E-01	0.3203E	0.6850E-05	0.2779E-10	0.2426E-10	0.5949E-16	0.5949E-16
0.9800	0.4084E-04	0.1818E-03	0.2821E	0.4723E-01	0.3312E	0.6372E-05	0.3104E-10	0.2742E-10	0.5251E-16	0.5251E-16
1.0000	0.4084E-04	0.1800E-03	0.2878E	0.4872E-01	0.3384E	0.6050E-05	0.2178E-10	0.1934E-10	0.1777E-16	0.1777E-16

EQUILIBRIUM MOLE FRACTIONS

ETA	C2H2	C3	C3H	C4H	HCN	H2	N	O	N2	O2
0.0	0.9537E-02	0.3253E-01	0.5208E-01	0.2244E-01	0.4510E-02	0.9320E-01	0.4667E-04	0.7752E-01	0.7150E-02	0.1104E-14
0.0050	0.6687E-02	0.3745E-01	0.4457E-01	0.2147E-01	0.5741E-02	0.9390E-01	0.6157E-04	0.1104E-01	0.6247E-02	0.2030E-14
0.0100	0.4552E-02	0.4185E-01	0.3661E-01	0.1661E-01	0.5741E-02	0.9390E-01	0.6157E-04	0.1104E-01	0.6247E-02	0.1904E-14
0.0150	0.2930E-02	0.4498E-01	0.2420E-01	0.1205E-01	0.3531E-02	0.9388E-01	0.1007E-03	0.2403E-01	0.4560E-02	0.3274E-14
0.0200	0.1754E-02	0.4559E-01	0.2621E-01	0.1205E-01	0.2836E-02	0.9388E-01	0.1007E-03	0.2403E-01	0.4560E-02	0.7031E-14
0.0231	0.1241E-02	0.4477E-01	0.1636E-01	0.5846E-02	0.2782E-02	0.9388E-01	0.1678E-03	0.4775E-01	0.3463E-02	0.5900E-14
0.0262	0.8395E-03	0.4233E-01	0.1234E-01	0.4059E-02	0.1802E-02	0.9388E-01	0.2014E-03	0.4775E-01	0.3463E-02	0.1571E-13
0.0294	0.5481E-03	0.3851E-01	0.9121E-02	0.2641E-02	0.1436E-02	0.9388E-01	0.2415E-03	0.4775E-01	0.3463E-02	0.2048E-13
0.0325	0.3402E-03	0.3356E-01	0.6581E-02	0.1621E-02	0.1079E-02	0.9388E-01	0.2967E-03	0.1234E-01	0.2653E-02	0.2824E-13
0.0356	0.2033E-03	0.2775E-01	0.3566E-02	0.9330E-03	0.6817E-03	0.9388E-01	0.3679E-03	0.1763E-01	0.2513E-02	0.5377E-13
0.0387	0.1163E-03	0.2172E-01	0.2407E-02	0.4950E-03	0.4155E-03	0.9388E-01	0.4604E-03	0.2552E-01	0.2433E-02	0.3663E-13
0.0450	0.3310E-04	0.1111E-01	0.7416E-03	0.1050E-03	0.3374E-03	0.9388E-01	0.7631E-03	0.5452E-01	0.2471E-02	0.2307E-12
0.0537	0.4285E-05	0.2934E-02	0.9488E-04	0.7073E-05	0.1373E-03	0.9388E-01	0.1675E-02	0.2169E-01	0.2950E-02	0.11790E-11
0.0625	0.4914E-06	0.5928E-03	0.5614E-05	0.3492E-06	0.5320E-04	0.9388E-01	0.1675E-02	0.2169E-01	0.2950E-02	0.1421E-10
0.0712	0.5825E-07	0.1112E-03	0.9558E-06	0.1762E-07	0.1530E-04	0.9388E-01	0.2734E-02	0.3581E-01	0.3964E-02	0.1217E-09
0.0800	0.7377E-08	0.2136E-04	0.1606E-06	0.8433E-09	0.6600E-05	0.9388E-01	0.1262E-01	0.1387E-02	0.3374E-02	0.9275E-09
0.0850	0.2331E-08	0.6622E-05	0.2931E-07	0.1730E-09	0.3434E-05	0.9388E-01	0.1585E-01	0.2739E-02	0.2739E-02	0.2734E-08
0.0925	0.4634E-09	0.2212E-05	0.4104E-08	0.6059E-11	0.1216E-05	0.9388E-01	0.2020E-01	0.7649E-02	0.1693E-02	0.1196E-07
0.1000	0.9420E-10	0.6446E-06	0.8604E-09	0.1674E-11	0.4417E-06	0.9388E-01	0.2324E-01	0.1783E-01	0.6745E-03	0.3967E-07
0.1100	0.1195E-10	0.1261E-06	0.2210E-10	0.8953E-13	0.6714E-07	0.9388E-01	0.2549E-01	0.3822E-01	0.3681E-03	0.9645E-07
0.1200	0.1670E-11	0.2596E-07	0.1078E-10	0.5330E-14	0.1577E-07	0.9388E-01	0.2702E-01	0.5335E-01	0.1686E-03	0.1635E-06
0.1300	0.2332E-12	0.5334E-08	0.1511E-11	0.8698E-15	0.5559E-08	0.9388E-01	0.2947E-01	0.6602E-01	0.4476E-04	0.1071E-06
0.1400	0.5893E-13	0.1736E-08	0.2685E-12	0.4276E-16	0.1814E-08	0.9388E-01	0.3357E-01	0.6334E-01	0.2393E-04	0.7630E-07
0.1500	0.1514E-13	0.5556E-09	0.5915E-13	0.5096E-17	0.7715E-09	0.9388E-01	0.4095E-01	0.6661E-01	0.1687E-04	0.5711E-07
0.1600	0.4575E-14	0.2083E-09	0.1564E-13	0.4426E-18	0.4437E-09	0.9388E-01	0.5369E-01	0.7609E-01	0.1566E-04	0.4633E-07
0.1700	0.1563E-14	0.8531E-10	0.4717E-14	0.2105E-18	0.2495E-09	0.9388E-01	0.7437E-01	0.7455E-01	0.1800E-04	0.4608E-07
0.1800	0.5751E-15	0.3697E-10	0.1540E-14	0.3705E-19	0.1711E-09	0.9388E-01	0.1052E-01	0.8022E-01	0.2400E-04	0.3941E-07
0.2000	0.3606E-16	0.6752E-11	0.1702E-15	0.2742E-20	0.8503E-10	0.9388E-01	0.2642E-01	0.9571E-01	0.4917E-04	0.4062E-07
0.2100	0.3019E-16	0.2632E-11	0.5154E-16	0.3094E-22	0.4136E-10	0.9388E-01	0.2675E-01	0.1050E-01	0.6782E-04	0.4391E-07
0.2200	0.1007E-16	0.9131E-12	0.1419E-16	0.2582E-22	0.3553E-10	0.9388E-01	0.3357E-01	0.1150E-01	0.8664E-04	0.4008E-07
0.2300	0.3011E-17	0.2756E-12	0.3356E-17	0.9489E-23	0.2351E-10	0.9388E-01	0.4027E-01	0.1250E-01	0.1092E-04	0.5270E-07
0.2400	0.7814E-18	0.7051E-13	0.6643E-18	0.5476E-22	0.1262E-10	0.9388E-01	0.4646E-01	0.1347E-01	0.1267E-04	0.5725E-07
0.2600	0.3042E-19	0.2623E-14	0.1313E-19	0.2528E-23	0.2537E-11	0.9388E-01	0.5604E-01	0.1513E-01	0.1445E-04	0.6418E-07
0.2800	0.1070E-20	0.4335E-16	0.3427E-21	0.3825E-23	0.3025E-12	0.9388E-01	0.6144E-01	0.1625E-01	0.1387E-04	0.6645E-07
0.3000	0.1853E-21	0.7131E-18	0.3560E-22	0.6377E-24	0.1529E-13	0.9388E-01	0.6346E-01	0.1676E-01	0.1194E-04	0.6372E-07
0.3300	0.1390E-22	0.2687E-21	0.8025E-22	0.2361E-22	0.5039E-16	0.9388E-01	0.6159E-01	0.1646E-01	0.2166E-04	0.5268E-07
0.3500	0.2686E-22	0.3050E-22	0.5356E-22	0.2270E-22	0.6227E-18	0.9388E-01	0.5926E-01	0.1616E-01	0.6153E-04	0.4532E-07
0.3800	0.1704E-22	0.2073E-21	0.3591E-22	0.1784E-21	0.2131E-18	0.9388E-01	0.5555E-01	0.1526E-01	0.4175E-04	0.3619E-07
0.4200	0.2109E-22	0.2305E-21	0.3238E-22	0.1760E-21	0.1413E-18	0.9388E-01	0.5115E-01	0.1441E-01	0.2690E-04	0.2839E-07
0.4400	0.2318E-22	0.2416E-21	0.3076E-22	0.1787E-21	0.1139E-18	0.9388E-01	0.4921E-01	0.1401E-01	0.2214E-04	0.2540E-07
0.4800	0.2606E-22	0.2557E-21	0.2553E-22	0.1780E-21	0.8839E-19	0.9388E-01	0.4712E-01	0.1358E-01	0.1803E-04	0.2756E-07
0.5000	0.2942E-22	0.2689E-21	0.2837E-22	0.1771E-21	0.7512E-19	0.9388E-01	0.4507E-01	0.1316E-01	0.1473E-04	0.2608E-07
0.5400	0.3371E-22	0.2859E-21	0.2750E-22	0.1785E-21	0.5292E-19	0.9388E-01	0.4292E-01	0.1271E-01	0.1195E-04	0.1776E-07
0.5600	0.3568E-22	0.2927E-21	0.2702E-22	0.1786E-21	0.4623E-19	0.9388E-01	0.4201E-01	0.1251E-01	0.1051E-04	0.1643E-07
0.6000	0.3766E-22	0.2995E-21	0.2655E-22	0.1767E-21	0.3235E-19	0.9388E-01	0.4113E-01	0.1232E-01	0.1059E-04	0.1590E-07
0.6200	0.4179E-22	0.3095E-21	0.2534E-22	0.1773E-21	0.2843E-19	0.9388E-01	0.3933E-01	0.1193E-01	0.5593E-05	0.1437E-07
0.6400	0.4179E-22	0.3095E-21	0.2534E-22	0.1773E-21	0.2843E-19	0.9388E-01	0.3933E-01	0.1193E-01	0.5593E-05	0.1437E-07
0.6600	0.4653E-22	0.3213E-21	0.2431E-22	0.1774E-21	0.2378E-19	0.9388E-01	0.3763E-01	0.1156E-01	0.7016E-05	0.1296E-07
0.7000	0.5129E-22	0.3320E-21	0.2337E-22	0.1777E-21	0.1806E-19	0.9388E-01	0.3612E-01	0.1123E-01	0.5995E-05	0.1175E-07
0.7400	0.5655E-22	0.3424E-21	0.2236E-22	0.1776E-21	0.1695E-20	0.9388E-01	0.3460E-01	0.1089E-01	0.5103E-05	0.1070E-07
0.7600	0.5655E-22	0.3424E-21	0.2236E-22	0.1776E-21	0.1695E-20	0.9388E-01	0.3460E-01	0.1089E-01	0.5103E-05	0.1070E-07
0.8000	0.6239E-22	0.3529E-21	0.2132E-22	0.1776E-21	0.4750E-20	0.9388E-01	0.3310E-01	0.1054E-01	0.4336E-05	0.9694E-08
0.8200	0.6239E-22	0.3529E-21	0.2132E-22	0.1776E-21	0.4750E-20	0.9388E-01	0.3310E-01	0.1054E-01	0.4336E-05	0.9694E-08
0.8600	0.2357E-21	0.6707E-21	0.6053E-22	0.5269E-23	0.2843E-20	0.9388E-01	0.3011E-01	0.0943E-01	0.3098E-05	0.788E-08
0.8800	0.2357E-21	0.6707E-21	0.6053E-22	0.5269E-23	0.2843E-20	0.9388E-01	0.3011E-01	0.0943E-01	0.3098E-05	0.788E-08
0.9200	0.2670E-21	0.6904E-21	0.5780E-22	0.5270E-23	0.2520E-20	0.9388E-01	0.2655E-01	0.0940E-01	0.2977E-05	0.7036E-08
0.9400	0.3032E-21	0.7113E-21	0.5454E-22	0.5269E-23	0.2169E-20	0.9388E-01	0.2701E-01	0.0903E-01	0.2135E-05	0.6255E-08
0.9600	0.1438E-22	0.1102E-21	0.5373E-22	0.5299E-23	0.3360E-21	0.9388E-01	0.2526E-01	0.0855E-01	0.1705E-05	0.5403E-08
1.0000	0.1625E-22	0.1162E-21	0.5249E-22	0.5286E-23	0.3540E-21	0.9388E-01	0.2412E-01	0.0836E-01	0.1467E-05	0.4476E-08

APPENDIX H

GRAPHICAL RESULTS OF CASES RUN

In Table 6.2. a tabular summary of the results of this study is given. This appendix includes figures corresponding to the summarized results of Table 6.2. Figures H-1 through H-8 present the temperature, velocity, velocity function, and radiative flux divergence for each case examined.

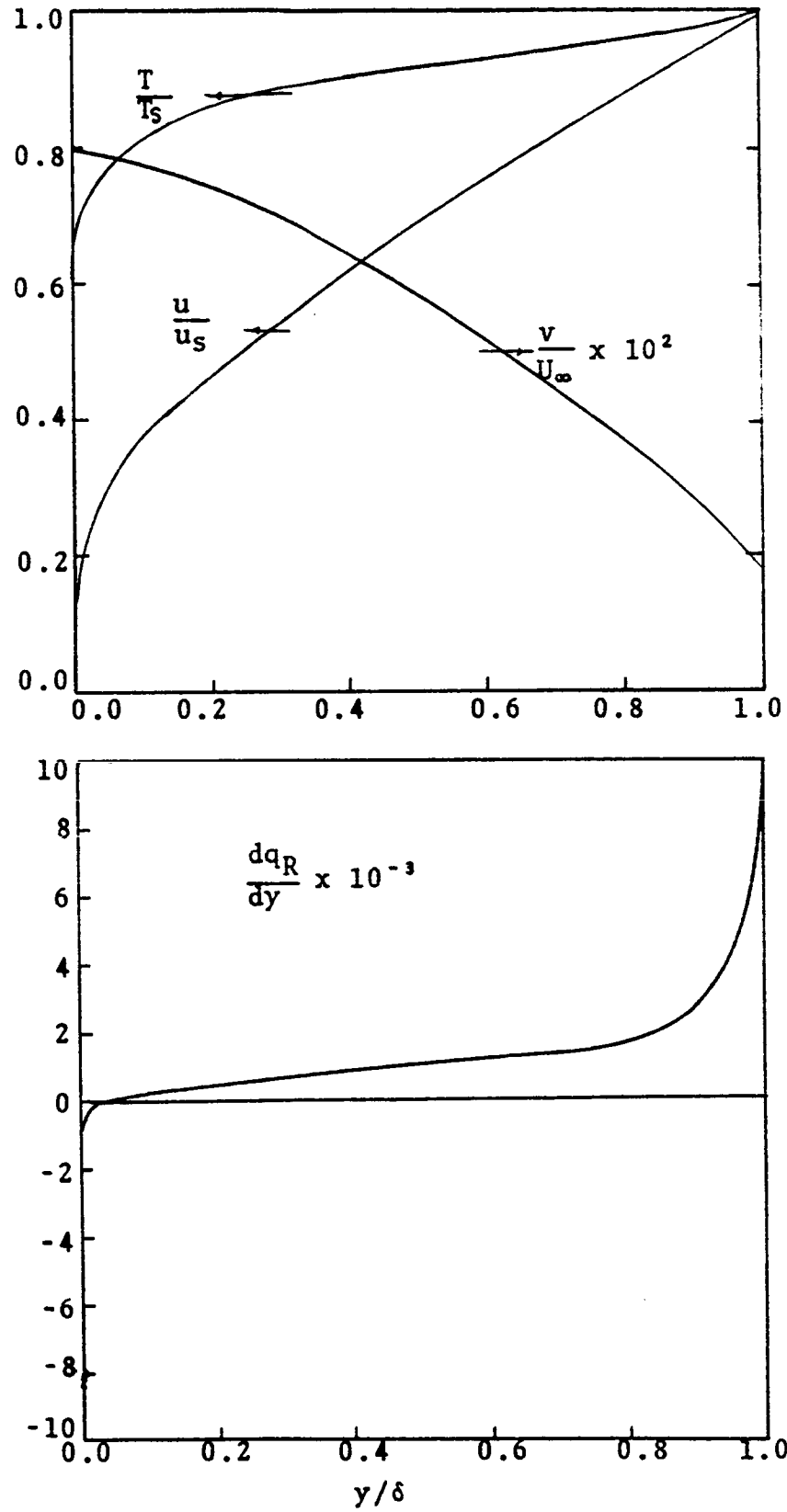


Figure H-1. Case Number 1.

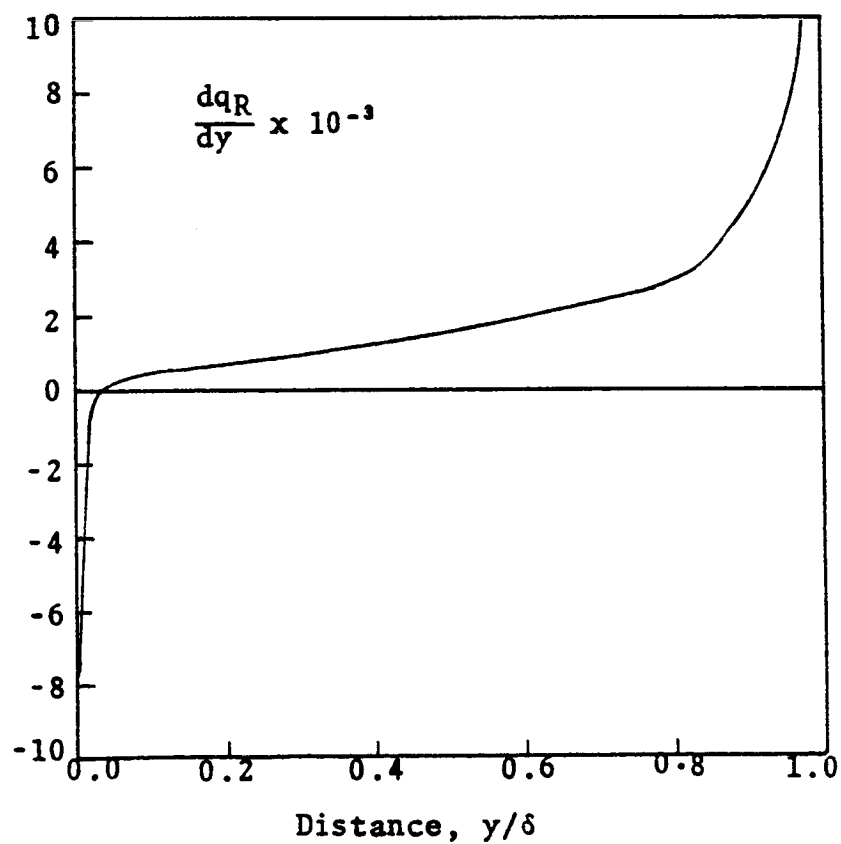
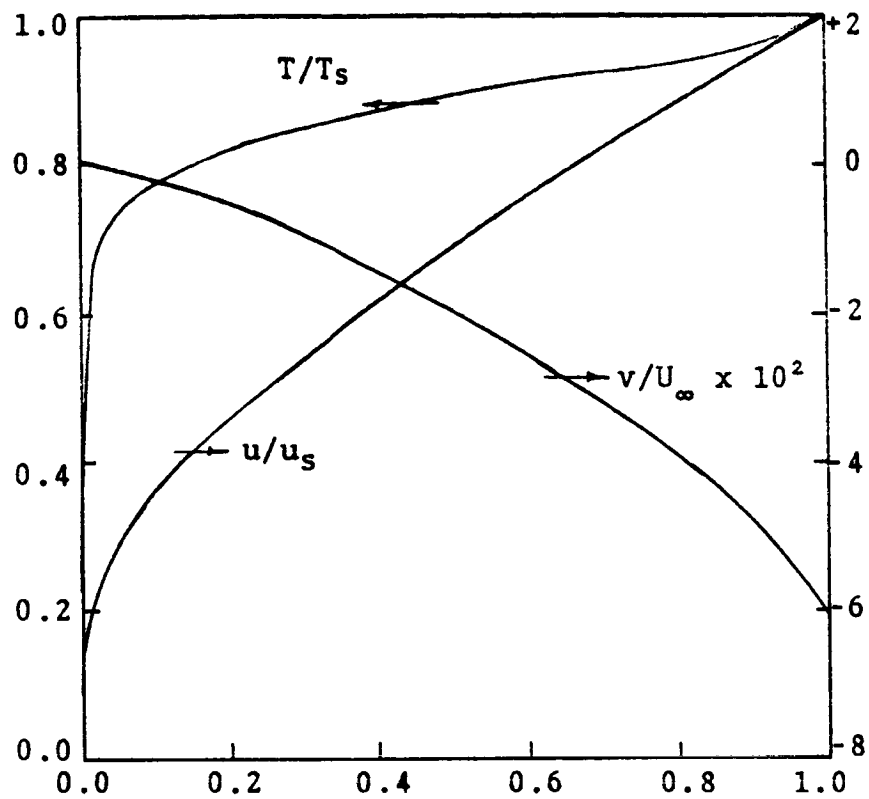


Figure H-2. Case Number 2.

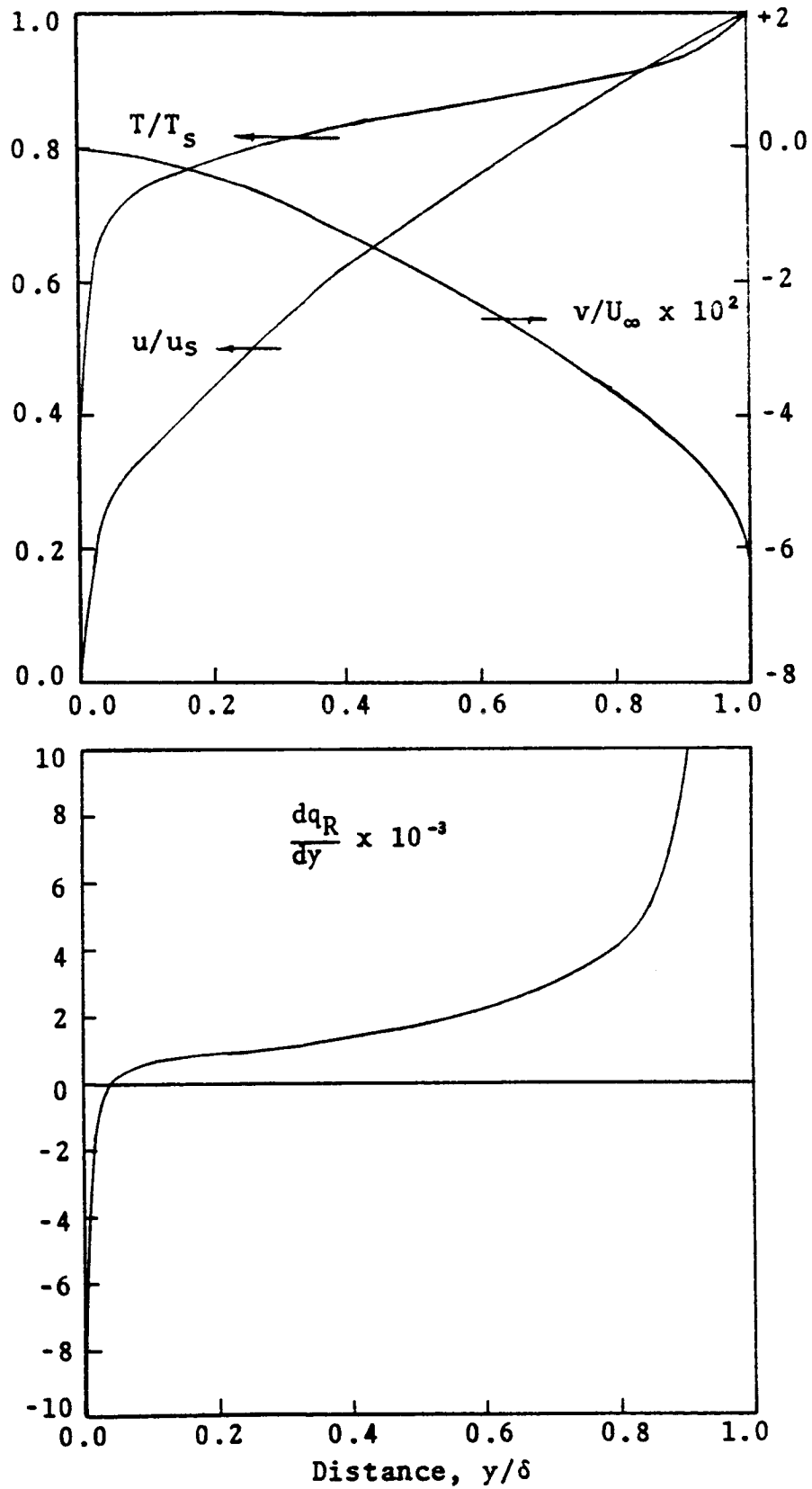


Figure H-3. Case Number 3.

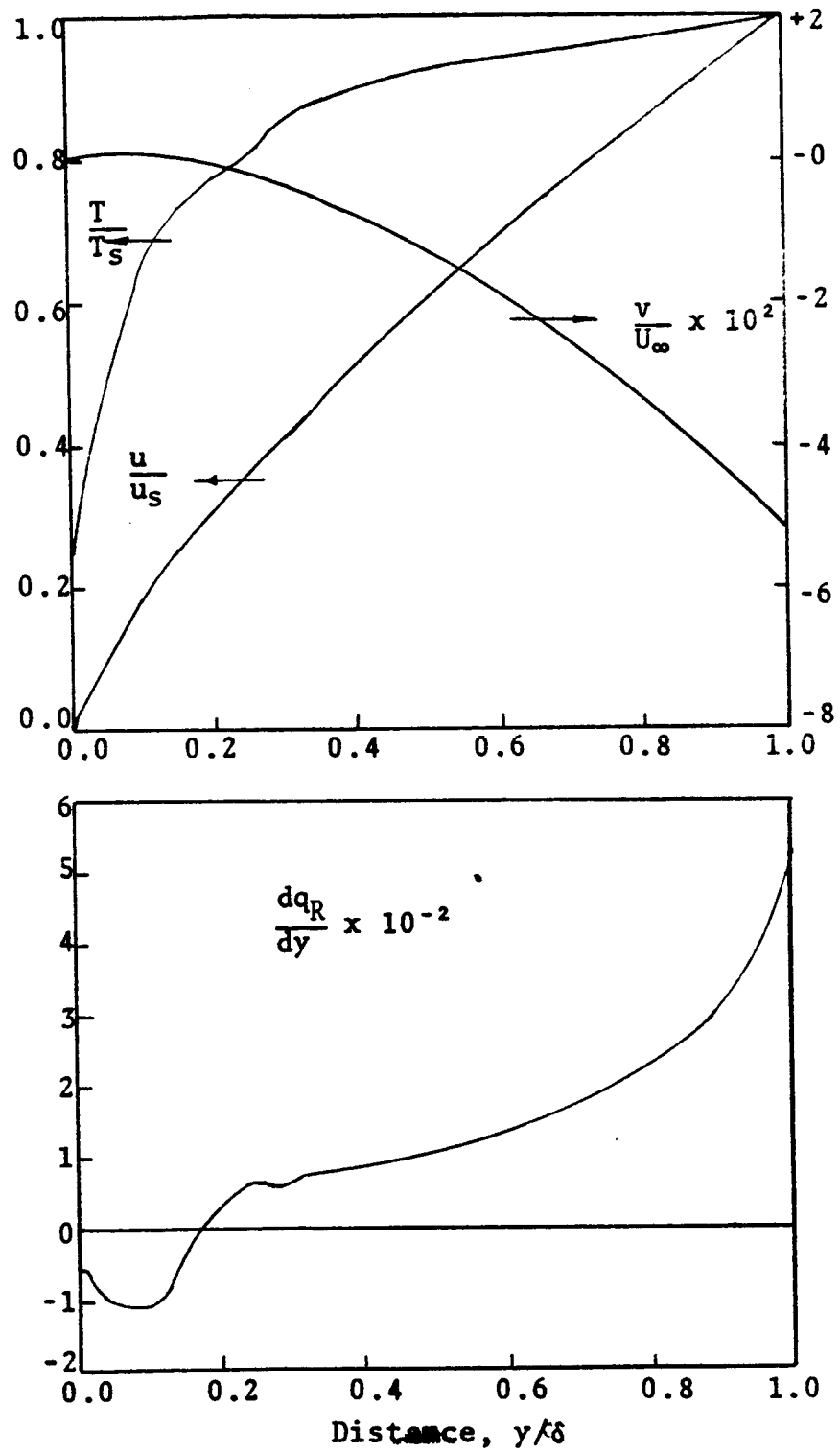


Figure H-4. Cases 4 and 5.

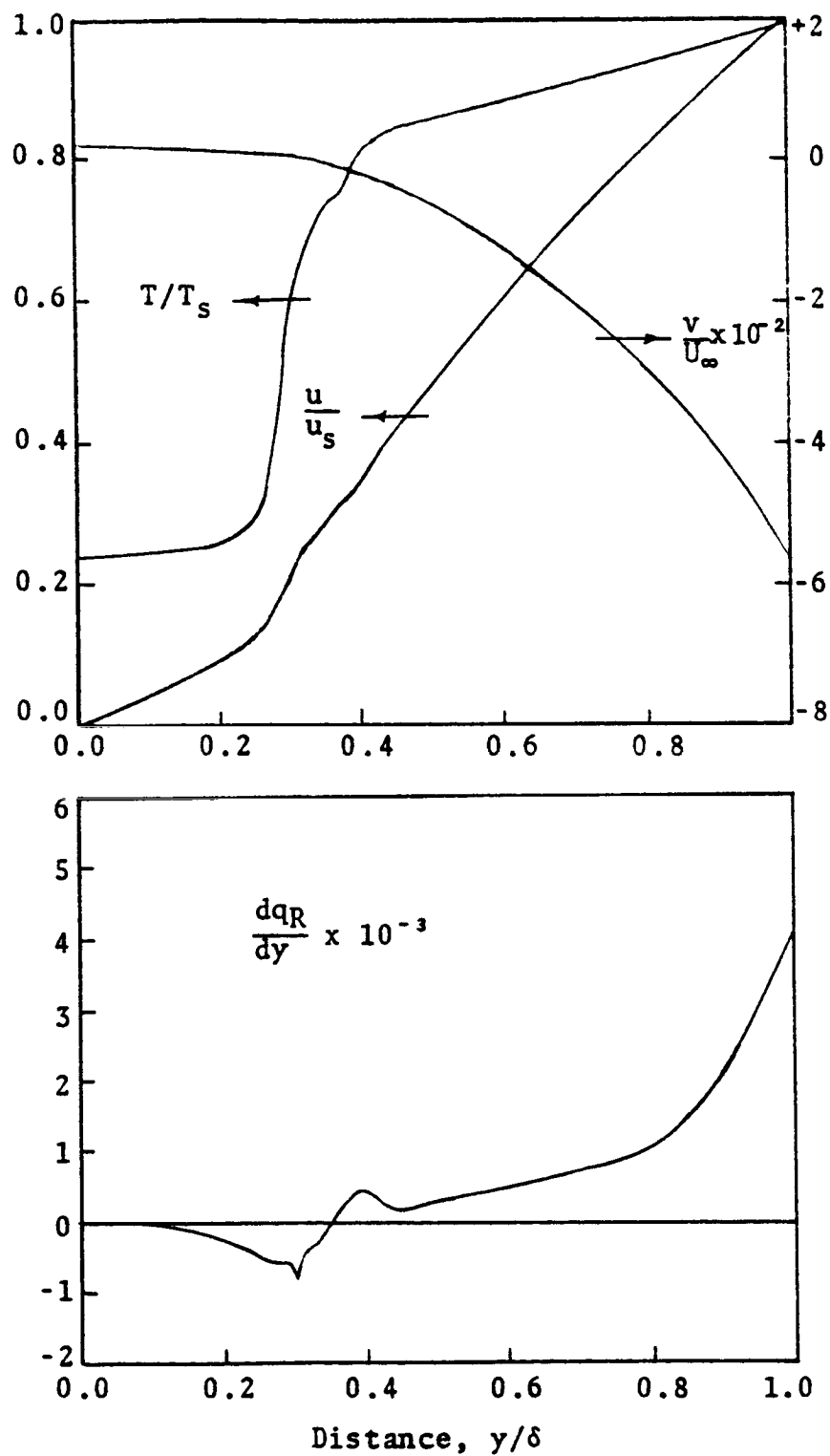


Figure H-5. Cases 6 and 7.

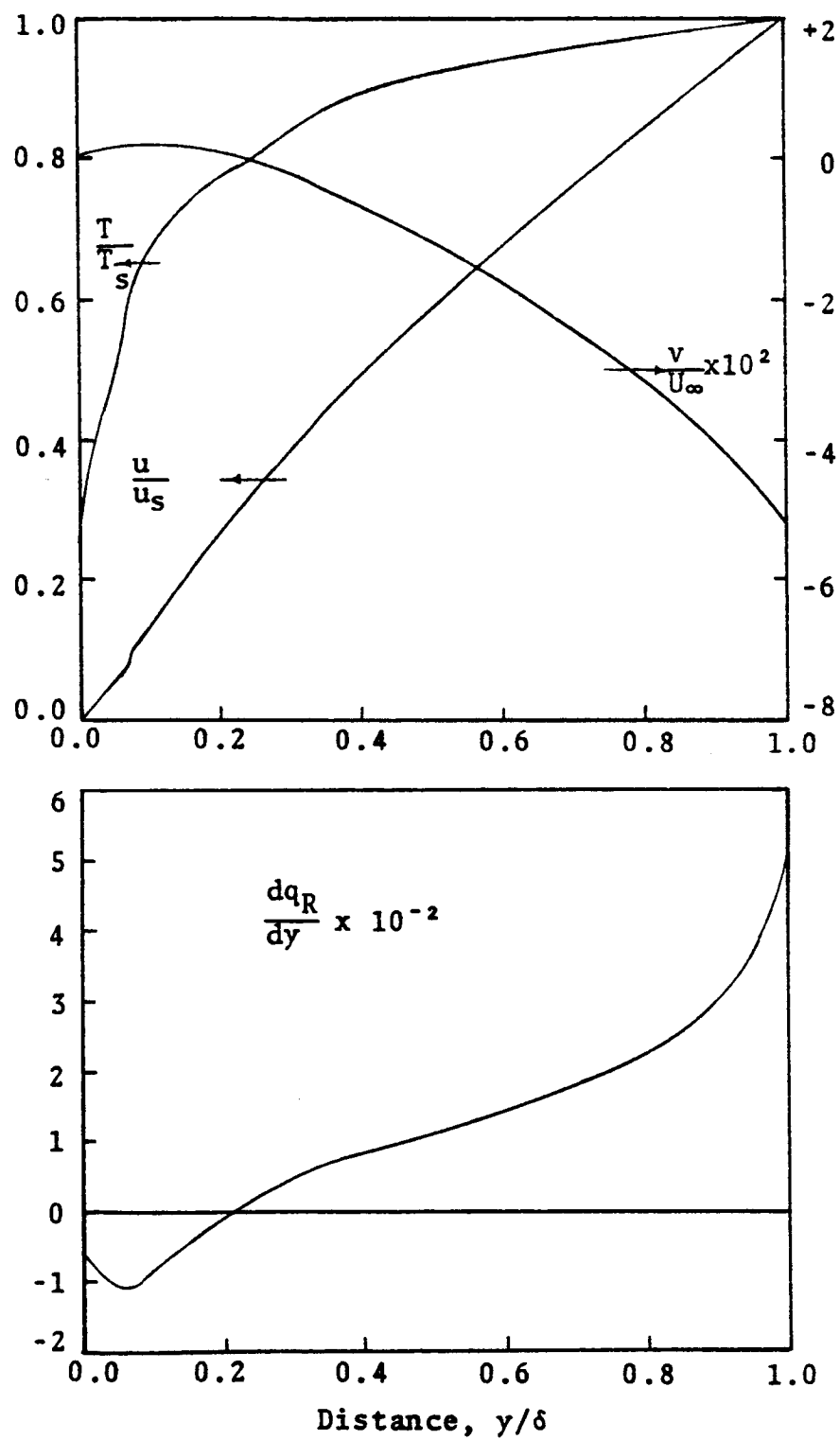


Figure H-6. Case Number 8.

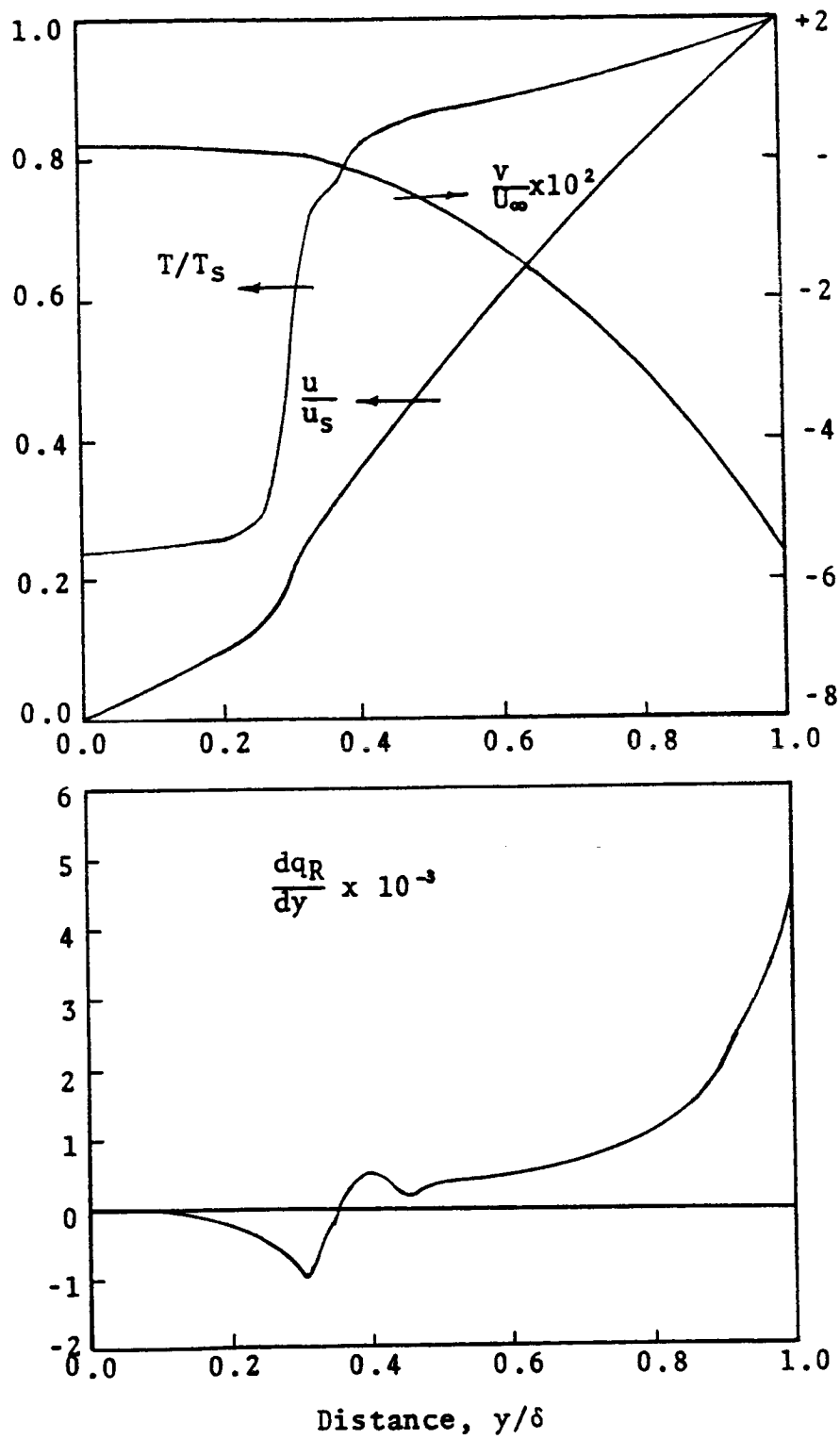


Figure H-7. Case Number 9.

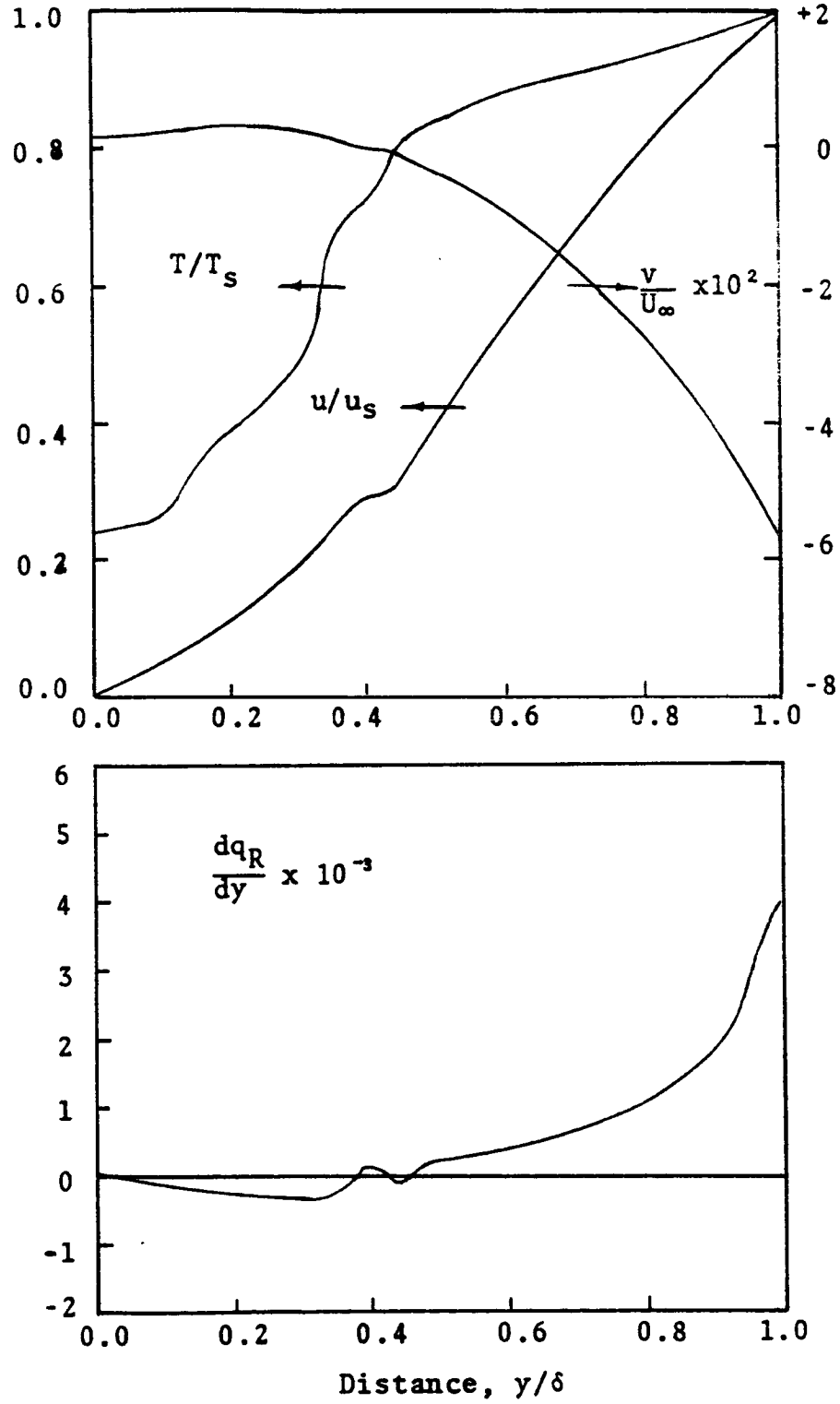


Figure H-8. Case Number 10.

APPENDIX I

POSTERIORI EXAMINATION OF SORET EFFECT

A conservative estimate of the maximum thermal diffusion effect that could be expected from the results of this study is given in this appendix. The examination proceeds as follows:

The contribution of temperature gradients toward mass diffusion is given by the following equation (from Eq. 2.1),

$$J_i = D_i^T \frac{d \ln T}{dy} \quad (I-1)$$

From Reference I-1, a large value of the binary thermal diffusion ratio ($M^2 D_A^T / \rho M_A M_B D_{AB}$) is seen to be on the order of 10^{-1} . Assuming that the molecular weights are of equal orders of magnitude,

$$\frac{D_A^T}{\rho \mathcal{D}_{AB}} \approx 10^{-1} \quad (I-2)$$

The most severe temperature gradient encountered in this study appeared in Case 6 (Figure H-5) at $y/\delta \approx 0.28$. The gradient in the log of the temperature at that point was computed to be 36.2°K/ft . At the same point,

a liberal estimate of the binary diffusion coefficient (D_{AB}) is 4.0×10^{-7} (D_{H-H}). From these estimates, and the corresponding value of the density, the non-dimensional mass flux ($J_i/\rho_s U_\infty$) was computed as $\approx 0.5 \times 10^{-5}$. In Table I-1, a tabulation of the predicted (multicomponent) mass fluxes is given for the same point of analysis. From these values, it is clearly shown that the maximum estimated mass flux due to thermal diffusion is at least an order of magnitude less than the significant species fluxes due to concentration differences.

TABLE I-1

MASS FLUXES OF PRINCIPLE SPECIES FOR CASE
NUMBER SIX AT $y/\delta = 0.28$

<u>Species</u>	<u>Mass Flux</u> <u>$J_i/\rho_s U_\infty$</u>
H ₂	0.3756×10^{-6}
N	-0.1555×10^{-4}
O	-0.4416×10^{-4}
N ₂	0.1110×10^{-4}
C ⁺	-0.1118×10^{-5}
H	0.1014×10^{-4}
C	-0.1568×10^{-3}
CN	0.2543×10^{-4}
CO	0.1562×10^{-3}
C ₂	0.1419×10^{-4}
C ₂ H	0.1092×10^{-6}

REFERENCES

- I-1. Bird, R. B., W. E. Stewart, and E. N. Lightfoot, Transport Phenomena, New York: John Wiley and Sons, Inc., 1966.

DISTRIBUTION

- 1 Headquarters Contracts Division
Code DHC-4
National Aeronautics and Space Administration
Washington, D. C. 20546
- 1 Mr. Robert T. Swann, Assistant Head
Thermal Protection Materials Branch
Langley Research Center
Hampton, Virginia
- 1 Mr. James N. Moss
Thermal Protection Materials Branch
Langley Research Center
Hampton, Virginia
- 1 Mr. K. H. Wilson
Lockheed Missles and Space Company
Palo Alto, California
- 1 Dr. W. S. Rigdon
Dr. R. B. Dirling
Dr. M. Thomas
McConnell Douglas Astronautics Company - Western Division
Santa Monica, California

Reacting Fluids Laboratory

- 4 Authors
- 1 Mr. G. Perez